



USMCA 2012



11th INTERNATIONAL SYMPOSIUM
ON NEW TECHNOLOGIES
FOR URBAN SAFETY
OF MEGA CITIES IN ASIA



USMCA 2012

(SEIKEN SYMPOSIUM 71)



ICUS Report 2012-03 (serial No.65)

*the 11th International Symposium
on New Technologies
for Urban Safety of Mega Cities in Asia*

October 10-12, 2012

The Government House, Ulaanbaatar, Mongolia

*Edited by
Eiko Yoshimoto*

*Organized by
The Mayor of Ulaanbaatar city,
Mongolian University of Science and Technology (MUST), Mongolia,
and
International Center for Urban Safety Engineering,
Institute of Industrial Science, The University of Tokyo, Japan*

*Sponsored by
The Office of the President of Mongolia,
The National Security Council of Mongolia,
The Government of Ulaanbaatar city, Mongolia,
and
The Foundation for the Promotion of Industrial Science, Japan,*

*Supported by
The President of Mongolia*

SYMPOSIUM ORGANISERS

STEERING COMMITTEE

E.Bat-uul, Mayor of Ulaanbaatar city, Mongolia
L.Erkhembayar, Adviser to the President of Mongolia
S.Dashdondog, Adviser to the Vice Prime Minister of Mongolia
Ts.Amgalanbayar, Director, National Emergency Management Agency, Mongolia
Yo.Jargalsaikhan, Senior Officer, National Security Council, Mongolia
N.Gantumur, Deputy Mayor of Ulaanbaatar city, Mongolia
B.Ganbold, Director, Asian Department, Ministry of Foreign Affairs, Mongolia
Ts.Bayarbat, Director, Policy Department of Construction, Buildings and Communication Infrastructure, Ministry of Construction and Urban Development
Bayarsaikhan, Director, Land, Construction, Geodesy Agency, Mongolia
B. Damdinsuren, Director, Mongolian University of Science and Technology
P.Otgonbayar, Director, School of Civil Engineering and Architecture, Mongolian University of Science and Technology
U.Sukhbaatar, Director, Research Center Astronomy and geophysics, Mongolian Academy of Science
Katsumi Mushiake, Foundation of River & Watershed Environment, Japan
Mehedi Ahmed Ansary, BUET, Bangladesh
Sudhir Misra, IIT Kanpur, India
Takeo Uomoto, Chief Executive, Public Works Research Institute, Japan
Yoshiaki Nakano, Director, IIS, the University of Tokyo, Japan
Tsuneo Katayama, Tokyo Denki University, Japan
Wei Cheng Fan, CPSR, Tsinghua University, China
Worsak Kanok-Nukulchai, AIT, Thailand
Yoshifumi Yasuoka, NIES, Japan

TECHNICAL COMMITTEE

E.Khurelbaatar, General Architect, Director of Construction and Urban Planning Department, Ulaanbaatar city, Mongolia
G.Nandinjargal, Head of Urban Policy Development Department, Ulaanbaatar city, Mongolia
R. Turbat, Director, E-School, Mongolian University of Science and Technology
E.Ninjarav, Vice director, School of Civil Engineering and Architecture, Mongolian University of Science and Technology
Chung Sung Gyo, Dong-A University, Busan, Korea
Chayanon Hansapinyo, Chiang Mai University, Thailand
Haruo Sawada, ICUS, IIS, the University of Tokyo, Japan
Kiang Hwee Tan, National University of Singapore, Singapore
Kimiro Meguro, ICUS, IIS, the University of Tokyo, Japan
Munaz Ahmed Noor, BUET, Bangladesh
Pennung Warnitchai, AIT, Thailand
Sommuk Tangtermsirikul, Thammasat University, Thailand
Srikantha Herath, United Nations University, Japan
Taikan Oki, IIS, the University of Tokyo

ORGANIZING COMMITTEE

M.Ulziibat, Head of Seismological Department, Research Center Astronomy and geophysics, MAS
T.Erdenetuya, General Engineer of Construction and Urban Planning Department, Ulaanbaatar city
T. Batbayar, Senior Specialist of Construction and Urban Planning Department, Ulaanbaatar city
M.Oyunchimeg, Associate Professor, School of Civil Engineering and Architecture, Mongolian University of Science and Technology
Akiyuki Kawasaki, ICUS, IIS, the University of Tokyo, Japan
Kohei Nagai, ICUS, IIS, the University of Tokyo, Japan
Shinya Kondo, ICUS, IIS, the University of Tokyo, Japan

PREFACE

On behalf of the Organizing Institutes of the 11th International Symposium on New Technologies for Urban Safety of Mega Cities in Asia (USMCA 2012), I express our sincere gratitude to all symposium participants and distinguished guests.

In the Asia and Pacific-Rim regions, rapid economic development along with population growth and concentration, are fast accelerating the pace of urbanization. Unfortunately, the rapid expansion of urbanization infrastructure is not adequately balanced with the appropriate measures for its maintenance and management, thereby resulting in serious urban disasters. During the last few years, several big disasters have occurred in Asia and the Pacific Rim regions, such as the killer cyclones Sidr in Bangladesh (2007), Nargis in Myanmar (2008), and Aila in Bangladesh and India (2009), and Typhoon Ketsna in the Philippines (2009), flooding in Mongolia (2009), Pakistan (2010) and Thailand (2011), the devastating earthquakes in Sichuan, China (2008), Sumatra (2009), Samoa (2009) and Japan (2011), and heat waves in Russia and Japan (2010). The number of fatalities and missing reported due to these disasters was well over 200,000. These unprecedented events have evidently shown us the significant importance of urban safety.

The International Center for Urban Safety Engineering (ICUS) was established in 2001 at the Institute of Industrial Science (IIS), the University of Tokyo, with the objectives of carrying out researches on urban safety and implementing them towards the realization of safer cities in the 21st century. For over a decade, ICUS has been actively tackling advanced researches, as well as the enhancement of networking, dissemination and information collection.

Based on ICUS's past ten-year activities, the "new" ICUS was launched in April 1, 2011. The purpose of the "new" ICUS is to identify, investigate, and resolve issues towards the realization of sustainable urban systems. Our goal is to build a prosperous and safe society, while we challenge socio-economic problems such as depopulation and aging of society, shrinking economic resources, advanced technology, environmental awareness and climate change, dense and decentralized urbanization, and so forth. Specifically, the three research divisions – "Urban Safety and Disaster Mitigation", "Environment Informatics", and "Social Infrastructure Management" – form the core of the "new" ICUS, with their activities in these fields intended to fulfill the objectives of "promotion of advanced research," "construction of networks," and "information collection and dissemination", as they take the above-mentioned socio-economic problems into account.

On March 11, 2011, a gigantic earthquake (officially named "The 2011 Tohoku region Off-Pacific Ocean earthquake") with moment magnitude (M_w) 9.0 occurred in the Tohoku (North-East) region of Japan. This largest earthquake in Japanese history generated a very huge tsunami with the highest run-up elevation reaching over 40 meters, which killed approximately 18,600 people and injured over 6,100 people. Over 400 thousand buildings and infrastructures, including nuclear power plants, were totally collapsed or heavily damaged due to the tsunami, fires, and ground motion. Due to the loss of emergency back-up power of the cooling systems in the nuclear reactor, the Fukushima I Nuclear Power Plant was also damaged severely, causing a large amount of radiation to leak out. Because of the accident, over 310 thousand people living around the power plant were forced to leave their houses for evacuation, and still have no choice but to keep living in refugee camps and temporal shelters. The total monetary loss by the earthquake estimated by the government was 16.9 trillion yen; nevertheless the indirect losses and damage due to the nuclear power accident were not included.

Issues related with the response, recovery and reconstruction of the affected areas are the typical purposes of the "new" ICUS. In order to fully realize the vision for safer cities in Asia and the Pacific Rim regions, ICUS has annually co-organized

USMCA since 2002 with its partners in the Asian region. In 2012, ICUS jointly organized the 11th USMCA in Ulaanbaatar, Mongolia, with the Mayor of Ulaanbaatar City and the Mongolian University of Science and Technology (MUST), also supported by the Office of the President of Mongolia, the National Security Council of Mongolia, the Government of Ulaanbaatar City and the Foundation for the Promotion of Industrial Science, Japan. The objectives of the symposium was to bring together decision makers, practitioners and researchers involved in the field of urban safety to share their expertise, knowledge and experience in tackling the critical issues for safer cities in Asia and the Pacific Rim regions. It also provided an environment to create and reinforce collaborative networks among experts in the fields relevant to urban safety.

During this two-day symposium, 62 papers in ten parallel sessions and 26 posters in poster session were presented with 5 papers by keynote speakers. Total participants were 153 from 14 countries, including Mongolia, Australia, China, Bangladesh, India, Indonesia, Japan, Korea, Nepal, Singapore, Sri Lanka, Thailand, USA, and Vietnam. The symposium focused on diverse issues: disaster response and recovery, risk assessment/prediction and early-warning, decision-making technologies, planning and development of urban infrastructure systems, life-cycle management of infrastructure systems, climate change mitigation and adaptation, development and application of sustainable technologies, and application of geospatial technologies.

I would like to thank all the members of the Steering, Technical and Organizing Committees, as well as the Symposium Secretariat for their hard work, time and effort in putting this symposium together. I would also like to thank all our sponsors for their generous support and contribution. Thanks are also due to those who have dedicated themselves to the success of this symposium.

Kimiro MEGURO

*Director of ICUS, IIS, The University of Tokyo
(Co-Chairman of Organizing Committee, USMCA 2012)*

Copyright and Reprint Permission:

Photocopy of an article is permitted for authors and other researchers for their own reading and research. Abstracting and indexing of the papers are permitted but acknowledgement should be given to “The 10th International Symposium on New Technologies for Urban Safety of Mega Cities in Asia” and the authors of each specific paper. Written permission should be obtained from the publishers prior to any other type of reproduction. Please contact:

*International Center for Urban Safety Engineering (ICUS),
Institute of Industrial Science (IIS),
The University of Tokyo, Japan*

Tel: +81-3-5452-6472

Fax: +81-3-5452-6476

ISBN: 4-903661-51-2

2012 Program Overview

<i>Time</i>	<i>Tuesday, 9 October</i>	
16:00-19:00	Pre-Registration (Bayangol Hotel Reception Desk)	
<i>Time</i>	<i>Wednesday, 10 October</i>	
08:00-09:00	Registration (Government House Reception Desk)	
09:00-09:10	Opening Ceremony (Room B) P.Tsagaan, Head, Office of the President, Message by The President of Mongolia to the 11 th International Symposium on New Technologies for Urban Safety of Mega Cities in Asia	
09:10-09:20	Opening speech E.Bat-Uul, Mayor of Ulaanbaatar City	
09:20-09:30	T. Shimizu, Ambassador of Japan in Mongolia	
09:30-09:40	Professor Kimiro Meguro, Director of ICUS Chair: D. Battulga: Ulaanbaatar city Parliament	
09:40-10:10	Keynote Speech (Room B) Prof.B.Damdinsuren, President of Mongolian University of Science and Technology and Prof. E. Ninjigarav Vice director, School of Civil Engineering and Architecture, Mongolian University of Science and Technology The role of universities in urban safety and security	
10:10-10:40	Dr. Yoshifumi Yasuoka, Center for Research and Development Strategy, Japan Science and Technology Agency Integration of urban service infrastructures with urban dynamics modeling and simulation platform	
10:40-11:10	Visiting Professor Yasuyoshi Ichihashi, ICUS Impacts of the Fukushima Daiichi NPS accident and Japan's long-term energy & environment policies Chair: Dr. Nagai, ICUS	
11:10-11:50	Group photo and tea-break (Chinggis Khan Monument in front of The Government house and visit the State museum)	
11:50-12:50	Special poster session (Exhibition Area)	
12:50-14:00	Lunch (Khuree restaurant)	
	2F Room A	2F Room B
14:00-15:50	Session 1 : <i>Urban flood risk management in changing climate</i> Special Presentation Prof. Srikantha Herath Session Chairs: Prof. Herath and Dr. Kawasaki	Session 2 : <i>Risk assessment 1</i> Special Presentation Prof. Mehedi Ahmed Ansary Session Chairs: Prof. Ansary and Prof. M.Ulziibat
15:50-16:05	Tea-break (Exhibition Area)	
16:05-16:55	Session 3 : <i>Development and application of sustainable technologies 1</i> Special Presentation Prof. Kimiro Meguro Session Chairs: Prof. Misra and Dr. Yasuoka	Session 4 : <i>Risk assessment 2</i> Session Chairs: Dr. Mishra and Prof. Koshihara
18:30-20:30	Symposium Banquet Main restaurant in Bayangol Hotel	

Time	Thursday, 11 October	
	2F Room A	2F Room B
08:30-10:15	Session 5 : <i>Disaster response and recovery</i> Session Chairs: Dr. Dutta and Prof. E.Ninjarav	Session 6 : <i>Planning and development of urban infrastructures systems 1</i> Session Chairs: Prof.V.Batsaikhan, NEMA and Dr. T. Kato
10:15-10:30	Tea-break (Exhibition Area)	
	2F Room A	2F Room B
10:30-11:55	Session 7 : <i>Development and application of sustainable technologies 2</i> Special Presentation <u>Prof. Tan Kiang Hwee</u> Session Chairs: Prof. Tan and Dr. Uomoto	Session 8 : <i>Application of geospatial technologies</i> Special Presentation <u>Prof. Haruo Sawada</u> Session Chairs: Prof. Huang and Dr. Chen
11:55-13:30	Lunch (Khuree Restaurant)	
13:30-14:35	Session 9 : <i>Development and application of sustainable technologies 3</i> Session Chairs: Prof. Meguro and Dr. Pradeep	Session 10 : <i>Planning and development of urban infrastructures systems 2</i> Special Presentation <u>Prof. Sudhir Misra</u> Session Chairs: Dr. Tanaka and Dr. Henry
16:05-16:20	Tea-break (2F Exhibition Area)	
16:20-17:20	Keynote Speech (Room B) Dr. S.Demberel, Research center astronomy and geophysics of Mongolian academy of sciences and T.Erdenetuya, General Engineer of Construction and Urban Planning Department, Ulaanbaatar city <i>Estimation of seismic risk for central Ulaanbaatar using building stock inventory</i> Dr. Taketo Uomoto, Chief Executive, Public work research institute <i>Importance of maintenance to utilize existing structures</i> Chair: Dr. Nagai, ICUS	
17:20-18:00	Closing ceremony (Room B) Dr. U. Sukhbaatar (award presenter and comment) Dr. Nguyen Hoang Giang (Announcement of USMCA 2013) Prof. Haruo Sawada(closing speech) Chair: Dr. Nagai.ICUS	
19:00-21:00	Closing Banquet Elite restaurant	

Time	Friday, 12 October
08:30-16:30	Excursion

Contents

Keynote Session

	<i>page</i>
The role of universities in urban safety and security <i>Bayanduuren Damdinsuren and Enebish Ninjigarav</i>	1
Modeling and simulation of urban dynamics for integration of urban service infrastructures <i>Yoshifumi Yasuoka, Kimiro Meguro, Akira Maeda, Koichi Honma, Junichi Toyouch, Takeshi Mori, Rika Takeuchi, Kotaro Katsuyama, Kenji Kaneko and Hidenori Kimura</i>	3
Impacts of the Fukushima Daiichi NPS accident and Japan's long-term energy & environment policies <i>Yasuyoshi Ichihashi</i>	5
Estimation of seismic risk for central Ulaanbaatar using building stock inventory <i>S. Demberel, T.Erdenetuya, Iu. Berzhinskii, L Bezhinskaia, O. Salandaeva, D Kiselev, D. Tulga and G. Tatkov</i>	21
Importance of maintenance to utilize existing structures <i>Taketo Uomoto</i>	23

Oral Session

Session 1:

Urban flood risk management in changing climate

Impact of urbanization on flooding and sustainable flood mitigation measures <i>Chen, Charng Ning</i>	31
Centralized and decentralized urban flood control measures under physical and societal constraints <i>Srikantha Herath, Socheat Penh, Hiroyuki Okui, Masahiro Imbe and Yoshihiro Kitagawa</i>	33
Disaster information collection by Thai and foreigners during the 2011 Thai flood <i>Michael Henry, Akiyuki Kawasaki and Kimiro Meguro</i>	43
A daily river system model for the Murray-Darling Basin, Australia <i>Dushmanta Dutta, Justin Hughes, Jai Vaze, Shaun Kim, Ang Yang and Geoff Podger</i>	55
Investigating potential climate change impacts on rainfall intensity duration frequency curves in Kathmandu, Nepal <i>Binaya Kumar Mishra and Srikantha Herath</i>	67

Flood hazard simulation for lower West Rapti river basin-Nepal under climate change impact	77
<i>Edangodage Duminda Pradeep Perera, Akiko Hiroe, Kazuhiko Fukami, Toshiya Uenoyama and Shigenobu Tanaka</i>	

Session 2:

Risk assessment 1

Community under fire threat: An assessment of fire hazard vulnerability of ward 65 in Dhaka City	87
<i>Special Presentation: Prof. Mehedi Ahmed Ansary and Naima Rahman</i>	
Vulnerability assessment of snow disaster based on traffic system: A case study of Chenzhou City in Hunan Province	103
<i>XU Xiaoge, Jing ai Wang and Takaaki Kato</i>	
The seismicity in Mongolia	115
<i>Baigalimaa Ganbat and Ulzibat Munkhuu</i>	
Seismic hazard of Ulaanbaatar City	123
<i>Odonbaatar Chimed</i>	
Capacity building of seismic disaster risk management in Ulaanbaatar City	125
<i>Masaru Arakida, Seiichiro Fukushima and Yujiro Ogawa</i>	
Evaluation of managed aquifer recharge methods to increase the groundwater resources for water supply Ulaanbaatar City and flow control Tuul river	133
<i>Nasanbayar Narantsogtyn</i>	
Hanoi environmental planning to build resilience to climate change hazards – A multi-institutional approach	145
<i>Lan Huong Nguyen, Viet Anh Nguyen and Viet Nga Tran</i>	

Session 3:

Development and application of sustainable technologies 1

Development of advanced composite material for seismic safety of non-retrofitted masonry housing schemes in urban and rural areas of development countries	153
<i>Special Presentation: Prof. Kimiro Meguro, Saleem Muhammad Umair and Muneyoshi Numada</i>	
Study on earthquake input motions for the structures in Ulaanbaatar City	165
<i>Ganzorig Erdene, Batsaihan Tserenpil, Tulga Gantumur and Altanzagas Ochirdorj</i>	
Numerical simulation of beam-column joint with simple reinforcement arrangement by three-dimensional RBSM	173
<i>Koichiro Ikuta, Daisuke Hayashi and Kohei Nagai</i>	
Contemporary middle-rise timber buildings in Japan	181
<i>Mikio Koshihara</i>	

Session 4:

Risk assessment 2

- Study on lightning risk assessment for oil tank area** 191
Hong Huang, Boni Su, Yuntao Li and Fanghui Luo
- Structural damage detection by using hybrid time reversal process method** 201
Usik Lee, Ilwook Park and Jungsik Choi
- Fire risk study of Ulaanbaatar City** 209
Bazarragchaa Sodnom and D. Bayan-Erdene
- The seismic-engineering survey among multi-store constructions within the territory of Ulaanbaatar City** 211
Batsaikhan Tserenpil, Sergei Serebrennikov and Baatarsuren Ganbold

Session 5:

Disaster response and recovery

- Study on recovery curves for temporary housing after the 2011 great east Japan earthquake** 221
Osamu Murao and Kazetaka Kotoku
- Disaster management of municipal governments on the Kii Peninsula after flood and sediment disasters caused by the 2011 Typhoon Talas** 229
Shinya Kondo, Kazuyoshi Ota and Yasuhiro Kataie
- Study on implementation of remote building damage assessment system during large scale earthquake disasters** 239
Makoto Fujiu, Miho Ohara and Kimiro Meguro
- News coverage concentration on specific municipalities: Analysis of TV report contents at 2011 Tohoku Earthquake** 249
Muneyoshi Numada and Kimoro Meguro
- Reconstruction of Kamaishi City after the 2011 Tohoku earthquake and tsunami** 257
Sae Shikita, Maria Bernadet Karina Dewi and Takaaki Kato
- Analysis of disaster information gathering behavior and language ability after the 2011 Tohoku earthquake** 263
Akiyuki Kawasaki, Michael Henry and Kimiro Meguro
- Analysis of traffic situation on urban road network after large-scale earthquake** 273
Shinji Tanaka, Daisuke Oshima and Takashi Oguchi

Session 6:

Planning and development of urban infrastructures systems 1

- Possibility of developing a new special economic zone in Ulaanbaatar City** 281
Oyuntsatsral Tseyenbaljir

Roadmap from smoke to the development: Airport city a win-win model for the eco-economical context of the capital city development <i>Davaanyam Surenjav</i>	289
Review on the definitions of vulnerability, resilience, and adaptation <i>Yuto Shiozaki and Takaaki Kato</i>	291
Ulaanbaatar City flat region acoustic <i>Barkhas Sukhbaatar and G. jambalsuren</i>	303
Eco fence-the improvement of the Ger district living environment <i>Ganbat Gantulga, G. Punsaldulam and Sh. Enkhtungalag</i>	309
Issues and challenge in legal framework related to urban redevelopment in Mongolia <i>Toshiaki Kudo and Tomoko Abe</i>	319
A challenge toward application of new urban redevelopment mechanism in Ulaanbaatar City <i>Tomoko Abe and Toshiaki Kudo</i>	329
 <u>Session 7:</u> Development and application of sustainable technologies 2	
Seismic vulnerability of gravity-load designed buildings <i>Special Presentation: Prof. Tan Kiang Hwee, T Balendra and Aziz Ahmed</i>	339
Study on the effects of chemical and physical properties of concrete on the behavior of internal water <i>Chohji Nakamura, Yuya Sakai and Toshiharu Kishi</i>	351
The fire resistance issue of reinforced concrete beam <i>Duinkherjav Yagaanbuyant and Erdenedavaa Bat-Ochir</i>	359
Modeling of diffusive and advective transport of ionic species in cemented soil <i>Hayato Ikoma, Taiju Yoneda and Tetsuya Ishida</i>	367
Shear performance of PVA-coarse aggregate-ECC beams under a rotating stress field <i>Yoshiyuki Takano, Benny Suryanto and Kohei Nagai</i>	375
Pushover analysis of RC bare frame: Performance comparison between ductile and non-ductile detailing <i>Rammancharla Pradeep Kumar and B. Narender</i>	385
 <u>Session 8:</u> Application of geospatial technologies	
How remote sensing data were used for the Tohoku Earthquake <i>Special Presentation: Prof. Haruo Sawada</i>	393
The investigation on a potential chemical incident risk in the area of Ulaanbaatar <i>Ganzorig Tsogtbaatar, Chimedtseren Purevjav, Sodnomragcha Dagva and Algirmaa Erdene-Ochir</i>	403

The application of geoinformation for emergency management and hazard <i>Sodnomragchaa Dagva</i>	417
Successful solution of water ecology and economy in consumption of apartment <i>Batbileg Enkhbat, Enkhtungalag SH and Bulgan Zorig</i>	427
Spatial distribution of heavy metal contamination in urban soil of Ulaanbaatar <i>Otgontuul Tsetsgee, Byambasuren Ts and Shabanova. L.B</i>	431
Estimation of global anthropogenic PM2.5 by integrating remote sensing and modeling <i>Hirothoshi Kishi, Wataru Takeuchi and Haruo Sawada</i>	441

Session 9:

Development and application of sustainable technologies 3

Reinforced soil walls damaged by tsunami impact in the 2011 Tohoku Earthquake <i>Jiro Kuwano and Junichi Koseki</i>	449
Evaluation of internal erosion by turbidity of drained water <i>Mari Sato and Reiko Kuwano</i>	459
Application of microbial calcite to hemp fiber reinforced soils to combat desertification <i>Seong R. Choi, Sookie S. Bang, Sangchul Bang, Josh Anderson, Seok J. Lee, Nam Y. Dho and Sung-Hwan Ko</i>	469
Sliding disaster in Vietnam and a new proposed design method of reinforced soil wall <i>Nguyen Hoang Giang and Jiro Kuwano</i>	477
Estimation of stress distribution in a model ground using bender elements <i>Reiko Kuwano and Sho Oh</i>	487

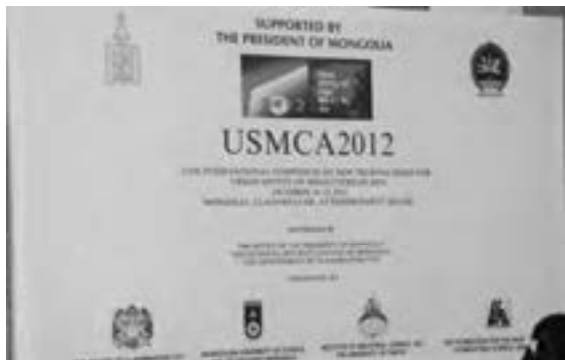
Session 10:

Planning and development of urban infrastructures systems 2

Regulatory framework for modern urban housing <i>Special Presentation: Prof. Sudhir Misra</i>	497
Conducting advanced technology of public transportation in Ulaanbaatar City <i>Munhjargal Victor</i>	503
The relationship between pedestrian perception and characteristics of sidewalk environment in case of the central area of Ulaanbaatar City <i>Amgalan Sukhbaatar, Noboru Harata and Nobuaki Ohmori</i>	519
Relation between urbanization and natural disaster risk in mega cities -Lessons from Tokyo- <i>Takaaki Kato</i>	529

Photograph

Welcome Boards and Registration



Registration at Bayangol Hotel

Bayangol Hotel

Inauguration Ceremony



Main Hall at Government House

Opening Speech



Mr. P. Tsagaan, Head Office of the President, Mongolia



Mr. E. Bat-Uul, Mayor of Ulaanbaatar City



Mr. T. Shimizu, Ambassador of Japan in Mongolia



Prof. K. Meguro, Director of ICUS

Invited Speakers (Keynote)



Prof. B. Damdinsuren, President of MUST



Dr. Y. Yasuoka, CRDS, Japan



Visiting Prof. Y. Ichihashi, ICUS



Dr. S. Demberel,



Dr. T. Uomoto, Chief Executive, PWRI, Japan

Special Presentation Speakers



*Prof. M. Ansary, BUET,
Bangladesh*



Prof. S. Herath, UNU, Japan



*Dr. D. Dutta, CSIRO,
Australia*



*Prof. E. Ninjigarav, MUST,
Mongolia*



*Prof. H. Sawada,
ICUS, Japan*

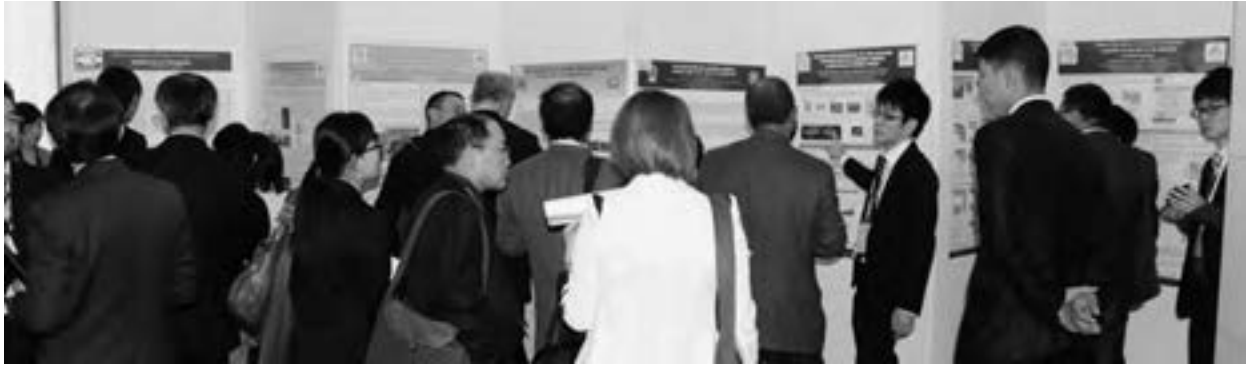


*Prof. K.H.Tan, NUS,
Singapore*



*Prof. S. Misra,
IIT, Kanpur, India*

Poster Session



Closing Ceremony at The Government House





*Dr. U. Sukhbaatar, MAS, Mongolia
as award presenter*



*Dr. N.G. Giang, NU, Vietnam
announces USMCA2013*



Young –Researcher-Award recipients with Dr. U. Sukhbaatar.

Poster presentation award: Dr. N.G. Giang, NU, Vietnam (left), Ms. X. Xu, The Univ. of Tokyo, Japan (second from left)

Oral presentation award: Dr. M. Henry, Hokkaido Univ., Japan, (third from left), Ms. Ts. Otgontuul, MAS, Mongolia (second from right), Mr. K. Ikuta, The Univ. of Tokyo, Japan (right)



Chair man: Dr. K. Nagai

Press Coverage by UBS and MNB



Break and Lunch Time



Banquet



Mr. E. Bat-Uul, Mayor of Ulaanbaatar City and Prof. K. Meguro, director of ICUS





Farewell party



Tour



Visit to Thermal Power Plant #4



Visit to Sun Bridge, a project built with Japanese Government Grant-aid project.



With Mongolian wrestlers at Guru camp



At Terelj National Park



Group photo of participants

Keynote Session

The role of universities in urban safety and security

Bayanduuren Damdinsuren¹, Enebish Ninjarav²

¹Professor, President of Mongolian University of Science and Technology(MUST), Mongolia

²Associate Professor, Vice director of School of Civil Engineering and Architecture, Mongolian University of Science and Technology (MUST)

ABSTRACT

Disasters and crimes are the threats. Urban security and urban crime and disasters affected to urban areas are spatial entities that are inherently tied to the urban structure that has been created in cities and are not philosophical phantoms that amorously float above cities. The urban environment encapsulates and defines the everyday lives of urban citizens. Megacity is facing the challenges and therefore should be taken all possible cares for urban inhabitants or must be provided urban security. Megacity security is essential issue most terrible things are any kind of disasters and crime for them. To avoid damage which takes place from disaster and crime or be affected to minimum damage megacity inhabitants necessary to possess an adequate knowledge and previously trained to protection techniques and should be done all possible measures against disaster and crime consequences. The education issue of inhabitants against disasters and crime is the role of the universities for megacity security. Universities should train people, include adequate disciplines in curriculum of university and do research. Universities should prepare well educated and highly skilled specialists in this concern, This is the contribution of universities in sustainable development of the nations or safety and secure live of urban area people. This paper looks at different kind of disasters, damage from them and the university role in megacity security.

Keywords: role, university, student, disaster, crime , urban ,citizen, urban safety, education, megacity security

Modeling and simulation of urban dynamics for integration of urban service infrastructures

Yoshifumi YASUOKA¹, Kimiro MEGURO², Akira MAEDA, Koichi HONMA,
Junich TOYOUCHI, Takeshi MORI, Rika TAKEUCHI, Kotaro KATSUYAMA,
Kenji KANEKO and Hidenori KIMURA
yyasuoka@ iis.u-tokyo.ac.jp

¹Center for Research and Development Strategy,
Japan Science and Technology Agency

²Director, Professor, ICUS, IIS, The University of Tokyo, Japan

ABSTRACT

In this presentation, we propose a strategy to establish an urban dynamics modeling and simulation system to evaluate, predict, and efficiently manage the dynamics of the urban service functions.

The Great East Japan Earthquake and the massive floods in Thailand revealed that urban service systems collapsed due to a single disaster. The risk of damage from earthquakes and floods is higher in cities with a higher concentration of people and functions in the world. There is fear that not only instant disasters but also climate change represented by global warming may heavily affect urban infrastructures in the medium and long terms. It is now urgent to promote urban studies, including how to build a future urban system; how to enhance the efficiency of urban service functions designed to deal with large-scale disasters, an aging society with fewer children, and the coming low carbon society and recycling-oriented society; and how to improve their robustness and resilience.

We propose a system to evaluate, predict, control, and manage those functions efficiently especially by virtually modeling the service functions of the service infrastructure systems essential to urban life, such as energy, water, transportation and logistics, and information and communications. This proposal features the modeling of urban functions in a virtual space (a cyber space) especially with the movements (dynamics) of people, goods, and land use as the core of the modeling. The challenges to be addressed are as follows.

- (i) Which part of the service functions should be measured and how? How should the measured data be used (measurement and analysis of urban dynamics)?*
- (ii) How should we model, predict, and evaluate service functions (modeling and simulation of urban dynamics)?*
- (iii) How do we establish a system to manage and control service functions (establishment of a basic system to integrate models in a virtual space [Urban Dynamics Platform; UrDYP])?*
- (iv) How do we establish a spatiotemporal theory for urban dynamics analysis?*

By addressing these challenges, we aim to establish a system to dynamically measure, model, and control and manage urban service systems.

Urban research has a long history. The supply system of drinking water and industrial and agricultural water has existed since ancient Greece and that of energy such as electricity and gas significantly developed in the modern era. However, each service has separately and independently developed because of their long histories, and they have not been integrated into a system linked with one another. For example, in the Great East Japan Earthquake, there was some confusion in infrastructure systems; trains being stopped while the electricity

was being supplied and water being cut off because the electricity went out. Such confusion caused the spread of the damage.

Taking energy supply as an example, urban energy is considered to be supplied with a distributed energy system utilizing several power sources in the future. However, it is essential to adopt a distributed integrated control system, such as a smart grid system to efficiently use energy from various power sources. Many studies on smart grids have begun in the world. As large-scale urban development is becoming increasingly harder with the economic slowdown not only in Japan but also in the world, integral linkage among urban service infrastructures will reduce the future burden.

This proposal aims to enhance the efficiency of urban service infrastructure functions and improve their robustness and resilience focusing on the dynamics of people, goods, and land use in cities. The methodologies of establishing new urban service systems proposed by this challenge are expected to accelerate not only efforts to deal with the coming aging society with fewer children but also efforts to achieve an energy-saving low-carbon city or a recycling-oriented city to tackle climate change. In addition, it is also expected that resilient cities will be built that are robust in the event of the large-scale disasters that are expected to occur. It will be significant if these methodologies contribute to the development of new cities not only in Asia but also in other countries in the world.

Keywords: *urban dynamics, urban infrastructure, systems analysis, modeling, simulation*

Impacts of the Fukushima Daiichi NPS accident and Japan's long-term energy & environment policies

Yasuyoshi Ichihashi
Visiting Professor, International Center for Urban Safety Engineering,
Institute of Industrial Science,
The University of Tokyo

ABSTRACT

The 3,11 Tohoku Earthquake and Tsunami caused level 7 nuclear disaster at Fukushima Daiichi Nuclear Power Station, and it brought most serious and complex challenge to Japan in the context of considerations on future energy and environmental situations. The author reports about the latest moves in Japan in regard to the government initiated policy reviews in the related areas.

1. 3.11 Earthquake & Tsunami

“Great East Japan Earthquake”

Earthquake

11 March 2011 (Fri), 14:46:23 JST

Magnitude: 9 (M_w) Duration: about 6 min

Epicenter: 38.6°N 142.52°E

(about 130 km off the Oshika Peninsula)

Depth: about 24 km

Type: Plate Boundary in the areas of Japan Trench (North American Plate, Pacific Plate)

Epicentral Area: Length about 450 km,

Width about 200 km

Seismic Intensity: JMA degree 7 (in Northern Miyagi area), quakes spread from Hokkaido to Kyusyu

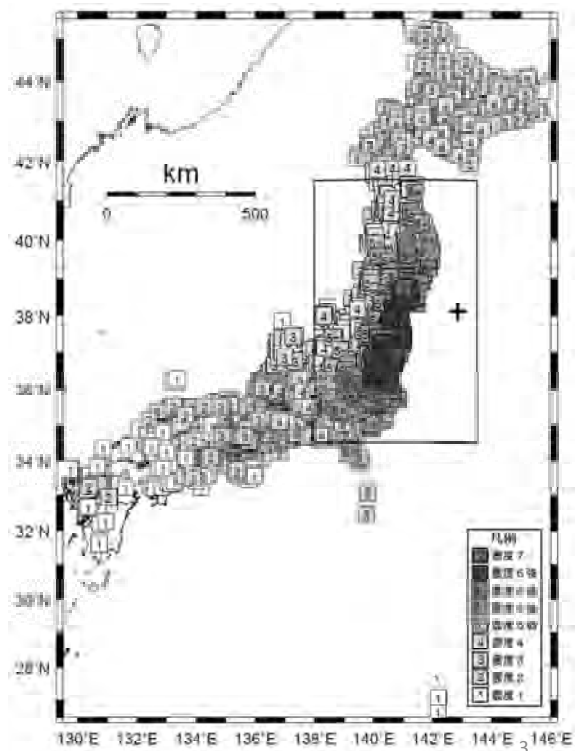
Tsunami

Max. Tide Height: 9.3 m (Souma, Fukushima)

Upstream Height: 40.5 m

Inland run: about 10 km (in Sendai Area)

Sea Water invasion area: 561 km²



Casualties & Situations that had to be dealt with

Death: 15,867 (over 90% by drowning, 65% above age 60), Missing:2906, Injured: 6109

Wholly destroyed & half damaged houses & buildings: more than 390,000

Electricity cut off: 8.91 mil. household

Water supply cut off: 1.8 mil. Household

Damaged Agricultural land: 23,600 ha

Damaged fishery vessel: 22,000

Evacuees: about 470,000 at peak

Direct damages: JP¥ 16-25 trillion

<Rescue Operations>

Police agency: total 307,500

Fire Defense Agency: 6,100

Marin Safety Agency: total 4413 vessels
total 1514 aircrafts

Defense Ministry: 100,000 at peak

Oversees Rescue teams: 28 countries, areas,
& int'l org. ; 128 countries & 33 int'l org
offered assistance; Operation "Tomodachi"
by U.S.Gov.

<Damages & Recovery of Infrastructures & lifelines>

Transport: railway, road, port, air services
each had severe damages and gradually
recovered. (In Tokyo, about 700,000 people
were not able to go home.)

Lifeline: electricity, gas, water supply, sewage,
telecommunication, broadcasting, oil refinery
etc. were damaged, and gradually recovered

Public buildings: about 6, 400 public schools
had damages, many waiting for reconstruction

Rivers, Agricultural facilities, Coastal & fishery
facilities: each had damages and many waits for
recovery

Immediate life assistance to the affected:

food 2.6 mil. meals, water 8 mil. bottles,
blanket 410,000 fuel 16.000 kl, medicine
240.000 boxes, etc.

<On-going process>

Recovery & Reconstruction Plans

Evacuees are still 340,000, hoping for going
home

Disposal of Debris: 24.9 mil. tons

4



5

2. Fukushima Daiichi NPS Accident

- Of the 6 Units, 3 (No.4, 5, 6) were not in operation
 - Units No.1, 2, 3 were automatically stopped immediately after earthquake. But supply of outer power was cut off, emergency generators could not continue supplying powers because of earthquake & tsunami, and non-electric cooling system also did not work.
 - Eventually this led to melt-down of fuels at all Units 1-3, and hydrogen gas exploded at Unit 1 (3/12), at Unit 3 (3/14), and at Unit 2 (3/15). Hydrogen Explosion also occurred at Unit 4 used fuel pool.
 - As a result, large amount of radioactive material were released into the air, onto the ground, and contaminated water used for cooling the fuel was also leaked into the seawater.
 - The government ordered evacuation of residents within 20 km radius area, and sheltering within 20-30 km radius area.
 - Thereafter tremendous amount of hard work and a long process were necessary to stabilize the fuel.
 - Nine month later, in Dec. 2011, the gov't declared that cold shut down was achieved on the site.
- <Investigation Committees>
- The government established Investigation Committee in June 2011, and the Committee submitted its final report in July 2012.
 - National Diet of Japan also established Independent Investigation Commission on Fukushima Nuclear Accident in December 2011, and the Commission submitted its final report in July 2012.
 - Both reports severely criticized TEPCO as well as the government for the disability to prevent level 7 nuclear accident. But both could not identify how the radioactivity was released in detail because of non-accessibility to the reactors.
 - All built-in safety measures were structured on the proposition " long-time all power loss is impossible", but it did take place. 6

Situations that had to be dealt with

- Care & assistance to evacuees (about 86,000) from the designated evacuation area (housing, including temporary shelters, medical care, schooling for children, guarded temporary visit to the original residence, etc.)
- Monitoring of radiation. Contamination was wide spread and monitoring posts & activities had to be expanded largely.
- Ban on shipment of some vegetables and fishery products, because of detected radiation. The government introduced a new criteria for the radioactive cesium in foodstuffs in April 2012.
- Insufficient supply of electricity, due to break down of NPS & other power plants. TEPCO carried out " Planned Electricity Outage" in March 2011. The Government (METI minister) ordered companies contracting more than 500w electricity to cut 15% usage in 2011 summer.
- Decontamination. A special law to carry out decontamination work was passed by the Diet. It requires huge amount of financial resources.
- Compensation for the economic & other damages caused by nuclear accident. For this purpose, a bill to establish Nuclear Damage Liability Facilitation Fund was passed in the Diet. Temporary payment has started, but total amount necessary is not known.
- Nationwide public views against restarting operations of NPSs. NPSs are obligated to go through maintenance programs after one year in operation. Accordingly, after Fukushima, all 54 NPSs stopped operations one by one, but because of the local government's oppositions, they were not able to restart operations. After introducing stress tests, the government decided to re-start two units at Oi NPS in Shiga Pref. Since then tens of thousand protesters started to gather in front of the Prime Minister's Office to make demonstrations.
- Separation of regulatory agency from nuclear promotional ministry (METI). IAEA also recommended separation. A new bill to create new nuclear regulatory body was passed by the Diet in June 2012. With this, a new independent Nuclear Regulatory Commission is to be established to replace previous Nuclear Safety Committee, and previous Nuclear and Industrial Safety Agency under METI will be re-organized to a new independent Nuclear Regulatory Agency under the Ministry of Environment. The new body is expected to introduce new safety guidelines of the NPSs. 7



3. Change of Public Views on NPSs

◉ A drastic change occurred in public views.

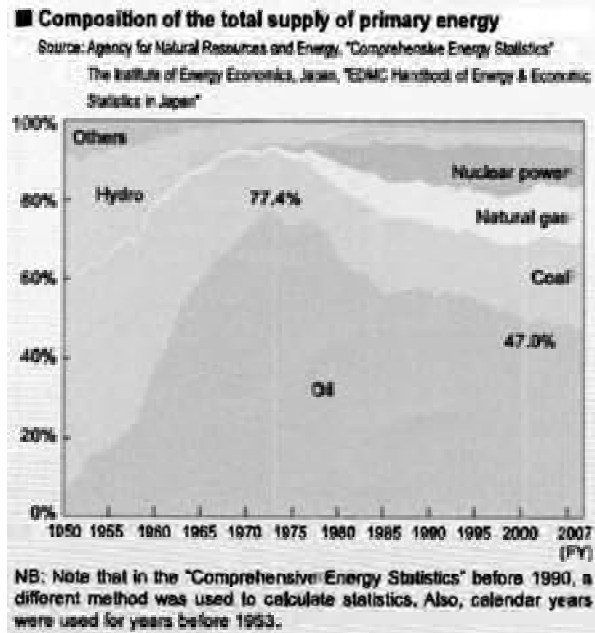
Public Opinion Polls by Cabinet Office							
Q: How do you think about nuclear power generation from now on ?							
(After Oil shock)		(After Three Mile & Chelnobyl)				(In global warming context)	
1976		1997		1999		2005	
Better develop more	50%	Better positively increase	5%	Positively increase	4%	Positively promote	8%
Better abandon	20%	Better cautiously increase	44%	Cautiously increase	39%	Cautiously promote	47%
Do not know	35%	Better not increase more	30%	Maintain current level	27%	Maintain current level	20%
		Better decrease	9%	Abolish in the future	19%	Abolish in the future	15%
		Better stop currently operating ones	2%	Abolish soon	2%	Abolish soon	2%
		Do not know	10%	Do not know	9%	Do not know	8%
Note that before 3.11, negative views were minorities							

NHK Survey	
Same Q:	
(After 3.11)	
Dec. 2011	
Should increase	1.9%
Maintain Current level	26.5%
Should decrease	50.7%
Should abolish all	20.3%
No answer	0.6%
Negative became 70%	

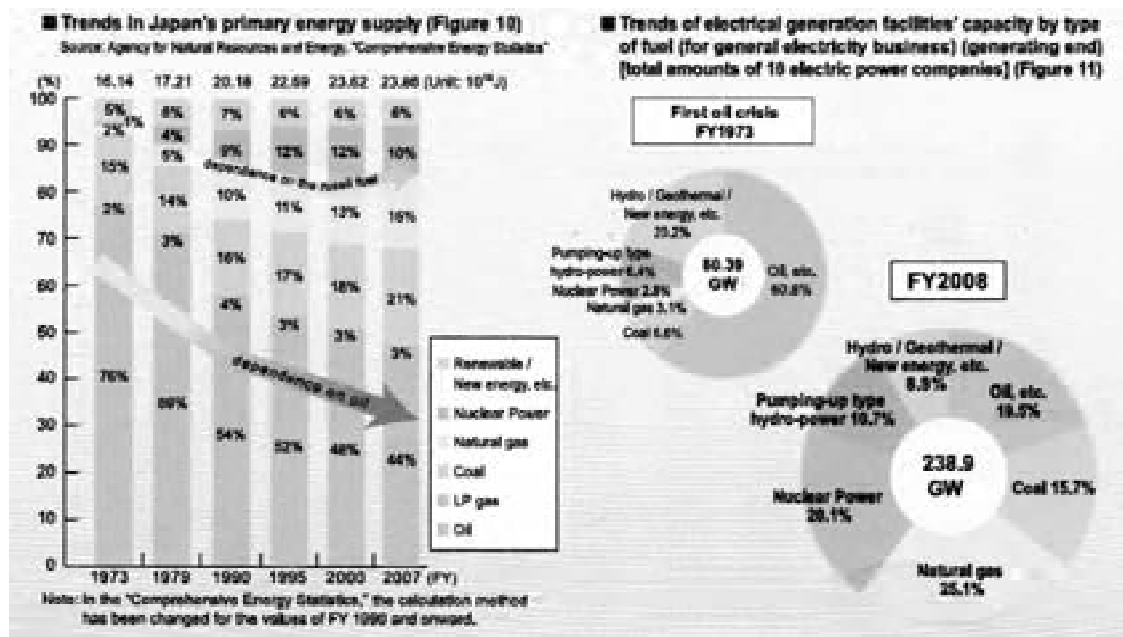
◉ This made reviews of long-term energy policy inevitable.

4. Impact on long-term energy policy

◉Historical transitions of energy resource composition in Japan

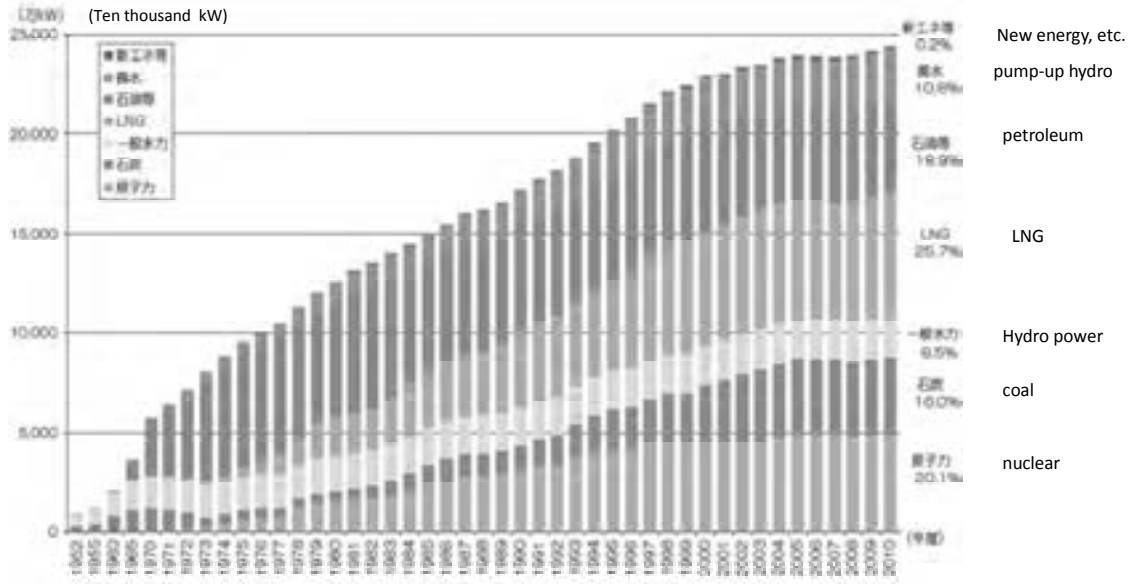


11



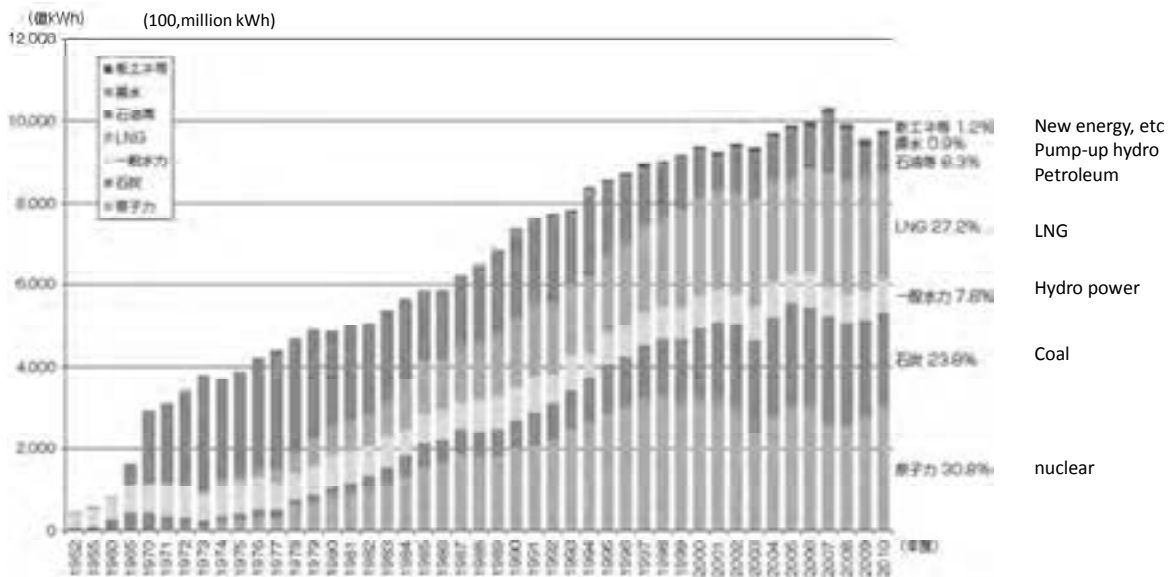
12

Transition in Power generation facilities capacity, year by year, by resources



13

Trends in generated electricity, year by year, by resources



14

- (1) Immediately after the war: hydro-power
- (2) Reconstruction period ('45-'62)
Coal as main
- (3) High-speed growth period ('62-'72)
Transition from coal to petroleum
- (4) After 1st & 2nd Oil Shock ('73-late'80s)
Weight on stable supply of resources, alternative energy resource development, and energy conservation measures
- (5) Since '90s
Need to adapt to global warming situation; "nuclear renaissance"
Technology development such as solar panel
2002.6 "Basic Act on Energy Policy"
Principles introduced were:
 - Stable supply
 - adaptation to environmental requirements
 - active use of market principles (deregulations)
- (6) According to the Basic Act, the government adopted Strategic Energy Plan in 2003, revised it in 2007, and made the second revision in 2010 (current plan). (Revision is required every 3 yrs.)

(7) The 2010 Plan laid emphasis on CO2 emission reduction, and called for the construction of 9 new or additional NPPs by 2020, and 14 or more NPPs by 2030. It was packaged with over 30% CO2 reduction by 2030. (See next graph)

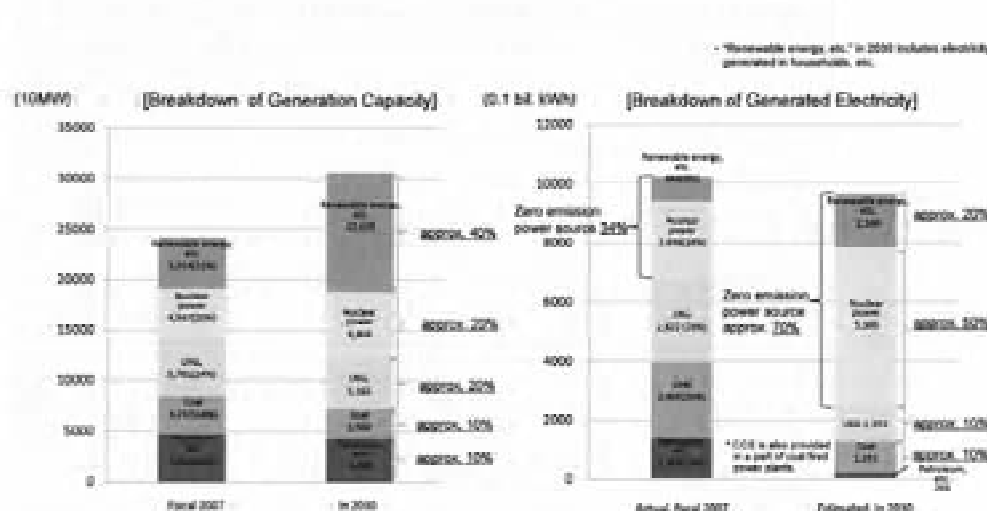
However, after 3.11, such Plan became obviously unsustainable, and the gov't decided that the Plan will be re-created from the scratch by summer 2012, one year earlier than the original timeline 2013.

15

◦ Following was the picture drawn in the 2010 Strategic Energy Plan

Balance of power generation Ref.

○ Zero emission power source ratio will become approx. 70%* (34% currently).



* This estimator is premised on considerable energy conservation, additional building (at least 14 plants) and increased facility utilization rate (approx. 80%) of nuclear power plants based on assured safety while acquiring understanding and trust of the public on installation location, etc., as well as introduction of renewable energy to the maximum extent. Scalability of the power system needs to be separately studied.

• Coal-fired thermal power plants assume that, in response to commercialization, CCS will be provided together with all power plants when they are replaced. It should be noted that the estimate may change depending on future technological development and security of CO2 storage facilities, etc.

(8) Regarding the use of nuclear energy, Atomic Energy Basic Law was enacted in 1955, and Japan Atomic Energy Commission (JAEC, for policies) was created, and later in '78, Nuclear Safety Commission (NSC, for regulation) were separated. (NSC is to be replaced by NRC from now on.)

AEC developed Long-term Basic Program for Development and Utilization of Nuclear Energy 9 times (approx. in every 5 years) since then, and in 2005, Framework for Nuclear Energy Policy was decided by the Cabinet.

(9) The 2005 Framework was to be reviewed after 5 years, and in 2010, AEC set up a New Nuclear Policy Planning Council.

However, after 3.11, consideration was suspended until summer 2012, due to change of the situation.

(10) Thus, 3.11 has impacted all-round Japan's energy and environment policies & necessitated reviews.

- (a) Advisory Committee on Energy and Natural Resources (Fundamental Issues Subcommittee), under Natural Resources and Energy Agency, METI, is to review alternative policy options for the current "Basic Energy Plan"
- (b) AEC, under Cabinet Office, is to review alternative policy options for the new "Framework for Nuclear Energy Policy"
- (c) Central Environmental Council, under Ministry of Environment, is to review alternative policy options for measures against global warming
- (d) The Energy & Environment Council (EEC or "Ene-kan"), set up in 2011 by the Cabinet Office, National Policy Unit, is to integrate these, and create "Innovative Strategy for Energy and Environment".

17

5. Process of the Review

◎ In July 2012, National Policy Unit of the Cabinet Office announced 3 options of the future energy composition in order to gather public views on them. Review process was scheduled as follows.



18

6 Three Scenarios

Following are three options as announced by National Policy Unit.

*The shares mean those in the electric energy generated. Figures in parentheses indicate changes from 2010 (before the Great East Japan Earthquake).

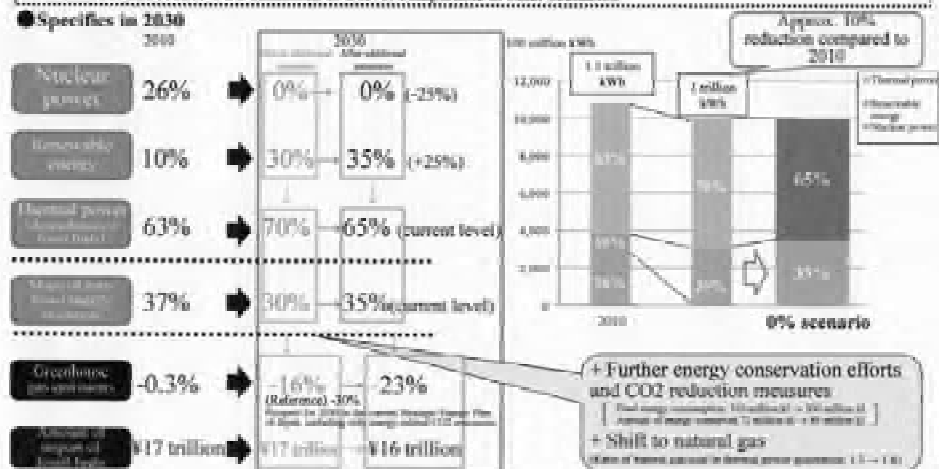
	2010	0% scenario		15% scenario	20-25% scenario	Reference (Current National Energy Plan of Japan)
		Before additional measures	After additional measures			
Share of nuclear energy	26% <small>Note 1</small>	0% (-23%)	0% (-25%)	15% (-10%)	20 to 25% (-5 to -1%)	45%
Share of renewable energy	10%	30% (+20%)	35% (+25%)	30% (+20%)	30 to 25% (+20 to +15%)	20%
Share of fossil fuels	63%	70% (+7%)	65% (Current level)	55% (-10%)	50% (-15%)	35%
Share of non-fossil energy resources	37%	30% (-7%)	35% (Current level)	45% (+10%)	50% (+15%)	65%
Electric energy generated	1.1 trillion kWh	Approx. 1 trillion kWh (-10%)	Approx. 1 trillion kWh (-10%)	Approx. 1 trillion kWh (-10%)	Approx. 1 trillion kWh (-10%)	Approx. 1.2 trillion kWh
Fossil energy consumption	300 million kl	Approx. 300 million kl (+0 million kl)	300 million kl (-0 million kl)	310 million kl (+12 million kl)	310 million kl (+12 million kl)	340 million kl
Greenhouse gas emissions (compared to 1990)	-0.3%	-16% (Reference: -30%)	-23% (-21%)	-23% (-22%)	-25% (-24%)	(Around -30%)

Note 1: The share of nuclear energy under the current Strategic Energy Plan of Japan (2010) is the share of large-scale power generation (including cogeneration and power-generating reactors). It ignores in particular small-scale units, energy-related CO₂ emissions.

19

0% Scenario

- Reduce the share of nuclear energy to 0% at the earliest possible time before 2030 and adopt the nuclear fuel cycle policy of direct disposal of spent nuclear fuel.
- Convert the energy structure to one consisting of renewable energy and fossil fuels in the end.
- Impose strict regulations, including restriction on/prohibition of sales of products with poor energy conservation performance, in broad fields, and implement a considerably drastic shift of energy sources to renewable energy, energy conservation and gas, even with a heavier economic burden, in order to reduce dependence on fossil fuels to the minimum and reduce CO₂ emissions to a level comparable to other scenarios.



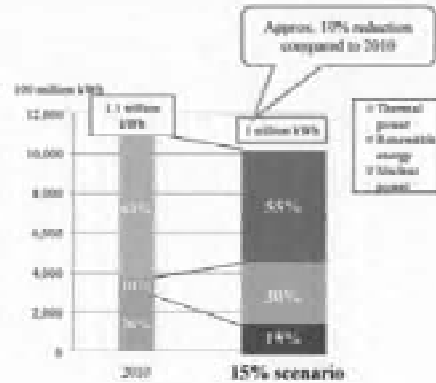
20

15% Scenario

- Steadily reduce dependence on nuclear energy to around 15% in 2030 and smoothly realize reduction of dependence on fossil fuels and CO₂ emission reduction
- Reprocessing and/or direct disposal are possible in relation to the nuclear fuel cycle policy.
- Utilize nuclear power, renewable energy, and fossil fuels through their combination and flexibly respond to various environmental changes, including those in the energy situation, in the international situation concerning the global environment, and in technological innovation

● Specifics in 2030

Nuclear power	2010: 26%	→	2030: 15% (-10%)
Renewable energy	10%	→	30% (+20%)
Thermal power (nuclear and fossil fuels)	63%	→	55% (-10%)
Share of coal in thermal energy	37%	→	45% (+10%)
Carbon dioxide emissions	-0.3%	→	-23%
Amount of investment of fossil fuels	¥17 trillion	→	¥16 trillion



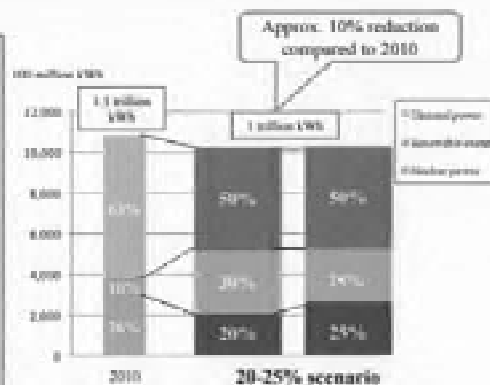
21

20-25% Scenario

- Keep a certain level of dependence on nuclear energy while slowly reducing it and achieve a share of nuclear energy in 2030 around 20-25%. Construction of new nuclear power plants and replace of existing plants are required.
- Reprocessing and/or direct disposal are possible in relation to the nuclear fuel cycle policy.
- Promote reduction of dependence on fossil fuels and CO₂ emission reduction from a more economic aspect.
- Strong public confidence in nuclear energy and administration thereof is the premise.

● Specifics in 2030

Nuclear power	2010: 26%	→	2030: 20% (-5%) to 25% (-1%)
Renewable energy	10%	→	30% (+20%) to 25% (+15%)
Thermal power (nuclear and fossil fuels)	63%	→	50% (-13%)
Share of coal in thermal energy	37%	→	50% (+15%)
Carbon dioxide emissions	-0.3%	→	-25%
Amount of investment of fossil fuels	¥17 trillion	→	¥15 trillion



22

7 Other Issues

- ◉ Decommissioning of Fukushima Daiichi NPS reactors. How? Development of technology required. Long time also needed. Huge money necessary.
- ◉ Also how to deal with decommissioning of other NPS reactors which reaches 40 years operating time limitation?
- ◉ How to deal with Japan’s long standing government policy of nuclear fuel recycling, including FBRs & pluthermal?
- ◉ Final disposal of the nuclear waste is also an unsettled issue.
- ◉ How to deal with existing power supply regime? Currently regional 10 electricity companies maintains regional monopoly of power generation, transmission and distribution. Is this system to be changed and deregulated more? Can separation of transmission bring competition with PPSs (Power Producer & Supplier, and be effective in supplying low-cost, stable powers?
- ◉ Higher electricity price is envisaged for both household & industry. And it may bring about more business/manufacturing companies escaping out of the country, decreasing domestic employment & worsening deflations. A vigorous new growth strategy is also needed.

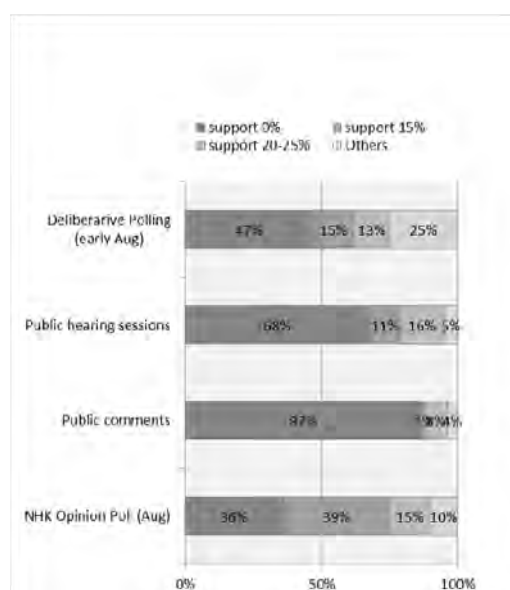
23

8 Latest Development

◉ On 4 Sep., Results of National Discussions were shown at Energy & Environment Council.

(examples)

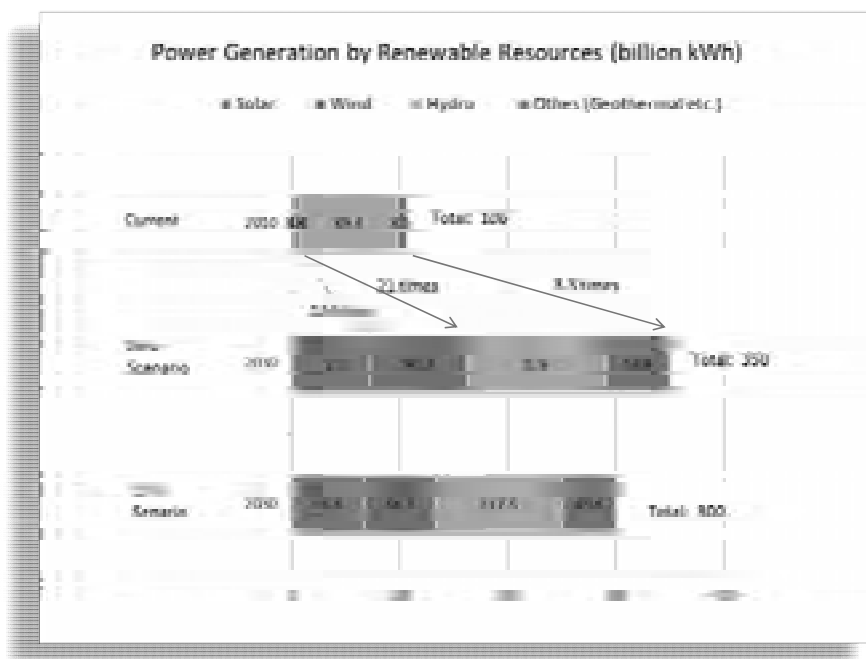
2030 Scenario	NHK Opinion Poll (Aug)	Public comments	Public hearing sessions	Deliberative Polling (early Aug)
support 0%	36%	87%	68%	47%
support 15%	39%	1%	11%	15%
support 20-25%	15%	8%	16%	13%
Others	10%	4%	5%	25%



24

- ◉ Summary of the National Discussion (by National Policy Unit)
 - Majority of the public are sharing broad direction toward a society away from dependency on nuclear power generation.
(Support for Zero scenario + 15% scenario was 70-80%)
 - About the time-frame & realizability of NPP non-dependency,
About half of the public hold certain concerns. Public does not yet have fixt view on “non-dependency by when”
 - Reasons of high support for immediate zero, or large-scale demonstrations against restarting NPP, should be seen in the context of non-confidence on the Government after 3.11, and concerns on NPPs.
- ◉ On 4 Sep., METI Minister reported about the challenges ahead in creating NPP non-dependency situation at EEC (Ene-kan).
 - Tighter electricity supply/demand→ Increase of electricity Price
(example: impact for household)(except single household)
2010 J¥16,900/month → 2030 max ¥32,243/month
 - Large requirement for new investment on renewable power generation (estimated ¥50 trillion required in 28 years)
(see next graph)
 - Issues of final disposal of fuel
 - Others

25



27

- ◎ Feed-in Tariffs for Renewable Energy has just started as of 1 July 2012.

Prices of Renewable Energy during July 2012 - March 2013						
Solar		≥10kW	<10kW			
	Price	¥42	¥42			
	Duration	20 years	10 years			
Wind		≥20kW	<20kW			
	Price	¥23.10	¥57.75			
	Duration	20years	20 years			
Hydro		≥1000kW <30,000kW	≥200kW < 1,000kW	<200kW		
	Price	¥25.20	¥30.45	¥35.70		
	Duration	20 years	20 years	20 years		
Geothermal		≥15,000kW	<15,000kW			
	Price	¥27.30	¥42			
	Duration	15 years	15 years			
Biomass		Biomass from sewage sludge & animals	Forest Thinnings	Whole Timber	Sewage Sludge & Municipal Waste	Construction Waste
	Price	¥40.95	¥33.60	¥25.20	¥17.85	¥13.65
	Duration	20 years	20 years	20 years	20 years	20 years

28

◎On 14 Sept. the government decided upon “Innovative Strategy for Energy and Environment”, at the Energy & Environment Council (“Ene-kan”) meeting.

-to aim at zero NPS operation in 2030’s

-3 principles: (1) 40 years operation limit for NPS to be strictly observed. (2) No new NPS construction. (3) Among existing NPSs, only those on which security is confirmed by new standard will be permitted to re-start.

-Nuclear fuel recycling will be continued. Researches & work on ways of direct disposal of spent fuel & disposal location will be immediately started. Aomori will not be final disposal location.

-”Monju” (prototype FBR) will finish its work within limited time-frame. (prototype → research only)

29

-Power generation by renewable resources will be 3 times more in 2030 than in 2010. 20% less greenhouse gas emission in '30 than in 1990. "Green Policy Framework" will be decided by the end of the year, including countermeasures against global warming.

-Power sector system reform plan will be made by the end of the year.

-Review from time to time.

◉ Later, on 19 Sept., the Government aimed to make a cabinet decision on the Innovative Strategy on Energy and Environment. However, due to oppositions from elsewhere, it could only decide to further examine the new strategy, making the Innovative Strategy as merely a reference.

30

◉ There are lots of domestic & international criticism on the new direction and the way the government handled the issue.

(Economic impact, Contradictions/dilemmas of zero NPS operations vs. continuation of recycling policies, accumulation of plutonium, and so on.)

◉ Meanwhile, elections of political party's presidency were held in both DP and LDP. In DP, PM Noda supported the government policy directions but 3 other candidates asserted earlier zero operation. In LDP, all 5 candidates asserted no hasty decision.

◉ It is anticipated that the issue may become a focal issue in the forthcoming general election.

◉ Meanwhile, on 2 Oct., Atomic Energy Commission decided to stop working on new "Framework for Nuclear Energy Policy", due to the Innovative Strategy on Energy and Environment, which required reviews on the way AEC operates, adding more confusions to the situation.

31

9 Conclusion

- ◉ 3.11 Earthquake/Tsunami and Fukushima Daiichi Disaster brought most serious challenge to Japan. Japan is at a crossroad toward the nation's future.
- ◉ Currently overall direction seems to be heading toward decreasing dependency on nuclear energy, eventually making it zero. But many questions still remain: How and in what pace? Does Japan really abandon all the industrial, technological and human resources base for the nuclear power generation in the country? How can Japan accommodate international requirements (CO2 emission, plutonium accumulation, developing countries' power needs, etc.
- ◉ Japan' forthcoming decision will no doubt have a far-reaching impact globally in the world-wide context of energy and environment.

32

Estimation of seismic risk for central Ulaanbaatar using building stock inventory

Iu. Berzhinskii¹, L. Berzhinskaia², O. Salandaeva³, D. Kiselev⁴,
S. Demberel, T. Erdenetuya⁵, D. Tulga⁶, G. Tatkov⁷

ABSTRACT

The seismic hazard in Ulaanbaatar City territory is related both to ground shaking from distant major earthquakes and active faults in the immediate vicinity of the city that are able to generate M 8.0 earthquakes. The design seismic intensity in the central part of the city is estimated at 7 to 8 on the MMSK-86 scale. In the last decade, the population of Ulaanbaatar city increased from 620 to 1,200 thousand inhabitants. There is a wide variety of modern housing developments. Besides precast concrete panel apartment buildings that were constructed in 1970-1990, the tower blocks are being built under the Japanese, Chinese and South-Korean homebuilder's projects. However, a half of the city population lives in yurts. Existing buildings inventory involved also the instrumental studies of dynamic characteristics of buildings at the micro-dynamic effect level, thus providing a possibility to estimate stiffness and strength. The accepted classification of buildings follows the Russian Seismic Intensity Scale standard MMSK-86 based on the notion of class of buildings according to the level of their seismic resistance. According to the level of seismic resistance, all residential buildings in Ulaanbaatar city may be divided into two major classes: C6 and C7. There is definite probability that some old buildings do not meet the requirements specified for class C6. A traditional national housing – well-built yurts – can be assigned to class C7. Seismic risk has been estimated using the model described in [Larionov et al., 2003]. The model was used to estimate economic risk for buildings of different types taking into account the buildings inventory data. The level of impact on population has been estimated through individual and collective risks. The value of seismic risk equal to 1×10^{-5} (1/year) was considered as acceptable one. Two scenario seismic events have been considered: earthquakes with intensity 7-8 according to the MMSK-86 scale. The results of computations have shown that an individual seismic risk considerably exceeds the accepted level. The value of seismic risk equal to 1×10^{-5} (1/year) was considered as acceptable one. Two scenario seismic events have been considered: earthquakes with intensity 7-8 according to the MMSK-86 scale. The results of computations have shown that an individual seismic risk considerably exceeds the accepted level. In case of an intensity 7 earthquake it is equal to 1×10^{-4} , and for an intensity 8 quake the level increases to 5×10^{-4} (1/year); a relative economic damage has been respectively estimated as 8% and 45%.

Larionov V., Frolova N. 2003. Peculiarities of seismic vulnerability estimations. In book: Natural Hazards in Russia, volume 6: Natural Risks Assessment and Management, *Publishing House "Kruk"*, Moscow, pp.120-131.

Importance of maintenance to utilize existing structures

Taketo UOMOTO
Chief Executive,
Public Works Research Institute

ABSTRACT

Many structures are being built in various parts of the world. To use these structures for long period of time, maintenance is one of the most important things. Usually, these structures can be used for more than hundred years, but due to deterioration, accidents, etc., some of the structures must be repaired within 50 years. This paper clarifies the causes of the deterioration and shows examples how to prevent the deterioration and how to deal with the problem after they are deteriorated.

1. INTRODUCTION

Japan experienced a rapid economic growth in the period of 1960 to 1990. More than 100million cubic meters of concrete were used to construct the structures such as buildings, bridges, tunnels, dams, roads, railways, etc. to support the activities of Japanese people. As a result, large stock of these infrastructures is reaching 50 years of service, and due to deterioration of the structures, maintenance of these structures has become a major interest among the owners and the civil engineers. In Japan, many different types of hazards attack every year on these structures, such as earthquakes, tsunamis, typhoons, etc. It is extremely important to prevent the structures collapse due to these hazards.

On March 11, 14:46, 2011, the massive³ “Great East Japan Earthquake” hit the country of Japan just off the Pacific coast. The magnitude of the earthquake was reported as 9.0, and shook Japan from Hokkaido to Nagoya City. The disaster was tremendous compared to Hanshin-Awaji Great Earthquake which took place in January 17, 1995. A large difference can be seen in not only the vibration of the ground caused by the earthquake, but the tsunami and nuclear power plant accident. Such earthquake disasters are occurring quite frequently compared to other countries. The data shows that the earthquake energy occurring in Japan is more than 10% of the whole earth.

On the other hand, population of Japan is estimated to reduce rapidly from now on because of fewer babies in a family (approximately 1.2 children per family) than needed to sustain the present population. Although high technologies have been developed in recent years, it is sure that fewer engineers will have to take care of this huge amount of structures from now on, which has never experienced in the

past. Due to reduction in the economical growth, the budget for both construction and maintenance will be reduced in the future.

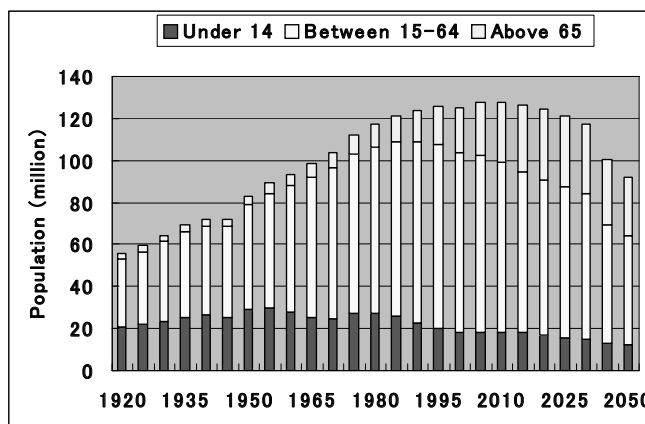


Figure 1 Percentage of different ages in Japan

Considering these situations, the maintenance of existing structures in Japan must be done with the following conditions: 1) rapidly increasing amount of existing structures reaching the age of 50 years, 2) less amount of engineers to maintain the structures, 3) less amount of budget to maintain the structures. Although there are many hazards in each country, concrete structures are expected to be safe for long period of time. These structures may deteriorate by many causes including chemical reactions, physical loads, etc., as time passes by.

If the structure is deteriorated before the hazards, the structure may easily collapse and it would be difficult to maintain the safety of the people. In order to keep the safety of urban area, it is important to study and investigate not only on hazards but also on durability aspects of existing structures. Even a small amount of concrete spalling may cause large scale traffic accidents as we experienced in Sanyo-Shinkansen in 1999. Considering these situations now, this paper explains what is happening now in Japan and how we are dealing with the problems through research and engineering.

2. GENERAL MAINTENANCE METHODS USED TILL NOW

The maintenance of concrete structures has been done mostly by the owners of the structures. In case of public structures, the ministries, etc. maintain the structure after the structures are completed. For the time being, the methods for the maintenance differ according to the owners of the structures. Although there are some differences, the main concept of the maintenance can be summarized as follows:

1. Periodic inspection and evaluation of deterioration degree
2. Detailed inspection and decision making
3. Repairing and strengthening of deteriorated structures

For periodic inspections, the inspectors inspect the structures visually, sometimes with the help of binoculars and hammers, once a year or once in several years according to the importance and time after the structure is completed. The

inspectors are mostly trained engineers with experiences. The detailed inspection is done when the estimated degree of deterioration exceeds certain limit, or when some new phenomenon is found during the periodic inspection. The detailed inspection is done by visual inspections with the aid of non-destructive tests or taking core samples out from the inspected structure. The purpose of the inspection is to decide the cause of the deterioration and also to evaluate whether repair and/or strengthening is needed or not.

To repair or strengthen the existing structures, it is important to design and select sufficient methods and materials. The most popular repair method for corrosion of steel bars due to carbonation is to eliminate the carbonated concrete and replace it by new concrete and apply coatings with and without FRP sheets. But in case of steel corrosion due to chlorides from the surrounding environment, the high chloride concentrated portions of concrete are taken out, anti-corrosive treatment is applied to the surface of the bar, and polymer cement mortar is generally used to repair the concrete before coating the concrete surface.



Figure 2 Deteriorated wharf due to chloride corrosion (Photo by Ema Kato)

3. STANDARD SPECIFICATION OF JSCE

After the investigations of many deteriorated concrete structures, the importance of durability was fully recognized by the civil engineers. To deal with the problem, not only JSCE, AIJ, and JCI have been recommending methods to deal with the problems but also the Ministries, and other authorities started to propose practical counter measures to cope with the situation. As a result, a large amount of researches has been done related to the durability of concrete structures including non-destructive inspection methods.

Among these authorities, the Concrete Committee of JSCE, the leading committee in the field of concrete in Japan, has published the translated version of “Standard Specifications for Concrete Structures-2002” in English to deal with the problems of durability. A new version of the Standard Specification was published in the

year 2007 in Japanese (JSCE, 2007a, 2007b and 2007c). The concept written in the specifications will surely be adopted by other institutions. (These standard specifications can be down loaded directly from the home page of JSCE: <http://www.jsce.or.jp/committee/concrete/e/index.html>)

The main proposals of the “Standard Specifications 2007” are the following two items:

- 1) Propose a new method to design and construct new concrete structures that can be used for specified lifetime without large amount of maintenance cost.
- 2) Propose an effective and economical system to maintain existing concrete structures with small number of engineers and workers.

The concepts of the new Standard Specifications are briefly explained in the following chapters.

3.1 DURABILITY DESIGN OF CONCRETE STRUCTURES FOR NEW STRUCTURES

Performance-based durability design was introduced to “Standard Specification of Concrete Structures” by the Concrete Committee of JSCE in the year 2000 and be translated to English version in 2005 (JSCE, 2005c). Although durability of concrete structures was considered important in the previous specifications, performance-based design method was not used. The previous specifications described the importance of durability by proposing that the concrete structures are durable for a long time when specified materials, mixes, covers, etc. are used. But these specifications did not mention about the duration of service time, etc.

The proposed performance-based new durability design can be summarized as follows:

1. The concrete structure must be quantitatively checked whether the structure possesses required performance within the designed period.
2. The degree of deterioration of the structure in service for a specified cause must be specified.
3. To maintain the structure above the specified degree of deterioration, the required performance must be specified.

To examine the performance on durability, a kind of limit state design scheme was introduced for the durability of concrete structures. The equation can be written as shown in Equation (1):

$$\gamma_i \cdot \frac{A_d}{A_{lim}} \leq 1.0 \quad (1)$$

where, A_d is designed performance of the structure at specified time considering the specified deterioration cause, A_{lim} is limit of the performance of the structure, and γ_i is coefficient of the structure considering the importance, etc.

Generally, performance of concrete has to be verified to satisfy the required performance. Not only resistances against deterioration but also mechanism

properties of concrete have to be verified as shown below.

1. Compressive strength
2. Carbonation rate
3. Diffusion coefficient of chloride ions in concrete
4. Dynamic modulus of elasticity
5. Resistance to chemical attack
6. Resistance to alkali aggregate reaction
7. Coefficient of water permeability of concrete
8. Fire resistance
9. Adiabatic temperature rise
10. Drying shrinkage characteristics
11. Setting characteristic

The Figure 3 shows an example of the calculated result for minimum cover thickness to prevent carbonation induced corrosion at different years of service for OPC concrete and BFSC concrete. As shown in the figure, the cover thickness required changes according to the type of cement to be used, water-cement ratio of concrete, years of service and exposed condition (wet or dry) of the structure to be constructed. When the structure is designed for long period of time, the cover thickness may become too large, and it is recommended to use other countermeasures such as Epoxy-coated bars.

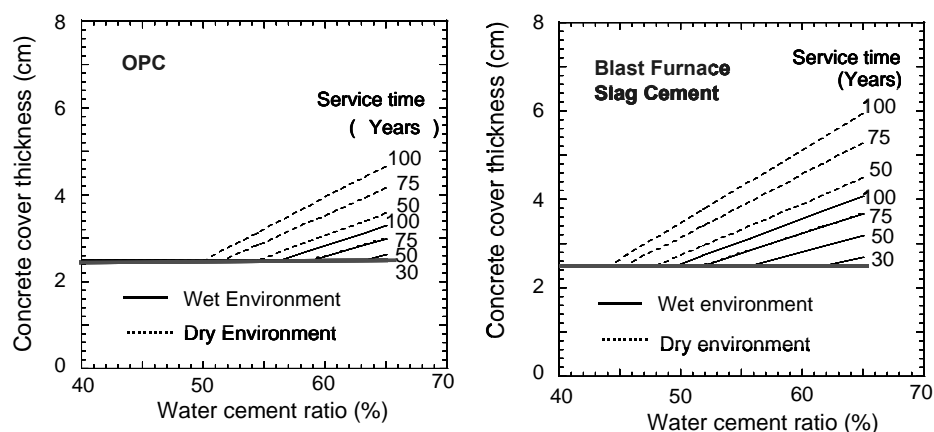


Figure 3: Calculated results of concrete cover according to JSCE Standard Specification

3.2 METHODS OF MAINTENANCE PROPOSED BYJSCE

The methods used in the new Standard Specification are basically the same as the conventional method. The differences are that the new method requires maintaining the structure within their required performances throughout their service life. Firstly, the listed below issues have to be clearly specified.

1. To maintain a structure, performances required for the structure must be clearly defined.
2. The performances required for general structures are “safety”, “serviceability”, “hazards to the public”, “aesthetics and landscape” and “durability”.

And the basic principles of maintenance works are as follows:

1. Structures must be maintained according to a designated maintenance category by formulating a maintenance program to retain the performance within the specified tolerances throughout their service life. And maintenance system includes adequate “initial inspection”, “deterioration prediction”, “inspection”, “assessment/judgment”, “remedial action”, and “record”.
2. To maintain a structure, in addition to the assessment and evaluation at the time of inspection, assessment and evaluation must be made throughout the service life of the structure based on prediction of deterioration.
3. To predict the deterioration, required performances of the structure must be clearly defined, and also the design service life must be made clear.
4. The records on design, construction, initial inspection, deterioration prediction, periodical inspection, assessment and/or evaluation, and remedial actions must be kept throughout the service life.

In detail, for an example, the standard method for chloride induced deterioration recommends the model to predict chloride ion diffusion, progress of steel corrosion, and correction of the prediction. Also the methods of initial inspection, routine inspection, periodic inspection, and detailed inspection as well evaluation and judgment method are also discussed. Finally, for recommendation remedial measures, information on measurements of both repair or strengthening also has to be recorded.

One of the difficulties is how to predict the degree of deterioration at the end of their service life. There are several researches being done to predict the deterioration in numerical manner. In the published Standard, several numerical prediction methods are introduced as references for structures suffering cyclic fatigue loads, carbonation induced corrosion and chloride induced corrosion. In case of cyclic fatigue, S-N curves are used to predict the service life. In case of carbonation induced and chloride induced corrosion of steel bars, diffusion equations for carbon dioxide and chloride are used to predict the degree of corrosion. Using these prediction methods, deterioration degree can be estimated to certain degree. (See Figure 4) But for other deterioration problems, which has not been studied numerically, a quantitative model has not been proposed yet. To deal with the problem, a qualitative method, namely “Grading method”, is introduced in the Standard.

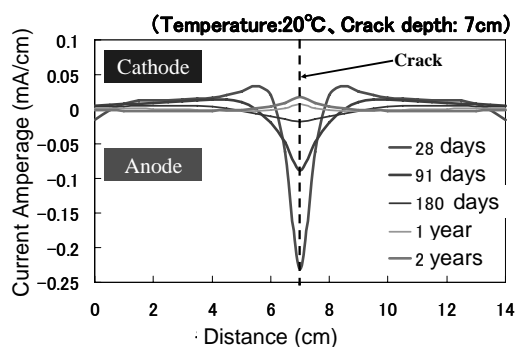


Figure 4: Quantitative prediction of corrosion in marine environment with cracks (Tsukahara et al., 2000)

4. PROBLEMS IN ACTUAL EXISTING STRUCTURES

One example of the problem is as follows: When a civil engineer is asked by the owner to check the safety of an old existing structure, one of the largest problems is that there are neither drawings nor construction records of the structure available. No problem may occur in case of important facilities, which is maintained with great care. But in case of normal structures, the owners do not know the importance of these documents.

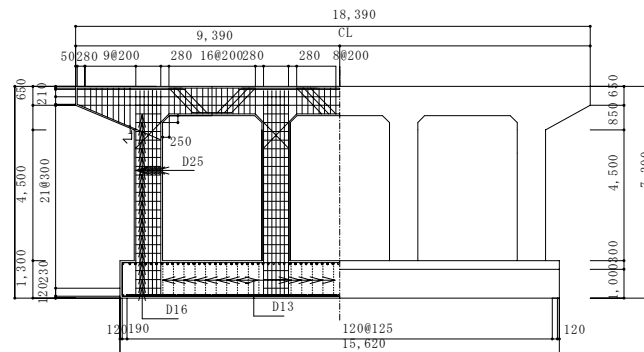


Figure 5: Re-designed reinforced concrete pier of a bridge (Okazaki, 2005)

To deal with the problem, NDI is not enough. Fortunately, our structures are not too old, and they are mostly designed and constructed by the method specified by JSCE, AIJ or other associations. Considering these, the only way is to re-design the structure again using the methodologies used at the time of construction. Figure 4 shows an example of re-designed bridge pier constructed about 35 years ago. From the figure, it is much easier for a civil engineer to check the safety of the structure under several hazards. It will become more important for the owners and engineers to keep these documents throughout the service life of a structure.

5. CONCLUDING REMARKS

Engineering is not always complete, and further research works are needed. To sustain existing structures, durability of the structure is important. One good method is to construct durable structures, but for the existing structures maintenance is the only way to deal with the problem. Although concrete committee of JSCE has set up a good system for maintenance of existing concrete structures, there are still many things to be done: not only researches but also education to the students and engineers about durability and maintenance. I hope this paper may become a help to the concrete engineers of the world who are trying to design, construct and maintain concrete structures.

REFERENCES

- Concrete Committee of JSCE, Standard Specifications for Concrete Structures-2007 “Design”. JSCE, Tokyo.
- Concrete Committee of JSCE, *Standard Specifications for Concrete Structures-2007, “Materials and Construction”*. JSCE, Tokyo.
- Concrete Committee of JSCE, Standard Specifications for Concrete Structures-2007 “Maintenance”. JSCE, Tokyo.
- Okazaki, S., 2005. *Development of monitoring system for RC bridge based on restoration design method*. Thesis submitted to the University of Tokyo for Master of Engineering degree.
- Tsukahara, E., Koyama, R., Hoshino, T., and Uomoto T., 2000. Estimation Method of Corroded Portion of Reinforcing Steel Bar by Natural Potential Measurement. *Non-destructive Testing in Civil Engineering 2000*, Elsevier.
- Uomoto, T., and Misra S., 2001. Role of Engineers to Improve Quality of Concrete Structures. *Proceedings of EASEC-8*, Singapore.

Oral Sessions

Impact of urbanization on flooding and sustainable flood mitigation measures

Charng Ning CHEN¹

¹Professor Emeritus, School of Civil & Environmental Engineering,
Nanyang Technological University, Republic of Singapore
chen@cnchen.com

ABSTRACT

Uncontrolled urban development invariably causes increase of flood risk and damages to the catchments. The increases in impervious covers and channelization are the key elements that cause increases in flood peak and volume, and reduction in base flow. Flood-plain encroachment, ground subsidence, and poor maintenance of drainage facilities also contribute to the flooding problems. The impact of these land-use related factors on the changes in flood characteristics are presented. Interest in mitigating the adverse impacts on water and land through innovative storm-water management approaches, such as the Low Impact Development (LID), are gaining broader acceptance worldwide. The approach emphasizes the conservation of natural systems and mimic the pre-development hydrologic function of a site, and thus reducing the flood peak and enhancing the base-flow. A similar approach- named as ABC (Active, Beautiful, and Clean) program, was introduced in Singapore, relying on the natural systems to detain, retain and treat storm-water on-site. Typical features include pervious pavement, green roofs, rainwater harvesting, rain gardens and green walls, vegetated and bio-retention swales and basins, and wetlands. Examples of LID/ABC practices in the U.S. and Singapore are presented. These practices have the benefits of achieving flood control, water augmentation and improvement to storm-water quality in a more sustainable manner.

Keywords: *urban flooding, impervious covers, channelization, flood-plain encroachment, ground subsidence, LID (Low Impact Development), ABC (Active, Beautiful, and Clean), water augmentation, water quality*

Centralized and decentralized urban flood control measures under physical and societal constraints

Srikantha Herath¹, Socheat Penh², Hiroyuki Okui³, Masahiro Imbe³
and Yoshihiro Kitagawa⁴

¹Academic Director, Institute for Sustainability and Peace,
United Nations University, Japan
herath@unu.edu

²Graduate Student, Institute for Sustainability and Peace,
United Nations University, Japan

³ Association for Rainwater Storage and Infiltration, Tokyo, Japan

⁴Professor, Kokushikan University, Tokyo, Japan

ABSTRACT

This research focuses on an alternative approach to flood control by combining centralized water retention systems with distributed onsite control using infiltration and facilities. The flood control requirements in upstream, midstream and downstream areas for an urban catchment in Tokyo were analyzed for different return periods. Various combinations of centralized flood control measures, notably the storage systems and onsite infiltration facilities were assessed that could meet the flood control demands. Then the least construction cost combinations of facilities meeting these requirements were identified. While the local government can implement the centralized control measures, the distributed implementation requires the consent and willingness of the residents of the catchment. This was assessed using a controlled household survey that also analyzed the effect of awareness building on increasing the willingness to participate. The study identified that implementing least cost solutions that meet both physical and societal constraints is possible if residents can be better informed of the environmental benefits of infiltration systems.

Keywords: urban flood control, public involvement, infiltration systems, least cost solutions, environment sustainability

1. INTRODUCTION

Urbanization adversely affect water cycle due to changes to hydrological processes. Concrete houses, building, pavement roads and other infrastructures have been built and constructed, which change natural land surface to impervious areas. Loss of natural retention areas and expansion of impermeable area cause increase the surface runoff volumes as peak discharges and constraint for natural infiltration to the ground (Hearth & Musiake, 1994). This phenomenon result in decreasing groundwater recharge leading to low river base flow as well as increase in surface runoff. When there is heavy rainfall, surface runoff increases

rapidly causing floods and inundations occur in downstream areas. According to Japan Sewage Works Association (2009), the rainfall intensity in urban areas of Japan has been increasing noticeably. Comparing rainfall intensity in the last ten years to those occurring last 30 years shows that rainfall intensity has been over 50mm per hour by a factor of 1.5, and this tendency exceeded the planned scale and capacity of drainage systems frequently.

Floods in urban area cause many problems for citizens and development activities. Moderate and frequent urban floods cause inconveniences for daily commuting to work, school, business, etc. Severe floods that significantly exceed drainage capacities causes large economic losses to individuals, business and infrastructure, etc. For example, in June 1999, Fukuoka suffered from a severe urban flood, which took place in the center of the city and storm water flooded underground, and repeated on July 19, 2003 (Herath, 2004). It is of great concern that these trends would continue become more serious under climate change conditions (Japan Sewage Works Association, 2009).

Flood countermeasures such as urban drainage and flood control have been developed and improved with various regulations enforced in rapidly urbanizing areas to deal with increased storm runoff (Herath and Musiaka, 1994). Direct flood countermeasures such as constructing storm water reservoirs, reinforcement of existing drainage system, and enhancing pumping stations have been expanded. However, these mitigation measures have constraints in field conditions due to limited land to be installed and large amount of finance to be committed. On the other hand, infiltration systems that consist of infiltration box, infiltration trench and permeable pavement, which have been installed and attached with households, building, and public roads have been utilized popularly and effectively to reduce storm runoff as a distributed counter measure. However, there are limited studies on the infiltration and storage systems for a whole watershed to control urban flood considering the different measures for upstream, middle stream and downstream. At the same time, there is an initiative to alter from the conventional measures to combination of infiltration and storage system (Japan Sewage Works Association, 2009).

The paper presents a case study of an urban catchment in the suburbs of Tokyo, where a combined system of flood storage using centralized systems with infiltration systems has been studied for optimum combination of the facilities in terms of construction cost and feasibility of participatory implementation.

2. METHODOLOGY

2.1 Study overview

An urban catchment in Tokyo metropolitan areas is selected for the study. The major components in the study are summarized as follows;

1. Analysis of food risk for different future return periods considering the current drainage capacity at upstream, midstream and downstream locations.

2. Analysis of feasible combinations of centralized storage facilities and decentralized infiltration systems to meet required flood reduction capacities for different design rainfall events
3. Analysis of implementing least cost flood control facilities with participatory flood management considering community willingness to engage.

2.2 Analysis of flood risk

Flood risk of the study area is analyzed using a physically based semi-distributed hydrological model. Similar Hydrologic Element Response (SHER) model that has been developed and used for the design of infiltration systems in the past (Herath, S, 1991, Herath et. al, 1992) was selected for the study. In applying the model, a catchment is divided in to a number of Similar Hydrologic Response Elements, based on soil type, depth to ground water and slope. The hydrologic

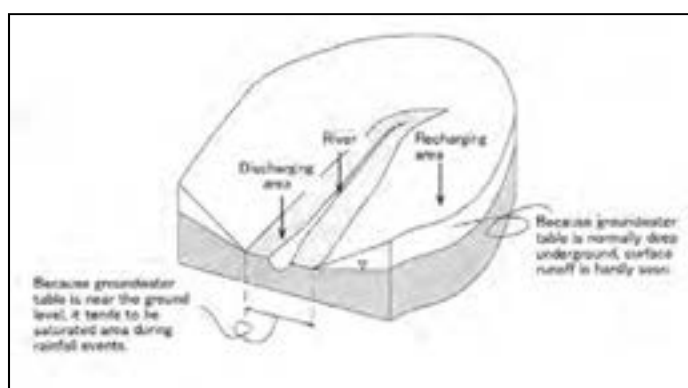


Figure 1. Schematic diagram of recharging and discharging areas (Source: Nippon Koei Technical report, 2011)

response of each block is estimated based on the land cover, and using surface routing, subsurface routing and ground water routing based on the saturated and unsaturated flow equations. The delineation of blocks also employs the concept of recharging and discharging areas as shown in figure 1. The current simulation has been carried out with the In the Extend SHER version (Herath, 1999), which has components such as rainfall block, surface flow and sub-surface flow block, evaporation block, underground flow block and river modeling block that can be graphically assembled to make the catchment simulation model. Setting of the model for a particular sub-catchment is shown in figure 2.

After setting up the model for the target catchment, calibration and validation, flood simulations are carried out for 1:10, 1:30 and 1:50 return period design rainfall events. The peak centered design rainfall pattern is given by,

$$r = b/T^{2/3} + a$$

where r : rainfall intensity (mm/h) and T : time (min). For Tokyo area the equations take the following form,

- 10 years return period: $r = 1500/T^{2/3} + 4.5$

- 30 years return period: $r=1800/T^{2/3}+4.5$
- 50 years return period: $r=1900/T^{2/3}+4.5$

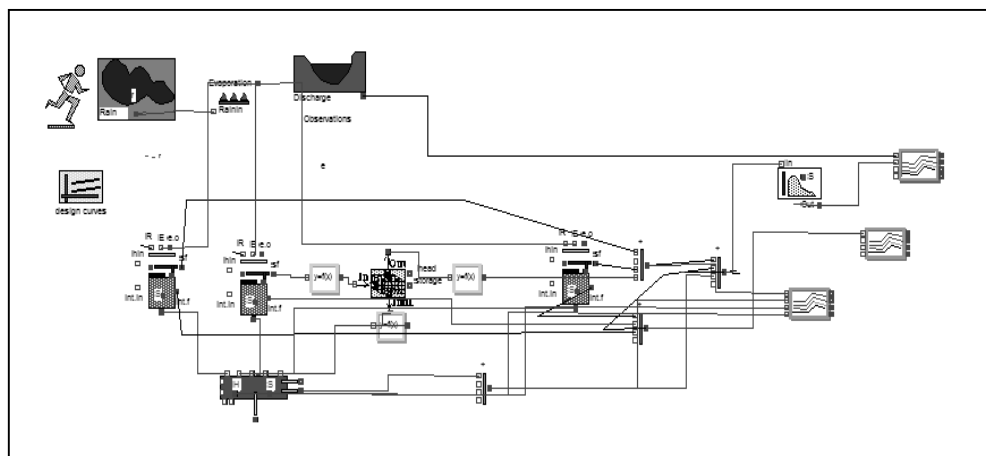


Figure 2. Setting up SHER-Extend model for a subcatchment

2.2 Feasible facility installation and cost estimation

In order to assess the feasible combination of flood control facilities, at first, all locations that can be used to install centralized storage facilities along the river as well as all locations that can be used to install onsite infiltration facilities in are identified from the detailed GIS of the catchment area. Then several sets of simulations are carried out to assess hydrological response of the study site under different combinations of storage and infiltration systems under selected design storms at upstream, midstream and downstream locations of the catchment.

2.3 Constructing Cost of Infiltration and Storage Facilities

In order to select the best combination with minimum construction cost, actual costs incurred in previous construction projects are used as average cost in this study. The construction costs for 2007 based on cost of different facilities in field installations are assumed to be valid for current too. The construction costs used in the study are shown in Table 1.

Table 1: Constructing cost of different types of facilities

Type of Facilities	Size (m)	Unit	Total Constructing Cost
Infiltration box	0.35*0.6	1	67,600 JP Yen
Infiltration trench	0.55*0.6*0.2	1m	29,900 JP Yen
Underground storage	1*1*1	1m ³	110,000 JP Yen

2.3 Assessment of participatory flood control management feasibility

While the centralized underground storage facilities can be installed by the local government in the public spaces identified in section 2.2, the infiltration facility installation at each individual house require residents willingness to install the infiltration facilities and maintain them. In this study we were interested in the

following 2 aspects of residents willingness to be engaged in the flood control using onsite facilities.

1. What percentage of residents are willing to install infiltration systems at their houses and their distribution in the upstream, midstream and downstream areas?
2. How can raising residents' awareness on environmental benefits of infiltration systems modify this willingness?

In order to address these issues, two sets of survey questionnaire were prepared. The questionnaires are identical except that one questionnaire has brochures and a CD as outlined in Table 2. The CD contains a movie clip which describe comprehensively about the change of water cycle due to urbanization, urban flood and the benefits of installing the infiltration facilities for reducing urban flood risks and improving groundwater table. The purpose of distributing two sets of questionnaires was to investigate whether promoting people's awareness of infiltration facilities affect on their decision to install the facilities.

Table 2: List of materials attached with questionnaire

Attached Stuffs	Without CD	With CD
Cover letter	✓	✓
Questionnaire	✓	✓
Infiltration and subsidy program	✓	✓
Information about Infiltration facilities		✓
Subsidy calculation	✓	✓
CD documentary		✓

The questionnaire was designed in two parts to collect information as outlined below;

Part 1: General information about respondents (gender, age, members of household) and Information about experiences with inundation (depth, duration, economic loss in overall)

Part 2:

Section A: For respondents who have known infiltration facilities

- For respondents who already installed the facilities
- For respondents who have not installed the facilities yet

Section B: For respondents who have not known infiltration facilities

- Reasons of installing the facilities
- Reasons of not installing the facilities

3. RESULTS

3.1 Study area

Figure 3 shows a map of Yato watershed, located in the Tokyo Metropolitan area, which was selected as the study site. There are four types of soil in Yato watershed, namely; Kanto loam, Alluvial lowland, Kazusa group, and Shimosa layer group. Most of the catchment is covered by Kanto loam, which is volcanic ash and appropriate for installation of infiltration facilities due to very high soil conductivity. The land use is categorized in to 15 types as forest, rice field,



Figure 3. Study Area

farming area, semi-developed area, unoccupied area, industrial area, residential area, commercial area, road, green space, public space, river, and others. Infiltration facilities are currently installed in some parts of the catchment as a result of local government initiative for installation of infiltration systems supported by a subsidy program.

3.1 Flood risk assessment

Prior to flood risk assessment it is necessary to check the accuracy of the modeling in a model validation process. The catchment was delineated to 4 sub catchments, according to the availability of observation data for simulation as shown in figure 4. The year 2009 rainfall and discharge records were used for the validation. The Nash-Sutcliffe coefficient(E) described by

the equation

below was used to assess modeling efficiency. The closer E is to 1, the higher the model efficiency in modeling the catchment response to a given rainfall input.

$$E = 1 - \frac{\sum_{t=1}^T (Q_o^t - Q_m^t)^2}{\sum_{t=1}^T (Q_o^t - \bar{Q}_o)^2}$$

Where E: model efficiency coefficient
 Q_o: observed discharge
 Q_m: modeled discharge

According to Table 3, the model performs well for both hourly and 10 min interval modeling, but modeling efficiency is higher for 10 minutes interval simulation than hourly interval simulation. This is consistent with the performance expected from a physically based model such as SHER model at higher temporal and spatial resolutions inputs.

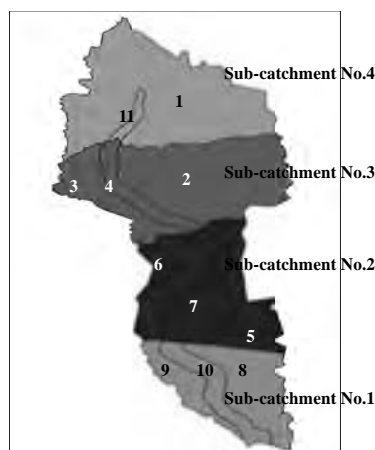


Figure 4. Sub-catchments and SHER blocks used in the simulation

Table 3: Accuracy of the modeling

Model efficiency	Sub-catchment No. 4	Sub-catchment No. 3	Sub-catchment No. 2	Sub-catchment No. 1
E (Hourly)	0.82	0.83	0.83	0.74
E (10 min)	0.848	0.95	0.93	0.957

After model validation the current drainage capacity of the study area for different design rainfall events has been assessed at each of the sub catchments. Figure 5 shows the river flows for different design rainfalls compared with current drainage capacity of the catchment

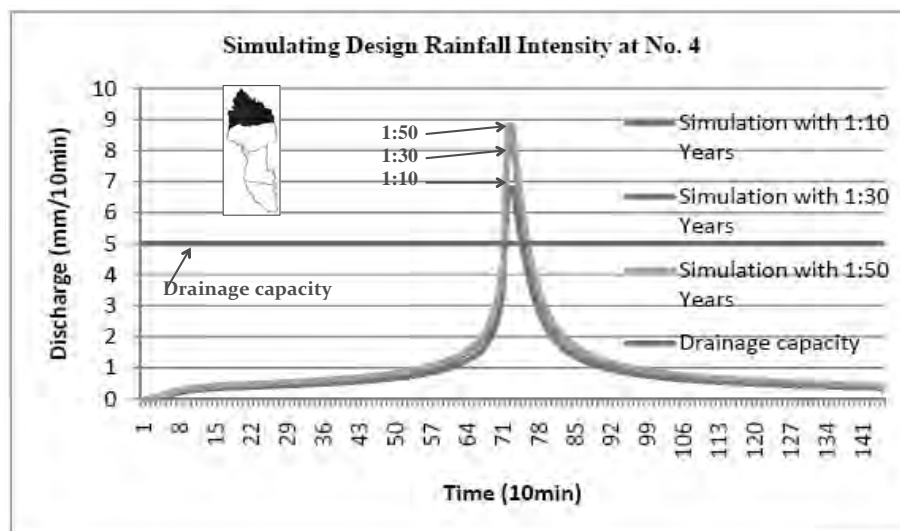


Figure 5. Flood discharge at different design rainfalls at sub catchment 4

3.2 Performance of flood control facilities installation costs

Flood control plans were developed to reduce the river flows to the drainage capacity level by the combined installation of infiltration and storage facilities. Obviously, infiltration trench and box are utilized as infiltration facilities. Table 4 shows characteristics of the infiltration facilities, such as types of infiltration facilities, dimension, infiltration capacity, and storage of infiltration facilities. In this study, residential areas, public facility areas, green areas, and roads are considered as feasible areas for installing the infiltration and storage facilities.

Table 4: Characteristics of infiltration facilities

Type of Infiltration Facility	Dimensions of Facility	Type of Soil	Saturated Hydraulic Conductivity (K _o , cm/s)	Infiltration Facilities		
				Infiltration capacity/unit (m ³ /s)	Void ratio	Storage (m ³)
Infiltration trench	Width: 0.55m, Height: 0.6m	Kanto loam	0.00275	0.0000899	0.4	0.132
		Alluvial lowland	0.001	0.0000327		
		Shimosa	0.00055	0.000018		
		Kazusa	0.001	0.000032		
Infiltration box	Width: 0.65m, Height: 0.7m	Kanto loam	0.00275	0.0000933	0.47	0.139
		Alluvial lowland	0.001	0.0000327		
		Shimosa	0.00055	0.000018		
		Kazusa	0.001	0.000032		

Table 5: Area of Land Use Types for Installing Infiltration Facilities

Total single houses (Unit)	4000
Complex building area (m ²)	298917
Unoccupied area (m ²)	153551
Road (m ²)	391325
Green space (m ²)	413283
Public facilities (m ²)	199131

Residential areas consist of single house and housing complexes. For single house land use type two units of infiltration box are installed, and for the rest of land use types, 500 meters length of trench can be installed in one hectare as per the guide lines adopted by Association for Rainwater Storage and Infiltration Facilities. The landuse types available for installation of infiltration facilities are given in Table 5.

The amount of storage or infiltration facilities that need to be installed so that the drainage capacity at a particular location along the river is not exceeded can be estimated by numerical simulation. The infiltration facility performance in flood control is estimated by the methodology outlined by Herath (1994). A given flood control objective can be achieved by various levels of combination of storage and infiltration facilities as shown in figure 6, where each point corresponds to the storage volume and infiltration capacity required to achieve drainage capacity of at sub catchment 4 outlet, for 1:10 year return period rainfall in the top figure for 1:50 year return period rainfall in the bottom figure. While 1:10 year design rainfall can be accommodated completely by either storage or infiltration facilities, it can be

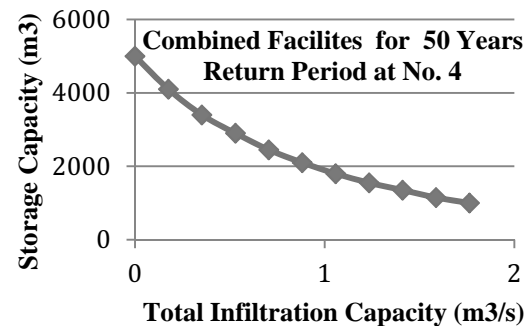
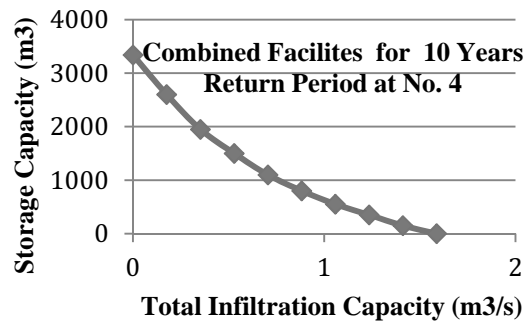


Figure 6. Feasible combinations of storage and infiltration facilities to achieve target flood control levels.

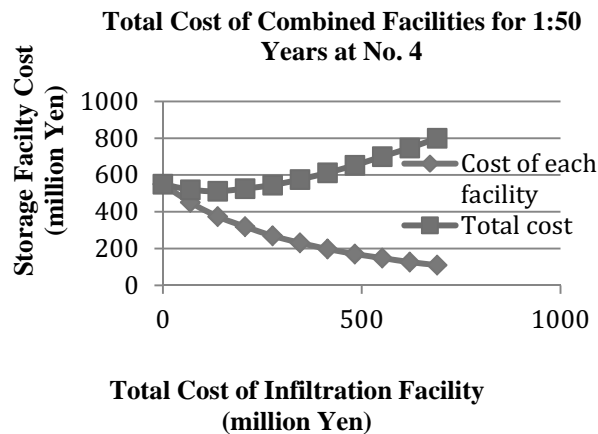
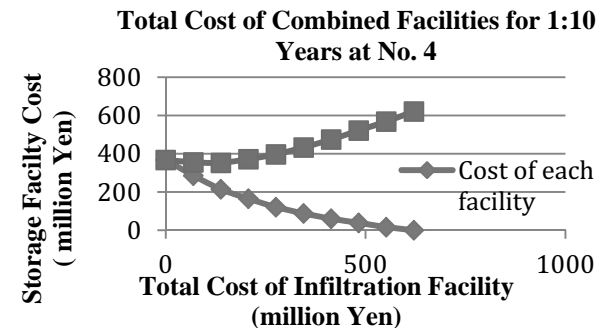


Figure 7. Installation cost of each type of facilities as well as total cost.

seen that 1:50 year event cannot be managed by infiltration facilities alone, even if maximum possible amount of infiltration facilities are installed.

Next the installation costs for each of the above configuration can be estimated from the values given in table 1. Figure 7 shows the total cost for infiltration and storage facility combinations according to the combined systems shown in figure 6. The least cost combination of facilities are summarized in table 6.

3.2 Survey results for participatory management

In order to engage the community in flood control and managing the water cycle through the installation of infiltration facilities the local government provides a subsidy for infiltration facility installation. Two infiltration boxes are recommended to be installed in each single house, and the local government covers 80% of total cost. Thus, for each single house the residents need to bear 20% of total cost which is about 30,000 Japanese Yen. To understand the willingness of the residents

to participate in the programme a household survey was carried out by distributing 1000 questionnaires among the 4000 single houses in the Yato watershed. 173 questionnaires were returned by Post, which is

Table 6. Optimum level of infiltration facilities to have least cost facility combination

Catchment No.	1:10 yr	1:30 yr	1:50 yr
Sub catchment 4	20%	20%	20%
Sub catchment 3	20%	20%	20%
Sub catchment 2	20%	20%	30%
Sub catchment 1	20%	20%	30%

17.3% of total questionnaires distributed. The figure 8 shows that at the current

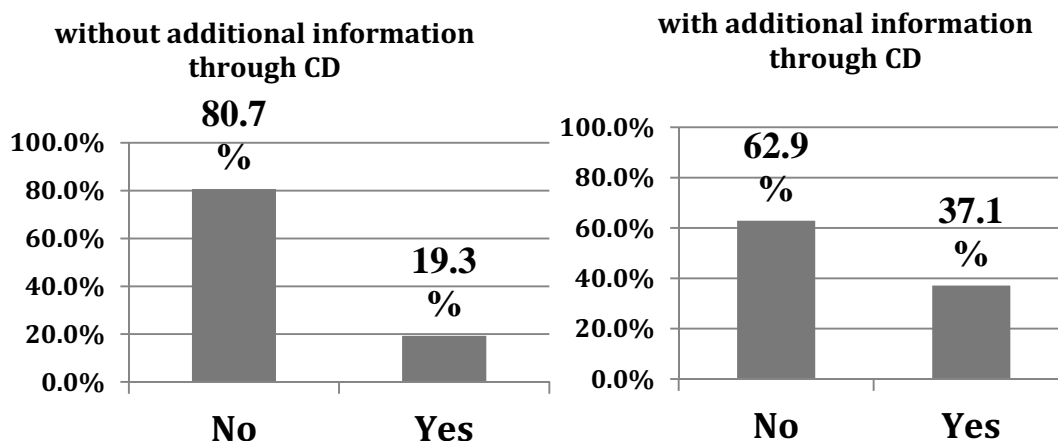


Figure 8. Willingness to install infiltration facilities according to survey results

level of awareness only about 19% of those responded were willing to participate in the programme. However, if the community can be made aware of the environmental benefits of infiltration systems, as was done through the CD distributed with the questionnaire, this number increased to 37%.

4. DISCUSSION AND CONCLUSIONS

The simulation study shows that least cost flood control systems for different parts of the catchment consist of having about 20-30% of flood volumes over the current drainage capacity taken by infiltration systems and the rest by centralized storage facilities. The survey of catchment residents on their willingness to participate in infiltration facility installation shows that in order to achieve this level of infiltration facility installation, the awareness of the residents on the environmental benefits of infiltration system installation need to be raised. While centralized storage facilities provide protection against river floods, infiltration facilities are effective in reducing surface floods. At the same time, centralized systems are more reliable in terms of long term maintenance of control and adjustments to suit changing rainfall and catchment conditions. Based on these considerations, it is recommended to provide a degree of redundancy in the flood control system by introducing additional protection by having 30-40% of excess reduction by infiltration systems and having about 70-80% protection from centralized storage systems.

REFERENCES

- Association for Rainwater Storage and Infiltration Technology. (1997). Engineering guideline for rainwater infiltration facilities. Infrastructure Development Institute, Japan
- Japan Sewage Works Association (2009). *Sewage Works in Japan*. Japan
- Herath S., Hirose N. and Musiaka K. (1990). A computer package for the estimation infiltration capacities of shallow infiltration facilities, *Proc. 5th International Conference on Urban Storm Drainage*, Japan, pp.111-118.
- Herath, S. (1991) A Physically based model for basin hydrological process simulation and its application to Hachioji New Town Project, *Nippon Koei Technical Bulletin*, No. 12
- Herath S., Musiaka K., Hirose N. and Matsuda S. (1992). A process model for basin hydrological modeling and its application, *Proc. Japan Annual Conference of Society of Water Resources and Hydrology*, pp.146-149.
- Herath S. and Musiaka K. (1994). Simulation of Basin Scale Runoff Reduction by Infiltration Systems, *Water Science and Technology Journal*, Vol.29, No. 102, pp267-276.
- Herath S. (1999) Design of Infiltration Systems, *UNESCO Workshop on Urban Storm Drainage Analysis and Modeling*, Hanoi, Viet Nam

Disaster information collection by Thai and foreigners during the 2011 Thai flood

Michael HENRY¹, Akiyuki KAWASAKI², and Kimiro MEGURO³

¹Assistant professor, Division of Field Engineering for the Environment,
Faculty of Engineering, Hokkaido University, Japan
mwhenry@eng.hokudai.ac.jp

²Project associate professor, International Center for Urban Safety Engineering,
Institute of Industrial Science, the University of Tokyo, Japan

³Professor and Director, International Center for Urban Safety Engineering,
Institute of Industrial Science, the University of Tokyo, Japan

ABSTRACT

From June to September 2011, heavy precipitation in Thailand led to flooding in the Chao Phraya River Basin. The floodwaters moved slowly south from the northern part of the country, eventually submerging the areas surrounding Bangkok and threatening the city itself by the end of October. Due to the ambiguity of the flooding progress, people invariably searched for information regarding the disaster so that they could better understand the developing situation and make decisions or preparations regarding whether to evacuate their homes or businesses. However, both Thai and foreigners alike experienced difficulties when it came to collecting accurate and up-to-date information on the flooding, such as incorrect or conflicting reports, false rumors, a lack of English-language updates, congestion in information networks such as hotlines, and so forth. In order to improve the dissemination of information after future flood disasters, a survey was conducted to understand how people residing in Thailand at the time of the flood collected their disaster information. This paper presents a summary of their responses and compares the results of Thai nationals with those of foreigners residing in Thailand in order to better understand the disaster information needs of each group.

Keywords: 2011 Thai flood, disaster information, foreigners, social media, traditional media

1. INTRODUCTION

From June to September 2011, the precipitation on the Indochina Peninsula was 1.2 to 1.8 times higher than average, with observed increases in Thailand of 134% in Chiang Mai and 140% in Bangkok. In addition, heavy rainfall continued over the Chao Phraya River basin into October. This heavy rain caused landslides and flash floods in the northern part of Thailand in August before starting to move slowly southwards (Figure 1, left). By mid- to late September, the inundation area had grown as dikes were destroyed in Nakhon Sawan and Chinart Provinces, and in early October floodwaters submerged several industrial complexes in

Ayutthaya Province. At the end of October, two flows of floodwater reached Bangkok, caused by overflow in the upstream Chao Phraya River which overtopped the King's Dike and by direct overflow from the Chao Phraya River where it runs along the Bangkok metropolitan area (Figure 1, right). Following the flooding of Don Muang Airport, 15 kilometers north of the city center, a temporary embankment was constructed north of the city and proper drainage of floodwaters into the Chao Phraya River began as the water level went down. Southward expansion of the floodwaters was finally halted at Bang Sue canal, about five kilometers north of the city center, in mid-November, and flooding of the city was prevented.

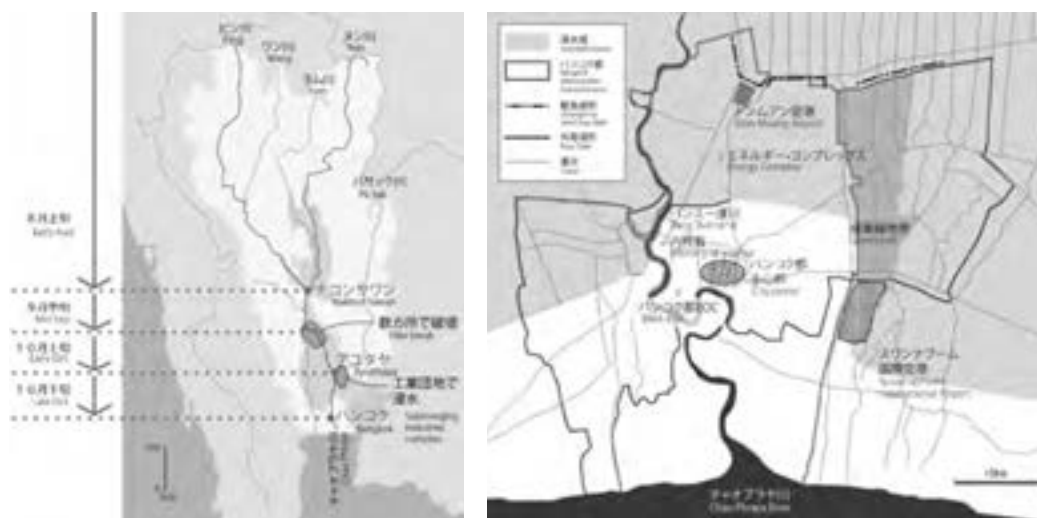


Figure 1: Flooding progress and estimated inundation areas in the Chao Phraya river basin (left) and Bangkok metropolitan area (right)

Unlike an earthquake or tsunami, the Thai flood lasted for several months, slowly progressing southwards from the northern part of the country. People were thus highly reliant upon disaster information in order to keep abreast of the flood's progress and to make decisions such as preparations for their home, the purchasing of supplies, whether to evacuate or not, and so forth. However, similar to the case of the 2011 earthquake, tsunami, and nuclear crisis in Japan (Kawasaki et al., 2011; Henry et al., 2011), people encountered many difficulties in obtaining the information they required. In the case of the 2011 Thai flood, some difficulties may have arisen from the inability to forecast how the flood would progress, leading to conflicting reports or false rumors about the predicted flooding level or path. Foreigners faced problems with obtaining information in a language which they understood. Other issues included congestion of information networks such as government hotlines or a lack of awareness of support systems.

With the increasing potential for devastating rainfall and flooding caused by changes to the global climate, it is important to prepare social response systems to mitigate the effects of future disasters. In order to improve disaster information dissemination after possible future floods in Thailand, a survey investigation on disaster information collection was carried out after the 2011 Thai flood. This investigation had three objectives: first, to clarify the disaster information

collection behavior and information-related difficulties of people living in Thailand at the time of the flood; second, to develop proposals for improving disaster information dissemination after future disasters; and third, to examine the differences in information collection behavior and difficulties between different disaster events and countries by comparing the results of the investigation in Thailand with a previous investigation conducted after the 2011 Tohoku Earthquake in Japan. This paper takes the first step towards these objectives by summarizing and discussing disaster information collection behavior considering the differences between Thai nationals and foreigners.

2. SURVEY METHODOLOGY

Data on disaster information collection behavior and information-related difficulties were collected using a survey. This survey was provided in three languages (Thai, Japanese, and English), and the contents were designed to clarify respondents' situation of flooding and evacuation, information collection activities, information difficulties, and demographics (Table 1). The survey was distributed via two methods: first, requests for participation in an online version of the survey were distributed through social and professional contacts and through direct contact with entities such as embassies; and second, a paper-based version of the survey was used to collect responses directly from people in the field. The online survey ran from March 12 to July 23, 2012, and the field survey ran from April 2 to 17 and from May 9 to 20, 2012.

Table 1: Survey questions

Theme	Questions
Flooding & evacuation	❖ Which of the following statements best describes your experience and response during the 2011 flooding?
Information collection	<ul style="list-style-type: none"> ❖ What information sources did you trust the most / the least during the 2011 flooding?* ❖ During the 2011 flooding, which media did you use to acquire information and in what language?* ❖ What types of information were most important for your decision to evacuate or not evacuate?*
Information difficulties	<ul style="list-style-type: none"> ❖ In general, what were the reasons why the above information was unclear or difficult to understand?* ❖ Were you aware that the public Thai PBS TV channel provided a special English news program on the flood every weekday night from October to December? ❖ Were you aware of the flood evacuation center for foreigners in Bangkok's Bang Na district?
Demographics	❖ Nationality, region of residence, gender, age, occupation

* These questions allowed for multiple responses

3. SAMPLE CHARACTERISTICS

3.1 Demographics

The survey received 975 responses representing 29 countries (Table 2). People from Thailand made up 78.5% of the total number of respondents. Among foreigners, Japanese made up the largest percentage with 38.6%, with respondents from India, Nepal, Bangladesh, and Vietnam totaling 29.0% and foreigners from other countries making up the remaining 32.4%. A majority of the represented countries received fewer than 10 respondents.

Table 2: Distribution of respondents by country of origin

Category (no. countries)	Countries (no. respondents)	% of total respondents	% of foreign respondents
More than 100 (1)	Thailand (765)	78.5%	-
50 to 100 (1)	Japan (81)	8.3%	38.6%
10 to 50 (4)	India (22), Nepal (15), Bangladesh (13), Vietnam (11)	6.3%	29.0%
Less than 10 (23)	Pakistan, The Philippines (9); Myanmar (8); Indonesia (6); Malaysia (4); Cambodia, France, Sri Lanka, UK, USA (3); China, Laos, Mongolia, Nigeria (2); Afghanistan, Australia, Austria, Bhutan, Canada, Denmark, Ethiopia, Niger, Vanuatu (1)	7.0%	32.4%

When asked what region of Thailand they were residing in before the flooding, 36.2% of Thai and 38.1% of foreigners responded that they were living in Bangkok and 43.1% of Thai and 56.2% of foreigners responded that they were living in the provinces in the Greater Bangkok region (Nakhon Pathom, Nonthaburi, Pathum Thani, Samut Prakan, and Samut Sakhon). The remaining 20.7% and 5.7% of Thai and foreigners, respectively, were residing in other regions of Thailand.

Among Thai respondents, 42.0% identified themselves as male and 56.7% as female, with 1.3% preferring not to answer. In contrast, 66.7% of foreigners identified themselves as male compared to just 32.9% as female and 0.5% preferring not to answer. The age distribution was more similar between Thai and foreign respondents, as shown in Figure 2, although foreign respondents skewed relatively younger, with 69.0% of respondents between 20 and 39 (compared to 58.0% for Thai) and Thai respondents skewed relatively older, with 38.8% of respondents aged 40 or higher (compared to 28.6% for foreigners). Respondents who preferred not to answer made up 0.4% and 0.5% of Thai and foreign respondents, respectively.

The distribution of respondents by occupation is given in Figure 3. For Thai respondents, a variety of occupations were represented, with the most working for foreign companies (28.5%), followed by Thai company employees (14.8%), students (14.5%), and freelance or self-owned businesses (11.0%). Conversely, the occupation held by the largest number of foreigners was "student" at 46.7%,

with foreign company employee in a distant second at 18.1% and foreign educational institution employee at 13.3%.

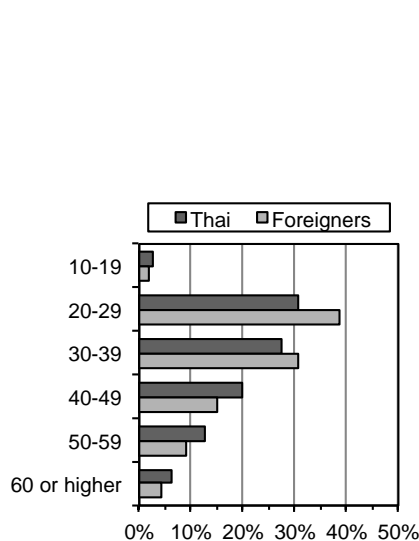


Figure 2: Distribution of respondents by age

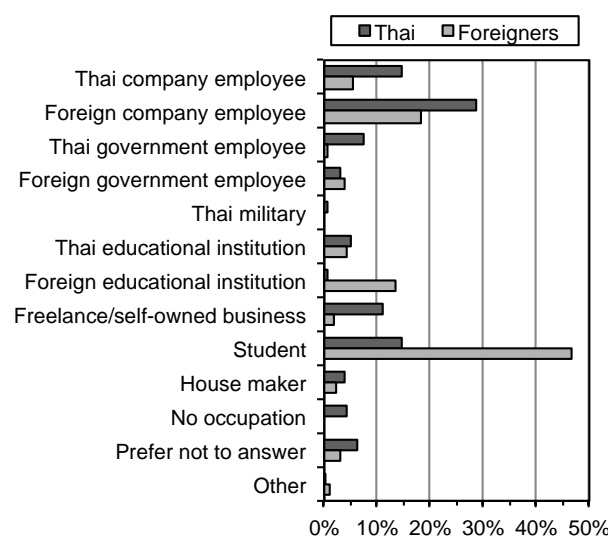


Figure 3: Distribution of respondents by occupation

3.2 Situation of flooding and evacuation

Respondents could be classified into groups depending on whether their residence was affected or not affected by flooding and whether they chose to evacuate or not evacuate. The distribution of respondents based on these four situations is summarized in Table 3. The percentage of respondents who were not affected by flooding and did not evacuate was similar between Thai and foreigners at 28.5% and 28.1%, respectively. The percentage was also similar for those who were affected by flooding and chose to evacuate, with 37.1% of Thai respondents and 40.0% of foreign respondents in that situation. However, more foreigners (28.1%) than Thai (6.9%) chose to evacuate even though their residence was not affected by flooding; conversely, more Thai (27.5%) than foreigners (3.8%) chose not to evacuate even though their residence was affected by flooding.

Table 3: Distribution of respondents considering flooding and evacuation

		Respondent action	
		Did not evacuate	Evacuated
Residence condition	Not affected by flooding	Thai: 218 (28.5%) Foreigners: 59 (28.1%)	Thai: 53 (6.9%) Foreigners: 59 (28.1%)
	Affected by flooding	Thai: 210 (27.5%) Foreigners: 8 (3.8%)	Thai: 284 (37.1%) Foreigners: 84 (40.0%)

4. SURVEY RESULTS

4.1 Disaster information sources

Figure 4 shows the most- and least-trusted sources of disaster information. For Thai respondents, the most trusted source was “Thai news sources,” with 44.7% of respondents, followed by “family, friends, colleagues, etc.,” with 37.6%. This order was reversed for foreign respondents, 43.3% of whom selected “family, friends, colleagues, etc.” as their most-trusted source, followed by “Thai news sources” at 40.0%. No other source was selected by more than 27% of respondents (either Thai or foreigner) as most-trusted, and nine of the 14 information sources received less than 20% from both Thai and foreigners. Large differences (albeit at low percentages) between Thai and foreigners could be seen for “district & sub-district government,” which was chosen as most-trusted by Thai respondents roughly five times more than by foreigners, and for “international organization,” “foreign government,” “foreign news source,” and “foreign research/academic institution,” which were chosen as most-trusted by foreign respondents between two and eight times more than by Thai. On average, Thai respondents selected 2.2 most-trusted sources, compared to 2.4 for foreigners.

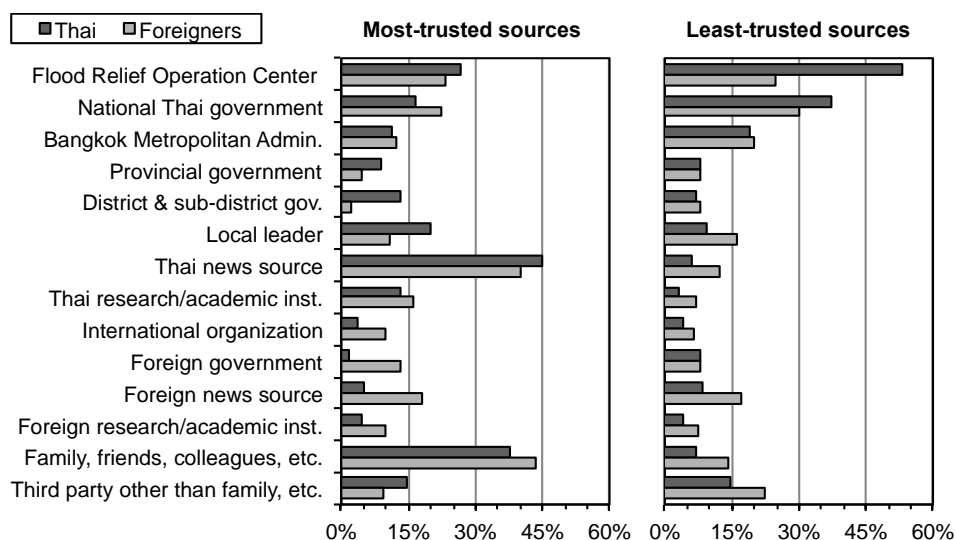


Figure 4: Most- and least-trusted disaster information sources

A much more pronounced difference between Thai and foreign respondents could be observed for least-trusted information sources. More than half (53.3%) of Thai indicated that they distrusted the “Flood Relief Operation Center,” followed by the “national Thai government,” which was selected by 37.4%. The next highest least-trusted source for Thai was the “Bangkok Metropolitan Administration” at just 19.2%; all other information sources were selected as least-trusted by fewer than 15% of Thai respondents. For foreigners, the top least-trusted information source was the “national Thai government” with 30.0% of respondents. The next three least-trusted sources, the “Flood Relief Operation Center,” “Third party other than family, friends, colleagues, etc.,” and the “Bangkok Metropolitan Administration” all fell between 25% and 20% of respondents. The largest difference between Thai and foreigners was seen for the “Flood Relief Operation Center”: even though it was the second least-trusted source for foreigners, more than twice as many Thai respondents (by percentage) indicated that they distrusted that information source. Also, while the top two least-trusted sources for foreigners were selected by between 24% and 30% of respondents, the top two

for Thai respondents were selected by between 37% and 54%. However, on average, foreign respondents indicated they had 2.0 least-trusted sources, compared to 1.9 for Thai respondents.

4.2 Media & language for disaster information acquisition

The media and language utilized for acquiring disaster information is shown in Figure 5. Thai respondents almost exclusively utilized Thai-language media, with respondents on average utilizing 3.6 different media modes in Thai compared to just 0.5 modes in English and less than 0.1 in other languages. “Television” was used by 90.3% of Thai for acquiring disaster information, followed by “inter-personal communication,” such as face-to-face and dial-in hotlines, and “traditional internet media,” such as websites and information portals, at 49.5% and 47.2%, respectively. The least-used media mode (in Thai), “direct communication tools” such as email, video chat, and instant messenger, was still used by nearly 20% of the Thai respondents.

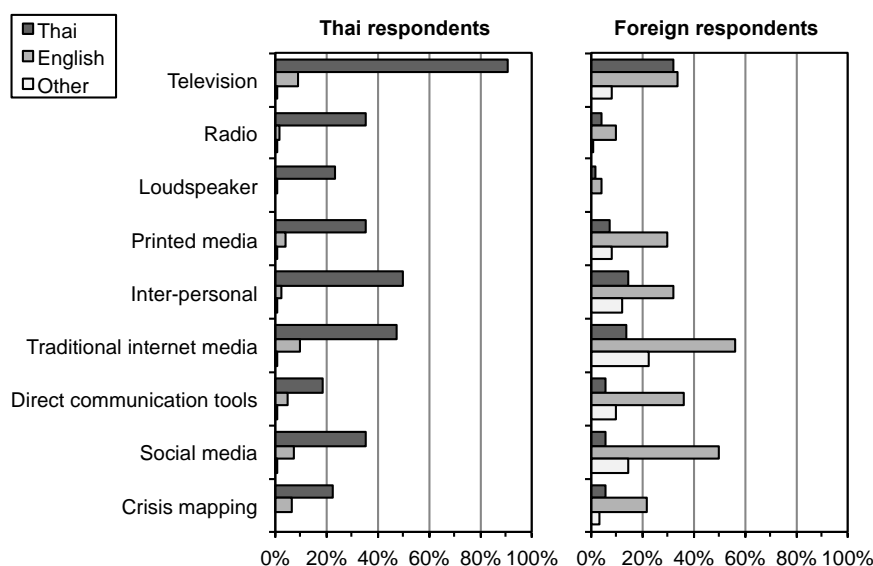


Figure 5: Utilized media and language for acquiring disaster information

Foreigners, on the other hand, utilized more languages but overall fewer media modes, averaging just 2.7 modes per respondent for English and 0.9 and 0.8 for Thai and other languages, respectively. English-language, internet-based media modes were used the most by foreign respondents, with “traditional internet media” at 56.2%, “social media” such as social networking sites and blogs at 49.5%, and “direct communication tools” at 35.7%. Roughly half of Thai respondents also utilized “traditional internet media” (albeit in Thai), but usage of other internet-based media modes in Thai among Thai respondents was less than the usage in English among foreigners. The most-utilized non-English media mode for foreigners was “television,” which only 32.4% of respondents reported they watched in the Thai language, compared to the more than 90% of Thai respondents who indicated they used Thai television. Foreigners also did not utilize audio-only media modes such as “radio” or “loudspeakers” as much as Thai respondents, 35.7% and 23.5% of whom used these two modes in Thai,

respectively, compared to just 9.5% and 4.3% in English among foreigners, respectively.

4.3 Important disaster information for decision-making

Figure 6 summarizes the importance of disaster information types for decision-making considering four different situations, which were introduced in Table 3. In this case, the decision-making is defined as whether the respondent chose to evacuate their residence or not, and this decision is examined depending on whether their residence was affected or not affected by flooding.

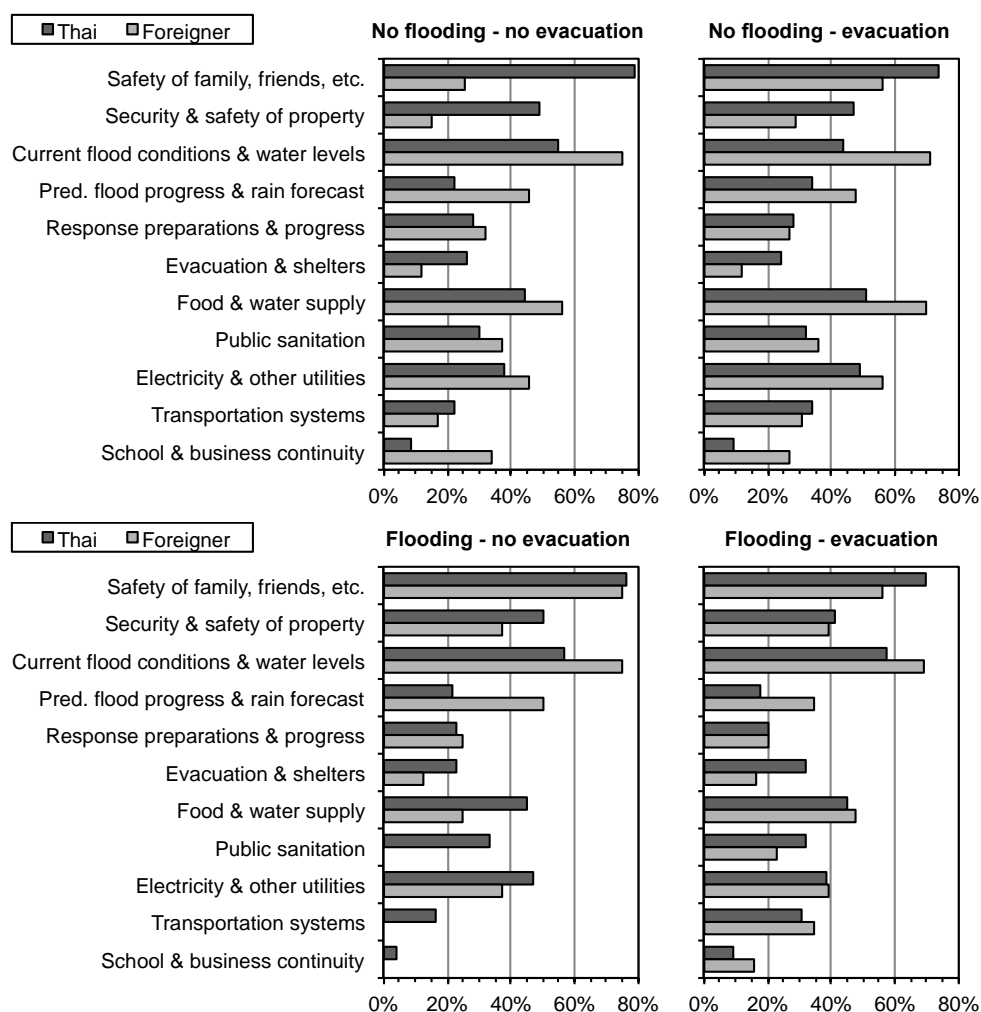


Figure 6: Importance of disaster information types for decision-making depending on flooding and evacuation situation

For Thai respondents whose residences were not affected by flooding, 78.9% indicated that they chose not to evacuate based on the “safety of family, friends, etc.,” followed by “current flood conditions & water levels” at 54.6% and “security & safety of property” at 49.1%. However, for foreign respondents whose residences were not affected by flooding, the top reason for choosing not to evacuate was “current flood conditions & water levels” at 74.6%, followed by

“food & water supply” at 55.9% and “predicted flood progress & rain forecast” and “electricity & other utilities,” both at 45.8%. In contrast to Thai respondents in this situation, few foreign respondents – only 25.4% and 15.3% – said that “safety of family, friends, etc.” and “security & safety of property,” respectively, were important for their decision not to evacuate, but more foreigners (45.8%) selected “predicted flood progress & rain forecast” as important than Thai (22.0%). On average, however, both Thai and foreigners cited the same number (4.0) of information types as important for their decision not to evacuate.

When looking at the situation where respondents chose to evacuate even though their residence was not affected by flooding, 73.6% of Thai said that “safety of family, friends, etc.” was important for their decision to evacuate. For foreigners, the most-cited important information for deciding to evacuate was “current flood conditions & water levels” at 71.2% of respondents. The second and third most-cited important information was, however, the same for both groups: “food & water supply” at 50.9% and 69.5% and “electricity & other utilities” at 49.1% and 55.9% for Thai and foreigners, respectively. Similar to the case in which their residence was not affected by the flooding and they chose not to evacuate, fewer foreigners selected “safety of family, friends, etc.” than Thai respondents, but the percentage was higher for the situation in which they evacuated (55.9%) than in the situation in which they did not evacuate. Again, the average number of selected important information types per respondent was similar for Thai (4.3) and foreigners (4.6).

In the situation where residences were affected by flooding and the respondents chose not to evacuate, it should be noted that the number of foreign respondents was only eight, compared to 210 Thai respondents in the same situation. Therefore, due to the small sample size for foreigners, it’s difficult to compare their important information with Thai respondents. For Thai respondents, however, 76.2% cited “safety of family, friends, etc.” as important for their decision not to evacuate, followed by “current flood conditions & water levels” at 56.7% and “security & safety of property” at 50.5%. On average, Thai respondents in this situation selected 4.0 important information types.

Finally, for Thai whose residences were affected by flooding and they chose to evacuate, “safety of family, friends, etc.” was cited the most by respondents, at 69.4%, as important for their decision to evacuate. For foreigners, however, “current flood conditions & water levels” was the most-cited important information at 69.0%. Conversely, the second most-cited reason for foreigners was “safety of family, friends, etc.” whereas for Thai respondents it was “current flood conditions & water levels.” Similar percentages of both Thai and foreign respondents selected “food & water supply,” “security & safety of property,” and “electricity & other utilities” as important for their decision to evacuate, and the average number of important information types (3.9 and 4.0, respectively) was also similar for Thai and foreigners in this situation.

4.4 Problems related to disaster information acquisition

The reasons why respondents encountered difficulties related to information acquisition are shown in Figure 7. For both Thai and foreign respondents, “confused by conflicting or differing information” was the most cited reason at 64.6% and 71.4%, respectively. “Misled or confused by rumors and/or exaggerated or false information” was the second most-cited reason for both groups, with 60.9% of Thai respondents and 59.5% of foreigners indicating they encountered this problem. Large differences between Thai and foreigners could be seen for “couldn’t understand information due to lack of language comprehension,” which was selected by around half of the foreign respondents but just over 10% of Thai. Conversely, 32.3% of Thai respondents reported that they were “unable to access information due to mobile congestion, power outage, etc.,” compared to just 5.2% of foreign respondents. Only 2.1% of Thai and 4.3% of foreigners indicated that they “did not have issues with unclear or difficult to understand information,” with Thai respondents citing 2.0 problems and foreigners citing 2.3 problems related to disaster information acquisition, on average.

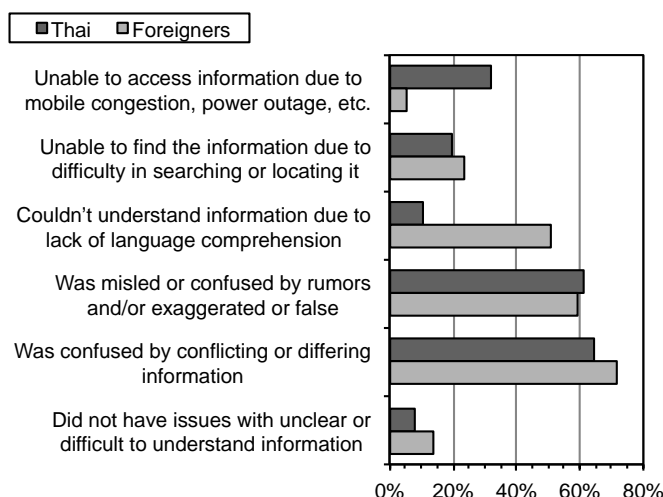


Figure 7: Reasons for problems related to disaster information acquisition

4.5 Awareness of disaster support for foreigners

The survey asked respondents whether they were aware that the public Thai PBS TV channel provided a special English news program on the flood and also if they were aware of the flood evacuation center for foreigners in Bangkok’s Bang Na district. The distribution of responses for foreigners for these questions is shown in Figure 8. In both cases there was a lack of awareness of these disaster support systems for foreigners, with 76% unaware of the English news program and 82% unaware of the foreigner-specific evacuation center.

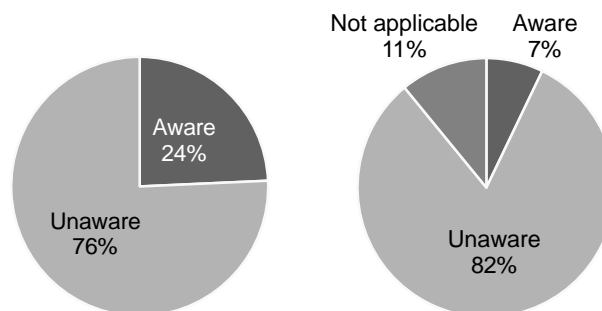


Figure 8: Awareness of foreign respondents of the Thai PBS English news program (left) and of the flood evacuation center for foreigners in (right)

5. DISCUSSION

Among the results summarized in this paper, several differences and similarities in the disaster information gathering behavior and information difficulties of Thai and foreigners could be observed.

First, there was a marked difference between Thai and foreigners regarding their flooding and evacuation situation. While similar percentages of respondents chose to not evacuate when their residence was not flooded and to evacuate when their residence was flooded, a much higher percentage of foreigners chose to evacuate even though their residence was not flooded and a much higher percentage of Thai chose to not evacuate even though their residence was flooded. In this situation, information on the current flood conditions and water levels was the most-cited important information, followed by food and water supply, safety of family, friends, etc., and electricity and other utilities, which were all cited by more than half of the foreign respondents. These results suggest that foreigners made their decision to evacuate, even though their residence was not currently being affected by the flooding, on the belief that they would be affected and that their safety and their needs for daily life would be threatened. Thai respondents whose residences were already being affected by the flooding and chose not to evacuate also cited the same reasons, including the security and safety of property, as the most important information for their decision not to evacuate even though their residence was affected. This suggests that Thai respondents may have believed that it was safer for them to remain at home or that they had sufficient supplies to continue daily life even though they were affected by the flood.

The results of this survey also confirmed that conflicting or differing reports and rumors, exaggerated, or false information were the main reasons for information difficulties among both Thai and foreigners. As Thai respondents almost exclusively utilized Thai-language media modes, and foreigners primarily used English media modes (with limited usage of Thai and other languages), these results suggest that the source of these difficulties was not caused by conflict between different language media (as in, reports in English versus reports in Thai), but rather by the information sources. Both Thai and foreigners highly trusted Thai news sources and family, friends and colleagues as information sources, but highly distrusted the Flood Relief Operation Center and the national Thai

government. Considering this stark distinction, these results may be interpreted as that people found the information given to them by their trusted sources to be most reflective of the situation they could observe for themselves, whereas the information given to them by the least-trusted sources conflicted with what they knew to be true, thus giving rise to the high citation of conflicting or differing reports and rumors, exaggerated, or false information as the main causes of information difficulties. High distrust in the national Thai government, however, may also have been caused by the policies the government implemented in order to prevent the flooding of Bangkok. These policies, which placed high priority on protecting the Bangkok city center, led to the large scale, long-term flooding of areas to the north of Bangkok. Analysis of the trust-worthiness of information sources considering the area of residence, such as Bangkok versus greater Bangkok area, may help to clarify this issue.

Lack of language comprehension also highly contributed to information difficulties for foreigners. English-language media were the main modes for foreigners when acquiring disaster information, except for Thai language television. As TV is primarily a visual medium, it's understandable that foreigners could utilize this media mode even without an understanding of the Thai language. However, the percentage of respondents using Thai television was still relatively low compared to the other media modes utilized in English such as traditional internet and social media, and much lower the percentage of Thai respondents who utilized Thai television. It was also found that foreigners were largely unaware of the English-language news program broadcast by the Thai PBS; if this awareness had been higher there may have been a higher percentage of respondents utilizing English television. This distinct lack of awareness extended to other support systems for foreigners as well, but it is unclear at this time why foreigners were unaware of these systems. Future analyses should consider how to clarify why foreigners were unable to find out about these disaster support systems and propose means for raising awareness.

In addition to the analyses proposed above, further analyses will also consider differences in disaster information collection and information difficulties considering income and education levels in order to explore differences which may arise when examining a population with a wide diversity of wealth and education.

REFERENCES

- Kawasaki, A., Henry, M., Meguro, K., 2011. Disaster information gathering behavior after the Tohoku Earthquake Part 1: Results of Japanese respondents. *2011 New Technologies for Urban Safety of Mega Cities in Asia (ICUS Report 2011-02)*, Chiang Mai, Thailand, 45-56.
- Henry, M., Kawasaki, A., Meguro, K., 2011. Disaster information gathering behavior after the Tohoku Earthquake Part 2: Results of foreign respondents. *2011 New Technologies for Urban Safety of Mega Cities in Asia (ICUS Report 2011-02)*, Chiang Mai, Thailand, 149-161.

A daily river system model for the Murray-Darling basin, Australia

Dushmanta DUTTA, Justin HUGHES, Jai VAZE, Shaun KIM, Ang YANG
and Geoff PODGER
CSIRO Land and Water, Canberra, ACT, Australia
Corresponding e-mail: Dushmanta.dutta@csiro.au

ABSTRACT

CSIRO has undertaken a research project to build a simplified daily river system model of the entire Murray Darling Basin (MDB). The basin has been divided into 17 regions for the development of the daily simplified MDB river model (SMDBRM). For each region, an individual model has been first built and then they are integrated. The key features of SMDBRM are a series of conceptual rainfall-runoff models for estimation of runoff contribution from gauged and ungauged basins, simplified node-link networks incorporating all major flow gauging stations for river flow routing, simplified approach for irrigation demand estimation, river-floodplain and river-groundwater flux exchange and a platform for integrating the 17 regional models using a CPU cluster for computational efficiency. The regional models have been calibrated for the period of 1975-1999 using an auto-calibration approach and the models are validated for the period of 2000-2009. The paper introduces the SMDBRM with a brief overview of the modelling framework and its development and presents key results from the calibration and validation of the rainfall-runoff and river routing models in different regions. The key advantages and current limitations of the model are also discussed.

Keywords: all small character (except a proper noun)

1. INTRODUCTION

The Murray-Darling Basin (MDB) is the largest Australian river basin covering an area of approximately 1 million km². The transboundary river basin, shared by four states and one territory, is Australia's most important agriculture region producing one third of Australia's food supply (CSIRO, 2008). The MDB Authority (MDBA) and various state water agencies are responsible for management of water resources within the basin. Different organisations use different river system models (such as IQQM by NSW and Queensland, REALM by Victoria, MSM-BigMod by MDBA and South Australia) that are appropriate for their modelling needs. Due to differences in modelling approaches and simulation time steps, it is cumbersome to combine these individual models to run together at a daily time step (Yang et al. 2012a). Predicted climate change impacts (CSIRO 2008) and sustainable diversion limits analysis (MDBA 2009) across MDB have highlighted the need for a whole of basin model that incorporates various physical and management characteristics for planning and operational

purposes. Addressing the need for a more streamlined model for various applications, this project has aimed to develop a simplified daily river system model with an auto-calibration procedure for the entire MDB, which has focused around using a daily time step and implemented it using the eWater Source integrated modelling software (Welsh et al. 2012). The auto-calibration procedures allows calibration of the model in a consistent, transparent and defensible manner applying best practice modelling principles (Black et al. 2011). The paper introduces SMDBRM, its development, testing and implementation with key results of calibration and validation for different modelling regions. The advantages and current limitations of the model are also discussed.

2. MODELLING REGIONS

The entire MDB was divided into 18 contiguous regions in the Murray-Darling Basin Sustainable Yields (MDBSY) Project (CSIRO 2008). These regions, namely Paroo, Warrego, Condamine-Balonne, Moonie, Border Rivers, Gwydir, Namoi, Macquarie-Castlereagh, Barwon-Darling, Lachlan, Murrumbidgee, Murray, Ovens, Goulburn-Broken, Campaspe, Loddon-Avoca, Wimmera and Eastern Mount Lofty Ranges, are primarily the drainage basins of the Murray and the Darling rivers and their tributaries (Figure 1). SMDBRM includes all regions except the Eastern Mount Lofty Ranges (EMLR) region in the far south west of the MDB, which represents less than 1% of the total area of the Basin and does not contribute significant water to the Murray River. An individual model was first built for each region and then all 17 regional models were integrated.



Figure 1: Maps of different regions of the Murray-Darling Basin (CSIRO 2008)

3. MODEL DEVELOPMENT

The SMDBRM has been developed using the node-link modelling concept employed in Source. In this modelling approach, a river system is schematised into a simplified river network using a node-link structure. The river network begins and ends with a node, and all nodes are interconnected by links. Runoff from gauged or ungauged tributaries or local contributing areas between two nodes is fed into the network as an inflow at the relevant location in the network.

Links represent a length of stream, which can be zero for near coincident processes, and are used for transfer of flow between two nodes with or without routing and transformation. Nodes represent a physical location along a river where flow either enters the system or is stored, extracted, lost or measured and can be used for the application of management rules. A set of nodes has been designed to represent functions of various physical and regulatory flow control processes in a river network. The details of links and nodes and their functionalities are elaborated in Welsh et al. (2012). The key components of SMDBRM are: i) Node-link networks, ii) Rainfall-runoff modelling, iii) Stream flow routing, iv) Irrigation demand modelling, v) Floodplain inundation modelling, vi) River-Groundwater flux modelling, vii) Auto-calibration procedure, viii) Reservoir operations and management rules and ix) Integration platform.

3.1 Node-link networks

The node-link network for each modelling region was set up based on the available storages, flow gauging stations and well-defined hydrologic sub-catchments in the MDBSY project (CSIRO 2008). It was aimed to incorporate all major stream networks, storages, major irrigation, environmental and urban demand and key resource indicator sites in Murray-Darling Basin. The hydrologic sub-catchments, geographic locations of gauging locations and high resolution remote sensing and aerial imagery (Google Earth Pro) were used to define the nodes for calibration and validation, links for modelling river reaches and contributing ungauged and gauged tributaries connecting to each modelling reach including confluences and distributaries. At present, SMDBRM includes a total of 477 nodes for calibration and validation (Table 1).

Table 1: Summary of node-links for 17 modelling regions in the current version of SMDBRM

Modelling region	No. of nodes	No. of reaches	No. of major storages	No. of confluences	No. of distributaries
Paroo	3	3	0	0	0
Warrego	8	8	0	0	2
Condamine-Balonne	28	31	2	3	3
Moonie	2	2	0	0	0
Border	24	26	3	5	3
Gwydir	19	22	1	3	6
Namoi	21	24	4	5	2
Macquarie-Castlereagh	50	52	3	8	8
Barwon-Darling	22	24	0	11	3
Lachlan	48	50	2	10	11
Murrumbidgee	57	58	4	5	6
Ovens	9	10	2	4	0
Goulburn-Broken	20	21	3	15	4
Campaspe	8	9	3	1	3
Loddon-Avoca	35	36	3	13	3
Wimmera	18	19	2	3	2
Murray	105	106	14	20	19
Total	477	501	46	106	75

3.2 Rainfall-runoff modelling

Rainfall-runoff (RR) modelling was undertaken to fill gaps and extend observed daily time series of gauged tributary inflow and to estimate the contribution of ungauged catchments in modelling reaches using a suite of six conceptual daily

RR models. The models are AWBM (Boughton, 2004), IHACRES (Croke et al., 2006), Sacramento (Burnash et al., 1973), SIMHYD (Chiew et al., 2002), SMARG (Vaze et al., 2004) and GR4J (Perrin et al., 2003), all of which have been applied in numerous studies both within Australia and internationally. In the RR model calibration, model parameters were optimised to maximise an objective function that incorporates the Nash-Sutcliffe efficiency (NSE) of daily runoff together with a constraint to ensure that the total modelled runoff over the calibration period is within 5% of the total recorded runoff (Viney et al., 2009). The model parameters are optimised using a global optimisation method (Shuffled Complex Evolution, Duan et al., 1993) followed by a local optimisation method (Rosenbrock, 1960). The best performed RR model is then incorporated in the final river system model.

3.3 Stream flow routing approach

Lag and linear Muskingum routing approaches are used in river flow routing to model travel time and attenuation. In the flow routing algorithm, river water (in-bank flow) fills the dead storage in a reach prior to propagating through the reach (Welsh et al., 2012).

3.4 Irrigation demand modelling

Two approaches have been used for estimation of irrigation water demands: i) linear regression model and ii) crop-water demand model. In the first approach, a set of linear regression models are established between the observed diversion and estimated crop-water demand based on rainfall, actual evapotranspiration estimated from MODIS and LANDSAT TM imagery (McVicar et al. 2011) and actual irrigation area for different reaches (BRS 2006) with diversions for a selected number of years with observed data. The established linear regression models are used to estimate irrigation diversions for the period of calibration and validation (Paydar & Pena Arancibia, 2012). This approach is currently implemented in monthly scale due to the limitation of the temporal resolution of the actual evapotranspiration derived from satellite imagery. In the second approach, irrigation demand is estimated using a daily crop-water demand model designed based on the concept of FAO-56 using reference evapotranspiration and crop coefficients (Allen et al. 1998).

3.5 Floodplain inundation modelling

For estimation of overbank flow from river to floodplain, an airborne scanning laser altimetry (LiDAR) digital elevation model (DEM) based rapid inundation model (LiDAR-RIM) is developed, which allows quick assessment of flood inundation area, volume, depth and duration for different flood events. Simulated results for different flood events are used to establish river stage-flooded area-flood volume (Hriv-Afp-Vfp) relationships for different modelling reaches. Zhang et al. (2012) have presented the methodology and its performance in the Murrumbidgee floodplain.

3.6 River – Groundwater interaction

A two-parameter monotonically increasing loss model is used to estimate flux loss from river to groundwater in losing streams. The approach uses a function, Monod equation, based on flow using the quantile-based approach. This is used to

reproduce the essential shape and features of the river to groundwater loss function, that is, a monotonically increasing function against flow based on the upper and lower bounds of annual observed/estimated flux. The approach is explained in Kim et al. (2012).

3.7 Auto-calibration procedure for river systems

An auto-calibration algorithm has been designed for calibration of SMDBRM. The calibration procedure is a stage wise approach that automatically calibrates routing and RR model parameters for river reaches (Fig. 2). The method is elaborated in Hughes et al. (2012). The main steps of the method are summarised below:

1. For a reach with ungauged headwater catchment, six RR models are used to estimate the ungauged inflow from upstream (Q_u/s). For any other reach in the middle of the network, simulated flow from the upper reach is used;
2. Q_u/s is adjusted for channel precipitation (P) and evaporation (E), which are estimated using climate data, channel cross-section, reach length and stream rating curves;
3. The estimated diversion (Q_{dv}) by irrigation demand model is abstracted from the adjusted upstream flow (step 2).
4. The resulting flow and gap-filled gauged tributary inflow (Q_{trib}) are routed to the downstream gauge using lag and Muskingum routing with parameters calibrated using a Monte Carlo simulation and three objective functions (NSE, %bias and modified Index of Agreement). Observed data at downstream of the reach (Q_d/s) is used for calibration of the lag and routing parameters;
5. Routed flow is adjusted for flux to groundwater (Q_{gw}), estimated by the groundwater loss model, and overbank flow to the floodplain (Q_{fp}), estimated using the established $H_{riv}-A_{fp}-V_{fp}$ relationships;
6. Each of six RR models is fitted to the residual of the routed flow and the observed Q_d/s using the area of contributing terrain and climate data to estimate ungauged local runoff (Q_{ug});
7. A loss/gain accounting function is derived to minimise bias by removing remaining unaccounted losses and gains.
8. Reservoir operations and management rules are incorporated to the calibrated regional models. The models are then recalibrated.

The auto-calibration approach can handle confluences and distributaries and it can be run together for an entire river network (Hughes et al. 2012). The model for each region is calibrated in three stages starting with the rainfall-runoff and river routing, then, the other components (simplified irrigation demands, SW-GW interactions, floodplain interactions and management rules) are added. This approach was adopted primarily for two reasons: to overcome the limitation of data for different components and to evaluate the performance of each modelling component. The three stages of calibration were:

- 1) calibration of streamflow routing & RR modelling of runoff from ungauged areas and assess unaccounted differences (steps: 1, 2, 4, 6 & 7).
- 2) stage 1 + crop water demand model + floodplain model + River-Groundwater model (steps: 1 to 7).
- 3) stage 2 + reservoir operations and management rules (all steps).

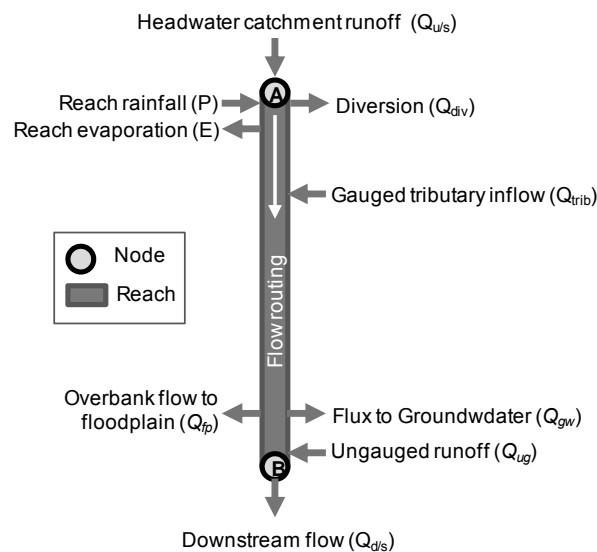


Figure 2: Conceptualisation of a river reach in SMDBRM for calibration using auto-calibration

3.8 Reservoir operations and management rules

SMDBRM includes all the major storages located in different regions (refer to Table 1). For calibration in stages 1 & 2, the simulated reservoir release is overridden by the observed reservoir release. In stage 3, the reservoir release is simulated based on the estimated irrigation demand and by introducing the reservoir operations and management rules. Many of the complex management rules are simplified before incorporating in SMDBRM and urban and environmental demands are included as pre-determined time series or patterns.

3.9 Integration platform for regional models

An integration platform was developed to integrate the individual river system models of the 17 regions using the command prompt version of Source. The platform parallelises the individual model runs to optimise the computational time. It includes a graphical user interface (GUI) and allows the integrated model to run in a CPU cluster. The key features of the integration platform are: parallel computing mechanism and daily feedback integration. Yang et al. (2012b) have elaborated the the integration platform and its performance.

The observed daily flow data, river cross-sections and rating curves at different gauging stations and reservoir storage levels for different regions were obtained from the databases maintained by the following agencies.

- Water Monitoring Data Portal, Department of Environment and Resource Management (DERM), Queensland (<http://watermonitoring.derm.qld.gov.au>)
- NSW Water Information (<http://www.waterinfo.nsw.gov.au>) and historic data dvd “PINEENA V9.3”
- Victorian Water Resources Data Warehouse (<http://www.vicwaterdata.net/>)
- Live river data, Murray-Darling Basin Authority (<http://www.mdba.gov.au/water/live-river-data>)

Diversions, water allocation, reservoir characteristics data for NSW, Queensland and Victoria were obtained from the State Water Corporation, the DERM and the DSE, respectively. SILO gridded climate data (Jefferey 2001) was used for fitting rainfall-runoff models. Data was available at 0.05° intervals, and was aggregated by contributing area to each stream gauge. In this way an area weighted climate file for each stream gauge was produced. These data were also used to gap-fill and extend the period of incomplete flow data at the headwater catchments and gauged tributaries. For consistency in calibration of the 17 regional models representing climatic and hydrological variability with both low and high flows, all the regional models were calibrated for the period of 1975-1999 (25 years). The calibrated models were validated with the daily observed flow for the more recent dry period of 2000-2009.

4. RESULTS

Figure 3 presents the summary statistics (of NSE and absolute bias in %) of stage 1 calibration and validation for all the regions except Murray. During the calibration, the model has performed reasonably well in all regions in the northern part of MDB (Paroo, Warrego, Condamine-Balonne, Moonie, Border, Gwydir, Namoi, Macquarie-Castlereagh and Barwon-Darling) with median NSE above 0.7 for all except for Gwydir (0.66). The median bias is less than 10% for all northern regions except for Moonie (12%). The performance of the model is less consistent in the southern regions. The model has performed worst in the Campaspe region with median NSE of less than 0.5 and median bias of above 40%. The median bias is less than 10% for the rests of the southern regions and median NSE is 0.7 for all regions except for Loddon-Avooca (0.66). Overall, the NSE values show highest variation in Gwydir, and Macquarie-Castlereagh regions of Northern MDB and Murrumbidgee, Campaspe and Loddon-Avooca of the Southern MDB.

The validation statistics are less satisfactory for several regions of both northern and southern MDB. In the northern regions, Paroo, Gwydir and Macquarie-Castlereagh regions have median NSE of less than 0.7 with median NSE of Macquarie-Castlereagh significantly lower than the other two. Median bias was less than 20% for all northern regions with Moonie and Macquarie-Castlereagh having median bias close to 20%, and the rests had median bias slightly above or below 10%. In the southern regions, median NSE was above 0.7 for Ovens region only. The model did not perform satisfactorily in the other regions having very low median NSE for Campaspe, Loddon-Avooca and Wimmera regions. The median bias was also very high for Wimmera region. For the rest, median bias was close or below 20% with less than 10% for Ovens.

It is worth highlighting the performance of the model in Barwon-Darling region, which is located downstream of 8 northern regions out of which seven regions contribute flow to this region. Simulated flows from the seven upstream regions were used as upstream boundary conditions at 13 inflow nodes in Barwon-Darling model. The statistics in Figure 3 show that the model has performed consistently well in Barwon-Darling region in both calibration and validation. This has clearly demonstrated that the loss/gain accounting functions (step 7 of auto-calibration)

minimise the propagation of error from upstream to downstream regions significantly.

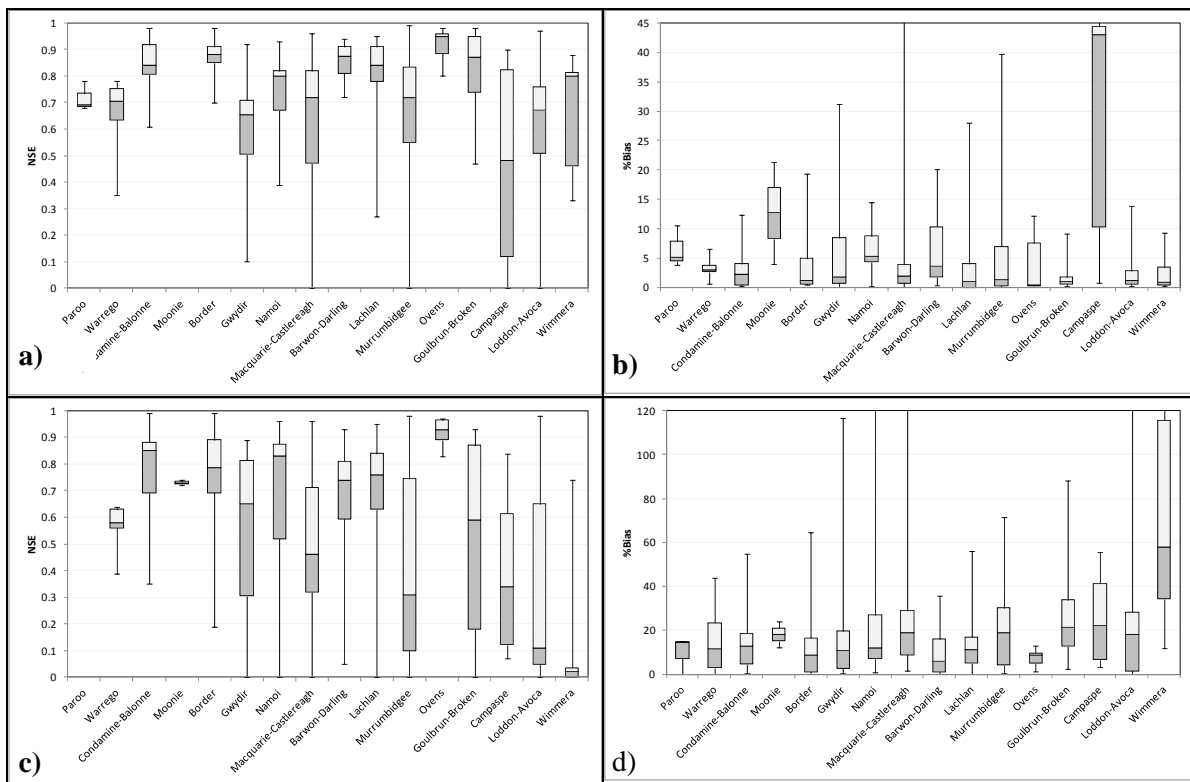


Figure 3: Boxplots showing the summary statistics of stage 1 calibration and validation of all nodes for different modelling regions: a) cal. NSE, b) cal. %bias, (c) val. NSE, d) val. %bias

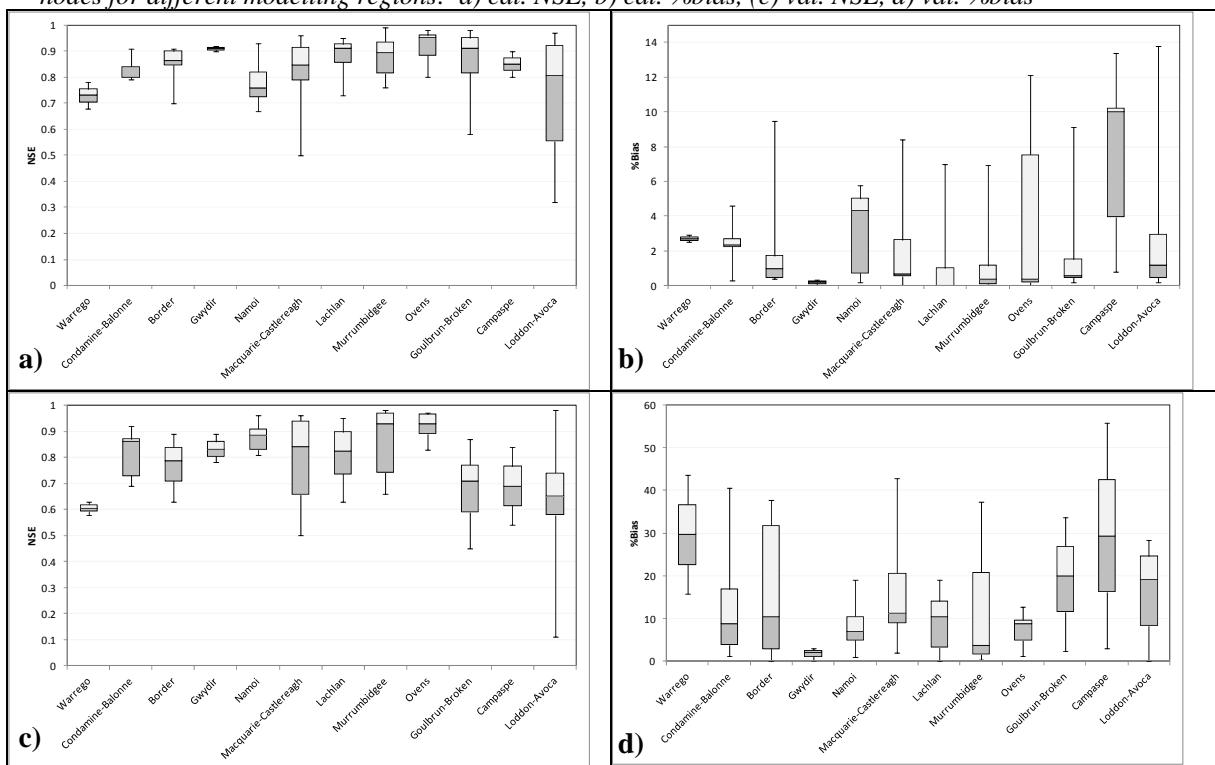


Figure 4: Boxplots showing the summary statistics of stage 1 calibration and validation of upper reaches of different modelling regions: a) cal. NSE, b) cal. %bias, (c) val. NSE, d) val. %bias

The variation in the performance of the model in different regions is influenced by several factors including irrigation diversion, overbank flow to floodplains, losses to groundwater and regulatory structures controlling flow based on water sharing and management rules. These components were not included in the stage 1 calibration and validation of the model. Figure 4 shows the summary of statistics (of NSE and absolute bias in %) for the upper reaches of the river systems above the floodplains with limited diversion in different regions (Paroo, Moonie, Barwon-Darling and Wimmera are omitted). The results for these reaches are significantly better for all regions for both calibration and validation periods. Median NSE was above 0.7 and bias was less than 10% for all regions during the calibration. During the validation period, the median NSE was above 0.6 for all regions and bias was less than 20% for all regions except for Warrego and Campaspe, which have median bias close to 30%. This results show that the diversion, groundwater losses and floodplain models need to be incorporated in the model calibration for the remaining reaches to improve the performance of the model. This is also apparent from the summary statistics of calibration and validation for the Ovens region (Table 2) with no diversion or, significant losses to floodplain in the modelling reaches in this region, the model has performed extremely well with NSE values above 0.8 for all gauges and bias was below 10% for most of the gauges. The unaccounted differences were less than 10% for all reaches except for the final reach. The low unaccounted differences demonstrate that the RR model was able to estimate the ungauged contributions satisfactorily for different reaches.

5. DISCUSSION

The results show that the model has performed well in stage1 auto-calibration in the upstream reaches of different regions (except in Murray, which is currently being calibrated) with limited diversion and overbank flow to floodplains. Hughes et al. 2012 have demonstrated that the auto-calibration approach can successfully calibrate model reaches with confluences and distributaries. In the case of distributaries, a split function is generated in the auto-calibration to estimate the flow in the distributaries as a proportion of total flow. The key advantages of the auto-calibration approach is that it is systematic, it explicitly accounts for different processes and allows consistency in calibrations of reaches in different regions across the whole MDB. That was not possible until now due to the differences in the existing models built for different regions of MDB.

The calibration approach needs to incorporate irrigation demand model and Hriv-Afp-Vfp relationships for obtaining better and satisfactory performance of the model in the lower reaches of different regions with high irrigation and losses to floodplains. Paydar & Pena Arancibia (2012) have demonstrated that the diversion can be well accounted for by the linear regression models established for different reaches in the irrigation districts of southern regions at a monthly scale. However, the approach does not work well in northern irrigation districts with large on-farm storages. It is expected that the daily crop model currently being built using FAO-56 concept will provide improved estimates of irrigation diversions in both northern and southern irrigation districts at a daily scale. Zhang

et al. 2012 have demonstrated that the LiDAR-RIM model can be effectively utilized for establishing H_{riv} - A_{fp} - V_{fp} relationships for different modelling reaches in floodplains using LiDAR DEM. The methodology is currently being revised to incorporate floodplain reaches without LiDAR DEM. It is expected that with incorporation of daily crop model and H_{riv} - A_{fp} - V_{fp} relationships for reaches in floodplains in the auto-calibration approach, the performance of the model will improve significantly in middle and lower reaches of different regions.

Yang et al. 2012b have shown that the run time of the integrated SMDBRM can be significantly improved using the CPU cluster in the integration platform. In addition, this approach of building SMDBRM with individual regional models first and then, their integration using the integration platform has other benefits such as:

- increase efficiency in development and implementation of the model at the regional scale;
- implementation of the auto-calibration procedure at the regional scale to overcome the complexity of optimisation of the whole system together; and
- the regional model can be implemented with different resource assessment and ordering systems for water allocations in different regions.

Although the auto-calibration of individual reaches are performed using R script, the node-link setup for different regions of SMDBRM are built in Source environment and stage 1 calibrated parameters and loss/gain accounting functions are transferred from R to Source. The simplified daily crop model and H_{riv} - A_{fp} - V_{fp} relationships can be easily incorporated in Source using its expression editor functionality. Presently no reservoir operations and management rules are included in the model. These can be done after completing stage 2 calibration of the model. Source includes functionalities for implementing complex reservoir operations and management rules in different regions of MDB, which have been rigorously tested in various trial applications (e.g., Dutta et al. 2012).

7. CONCLUSIONS

The paper has introduced the daily simplified river system model developed for the entire MDB. The results of stage 1 calibration have demonstrated that the model has performed well in upper reaches of regions where there are limited diversion and floodplain interactions. It is expected that the performance of the model will improve in lower reaches with diversion and floodplain losses after incorporation of daily irrigation demand model and H_{riv} - A_{fp} - V_{fp} in the stage 2 calibration of the model. The auto-calibration approach included in the model allows systematic calibration in a consistent manner across the basin. The model allows explicit accounting of different processes in each modelling reach and thus, making the outputs transparent. The integration platform of the model allows to optimise the run time of the model making it suitable for basin-wide applications for various planning and management purposes.

REFERENCES

- Allen RG, Pereira LS, Raes D, Smith M (1998). Crop Evapotranspiration—Guidelines for Computing Crop Water Requirements, Irrigation and Drain, Paper No. 56. FAO, Rome, Italy, p. 300.
- Black D, Wallbrink P, Jordan P, Waters D, Carroll C, Blackmore J (2011). Guidelines for water management modelling: Towards best-practice model application, eWater CRC.
- Boughton WC (2004). *The Australian water balance model*, Environmental modelling and software, 19: 943-956.
- BRS (2006). Final report: 1992/93, 1993/94, 1996/97, 1998/99, 2000/01 and 2001/02 land use of Australia, version 3, Bureau of Rural Sciences, Canberra.
- Burnash, RJC, Ferral RL, McGuire RA (1973), *A generalised stream-flow simulation system: conceptual modelling for digital computers*. Technical report, Joint Federal & State River Forecast Center, Sacramento.
- Chiew FHS, Peel MC, Western AW (2002). *Application and testing of the simple rainfall-runoff model SIMHYD*, Water Resources Publications, Littleton, USA, pp. 335-367.
- Croke, BFW, Andrews F, Jakeman AJ, Cuddy SM, Luddy A (2006). *IHACRES Classic Plus: A redesign of the IHACRES rainfall-runoff model*. Environmental Modelling & Software 21: 426-427.
- CSIRO (2008). *Water availability in the Murray-Darling Basin. A report to the Australian Government from the CSIRO Murray-Darling Basin Sustainable Yields Project*. CSIRO, Australia.
- Duan QY, Gupta VK, Sorooshian S (1993). Shuffled complex evolution approach for effective and efficient global minimization. *Journal of Optimization Theory and Applications* 76(3):501-521.
- Dutta D, Welsh W, Cetin L (2012). Implementation of Continuous Sharing Resource Assessment System in Source: An Application in the Macintyre Brook River, HWRS2012 (submitted).
- Hughes J, Dutta D, Kim S, Vaze J, Podger G (2012). *An automated calibration procedure for a river system model*, Proceedings of the National Conference on Water and Climate: Policy Implementation Challenges, Engineers Australia, Canberra, CD-ROM version (8pages).
- Jeffrey SJ, Carter JO, Moodie KB, Beswick AR (2001), *Using spatial interpolation to construct a comprehensive archive of Australian climate*. Environmental Modelling and Software, 16:309-330.
- Kim S, Vaze J, Dutta D, Hughes J, Dawes W. (2012). Investigation of different loss and gain accounting methodologies for river system modelling, HWRS 2012 (submitted)
- McVicar TR, Van Niel TG, Li LT, Emelyanova IV, Donohue RJ, Marvanek SP, Van Dijk AIJM, Guerschman JP, Warren GA (2011). Estimating actual evapotranspiration of lateral inflow receiving areas in rural landscapes across Australia. WIRADA Science Symposium, Melbourne 2011.
- MDBA (2009). Development of Sustainable Diversion Limits for the Murray-Darling Basin, Issues Paper, November 2009, MDBA publication no. 48/09
- Paydar Z, Peña Arancibia JL (2012). Irrigation demand modelling using remote sensing data. CSIRO: Water for a Healthy Country National Research Flagship.
- Perrin C, Michael C, Andreassian V (2003). Improvement of a parsimonious model for streamflow simulations. *Journal of Hydrology*, 279:275-289.
- Rosenbrock HH (1960). An automatic method for finding the greatest or least value of a function. *Computer Journal*, 3:175-184.
- Vaze J, Barnett P, Beale GTH, Dawes W, Evans R, Tuteja NK, Murphy B, Geeves G, Miller M (2004). Modelling the effects of landuse change on water and salt delivery from a

catchment affected by dryland salinity in south-east Australia, *Hydrological Processes*, 18:1613-1637.

Viney NR, Perraud JM, Vaze J, Chiew FHS, Post DA, Yang A (2009). *The usefulness of bias constraints in model calibration for regionalisation to ungauged catchments*, in 18th World IMACS/MODSIM Congress, Cairns, Australia, 13-17 July.

Welsh W, Vaze J, Dutta D, Rassam D, Rahman J, Jolly I, Wallbrink P, Podger G, Bethune M, Hardy MJ, Teng J, Lerat J (2012). An integrated modelling framework for regulated river systems, *Environmental Modelling and Software*, doi:10.1016/j.envsoft.2012.02.022.

Yang A, Podger G, Seaton S, Power R (2012a). *A river system modelling platform for Murray-Darling Basin, Australia*. *Journal of Hydroinformatics* (in press).

Yang A, Dutta D, Vaze J, Kim S (2012b). *A River Modelling Platform for Building a Simplified Daily River System Model for the Murray-Darling Basin*, HWRS 2012 (submitted).

Zhang Y, Dutta D, Vaze J (2012). *Rapid inundation modelling using LiDAR-DEM in the Mid Murrumbidgee floodplain*, HWRS2012 (submitted).

Investigating potential climate change impacts on rainfall intensity duration frequency curves in Kathmandu, Nepal

Binaya Kumar MISHRA¹ and Srikantha HERATH²

¹Research Associate, Institute for Sustainability and Peace
United Nations University, Tokyo, Japan
mishra@unu.edu; mishra_binaya@hotmail.com

²Senior Academic Programme Officer, Institute for Sustainability and Peace
United Nations University, Tokyo, Japan

ABSTRACT

Stationary assumption of rainfall IDF curves is not valid under climate change scenario. Objective of this study is to assess the change in IDF curves for stormwater management in Kathmandu, Nepal under climate change scenario. The study area was found to have very few short duration rainfall data, and hence a simple scaling theory was applied for deriving the short duration rainfall intensities from daily rainfall data. The scaling behavior of observation rainfall intensities was examined and it was revealed that the statistical properties of observation rainfall follow the assumption of simple scaling. We employed 20-km daily global climate model (GCM) rainfall output of Meteorological Research Institute (MRI), Japan for investigating the climate change impact. Using regionalized quantile-quantile bias-corrected annual maximum rainfall data of 1979-2003 and 2075-2099 periods as present and future climate respectively, potential climate change impacts on IDF curves were assessed. A total of six different durations (1, 2, 3, 6, 12 and 24-hrs) for return periods of 2, 5, 10, 25, 50 and 100 years were analyzed for preparing the IDF curves. Comparison of IDF curves for present and future climate indicated a significant increase in maximum rainfall intensities which has major implications on planning and design of urban stormwater drainage systems.

Keywords: *Bias correction, climate change, rainfall IDF curves, simple scaling*

1. INTRODUCTION

Rainfall intensity duration frequency (IDF) curves are important in design of urban stormwater management infrastructures such as flood detention reservoirs, sewer systems etc. Rainfall IDF curves provides the estimates of rainfall intensities for different durations and return periods. Annual extreme rainfall intensities corresponding to particular durations are fitted to empirical or theoretical probability durations for preparing the rainfall IDF curves. One of the basic assumptions in preparation of rainfall IDF curves is that historic extremes will characterize the extremes of future rainfall. However, this assumption is not valid under changing climatic scenario which will bring change in the magnitude and frequency for extreme rainfall. Such changes in extreme rainfall pattern point

out for new design and regulations in urban stormwater infrastructures management. Stormwater management has been a major problem in urban areas of Nepal especially in Kathmandu valley. Twenty-five per cent of households in Kathmandu have been flooded due to inadequate drainage as storm water no longer drains away as it used to and the technical systems put in place are not sufficiently flexible to deal with a changing climate (IIED report, 2009).

Objective of this research is to assess climate change impact on rainfall IDF curves in urban Kathmandu valley, Nepal. Assessment of climate change impact on rainfall IDF curves includes the following major steps: (i) bias correction of global climate model (GCM) rainfall projections for current and future climate period; (ii) derivation of rainfall IDF relationships for short-duration rainfall from daily rainfall data; and (iii) comparative analysis for rainfall IDF curves.

Climate change projections are widely used to assess likely changes in rainfall pattern in future. Global climate models (GCM) are currently the most credible tools available for simulating the response of the global climate system to increasing greenhouse gas concentrations, and provide climatic variables such as temperature, rainfall etc. These projections are available for current and future climate. A very high resolution global climate model (GCM) rainfall projections of Meteorological Research Institute (MRI), Japan has been employed for assessing the climate change impact. MRI-GCM is a very high resolution atmospheric model with 20 km spatial and daily temporal resolution (Kusunoki et al., 2008).

Because of flaws in model structure and coarse resolution input, GCM outputs are found to be largely biased when compared with observation data (Sperna Weiland et al., 2010). Therefore, direct use of GCM outputs may not suitable for the climate change impact assessment at basin level. Downscaling enables GCM outputs to be used for local/basin scale climate change impact assessment. There are several downscaling techniques available to transform GCM outputs to local scale for reliable impact assessment (Coulibaly and Dibike, 2004; Hansen et al., 2006). Downscaling techniques are broadly classified into dynamical and statistical types. Dynamical downscaling technique converts GCM outputs into local climate data by using a regional climate model (RCM). RCM enhances the simulation of atmospheric circulations and climate variables at finer spatial scales. Statistical downscaling techniques use models of correspondence between GCM contemporary climate scenarios data and real world data. GCM projection climate scenario data is used as input to correspondence models to predict the expected future real world data. Fundamental assumption is that statistical relationship will remain valid under future climate change scenario.

The statistical downscaling is much less computationally demanding as well as simple than the dynamical downscaling. In many cases, the statistical downscaling technique can provide similar or better accuracy than that of dynamical downscaling (Murphy, 1998; Haylock et al., 2006). The most commonly used statistical techniques are regression, stochastic weather generator, weather typing, spatial disaggregation and bias correction. Among these techniques, regression, stochastic weather generator and weather typing are used for transforming coarse GCM output to observation locations. Disaggregation is employed for transforming coarse GCM output to fine resolution output. Bias correction techniques are employed for transforming GCM output to point as well as grid cell scale.

In this study, bias corrected daily GCM rainfall data for Upper Bagmati river basin (U/S of Pandhero Dovan) was used for assessing climate change impact on rainfall IDF curves in Kathmandu urban valley.

In this study, regionalized quantile-quantile bias corrected data has been used (Mishra and Herath, 2011). In this technique, a GCM grid cell is linked to neighboring observation stations data. We have proposed delineation of homogeneous rainfall regions to link neighboring observation rainfall stations to a GCM grid cell. Calibration and validation of regionalized quantile-quantile bias correction technique was performed for 1979-1993 and 1994-2003 periods respectively. Using bias-corrected data of 1979-2003 and 2075-2099 as current and future climate respectively, climate change impact assessment on rainfall IDF curves in Kathmandu valley has been made.

Establishment of IDF relationships goes back to the 1930's (Bernard, 1932). Since then, different forms of relationships have been constructed for several regions of the world. Bell (1969) and Chen (1983) derived the IDF formulae for the United States based on statistical analysis. Koutsoyiannis et al. (1998) proposed a new generalizing approach to the formulation of IDF curves using efficient parameterization. Sub-daily rainfall data of longer periods is rarely available, which will be enough to prepare rainfall IDF curves, at most of the stations in several developing countries including Nepal. Because daily rainfall data is the most accessible and abundant source of rainfall information, it is natural to develop and apply methods to derive the IDF characteristics for short duration events from the daily rainfall statistics. The IDF formulae are empirical equations representing a relationship among maximum rainfall intensity as dependent variable and rainfall duration and frequency as independent variables. All forms of the generalized rainfall IDF relationships assume that rainfall intensity is inversely related to the duration of a storm raised to a power, or scale factor. Use of scaling properties for deriving the IDF characteristics of sub-daily rainfall from daily rainfall is largely popular. Menabde (1999) applied simple scaling theory to describe rainfall IDF in Australia and South Africa. It was shown that the cumulative distribution function for the annual maximum rainfall had a simple scaling property over the range of 30 min to 24 hours and in some instances to 48 hours. Nhat et al. (2006) derived rainfall IDF relationships for short-duration rainfall from daily rainfall in Yodo river basin, Japan. Bara et al. (2009) applied the simple scaling theory to the intensity-duration-frequency (IDF) characteristics of short duration rainfall in Slovakia. The IDF relationships, which were deduced from daily rainfall, showed acceptable results in comparison with the IDF curves obtained from at-site short duration rainfall data. In this study, scaling properties of extreme rainfall are examined at Kathmandu airport in order to establish scaling behaviour of statistical moments. Such scaling approach will enable to derive rainfall IDF for shorter durations.

2. STUDY AREA

Kathmandu Valley has been considered for the study. The study area is situated in Kathmandu, Lalitpur and Bhaktapur districts of Nepal. The valley with area of roughly 500 km² lies between 27° 32' N to 27° 49' N and 85° 11' to 85° 32' E. Kathmandu valley is situated inside Bagmati river system. The valley has a

centripetal drainage system. The climate of the valley is subtropical to monsoon with hot and wet summer and cold and fairly dry winter. The maximum and minimum temperatures are 35°C and -2.5°C respectively. About 80% of the total annual rainfall occurs during the months of June to September. Winter rainfall is common but not heavy. The average annual rainfall in the basin is 1650 mm. bias corrected GCM data of Meteorological Research Institute, Japan; climate change impact assessment is intended using bias corrected MRI-GCM daily rainfall values of 1979-2003 and 2075-2009 periods as current and future climate respectively. Urban Kathmandu valley is in 4 numbers of MRI-GCM grid cells (Figure 1). The grid cells are numbered similar to Mishra and Herath (2011).

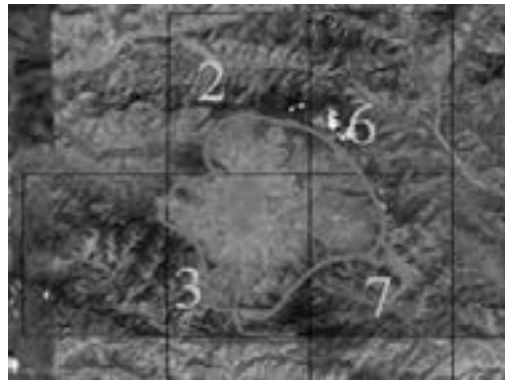


Figure 1: Location of urban Kathmandu valley inside MRI-GCM cells

3. SIMPLE SCALING OF RAINFALL INTENSITY

Scaling properties of extreme rainfall are examined to establish scaling behavior of statistical moments over different durations. Such scaling or scale-invariant models enable to scale data from one temporal resolution to another, and thus help to overcome the lack of extreme rainfall data of sub-daily durations.

Based on empirical evidence, it is assumed and verified that random variable I_d and I_D as annual maximum rainfall intensities over time duration d and D respectively can have the following scaling property (Menabde et al., 1999):

$$I_d = \left(\frac{d}{D}\right)^{-\eta} I_D \quad (1)$$

In equation 1, the equality refers to identical probability distribution for both variables and η represents the scaling exponent. The relationship between the moments of order q can be obtained by raising both sides of equation to power q and taking the expected values of both sides (equation 2).

$$E[I_d^q] = \left(\frac{d}{D}\right)^{-\eta(q)} E[I_D^q] \quad (2)$$

Estimation of scaling exponent η is illustrated in Figure 2 which includes (i) log-log graph of moments $E[I_D^q]$ versus durations of different order q ; and (ii) linear graph of slopes (of moments versus duration lines) and moment order q . If the

resulting graph is a straight line i.e., value of η (slope) remain same for different values of q , it is of simple scaling otherwise it is of multi-scaling.
 In this study, rainfall data of 25 years record length ranging from 1979-2003 at Kathmandu airport were collected for confirming the simple scaling properties. Menabde et al. (1999) found simple scaling property over the range 30 min to 48 hours. Rainfall intensities of 24-, 48- and 72-hour durations were tested to investigate the scaling properties as sub-daily rainfall was not available for longer periods. A log-log plot of the moments against their durations were examined for moment order $q=1, 2, 3, 4$ and 5. Figure 3 illustrates q^{th} moment of the rainfall intensities (mm/h) against different durations.

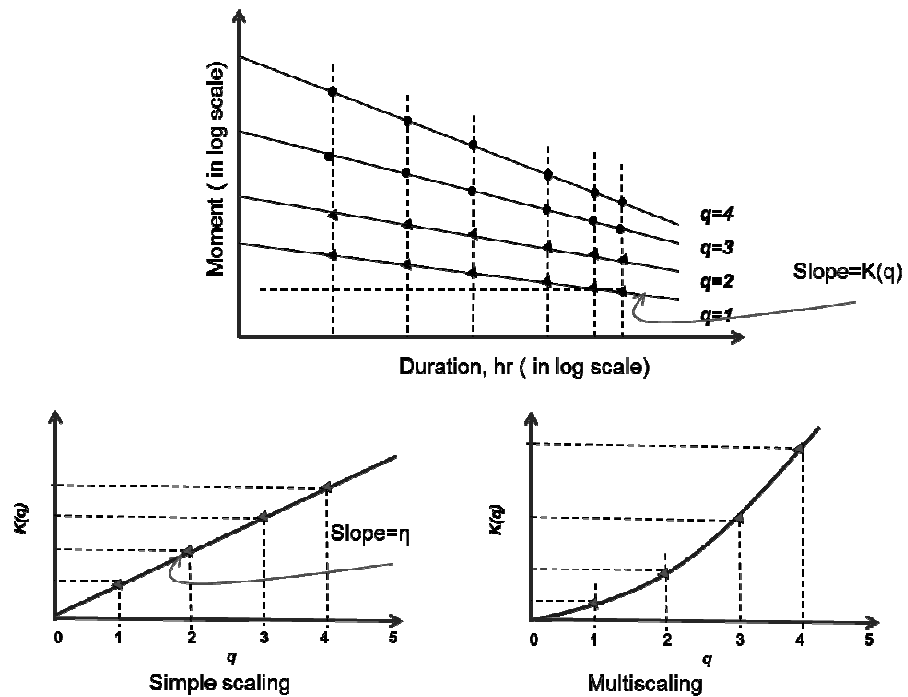


Figure 2: Illustration for simple and multi-scaling properties (Nhat et al., 2007)

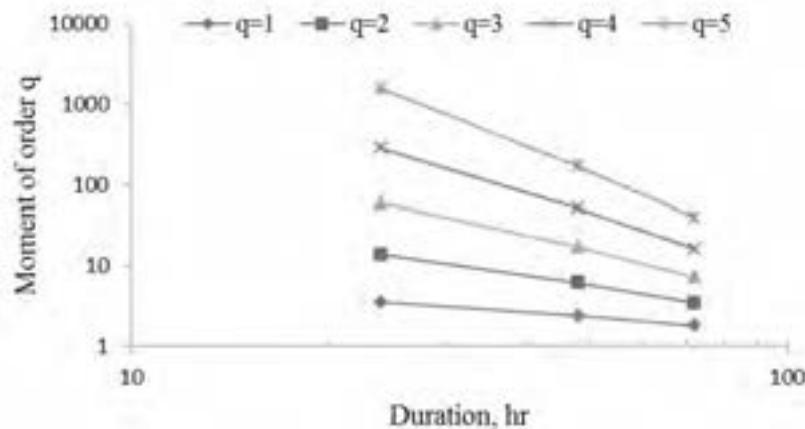


Figure 3: Scaling of the moments at Kathmandu airport

In order to determine if the data follows simple scaling or multi-scaling, slopes $K(q)$ of moment *versus* duration lines was plotted against the moment order q . Figure 4 shows linear dependence, thereby confirming about simple scaling. Hence, simple scaling can be assumed for estimation sub-daily rainfall intensity duration frequency curves in urban Kathmandu valley. Scale factor is estimated by slope of the regression line as 0.6761.

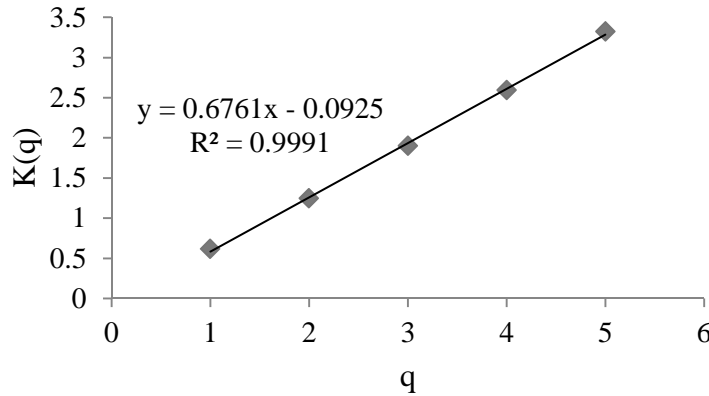


Figure 4: Simple scaling shown by linear regression at Kathmandu airport

4. DERIVATION OF SUB-DAILY RAINFALL IDF RELATIONSHIP

Menabde et al. (1999) also showed that the scaling behavior can be found for the parameters of a fitted CDF and for the quantiles estimated from the fitted CDF, corresponding to different return periods T .

General form of IDF relationship (Koutsoyiannis et al., 1998) with i as rainfall intensity, T as return period and d as duration of extreme event can be expressed in the following form (equation 3):

$$i = \frac{a(T)}{b(d)} \quad (3)$$

The function $a(T)$ can be determined from the probability distribution function of the maximum rainfall intensity, and the function $b(d)$ is sought in the form (equation 4):

$$b(d) = (d + \theta)^\eta \quad (4)$$

where θ and η are phenomenological parameters to be estimated. Considering the annual maximum rainfall intensity I_d over the time period d characterised by CDF $F_d(i)$ by equation 5:

$$F_d(i) = \Pr(I_d < i) = 1 - 1/T \quad (5)$$

Applying scaling theory in terms of CDF:

$$F_d(i) = F_D\left(\left(\frac{d}{D}\right)^{-\eta} i\right) \quad (6)$$

Assuming the CDF of extreme events in standardized functional form:

$$F_d(i) = F\left(\frac{i - \mu_d}{\sigma_d}\right) \tag{7}$$

where F is some function, independent of d . Further assumption of scaling theory will result the following formulae (equation 8 & 9):

$$\mu_d = \left(\frac{d}{D}\right)^{-\eta} \mu_D \tag{8}$$

$$\sigma_d = \left(\frac{d}{D}\right)^{-\eta} \sigma_D \tag{9}$$

Substituting equations (7), (8) and (9) in formula (5) and inverting it in respect to i , we get the following IDF general relationship (equation 10):

$$i = \frac{\mu + \sigma F^{-1}\left(1 - \frac{1}{T}\right)}{d^\eta} \tag{10}$$

where $\mu = \mu_D D^\eta$ and $\sigma = \sigma_D D^\eta$. Equation 10 shows that the scaling assumption leads to $\theta=0$ in the general form (equations 3 & 4).

6. RAINFALL EXTREME UNDER CHANGING CLIMATE

With application of the simple scale scaling model for rainfall intensities at Kathmandu airport station, the scale factor was estimated to be 0.6761. The rainfall IDF for sub-daily duration rainfall intensities can be estimated using equation (10). Daily rainfall data for 4 numbers of MRI-GCM covering urban Kathmandu valley of 25 years length ranging from 1979-2003 and 2075-2099 as current and future climate respectively yielded following mean and standard deviation values (Table 1):

Table 1: Mean and standard deviation of annual maximum rainfall intensities

MRI-GCM grid cell number	Present climate (1979-2003)		Future climate (1979-2003)	
	Mean, $\mu_{D=24h}$	S.D., $\sigma_{D=24h}$	Mean, $\mu_{D=24h}$	S.D., $\sigma_{D=24h}$
2	4.2	1.1	4.5	1.6
3	3.2	1.1	3.5	1.3
6	4.0	1.3	4.6	1.4
7	3.7	1.2	4.1	1.7

Assuming Gumbel distribution as suitable candidate in equation 10, the following simple rainfall IDF can be derived (equation 11):

$$i = \frac{\mu_D D^\eta - \sigma_D D^\eta \ln\left(-\ln\left(1 - \frac{1}{T}\right)\right)}{d^\eta} \tag{11}$$

Equation 11 enabled generation of rainfall IDF curves for present and future climate over Kathmandu value by smoothing maximum rainfall intensities over d

= 1, 2, 3, 6, 12 and 24 hours. Figure 5 & 6 show rainfall IDF curves estimated for 2-, 5-, 10-, 25-, 50- and 100-years return periods. Change in rainfall intensities for different duration and return periods are shown in Table 2. An important observation is made by visual as well as tabular inspection for all return periods, for all durations that rainfall intensities are significantly greater for future climate than present climate. Table 2 points out that there will be an average increase of 18.9% ranging from 10.9% to 22.2% in extreme rainfall intensities. These observations have major implications for the design, operation and maintenance of storm water infrastructures in urban Kathmandu valley.

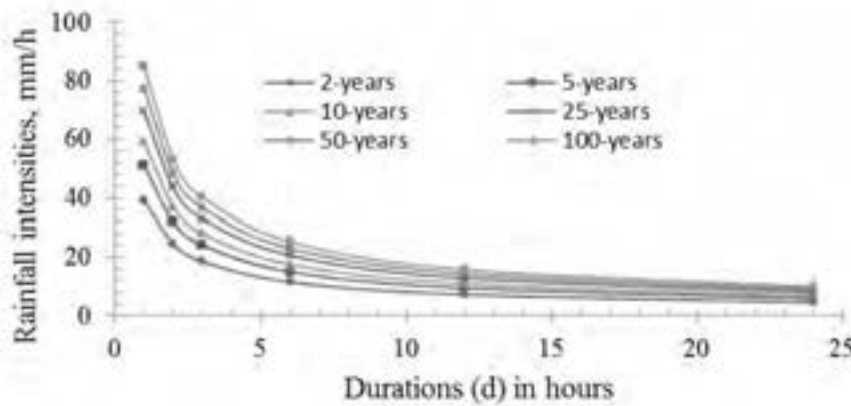


Figure 5: Rainfall IDF curves at urban Kathmandu valley for present climate

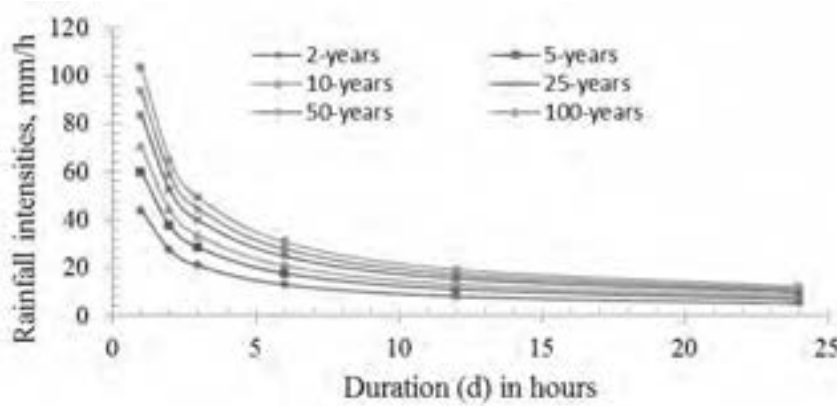


Figure 6: Rainfall IDF curves at urban Kathmandu valley for future climate

Table 2: Percentage change in rainfall intensities at urban Kathmandu valley

Durations (d) in hour	Change (%)					
	Average rainfall intensities (mm/h) for return periods					
	2	5	10	25	50	100
1	12.5	17.7	19.1	20.6	21.4	22.1
2	12.2	17.9	19.2	20.7	21.6	22.1
3	12.4	17.8	19.2	20.6	21.3	22.1
6	12.9	17.9	19.3	20.3	21.3	22.2
12	12.3	17.9	19.1	20.9	20.8	22.2
24	10.9	18.6	18.8	21	21.1	22.2

6. CONCLUSIONS

Potential impact of climate change on rainfall extremes have been studied by analysing rainfall IDF curves for present and future climate at urban Kathmandu valley, Nepal. The assessment has been made by using 20-km daily MRI-GCM rainfall projections over the Kathmandu valley. Regionalized quantile-quantile bias correction successfully reduced any significant biases in the MRI-GCM rainfall projections. The properties of the time scale invariance of selected rainfall quantiles were investigated at Kathmandu airport. It has been shown that the rainfall at Kathmandu airport follow assumption simple scaling properties. Accordingly, following the revision of Menabde et al. (1999), it was possible to derive the rainfall IDF curves for shorter durations from daily rainfall intensities. Results of this study are of significant practical importance for design, operation and maintenance of storm water management infrastructures under changing climate scenario.

REFERENCES

- Bara, M., Kohnova, S., Gaal, L., Szolgay, J. and Hlavcoval, K., 2009. Estimation of IDF curves of extreme rainfall by simple scaling in Slovakia, *Geophysics and Geodesy*, 39(3), 187-206.
- Bell, F. C., 1969. Generalized rainfall-duration-frequency relationships, *Journal of the Hydraulic Engineering*, 95(1), 311– 327.
- Chen, C.L., 1983. Rainfall Intensity-Duration-Frequency formulas, *Journal of Hydraulic Engineering*, 109(12), 1603– 1621.
- Coulibaly, P. and Dibike, Y.B., 2004. Downscaling of global climate model outputs for flood frequency analysis in the Saguenay River System, Department of Civil Engineering, McMaster University, *Hamilton*, Project no. s02-15-01.
- Hansen, J.W., Challinor, A., Ines, A., Wheeler, T. and Moron, V., 2006. Translating climate forecasts into agricultural terms: advances and challenges, *Climate Research*, 33, 27-41.
- Haylock, M.R., Cawley, G.C., Harpham, C., Wilby, R.L. and Goodess, C.M., 2006. Downscaling heavy precipitation over the United Kingdom: a comparison of dynamical and statistical methods and their future scenarios, *Int. J. Climatol.*, 26, 1397-1415.
- IIED report, 2009. Climate change and the urban poor: Risk and resilience in 15 of the world's most vulnerable cities (<http://pubs.iied.org/pdfs/G02597.pdf>).
- Kusunoki, S., Yoshimura, J., Yoshimura, H., Mizuta, R., Oouchi, K. and Noda A., 2008. Global warming projection by an atmospheric global model with 20-km grid, *Journal of Disaster Research*, 3(1), 4-14.
- Koutsoyiannis, D., Kozonis, D. and Manetas, A., 1998. A mathematical framework for studying Intensity-Duration-Frequency relationships, *Journal of Hydrology*, 206, 118– 135.
- Menabde M., Seed A. and Pegram G., 1999. A simple scaling model for extreme rainfall, *Water Resour. Res.*, 35, 1, 335– 339.
- Mishra, B.K. and Herath S., 2011. Climate Projections Downscaling and Impact Assessment on Precipitation over Upper Bagmati River basin, Nepal,

- Proceedings of 3rd International Conference on Addressing Climate Change for Sustainable Development through Up-Scaling Renewable Energy Technologies*, 275-281 (<http://cecar.unu.edu/groups/cecarweb/blog/?tag=research+article>).
- Murphy, J., 1998. An evaluation of statistical and downscaling techniques for downscaling local climate, *Journal of Climate*, 12, 2256-2284.
- Nhat L. M., Tachikawa Y., Sayama T. and Takara K., 2007. Regional rainfall intensity duration-frequency relationships for ungauged catchments based on scaling properties, *Annuals of Disas. Prev. Res. Inst.*, Kyoto Univ., 50B, 33-43.
- Sperna Weiland, F.C., van Beek, L.P.H., Kwadijk, J.C.J. and Bierkens, M.F.P., 2010. The ability of a GCM-forced hydrological model to reproduce global discharge variability, *Hydrol. Earth Syst. Sci. Discuss.*, 7, 687-724, doi:10.5194/hessd-7-687-2010.

Flood hazard simulation for lower West Rapti river basin-Nepal under climate change impact

Edangodage Duminda Pradeep PERERA¹, Akiko HIROE², Kazuhiko FUKAMI³,
Toshiya UENOYAMA⁴, Shigenobu TANAKA⁵

¹Research specialist, International Centre for Water Hazard and Risk Management under the auspices of UNESCO, PWRI, 6-1 Minamihara, Tsukuba, Ibaraki, Japan
perera55@pwri.go.jp

²Researcher, International Centre for Water Hazard and Risk Management under the auspices of UNESCO, PWRI, 6-1 Minamihara, Tsukuba, Ibaraki, Japan

³Chief Researcher, International Centre for Water Hazard and Risk Management under the auspices of UNESCO, PWRI, 6-1 Minamihara, Tsukuba, Ibaraki, Japan

⁴Senior Researcher, International Centre for Water Hazard and Risk Management under the auspices of UNESCO, PWRI, 6-1 Minamihara, Tsukuba, Ibaraki, Japan

⁵Deputy Director, International Centre for Water Hazard and Risk Management under the auspices of UNESCO, PWRI, 6-1 Minamihara, Tsukuba, Ibaraki, Japan

ABSTRACT

We focused on integrating AGCM results with a river discharge model and an inundation model to carry out a descriptive present and future flood hazard study for lower West Rapti river basin. In this study, bias corrected high resolution AGCM precipitation outputs of Meteorological Research Institute, Japan Meteorological Agency (MRI-AGCM 3.1s and 3.2s) for IPCC Special Report on Emission Scenario A1B were utilized to obtain the precipitation patterns over West Rapti river basin for Present (1980 – 2004), Near Future (2015 – 2039) and Future (2075 – 2099) time durations. PWRI-distributed hydrologic model ver.2 (PDHM) was employed to obtain the river discharges for above mentioned time durations followed by frequency analyses for 25 and 50 years return periods flood discharges. The frequencies and intensities of calculated return period flood discharges showed increments in ratios when the Future values were compared with the Present values for both MRI-AGCM 3.1s and 3.2s. Flood frequency increment ratios for AGCM 3.1s and 3.2s were 1.4 and 2.2 respectively while for the flood discharges, ratios were 1.1 and 1.9 for 50 years return periods flood discharges. Flood inundation simulations of 50 years return period events for Present and Future were carried out by rainfall, runoff and inundation model (RRI model) followed by an assessment for the flood hazards based on the simulated flood depths and distributions at several residential locations of the target area. Future flood depths in the area show a significant increment compared to the Present situation. These variations in Future climate will cause complex implications on the socio-economic conditions of the target area such as irrigation, agriculture, livestock, education, health and transportation.

Keywords: climate change, flood hazards, hydrological modeling, inundation

1. INTRODUCTION

Nepal’s vulnerability to climate-related disasters is likely to be exacerbated by the increase of intensity and frequency of water hazards induced by climate change (IPCC, 2007). Nepal has been identified as a frequent disaster spot in the developing world and consequently in the Global Natural Disaster Analysis Report (Dilley et al., 2005). Nepal was ranked at 11th place on disaster vulnerability in the world. Most known water hazards in Nepal are floods, landslides, debris flows, droughts, snow avalanches and glacier lake outbursts (GLOF). In a humid climate like that of Nepal, there will be changes in the spatial and temporal distribution of temperature and precipitation due to climate change, which in turn will increase both the intensity and frequency of extreme events like droughts and floods (Mahtab, 1992). The majority of Nepal’s present population depends on agriculture for their subsistence but still about 63% of the agricultural lands are deprived of modern irrigation facilities (FAO, 2004). The increased precipitation variability may create difficulties in cultivating these lands and could result in probable food scarcity for the population. Currently, about 31% of Nepal’s total population is below the poverty line and 95% of them live in rural areas (MOF, 2005). The poor people are more vulnerable to climatic extremes as well as gradual changes in climate than the rich because they have less protection, less reserves, fewer alternatives and a lower adaptive capacity since they are more reliant on primary productions (AfDB et al., 2003).

2. STUDY AREA

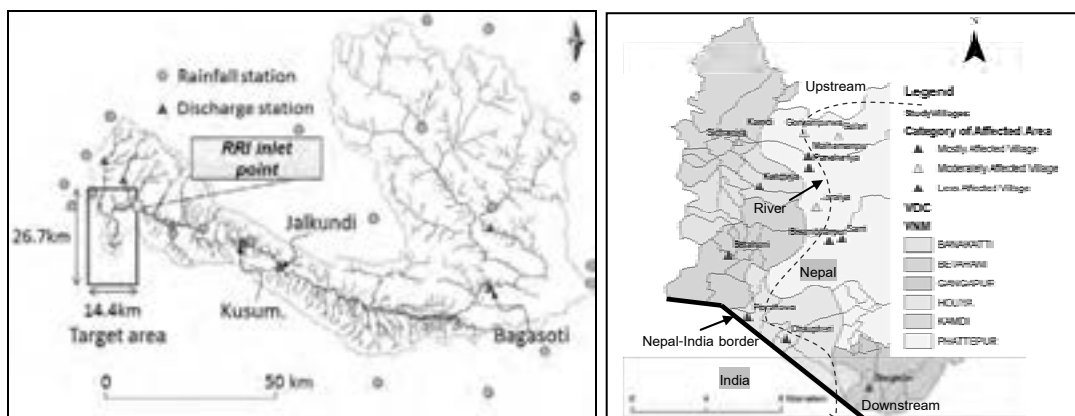


Figure 1: West Rapti river basin and target area Figure 2: VDCs of target area

The West Rapti river basin is an important river basin concerning its significance in water supply for agriculture, irrigation, and domestic uses to the West Tarai region of Nepal. It covers about 6450 km² and has the total population of approximately 1,046,000 (CBS, 2001). The West Rapti river originates from the Mahabharat range in Nepal with the average altitude of about 3000 m. According to the topographical profile, the basin can be broadly categorized as upper (hilly) and lower (Tarai – plain). Springs and monsoon precipitations are the main contributors for the water budget of the river. The annual average precipitation is about 1500 mm. Observations of daily precipitation at 21 rainfall stations which are located inside or

around the basin and daily discharges at 3 river gauging stations (Bagasothi, Julkundi, and Kusum) are available for this study (Figure 1).

The study area is located in the lower West Rapti river basin near the Nepal-India border, (Figures 1 and 2) Nepalgunj in Banke district, Nepal which faces recurrent flood disasters where significant losses of properties, lives and livelihood of the local population occur. Recent extreme flood events in lower West Rapti were reported in 1984, 1989, 1998, and 2007. Flood inundations are generally caused by both the mainstream of the river and local heavy rainfalls, contributing to high flows in the tributaries. It is reported that the inundation problem has been worsened by the construction of the Laxmanpur barrage and Kalkaluwa afflux bund in Indian territory near to the Nepal-India border, since it obstructs the natural drains and flows from West Rapti river (UNDP, 2009). In future anticipated climate change induced high precipitations will intensify the flood inundations in this area. The study area covered six Village Development Committees (VDCs) namely Kamdi, Bankatti, Phattepur, Betahani, Holiya and Gangapur in the lower West Rapti basin (Figure 2). Those VDCs were categorized as most affected, moderately affected, and less affected according to the historical inundation severity based on the information received during the field surveys conducted by the authors in June and December of 2011 and previous literature (Osti, 2008). Agriculture-based economy prevails in the area, and the population was approximated as 45,000 in 2001 (CBS, 2001). The land cover is mainly consisted of farmlands, forests, and villages. As categorized in Figure 2, the villages located near Nepal-India border are quite vulnerable in terms of floods. Likewise, the villages located in the upstream, are moderately vulnerable whereas the villages located in the middle part are less vulnerable in comparison to the visited VDCs of downstream and upstream.

3. METHODOLOGY

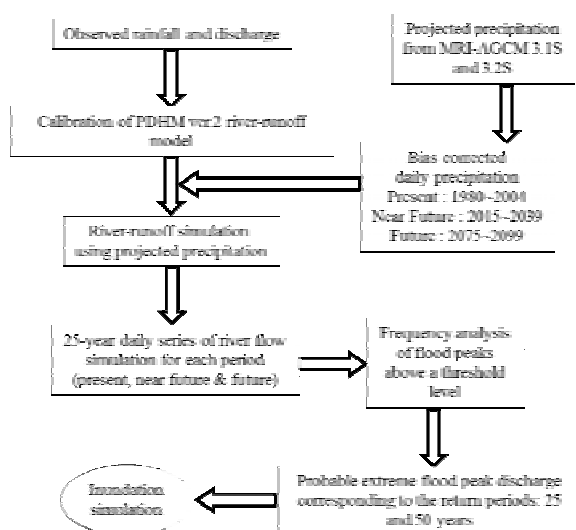


Figure 3: Flow chart of the modeling process

The complete methodology of the study is explained in Figure 3. PWRI-Distributed Hydrological Model ver.2 (PDHM) (Sugiura et al., 2008) was calibrated using observed rainfall and discharge data of Bagasothi and Julkundi stations. The calibrated PDHM was run with the 20 km x 20 km mesh based rainfall outputs of AGCMs to obtain the river runoff at the boundary (RRI inlet) of the target inundation simulation area. River runoff simulation with AGCM outputs were carried out for Present (1980 – 2004), Near Future (2015 – 2039) and Future (2075 – 2099).

Frequency analyses were carried out for the 25 years sets of river run off results of the RRI inlet point using peaks over threshold (POT) method to obtain the 25 years and 50 years return periods' peak discharges. Finally inundation simulations were conducted for obtained 25 and 50 years return periods flood events to understand the inundation distribution and depths at the selected area.

3.1 MRI-AGCM outputs and bias correction

MRI-AGCM 3.1S provided information on possible climate change induced by global warming, including future changes in tropical cyclones, the East Asia monsoon, extreme events, and blocking anticyclones (Mizuta et al., 2006). MRI-AGCM 3.2S is the improved version of MRI-AGCM 3.1s with the introduction of various new parameterization schemes, and shows improvements in simulating heavy monthly-mean precipitation around the tropics on the Western Pacific, the seasonal pattern of the East Asian summer monsoon, and so on (Mizuta et al., 2011). As the lower boundary condition, these climate experiments were performed with the observed sea surface temperature (SST) and SST change projected by atmospheric-ocean coupled models. These boundary conditions were common for both MRI-AGCM 3.1S and 3.2S. The future climate experiments are called as SFOAC and SFAC, while the present climate runs are called as SPOAC and SPAC with MRI-AGCM 3.1S and 3.2S, respectively. For near future, they are as NFOAC and NFAC. Bias correction was needed to remove the bias in the GCM outputs. In this study a statistical bias correction method developed by Inomata et al., 2009 was applied. The main objective of the bias correction method is to correct intensity of GCM daily precipitation samples to express both seasonal patterns and extreme values appropriately. The basic idea of the bias correction is to adjust the probability distribution of GCM daily precipitation to that of its observed counterparts. The bias corrected rainfall data was applied to PDHM model to generate the river discharge.

3.2 PDHM

PDHM is a conceptual model with three tanks to represent surface flow (surface tank), groundwater flow (lower tank) and river discharge (river course tank). The simultaneous flow exchange between tanks is controlled by various parameters. The distributed nature of tanks within the model area gives freedom to consider various land uses as well. PDHM model with 800 m x 800 m resolution and simulation time interval as 1 day was calibrated for the river discharge data for 2006 and 2008 at two river discharge gauging points using measured rainfall data obtained from rainfall stations shown in Figure 1. Flood events of 2006 and 2008 which had peak discharges above 1000 m³/s at Kusum station were selected for the calibration. PDHM model's parameters were tuned by trial and error method to achieve the differences between observations and simulations minimum for the selected flood events at Bagasothi, Julkundi and Kusum river gauging stations.

3.3 RRI model

RRI model simulates the processes of rainfall-runoff and inundation simultaneously based on two-dimensional diffusion wave equations. The model deals with slopes and river channels separately. The inflow-outflow interaction between the slope and river is calculated based on different overflowing formulae depending on water-level and levee-height conditions. A storage cell based inundation model suggested by Hunter et al., 2007 has been applied to calculate lateral flows on slope grid cells. The model equations are derived based on mass balance equation and momentum equation for gradually varied unsteady flow (Sayama et al., 2011). Topographic

data used in this study were obtained from HydroSHEDS (3-s resolution) (Lehner et al., 2008). The resolution corresponded approximately to 90 m x 90 m in this region; length and width of the inundation model were 26.7 km and 14.4 km. The number of grid cells was 47520 in the modeled area. The inundation model area was 384.5 km². The model requires information of the river channel locations and cross sections. We used flow accumulation datasets included in HydroSHEDS. For the river cross sections, 500 m width and 1 m depth of cross section was used for the simulation based on available field measurements. RRI model was employed to simulate the inundations for 25 years and 50 years return periods floods in this study. In the simulation of 2007 flood, three rainfall stations were used while in simulating the future flood events 20 km x 20 km mesh based rainfall data was employed. The land use of the area was mainly consisted of agriculture and small amount was allocated for residential area. The topography of the model area was consisted of plane and mountainous areas with lowest elevation of 116 m and highest of 422 m elevation.

4. RESULTS AND DISCUSSION

4.1 Inundation results for 2007 flood

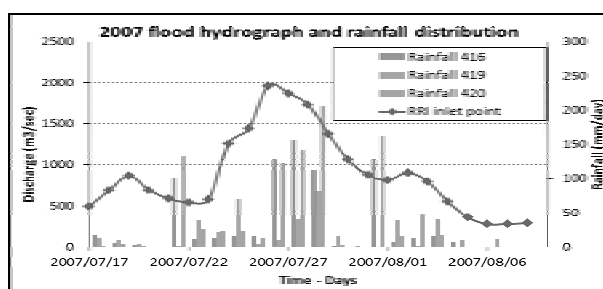


Figure 4: Discharge hydrograph at RRI inlet

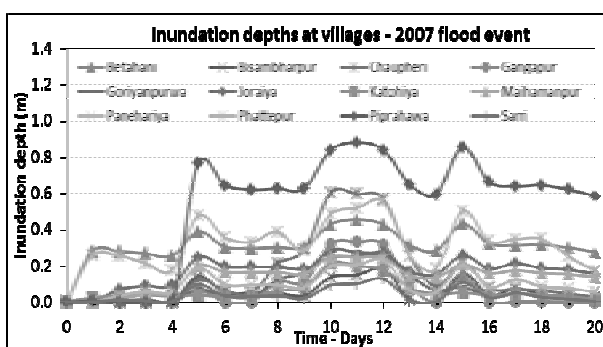


Figure 6: Inundation depths at villages in the target area

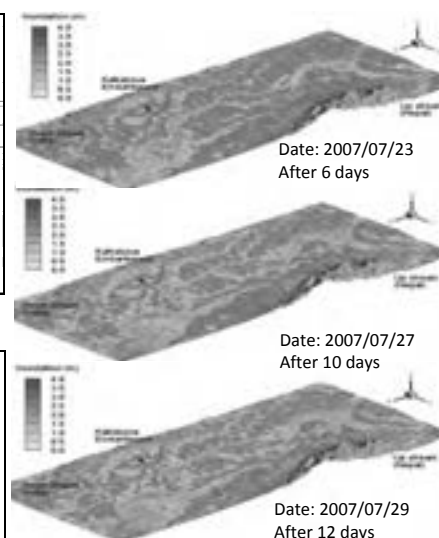
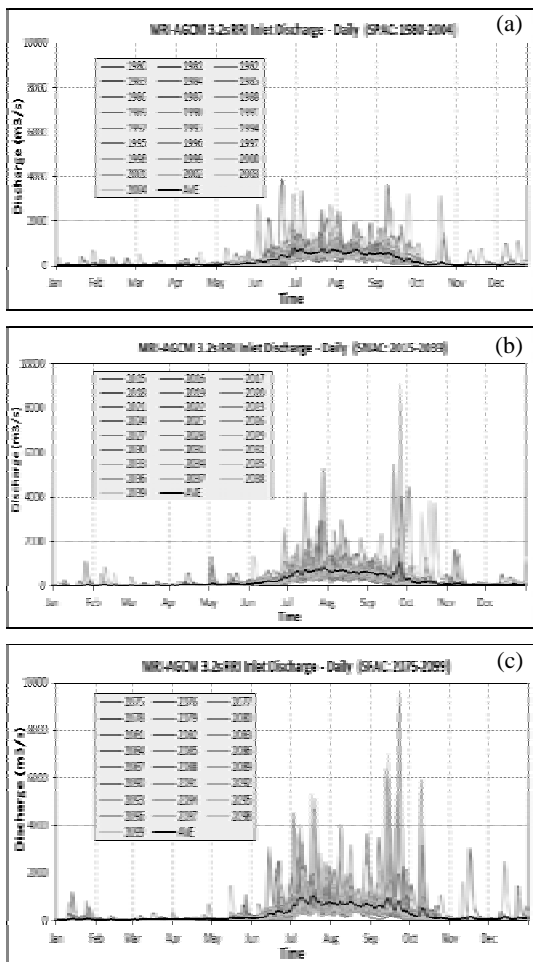


Figure 5: Inundation maps

According to the historical information, there was a significantly larger flood had occurred in 2007 with severe damages to the residents of the area. As mentioned in the introduction, the households in the area were divided in three groups as most affected, moderately affected and less affected. In our study we simulated the inundation for 2007 flood event based on available rainfall data and PDHM model outputs for river discharges. Simulation results also show that most affected areas with higher flood levels. Flood depths of moderate and less affected areas show comparative depths according to their classification. Figure 4 shows the hydrograph of RRI inlet point which was obtained from PDHM and rainfalls of field measurements. 2007 flood event lasted for about 2 weeks started from July 17th to

August 6th of year 2007. The peak was approximated as 2000 m³/s and the maximum rainfall occurred was 190 mm/day. Figure 5 depicts a series of inundation maps which clearly explains the flood hazard of 2007. In the simulation results, the maximum inundation distribution was occurred from 25th to 29th July of 2007. The observed rainfalls around the simulated area were also shown above 100 mm/day during that period. Figure 6 explains the simulated flood depths at the VDCs located in the modeled area. The VDCs of Piprahawa, Chauperi and Phattepur show the higher flood depths compared to other villagess in the area. The maximum flood depth was at Piprahawa and it was close to 1.0 m. According to the field survey information, flood depth of above 30 cm can cause significant damages for agriculture and household properties of this area. The distribution of flood depths in the modeled area is reasonably agreed with the village classification of mostly, moderately and less affected.

4.2 Inundation simulations for Present and Future flood events based on frequency analysis.



In the present paper, the focus is on the simulation results which were based on MRI-AGCM 3.2s. Figure 7 shows RRI inlet discharges which were simulated by PDHM model based on the bias corrected MRI-AGCM 3.2s output precipitations. It can be clearly seen that the river discharge at the RRI inlet point has increased twice from Present (SPAC) to Near Future (SNAC) and Future (SFAC). An overall increment of discharges can be seen compared to the Present time period. In SPAC the peaks have occurred in June or July most of the times, however for SNAC and SFAC the appearances of high peaks have been shifted to September and October. In SPAC, the peak events' discharges were less than 4000 m³/s however in SNAC and SFAC, the frequencies of peaks above 4000 m³/s are significantly higher. Frequency of occurrence of flood discharges more than 1500 m³/s in SFAC has increased by 2.2 times compared to SPAC. Similarly the discharges for 25 and 50 years quantiles have been increased close to two times. These results show the possible Future climate changes compared to Present situation.

Figure 7: Daily discharges at RRI inlet point for SPAC (a), SNAC(b) and SFAC(c)

Table 1: Frequency analysis results for RRI inlet point discharges

Type of GCM	Time period	Frequency in 25 years	Probable peak discharge (m ³ /s)	
			1/25	1/50
MRI-AGCM 3.1s	SPOAC	38	3270	3630
	SNOAC	38	4090	4600
	SFOAC	53	3540	3910
MRI-AGCM 3.2s	SPAC	30	4100	4660
	SNAC	37	7060	8170
	SFAC	66	7720	8810
PDHM discharge (based on observed rainfall)		43	3910	4350

Table 1 shows the results of frequency analysis which was carried out to obtain the discharge quantiles for 25 and 50 years return periods for RRI inlet point based on MRI-AGCM 3.1s and 3.2s precipitation outputs. The obtained POT values were fitted to exponential distribution to obtain 25 and 50 years return periods floods. According to Table 1, it can be seen that the MRI-3.1s' quantiles show lower values than MRI-3.2s. Probable peak discharges increase remarkably in Near Future and they change slightly at the end of 21st century for MRI-3.2s. Frequency of flood increases in Near Future and Future. 25 and 50 years peak discharges which were calculated based on PDHM output discharges under the observed rainfalls, have the values of 3910 m³/s and 4350 m³/s respectively. The 50 years return period flood of MRI-3.2s is more than double of the peak discharge value based on observed rainfalls.

4.3 Inundation results of SPAC and SFAC for 50 years return period flood

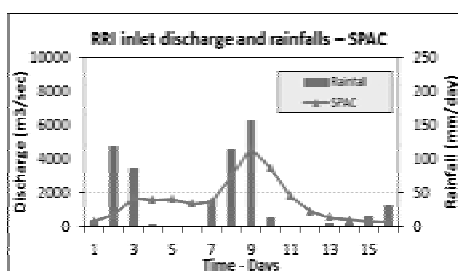


Figure 8: Discharge hydrograph at RRI inlet for SPAC

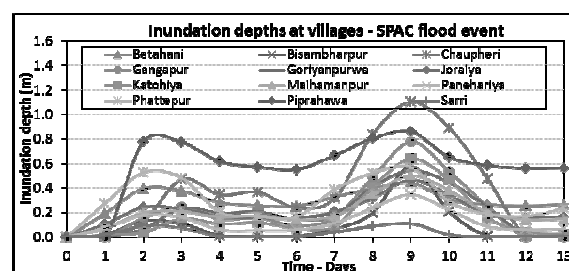


Figure 9: Inundation depths at villages in target area for SPAC

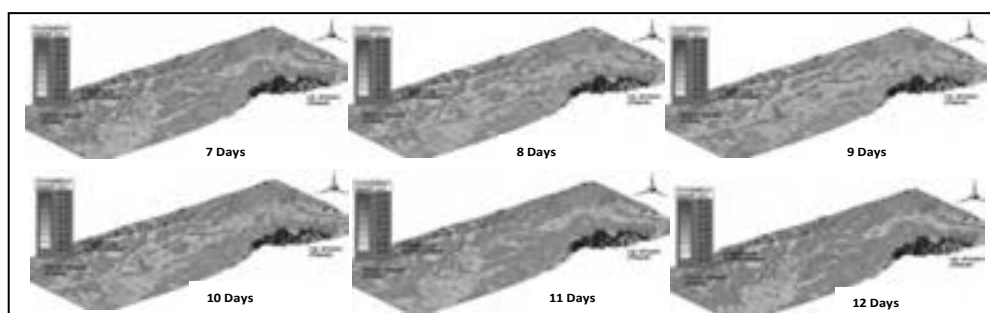


Figure 10: Inundation maps for SPAC flood event

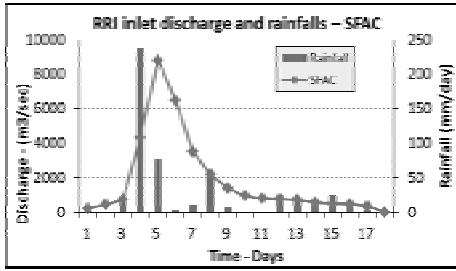


Figure 11: Discharge hydrograph at RRI inlet for SFAC

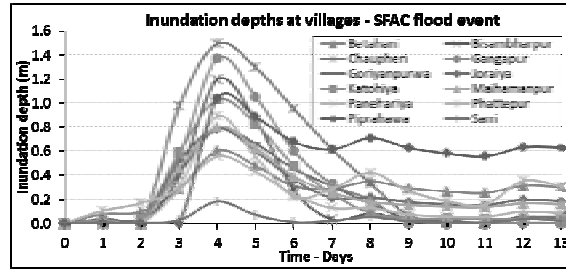


Figure 12: Inundation depths at villages in target area for SFAC

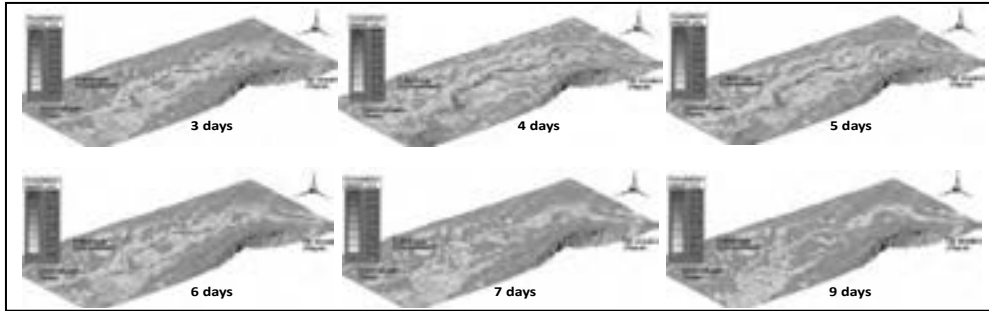


Figure 13: Inundation maps for SFAC flood event

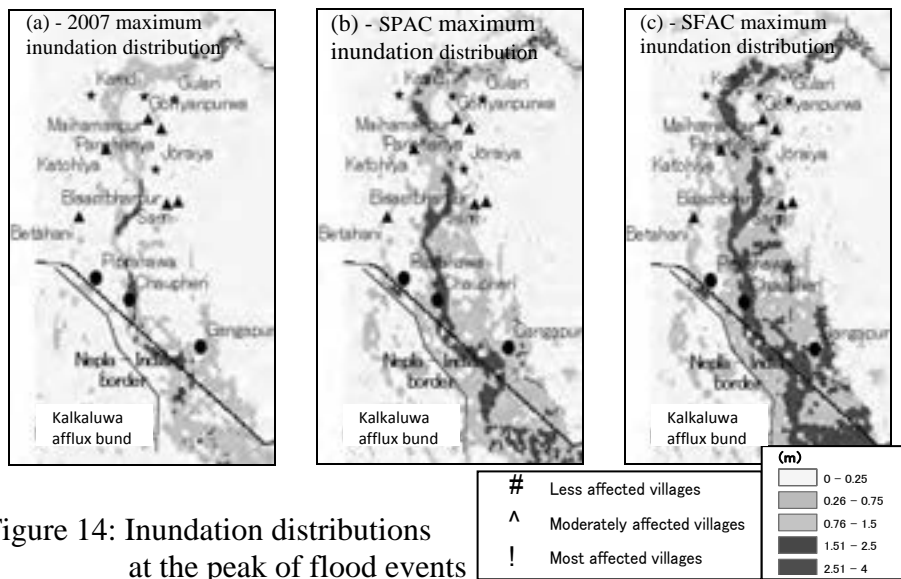


Figure 14: Inundation distributions at the peak of flood events

Table 2: Inundation area where the flood depths equal or exceed 30 cm at the peak

2007 flood, A_{2007} (km ²)	SPAC flood, A_{SPAC} (km ²)	SFAC flood, A_{SFAC} (km ²)	$\frac{A_{SPAC}}{A_{2007}}$	$\frac{A_{SFAC}}{A_{2007}}$
60	106	133	1.8	2.2

The figures in section 4.3 explain the simulation results of Present and Future inundations of 50 years return period floods. The variation of flood depths in SPAC and SFAC (Figure 9 and 12) shows that the villages located in most affected VDCs such as Piprahawa, Chaupheri and Gangapur have shown high flood levels compared to 2007 flood. For Chaupheri, in 2007 it was about 0.6 m and for SPAC

and SFAC cases the flood depths have been increased to 1.1 m and 1.5 m respectively. Therefore, in future the anticipated flood depth at Chaupheri will be increased more than twice of 2007 flood depth. Gangapur which is located close the river channel will be also severely affected in future since its flood depth in SFAC is 1.4m while in SPAC and 2007 flood the depths are 0.8 m and 0.3 m respectively. Similar tendency can be seen in other villages also. Therefore in Future the flood vulnerabilities of the villages which were categorized as mostly affected VDCs, will be significantly increased. The possible reason for the high flood levels in Piprahawa even though it is located somewhat away from the main channel can be explained as due to the afflux bund in the Nepal-India border. Figure 14 shows the Nepal-India border and the location of Kalkaluwa afflux bund. This afflux bund was constructed very near to the border and during the field survey, it was heard that during the 2007 flood event also it was one of the cause of inundation especially in Piprahawa area. However, to understand the behavior of this bund in a flood event a very detailed simulation study should be carried out.

Figure 14 depicts the inundation distribution at the peak flood levels of 2007 flood, SPAC and SFAC 50 years return period floods. In 2007 the peak discharge was about 2000 m³/s, in SPAC it was 4660 m³/s and for SFAC it was 8810 m³/s. The inundation distributions for above mentioned flood peaks show their impacts to the target area clearly. In the target area, when the flood depth exceeds 30 cm, the property and agricultural damages are high according to the field survey. In Table 2, the inundation areas which exceed the 30 cm flood depth are shown with ratios comparing with 2007 flood. It is noticed that in Future the inundation area exceeding 30 cm will be doubled compared to 2007 flood. When the flood discharge becomes higher the VDCs which were classified as less or moderately affected are also showing high level of floods which can be lead to severe disasters in future. Consequently, there will be more damages to human lives, livestock and properties in the area if adaptation and mitigation measures are not taken in time.

5. CONCLUSION

The impact of climate change on flood hazards in lower West Rapti river basin in Nepal was analyzed by feeding present, near future and future climate, projected precipitations into a distributed hydrological model to achieve the river runoff. Employment of the obtained river runoff to an inundation model was carried out to simulate the flood hazards at different time intervals in present, near future and future periods.

When the daily discharge values of SPAC, SNAC and SFAC were compared a significant increase of the magnitude and frequency of high discharges were noticed in near future and future than present. Moreover shifting of high discharge seasons from June/July to September/October was seen implying the potential of varying the climate patterns in future. Such a phenomenon will seriously affect to the agriculture in the target area. In the comparison of inundation areas which exceed 30 cm flood depth, in future the ratio is more than twice compared to 2007 flood. The flood hazards in the highly affected areas will be increased significantly in future as a result of increased flood depths in most of the villages in the target area. Profound countermeasures should be implemented to reduce the flood induced damages.

REFERENCES

- AfDB, DFID, EC, BMZ, OECD, UNDP, UNEP and the World Bank, 2003. *Poverty and climate change: reducing the vulnerability of the poor through adaptation* [Sperling, F.(ed.)], Bonn.
- CBS, 2001. *Statistical Year Book of Nepal*, Central Bureau of Statistics, National Planning Commission, Government of Nepal, 445-446.
- FAO, 2004. *Compendium of food and agriculture indicators 2004 – Nepal*. (www.fao.org/es/ess/compendium_2004/pdf/ESS_NEP.pdf)
- Dilley, M., Chen, R. S., Deichmann, U., Lerner-Lam, A. L., and Arnold, M., 2005. *Natural Disaster Hotspots: A global Risk Analysis*. The World Bank Group, Washington, DC.
- Hunter, N. M., Bates, P. D., Horritt, M. S., and Wilson M. D., 2007. Simple spatially-distributed models for predicting flood inundation: a review, *Geomorphology* 90, 208-225
- Iomata, H., Takeuchi, K., and Fukami K., 2009. Development of a statistical bias correction method for daily precipitation data of GCM20. *Annual Journal of Hydraulic Engineering, JSCE* 55, 247-252.
- IPCC, 2007. Summary for Policymakers, In: *Climate Change 2007: The Physical Science Basis. Contribution of Working Group I to the Fourth Assessment Report of the Intergovernmental Panel on Climate Change*. Cambridge University Press, U K.
- Lehner, B., Verdin, K. and Jarvis, A. 2008. New global hydrography derived from space borne elevation data. *Eos, Transactions, AGU* 89(10), 93-94.
- Mahtab, F. U., 1992. The delta regions and global warming: impact and response strategies for Bangladesh. In: *The regions and global warming: impacts and response strategies* [Schmandt, J. and J. Clarkson (eds.)], Oxford University Press, New York.
- Mizuta, R., Oouchi, K., Yoshimura, H., Noda, A., Katayama, K., Yukimoto, S., Hosaka, M., Kusunoki, S., Kawai, H., and Nakagawa, M., 2006. 20-km-mesh global climate simulations using JMA-GSM model - mean climate states. *Journal of Meteorology Society of Japan* 84, 165–185.
- Mizuta, R., Yoshimura, H., Murakami, H., Matsueda, M., Endo, H., Ose, T., Kamiguchi, K., Hosaka, M., Sugi, M., Yukimoto, S., Kusunoki, S., and Kitoh, A., 2011. Climate simulations using MRI-AGCM3.2 with 20-km grid, *Journal of Meteorology Society of Japan* 90A, 233-258.
- MOF, 2005. *Economic Survey – Fiscal Year 2004/05*. Ministry of Finance, Nepal, Kathmandu.
- Osti, R., 2008. *A feasibility study on integrated community based flood disaster management of Banke district, Nepal phase I(a): Baseline study*. Technical note of PWRI No. 4122, Public Works Research Institute, Tsukuba, Japan.
- Sayama, T., Ozawa, G., Kawakami, T., Nabesaka, S., and Fukami, K., 2012. Rainfall-runoff-inundation analysis of Pakistan flood 2010 at the Kabul river basin, *Hydrological Science Journal* 57-2, 298-312
- Sugiura, T., Fukami, K., Fujiwara, N., Hamaguchi, K., Nakamura, S., Hironaka, S., Nakamura, K., Wada, T., Ishikawa, M., Shimizu, T., Inomata, H., Itou, K., 2008. Development of an Integrated flood analysis system (IFAS) using satellite-based rainfall data (Japanese), *Journal of River Technology – JSCE* 14, 53-58.
- UNDP, 2009. *Nepal Disaster Report*. Ministry of Home Affairs - Nepal and Nepal Disaster Preparedness Network, Nepal.

Community under fire threat: an assessment of fire hazard vulnerability of ward 65 in Dhaka City

Naima RAHMAN
Research Planner, BNUS, Dhaka, Bangladesh
naima.rahman05@gmail.com

Mehedi Ahmed ANSARY
Professor, Department of Civil Engineering, BUET, Dhaka, Bangladesh
ansary@ce.buet.ac.bd

ABSTRACT

In the last few years Dhaka City has been experiencing many fire accidents due to lack of proper precautionary measures, institutional inefficiency, insufficient equipment support and lack of public awareness. In this study, a traditional community of ward 65 of Dhaka has been selected for vulnerability assessment using Community Vulnerability Assessment Tool (CVAT). From the fire vulnerability analysis it has been found that most of the buildings of the study area are highly vulnerable. 27% critical facility was found to be within the highly fire vulnerable areas. High population density in the high risk zone and plastic recycling and processing industries make the area socially vulnerable to fire hazard. 20 % buildings have plastic manufacturing and processing industries which is highly vulnerable to fire hazard. Most of the buildings (42%) have 3 feet wide staircase. 19% households have only 0-5 feet roads in front of their houses which is inaccessible for fire truck. Besides, electric pole is located in front of 14% buildings and transformer is located in front of 11% building. 97% buildings of the study area have different type of fire sources. In this respect this community is vulnerable to fire hazard. The land use pattern of ward 65 indicates also the possibility of this kind of hazard. As being a mixed use residential area, the loss due to fire may be catastrophic. To increase resiliency of the community in case of fire hazard some steps should be taken such as change in present land use pattern, relocation of chemical factory and plastic factory, and widening of road network and staircase of building.

1. INTRODUCTION

Dhaka City has been experiencing many fire accidents at present and in most cases lack of proper precautionary measures along with the institutional inefficiency, insufficient equipment support and lack of public awareness are making the situation worse. To mitigate the impact of fire at

community level, public participation is important. As a high risk area of fire hazard, no vulnerability assessment has been conducted in Dhaka City. In this study, a traditional community of ward 65 of Dhaka has been selected for vulnerability assessment. Community Vulnerability Assessment Tool (CVAT) (Lisa et al, 2002) method has been applied to assess vulnerability of the community to fire hazard. At first, a hazard map showing the different risk zones of fire has been developed by land use in the study area. Then four vulnerability analyses have been conducted namely social vulnerability, critical facilities vulnerability, economic vulnerability and structural vulnerability. To accomplish these vulnerability analyses different field surveys have been conducted for getting complete scenario of the community. By using some parameters and attributes, community vulnerability has been evaluated with respect to fire hazard. Finally some recommendations have been provided to improve the present condition of the community.

2. BACKGROUND

The A fire hazard is any situation in which there is a greater than normal risk of harm to people or property due to fire. The physical vulnerability of the country’s population and infrastructure is compounded by economic vulnerability. Extensive fire inevitably causes upheavals not only in the physical but also in the social and economic context where it occurs. Urban fires have devastating impact on the communities. An analysis of disaster impacts on urbanizing areas show that fires cause the greatest loss of life and property. Fires hazards occur frequently in Bangladesh especially in urban areas. Table 1 describes number of fire accidents originated by various causes in the last three years in Bangladesh. Electric fault, kitchen fire, cigarette, naked fire, burning ash, fireworks, friction of machine, sabotage, mob, unknown and misc (engine misfire, spontaneous ignition, and chemical reaction) are different causes of fire. Among these most of the fire occur due to electric fault and kitchen fire.

Table 1: Causes of Fire in Bangladesh

SL	Cause of Fire	Number of Fire Incident					
		2009		2010		2011	
1	Electric Fault	3754	43.27%	3188	39.44%	3760	43.86%
2	Kitchen Fire	2254	25.98%	2166	25.67%	2137	24.89%
3	Cigarette	865	9.97%	789	9.75%	828	9.64%
4	Naked fire	542	6.24%	528	6.52%	450	5.24%
5	Burning Ash	229	3.41%	267	3.16%	358	4.17%
6	Fire Works	162	2.41%	204	2.41%	161	1.87%
7	Friction of Machine	134	1.99%	170	2.01%	244	2.84%
8	Sabotage	85	1.26%	149	1.76%	104	1.21%
9	Mob	113	1.68%	241	2.85%	78	0.90%
10	Unknown	868	-	1105	-	726	-
11	Misc (Engine misfire, spontaneous ignition, Chemical reaction)	536	6.17%	389	4.61%	464	5.40%
	Total	12182		14682		13041	

Source: Bangladesh Fire Service and Civil Defense, 2012

Residential fire events are increasing in every year tremendously and it causes loss of property and injures many people badly. Industrial fire is also in increasing trend. (Bangladesh Fire Service and Civil Defense, 2011) Economic loss due to fire incidents is high. Figure 2 describes amount of loss due to residential fire in Taka crore from 2002 to 2010. Among these years the highest amount of loss (Tk. 272.64 crores) is seen in 2005. In most of the years the loss amount is above Tk. 100 crores. As Bangladesh is a developing country it cannot afford the huge amount of loss due to fire accidents every year.

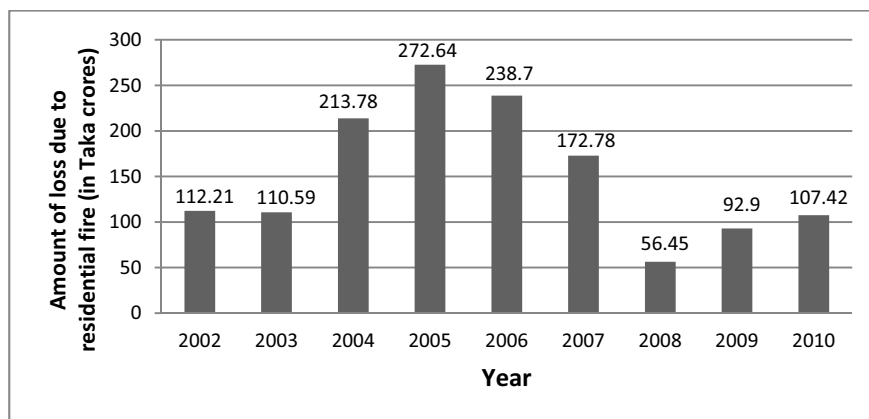


Figure 2: Extent of losses due to fire hazards in recent years
(1 Million USD = Taka 8.6 crore)
(Source: Bangladesh Fire Service and Civil Defense)

Dhaka the capital of Bangladesh often faces fire hazards due to its dense building concentrations, narrow roads, flammable building materials, aging water supply and electrical wire, chemical factory in residential areas as well as the lack of preparedness and response skills among local people and the fire authority. Figure 3 shows the trend of fire in Dhaka City in the last six years. Most of the fire events occurred in 2010 than the other statistical year.

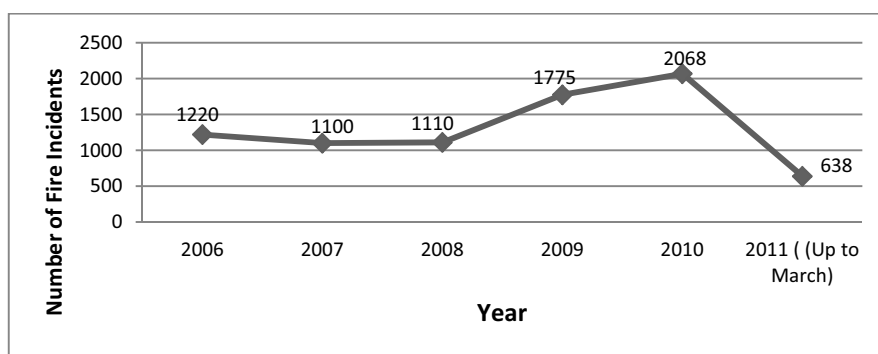


Figure 3: Number of fire event in Dhaka city
(Source: Bangladesh Fire Service and Civil Defense, June 2011)

In 3rd June 2010, a devastating fire broke out in the densely-populated part of Old Dhaka city at Nimtoli. Fire killed at least 117 people and caused injury to a hundred people. Most of the affected peoples were women and

children. Initially it was thought that explosion of two transformers at Nimtoli started the fire but later it has been known the fire originated from an oil stove and spread to the chemical warehouses nearby and resulted high casualties and damages.

Two back to back fires occurred in 15th and 16th January 2012 in Islambag and Labag areas in Ward 65 in Old Dhaka. The first incident occurred in a plastic warehouse near the Eidgah ground in West Islambag at around 10:45 PM started from a gas stove. The next day again at the same time another fire occurred in Shahid Nagar area at Labag around 10:30 PM. In this case fire originated from a tin shed house. Around 100 shanties, five shops and a printing press caught by fire. (BNUS field Survey, 2012).

This is a common situation in Old Dhaka where most of the buildings have small factories like chemical, plastic, rubber etc., and Warehouse and food shops up to second floor of the residential building. In Old Dhaka no house is equipped with fire fighting equipments like extinguisher, hose pipe etc. They don't have sufficient width of staircase let alone the emergency exit. In this respect, assessment of fire hazard vulnerability in Dhaka City especially in the old part is very important. The old part 'Puran Dhaka' is the most vulnerable area in Dhaka City. In this study Ward 65 (Map 1) of Old Dhaka is selected for the vulnerability assessment. This ward is one of most vulnerable to fire hazard than other because of its traditional land use and population density. Fire incidents are very common phenomenon in this area. It is also one of the oldest areas of Dhaka City. This ward is mainly used as manufacturing industrial area. Besides several land uses like Warehouse, commercial use, chemical shop, clamber storage and processing shops are also prominent. Land use of this area makes it more unique than the other area of Dhaka City. In this study, assessment of fire hazard vulnerability of the community has been conducted to examine the existing risk of fire in the area and prepare the residents to face this sort of disaster.



*Map 1: Study Area (ward 65 of Dhaka city)
Source: Dhaka City Corporation*

3. METHODOLOGY

3.1 Study Design

For achieving the objectives, depending on the literature review a checklist for the study has been designed which has been modified on the basis of findings from pilot survey. The checklist is given in Appendix-A.

3.2 Study Area Selection

The Ward 65 of Old Dhaka is selected as the study area to assess the fire hazard vulnerability. The study includes the vulnerability assessment of the building stocks. Buildings adjacent to the roads were surveyed.

3.3 Sampling

The total number of buildings of Ward 65 is 3210. For this sample size, total 1078 buildings survey has been conducted keeping the confidence level at 95% and confidence interval is 2.43.

(<http://www.surveysystem.com/sscalc.htm>, accessed on 25th March, 2011).

3.4 Data Collection

3.4.1 Base map collection and updating map from field survey

A base map of the study area was collected from Dhaka City Corporation (DCC) office to become familiar with the environment of the study area. Field survey of the buildings was conducted on the basis of the DCC base map.

3.4.2 Primary Data Collection

A checklist survey was conducted in the study area to find out the existing socio-economic condition of the residents.

3.5 Data Processing and Analysis

Through data collection, raw data have been collected. Information collected from the survey, have been inputted in MS Access and then converted to SPSS 12 for processing and analysis.

3.5.1 Fire hazard vulnerability analysis

To assess the community vulnerability of Ward 65 in Old Dhaka, Community Vulnerability Assessment Tool (CVAT) is used to find out the existing scenario of the area. This tool has 7 steps including:

- Hazard identification
- Hazard analysis
- Critical facilities analysis
- Social analysis
- Economic analysis
- Environmental analysis
- Mitigation opportunities analysis

In this study only critical facilities analysis, social vulnerability analysis, economic vulnerability analysis and in addition structural vulnerability analysis has been done to assess the vulnerability of the community. The

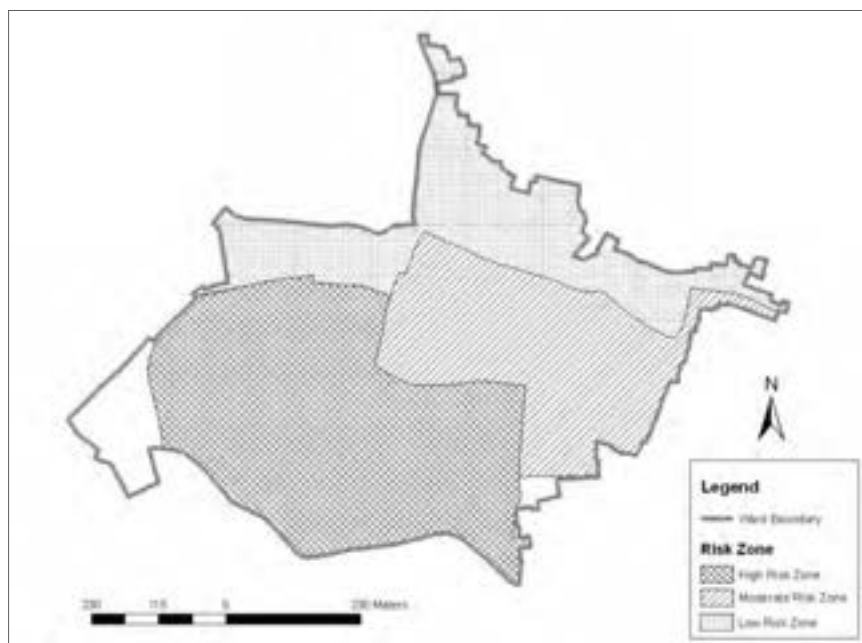
tools and methodologies used in this analysis consist of GIS and spatial mapping analysis.

3.6 Preparation of Final Report

All information and finding are gathered and presented by tables, graphs and maps to prepare the final report. Some recommendations based on the findings are provided to improve the overall conditions of Ward 65 in the report.

4. FIRE HAZARD VULNERABILITY ANALYSIS

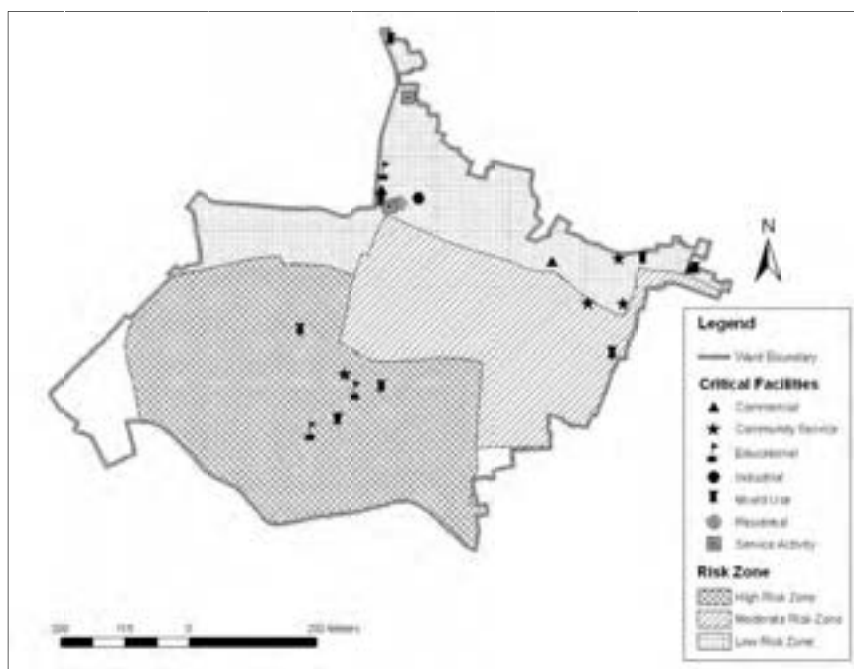
The study area is divided into three risk zones including high risk zone, moderate risk zone and low risk zone according to their land use from expert opinion. Land uses of various risk zones differ from other (map 3). The total area of Ward 65 is 118.1668 acres (0.478 Square Kilometer). Among this, high risk zone is 52.84 acres (44.72%), moderate risk zone is 30.89 acres (26.14%) and low risk zone is 27.95 acres (23.65%). (From GIS Map) The livelihoods of the inhabitants of a zone are primarily based on plastic processing industries like plastic manufacturing, recycling and processing factories. This zone is considered as high risk area. The name of this portion is Islambag. The zone also displays a high building density with multi-storey buildings and very few urban public spaces left. In the moderate risk area processing factory and different Warehouse (plastic Warehouse, cattle food storage) are dominant. Residential use with commercial (retail shop, office, bank and storage) use is considered as the low risk area.



Map 3: Fire risk zone in Ward 65

4.1 Critical Facilities Analysis

The critical facilities in ward 65 were identified and a complete inventory of these facilities was prepared. There are total 22 numbers of critical facilities in the study area. Then critical facilities that are in and within close proximity to high risk areas were identified by overlying the critical facilities location over the map of fire vulnerable areas. Map 4 shows critical facilities map in Ward 65. The most common critical facilities in the area are as follow:



Map 4: Critical facilities Map in Ward 65

Figure 4 shows that 27.27% critical facilities are located at the high risk, 9.09% are located at moderate risk area and 63.64% are located at low risk zone. The critical facilities are mainly educational institution and religious center. Most of the critical facilities are located in the Lalbagh area which is comparatively low risk zone. In this area land use is mainly residential and in some case mixed (residential, retail shop, commercial) and the people in this area are less vulnerable to fire hazard. In high risk zone i.e. Islambag, plastic industries are located to very close proximity to critical facilities.

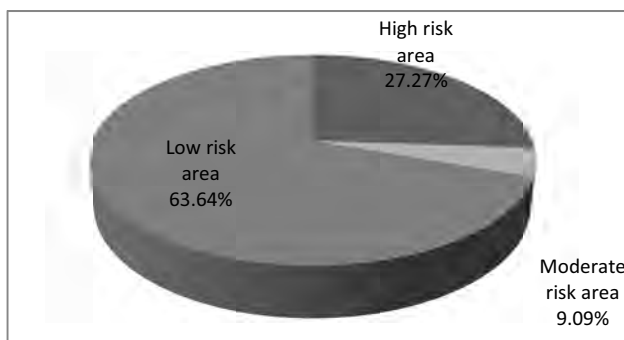


Figure 4: Percentage of critical facilities in different risk zones

Critical facilities of the study area are not vulnerable to fire. Besides these are located mainly adjacent to wider roads. In case of any fire, these can be used as shelter for the inhabitants.

4.2 Social Vulnerability Analysis

Number of population in any building of the study area varies from 0 to 400. Most of the buildings (28.53%) have 11 to 20 people. 22.03% have 21 to 30 persons and 18.93% have 6 to 10 persons. Building having population more than 100 is very low (1.6%). But most of the densely populated buildings are situated in the high risk zone (Map 5) which mainly consists of plastic recycling and processing factories. In these factories generally woman and child laborers work. With respect to these conditions of the area it can be said that the area is vulnerable to fire hazard.

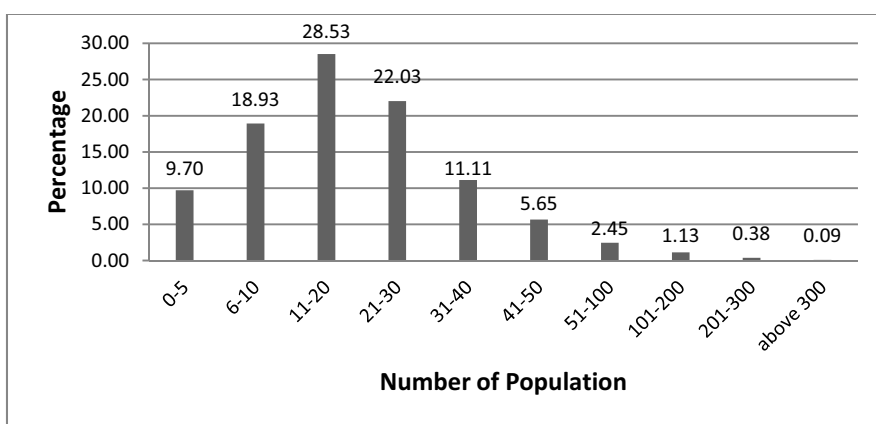
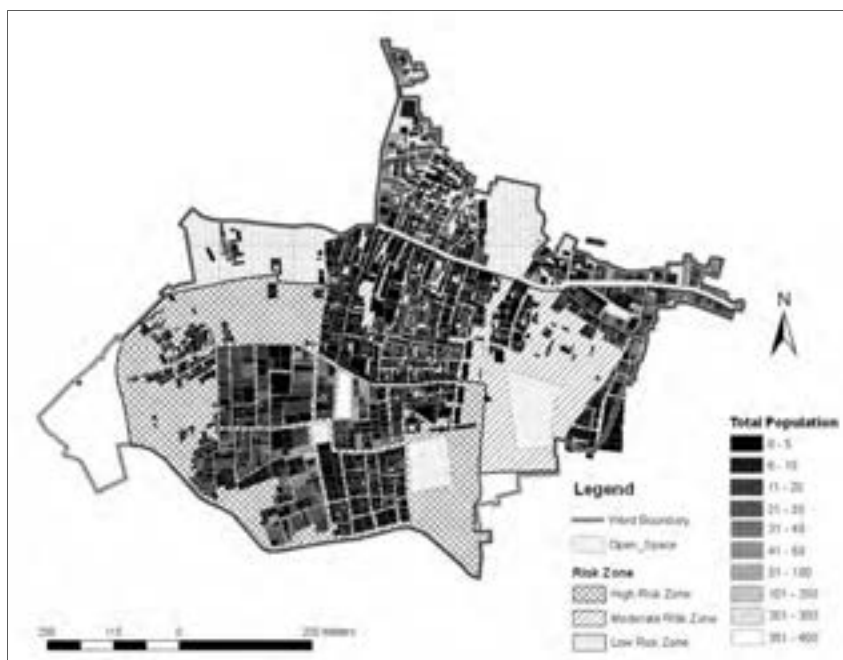


Figure 5: Population distribution in Ward 65.



Map 5: Population Map of Ward 65

4.3 Economic Vulnerability Analysis

Among the surveyed households, 57.22% have different types of economic activities. Plastic manufacturing and processing industry is dominating (20.22%); others are different type of factory (15.19%), warehouse (8.95%), iron/metal shop/factory (2.8%), gold and silver shop (1.49%), electric goods shop (1.3%), chemical shop/factory (1.21%) and other (6.06%) etc. Grocery shop, grocery shop and bank, medicine shop, tailoring shop/laundry, clamber storage, paper shop, bank/services, cloth store, hotel, market and phone shop are in other category. Figure 6 shows different types of economic activities of the study area.

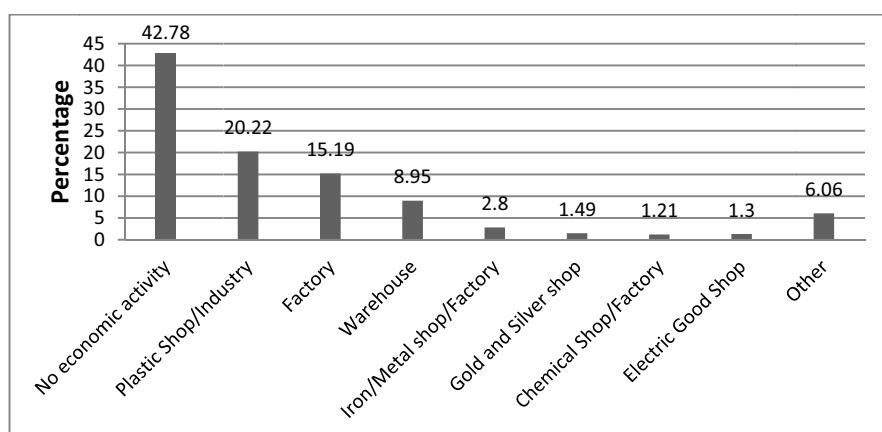


Figure 6: Economic Activities of the Study Area

Some economic activities makes the study area vulnerable to fire hazard. Among them plastic manufacturing industry is totally based on chemicals which promote fire to spread within few seconds to the locality. From land use survey, it is found that the area is mainly a residential area (36.9%). Mixed activity is found in four categories: 1. residential and commercial (31.87%), 2. residential and industry (16.4%), 3. commercial and industry (0.93%), and 4. residential and education (0.1%). Figure 7 shows the present land use of the study area.

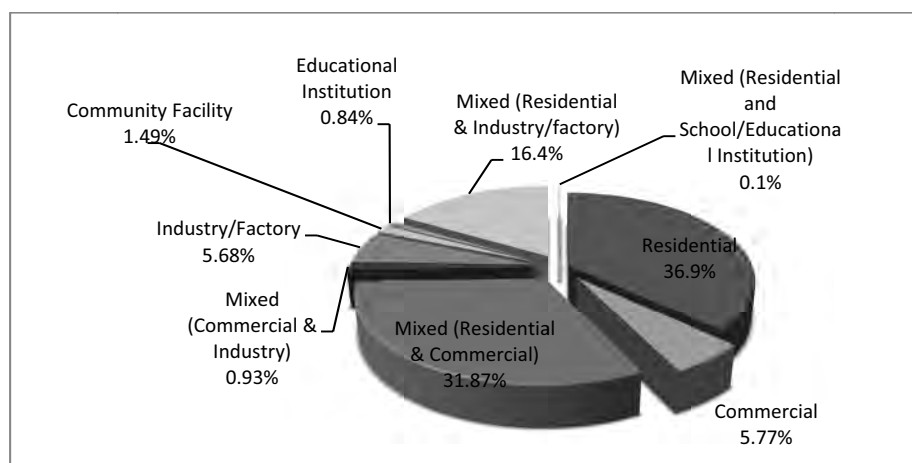
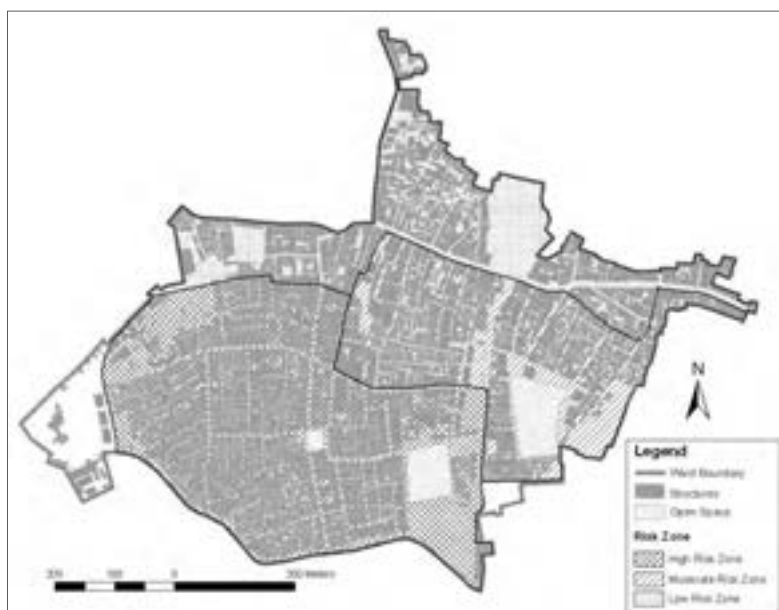


Figure 7: Present Land Use of the Study Area

4.4 Structural Vulnerability Analysis

There are other factors in the area which makes it vulnerable to fire hazard. These factors are width of staircase, road width of the area and accessibility to the building, position of transformer and electricity pole. If the roads are not accessible to fire service vehicle to douse/ put off the fire it may cause a loss to the community. For the emergency evacuation process staircase width is a vital issue to the resident of a building. That's why these factors get importance to the vulnerability assessment. The area consists of total 3210 structures. Among these, 55.66% of the structures are situated in high risk zone; 24.45% structures are situated in moderate risk zone and 19.89% structures are situated in low risk zone. (Map 6)



Map 6: Structure Map of Ward 65

4.4.1 Age of Structure

From the field survey, 2011, it is found that Ward 65 is composed of both old and newly developed buildings. 23.3% of surveyed buildings have been constructed 0-10 years ago. These are the newest structures of the area. Most of the buildings have been constructed around 11-20 years ago (25.7%). 23.2% and 11.6 % structures have been built 21-30 years and 31-50 years before respectively. 15.9% building are 51-100 years old and 0.4% buildings are more than 100 years old.

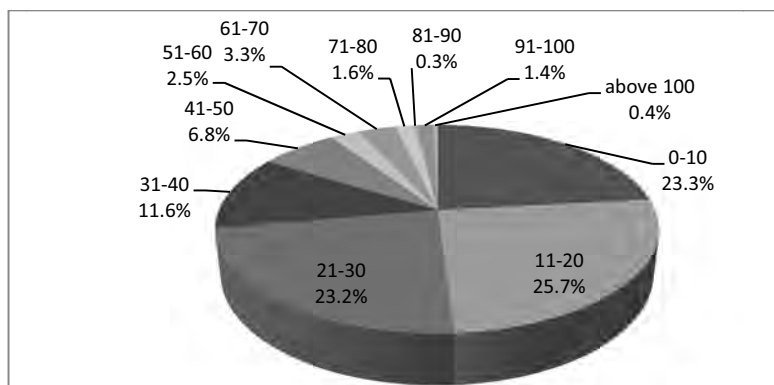


Figure 8: Age of building in the study area

4.4.2 Number of Floor

From field survey it has observed that in the study area most of the buildings (29.64% of surveyed buildings) are one storied. These buildings are mainly used as clamber storage and processing activity and plastic manufacturing and processing. In these structures fire can propagate very swiftly. 22.27% buildings are two storied and mainly used as residential and plastic processing activity. 3 storied are 14.35%, 4 storied are 13.05%, 5 storied are 12.3% and 6 to 14 storied are 7.36%. 1.03% buildings are under construction.

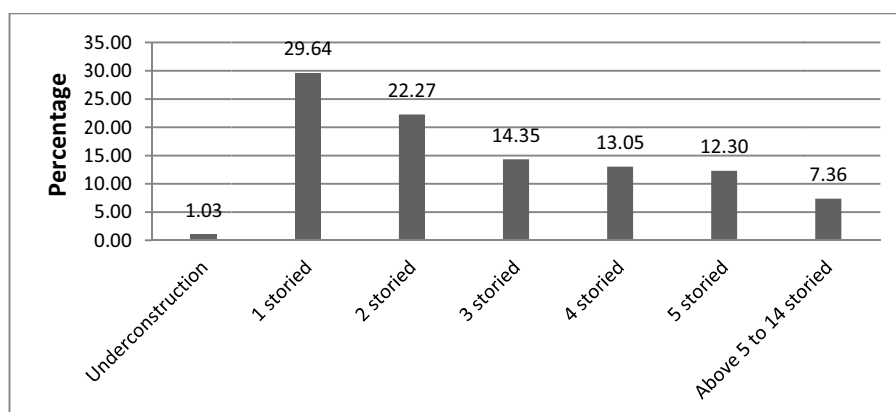


Figure 9: Number of floor of the building in the study area

4.4.3 Staircase Width

In the older portion of Dhaka city it is a tradition that the width of staircase is smaller than the new part of Dhaka. From the field survey it has been observed that staircase width of buildings varies from 1-5 feet. Most of the buildings (41.82%) have 3 feet wide staircase. 4 feet wide staircases are seen in 28.09% buildings. In case of some newly constructed buildings the width is 5 feet (11.73%). Wider staircase is essential for any building during the evacuation process for any disaster. For fire hazard it gets special priority because fire spreads very quickly in a building. So people need to protect themselves from the rage of fire in a very short time. In this respect the study area is vulnerable to fire hazard.

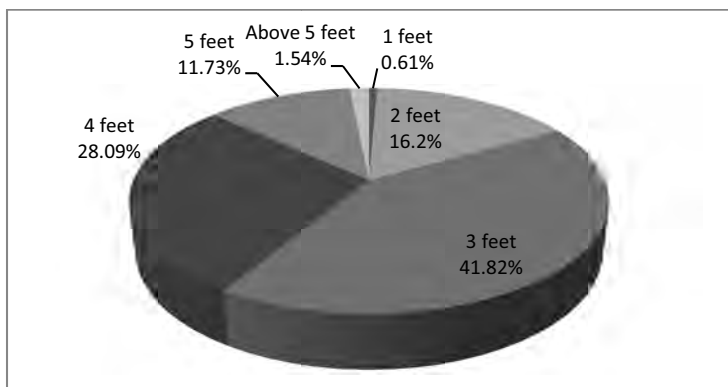
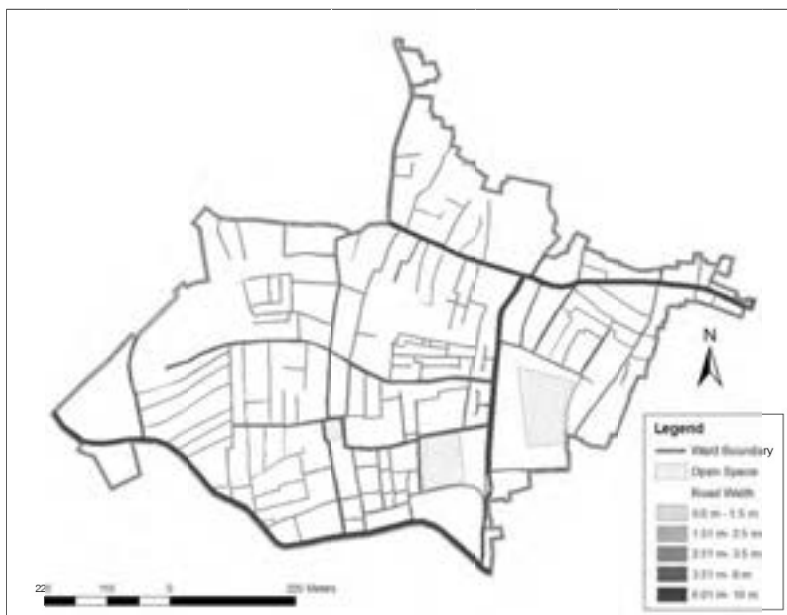


Figure 10: Staircase width (feet) of building in the study area

4.4.4 Road Width/ Accessibility to Building

For emergency response during any disaster road width is an important factor. If the road is not sufficiently wide to move fire service’s vehicle it may cause another disaster to the people and it may extend the loss. Building fire can spread very quickly and can overwhelm properties and life. In the study area accessibility to each household is not good. The main roads are wide and accessible to the fire service vehicle but the local roads and connecting roads to the buildings are not accessible to the vehicle. (Map 7)



Map 7: Accessibility Map of Ward 65

Road width varies from 1-40 feet in the study area. Most of the residents have 6-10 feet roads in front of their houses (44.73%). 16.31% have 11-15 feet roads and 20.42% have above 15 feet roads. 18.55% households have only 0-5 feet roads which is inaccessible for fire truck. These narrow roads are totally impossible for evacuation and rescue process. In this respect this community is also vulnerable to fire hazard. They are not aware about widening the road.

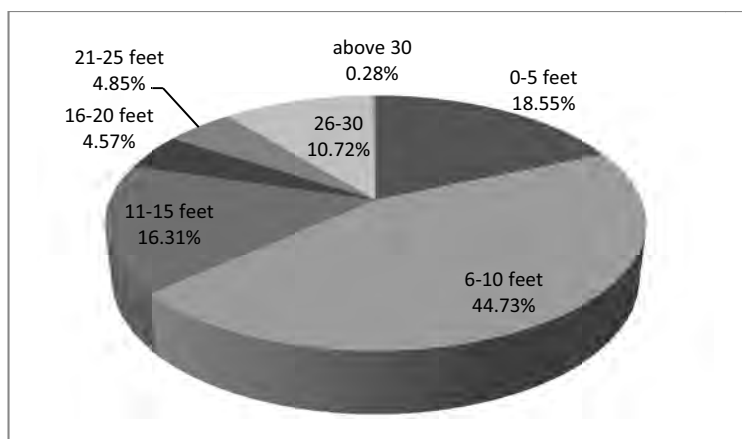


Figure 11: Road width (feet) / accessibility to building in the study area

4.4.5 Transformer and Electricity Pole

Position of transformer and electricity pole to a building is also assessed in this study because these may cause serious fire hazard to the locality. Recently in old Dhaka a fire incident occurred due to the blast of a transformer. The buildings in this area are constructed very closely to each other. So that fire can spread out to another building. Among the surveyed buildings electric pole is located in front of 13.51% buildings and transformer is located in front of 11.37 % building.

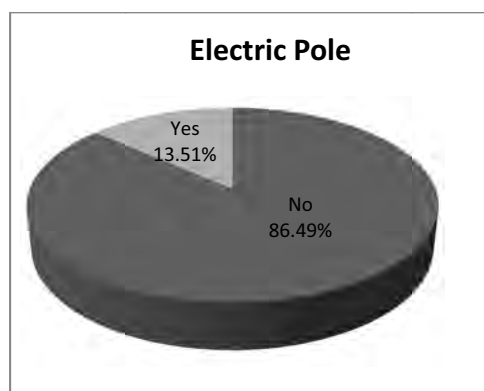


Figure 12: Electric pole in the study area

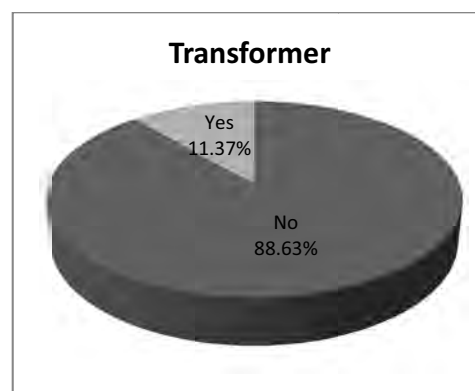


Figure 13: Transformer in the study area

4.4.6 Existence of Fire Source

Most of the buildings of the study area have different type of fire sources. Gas stove, electric wire, chemical factory and plastic factory are the main sources of fire. Besides, there are also some ornament factories, metal factories, recycled plastic shop, printing press and wholesale paper market in the area all of which can be source of great fire hazard. Residential houses are vulnerable due to gas stove (38.4%) and electric wire (15.84%). Households with mixed use are mainly vulnerable due to plastic factory (17.8%), chemical shop (16.59%), metal factory (2.8%) and gold ornament factory (1.5%). 3.26% buildings have no fire source.

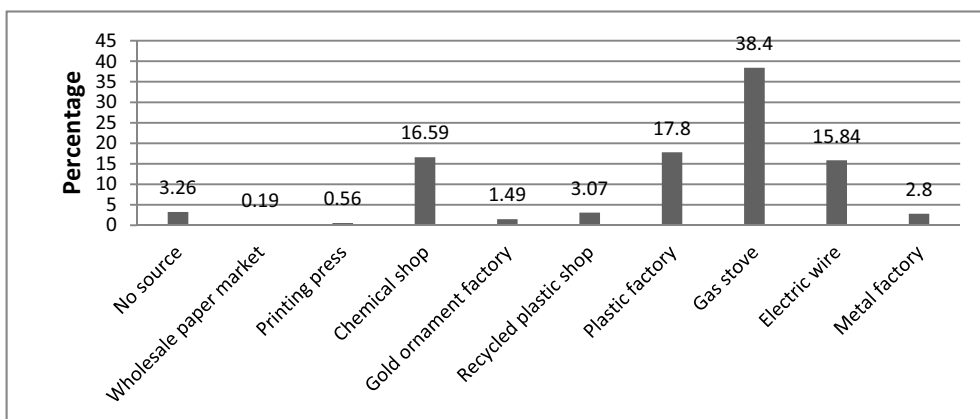


Figure 14: Existence of fire sources in the study area



Figure 15: Electric pole and transformer in front of building



Figure 16: Narrow road within buildings

5. MAJOR FINDINGS

Severe fire incidents have occurred in ward 65. From the fire vulnerability analysis it has been found that maximum numbers of buildings of the study area are highly vulnerable (55.66%). Most of the highly fire vulnerable buildings are located in Islambag Road. Buildings of Water works Road and Lalbag area are less vulnerable because of being residential areas with mixed commercial use.

27.27% critical facility was found to be within the highly fire vulnerable areas. Most of these facilities (63.64%) are situated in the low risk zone. So critical facilities of the study area are moderately vulnerable to fire.

Population density in the high risk zone is high and the area consists of plastic recycling and processing industries. In these factories generally woman and child labors work. So it can be said that the area is socially vulnerable to fire hazard.

Most of the buildings of the study area have different kind of economic activities. Only 36.9% buildings are residential with no economic

activity. 20.22% buildings have plastic manufacturing and processing industries which is highly vulnerable to fire hazard.

Most of the buildings (41.82%) have 3 feet wide staircase. 18.55% households have only 0-5 feet roads in front of their houses which is inaccessible for fire truck. Besides, electric pole is located in front of 13.51% buildings and transformer is located in front of 11.37 % building. 96.74% buildings of the study area have different type of fire sources. In this respect this community is vulnerable to fire hazard.

6. CONCLUSIONS

Urban fire incidents have been determined to have a high likelihood of occurrence in our country. But no mentionable fire risk assessment has been performed although fire hazard characterization information is available in the Fire Service and Civil Defense (FSCD). In this study after conducting vulnerability assessment using Community Vulnerability Assessment Tool (CVAT), it is found that ward 65 is vulnerable to fire hazard. The land use pattern of ward 65 indicates the possibility of this kind of hazard. The area comprises of residential use as well as commercial and industrial uses like plastic manufacturing and processing factory and chemical factory which may induce massive fire. As being a mixed use residential area, the loss due to fire may be catastrophic. To minimize the social and economic loss, Mitigation Planning is required. A change in present land use pattern is required. Chemical factory and plastic factory should be relocated. Road network as well as staircase of building should be wider to evacuate the community people. Community awareness should be raised. Although CVAT has been applied in this small area of Dhaka city, it can be applied to any type of hazard in any location of the country both at micro and macro levels.

REFERENCES

Lisa, K. Flax, Russell, W. Jackson and David, N. Stein (2002) "Community Vulnerability Assessment Tool Methodology" *Natural Hazards Review* Vol. 3 (ISSN 1527-6988), 162-176.

<http://www.surveysystem.com/sscalc.htm>, accessed on 25th March, 2011.

BNUS field survey, 2012.

Vulnerability assessment of snow disaster based on traffic system: A Case Study of Chenzhou City in Hunan Province

Xiaoge XU¹, Jing'ai WANG², and Takaaki KATO³

¹ Graduate Student School of Eng., The University of Tokyo, Japan
xuxiaoge@city.t.u-tokyo.ac.jp

² Professor, School of Geography, Beijing Normal University, China

³ Associate Professor, ICUS, IIS, The University of Tokyo, Japan

ABSTRACT

From January to February in 2008, a 50-year snow disaster was occurred in South China, and Chenzhou City, which is located in the southeast of Hunan Province, became one of the hardest affected areas in this disaster. The paper establishes pattern of urban snow disaster system based on the theory of regional disaster system, which consist of factors concerning hazards, hazard-formative environments and disaster affected bodies. The disaster chain is also drawn and indicates that traffic system and lifeline system which are the primary disaster affected bodies in urban areas are also the medium exacerbating damages. In this case, the paper sets up a vulnerability assessment index framework mainly based on traffic system, and applies it in Chenzhou City. The results of assessment indicate that obvious geographical differences exist in the vulnerability of snow disaster affected bodies. Furthermore, improved model involving meteorological index is also used to assess the vulnerability of disaster affected bodies under diverse hazardous conditions considering the dynamic characteristic of hazard-formative environments. The data shows that the vulnerability of traffic system in Chenzhou City obviously increases in 2008 winter compared with 2007.

Keywords: urban snow disaster system, disaster chain, vulnerability assessment of lifeline, China.

1. INTRODUCTION

The 50-year snow disaster occurred from January to February in 2008, affected 17 provinces and more than 100 millions victims were affected in South China. Chenzhou City, which is located in the south-east of Hunan Province, was one of the hardest affected disaster areas. Over 4 millions victims were affected in this city, and the constant snow led the city become an isolated island because of the interruption of traffic and electricity system.

The problem of urban snow disaster has been increasingly prominent; however, compared with other types of disasters, the research on urban snow disaster is much fewer at present. Existing study of snow disaster is focused on climate change and disaster prediction (Weisman, 1996; Onton, 2001) or the pollution problem of urban snow remnants (Viklander, 1996; Engelhard and de Toffol,

2007). Japan, as a high-urbanization and snowstorm-prone country, is more mature in the field of urban snow disaster. Urano et al. (1987) studies the impact of snow slide on urban area based on runoff characteristics; Tomabechi et al. (1997) pointed out that snow damages caused by snowstorms are strongly influenced by the wind velocity and temperature and snow disaster break out more easily in Hokkaido than in the Hokuriku districts according to the survey from 1971 to 1990; Kaneda et al. (1997) focused on the evacuation facilities under the situation of snow disaster; Sugimori and Sano (2002) set up the theory of urban snow disposal system and applied it in Tokamachi. There are also some studies on the evaluation of the damage of urban snow disaster, which mainly focus on the extent of economic losses (Umemura et al., 1993) or the extent of buildings affected snow pressure (Suzuki et al., 1991). Research on the vulnerability of natural disasters in China began in the 1990s; however, the research was primarily aimed at other types of disaster, such as drought (Sang and Shi, 1998), earthquake (Xu et al., 2004), fog (Wang, 2004), etc. Hao et al. (2003) used the example of pastoral areas of Inner Mongolia to assess the vulnerability of animal husbandry, but the urban disaster affected bodies are completely different from the ones in pastoral areas, and the evaluation model cannot directly be applied in urban areas.

As stated above, the damage of urban snow disaster has been aggravated, while the research on this problem is still little concerned about. In this situation, the paper establishes the patterns of urban snow disaster system and disaster chain based on the theory of regional disaster system (Shi, 1996). In addition, the paper sets up the vulnerability assessment index framework mainly based on traffic system, and applies them in Chenzhou City, so that to provide scientific basis for disaster reduction decision-making.

2. URBAN SNOW DISASTER SYSTEM AND SNOW DISASTER CHAIN

2.1 Urban snow disaster system

Based on the theory of regional disaster system (Shi, 1996), urban snow disaster system consists of hazards, hazard-formative environments and disaster affected bodies (Figure 1). Hazards (H) mainly refer to the persistent large-scale snowfall. Hazards factors include intensity (H_1), frequency (H_2), duration (H_3), regional range (H_4) of the snowfall, snow depth (H_5), land surface temperature (H_6) and the land surface slippery level (H_7).

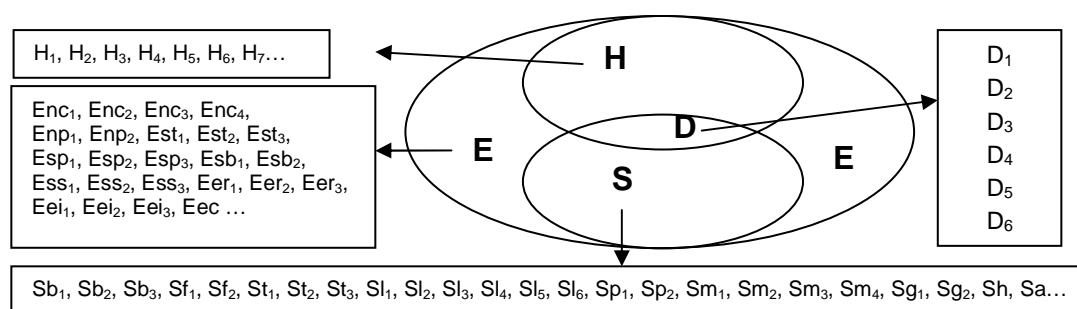


Figure 1: Urban snow disaster system

Hazard-formative environments (E) include natural environment (En), social environment (Es) and economic environment (Ee). Natural environment is concerning with the climatic condition (Enc) and the topography condition (Enp): the former involves average winter temperature (Enc₁), winter precipitation (Enc₂), average annual humidity (Enc₃) and average annual wind velocity (Enc₄); the latter contains slope (Enp₁) and aspect (Enp₂). In social environment, disaster is mainly affected by traffic system (Est, Est₁-Traffic density, Est₂-Accessibility, Est₃-Distribution of street trees), urban population (Esp, Esp₁- Population size, Esp₂-Population density, Esp₃- percentage of vulnerable people), structures (Esb, Esb₁-Density of structures, Esb₂- Constructions of structure) and administrative measures (Ess, Ess₁-Disaster-related laws, Ess₂- Public awareness of disaster, Ess₃-Scientific research on disaster reduction). Economic environment (Ee) mainly refer to disaster preparedness (Eer, Eer₁-Per capita GDP, Eer₂- Industrial output value, Eer₃-Relief supply reserves), inputs of disaster relief (Eei, Eei₁-Relief funding, Eei₂-Relief supplies, Eei₃-the number of labor input) and disaster recovery capabilities (Eec). Urban snow disaster affected bodies (S) cover fixed class and movable class (Table 1).

According to the theory of regional disaster system (Shi, 1996), Damage (D) is the product from mutual combination of hazards, hazard-formative environments and disaster affected bodies. In this urban snow disaster system, damage includes traffic system damage (D₁), human’s health damage (D₂), animals and plants’ health damage (D₃), lifeline system damage (D₄), residents stranded (D₅), structures damage (D₆), etc.

Table 1: Classification of urban snow disaster affected bodies

Fixed Class	Structures (Sb)	Residing house (Sb ₁), Office(Sb ₂), Historical relic (Sb ₃)
	Factories (Sf)	Production line (Sf ₁), Industrial equipment (Sf _s)
	Traffic system (St)	Highway (St ₁), Railway (St ₂), Airport(St ₃)
	Lifeline system (Sl)	Water supply pipes (Sl ₁), Drains piping (Sl ₂), Cable (Sl ₃), Communication network (Sl ₄), Oil and gas pipeline (Sl ₅), Heating pipe (Sl ₆)
	Plants (Sp)	Street tree (Sp ₁), Frost tree (Sp ₂)
Movable Class	Transport machinery(Sm)	Aircraft (Sm ₁), Train (Sm ₂), Car (Sm ₃), Cycling (Sm ₄)
	Flow of goods(Sg)	Transporting goods (Sg ₁), Storage of goods (Sg ₂)
	Human being (Sh), Animals (Sa)

2.2 Urban snow disaster chain

In order to analyze the interaction among hazards, hazard-formative environments and disaster affected bodies, the disaster chain is drawn. Disaster chain is a series of disaster phenomenon caused by some hazard factors, and usually includes serial disaster chain and simultaneous disaster chain. Urban snow disaster chain is initially established by summarizing massive snow disaster cases the disaster system theory (Figure 2).

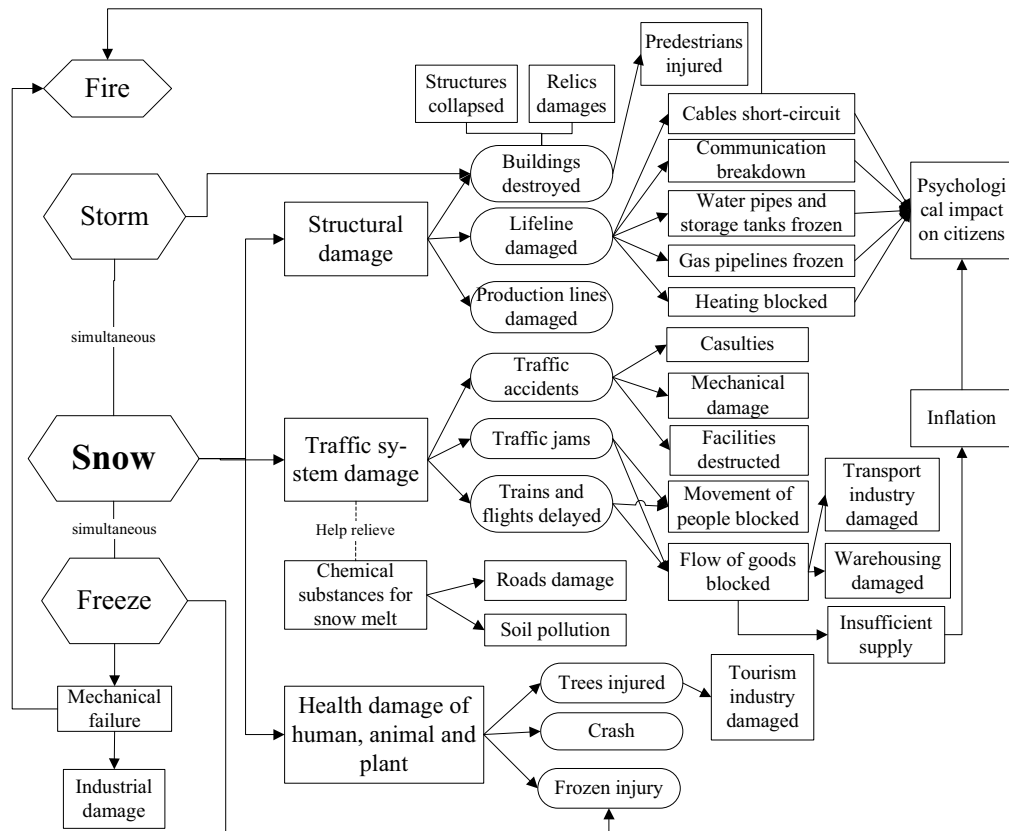


Figure 2: Urban snow disaster chain

From the disaster chain, the urban snow disaster is usually complicated by freeze or storm, brings about a series of secondary disasters such as traffic jams, structural damage, environmental pollution through chain reactions, in which the damage of traffic system and lifeline system is the main cause to exacerbate and enlarge the effects of disaster, blocking the flow of people, goods and information, resulting in casualties and property losses.

3. VULNERABILITY ASSESSMENT INDEX FRAMEWORK OF SNOW DISASTER BASED ON TRAFFIC SYSTEM

3.1 Vulnerability assessment model

Vulnerability assessment methods can be divided into two types: generalized vulnerability assessment which evaluates the whole regional disaster system, and special vulnerability assessment which only focuses on the sensitive extent of human related social and economic system to hazard factors. This paper adopts the generalized one proposed by Shi (2002), as follows (equation 1):

$$V = V_{SE} \cap V_E \cap V_{ST} = f(H, E, \phi, \lambda, h, t) \quad (1)$$

In which V_{SE} is the regional spatial and temporal vulnerability, V_E is the vulnerability of hazard-formative environment, V_{ST} is the vulnerability of disaster

affected body, H is the human system, E is the natural environment system, φ is latitude, λ is longitude, h is the height and t is the time (Shi, 2002). Considering the dynamic characteristic of hazard-formative environments, the urban snow disaster vulnerability assessment model is built up as follows (equation 2 and equation 3):

A. Vulnerability of traffic system under the same hazards condition:

$$V_S = \sum N_{ik} \times W_i \quad (2)$$

In which V_S is the vulnerability of assessment unit k in the same hazard-formative condition, N_{ik} is the normalization value of the disaster affected body vulnerability factor i in assessment unit k , W_i is the corresponding weight of factor i .

B. Vulnerability of traffic system under the diverse hazards condition:

$$V_D = \sum N_{ik} \times W_i + \sum H_{ik} \times W_i \quad (3)$$

In which V_D is the vulnerability of assessment unit k in the diverse hazard-formative condition, N_{ik} is the normalization value of the disaster affected body vulnerability factor i in assessment unit k , H_{ik} is the normalization value of the hazard-formative environment vulnerability factor i in assessment unit k , W_i is the corresponding weight of factor i .

3.2 Vulnerability assessment index of snow disaster based on traffic system

3.2.1 Characteristics of urban traffic disaster affected body

Blaikie et al. (1994) point out that, the key of disaster mitigation is to reduce the vulnerability and increase the resilience capacity of disaster affected bodies due to the difficulty of changing hazard factors. As stated above, according to studies of a great many snow disaster cases, urban snow disaster is exacerbated mainly through the traffic system. Traffic system, which is one of the main disaster affected bodies in urban snow disaster has the following attributes: (1) highway develops fast but also enjoys larger blocking risk than regular roads, especially in snowy and rainy conditions; (2) car traffic is more vulnerable compared to non-motor vehicles or trans; (3) vulnerability of traffic system is closely related to slope of the road: the higher the slope, the larger the vulnerability; (4) vulnerability of traffic system is positively related to the height: the bigger the height, the lower the temperature, the higher the humidity, and the easier for the road surfaces to form ice layer

3.2.2 Vulnerability assessment index

According to the attributes of traffic system as stated above, this paper builds up a vulnerability assessment index framework of urban snow disaster where traffic system is seen as the main disaster affected body. The vulnerability of traffic system is mainly concerned with terrain, topography and traffic capacity. Under some particular conditions such as rain or snow weather, the outage risk of different types of roads should also be considered in the index framework. In addition, according to different snowmelt rates in different aspects, the aspect factor is also involved in the assessment. Follow the principles of importance, comparability and quantitative assessment, five factors is selected: altitude (Al), slope (Sr), aspect (As), regular traffic capacity (Ch), and outage probability (Rt).

Firstly, altitude (Al) is negatively related to road surface temperature and thus the high-altitude area is easily blocked due to snow thawing and accumulating. Secondly, slope (Sr) directly influence the speeds of cars, the larger the road gradients, the slower the cars run and the easier the traffic jam occurs, and in special weather conditions, cars cannot even run in areas where slopes are too large. Thirdly, aspect (As) of road is mainly related to the speed of snow melting. Generally speaking, snow in sunny slope melt faster than those in shady slope, while the half sunny, half shady slope thaws in a medium speed. Fourthly, regular traffic capacity (Ch) is used to measure the transmitting ability of roads in each grade without hazards. Transmitting ability, which is also named road capability or traffic capability means the possible largest number of transmitting objects, including cars or people, in certain position, roadway or fragment, in a time unit. The transmitting ability is designed to be different for railroads or highways in different grades. Lastly, outage probability (Rt) means the possible traffic control that would results in disasters such as road and passenger blocking in special weather conditions including snow and rain. Furthermore, as stated above, snow disaster is mainly caused by the spatio-temporal difference effect of the hazards' intensity and disaster affected body's vulnerability. Considering the dynamic characteristics of hazard formative environment, the paper picks up winter precipitation anomaly percentage (Pw) and winter temperature anomaly percentage (Tw) to investigate the regional diversity of vulnerability under different levels of hazards' intensity.

3.3 Distribution and grading of vulnerability assessment index weights

The assignment of index weight uses the method combined of AHP (Analytical hierarchy process) and expert making method. AHP is a decision-making methods that combines qualitative and quantitative analysis. It is a process that models and quantifies the decision-making person's thinking process of a complex system. The paper compares the related elements in the system, constructs the judgment matrix based on relative importance, and then uses MATLAB programming to calculate the weights. The results would be taken consistency test to ensure the realism of evaluation thinking finally. The weight is shown in Table 2.

Table 2 Vulnerability assessment index and weight of urban snow disaster

Factor	Assessment Index	Symbol	Weight	
			V ₁	V ₂
Vulnerability of regional disaster bearing body	Altitude/m	Al	0.2142	0.1273
	Slope/%	Sr	0.1211	0.0725
	Aspect/°	As	0.0765	0.0462
	Regular Traffic Capacity/ cars per hour	Ch	0.3892	0.2192
	Outage Probability	Rt	0.1990	0.1385
Intensity of Regional Hazards	Winter Precipitation Anomaly Percentage/%	Pw		0.1273
	Winter Temperature Anomaly Percentage/%	Tw		-
				0.2686

Note: V₁ – the same hazard condition; V₂ – diverse hazards condition.

There still remains the problem of unify the dimensions during multi-index modeling. Quantify and grade the above evaluation indexes to unify the dimensions of variable indexes. The value of each grade is assured according to analysis of a great many snow disaster cases. Take slope (SI) for example. Its largest value recommended is 4% and the limitation is 6% when the car speed is 80km/h. While when the car runs at the speed of 20km/h the recommended largest gradient is 8% and the limit is 9%. Besides, the designing standard of regular auto vehicles limits its capable slope at the value of 15%. Therefore, the paper divides slope into four grades: (1) 0% -4%; (2) 4%-8%; (3) 8%-15%; (4) more than 15%.

4. CASE STUDY IN CHENZHOU CITY

4.1 Overview of the study area

Chouzhou City, located in the southeast of Hunan Province, China, is a mountainous area and the terrain of southeastern part is higher than the one of northwest. The cold air is always easily accumulated in the foot of mountains, while the warm air is strong in the high altitude area. The two flows of air are gathered together to become “the Lanning Stationary Front”, which lead Chenzhou to the frozen-prone area. The distribution map of aspect, elevation and slope in Chenzhou is shown as Figure 3. The data of map is calculated using ArcGIS based on DEM data (1: 250000 in 2007) and overlapped with district map.

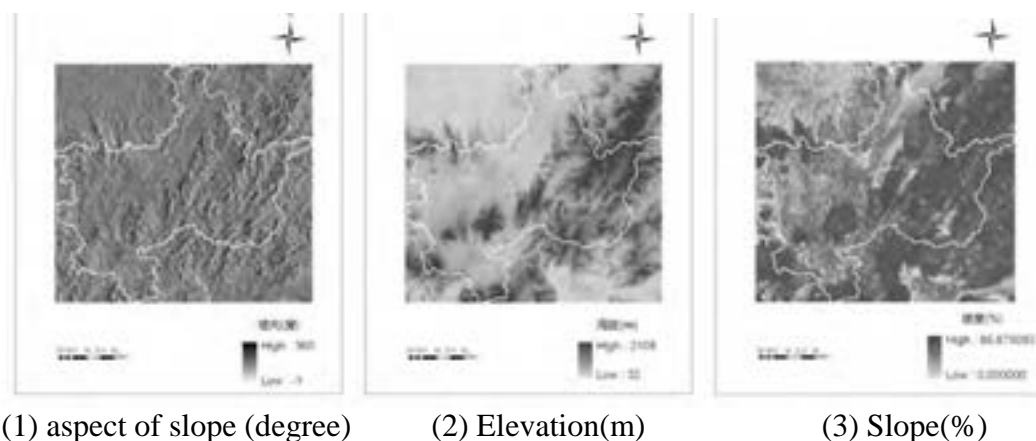


Figure 3: The terrain condition of Chenzhou City

On the other hand, as an inland area with undeveloped water carriage, the main connecting methods of Chenzhou with outside are railroads and trans-territory roads. The traffic system of Chenzhou City has developed fast and its road turnovers have been remaining a constant high growing speed. In the end of 2007, the cargo turnovers of the urban roads reached 8970 million ton km, and its passenger turnovers reached 3940 million person km. The road traffic supports the flows of the whole area, and its influence on the urban disaster affected body in snowy low-temperature weather is direct and huge. In the snow disaster occurred in Jan.2008, road surfaces of highway in length of more than 80 km were covered by ice, and approximately ten thousands of cars and people were blocked in Chenzhou areas.

4.2 Assessment results in Chenzhou City

According to the urban snow disaster vulnerability assessment model, the paper assesses the vulnerability of the main traffic network in Chenzhou for 350m*350m grid as an evaluation unit. The maps use the super-scale to show the roads, which is 10–50 times larger than the original roads. ArcGIS is used to do grid computing, and the distribution map of vulnerability of Chenzhou city under the same hazard condition is drawn. (see Figure 4). The map shows following facts under the same hazard condition. Vulnerability of Chenzhou section of the Beijing-Zhuhai expressway that above 0.3 is the highest in Chenzhou city and the maximum value is 0.360. The total length of roads whose vulnerability above 0.3 in the whole area is 52.5 km, and the Guidong – Qingguangping part of 106 State Road, Mangshan Farm section in Yizhang County, Tuqiao – Yijiang section in Rucheng County and Yangtougiao – Shen-ao part in Zhixing city belong to this high-vulnerability interval. Minimum value in Chenzhou is 0.116, and total length of roads whose vulnerability below 0.2 is 593.6 km. The vulnerability of lateral roads in southwestern region is less than 0.2. Under the same hazard condition, the average vulnerability of Chenzhou city is 0.210.

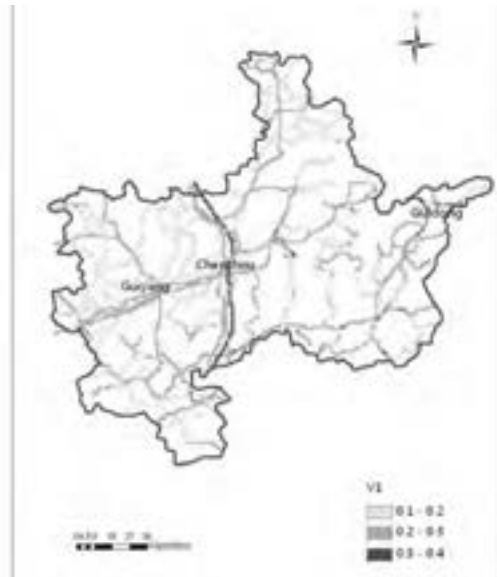


Figure 4: Vulnerability distribution of traffic system under the same hazard

The distribution maps which under diverse hazards condition (data in 2007 and 2008 winter) are also made (Figure 5). Under diverse hazards condition, the maximum value of vulnerability of all research area is 0.228 in 2007 winter, and the region with the maximum value is Guidong –Chetouao section. The total length of roads whose vulnerability above 0.2 is only 8.75 km. The vulnerabilities of Chenzhou section of Beijing-Zhuhai expressway and Chenzhou–Zhixing expressway, main roads in Rucheng County and Mangshan Farm section in Yizhang County are at interval of 0.1–0.2, and the total length in this interval is 300.3 km. Vulnerabilities of roads in most of the southwestern region are less than 0.1, and the total length of roads whose vulnerability below 0.1 reaches 949.2 km, up to 75.4 % of the total length of Chenzhou. The average vulnerability in 2007 is 0.074. In 2008 winter, due to the heavy rainfall and low-temperature, average vulnerability of Chenzhou city obviously increases to 0.219. Max value regions lie in Yizhang–Yongxing section of Beijing-Zhuhai expressway and Datang–Qingguangping section in Guidong County, and the maximum value is 0.335. The total length of roads whose vulnerability above 0.3 reaches 36.05 km. Except for Guiyang County and Anren County which are located in southwest, the vulnerability of main roads in other counties are all more than 0.3. The minimum value of vulnerability in 2008 is 0.122, while the minimum in 2007 is just 0.007.

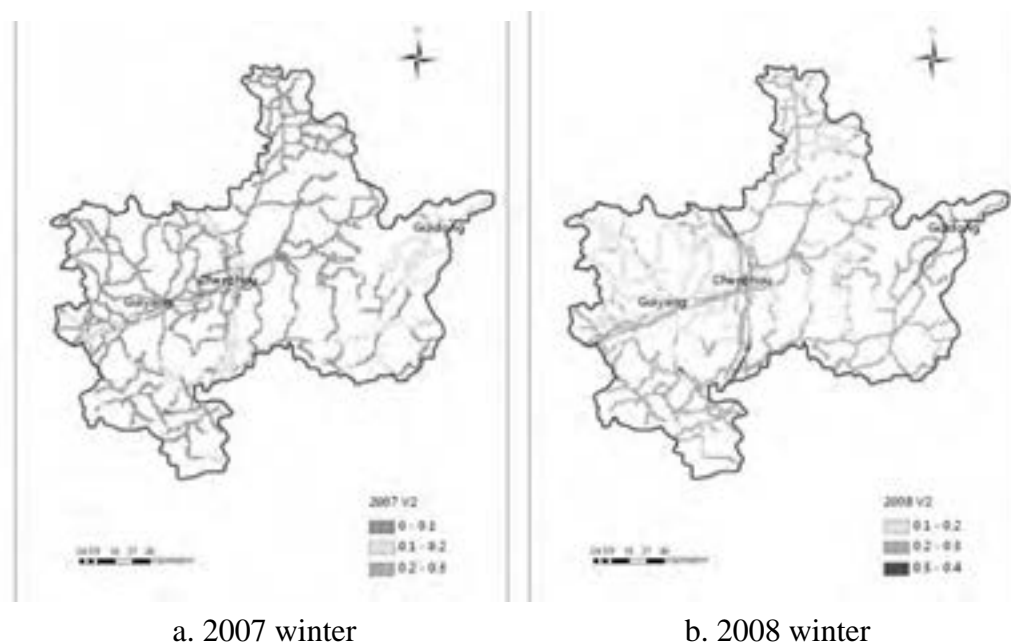


Figure 5: Vulnerability distribution of traffic system under diverse hazards

The assessment result of traffic system in Chenzhou city is shown in Table 3. The results of assessment indicate that obvious geographical differences exist in the vulnerability of snow disaster affected bodies. Firstly, vulnerability of Chenzhou section of the Beijing-Zhuhai expressway is the highest in Chenzhou city, which is due to its higher outage probability and higher traffic capacity. Secondly, the southeastern counties are more vulnerable than the northwest region. This is because the altitudes and slope in south eastern counties such as Gongdong County and Rucheng County are higher than the ones in northwest, and the aspects of roads in southeast are mainly ubac or half shady slope. Finally, according to the snow disaster vulnerability dynamic process analysis, the vulnerability of Chenzhou city had an obvious increase in 2008 winter compared with that in 2007 winter. This is decided by the weather of low-temperature and heavy rainfall.

Table 3: Vulnerability assessment results of traffic system in Chenzhou

Hazards condition	Vulnerability distribution of traffic system							
	Percentage of the interval covers the total length of roads (%)				Max.	Min.	Average	
	0-0.1	0.1-0.2	0.2-0.3	0.3-0.4				
V ₁	0	46.11	49.81	4.08	0.360	0.116	0.210	
V ₂	2007	75.44	23.87	0.69	0	0.228	0.007	0.074
	2008	0	35.47	61.66	2.87	0.335	0.122	0.219

5 SUMMARY AND CONCLUSION

The paper based on a large number of urban snow disaster cases, establishes urban snow disaster system and urban snow disaster chain for the first time, which reveals the mechanism of snow disaster and how it was affected by hazards, hazard-formative environment and disaster affected body. The disaster chain

indicates that the vulnerability of traffic system and the lifeline system is the main respect to exacerbate the snow disaster. The vulnerability assessment index system of urban snow disaster based on traffic system is set up for the first time. The assignment of index weights uses the method combined of AHP and expert rating, and then the paper builds up the urban snow disaster vulnerability assessment model, which provides the foundation for evaluation. The paper applies the vulnerability assessment model in Chenzhou city, Hunan, China. The assessment results show that obvious geographical differences exist in the vulnerability of snow disaster affected bodies, which mainly due to the topography diversity. According to the snow disaster vulnerability dynamic process analysis, the vulnerability of Chenzhou city obvious increases in 2008 winter compared with 2007 winter, because of the weather of low-temperature and heavy rainfall in 2008 winter.

For the reason of data acquisition difficulty, the paper is still insufficient in vulnerability assessment of traffic system. The next step on this research is to consider include the buffer zone of roads, its population density and economic index. The evaluation objects will also be extended to urban lifeline systems and structures to further improve urban snow disaster vulnerability assessment index system, and to make it more applicable.

REFERENCES

- Blaikie, P.T. Cannon, I. Davis and Wisner B., 1994. *At Risk: Natural Hazards, People's Vulnerability, and Disasters*, Routledge, London,
- Engelhard, C. and de Toffol S, 2007. Environmental impacts of urban snow management- The alpine case study of Innsbruck [J]. *Science of the Total Environment*, 382:286-294.
- Hao L., Wang J. and Shi P., 2003. Vulnerability assessment of regional snow disaster of animal husbandry: taking pasture of Inner Mongolia as an example [J]. *Journal of Natural Disasters*, 12(2):51-57. (In Chinese)
- Kaneda Y., Masamichi E. and Aratani N., 1997. Evacuation plan in the snowy areas[R]. *Science Synopsis Album.D-1*, (9):949-952. (In Japanese)
- Onton D.J. , 2001. Diagnostic and sensitivity studies of the 7 December 1998 great Salt Lake-effect snowstorm[J]. *Mon. Wea. Rev.*, 129:1318-1338.
- Maria Viklander, 1996. Urban snow deposits-pathways of pollutants[J]. *The Science of the Total Environment*,189/190:379-384.
- Sang,Y., Shi, P.,1998. Discussion on the role of anthropogenic factors in the forming of agricultural drought disaster process[J]. *Journal of Natural Disasters*, (4):35-43. (In Chinese)
- Shi, P.,1996. Theory and practice of disaster study[J]. *Journal of Natural Disasters*, 5(4):6-17. (In Chinese)
- Sugimori, M. and Sano,H., 2002. Theory and application of network analysis of urban snow disposal system[C].*Proceedings of Urban Forum in the northern Aomori Cities*:17-20. (in Japanese)
- Suzuki, T. Kitara, M. and Takahashi A., 1991. Study on Evaluation of Urban Snowy Risk for Each District[R]. *Journal of Archit.Plann. Environ. Engng. AIJ.B*, (9):59-62. (In Japanese)

- Tsukasa,T., Yamagata,T. and Yamamoto, H., 1993. Analysis of snow damages from the planning of a region development and construction [J]. *Journal of Archit.Plann.Environ.Engng.AIJ*, 447(5):61-68. (In Japanese)
- Umemura,T., 1993. Study of Amount of Snow Damage in an Urban Area with Heavy Snowfall [J]. *Japan Society for Natural Disaster Science*, 14(1):77-86. (In Japanese)
- Urano,S. Takeshi,T. and Yamamoto,H.,1987. Runoff Characteristics of the Toyohora River and Effects of Snow Dumping on Them, in the Sapporo Urban Area[J]. *Journal of Environmental Science in Hokkaido University*, 3:49-60. (In Japanese)
- Wang, Z. and Wang, J., 2004. Discussion on several relative problems of fog disaster[J]. *Journal of Natural Disasters*, 13(2):134-139. (In Chinese)
- Weisman.R.A., 1996. The Fargo Snowstorm of 6-8 January 1989[J].*Weather Forecasting*, 11:198-216.
- Xu,W., Wang, J. and Shi,P., 2004. Hazard degree assessment of urban earthquake disaster in China[J]. *Journal of Natural Disasters*,13(1):9-15. (In Chinese)

The seismicity in Mongolia

Baigalimaa GANBAT

Researcher, Research Center Astronomy and Geophysics Of Mongolian
Academy of Sciences, Ulaanbaatar, Mongolia

baigalaa@rcag.ac.mn

Baigalimaa GANBAT¹, Ulziibat MUNKHUU²

¹ Researcher, Research Center Astronomy and Geophysics Of Mongolian
Academy of Sciences, Ulaanbaatar, Mongolia

baigalaa@rcag.ac.mn

² Head of Seismological Department, Research Center Astronomy and Geophysics
Of Mongolian Academy of Sciences, Ulaanbaatar, Mongolia

ABSTRACT

The Mongolian Seismological Observatory was established in 1957 – the International Year of Geophysics – with an analog seismic station (SKM-3) on the foundation of our center (Research Center of Astronomy and Geophysics of Mongolian Academy of Sciences - RCAG, MAS). The same year, the 4 December 1957, the strong Gobi-Altay earthquake occurred ($M_w=8.1$). It confirmed the high seismic activity (three other events with magnitudes more than 8 occurred the 1905/07/9, the 1905/07/23 and the 1931/08/10) and the hazard associated with it in Mongolia despite this high activity, associated with India-Asia collision, seems to be abnormally high during the XX century.

Seismic activity of Mongolia is associated with the deformation induced by the world largest collision, the collision between India and Eurasia. Mongolia is located at the transition between compressive structures associated to India-Eurasian collision and extensive structures localized in north of the country as Hövsgöl area and Baykal rift Unlike earthquakes that occur along plate boundaries, continental earthquakes are widely distributed over large regions and typically have shallow depths, in the range of 10 to 25 km beneath the surface. Major continental earthquakes usually occur along seismically active faults, which individually have very long recurrence intervals (in the range of several thousand years). Late Quaternary deformation in Mongolia is distributed over a vast region, and includes a full spectrum of deformation styles and structural orientations. At the north, the activity is dominated by the Baikal rift and the Hövsgöl, Busiingol and Darhad grabens with a transfer zone following the Tunka Basin. At the west, the activity is related to the deformation of the Altai range, characterized mainly by right lateral strike-slip motion. The occurrence and distribution of strong earthquakes are related to these widespread and varied styles of deformation.

Keywords: seismicity, seismic activity

1. INTRODUCTION

Since 1957 is started instrumental seismological study in Mongolia. Mongolia has experienced four major earthquakes ($M_s > 8$) and many more moderate earthquakes (M_s 5.3-7.5) in this century. The seismic activity in Mongolia is related to its location between the compressive structures associated with the collision of the Indian and Eurasia plate with the Eurasian plate on the one hand and the extensional structure associated with the Baykal rift system on the other. The historical records (1903 onward) of the seismicity in Mongolia show a high concentration of seismic activity along the Mongolian-Altay, Gobi-Altay, Khuvsgul Darkhad, Bolnay ranges and around Mogod east of Hangay mountain.

2. SEISMIC STATION NETWORK

In the Mongolian seismic station network has running renewed digital regional 9 seismic stations with one component short period seismometer, surrounding Ulaanbaatar has working 5 telemetric digital stations. Since 2000, we have installed 5 mini array with seismic, infrasound, radionuclide stations and in real time to MNDC. And now has working 6 accelerographs, surrounding Ulaanbaatar has working 3 accelerographs and in the west part of Mongolia has working 3 accelerographs. Data acquisition and interpretation of all stations are going on Mongolian National Data Center of Research Center of Astronomy & Geophysics of Mongolian Academy of Sciences (MNDC, RCAG, MAS). The quality of research study is improving by influence of enlargement of seismic station network with modern high sensibility seismic station and great seismic database. (Figure.1)



Figure.1 Seismic station network of the Mongolia

3. SEISMIC ACTIVE ZONE OF MONGOLIA

Most events are located in the west and the north Mongolia as the Khuvsgul active rifting zone and the Altay transpression zones. In the south Mongolia, the active is concentrated near the Gobi-Altay zone. The center of Mongolia, the Hangai dome, looks relatively a seismic and we can clearly track the boundary of the dome by its seismic activity as at the north and east border of Hangai dome where are active Bolnay and Mogod zones. South of Ulaanbaatar, at around 180-250 km, is a clear EW seismic elongated zone near the Deren city. In the eastern part of Mongolia, the seismic activity is low. (Figure.2)

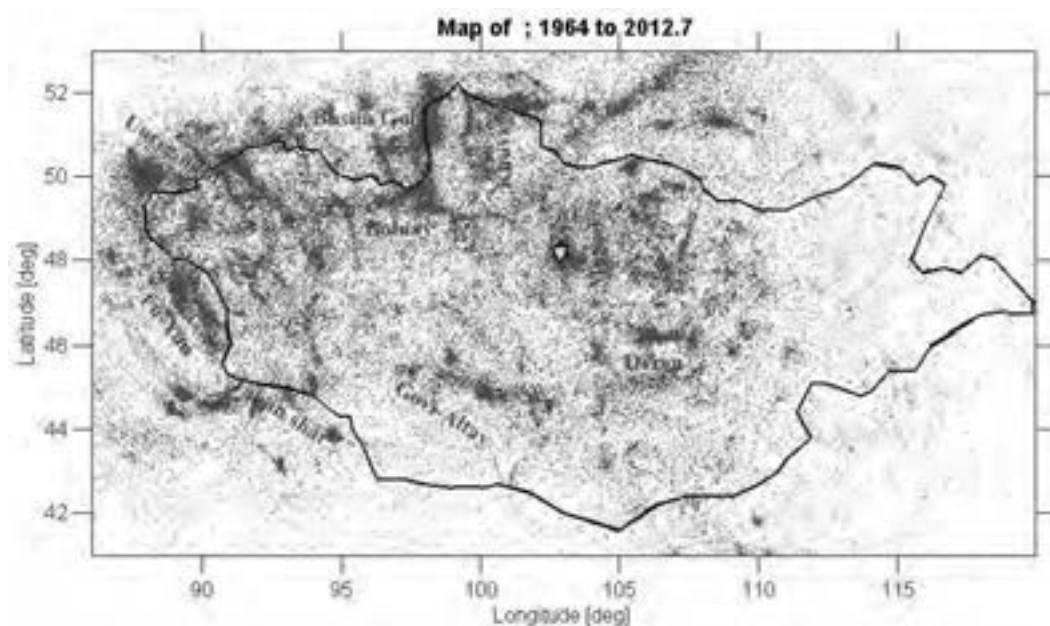


Figure.2 Seismic activity zone

Gobi-Altay

The Gobi-Altay zone is oriented EW active faults connected or parallel to the Bogd fault which ruptured during the Gobi-Altay earthquake (4 December 1957) with $M_w=8.1$ and 270 km of surface rupture. They are all oriented EW, associated to left lateral strike-slip with a small reverse component. The geodynamic behavior of all this area is considered homogeneous. The eastern end has been defining where there is no any large known structure (more than 100 km long) and where the EW morphology of the Gobi-Altay range disappears. We extended the zone to the east of Dalanzadgad by 150 km. Bayasgalan et al., (1999) showed that the end of large strike-slip faults often turn and are associated with thrust faulting. The Unegtei and the Buuryn Hyar active faults are most likely the eastern limit of Gurvan Saihan faults zone. Nevertheless, we extended the eastern limit of the Gobi Altay zone more to the east in order to assure that large Gurvan Saihan strike-slip faults zone is taken into consideration.

Bolnay

The Bolnay zone lies between Hangai Dome and Khuvsgul extensional zone. From geological and seismotectonic data, the left lateral strike-slip fault is predominant. In this zone occurred two large earthquakes, Tsetserleg earthquake (July 9 1905) with $M_w=8.0$ and 190 km of surface ruptures and the Bolnay earthquake with $M_w=8.3$ and 455 km of surface ruptures (Schlupp 1996). The seismicity seems connect the Tsetserleg fault with the Busiin-Gol rifting. The seismicity recorded along Bolnay fault is more concentrated in the middle of the structure.

Hangay

Khuvsgul and Busiin-Gol zone is one of extension zone. The area produces high seismic activity and the largest earthquake occurred on 27th December, 1991, called Busiin-Gol, with magnitude of $M_w=6.5$. The seismicity of Khuvsgul zone is complex. There are three seismic NS basins: Busiin-Gol, Darhad and Khuvsgul lake area. Most of epicenters are concentrated in the Busiin-Gol zone connected with the Sayan active zone to the west and the Baikal active rifting zone to the NE.

Mogod

The Mogod zone is oriented NS with right lateral active faulting. On the 5th January, 1967 a large earthquake occurred with $M_w=7.2$ and produced more than 45 km of surface rupture (Bayasgalan, 1999). Mogod zone shows a local high concentration of earthquakes.

Ulaanbaatar

Ulaanbaatar seismotectonic zone contains a large and wide topography, clearly different from adjacent zone. The main orientation of this smoothed relief is N30. The geodynamic behavior seems to be related with some recent general uplift as indicated by several rivers incising the relief. We include into this zone the seismic active area of Deren where took place a recent event felt at Ulaanbaatar ($M_w=5.6$, 1998/09/24; $M_s=5.2$, 2010/01/09;). This zone is located around 180 km south from Ulaanbaatar city. The seismic activity Deren zone is oriented EW.

4. SEISMICITY

The map of “One century of seismicity in Mongolia 1900 - 2000”, published by RCAG in collaboration with DASE, displays the known seismic activity of the whole Mongolia during the XX century and shows several characteristics of the area. (Figure.3) We collected three kinds of seismic data: international published data (before 1964), seismic data recorded by the Mongolian seismic network consisting in 10 analogical seismic stations (1964-2000) and completed since 1994 by several digital telemetric stations widespread around Ulaanbaatar city and in western Mongolia.

The largest known historical earthquakes in Mongolia area was the 10 August 1931, 09 and 23 July, and 04 December 1957 which are called Mongol-Altai (Fu-Yun), Bulnai, Tsetserleg and Gobi-Altay earthquakes whose size (estimated moment magnitudes more than 8) and location (somewhere in western Mongolia). The largest instrumentally recorded natural earthquake in Mongolia was a magnitude 7.0 in 05th January, 1967; Tsagaan shiveet 1970, magnitude 7.0; Tahiin-Shar 1974, magnitude 6.7; Buteel 1989, magnitude 5.6; Busiin-Gol 1991, magnitude 6.5; Deren 1998, magnitude 5.6.

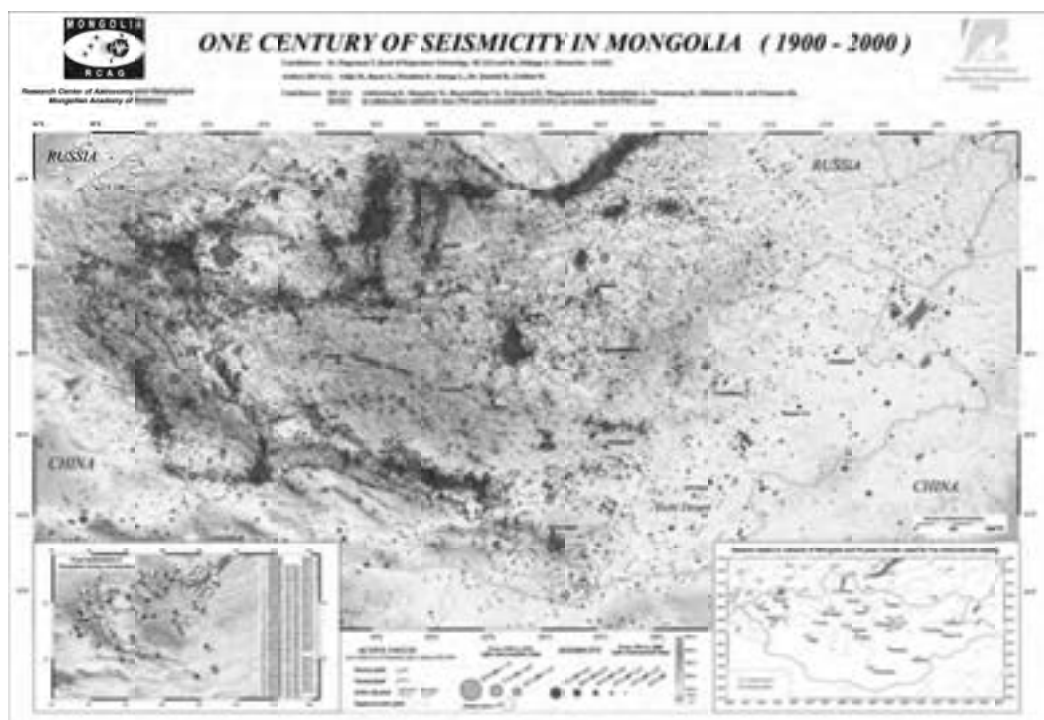


Figure.3 Seismicity of Mongolia (1964-2000 $M_I \geq 2.5$)

Since 2000, moderate earthquakes occurred Chuya 2003, magnitude 7.3; Bogd 2006, magnitude 5.8; Tushig 2006, magnitude 5.2; Gobi-Altay 2007, magnitude 5.4; Bayanteeg 2009, magnitude 5.15; Deren 2010, magnitude 5.0; Gobi-Altay 2011, magnitude 5.19; Bayantsagaan 2011, magnitude 5.2; Khankhnogor 2011, magnitude 5.8; Nomgon 2012, magnitude 5.1; Fu-Yun 2012, magnitude 5.4. (Figure.4)

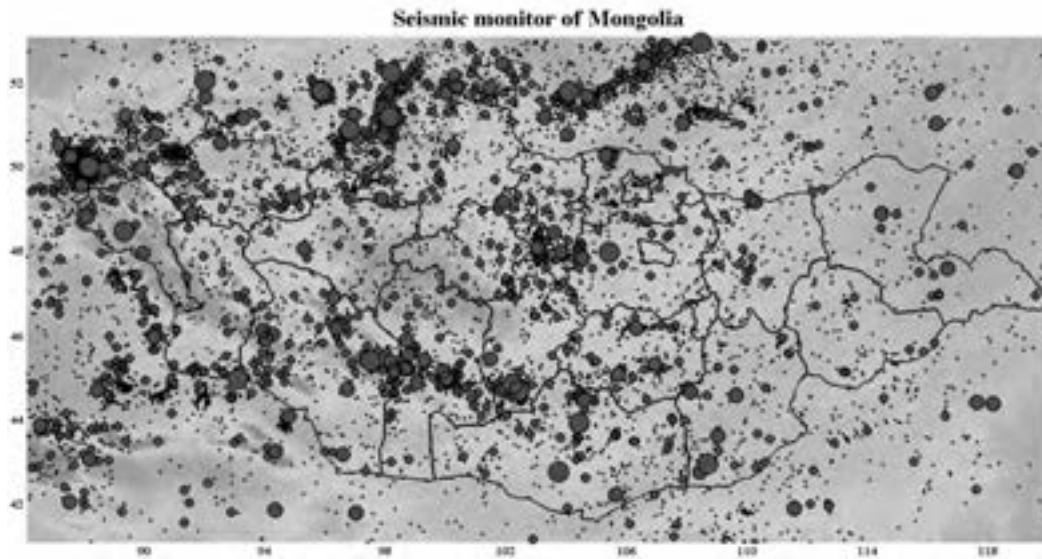


Figure.4 Seismicity of Mongolia (2001-2012.07 MI \geq 2.5)

The Figure.5 shows Gutenberg-Richter relation calculated magnitude between 1900 to 2012.07. We can obtained $a=6.07$ and $b=0.678$ for magnitude. This low value of b is consistent with relatively high number of large earthquakes and parameter “ a ” characterized the number of events.

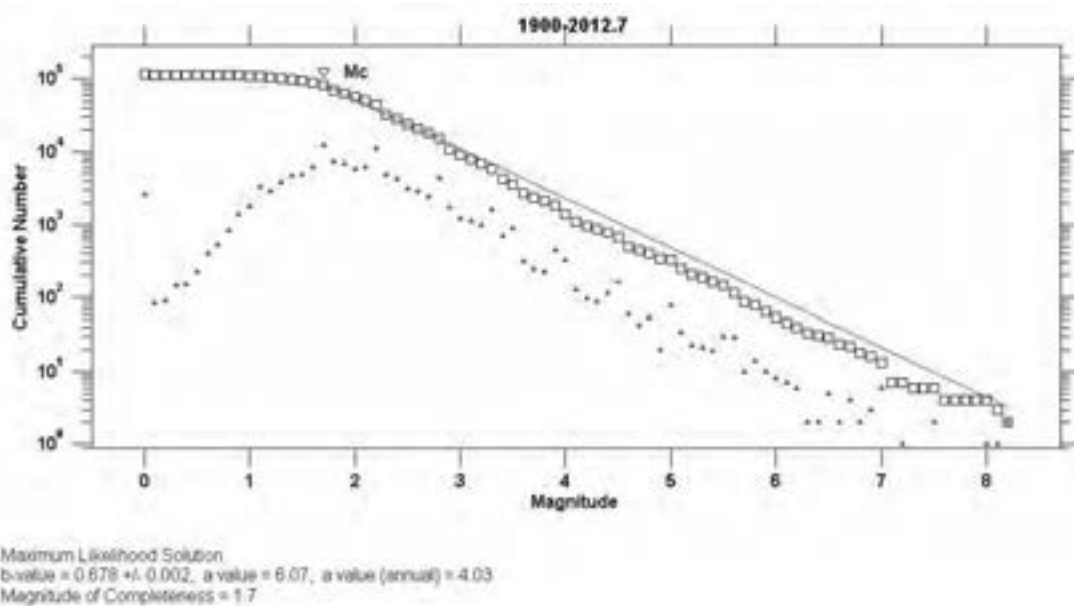


Figure.5 Gutenberg-Richter relation using magnitude between 1900 to 2012.07.

From 1900 to 1963 are reported more than 300 earthquake, with magnitude 3.5 and 8.2 including four large events. The Figure.6 shows the maximum magnitude distribution with time. (1902-2012.07)

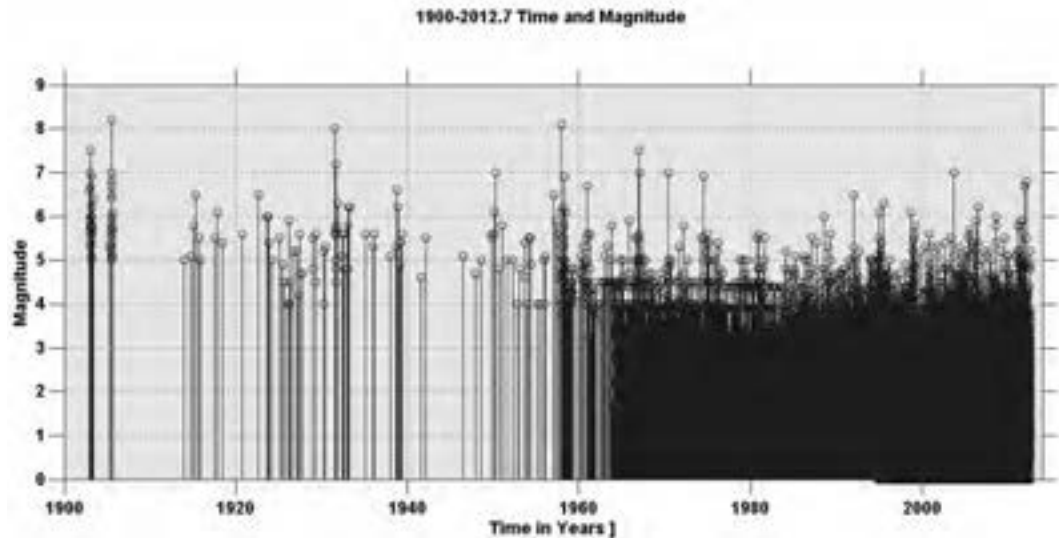


Figure.6 Distribution of the magnitude and time in Mongolia (1902-2012.07)

The Figure.7 shows the cumulative number of events function of time. We can see the increasing of detected event starting from 1994, when our network upgraded. The increasing in 1991, 2003 are related to the numerous aftershock related to the magnitude 6.5 event.

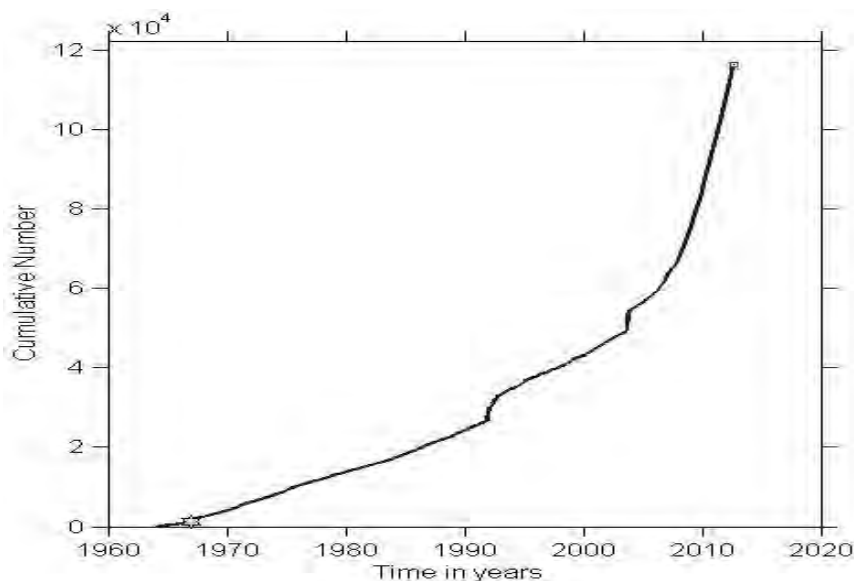


Figure.7 Cumulative number of events time (1902-2012.07)

REFERENCES

Baljinnyam, I., A. Bayasgalan, B.A. Borisov, A. Cisternas, M.G. Dem'yanovich, L. Ganbaatar, V.M.Kochetkov, R.A. Kurushin, P. Molnar, H. Philip, and Y.Y. Vashchilov (1993), Ruptures of Major 50th anniversary earthquake conference commemorating the 1957 Gobi- Altay earthquake July 25 – August 08, 2007, Ulaanbaatar - MONGOLIA 11 Earthquakes and Active Deformation in Mongolia and its Surroundings. Vol. Memoir 181 of Boulder, Colorado: The Geological Society of America, Inc.

Bayasgalan, A., Jackson, J., Ritz, J.F., and Carretier, S (1999), Field examples of strike-slip fault terminations in Mongolian and their tectonic significance, *Tectonics*, 18, 394-411.

Bayasgalan A and J. A. Jackson (1999). A re-assessment of the faulting in the 1967 Mogod earthquakes in Mongolia, *Geophys. J. Int.* 138, 784-800.

Khilko S.D., R.A. Kurushin, V.M. Kochetkov, L.A. Misharina, V.I. Melnikova, N.A. Gilyova, S.V. Lastochkin and D. Monhoo, (1985). Earthquakes and the base of the seismic zoning of Mongolia. Vol. 41 of The joint Soviet-Mongolian scientific - Research Geological Expedition. 225 p.

ONE CENTURY OF SEISMICITY IN MONGOLIA (1900–2000): Coordinators : Dr. Dugarmaa T., and Dr. Schlupp A. ; Authors : Adiya M., Ankhtsetseg D., Baasanbat Ts., Bayar G., Bayarsaikhan Ch., Erdenezul D., Mungunsuren D., Munkhsaikhan A., Munkhuu D., Narantsetseg R., Odonbaatar Ch., Selenge L., Dr. Tsembe B., Ulziibat M., Urtnasan Kh. and in collaboration with DASE since 1994 and its scientific (DASE/LDG) and technical (DASE/TMG) teams., Research Centre of Astronomy & Geophysics of the Mongolian Academy of Sciences (RCAG), Mongolia and Laboratoire de Teledetection et Risque Sismique, BP12, Bruyeres le Chatel, France 2003

Schlupp A. (1996): Neotectonic of western Mongolia using field, seismological and remote sensing data. Laboratoire de Sismologie et de Physique de la Terre, Ecole et Observatoire de Physique du Globe de Strasbourg - Université Louis Pasteur de Strasbourg, PhD, 1 map, 270 pages, in french.

Schlupp A and Cisternas A. (2007), Source history of the 1905 great Mongolian earthquakes (Tsetserleg, Bolnay), *Geophys. J. Int.* (2007) 169, 1115–1131, doi: 10.1111/j.1365-246X.2007.03323.x

Ulziibat M, (2006) The 2003 Chuya sequence “North Altay range”, PhD, Doctor of Sciences, University of Nice, Geosciences Azur, France, 172 p.

Seismic hazard of Ulaanbaatar City

Chimed ODONBAATAR

Project Researcher, Research Center Astronomy and Geophysics Of Mongolian Academy of Sciences,
Ulaanbaatar, Mongolia
odon@rcag.ac.mn

ABSTRACT

The main active faults near the capital of Mongolia, Ulaanbaatar with about 1.2 M inhabitants, are located at less than 20 km and could produce large earthquakes with magnitude up to 7.5. This active fault can produce ground motion intensity VII-IX at the Ulaanbaatar basin area. Another hand the city is built on a sedimentary basin, of a thickness up to 100 meters, which may generate site effects. To quantify their impact on the amplitude and the duration of the ground motion, according to the frequency, I used weak motion, at 32 sites, and ambient noise records, at 104 sites. For that, I applied horizontal to vertical (HV) and sedimentary to rock site (SSR) spectral ratio. An analysis of the reliability of the results shows that the HV ratio amplitude varies in relation to the noise level and that when there is a particular local noise source the amplified frequency polarizes itself perpendicularly to the source direction.

A velocity structure of the basin, determined by 3 microtremor array measurements, and a 3D digital model of the basin were used to produce 1D and 2D simulations. The amplified frequency (HV) is well explained by the 1D simulation but the shape of the peak (SSR) fits better with the 2D simulation. At the end amplified frequency zoning deduced from observation and theoretical calculation results.

Capacity building of seismic disaster risk management in Ulaanbaatar City

Masaru ARAKIDA, Sei'ichiro FUKUSHIMA, Yujiro OGAWA
JICA Expert Team, The Project for Strengthening the Capacity of
Seismic Disaster Risk Management in Ulaanbaatar City, Mongolia
ma-arakida@adrc.asia

ABSTRACT

Government of Mongolia and government of Ulaanbaatar city are promoting Earthquake Disaster Management in Ulaanbaatar city since several active faults near Ulaanbaatar city were found recently. In this paper, Project titled as "CAPACITY BUILDING OF SEISMIC DISASTER RISK MANAGEMENT IN ULAANBAATAR CITY" which is now implementing as by JICA is introduced. The Project consists of Earthquake Risk Assessment in UB city, Building Construction Guideline, Urban planning for safer city and Earthquake disaster education.

Keywords: Mongolia, earthquake, risk management, risk map, education

1. INTRODUCTION

In UB, the capital of Mongolia, the number of unfelt earthquakes has been increasing since 2005; especially its trend has been more obvious after 2009. A French research institute pointed out in 2010 that UB City and its suburbs are surrounded by 4 faults including newly discovered ones which might cause the earthquakes of Magnitude 7 (M7) level. Also according to the 2000 simulation by National Academy of Mongolia, it is predicted that approximately 300 buildings and 60,000 citizens would be affected if the M7 level earthquake hits UB City.

2. PROJECT OUTLINE

2.1 Objectives

To strengthen the capacity for seismic disaster risk management in UB City and to transfer relevant skills and technologies to personnel concerned with the Project

2.2 Remarkable Outcomes

Followings are outcomes of this project;

- Formulation of integrated seismic risk map for UB,
- Revision of regional seismic disaster risk management plan,
- Preparation of the draft construction guideline for middle-high storied building considering seismic disaster risk resilient urban development, and,
- Capacity development of the relevant authorities and citizens in seismic disaster risk management.

2.3 Project Implementation Policy

Eleven policies listed below are employed in conducting the project;

- Maximum utilization of existing technology in Mongolia,
- Formulation of achievable seismic disaster risk management plan,
- Utilization of ground motion Intensity map by Mongolia Academy of Science,
- Proposal of early warning system utilizing existing infrastructures,
- Establishment of scenario earthquakes,
- Enhancement of ownership by participation of CPs and promotion of close cooperation among relevant organizations,
- Importance of capacity development and implementation of capacity assessment,
- Fulfilling publicity activities utilizing media such as TV, Radio and Internet,
- Importance of emergency drill and education at schools,
- Seismic Risk Mitigation Awareness Campaign in UB City, and,
- Establishment of SC and WG

2.4 Project Schedule

Figure 1 shows the brief schedule of the project.

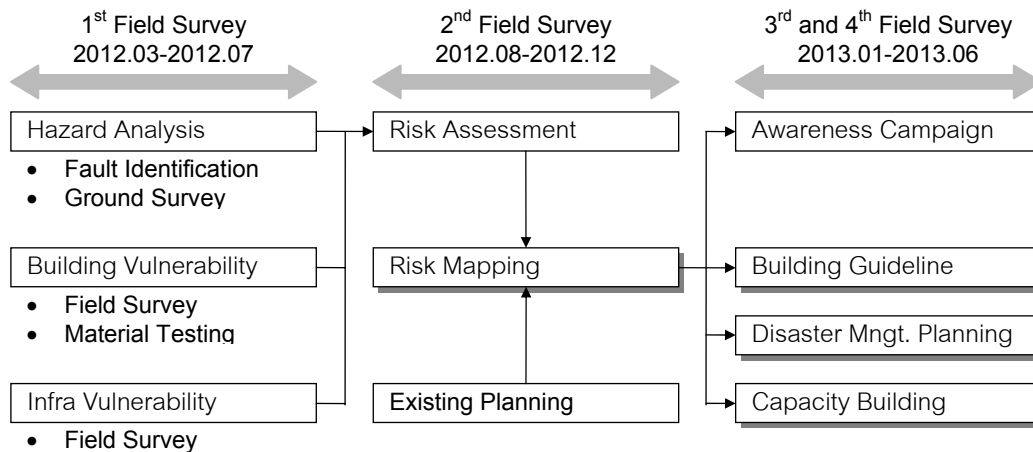


Figure 1 Project Schedule

3. OBJECTIVE AND METHODOLOGY

3.1 Risk Evaluation

3.1.1 Earthquake Scenario

Two scenarios are employed in this project; (1) ground motion by Hustai Faults, and (2) larger ground motion by Emeelt Fault or Gunjiin Fault. The former corresponding to the current ground motion intensity in UB, and the latter is employed as the worst case.

The characteristics of the faults are summarized in Table 1 with moment magnitude M_w estimated from the size of the fault. Also, Locations of the faults are shown in Fig.1.

Table 1 Characteristics of faults

	Hustai Fault	Emeelt Fault	Gunjiin Fault
Location	Extending to southwest from about 30 km southwest from central Ulaanbaatar city	southwest 15 km from Ulaanbaatar city	Extending to northeast from 5km northeast distance from Ulaanbaatar city
Strike	NE-SW	NW-SE	NE-SW
Dip	SE	NE	unknown
Length	80 km	About 30 km	15-20 km

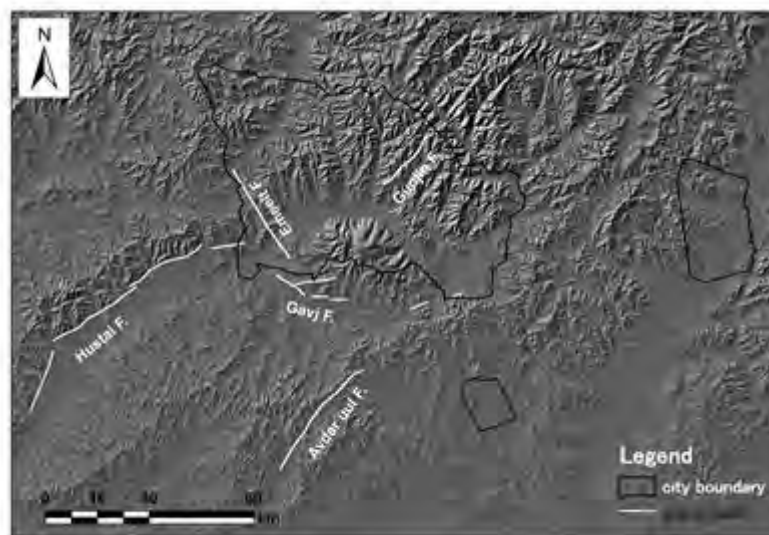


Figure 2 Locations of faults

3.1.2 Ground Motion Estimation

The empirical method that gives the stable results are employed to estimate ground motion parameters at given location. The formula by Kanno et al. (2006) is selected for the following reasons;

- It gives peak ground acceleration almost identical to the one used in the existing seismic hazard map,
- It evaluate not only peak ground acceleration but also peak ground velocity and spectral acceleration, which are compatible to the risk assessment of buildings and infra-structures, and,
- Amplification effects of surface soil can be considered by the parameter of AVS30 that is the mean shear wave velocity of the surface soil up to the 30m depth.

3.1.3 Surface Soil Survey

For grapes the ground condition of the study area, we plan to conduct boring survey with standard penetration test and PS logging, surface wave survey, microtremor measurement. Considering existing boring points and ground conditions, we planned surveying points shown as in Figure 3. However, about the satellite districts, for check ground conditions in residential area, we set the survey points shown as figure 4.



Figure 3 Survey point in Central UB



Figure 4 Survey point in satellite districts

The boring points and geophysical surveying points maybe changed depending on the results of permission from authorities and owner.

3.1.4 Expected Outcome

Comprehensive risk seismic hazard maps are provided, by which the existing disaster prevention/reduction planning will be reviewed appropriately. Also relevant techniques and knowledge are transferred to CPs. Figures 5 and 6 show the tentative results, which will be modified after completion of ground survey.

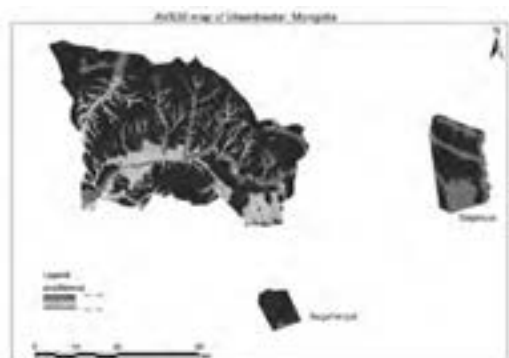


Figure 5 Distribution of AVS30

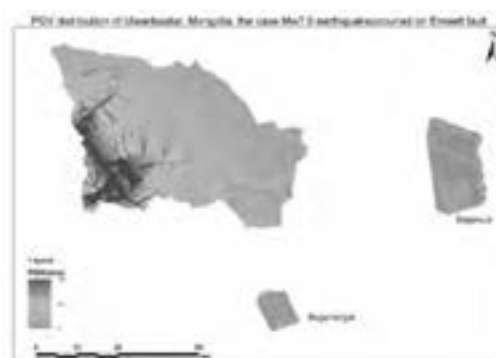


Figure 6 Distribution of PGV by Emeelt Fault

3.2 Seismic Capacity of Buildings

Damage of building is estimated by comparing the deformation under seismic loading and allowable deformation. Among various methods to estimate deformation are proposed, such as static push-over analysis or dynamic response analysis, employed is the method recently proposed in Japan to check the ultimate capacity of building.

3.2.1 Methodology

Given the scenario earthquake, spectral acceleration at a site is calculated and is converted to the complex spectrum, which shows the relationship between spectral displacement S_D and spectral acceleration S_A . The conversion is based on the following formula,

$$S_A = \omega^2 S_D,$$

where, ω is circular frequency and is derived from natural period.

On the other hand, building is modeled as an equivalent single freedom system with nonlinear displacement-force relationship called as a skeleton curve. Dividing force by mass, the skeleton curve is converted to the relationship between displacement and acceleration, so that this relationship can be overlaid on the complex spectrum.

An intersection point shows the displacement and acceleration of the building under the earthquake loading. It is noted that the complex spectrum may be modified reflecting the increment of damping due to non-elastic behavior. The outline of the ultimate capacity design is illustrated in Fig. 7.

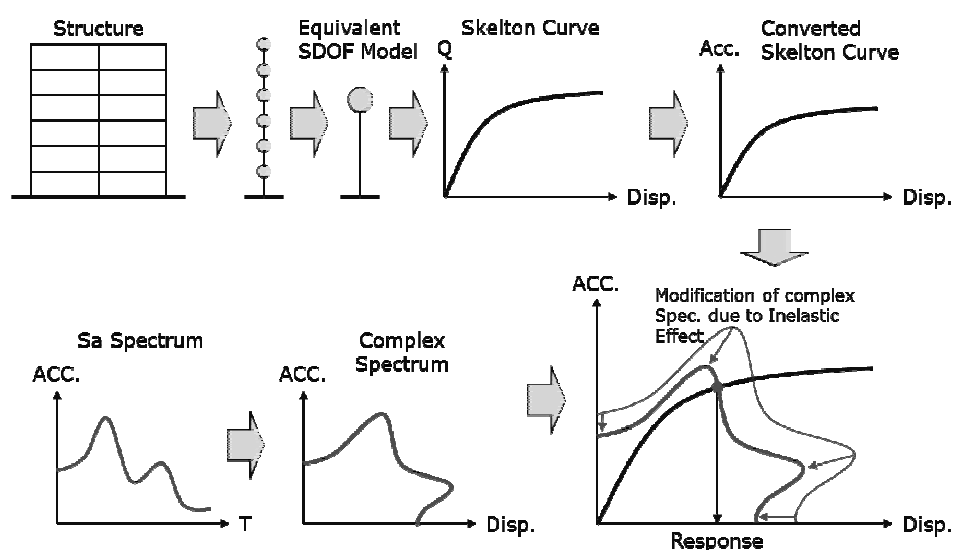


Figure 7 Outline of ultimate capacity design

3.2.2 Expected Outcome

UB city will be able to establish appropriate earthquake disaster management plan and urban plan to reduce earthquake damage by utilizing earthquake risk evaluation. Also relevant techniques and knowledge are transferred to CPs.

3.3 Fire Risk of Ger Area

3.3.1 Introduction

The population in UB city has rapidly increased from 0.65 million to 1.22 in 2012. As it is not easy to supply houses for half of million new residents only in about decade, residential area is expanded to the suburbs of UB city and most of them lives in traditional Ger. Ger is made of wood and cloth with coal stove. According rapid expand of Ger area, there is no city planning to construct road as well as water supply system, sewage system except electric power supply in the area.

3.3.2 Methodology

Fire risk should be considered high in Ger area in this situation. To identify the risk in Ger area should be divided to risk of fire break and risk of fire spread. Not only Ger but also wooden houses and brick or concrete made houses are increasing in Ger area.



Figure 8 Ger area near center



Figure 9 Ger area in suburb

3.3.2.1 Fire Break Risk

Fire break risk is based on method developed by Tokyo Fire Department.

- Total number of fire break is sum of fire from collapsed house and fire from facilities using fire.
- Number of fire break from collapsed houses is sum of fire from electric equipment and fires from electric line.
- Fire break possibility of each case is used past statistic data developed by Tokyo Fire Department because of no statistical data in Mongolia.

3.3.2.2 Fire Spread Risk

There are several fire spread risk methods. Among them, Fire Spread Cluster Method which developed by Tokyo Fire Department is used. This method is to identify area (cluster) which will be burned by one fire.

3.3.3 Expected Outcome

UB city will be able to establish appropriate earthquake disaster management plan and urban plan to reduce earthquake fire damage by utilizing earthquake fire risk evaluation.

3.4 Disaster Education

3.4.1 Background

In 2010, NEMA and ADRC cooperated in conducting the disaster reduction related seminar and the emergency drill for teachers and students in 2 schools in UB City according to Japan cabinet office project "Transfer of Japanese Disaster Reduction Related Technique". This activity consisting of lectures and game-like drills obtained good reputations from both NEMA and schools' teachers and students, so the activity is recognized as an effective way to increase citizens' sense of danger.

In this project, JICA project team and UB city are planning to conduct "Seismic Risk Mitigation Awareness Campaign" in UB.

At first, project team conducted evacuation drill and disaster prevention workshop during the Japan-Mongolia Joint Seminar on Preparedness and Mitigation to the Seismic Disaster on March 2012 in Mongolia.

3.4.2 Methodology

The working group (WG) of disaster education, consist of JICA project team and UB city, are planning to have a workshop (WS) on 17-18 September 2012 for more discussion and sharing information. It is a part of preparation of "Seismic Risk Mitigation Awareness Campaign" on June 2013. In this WS, we'll have some lectures and technical discussions of disaster education structure for effective outcome, and also have some demonstrations of disaster education program for better understanding.



Figure 10 Activities of "Iza-Kaeru Caravan" Performed on Feb. 2011 in UB City

One of the disaster education program which the Campaign will be based on, is the "Iza-Kaeru Caravan", the new style emergency drill conducted at 2 schools in UB City by ADRC in 2011.

"Iza-Kaeru Caravan" is a game-like emergency drill, through which people can learn a variety of knowledge and techniques related to disaster management with fun. This drill was developed by Plua-arts, the NPO, aiming more attendance of the generations not interested in emergency drills. This activity has already been incorporated in JICA Hyogo Center and was successfully introduced to Indonesia, Guatemala, El Salvador and Costa Rica. This activity also had a good reputation from teachers and students in the implementation in Mongolia in Feb. 2011 with recognition as an effective tool to increase citizens' sense of crises, and is now examined its development in Mongolia, so such a situation is duly considered in the Project.

The WG estimates 200 participants in the drill with examination of the method of recruitment. Cooperation with other events such as local festivals will also be examined.

WS combined with the trainers training of local staffs are implemented to incorporate the local needs and to develop the facilitators for the Campaign to be held in 2013. Preparation for the Campaign is also done by the developed facilitators.



Figure 11 Learned from “Great Hanshin-Awaji earthquake in 1995” on Mar. 2012 in UB City

3.4.3 Expected Outcome

The mechanism of earthquake and necessary preparations will be recognized to the participants of the Campaign.

UB city will be able to conduct disaster education in local level by utilizing disaster education tool developed in this project.

Schools will be able to conduct disaster drill and training to school children by utilizing disaster education tool developed in this project.

REFERENCES

- Activities for communities, 9 May 2011, Asian Disaster Reduction Center, The report of “Project on Transfer of Disaster Management Measures of Japan to Enhance DRR Capacity in Asia 2010”, Mar. 2011, Urban Disaster Research Institute
- Amornthip P., Research Paper, Study on Dissemination of Disaster Prevention
- Kanno T. et al., A New Attenuation Relation for Strong Ground Motion in Japan Based on Recorded Data, Bull. of the Seismological Society of America, Vol.96, No.3, pp.879-897, June 2006.

Evaluation of managed aquifer recharge methods to increase the groundwater resources for water supply UB City and flow control Tuul river

Narantsogtyn NASANBAYAR

Lecturer, Hydraulics and Hydro construction, EED, SCEA, MUST, Mongolia

nnasan_4@yahoo.com

ABSTRACT

Ulaanbaatar as the capital city of Mongolia is the primary hub for commerce and industry and generates nearly 70 percent of Gross National Product (GNP). More than a million inhabitants, 20,000 factories and businesses, 400 hectares of irrigated farms, 330,000 livestock and 3 power plants in Ulaanbaatar rely on water supplied from Tuul river.

Research objectives are to find the suitable methods of artificial ground water recharge for the Mongolian harsh continental weather conditions, aquifer recharge management possibilities like aquifer infiltration from precipitation and surface flow during wet seasons summer and autumn collect groundwater in artificial recharged aquifer, aquifer storage possibilities of surface water by infiltration in flooding season in order to use in low flow period like winter and spring, also increase or decrease of ground water resources by pumping from aquifer during the winter cold season to make ice storage in order to reflowing river by melting in dry season March and April where Tuul river doesn't flow, research surface water evaporation in winter season and absorbing smoke in air decrease it by snowing.

Keywords: *Managed Aquifer recharge, basin, injection well, flood, humidity*

Introduction

Ulaanbaatar's current and future water supply options depend wholly on the Tuul river. To date the city has been supplied deep wells that draw on groundwater sources from an unconfined aquifer that runs along the bed of the river or on exploiting additional alluvial- proluvial deposits from the Tuul's tributaries.

Ulaanbaatar's water supplies are extracted from deep wells, located in 4 sites: the "upper source" just below the confluence of the Terelj and Tuul Rivers in the upper basin, and 3 sources in the city itself "central", "industrial", and "meat factory" . Ground water is the only source of drinking water supply capital city of Mongolia.

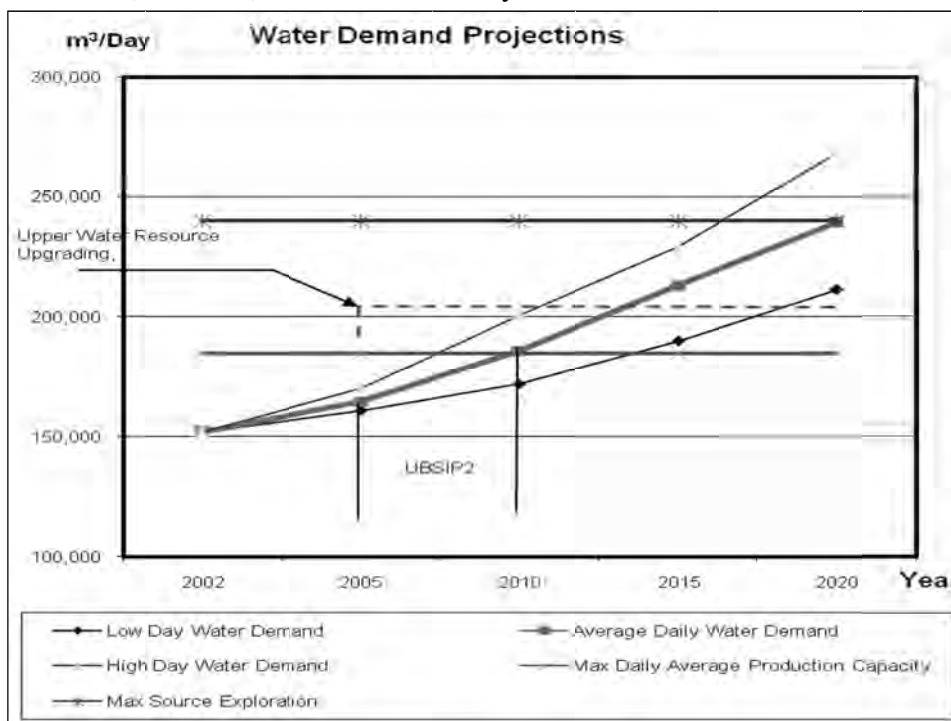
The under groundwater sources for water supply of Ulaanbaatar city monitored in 4 points. Every year in February, March and April ground water table drink water sources decrease to minimum 14-15m from surface, in June, July and August reach to highest level 2-3m deep from earth surface. The data's from Ulaanbaatar

water supply groundwater monitoring stations at upper source, shows that ground water table decrease every year.

The data shows ground water table level decrease 2.7m from the year 2001 to 2008 .

Ground water abstraction is expected to increase in the future because of expected population growth, and industrial development in the city. Due to possible increase in temperature caused by climatic change, evaporation is also expected to increase. All these effects may lead to a lower ground water recharge and a reduction of sustainable ground water resources availability.

Groundwater tables in Ulaanbaatar have been showing a marked decline over the last 50 years. Water is being abstracted faster than the rate of recharge. As the city grows and water demand increases, this problem is intensifying. According to government figures, water use is estimated at 212,000 cubic meters per day and is predicted to reach 286,000 cubic meters in 2010, 438,000 cubic meters in 2020, and 708,000 cubic meters by 2050.



Graph 1 Water Demand Projections

/ The study on water supply system in Ulaanbaatar and surroundings /1993-1995, JICA/

Seasonal water shortages are growing even more common, and various studies warn that sometime within the next 10 years the city will be facing a critical shortfall in water availability.

Water supply every days is increasing with the development of city, industries and growth population but ground water source is decreasing by the climate change and last decade year flow of TUUL river during the every spring in March and April come off or doesn't flow. Therefore, we need decide this problem by building complex of hydraulic structures, flow control and build some artificial groundwater recharge systems like drainage or flooding area near drink water extraction wells.

Main Part.

1.1 The Managed Aquifer Recharging methods.

The Artificial underground water resource recharging for water supply has significant role for decision problems for human life condition development.

Recharge occurs both naturally (through the water cycle) and anthropologically (i.e., "artificial groundwater recharge"), where rainwater and or reclaimed water is routed to the subsurface.

Groundwater is recharged naturally by rain and snow melt and to a smaller extent by surface water (rivers and lakes).

The Artificial Recharging Ground water Recourses or Managed Aquifer Recharge is a engineering and technical complex provision for building new reserve of fresh water resources cohering and combining its natural ground water alimentation of surface water. Recharge refers to the replenishment of an aquifer's groundwater. An aquifer is a layer of underground sand, gravel or spongy rock where water collects. Groundwater recharge or deep drainage or deep percolation is a hydrologic process where water moves downward from surface water to groundwater. This process usually occurs in the vadose zone below plant roots and is often expressed as a flux to the water table surface.

This method has economical benefits for drinking water supply system constructing and utilization expenditure, because reduce water supply system and transport capital and shortening constructing term. This method useful for constructing new water intake abstraction structure and improving water extraction structure.

Main structure of Artificial Recharging ground water resources is a spreading structure.

There are 2 types of percolation structure:

1. Surface spreading structure. Recharge basin, spreading channel and flood area
2. Subsurface spreading structure. Injection well, Filtration bore and shaft

Surface spreading methods require extensive land areas, permeable surface materials with high vertical permeability, periodic maintenance to prevent clogging, and little or no water retreatment (Kimrey, 1989). On the other hand, high evaporation losses and groundwater vulnerability to surface contamination make these methods inapplicable for nearby land use. In the case of subsurface spreading, evaporation losses and required land area are minimized but initial costs are increased. Besides, it is difficult to clean these structures (Reddy, 2008).

Disadvantage of surface recharge structure are that is occupying large area of intake structure, and dependence of natural climate condition is more therefore in cold season covering with ice has bad air change. Therefore temporary work out in short cold season area or warm land is applicable.

1.2 Direct Injection

Another method of artificial recharge is direct injection. Recharge wells and aquifer storage and recovery (ASR) wells are examples of direct injection methods, where water is injected into the aquifer (Philipps, 2003). Figure 2.2 shows examples of both recharge and ASR wells. The recharge well and its

purpose were briefly described with equations derived from idealized boundary and permeability conditions by Thiem (1923). Simpson (1948) described the factors affecting recharge rates in wells. Dewey (1933) summarized the conditions where recharge wells can be used successfully.

Subsurface spreading structures can be used to protect from becoming salty and polluting aquifer in operation, cool industrial apparatus, re-use underground water using air conditioning equipment many times and flow transferring water to the aquifer in operation from stratum with adequate watering in water intake with low productivity of industrial and household water supply. But it must be transferred from aquifer with water of high quality. It is impossible to use this method in permafrost grounds or long term frozen grounds in winter and autumn.

Table 1. Advantages and disadvantages of artificial recharge methods.

	WATER SPREADING METHODS		DIRECT INJECTION METHODS
	SURFACE SPREADING METHODS	SUBSURFACE SPREADING METHODS	
ADVANTAGES	<ul style="list-style-type: none"> • Initial low capital cost • Simple maintenance • Low operation and maintenance costs 	<ul style="list-style-type: none"> • Used where surface layers of low permeability preclude surface infiltration • Co-exists with other surface urban uses • Minimize evaporation losses 	<ul style="list-style-type: none"> • Used where vertical permeability is limited • Occupy small surface areas • Fit in most land patterns • Utilize existing water supply infrastructures
DISADVANTAGES	<ul style="list-style-type: none"> ❖ Require: <ul style="list-style-type: none"> ➢ Near surface aquifer ➢ Permeable soil profile with high vertical permeability ➢ Frequent maintenance to prevent clogging ❖ High evaporation losses and groundwater vulnerability to surface contamination 	<ul style="list-style-type: none"> • Higher initial capital cost • Limited aerial extend • Difficult to clean/ maintain 	<ul style="list-style-type: none"> ❖ High: <ul style="list-style-type: none"> ➢ Capital cost ➢ Energy requirements ➢ Operation and maintenance costs ❖ Require: <ul style="list-style-type: none"> ➢ Frequent pumping to remove clogging ➢ Pretreatment prior to recharge

1.3 Underground Dam

Underground dams are also considered as an artificial recharge method, which prevent groundwater flow and store water beneath the ground (Nilsson, 1988). They are used where surface storage becomes impractical owing to high evaporation rates, reservoir siltation, pollution risks, etc (Boochs and Billib, 1994). efficiency and simplicity has revived interest (Foster and Tuinhof, 2004).

Detailed information about physical conditions, design and construction of underground dams are given by Nilsson (1988). Underground dams are usually constructed in arid regions, where irregular rainfall is observed. Well defined and narrow valleys, natural dikes are preferred for locating underground dams. In hydrogeological point of view, the river beds consisting of sand and gravel are considered as best localities, where suitable storage and flow characteristics are observed.

Research purpose:

“Management of Aquifer recharge” is known in Mongolia as well as but we are lacking of experience and practice in this field of work.

Purpose and Scope:

- Provide information for future improvement in solving the water supply related issues in Ulaanbaatar to find simple, low needed capital costs, cheapest and reliable method.
- Research the balance between consumption and recharge in order to develop strategies to solve water shortages using managed aquifer recharge.
- Study the feasibility of flow control methods to eliminate discontinuance Tuul river in dry season.
- Research humidity and evaporation from water storage in winter cold season to absorbing smoke Ulaanbaatar city decrease air pollution by snowing.

Research Objectives:

Due to over purposes in the Ulaanbaatar water supply Central source must study following researches:

1. Research aquifer storage possibilities of surface water by infiltration in flooding season in order to use in low flow period like winter.
2. Research aquifer recharge management possibilities, also increase or decrease of ground water resources by artificial recharging during the winter cold season
3. Research aquifer infiltration from precipitation and during wet seasons. building artificial recharge basin to study percolation of monitoring of underground water flux control in Mongolian weather condition.
4. In winter cold season making ice storage by pumping ground water from artificial sources in order to using reflow river flow by melting in dry season in March and April.
5. Research the balance between consumption and recharge in order to develop strategies to solve water shortages using managed aquifer recharge.
6. Determine the most suitable and efficient method of Injection wells or Recharge basins in Mongolian extreme weather conditions.
7. Making fog from artificial water storages and search air pollution decreasing by humidity in winter season.

2. Managed Aquifer Recharge water sources.

2.1 Central source upper side A zone.

The drinking water supply system Central source of the city Ulaanbaatar was put into operation in year 1959. Drinking water extraction comes from 93 ground water wells with deep well pumps, 7 booster pumping station. The capacity of source reserve is 114000 m³/day, nowadays water extraction 87-90 thousand.m³/day from 70-80 wells supply to capital city.

/The report of feasibility study of Multi purpose dam on the Tuul river "MONHYDROCONSTRUCTION" LLC 17p/

The research work will be conducted through central source branching Tuul river near Gachuurt, derivate flowing into the old river channel, making percolation channel, recharge basin and injection funnel well and using methods to increase water resource. It includes of digging channel to take water in the river bench, flowing into the river channel, building earth dam and flowing into the old channel.



Figure-1. Derivation area Gachuurt of Tuul river side.

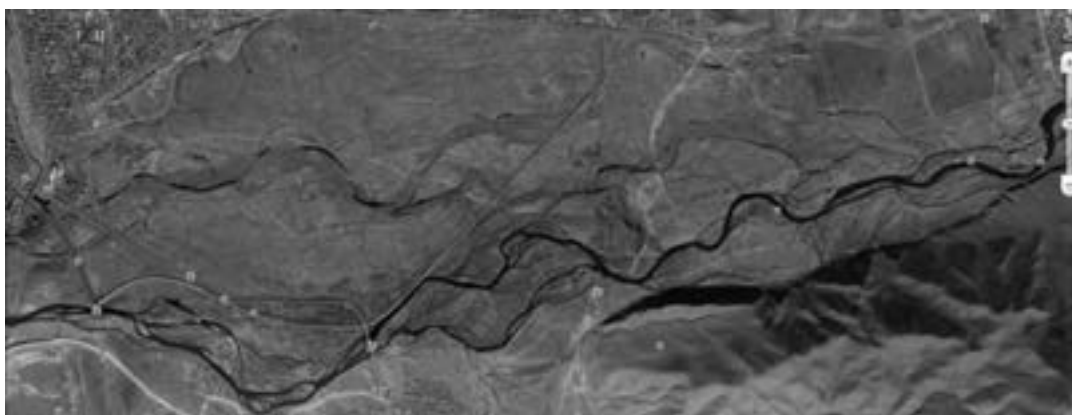


Figure-2 Central source Gachuurt-Uliastai /Google Earth/

Channel will be digged in the bench of river bank from the upper side of the Central source or lower part of Mongol shiltgeen near Gachuurt and water will be derivate flown into the old channel. In order to flow by the old channel additional embankments will be built in three places to flow into the currently existing channel of old river channel. Also water abstraction structures will be made in two places of currently existing embankment. In this way water will be brought by the old channel into the initial operating wells of the Central source and discharged water by the water abstraction structure under the embankment

1. will be given to the recharge basins through stream channel
2. plain between wells located in the part of Tuul river will be flooded
3. water will be given by the subsurface spreading well funnel shaft into wells located upper percolation channel.

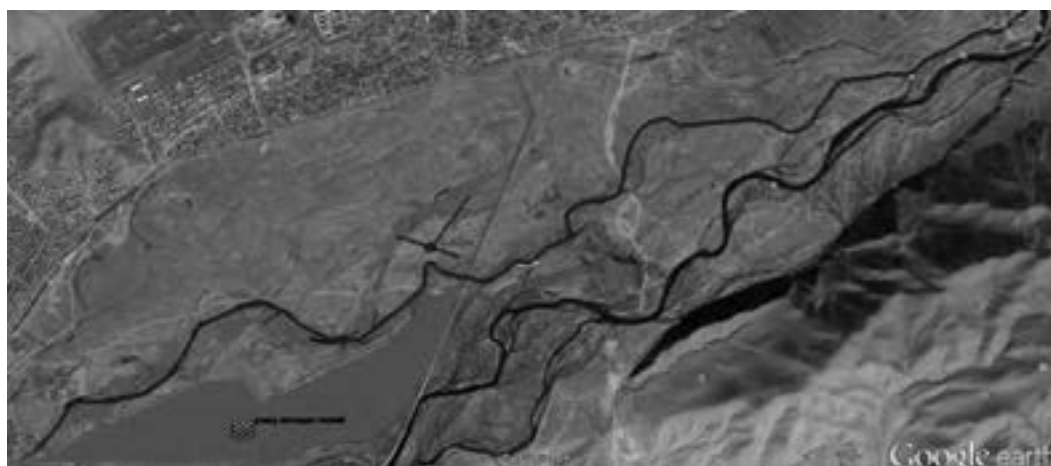


Figure-3. Variant of Managed Aquifer Recharge /MAR/ in Central source upper side of Ulaanbaatar water supply system. /Google Earth/

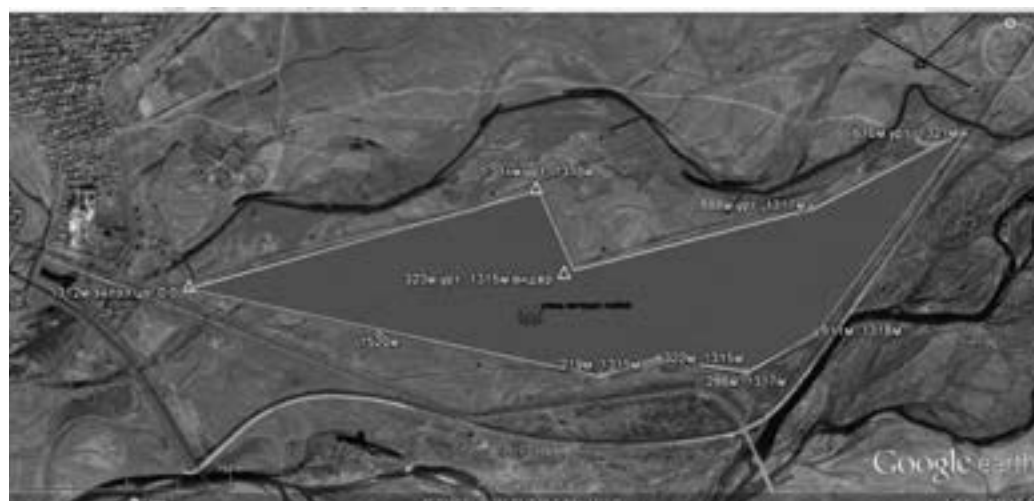


Figure-4. Perimeter and square measuring of flooding area. /Google Earth/
 In this area flooding field perimeter 5678m, flooding square 949285m² or 95 hectare. Flooding area water storage capacity 189651m³ or 1.9 million.m³.

In the Khujirbulan side from Gachuurt to Bayanzurkh Bridge of Central source has 20-30 thousand.m³/day, 600-900 thousand.m³/month available dynamic reserve. Available storage capacity of flooding area 189651m³ it's enable to alimentation by melting ice storage in low flow months March and April when make ice storage in cold winter times through pumping artificial resources of underground water.

2.2 Central source B zone.

In Central source area down side for water supply UB city will be built surface spreading recharge basin, injection well, funnel shaft, flooding area, **underground dam** combined with National Garden Park construction .

2.3 Industrial source recharge methods.

Flow of Selbe and Tuul rivers and water resource will be used to take measures to artificially increase underground water resource in the Water supply industrial part. In order to do it underground water resource will be increased through flowing water by derivation channels to the operating injection wells by water volume of industries or 3rd and 4th power plants and infiltrating it. Water will be intake from the bench of Selbe river on the northern west part of the 3rd power planet by the derivation channel and brought into water supply wells of the power plant and water will be brought by the percolation channels into the recharge basins and each well.



Figure-5. The version of artificial recharging ground water Industrial zone water supply wells through derivation channel, recharge basins. /Google Earth/

Let's choose cheap and economically efficient version to derivate flow of Selbe river in order to be flooded in the square enclosed by embankments of water supply of 3rd and 4th power plants to protect from flood.



Picture-6. The flooded area version of Industrial water supply wells. /Google Earth/

The Industrial source for water supply was established 1961 operating 16 deep water pumping wells, 4 booster pumping station. 25-30 thousand.m³/day water extracts and supply to capital city.

/The report of feasibility study of Multi purpose dam on the Tuul river "MONHYDROCONSTRUCTION" LLC 17p/

The Industrial source side of water supply where tributary Selbe river to Tuul river flooding area perimeter 3887m, water storage area length 1819m, flooding square

$$S_2 = 180553i^2 + 642130i^2 = 822683i^2,$$

$$S_3 = 207870i^2 + 333882i^2 + 191395i^2 = 733147i^2,$$

Totally 1555830 i² or approximately 155.58 hectare will be flooded.

Available storage volume of flooding area

$$W_1 = S_1 \cdot \frac{2}{3} + S_2 \cdot \frac{1}{3} = 180553 \cdot \frac{2}{3} + 642130 \cdot \frac{1}{3} = 2260802 i^3$$

$$W_2 = S_1 \cdot 3 + S_1 \cdot \frac{1}{3} + S_2 \cdot 2 + S_3 \cdot \frac{1}{2} = 103935 \cdot \frac{10}{3} + 2 \cdot 437817 + 191395 \cdot \frac{1}{2} = 1317781.5 i^3$$

Volume of the artificial water pool flooded in water from bridge of Selbe river to the inward zone to Tuul river is 3.58 millions .m³ and during the low flow period in spring time or in March and April water resource in the draining part of Selbe river of industrial water supply source will be collected, frozen and during the melting period in spring it is possible to replenish underground water supply by water of above mentioned melted ice in February.

3. Flow control of TUUL river.

In order to improve flow of Tuul river and increase flow in the low flow period in spring will be built overflow dam or barrage with water abstraction structures upper the bridge of Yarmag using closed industrial water supply protection embankment.



Picture7. Tuul river bed. 2012.04.14.



Figure 8. Flow control water reservoir-I /Google Earth/
Water reservoir for flow control Tuul river between 2 bridges Yarmag and Songolon will be with length 2470m, perimeter 5571m.

Water submerged area will be:

$$S_4 = S_1 + S_2 = 1748 \cdot \frac{721+341}{2} + \frac{721 \cdot 771}{2} = 928188 + 277945 = 1206133.5 \text{ } i^2$$

Totally 120.6 hectare and volume of the reservoir would be.

$$W_4 = S_1 \cdot 6 + S_1 \cdot \frac{1}{2} + S_2 \cdot \frac{2}{3} = 928188 \cdot 6.5 + 277945 \cdot \frac{2}{3} = 6125870.34 \text{ } i^3 \text{ or } 6,13 \text{ million.} m^3$$

The minimum flow rate of river Tuul in dry season is 2.0m³/s. This will be reserve in cold season in the reservoir-I between bridges of Yarmag and Songolon and it will shed by ice melting in March and April during the cut off period of Tuul river: 6125810.34/60days/24hours/60minute/60second=1.18i³/ñ it's low than dry season flow of Tuul river than one more reservoir need to be enable water flow in dry season for flowing Tuul river.



Figure-9. Flow control water reservoir-II of Tuul river. /Google Earth/

The area between next two bridges Bio and Songolon will be submerged 4507m length, perimeter 14639m. Submerged square of flow control reservoir Tuul river is

$$S_{\text{àèi-ñiñ}} = S_1 + S_2 = 3151 \cdot \frac{1954+3053}{2} + \frac{3053 \cdot 1356}{2} = 7888528.5 + 2069934 = 9958462.5 \text{ } i^2 = 996 \text{ hectare}$$

The volume of submerged area of flow control reservoirs:

$$W_4 = S_1 \cdot 2 + S_1 \cdot \frac{10}{2} + S_2 \cdot \frac{2 \cdot 2}{3} = 55219699,5 + 2069934 \cdot \frac{4}{3} = 55219699,5 + 27599 = 57979611.5 \text{ } i^3 = 57.979 \text{ million.} m^3$$

Ice will be frozen and reserved in the valley between bridges of Tuul river and Bio-Songolon and it will shed by ice melting in March and April during the cut off period of Tuul river. It would be:

$$57979611.5 \text{ } i^3 / 60 \text{ days} / 24 \text{ hours} / 60 \text{ minute} / 60 \text{ second} = 11.18 \text{ } i^3 / \text{ñ}$$

It is more than annual average run-off of month April 6.431 i³/ñ, therefore must be built flow control structure embankment dam in the valley between bridges of Tuul river Bio Complex and Songolon.

4. Smoke absorbing method.

The water reservoir in the submerged area has significant role for flow control Tuul river. In watery and rainy season collect and store water in reservoir and use it in dry season to annual run-off possibilities Tuul river. Let's take absorbing methods in air pollution after the built flow control reservoir and surface spreading structures and reduce air pollution.

Table.2. Annual evaporation distribution in cold season of Tuul river.

No	Month	I	II	III	X	XI	XII	season
1	Evaporation	0	1.0	1.3	2.0	1.2	1.0	6.5%
2	Evaporation layer (E) _{ii}	0	2.92	3.8	5.8	3.6	2.9	19.02

To calculate difference of evaporation or winter steam formation 19.02 mm of it forms from the area of 24.56 km²:

Will be from the flooded area by water

$$S_1=949285\text{m}^2 \text{ or } 0.95 \text{ km}^2 \text{ of square } \mathbf{11.89\text{km}^2}$$

$$S_2=822683\text{m}^2, \text{ or } 0.82 \text{ km}^2 \text{ of square } \mathbf{23.7\text{km}^2}$$

$$S_3=733147\text{m}^2, \text{ or } 0.73 \text{ km}^2 \text{ of square } \mathbf{9.14\text{km}^2}$$

$$S_4=12061335\text{m}^2 \text{ or } 12.1 \text{ km}^2 \text{ of square } \mathbf{151.4\text{km}^2}$$

$$S_5=9958462.5\text{m}^2 \text{ or } 9.958 \text{ km}^2 \text{ of square } \mathbf{124.6\text{km}^2}$$

TOTAL 320.73mm

It is definite to form great amount of steam in the winter time. This steam will be fully absorbed capital city's smoke itself in the winter time and become frost snow and landed to the earth. Above mentioned items were observed on 01 and 02 January 2012.

On 31 December 2011 fog landed and tomorrow morning frost landed and the morning became clear without smoke. It was happened next day again.

In this way in the winter time water reservoir evaporation and fog loss absorbs smoke of Ulaanbaatar city, becomes frost and snow and lands in the earth and it will be most ordinary, efficient and optimal version to eliminate air pollution of Ulaanbaatar city.

The above mentioned table has been shown that in case water pool is built, water loss losing from water pool will be increased evaporation into Tuul river a year and precipitation will be increased in this amount. Evaporated water is lost under the wind influence and but it is comparatively less and dominating directions are from eastern and western directions. Also evaporated water by air pressure difference will move into the higher part of Khentii mountain and it will become clouds there and precipitation will become and be landed back.

It will feed rivers of Khentii mountain to consist source of flow of Tuul river and Terelj river and as well as it will influence in flow of Tuul river well and natural flow adjustment will be done.

Also during the low flow period in spring evaporation conducts regularly and it will become the main factor to create favorable and humid climate to remove dust of the capital city and grow greenery.

Conclusion:

Choice of methods to artificially increase underground water resource of water supply sources of Ulaanbaatar city and research work on Tuul river flow adjustment aims at solving the pressing issues of water supply of population of the capital city in the most ordinary and low invested and cheapest method and restore flow of Tuul river during the low flow period in spring and the following conclusions have been made.

1. It is fully possible to use water resource of non-using wells in water supply sources located in the valley of Tuul river
2. It is possible to build water pool using increased flow of Tuul river and during the months of much more precipitation and increase underground water artificially
3. It is possible to collect and froze flow of surface in the winter's cold time and use it during the low flow period of spring
4. Based on the modeling of underground water of water sources of Ulaanbaatar city it has advantages to choose the most efficient version, determine increasing amount and increase water resource feeding conditions and utilization balance through using method to artificially increase underground water resource artificially and funnel percolation shaft, percolation water pool and method to be flooded by water.
5. It is possible to make flow adjustment to eliminate cut off of Tuul river.
6. Evaporation evaporated from recharge basin of Tuul river will be increased precipitation and create humid environment to the climate of the capital city.
7. It has advantages that in the winter time fog evaporated from the will eliminate smoke of the capital city and become frost and land to the earth and clean air.

These planned work will either increase flow of Tuul river during the low flow period or be formed frost in the winter, absorb smoke of the capital city itself and clean air and in summer evaporation will be increased, precipitation will be increased, watering of greenery of the capital city and favorable conditions to plant trees and plants will be created.

REFERENCES

1. *The final results report of feasibility study Multi purpose dam built on the Tuul river* "MONHYDROCONSTRUCTION" LLC
2. Geocology Institute. *The report of water quality, aquatic environmental ecology study*. 2003.
3. Geocology Institute. *The report study works of Tuul river water reserves decreases reason, protection provision*. UB. 1997
4. Geocology Institute. *"The ecological assessment of Tuul river"* UB 1999
5. B.Myagmarjav, M.Davaa. *Surface water of Mongolia*. Ulaanbaatar .1999
6. *Mongolian climate and surface water reserve atlas*. UB. 1985
7. *Mongolian National Atlas*. UB. 1990
8. *Google Earth*

Hanoi environmental planning to build resilience to climate hazards – A multi-institutional approach

Lan Huong NGUYEN¹; Viet Anh NGUYEN²; Viet Nga TRAN³

¹ Lecturer, Researcher, IESE, National University of Civil Engineering, Vietnam
lanhuong1184@gmail.com

² Associate Professor, Vice Director, IESE, National University of Civil Engineering, Vietnam

³ Lecturer, Researcher, IESE, National University of Civil Engineering, Vietnam

ABSTRACT

Hanoi city lies in the centre of the Red River Delta, one of the most seriously affected areas by climate hazards. This paper focuses on the Hanoi government's multi-institutional approach in Environmental planning for adaptation and mitigation against climate hazards. By discussing the vulnerabilities to climate hazards of Hanoi city, the paper emphasizes that to minimize the impacts of climate change and natural disaster affected to humans as well as to the process of economic development of Hanoi, both adaptation and mitigation of climate hazards should be implemented simultaneously. The framework proposed consists of four main groups of measures to cope with climate change and natural disaster namely: Environmental planning, construction planning, institutional and mechanism tools, and multi sectoral planning. Finally the paper highlights the prioritized programs should be implemented for Hanoi to build resilience to climate hazards to year 2020 with vision to 2030.

Keywords: Urban environmental planning, resilience, climate hazard.

1. INTRODUCTION

Hanoi is the capital city and the second largest city in Vietnam that contributes 12.73% GDP of the country (2010). Hanoi has undergone large urban sprawl with the urbanized area doubled from 1991 to 2004. Despite fast socio-economic growth, Hanoi is considered as flood prone and seriously affected by climate hazards. The city lies in the centre of Red river delta; the region has highest vulnerability level of exposure to storm and flooding (MONRE). In addition, vulnerabilities of lives and livelihood to climate risks are primarily the result of inadequate and unsustainable urban planning practices that does not account climate hazards risks management and planning in the socio-economic development of the city .

2. VULNERABILITY OF HANOI TO CLIMATE HAZARDS

To access vulnerability of Hanoi to climate hazards, we emphasize on the variation of climate components such as temperature, precipitation that results in

occurrence of flooding, landslides, water stresses and the impact to the city socio-economical development as well as impact to livelihoods.

2.1 Climate components variability

Hanoi lies in the centre of the Red River Delta Vietnam, experiences typical Northern region climate with summers are hot and humid, and winters are relatively cool and dry summers, lasting from May to September, receiving the majority of the annual 1,680 millimeters (66.1 in) of rainfall. The winters are short, the temperature could sometime drop below 10°C. For the period of 50 years to date, the temperature of Hanoi areas has increased together with the increasing of overall temperature of Vietnam by 0.5°C but with faster pace compare to other regions in the country. The frequency of cold fronts decreased, numbers of extreme cold days recorded decreased. Meanwhile the sustained period of a cold front increase with the highest recorded in 2011 (1 month).

Data from the Climate Change Scenarios for Vietnam (2009) for Low emission (B1) and High emission (A2) scenarios show that within the next 50 years, the temperature of the North Delta (including Hanoi area will projected to increased 1.4 - 1.6 0C.

Rainfall in dry season would decrease and increase in rainy season. By year 2060, annual rainfall of the North Delta would increase, relative to the period of 1980-1999 about 4.5% (scenario B1) and 5% (Scenario B2). Rainfall in period of March to May would decrease about 3-6%, whereas rainfall in middle of the rainy season would increase for 7-10% by the year of 2100.

2.2 Flood and inundations

According to Vu Dinh Thanh et al (2011), in three decades, the Red- Thai Binh River - has experienced three major floods (1996, 2002 and 2007) with water level of peak flood in Hanoi was 12 meters causing breaking of dikes. In addition, heavy rains in 2003 and 2008 caused severe flooding in the Red River Delta, damages to people and properties. Particularly the Red river large flood in 8/1996 with the peak flood over the alert level 3 causing landslide and breaking of more than 390 dykes, with a total length of 142 km (119 km including 23 km of dykes and embankments); total life loss is 60 people, thousands of homes were swept away, damaged and flooded, the damage estimated up to 730 billion. Unexpected heavy rains occurred in November 2008 was recorded as largest in recent 35 years in Hanoi. Total damage caused to the northern provinces are tremendous, as 101 people found dead, estimated loss of 8590 billion VND (500mil.USD , 2009 equivalent).

In the urban districts of Hanoi, there are remaining 25 local flooded areas to 50-100mm rainfall per hour. There are flood prone areas in other urban centers of the city.

Inundation is a stress to Hanoi, given as following reasons:

- Gaps between urbanization and drainage infrastructure development.
- The old and low capacity of underground sewage irrigation is unable to discharge water when rainfall is higher than 100 millimeters per hour;
- The design drainage capacity for rain with frequency of 2-5 years leading to insufficient capacity (canals, irrigation pumping stations).

- Due to urbanization, ponds and lakes in Hanoi has been replacing with residential areas and roads, reduction of permeability and water restoration capacity
- The urbanization boom has led to inefficient solid waste disposal, resulting in inundation and stagnation of underground water
- New urban planned areas relating to elevation system of urban infrastructure are usually higher than the older part, causing difficulties for rainwater to drain leading to flooding.

Table 1: Flood prone areas in Hanoi

No	Year	Flooded area (ha)			Notes
		Left Day river bank	Right Day river bank	Northern Hanoi	
1	2004	60,972	2793	7560	
2	2006	58,740	6813	8450	Severe flooding in Hadong district
3	2008	56,500			Severe flooding in the South. Nhue river, exceeding drainage pump capacity

(Source: Drainage planning of Hanoi capital in 2030, Vision 2050)

2.3 Surface water depletion

According to experts, under the impact of climate change, water demand increases during the dry season, while decreases capacity of soil moisture and groundwater recharge. The river flow regimes become higher in the rainy season and lower during the dry season, causing urban flooding, salinity and ground water degradation.

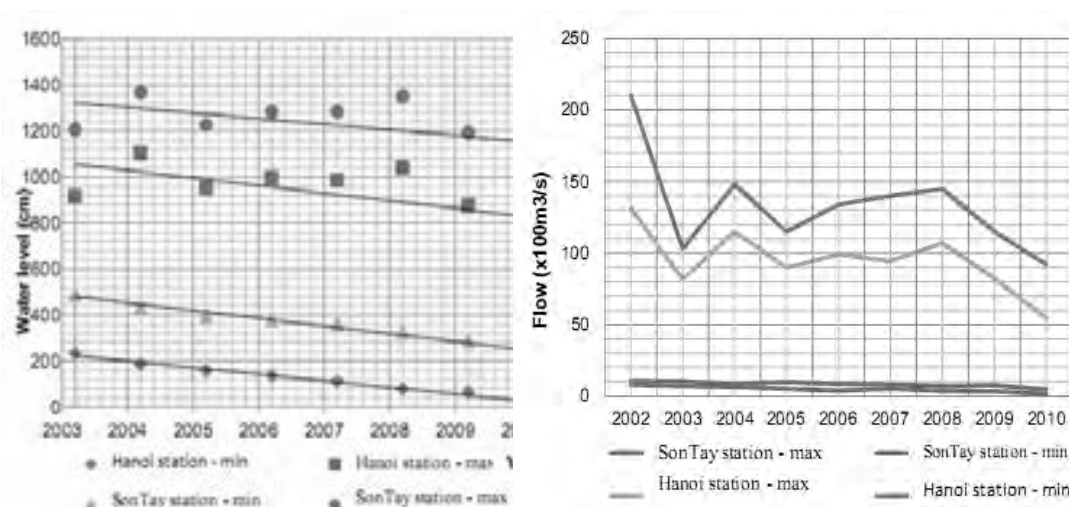


Figure 1. Water level and Flow of Red River (2003-2010)

Source: Hanoi Statistical Yearbook

Regulation of the river water in the reservoir in the dry season seems to be improving the condition of lower stream. However, the water downstream of Red River and Thai Binh is recorded to drop sharply, which might be due to the regulations that are not in accordance with current legislation. In addition, the regulation regimes of Hydropower reservoirs of Red River upper streams contribute to downstream water depletion in the dry seasons. Particularly from January to mid March / 2007, the amount of Red River water depletion has dropped 45-55% in Hanoi. Daily average water level decreased to 1.95 m, the minimum water level was 1.21 m (lower than the period 1956-1985 is 1.11 m), average daily flow is 797m³ / s (less than the period from 1956 to 1985 is 166m³ / s) (Hanoi Statistical Yearbook 2010 2011).

2.4 Landslide

Climate change is showing its clear signs under forms of natural disasters in the capital. Many dykes are at risk of facing landslides due to more floods from the systems of Hong (Red), Da and Duong Rivers, which can threaten lives of residential areas along the rivers, the department elaborated. Especially, heavy rains and floods also cause difficulties for drainage, resulting in prolonged serious submergences in the city (DONRE). Hanoi government has put much effort to construct embankments and relocating houses, many anti-landslide projects over the past years as well as implemented projects on upgrading river dyke systems by 2020. However, number of landslide prone spots is increasing. Climate change is showing its clear signs under forms of natural disasters in the capital. Many dykes are at risk of facing landslides due to more floods from the systems of Hong (Red), Da and Duong Rivers, which can threaten lives of residential areas along the rivers, the department elaborated. Especially, heavy rains and floods also cause difficulties for drainage, resulting in prolonged serious submergences in the city, the department added. To mitigate impacts of climate change, Hanoi has invested in many anti-landslide projects over the past years as well as implemented projects on upgrading river dyke systems by 2020.

2.5 Climate hazards impact to socio-economic development and environmental protection

These climate related events cause a multitude of potential impacts and risks not only to natural areas but specifically to populations of densely built up metropolitan areas of Hanoi. Negative effects such as severe urban floods, disturbances of the energy supply or public transport systems in urban areas lead to decrease of GDP of the city. The table below describes climate related impacts in urban areas in order to estimate the possible damages that might arise for human-influenced systems by climate change, including climate hazards. There are two elements that are classified into columns and rows: first, the probability of the occurrence of the events and second the "elements" at risk. Events to be included are flood, water depletion and landslide. "Elements" at risk are institutional bodies including urban infrastructure services or economic losses, human health or livelihood. The goal of this matrix is to visualize climate hazards impact to inform decision makers and the general public about climate change risks, and to increase their capacity to implement necessary adaptation measures and to increase the resilience of the urban system of Hanoi.

Table 2. Climate hazards impacts to socio-economic development and environmental protection

Sectors affected	Surface water depletion	Flooding	Landslide
Water Resources and Environment	Red River water depletion	Change of hydrological regime of the river, promoting extremist phenomenon, increasing the average number of flood, flashflood	
Industry	Water shortage for industrial production, cooling system	Scarcity of materials and delay of processing due to traffic disturbance by flooding	
Transport	Irrigation water shortage	Damages to railway lines, roads, river ports.	Flooding of river ports.
Agriculture	Water quality: polluted with urban wastewater.		Serious erosion leading to loss of agriculture land and crops
Construction, infrastructure, urban development		Increase in flooding in the city and the surrounding urban	Damage to roads, infrastructure along riverbank
Health, public health		Increased exposure to water borne diseases such as gastrointestinal diseases, skin diseases Increased risk of injury or death from storms, flood.	Life and properties losses due to landslides
Business services, trade, tourism	Loss due to water shortage	Reduce recreational activities, outdoor service Disrupted communications affect tourist	
Energy	Water shortage for hydropower generation	The amount of electricity generated per year increased to about 0.8% of total electricity generation capacity (scenario B2)	
Water Supply	Lack of water for water supply and waste water for daily consumption , production of urban areas	Exceeds capacity of the treatment plant and pumping stations when heavy rainfall occurs	

3. INSTITUTIONAL APPROACH TO BUILD RESILIENCE TO CLIMATE HAZARDS

After an international workshop on flood mitigation, emergency preparedness, and flood disaster management in Hanoi in 1992, the First National Strategy and Action Plan for Disaster Mitigation was developed and approved in 1994 (updated 1995). Since then, the central government and city authorities has made much effort to strengthen capacity for climate change adaptation. Taking basic principle to cope with climate hazards, Hanoi is engaging in the following adaptation activities (Box 1):

- ✦ Actively improve the food preparedness and prevention standards for sustainable development.
- ✦ Current food prevention probability level is 0.8 percent, but the target is 0.4 percent and then 0.2 percent in the future;
- ✦ Strengthen the dike system to protect the right bank of the Red River (Asian Development Bank project);
- ✦ Strictly monitor, investigate, and respond to dike emergencies through institutional strengthening;
- ✦ Clear river bed and unlock river flows to ensure prompt food discharge in the Red River, including lifting collapsed war-damaged bridges, lowering the elevation of inner dikes, relocating houses and construction from the restricted barrier of foods, and dredging river estuar deposits;
- ✦ Build upstream water reservoirs to control the flood pressures for Hanoi;
- ✦ Strengthen flood discharge and construction (following design procedures) to protect Hanoi in flood emergencies. Issue detailed socio-economic policies for flood discharge and control processes to ensure social equity;
- ✦ Plant and protect upstream forests (e.g., 5 million hectares forestation program with targets an increase in forest coverage up to 40 percent by 2010); and
- ✦ Implement “channelization” initiative for selected parts of the Red River that flow within the Hanoi zone.

Source: The World Bank, 2009

Investment has been made to the city’s flooding prevention activities; however the city still suffered from flood and inundation when heavy rain occurs. Climate change adaptation and mitigation grow much attention from city residents and authorities, pressing urban planners to search for solutions. The environmental plan for Hanoi for the period 2015-2020 with vision to 2030 addresses the issue of climate hazard adaptation planning with the multi-institution approach. This approach is base on principle of building resilience city to climate change by enhancing the capacity of people and communities to adapt to and cope with climate hazards (Figure 2.)

Measures to cope with climate hazards adaptation is divide into 5 groups of structural and non-structure including

- ✦ Planning and design focus on water supply and drainage system; cooperation between ministries, neighboring provinces and cities in regulating water regimes of Red River system, especially irrigation

- headwork, hydro power reservoirs; renovating and conservation of lakes and rivers; land use planning
- ✦ Construction measures focus on constructing of complete dyke systems including emergency spillways along the dikes for selective filling of flood retention basin; completing drainage systems, irrigation dams and reservoir to uptake over flow storm water, protection of urban areas.
- ✦ Non-structural measures: institutional strengthening including completing city’s legal documents such as Regulation on Flood and Storm warning, prevention and disaster relief; facilitate green industry, energy saving and environmental industries (focuses on taxes and subsidies); mobilizing investment from public and private sectors; public awareness raising through official education, propagandas, media...

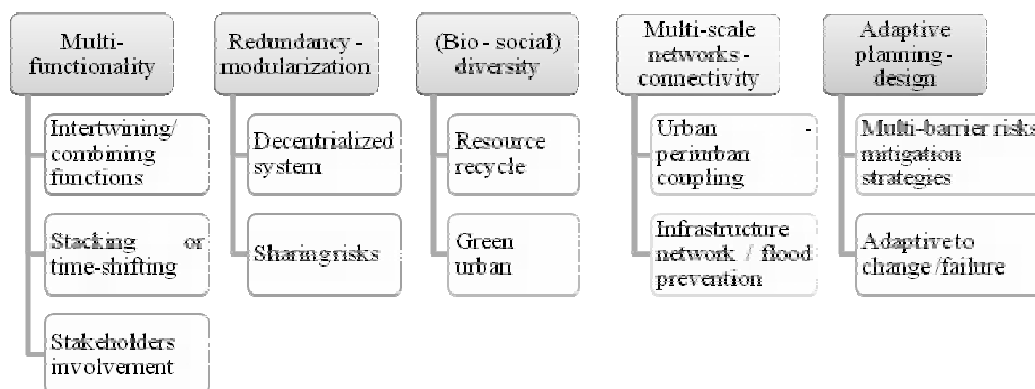


Figure 2: Principles of building resilience city to climate change

- ✦ Measures by sectors: focus on sectors that are affected by climate hazards (from table 2)
- ✦ Finance and businesses with climate change: investment strategies for both adaptation and mitigation of climate change encourage, ensuring competition and large-scale investment. Mitigating climate change should be considered as economic opportunity, social and environmental. Reducing carbon emissions per unit of GDP should be the approach of Hanoi. There is a need for modification and amendment of current financial policies (especially energy subsidies and taxes)

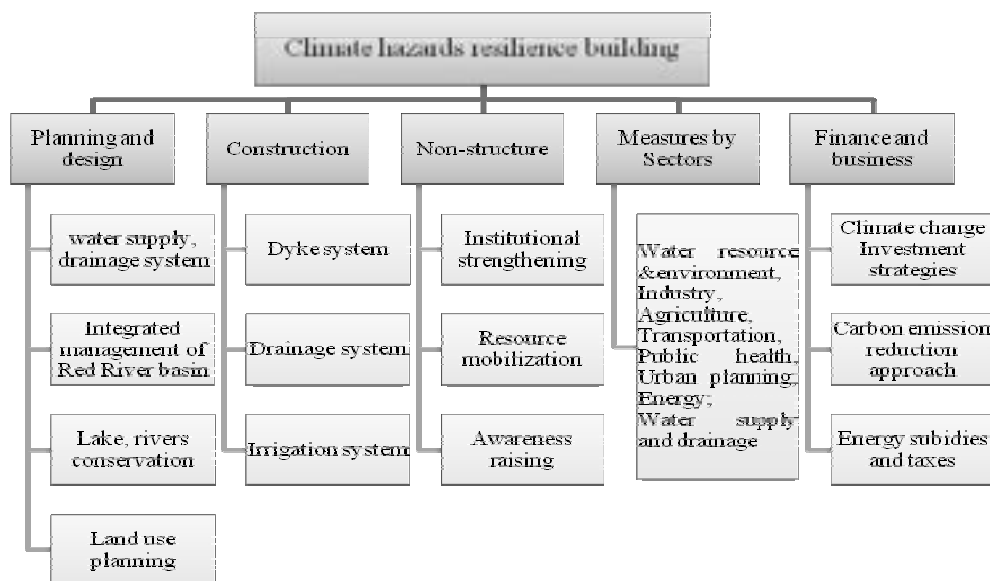


Figure 3. Multi-institutional approach for Hanoi Climate Change planning

REFERENCES

- Hanoi Statistical Department, 2011. *Hanoi Year book 2010*. Hanoi: Statistical Publishing House.
- Dinh Vu Thanh, Nguyen Van Viet, 2011. *Socio-economical losses account for natural disaster, climate change and relocation in Vietnam*. National Conference on Hydro-meteorology, Environment and Climate Change.
- Le Bac Huynh, Bui Duc Long, 2011. *Initial steps for Climate Change impact assessment relating to flood, flash flood and drought in Vietnam*. National Conference on Hydro-meteorology, Environment and Climate Change.
- Luong Tuan Anh, Hoang Thi Thanh Thao, 2011. *Water utilization of upper stream and Red river basin resource impact assessment report*. Institute for Hydro-meteorology and Environment.
- Nguyen Cong Kien, 2008. *Assesment of stability of the Red River embarkment in Hanoi downtown areas*.
- Nguyen Nhu Y, Le Van Linh, Nguyen Thanh Son, Tran Ngoc Anh, 2011. *Climate Change Impact to Day River flow regime in the Hanoi area*. Science and Technology Journal.Vietnam National University, 27: 192-199.
- Hanoi People’s Committee, 2012. *Hanoi Drainage and Sewerage plan to year 2030 , with a Vision to 2050*. Hanoi Plan: Hanoi People’s Committee
- Tran Thanh Xuan, Tran Thuc, Hoang Minh Tuyen, 2011. *Climate Change Impact on Water resource in Vietnam*. Science and Engineering Publishing House..
- The World Bank, 2009. *Climate Resilient Cities: A Primer on Reducing Vulnerabilities to Disasters*. The World Bank.

Development of advanced composite material for seismic safety of non-retrofitted masonry housing schemes in urban and rural areas of developing countries

Saleem Muhammad Umair¹

PhD Candidate, Department of Civil Engineering, The University of Tokyo
mumair@iis.u-tokyo.ac.jp

Muneyoshi Numada

Research Associate, ICUS, IIS, The University of Tokyo, Japan
numa@iis.u-tokyo.ac.jp

Kimiro MEGURO

Professor, Director, ICUS, IIS, The University of Tokyo, Japan
meguro@iis.u-tokyo.ac.jp

ABSTRACT

The present study deals with the earthquake disaster reduction by the development of new composite material to mitigate the collapse of unreinforced masonry structures (URM) in urban and rural areas in developing countries. Collapse of unreinforced masonry walls causes a large number of human casualties due to a strong ground motion. Masonry walls are relatively strong for in-plane shear and much weaker in out of plane direction resulting collapse of masonry structure. Being highly expensive, FRP is a strong material and can significantly increase the out of plane bending strength of masonry walls. Being an expensive material, FRP exhibits a highly catastrophic brittle failure under extreme loading leaving no warning and evacuation time for residents. On the contrary, polypropylene band (PP-band) is a cheap material with much larger ductility and holding capacity to avoid sudden failure, caused by the breaking of wall into small fragments which has been found as a major cause of casualties. In this study, an attempt has been made to find a composite material by using FRP and PP-band to increase the shear capacity and to avoid the catastrophic brittle failure of masonry walls under strong ground shaking. In order to achieve required objectives, out of plane load tests have been carried out using six masonry wallets consisting of three non-retrofitted masonry wallets, PP-band retrofitted masonry wallet, FRP retrofitted masonry wallet and FRP+PP-band retrofitted masonry wallet. Behavior of wallets has been carefully observed in terms of peak strength, deflection and deformation capacity. It has been found that retrofitting of masonry walls using FRP and PP-band is much viable solution as compared to conventional retrofitting techniques because FRP+PP-band reduced the overall cost of retrofitting due to confining and holding effect of PP-band which is a very low cost material.

Keywords: retrofitted, composite, polypropylene, fiber reinforced polymer

1. INTRODUCTION

1.1 General

Masonry is one of most popular and oldest construction material. Because of its low cost and local availability, its significance as a construction material has become more relevant. Better aesthetics, good heat and sound insulation, high fire rating and economical construction are some of additional inherent advantages of masonry construction. Masonry contributes a large number of structures in world's inventory of non-engineered construction and almost all of the construction is composed of unreinforced masonry (URM). Seismic vulnerability of URM is highly questionable in the region of high seismic activity. According to Coburn and Spence [Coburn and Spence, 1992], collapse of URM masonry houses is the biggest cause of human casualties in under developed parts of world during earthquake hazards. Understanding and realizing the shortcomings of URM masonry, many researches worldwide started efforts to strengthen and retrofitting of existing masonry construction. In this regards many retrofitting techniques have been developed such as adding concrete frames, masonry jacketing, ferrocement coatings, applying near surface mounting sheets or members using wire mesh. Most of these methods are expensive, aesthetically not good and add mass to the masonry wall system.

Masonry walls are strong enough in in-plane direction of seismic force. On the other side, out of plane failure of masonry wall system is hazardous and explosive causing almost complete collapse of masonry structure [Bruneau, 1994]. There is no doubt to say that URM is more vulnerable when seismic force is acting in out of plane or perpendicular to longitudinal axis of wall. It is the idea of many researches that behavior of masonry walls in out of plane direction requires more experimental and theoretical investigation. [Flagan et al 1993, Drysdale et al 1994].



Fig (a): Canterbury, New Zealand



Fig (b): Gedikbulak, Turkey

Figure 1: Typical out-of-plane failure of an unreinforced masonry.

Figure 1(a) shows typical out-of-plane failure of an unreinforced masonry wall on the second level of 146 Kilmore Street in Canterbury New Zealand [EERI, 2012]. The light blue concrete column, hanging from the second floor, has no reinforcement. Figure 1(b) shows the out of failure of masonry house during Van, Turkey Earthquake of October 23, 2011. [EERI, 2012].

1.2 Literature Review

Among some of recent retrofitting methods Fiber Reinforced Polymers (FRP) has become very popular because of its less retrofitting time, better aesthetics, high strength and ease in application over the masonry surface. On the other hand, FRP can increase the initial shear strength and out of plane bending strength to the great extent.

Meguro and Mayorca [Meguro and Mayorca, 2003] have developed polypropylene band (PP-band) retrofitting method considering economic affordability, local acceptability, material availability and technological applicability required for retrofitting. PP-band is a very cheap material with fairly large deformation capacity. Main objective of PP-band retrofitting is to hold the masonry components into a single unit and to prevent the collapse of masonry structure. After carrying out a series of experiments ranging from small-scale model to full-scale masonry house, it was found that PP-band retrofitted walls can withstand much stronger input ground motion without collapse [Meguro et al, 2005].



(a): PP-band retrofitting of a masonry house in Indonesia



(b): PP-band retrofitted wall in the laboratory.

Figure 2: Retrofitting of masonry wall using PP-band in the field and laboratory.

1.3 FRP and PP-band Composite Retrofitting Technique

In this research we proposed a new retrofitting material which is a composite of Polypropylene band and Carbon Fiber Reinforced Polymer (CFRP). Both of these materials are applied on masonry wall system as a composite material and this composite not only increases initial shear strength but also serve satisfactory to keep integral the structural system by providing sufficient deformation and energy

dissipation capacity. FRP is a brittle material and has ultimate tensile strain ranging from 2 to 4% [V. Turco and S. Secondin, 2005]. Whereas, PP-band cannot increase significantly initial strength of non-retrofitted masonry, it can enhance the structural deformation capacity up to 50 times larger than that of non-retrofitted one [Meguro et al, 2005]. FRP can serve satisfactory if it is applied completely or fully wrapped to hold the brick units which can increase tremendously the retrofitting cost and still do not allow the structural system a reasonable deformability, while PP-band is not only a fairly ductile and deformable but can also be wrapped completely to the wall system because of very low retrofitting cost.

In order to achieve the required objectives, a series of out of plane load tests are carried out using different wallet schemes. A total of six masonry wallets are tested, three non-retrofitted and three are retrofitted. Among retrofitted masonry wallets, one is PP-band retrofitted masonry wallet, one is CFRP retrofitted masonry wallet and one is CFRP+PP-band retrofitted masonry wallet. The main objective of this study was to investigate the effect of PP-band and CFRP composite on increasing bending strength and deformation and energy dissipation capacity in the out of plane direction of masonry walls.

2. EXPERIMENTAL PROGRAM

2.1 Material testing

2.1.1 Properties of masonry

Compression, Shear and bond tests are carried out in order to determine the properties of brick, mortar, and masonry. Table 1 shows the properties of different materials used for construction of masonry wallets. Bricks compressive strength is determined according to ASTM C-67. Three samples of burnt brick were tested under direct compression. Three mortar cubes of 50mm×50mm×50mm containing a weight mixed proportion of cement, lime and sand (250g: 1,000g: 2,800g) were tested with 0.25 water/cement ratios according to ASTM C-109. Three samples of brick triplets, each triplet consisting of three bricks joined together by 5 mm mortar thickness were prepared to evaluate the shear strength of masonry units. Three masonry prisms each consisting of five bricks were tested according to ASTM C-1314.

Table 1: Characteristics of materials used in experiments

Test	Compressive strength of brick	Compressive strength of mortar cube	Compressive strength of masonry prism	Shear strength of mortar	Bond strength of mortar
Specimen	(MPa)	(MPa)	(MPa)	(MPa)	(MPa)
1	25.10	1.08	15.95	0.24	0.0040
2	26.60	1.07	11.60	0.15	0.0050
3	26.70	1.34	13.25	0.21	0.0040
Average	26.10	1.16	13.60	0.20	0.0043

2.1.2 Axial tensile test on polypropylene (PP) band

Three sample of PP-band with 6mm×0.6mm in nominal area of cross section and 150mm in gauge length are tested under uniaxial tensile loading using displacement control universal testing machines (UTM). Table 2.0 shows the tension test results of PP-band.

Table 2: Polypropylene band tension test results

Specimen	Maximum Axial Stress (MPa)	Initial Modulus (GPa)	Residual Modulus (GPa)	Failure Strain (%)
PP-1	254.20	7.38	1.91	12.30
PP-2	246.50	6.95	2.06	12.67
PP-3	234.40	6.42	1.96	11.91
Average	245.03	6.92	1.98	12.29

2.1.3 Properties of CFRP and epoxy

Properties of CFRP and epoxy are provided by the supplier of these materials. Bi directional type of fiber layout is used in CFRP. Thickness of CFRP sheet is 0.5mm. Bond E-250 epoxy is used to apply CFRP over the brick surface. Table 3 and Table 4 show the properties of CFRP and epoxy. All epoxy strength parameters are examined at temperature of 20±1°C after curing time of 7 days.

Table 3: Material properties of CFRP

Material	Tensile modulus (GPa)	Bending strength (MPa)	Bending modulus (GPa)	Compressive strength (MPa)	Ultimate Elongation (%)
CFRP	120	130	90	900	2

Table 4: Material properties of Epoxy

Material	Tensile strength (MPa)	Tensile shear bond strength (MPa)	Bending strength (MPa)	Compressive strength (MPa)	Compressive shear bond strength (MPa)
Epoxy	20	9.6	45	50	21

2.2 MAOSNRY WALLETS TESTING SCHEME

2.2.1 Masonry wallets testing and experimental setup

Four types of masonry wallets are shown in the Fig 3. Size of masonry wallet is 475mm x 238mm x 50mm. All of these wallets are constructed using 75mm x 37mm x 50mm burnt brick units. Cement lime mortar with a weight mixed proportion of cement, lime and sand (250g: 1,000g: 2,800g) is made with 0.25

water/cement ratios. Masonry wallets are constructed, cured and tested under similar conditions. In case of CFRP and CFRP+PP-band retrofitted masonry wallets, CFRP is pasted on wallet surface with the help of strong epoxy and cured for 24 hours whereas PP-band and CFRP+PP-band retrofitted, PP-band is applied on both faces with the help of ultrasonic welder and also connected in out of plane direction.

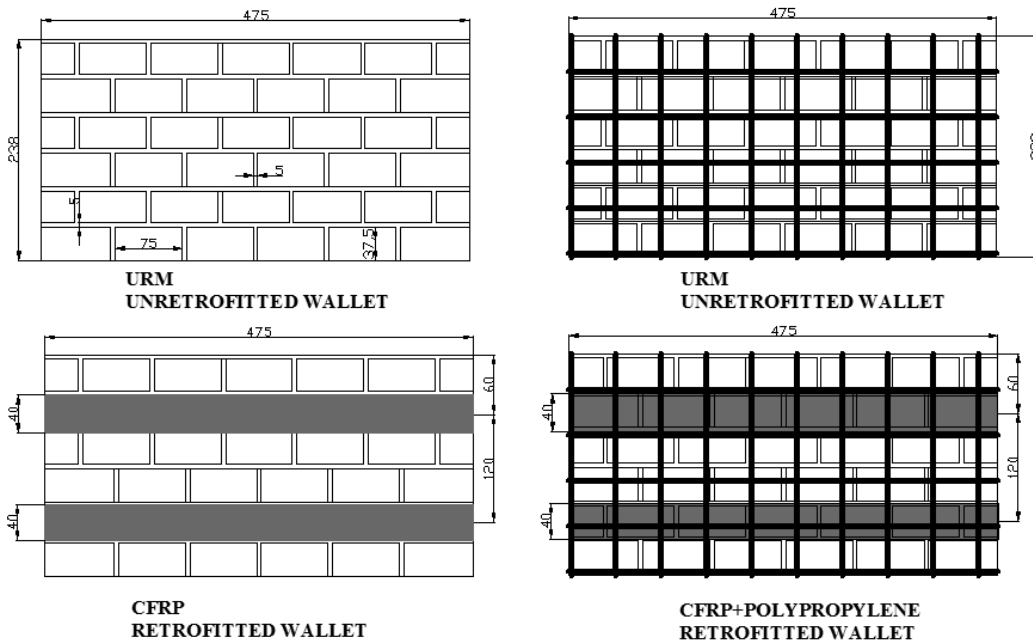


Figure 3: Masonry wallets retrofitting scheme for out of plane load test.

Three of the masonry wallets are retrofitted using different retrofitting schemes. One is PP-band retrofitted, one is CFRP retrofitted and one is CFRP+PP-band retrofitted. Two CFRP strips of dimension 475mm x 40mm x 0.5mm are used on both faces of CFRP and CFRP+PP-band retrofitted masonry wallets. PP- band mesh pitch of 50mm is used for PP-band retrofitted and CFRP+PP-band retrofitted masonry wallet.

2.2.2 Test Setup

Each of the wall specimen was tested like a simply support beam of center to center span of 440mm with one displacement at the center of span in the form of line load throughout the width of the masonry wallet as shown in Fig 4 (a) and (b). Total size of masonry wallet is 480mm from edge to edge of specimen. Vertical displacement is applied at center of the specimen at a loading rate of 0.1 mm/min. Two LDTV displacement transducers with 500×10^{-6} /mm sensitivity are used at quarter span to measure the deflection. Wall specimen is simply supported on two steel rollers and displacement is transferred from machine to specimen with the help of steel roller and a cap plate. A small initial displacement is applied to assure the full contact of the wallet and loading arrangement. Specimens were completely inspected in throughout the length of loading increments. Different displacement loading rates are selected depending upon the failure displacement

and duration of test. All displacement and loading data is recorded in a computerized digital acquisition system.

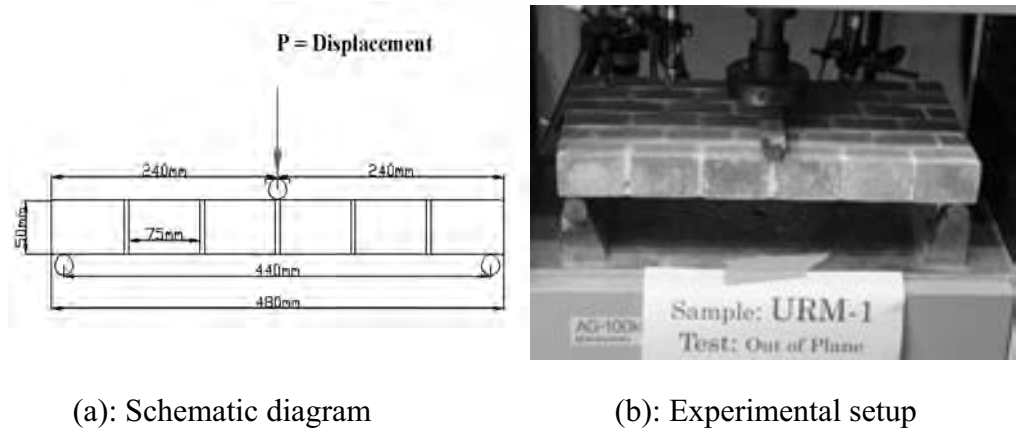


Figure 4: Test setup of out of plane load test

3. TEST RESULTS

3.1 Non-retrofitted masonry wallet

One of the main focuses of experimental results was load-displacement curves of masonry wallets. Figure 5 shows the load displacement curve of non-retrofitted masonry wallets. All URM specimens are tested using same loading rate of 0.1mm/min. Although preparation, curing and testing conditions of masonry wallets were similar still the non-retrofitted wallets show a variety of peak strength with an average value of 0.7 kN with almost similar initial stiffness. Behaviour of wallets was almost linear up to the peak value. Sliding type of failure has been observed exhibiting a weak brick mortar joint at vertical displacement range from 0.6mm to 1.2mm as shown in Fig.5 (a).

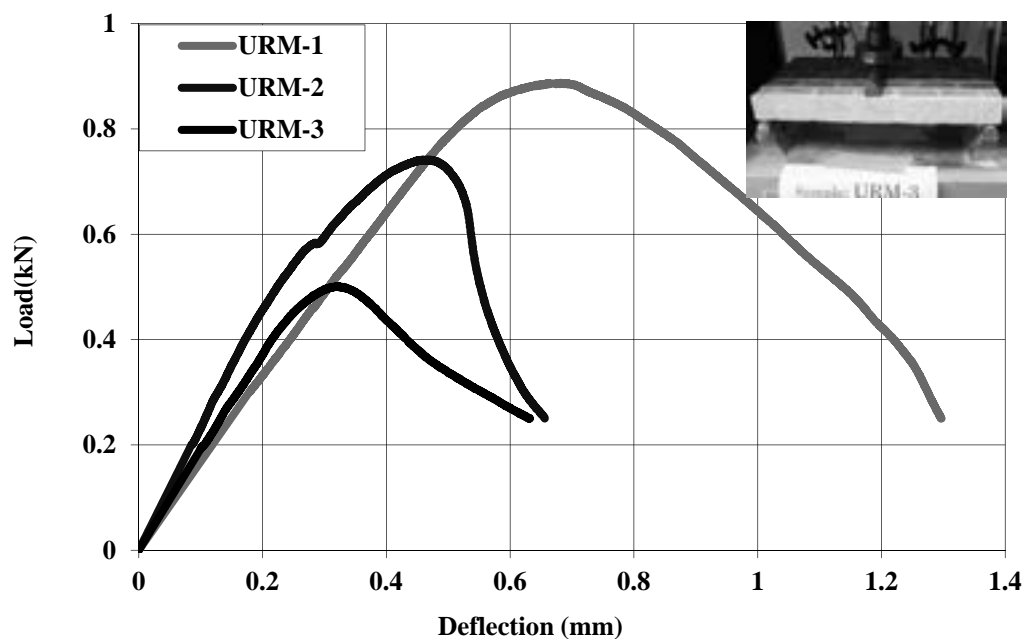


Figure 5: Load-displacement curves of non-retrofitted masonry wallets.

3.2 PP-band retrofitted masonry wallet

Figure 6 shows the load displacement curve of PP-band retrofitted masonry wallet. It has shown almost similar initial stiffness and peak strength of 0.79 kN which is almost same as that of non-retrofitted masonry wallet. Up to initial peak loading rate of 0.1mm/min is used and after that the test was continued at a loading rate of 2.0 mm/min. In case of PP-band retrofitted masonry wallet after the displacement of 1.2 mm/min the sample again started taking load with some reduced stiffness, even it has gone up to a displacement of 57.7 mm with a load value of 0.88 kN. PP-band retrofitted masonry wallet has shown a fairly long deflection and deformation as compared to URM masonry wallets

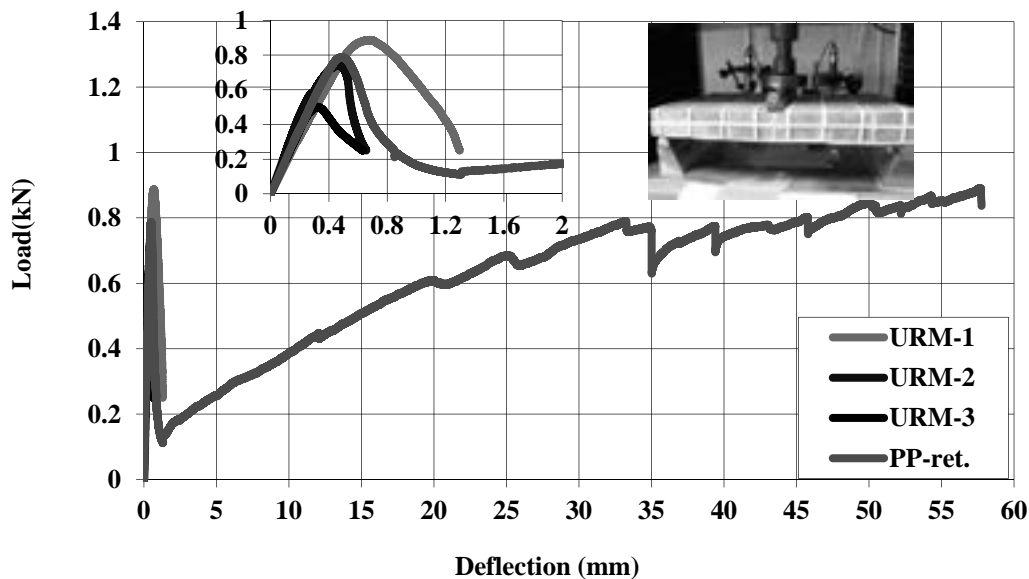


Figure 6: Load-displacement curves of non-retrofitted masonry wallets and PP-band retrofitted masonry wallet.

3.3 CFRP retrofitted masonry wallet

Figure 7 shows the load displacement curve of non-retrofitted masonry wallet, PP-band retrofitted and CFRP retrofitted masonry wallet. CFRP retrofitted masonry wallet is tested at a loading rate of 0.25mm/min and use of CFRP has increased initial peak strength of non-retrofitted masonry wallet from 0.8 kN to 8 kN. CFRP retrofitted masonry wallet has shown a high initial stiffness as compared to URM and PP-band retrofitted masonry wallets. Use of CFRP has also increased the mid span deflection from 1.2 to 5.0 mm but it is far less than PP-band retrofitted case. PP-band retrofitted masonry wallet has increased the displacement from 1.2mm to 58 mm. It can also be seen from figure 7 that CFRP retrofitted wallet has shown a sudden drop in strength from 1.6 kN to 1.0 kN at a displacement of 0.65mm. This sudden drop was due to detachment and falling of one layer of brick at the inner edge of masonry wallet. After that it again started taking load and reached to peak strength of 8.0 kN. CFRP was acting just like tension reinforcement on tension face of a simply supported beam and bricks were taking care of compression just like a simply supported beam having reinforcement on both of the faces.

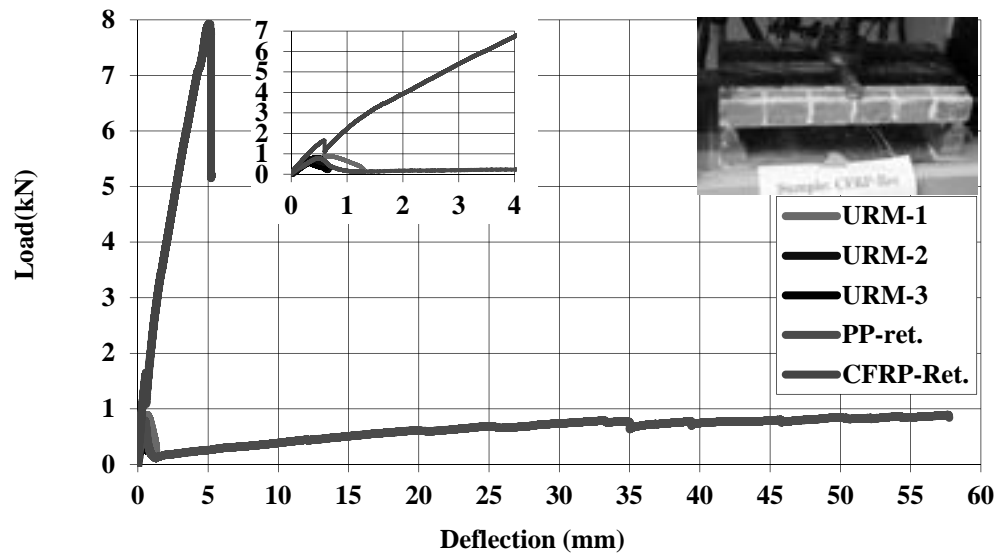


Figure 7: Load-displacement curves of non-retrofitted masonry wallets, PP-band retrofitted and CFRP retrofitted masonry wallet.

3.4 CFRP+PP-band retrofitted masonry wallet

Figure 8 shows the load-displacement curve for URM, PP-band retrofitted and CFRP+PP-band retrofitted. In case of CFRP+PP-band retrofitted masonry wallet initial strength of URM is increase from 0.8 kN to 5.5 kN and displacement carrying capacity is also increased from 1.2mm to 62mm. After the peak strength of 5.5 kN, there is a sudden drop but still CFRP+PP-band retrofitted masonry wallet has shown a good residual strength up to the final failure of wallet. Proposed composite material has increased initial strength, deformation capacity, and residual strength of non-retrofitted masonry wallet.

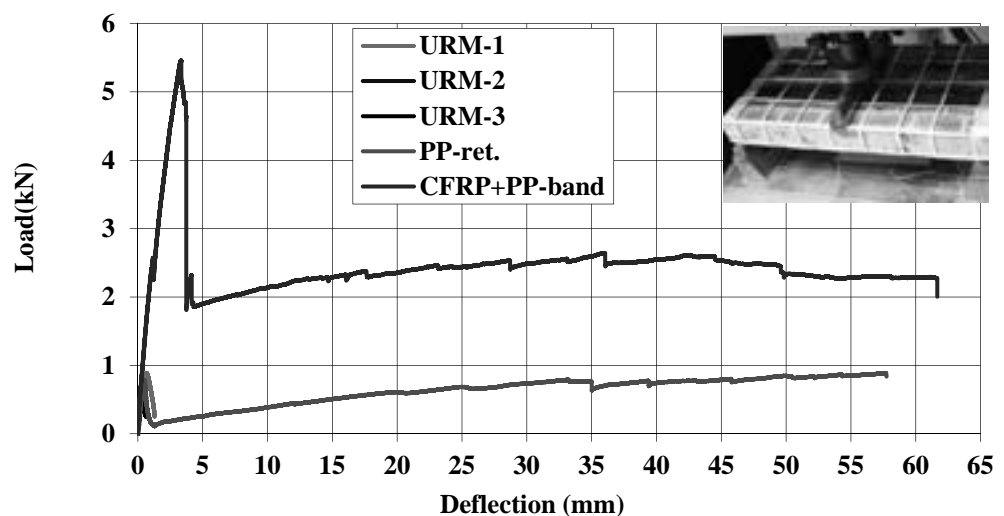
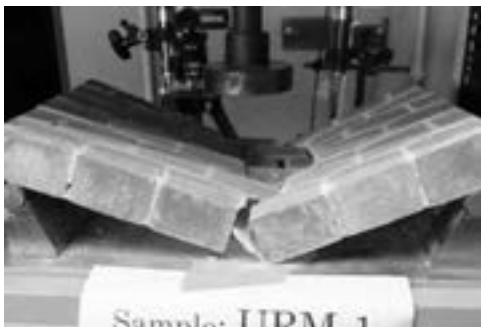


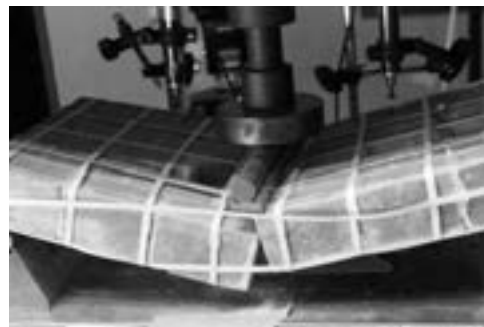
Figure 8: Load-displacement curves of non-retrofitted masonry wallets, PP-band retrofitted and CFRP+PP-band retrofitted masonry wallet.

4. FAILURE MODES

Figure 9 shows that failure pattern of different type of masonry wallets under out of plane loading. Figure 9 (a) shows a pure bending type of failure with major central cracking with spalling of bricks in the central part of masonry wallets. There were no signs of shear failure near supports. Figure 9 (b) shows that PP-band retrofitted masonry wallet failure. It is almost same type of failure as that of URM but PP-band kept holds the masonry units. As PP-band is attached with the out of plane connectors, so it has not provided any increase in bending strength but after the peak, it kept the brick unit as single mass to further take load up to a displacement of 58 mm as shown in Fig 6. Figure 9 (c) shows the failure the failure of CFRP- retrofitted masonry wallet. CFRP- retrofitted masonry wallet has shown a step wise failure initiated with the fall of inner and outer brick layers. Failure of wallet was mainly due to detachment and debonding of CFRP from brick surface. CFRP+PP-band retrofired masonry wallet failure has shown in the Fig 9 (d). Use of PP-band along with the CFRP has changed the failure mode of only CFRP retrofitted masonry wallet as the step was failure is vanished. In CFRP retrofitted case the wallet was disintegrated into longitudinal strips but CFRP+PP-band retrofitted masonry wallet has avoided the delamination of brick layers form the wallet. It kept hold the entire brick mas into a single system even upto the final failure of masonry wallet.



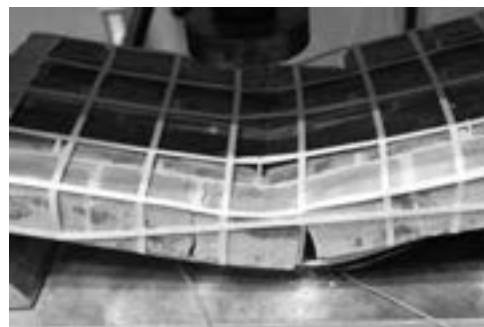
(a) Failure pattern of URM



(b) Failure pattern of PP-band retrofitted masonry wallet



(c) Failure pattern of CFRP-retrofitted masonry wallet



(d) Failure Pattern of CFRP+PP-band retrofitted masonry wallet

Figure 9: Failure pattern of different types of masonry wallets under out of plane loading.

5. CONCLUSIONS

FRP is an expensive and has very high initial stiffness with a failure strain ranging from 2-4% whereas PP-band is a cheap material with very high failure strain ranging from 12-14%. Non retrofitted masonry wall has shown very sudden failure breaking the wall into small pieces. PP-band has provided very high deformation and energy dissipation capacity but the release of energy through proper crack distribution on all over the masonry wall units. CFRP has increased the initial strength of masonry wall but it could not increase the deformation and energy dissipation capacity of masonry wall exhibiting a very high brittle failure. Failure of CFRP was mainly due to debonding of CFRP strips from the brick surface. In order to further increase the performance of masonry wall units less thickness with more surface area with good brick surface conditions are recommended. CFRP+PP-band together have not only increased the initial strength, deformation capacity, energy dissipation capacity but also the residual strength of masonry wall in post peak behaviour. This increase in residual strength is due to holding effect of PP-band provided to the bricks and CFRP and it reduces the chances of further detachment of CFRP from brick surface as wall undergoes further displacements. CFRP+PP-band retrofitted has changed the mode of failure of CFRP retrofitted wall from sudden brittle failure to gradual ductile failure. Use of both the materials has given a very high performance and cost effective technique for retrofitting of masonry structures which can save property and human life during a seismic hazard.

REFERENCES

- Coburn A., Spence R., 1992. *Earthquake protection*. Wiley. Chichester.
- Bruneau, M., 1994. Seismic evaluation of unreinforced masonry building: A state of art report. *Can J. Civ. Engrg., Ottawa*, 21, 512-539.
- Flanagan, R. D., Bennett, R. M., and Beavers, J. E., 1993. *Seismic behavior of unreinforced hollowclay tile infilled frames*. *ASTM design and construction problems and repair, ASTM STP 1180*. ASTM, West Conshohoken, Pa.
- Drysdale, R. D., Hamid A. A, and Bake, R.L., 1994. *Masonry structures behavior and design*. Prentice- Hall, Englewood Cliffs, N.J.
- EERI special earthquake report, 2012. The M_w 7.1 Erciş-Van, Turkey Earthquake of October 23, 2011.
- Mayorca, P., and Meguro K., 2003. *Strengthening of Masonry Structures using Polypropylene Bands*. Proc. of the 58th Annual Conference of the JSCE, CD-ROM.
- Meguro K., Mayorca P., Sathiparan N., Guragain R., Nesheli N., 2005. *Shaking table tests of 1/4 scaled masonry models retrofitted with PP-band meshes*. Proceedings of the Third International Symposium on New Technologies for Urban Safety of Mega Cities in Asia, Singapore. 1, 9-18.
- Turco V., Secondin S., Morbin A., Valluzzi M.R., Modena C. 2006. *Flexural and shear strengthening of unreinforced masonry with FRP bars*. *Composites Science and Technology*. 6:1, 289–296.

Study on earthquake input motions for the structures in Ulaanbaatar City

GANZORIG Erdene¹, BATSAIHAN Tserenpil², TULGA Gantumur³
and ALTANZAGAS Ochirdorj⁴

¹ Ph.D., Ass. Professor on Structural Engineering, School of Architecture
and Civil Engineering, MUST, midiid@magicnet.mn

² Ph.D., Head of Seismology Division, Research Center for Astrology and
Geophysics, Mongolian Academy of Science, batsaihan523@yahoo.com

³ Structural Consultant, Tulga Project LLC, Mongolia,
tulproject@yahoo.com

⁴ Lecturer, Department of Structural Engineering, School of Architecture
and
Civil Engineering, MUST, oaltanagas@yahoo.com

ABSTRACT

For design of high rise buildings, Mongolian National Design Code is required to perform an analysis using time histories and its response spectrum curve of earthquake excitations. Time Histories and Response Spectrums are must be developed for the real building site. In the Code also stated that, the requirements for the time histories and response spectrums are must be established from Central Government organization. In this paper, carefully studied are internationally common requirements for the time histories and its response spectrums and first time developed are the requirements in Mongolian condition. Developed are the requirements for design response spectrum, on basis of the requirements in codes of Russian Federation, USA, Japan, China and Turkey etc. Developed are first time in Mongolia, in Ulaanbaatar, real time histories and response spectrums on site of 25 story Hotel Building of Tuushin Company, using up-to-dated common approaches in international practices. As the case studies, performed are structural calculations using these records and curves and discussed the results, compared with the results of conventional design response spectrum method calculations. Discussed are further research needs for the developments of local requirements for the time histories and response spectrums.

1. PRESENT CONDITION OF THE STUDY

In “Design of Buildings and Structures in Seismic Region”, BNbD 22.01*/2006 of Mongolia, it is specified that “To design of important and high-rise buildings (higher than 16 story), seismic analysis of the building shall be performed using ground motion records of base soil as well as synthesized accelerogram. In those cases maximum amplitude of the base soil acceleration shall be at least 100, 200 and 400 cm/s² apparently taking into consideration of 7, 8 and 9 grade of

earthquake intensity of the site” [1]. Synthesized accelerogram is an artificial acceleration record that may generated from the probable earthquakes on the site [7].

In the above provision it is specified to use two different types of accelerograms including the historic seismic events and artificial records in the analysis of one building. This provision has been included in the code since 1981 but it has not been required to use this provision up to the recent period. Once there was no demand therefore almost no research has been conducted in this area. Moreover seismic data in the national code of Mongolia has been just adopted from the Code Russian Federation.

Today when structural design analysis theory and tools are rapidly developing, it has been common that codes and regulations of foreign countries have required use of records of potential earthquakes on that area and similar earthquakes that occurred in a different area in the seismic analysis. This requirement has been widely put not only on the high-rise building but also low rise buildings [5]. Therefore many studies on accurate development of seismic data and characteristics and effective usage in the design, have been carried out in foreign countries [3].

It is clear that seismic source, propagation condition and soil characteristics that apply to the design of building are different on every building. Those factors are definitely within territory of Mongolia. Particularly, only an earthquakes within 300 and 400 km is hazardous for building that is being designed in Ulaanbaatar. Therefore, we need to have seismic data and parameters of own country to be used in the structural analysis. Aim of this paper is definitely directed to it.

On the other hand, many buildings higher than 16 stories have been designed and built recently in Ulaanbaatar. Thus, we are required to implement the above requirement of our code in actual structural design of the high-rise buildings.

In order to describe in input motion and its synthesized record, micro seismic study and measurements are carried out in the site of the building. The record vary depends on many factors, such as seismic history, potential sources, tectonic formation of soil, hazard level, water table, thickness and density of base soil layers of the site.

Synthesized accelerogram is developed mostly in bed rock or in the alluvial soil surface. Accelerogram is developed using an earthquake source model, historical earthquakes, travel condition, soil geotechnical characteristics and geophysical parameters of the site [11].

This accelerogram is corrected by using the acceleration records of the actual earthquakes in order to match with the design response spectrum of the Code by many indicators such as duration and energy contents etc. It is the main difficulty to develop the accelerogram [6].

The acceleration record of the historical earthquakes is taken from the record bank and it is an important input data for the analysis and research, because it contains mechanism of earthquake and process and all indicators of the soil excitation (e.g. amplitude, frequency, energy contents, duration and phase etc). It is also proper to reflect all factors including the earthquake source, propagation ways and soil characters of the site in the analysis. Also the accelerogram can be used in the analysis by scaling the amplitude and correct reflecting attenuation law.

It is complicated to choose proper accelerogram developed by the micro seismic investigation for the analysis. In the code it is specified that state administrative

organization is in charge for establishment of requirements on the accelerogram and its response spectrum curve to be used in the analysis. In the most codes it is specified to use several accelerograms in the analysis of one building.

2. MICRO SEISMIC STUDY OF THE SITE OF TUUSHIN HOTEL BUILDING

Seismic hazard assessment of the site of 25 story hotel building of “Tuushin” LLC to be built in the territory of Sukhbaatar district of Ulaanbaatar city was executed based on geophysical measurement, fund materials, analysis methodology and basic hazard study [4].

Client provided topography and required information on engineering–geology and hydro geology.

View and model for the structural analysis of the hotel building of Tuushin LLC are shown in Figure 1.



Figure 1. 3D view and model of the structural analysis of the hotel.

Propagation velocity of primary and shear waves were determined till the bedrock depending on the depth in the site of the hotel building. Etalon velocity of the seismic wave that is observed in the bedrock in the vicinity of Ulaanbaatar city was chosen and the seismic model of the site was developed.

Horizontal gradients of the basic signal of potential strong earthquake was developed by the first step. Strong earthquake accelerogram to hazard the base, its response spectrum and frequency characteristics are estimated and developed on horizontal (EW) and vertical (Z) gradients (Figure 2).

Basic input data of the seismic actions are within the following limit: seismic hazard intensity is 8.1 grade according MSK scale. Maximum amplitudes of the acceleration to be observed by the strong earthquake is 213 and 127 cm/s² on horizontal (EW) and vertical (Z) direction respectively. Maximum amplitude of the acceleration response spectrum is 1,4; 3,3 in the horizontal and 1,27 Hz on the vertical and they are 51,6 and 27,7 cm/s on horizontal (EW) and vertical (Z) directions respectively.

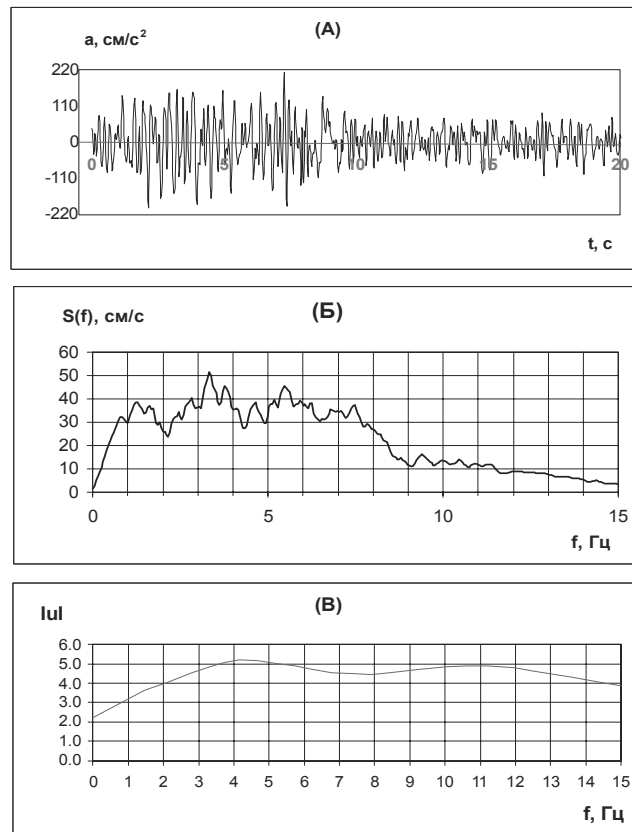


Figure 2. Accelerogram and its response spectrum, frequency characteristics in horizontal direction

Intensity of the seismic action was determined based on assumption that soil deformation is elastic and bases on the intensity scale descriptions.

3. ANALYSIS OF THE STRUCTURE OF TUUSHIN HOTEL

The accelerogram and its response spectrum developed by the micro seismic study of the site were taken as example and used in the analysis of the structure.

Structural system consists of cast-in situ RC core, shear walls, SRC frame system with shear walls, and lateral loads resisted mainly by RC core and shear walls.

Concrete grade is B30, compressive strength is 224 kgs/cm^2 , Young's modulus – $3.3 \times 10^5 \text{ kg/cm}^2$ and Poisson's ratio - 0.2 in the design. Column section is composite from H type steel section and cast in place external concrete part. Strength of the column and beam steel was taken as 3000-3300 kg/cm^2 depending on its thickness.

Foundation is 2 m thick cast-in situ RC raft foundation. Structural analysis model of raft foundation is taken as the slab on Winkler sub grade. Earthquake intensity of the site was grade 7 by micro zoning and grade 8 by micro seismic study.

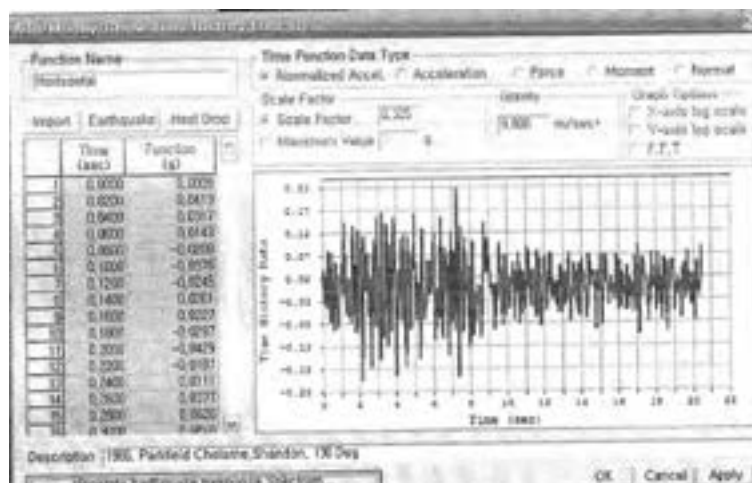


Figure 3 . Structural analysis using an accelerogram by MIDAS program

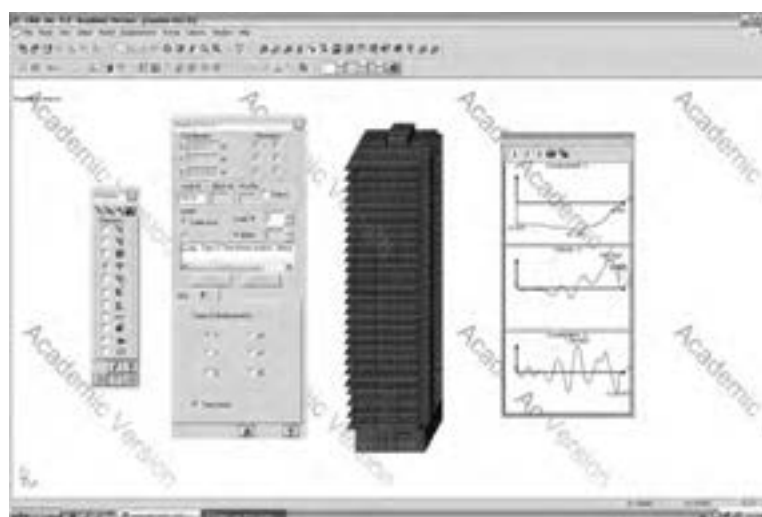


Figure 4. Structural analysis using an accelerogram by LIRA program

The structure was analyzed for the seismic actions at IST construction consulting company of Republic of Korea using MIDAS program [13]. Also it was analyzed at design company Goo Van Consulting of Mongolia using LIRA - 9.4 program [9]. First, structural analysis used the design response spectrum by conventional response spectrum method on both of the above two companies. Next analysis was calculated using the accelerograms by MIDAS program and mode superposition method (Figure 3). Also analysis was made by direct integration of differential equation of the motion method and mode superposition method by LIRA program (Figure 4).

4. RESULTS OF THE STUDY

Commonly used international requirements are studied and the requirements for Mongolia are developed for the first time. Also the requirements on the response spectrum curve to be used on the analysis of the high-rise building were

determined and proposed based on experiences of Russian Federation, USA, Japan, P.R. C and Turkey [10].

Following the above requirements potential seismic record and response spectrum curve were developed on case of Ulaanbaatar city in accordance with internationally used methodology.

Also the results analyzed by using the Time Histories and compared to the results analyzed by the conventional Response Spectrum Method. The results used MIDAS program was 60 – 70% and LIRA program was 40 – 50% of this result. From this, results of the analysis are more less than the conventional response spectrum results and it proves ineffectiveness of the analysis using this accelerogram.

According the accelerogram developed by Research Center for Geophysics Astrology and predominant frequency is observed to be 0.2-0.3 seconds but the response spectrum curve given relatively wide range and takes the maximum value between 0.1-1.0 seconds and it shows inappropriateness between them. Also as for the response spectrum curve its form is much different than MNCN code of Moscow and Japanese code shown in the Figures. (Figure 5,6,7).

Also it is needed to clarify reason for high amplitude of the response spectrum curve. It is needed to study experiences and methodology of foreign countries.

Low predominant frequency of the accelerogram results in relatively low analysis result of the analysis used the accelerogram. Therefore, it is required to consider an amplification of base layers, methodology to choose earthquake that potential to be hazardous for that building from earthquakes that occurred in foreign countries or internationally used earthquakes and solve the problem urgently.

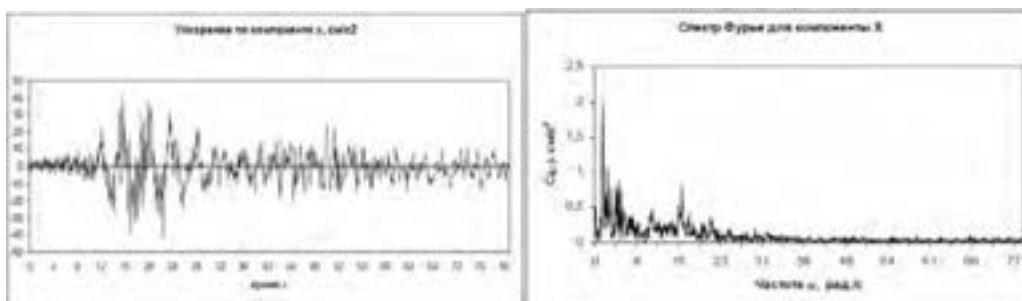


Figure 5. Registered in Moscow acceleration record and its Furies spectrum, MNCN code, 4th of March, 1977. Moscow

Etalon record developed on bedrock is must be same on total territory of Ulaanbaatar city thus it is insufficient to reduce and increase the amplitude depending on the intensity of the site not considering amplification of the base layers. Also, the accelerograms are varied only by their amplitudes along the horizontal and vertical directions.

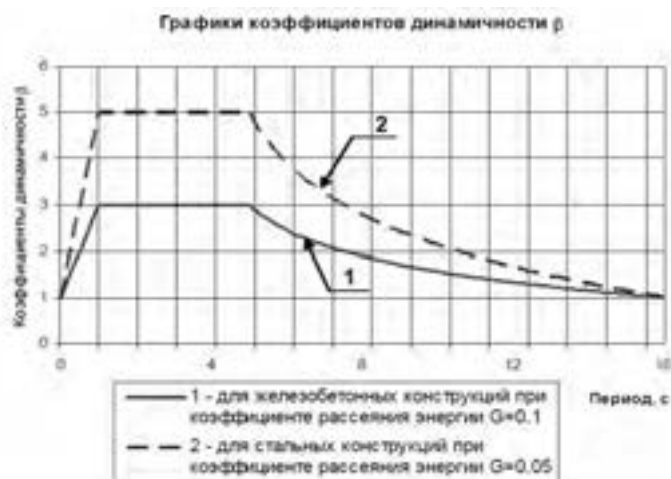


Figure 6. Design Response Spectrum curve for the analysis, MNCN code, Moscow.

Period (seconds)	Acceleration response spectrum (unit: m/sec ²)	
	Earthquake motion that occurs rarely	Earthquake motion that occurs extremely rarely
$T < 0.16$	$(0.64 + 6T) Z$	It shall be a value equal to 5 times the acceleration response spectrum of earthquake motion that occurs rarely
$0.16 \leq T < 0.64$	$1.6Z$	
$0.64 \leq T$	$(1.024 / T) Z$	

In this table, T and Z shall represent the frequency of the building (unit: seconds) and the value of Z stipulated in Article 88 paragraph 1 of the Order respectively.

Figure 7. Design Response Spectrum for the analysis of high-rise buildings, notification #1461,2001 by MLIT Japan

Another requirement on the accelerogram is its duration. For example, duration is 80 sec in MNCN code of Moscow, 56 – 160 sec in DBN code of Ukraine, at least 1 minute in BSL code of Japan and 30 sec in DBYBHY code of Turkey while period of our accelerogram is 23 sec and it is seems insufficient [5].

It is needed to compare with scenario earthquake of Ulaanbaatar city by professor N. Kawase and others [12].

Also it is required to provide fundamental period base layer of the site and direction of earthquake excitation.

Result of the study is determined and further concerning issues in this are developed.

5. CONCLUSION

1. Etalon record developed on bedrock is must be same on total territory of Ulaanbaatar city thus it is insufficient to reduce and increase the amplitude

- depending on the intensity of the site not considering amplification of the base layers.
2. According to the above mentioned conclusion only one accelerogram can be used in the site with same earthquake intensity. Therefore it is needed to develop at least several accelerograms and use two or three of them which are seems more hazardous to the structure.
 3. To increase relatively less duration time of the accelerogram compared to foreign countries.
 4. To develop a national code or regulation to carry out micro seismic investigation of the site urgently. In other words, it is required to set requirements on accelerograms and site response spectrum to be used in the design of buildings and structures.
 5. To continue the research further and develop the design response spectrum curve to be used in the analysis of the high-rise structures and have it approved by the central government organization.

REFERENCES

- [1]. "Design of Buildings and Structures in Seismic Region", BNbD 22.01*/2006, Mongolia
- [2]. E. Ganzorig and others, "Commentary to the Code for Design of Buildings and Structures in Seismic Region, BNbD 22.01*/2006", BD 22-101-07
- [3]. Ts. Batsaikhan. *Geophysical investigation of seismic hazard level of Ulaanbaatar city*. Dissertation for Ph.D., Irkutsk, Russia, 2006.
- [4]. Ts. Batsaikhan, B.E. Jurik,, *Earthquake hazard assessment of the construction site of the hotel of "Tuushin" LLC to be built in the territory of Sukhbaatar district of Ulaanbaatar city*, 2009
- [5]. *International Association for Earthquake Engineering, Regulations for Seismic Design*, A World List - 2006, Tokyo, Japan, 2006
- [6]. Seismology Committee, Structural Engineers Association of California, *Recommended Shear Force Requirements and Commentary*, 1996, Sixth Edition
- [7]. *Earthquake Motion and Ground Conditions*, Architectural Institute of Japan, Tokyo, 1993
- [8]. Anil K. Chopra, *Dynamics of Structures. Theory and Applications to Earthquake Engineering*. Prentice Hall, 2001
- [9]. Gorodetski A.S. and others. "Structural analysis of cast in-situ high-rise buildings". Kiev, Publisher Fact, 2004
- [10]. B.N. Gordiev and others, *Loads and effects on Structures*. Publisher ASB, Moscow, 2007
- [11]. Yasin M. Fahjan, "Selection and Scaling of Real Earthquake Accelerograms to fit the Turkish Design Spectra, Digest 2008" - Technical Journal, Turkish Chamber of Civil Engineers, Volume 19, December 2008
- [12]. UN Habitat Project MON 99/301, *Earthquake "Disaster Risk Management Scenario For Ulaanbaatar, Mongolia, Final Report*, 2001
- [13]. "Analysis Manual for MIDAS/Gen", MIDAS IT Co.Ltd., 2006

Numerical simulation of Beam-Column joint with simple reinforcement arrangement by three-dimensional RBSM

Koichiro IKUTA¹, Daisuke HAYASHI², Kohei NAGAI³

¹ Graduate Student, School of Engineering, The University of Tokyo, Japan
ikuta@iis.u-tokyo.ac.jp

² Project Researcher, IIS, The University of Tokyo, Japan

³ Associate Professor, ICUS, IIS, The University of Tokyo, Japan

ABSTRACT

Structural performance at beam-column joint varies much depending on the arrangement of reinforcement steel bars at joints. To investigate the influence of the bending radius of reinforcement bars at beam-column joints on rigid frame and study the failure mechanisms of beam-column joints, analyses were carried out by three-dimensional Rigid Body Spring Model (RBSM). Simulations of L beam-column joints with simple reinforcement arrangement were carried out to examine the failure pattern at L beam-column joints. In this paper, only monotonic loading (two types, open and close) to the joint part was carried out. These simulations showed the different crack patterns and failure modes according to the loading direction. These results would be beneficial to improve the analysis model for further proper numerical simulations of L beam-column joints.

Keywords: RBSM, crack pattern, beam-column joint, bending radius

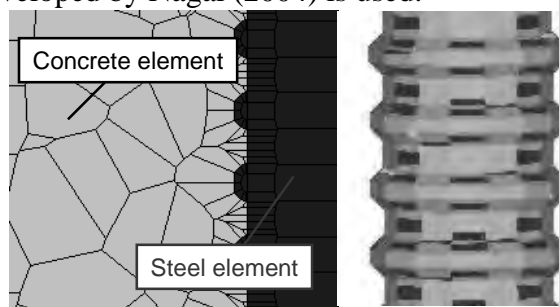
1. INTRODUCTION

Nowadays in Japan, seismic design code is becoming more stringent. To satisfy the stringent requirements, larger amounts of reinforcement must be placed, resulting in increased reinforcement congestion. This problem particularly occurs at beam-column joints, where reinforcements meet from many different directions. As a result, it becomes difficult to ensure proper concrete compaction and hence poorer concrete quality may result. Moreover at the L beam-column joints, structural performance is thought to change depending on the arrangement of reinforcement. However, it is difficult to clarify the structure performance on complicated bar arrangement like beam-column joints, so only little analysis have been done for the beam-column joints. In this study, numerical simulations are carried out to investigate the influence of the bending radius of reinforcement at the L beam-column joints by Rigid-Body Spring Model (RBSM), which is a kind of discrete analysis.

2. ANALYSIS METHOD AND MODEL

2.1 Analysis method

In this study, analysis is carried out by 3D RBSM approach, proposed by Kawai (1978). Two types of elements, namely concrete and steel elements, are used to define the geometry of a specimens embedded reinforcing bar. The concrete elements size is set smaller than the maximum aggregate size, while the steel element size is set according to geometric complexity of the reinforcing bar (Figure 1). Three springs (one normal direction and two shear directions) are assumed to connect each face of the elements. The properties of the springs are determined so as the elements, when combined together, enable accurate prediction of the response of laboratory-scale material test. In this study, simulation system developed by Nagai (2004) is used.



(a) Cross section of elements (b) 3D Rebar shape

Figure 1: Modeling of geometric rebar shape

2.2 Constitutive models

Two elements are used to represent the behavior of reinforced concrete:

(1) Steel element for steel bars

The geometry of the steel elements is modeled in an accurate manner to properly account for the interlock between reinforcement and concrete. Figure 1 illustrates typical reinforcement geometry used in analysis. Bi-linear model is adopted for the steel elements to reproduce the yielding of steel.

(2) Concrete element

The shape of concrete elements is determined by using the Voronoi diagrams, except those nearby the steel elements which were constructed manually following the geometry of the steel elements. Random element generation is considered to reasonably replicate concrete fracture process.

The concrete constitutive models for the normal and shear spring are shown in Figure 2. The normal springs are assumed to behave elasticity both in compression and in tension. After reaching its strength in tension at f_t , the stress in the springs is assumed to decrease linearly to zero at the maximum crack width w_{max} (assumed to be 0.003mm, Figure 2(a)). The shear spring is assumed to behave in an elastic-plastic manner (Figure 2(b)), with a yield strength computed from Equation 1 (adopted from Muto et al.(2004), Figure 2(c)). Here, $\phi = 37^\circ$.

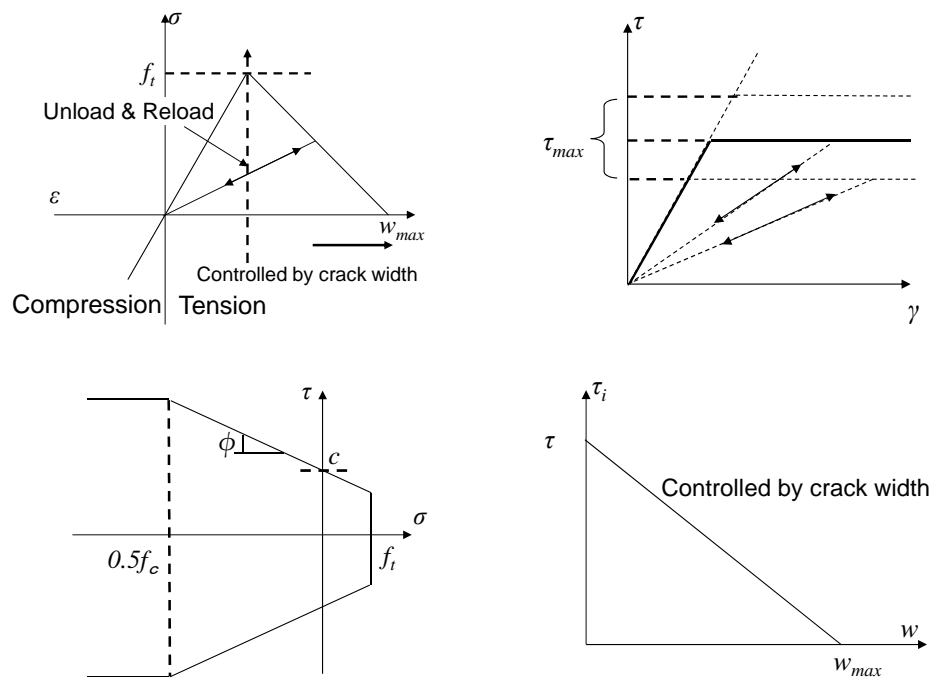
$$\tau = \begin{cases} c - \sigma \tan \phi & (\sigma \geq 0.5f_c) \\ c - 0.5f_c \tan \phi & (\sigma < 0.5f_c) \end{cases} \quad (1)$$

$$c = f_t(1 + \tan \phi)$$

For regions within 1D (D: bar diameter) from the reinforcement surface, the concrete constitutive model is modified to account for interfacial zone between the reinforcement and the concrete (Salem et al. (2005)). In this zone, the elastic modulus of the spring is assumed to be a half of the original value.

(3) Steel-Concrete interface

At steel-concrete interface, the normal spring is considered to be the same to that of the concrete element (Figure 2(a)), but with a tensile strength of only a half. The shear spring is assumed to behave elastic-plastic, with the yield strength calculated from same concept of criteria to concrete element. Moreover, the shear strength of the interface spring is assumed to decrease according to crack width to represent interface fracture (Figure 2(d)).



(a) Model of normal spring of concrete (b) Model of shear spring of concrete
(c) Failure criterion of concrete (d) Model of shear reduction of concrete

Figure 2: Constitutive models of springs

3. L BEAM-COLUMN JOINT SIMULATIONS WITH DIFFERENT BEND RADIUS FOR BENDING BAR

3.1 Analysis cases

The arrangement of reinforcement at the joint part is thought to have a significant influence to the structural performance of beam-column joints. To investigate the influence of the bending radius of the steel bar to the structural performance at the

L beam-column joints, in this study the several simulations with different bend radius at the corner, 25mm(1D), 75mm(3D), 200mm(8D), were analyzed. Here, D means diameter of steel bar. The arrangement of reinforcement is simplified than the practical due to calculation cost. Table 1 shows all simulation cases. The models used in analysis are shown in Figure 3. Reinforcing steel bars in the model are diameter 25mm and 10mm deformed bars.

The boundary condition considered in the analysis is shown in Figure 4 Displacement controlled monotonic loading was applied to the left surface of specimen, with an increment of 0.1mm for each steps and all elements on the bottom surface were fixed. Two types of loading, *Open* and *Close*, were carried out. *Open* means pull the left surface to left direction, and *Close* means push the left surface to right direction.

Table 1: Analysis cases

Case	Open or Close	Bend Radius	Concrete		Steel bar		Number of elements	Maximum Load in analysis (kN)
			Strength (N/mm ²)		Elastic modulus (kN/mm ²)	Yielding Stress (MPa)		
			f_c	f_t				
C1	Close	25(1D)	25	2.5	190	600	222871	207.7
C3		75(3D)					198837	198.3
C8		200(8D)					176451	196.9
O1	Open	25(1D)	25	2.5	190	600	222871	122.6
O3		75(3D)					198837	119.8
O8		200(8D)					176451	169.9

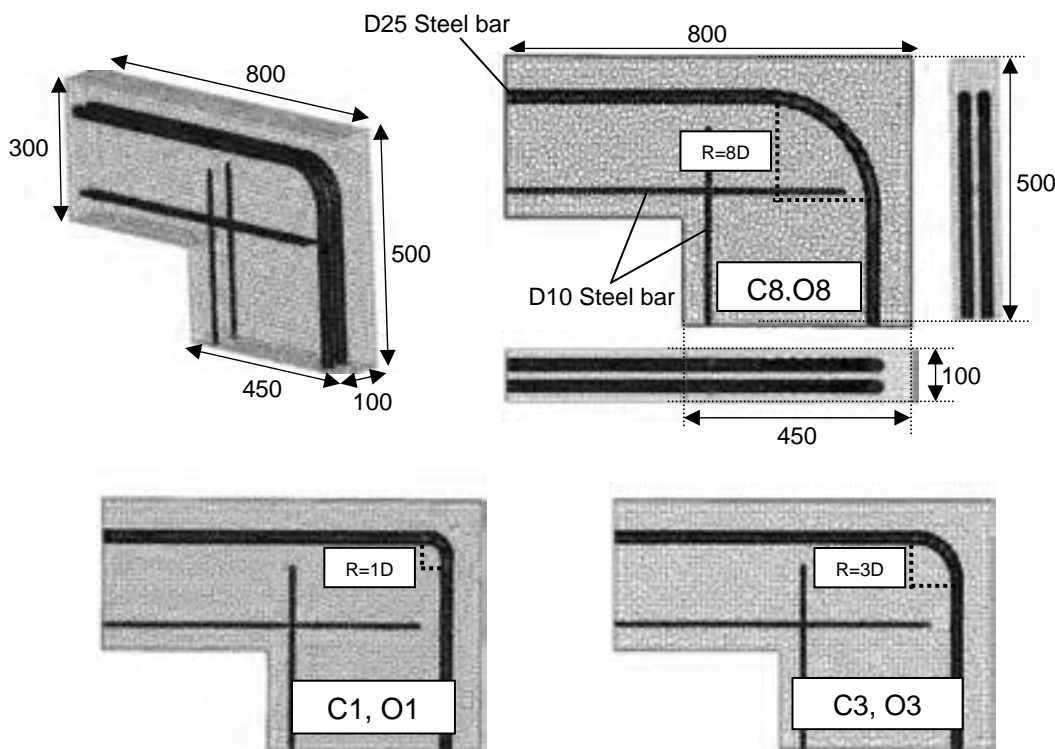


Figure 3: Analysis models

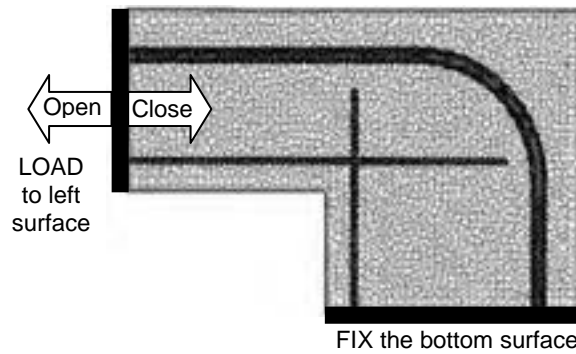


Figure 4: Boundary condition

3.2 Analysis result

3.2.1 Crack pattern

Figure 5(a) shows the crack pattern for close cases at the maximum load and Figure 5(b) shows the crack pattern for each open cases at the displacement of 1.3mm. Deformation is enlarged 25 times.

In all close cases (Figure 5(a)), shear cracks were formed from the bottom-right side to top-left side and only few bending cracks on the top surface were observed. This means all three cases had shear failure at the column area. At first, shear cracks occurred at column part from the bottom-right side and then it propagated to the beam part. In these analyses, almost all cracks concentrated on only column part, and no cracks occurred at bending reinforcement area. The reason of this behavior is a boundary condition introduced to this model. In this analysis all bottom surface elements were fixed and could not rotate, as a result stress concentrated at column area and it led to the failure at column area before cracks occurs at the joints.

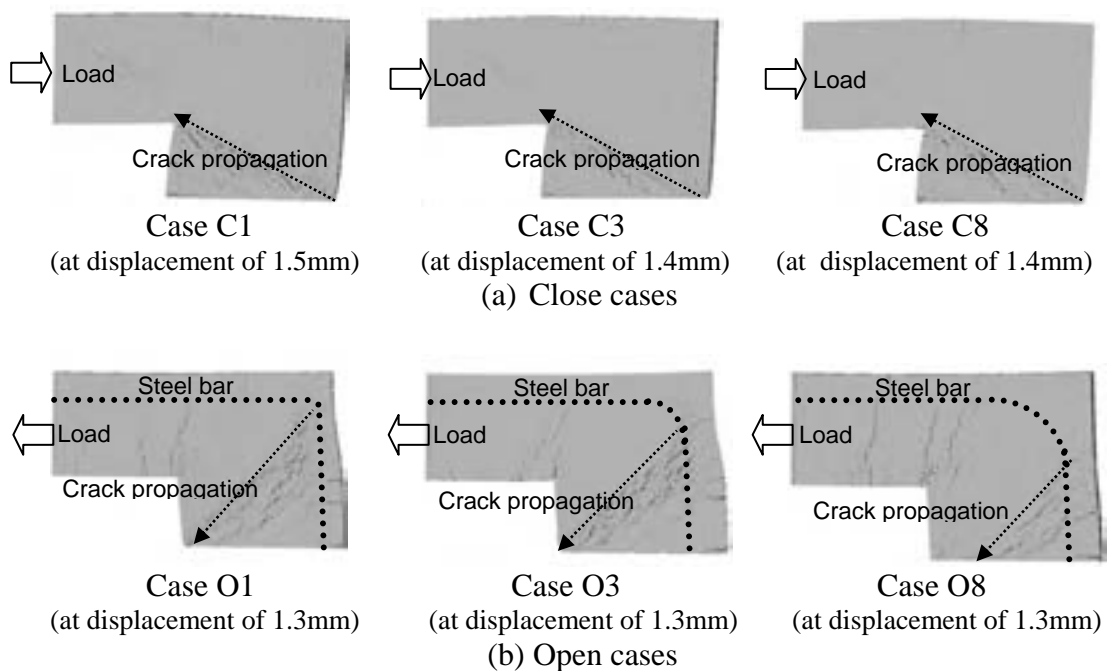


Figure 5: Cracks pattern

In all open cases (Figure 5(b)), shear cracks occurs from the bending point of reinforcement bar to the bottom surface and these shear cracks propagated in around 45 degree direction. These analyses shows that location of the crack changes depending on the bending radius of reinforcement and the cracks start from the bending start point.

3.2.2 Load-Displacement Relationship

The load-displacement relationships from analysis are shown in Figure 6. In all close cases (Figure 6(a)), the load-displacement relationship is not so different although the bending radius is different. Figure 7 shows the stress distribution for close cases at the maximum loading. In all cases, compression stress formed diagonally from the bottom of column to the loading side. Tensile stress generated around the bending reinforcement area. Shear failure occurs in column in all three cases, so the maximum load of 3 cases is almost same.

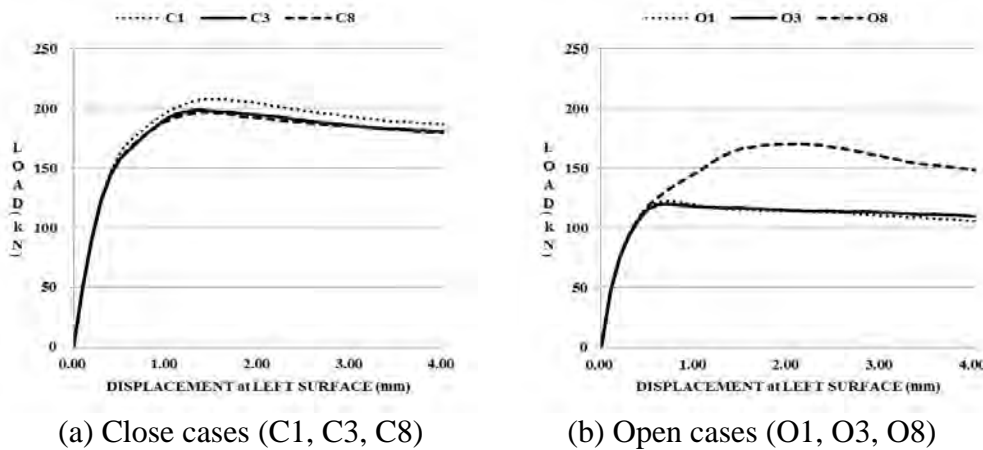


Figure 6: Load-displacement

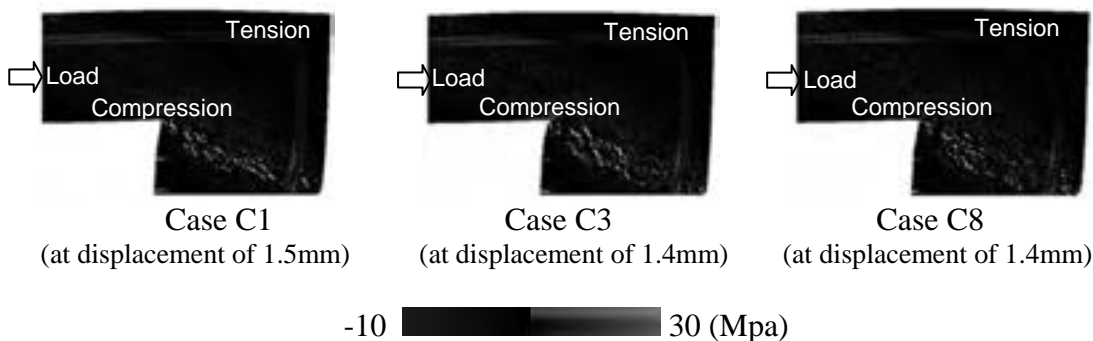


Figure 7: Stress distribution of close cases

In open cases (Figure 6(b)), the load-displacement relationship of O1 and O3 were almost same, but O8 was different: the maximum load of O8 (169.9kN) was larger than other two (O1:122.6kN, O3:119.8kN).

Figure 8 shows the stress distribution of 3 open cases when displacement is 1.3mm (O1 and O3 is after maximum loading, O8 is before maximum loading). In all cases, compression strut was formed from the bending part of steel bar. In this

analysis, it seems that width of the compression strut is defined by the bending reinforcement area. It means that compression strut area is influenced by bending radius of steel bar. As a result, the size of compression strut of O8 is larger than other two and this may be a reason for the increment of maximum loading.

Figure 9 shows the shear stress distribution of 3 open cases. Shear stress area is different and in all cases shear stress is from bending start area of steel bar to bottom surface in around 45 degree direction. The shear stress area accords with the internal crack area also (Figure 10). In case O1 and O3, shear cracks reach almost corner, left side of bottom, of the column, so the stress transfer only along the shear cracks. However in case O8, shear cracks does not reach the corner and stops at bottom surface which is fixed, so the stress can transfer from bending bar to the bottom surface through compression strut widely. This may be the reason for that the load of O8 is still increasing at the displacement of 1.3mm.

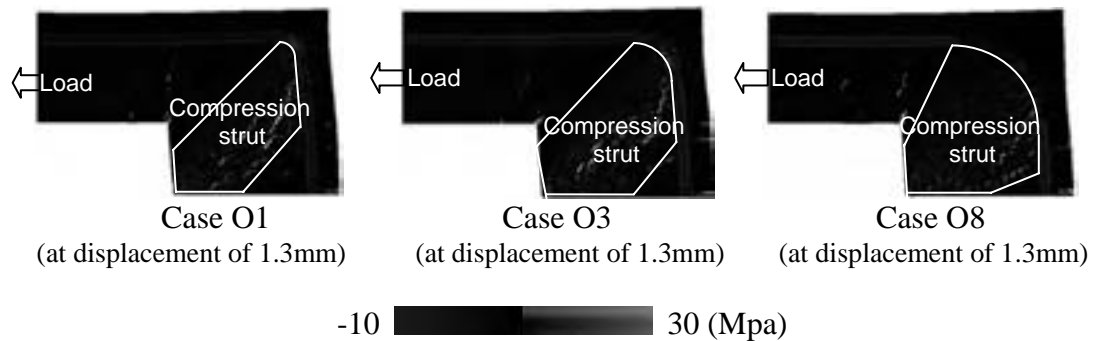


Figure 8: Stress distribution of Open cases

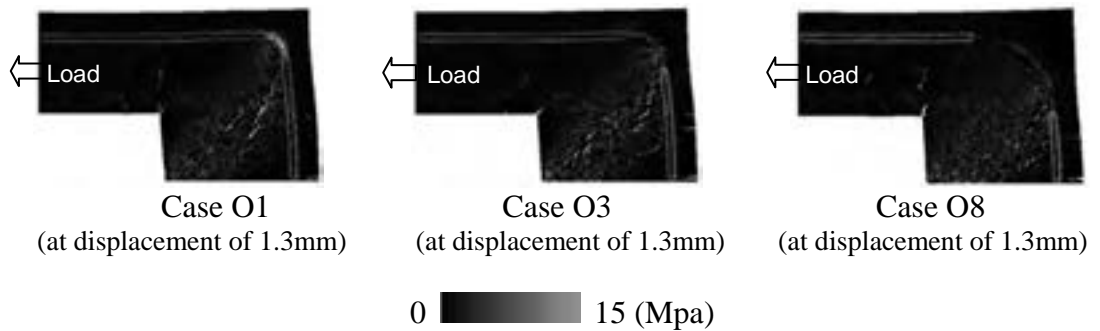


Figure 9: Shear Stress distribution of Open cases

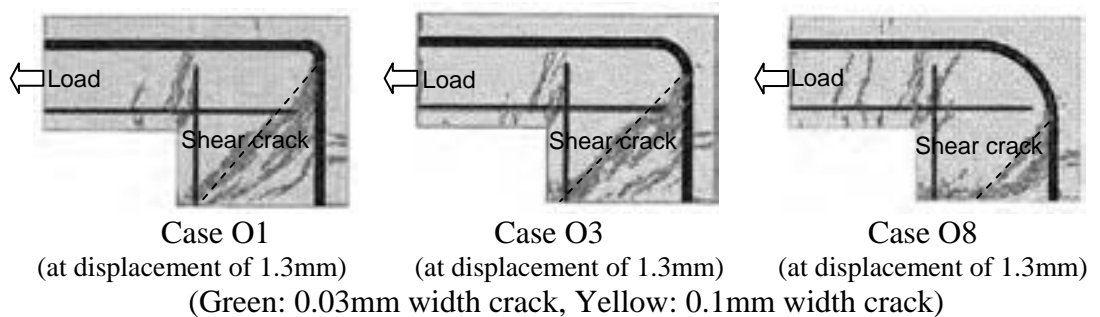


Figure 10: Internal cracks for Open cases

4. CONCLUSIONS

From the result of simulations investigating the influence of reinforcement arrangement to the L beam-column joints, the following conclusions are made.

(1) The analysis of RBSM for L beam-column joints simulated the different crack patterns according to the loading direction and boundary condition.

(2) The analysis of loading *Close* direction could not simulate the cracks in joint area because of the boundary condition problem. This boundary condition problem should be solved next.

(3) In the analysis of *Open* direction, compression strut was formed and the size of the strut depends on the bending radius of steel bar that caused the difference of maximum loading capacity.

REFERENCES

Salem H, M. and Maekawa, K., 2004. Pre-and Postyield Finite Element Method Simulation of Bond of Ribbed Reinforcing Bars, *Journal of Structural Engineering*, ASCE, 671-680.

Kawai, T., 1978. New Discrete Models and Their Application to Seismic Response Analysis of Structure, *Nuclear Engineering Design* 48, 207-229.

Muto, S., Worapong, S., Nakamura, H. and Kunieda, M., 2005. Analysis of Bond Characteristic between Concrete and Deformed Bar by Meso-scale Analysis. *Proceedings of JCI*, Vol.27. No.2, 763-768.

Nagai, K., Sato, Y. and Ueda, T., 2005, Mesoscopic Simulation of Failure of Mortar and Concrete by 3D RBSM. *Journal of advanced concrete technology*, Vol.3, No.3, pp.385-420.

Contemporary middle-rise timber buildings in Japan

Mikio KOSHIHARA
Professor, IIS, the University of Tokyo, Japan
kos@iis.u-tokyo.ac.jp

ABSTRACT

Buildings in Japan have been constructed using timber since olden times. At the same time, Japan is a country beset by earthquake and timber buildings were weak against fire. So, from 1950 to 1987 wooden buildings over 13m height were prohibited by law. Revision of the Building Standards Law 2000 allowed the construction of buildings four-story or taller with fire-resistance performance. M-Bldg. built in 2005 is the first five-storied timber building after established Building Standard Law in Japan. The possibilities of middle-rise and high-rise timber buildings in Japan are extended by completion of this building and some middle-rise timber buildings were built.

This paper describes the detail of three middle-rise timber buildings below. Eastern Saitama Regional Development Center “Kasukabe Convention Hall” is six storied mix structure convention hall. From 1st to 4th stories of this building are steel structure and top of 2 stories are timber structure. “Wood Square” is four storied timber based hybrid structure office building. “Shimouma Project” is five storied timber apartment house.

Keywords: seismic performance, fire resistance performance

1. INTRODUCTION

Buildings in Japan have been constructed using timber since olden times. Traditional timber temples and shrines, such as the Horyu-ji Temple, look the same as they did when constructed more than 1400 years ago. Many large-scale timber buildings were constructed during that time, and include the Hall of the Great Buddha in Todai-ji Temple (height: 46.8 m, area: 2878 m²) and the five-story Pagoda in Toji Temple (height: 54.8 m). Even after the Meiji Era, four and five-story timber buildings were used as factories, warehouses, and inns, until the construction of large-scale timber buildings was restricted by the Urban Building Law of 1919, and the Building Standards Law of 1950 further restricted the construction of large-scale timber buildings. In 1959, the Architectural Institute of Japan carried a resolution against timber construction to prevent fire, storm, and flood damage, making it impossible to construct large-scale timber buildings. Timber building height restrictions were loosened in 1987, allowing the construction of three-story structures and buildings taller than 13 m. Eaves having a height of more 9 m were also permitted using large sections of laminated timber. Revision of the Building Standards Law in 2000 allowed the construction of buildings four stories or taller with fire-resistance performance. The present study

reports the structural and fire resistance characteristics of the first timber-based hybrid structure in Japan, the five-story Kanazawa M building (Kanazawa M Bldg.), constructed in 2004.

2. KANAZAWA M BUILDING

2.1 Outline of the building

The five-story Kanazawa M Bldg. (height: 14.237 m, area: 6.195 m x 12.100 m) was constructed in Kanazawa City, Ishikawa Prefecture. (Photo 1) The first story has a Reinforced Concrete structure and the second to fifth stories have a timber-based hybrid structure with built-in steel materials. Building data are listed in Table 1, and the floor plan and elevation are shown in Figure 1 and Figure 2.

Table 1: Building data

Architect	-architect office- Strayt Sheep
Structural Design	Kirino Structural Engineering Office
Area	374m ² (total floor) / 74.96m ² (building)
Use	School
Height	14.237m
Number of stories	5th stories
Structure	RC construction(first story) Timber-based hybrid construction(2-5 storied)



Photo.1: External view of Kanazawa M Bldg.

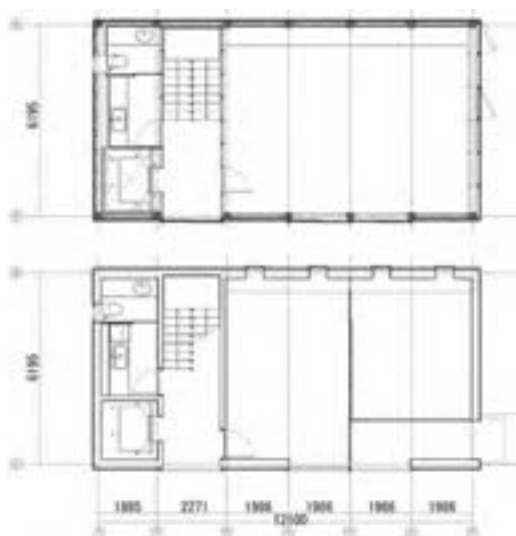


Figure 1 : Floor plan

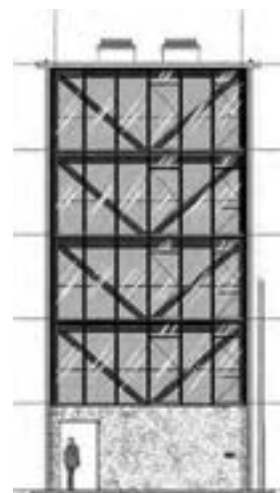


Figure 2 : Elevation

2.2 Members

The building mainly uses the structural members listed below to satisfy the requirements for vertical load performance, seismic performance, and fire resistance. This building is required fire resistive construction, and structural elements are required 1 hour fire resistive period.

(1) Column, beam, and brace

The building uses laminated timber with built-in steel materials for columns, beams, and braces to satisfy the structural and fire resistance requirements of a five-story building. The cross section of each member is shown in Figure 3.

The column is square laminated timber (larch E105-F300, 200 x 200 mm) with built-in square steel bars (SS400, 65 x 65 mm). The beam is laminated timber (200 x 330 mm) with steel plates (SS400, PL-22x300). The cross section of a brace looks identical to that of a column, which is necessary for fire resistance certification.

(2) Floor and roof

The floors and roofs are made of reinforced concrete slabs joined together with lag screws and steel plates built into the beams.

(3) Wall

The longitudinal walls are load-bearing and made of nailed plywood. The lateral walls are non-load-bearing, because of setting braces.

(4) Stairs

The stairs are made of steel frames.

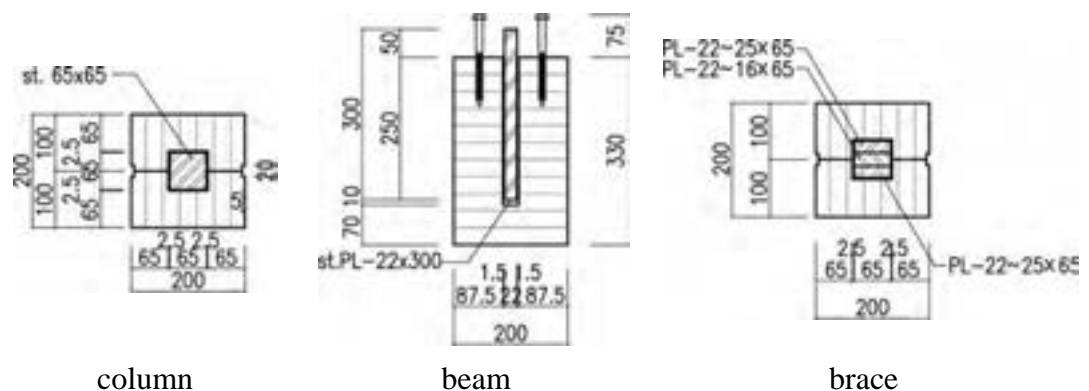


Figure 3 : Cross sections of column, beam, and brace

2.3 Structural planning

Similar to ordinary timber buildings, a five-story timber-based hybrid structure requires verification of its safety against self weight, live load, vertical load by snow coverage, and horizontal load under a horizontal force, such as an earthquake or wind. Fire resistive buildings are also required to maintain building integrity in the event of a fire. Based on these structural performance requirements, the following structural verification was conducted on the Kanazawa M Bldg.

2.3.1 Vertical Load

The timber and steel frame function together as a structural member in the second to fifth stories of a timber-based hybrid structure. To clarify the function of the timber and the steel frame about each member, the joint was designed as follows:

(1) Beam

Since the vertical deformation is equal between the timber and the steel frame, vertical load should be shared depending on their ratio of flexural rigidity, EI (E: Young's modulus, I: Geometric moment of inertia). The flexural rigidity ratio EI / ΣEI is shown in Table 2.

Table 2: Flexural rigidity ratio of timber and steel frame

	E (N/mm ²)	I (mm ⁴)	EI (Nmm ²)	EI/ ΣEI
Timber frame	1.05x10 ⁴	5.55x10 ⁸	0.583x10 ¹³	0.366
Steel frame	2.05x10 ⁵	4.95x10 ⁷	1.01x10 ¹³	0.634

The flexural rigidity ratio EI / ΣEI is shown in Table 2.

The timber and steel frame of the beam are joined at a beam edge using drift pins to transmit the load from the timber to the steel frame, so the steel frame bears all the shear force at the edge. The gusset plate from the steel frame of the column and the steel frame of the beam are joined with high tension bolts for the column-beam connection. The holes in the side of the timber frame are filled with timber after high tension bolts are clamped. (Figure 4).

Snow load stress on both the timber and steel frame of the beam are designed not to exceed the short-term allowable limit, even in the very rare case of a snow load with a vertical depth of 1.2 m (multiplied by 1.4).

(2) Column

Vertical load is transmitted to the steel frame of a column through a gusset plate, and vertical loading of the timber is avoided using a 3 mm clearance, which is essential for combining the timber with the steel frame. The timber of the column functions as a buckling restraint for the steel frame, and, as the structural experimentation, alone, the steel frame of the column buckles at about 20% of the yield stress. However, the timber-based hybrid column did not buckle when the steel frame yielded to axial force compression because the timber functioned as a buckling restraint.

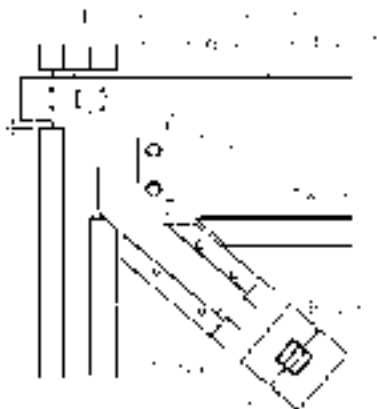


Figure 4 : Joint (Lateral)

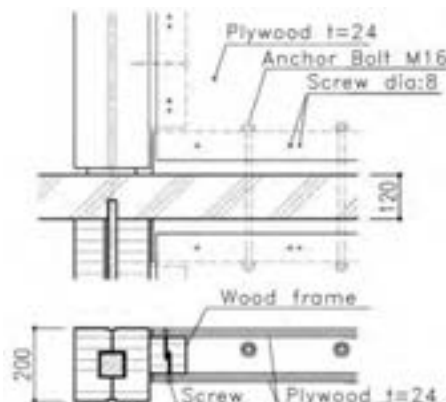


Figure 5 : Joint (longitude)

2.3.2 Horizontal load

The structural planning of the building is different from each direction. A timber-based hybrid beam is suspended laterally and supported by columns of identical material, and the longitudinal beam is built in a reinforced concrete slab. Damage limit seismic force produces greater horizontal force than the load exerted by very rare wind, as prescribed in the Building Standards Law, so horizontal resisting elements are braces the lateral roof face and the longitudinal plywood (load-bearing) walls.

(1) Beam

A lateral timber-based hybrid beam bears axial force and produces a reaction force of braces during an earthquake. The steel frame bears axial force, the timber frame functions as a buckling restraint, and calculations confirmed the absence of buckling within the safety limits of applied axial force.

(2) Column

During a lateral earthquake, a timber-based hybrid column produces a reaction force of braces. This column does not buckle when the steel frame yielded to axial force compression as mentioned above.

During a longitudinal earthquake, vertical shear force is transmitted from the plywood bearing wall to the timber of the column through the vertical frame (Figure 5). The timber has a bearing plate of the steel frame (PL-19) at both ends of the timber of the column, and when the timber collides against the bearing plates, axial force is transmitted to the steel frame of the column. Therefore, during an earthquake, the timber functions as a buckling restraint.

(3) Brace

A brace bears axial force during a lateral earthquake. Only one steel frame (PL-22x65), at the center, contributes to the structure as the steel frames. Buckling of the brace was not observed under significant plastic deformation of the steel frame by compression axial force.

(4) Plywood bearing wall

A plywood bearing wall bears horizontal force during a longitudinal earthquake, and consists of structural plywood (thickness: 24 mm), screws (diameter: 8 mm) and both vertical and horizontal frames of laminated timber arranged around the plywood (Figure 5). Vertical shear force of the plywood bearing wall is as mentioned in Section (2), and horizontal shear force is transmitted from the structural plywood to both the horizontal frame and the downstairs plywood bearing wall through anchor bolts (M16) embedded in the reinforced concrete slab.

2.3.3 After Fire

(1) Beam

Only the steel frame bears vertical load on the assumption that the timber had burnt completely. Although timber actually stops burning, the remaining timber cannot be used as a structural member under present law. The vertical load is assumed to be the same as before a fire, and for safety reasons, the steel frame stress should not exceed the long-term allowable limit.

(2) Column

The column also bears vertical load only using the steel frame and the stress applied should not exceed the long-term allowable limit for buckling.

(3) Brace

The timber of a brace is also assumed to have completely burned. The wind pressure, at the maximum momentary wind velocity of 15 m/s, is set as the constant wind load, and both brace tension and beam bending resist the lateral horizontal force. In this case, the steel frame stress is prevented from exceeding the short-term allowable limit.

(4) Plywood bearing wall

A plywood bearing wall is assumed to have completely burned.

(5) Longitudinal RC beam

An RC slab has a built-in longitudinal RC beam, as shown in Figure 5. The rigid frame structure, consisting of the RC beam and the steel frame of the column, resists the longitudinal horizontal force produced by the constant wind.

2.4 Calculation of response and limit strength

We created an analytical model of the building based on the experimental results, and verified the safety against seismic force by predicting response deformation using the performance-based design method (“Calculation of Response and Limit Strength”).

2.4.1 Verification by Safe Limit Strength Calculation

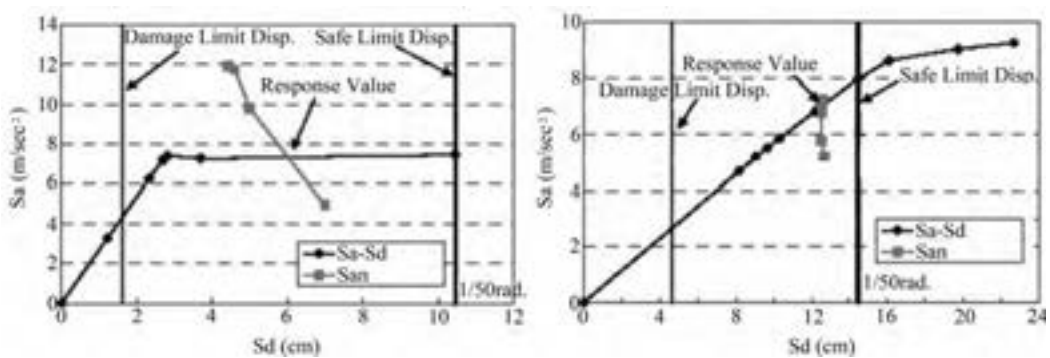
(1) Safe limit drift angle

A safe limit drift angle of 1/50 was set for both the lateral and longitudinal directions. Since the strength of longitudinal plywood bearing wall rose to a drift angle of approximately 1/20, 1/50, as a safety margin, is more than adequate. This margin was set in accordance with the deformation tracking performance of a sash window used for an outside wall of an ordinary building.

(2) Calculation of response

The experimental and analytical safety limit strength exceeded the required safety limit strength, and the true response value is calculated as follows:

- a) Creating a relation diagram of the load-deformation curve (Sa-Sd) at the representative material point of the building
- b) Calculating the acceleration (San) of input into the building at equivalent cycles by considering building attenuation at each step
- c) Plotting San on a straight line connecting Sa-Sd (load deformation of the building) and the origin at the step



lateral direction

longitudinal direction

Figure 6 : Prediction of responses at the time of an earthquake

- d) The true response value is the intersection of the San curve at each step (demand curve) and the Sa-Sd curve of the building.

Results of the calculation are shown in Figure 6. The safety against seismic force both direction was verified. In the lateral direction, strength hardly increases after the yielding of horizontal resisting elements. In the longitudinal direction, the plywood bearing wall is in an elastic area, up to 1/50 of the safe limit drift angle.

2.5 Performance of M Bldg.

Besides verifying the safety against seismic force, to satisfy the fire resistance performance required for fireproof buildings, we verified fire resistance using a beam-loaded heating test, a column-loaded heating test, and a joint heating test. Based on the results of structure and fire resistance research, Japan's first building using a timber-based hybrid structure, having 1-hour fire resistance, was completed in Ishikawa Prefecture in 2005,

3. “Kasukabe Convention Hall” building

The Eastern Saitama Regional Development Center “Kasukabe Convention Hall” was constructed in Kasukabe City, Saitama Prefecture in 2011.(Photo 3) This



Photo 3 : “Kasukabe Convention Hall” Bldg.
(Photo by YAMASHITA SEKKEI INC.)

Table 3: Building data

Architect	YAMASHITA SEKKEI INC.
Structural Design	YAMASHITA SEKKEI INC.
Area	10529.08m ² (total floor) / 2848.04m ² (building)
Use	Convention hall
Height	27.086m
number of storeys	6 stories
Structure	Steel structure (1st-4th stories), Timber structure (5th-6th stories)

building is six storied mix structure convention hall. From 1st to 4th stories of this building are steel structure and top of 2 stories are timber structure. Feature of this building is that 2x80mm thick wall is used as shear walls. This wall is made of LVL (Laminated Veneer Lumber). These seismic elements are allowed lower fire resistance than column, beam and floor which support vertical load, such as self weight or live load. So these members can be exposed itself without fireproof coating and can be used as a finishing material.

4. “WOOD SQUARE” building

The “WOOD SQUARE” Bldg. was constructed in Koshigaya City, Saitama Prefecture in 2012.(Photo 3) This four storied timber building have a timber-based hybrid structure with built-in steel materials same as M Bldg.



Photo 3 : “WOOD SQUARE” Bldg. (left: exterior, right: interior)
(Photo by POLUS)

Table 4: Building data

Architect	JR EAST DESIGN CORPORATION
Structural Design	JR EAST DESIGN CORPORATION
Area	6592.63m ² (total floor) / 1353.51m ² (building)
Use	Office
Height	21.000m
number of stories	4 stories
Structure	Timber-based hybrid construction

This building use the maximum timber-based hybrid beam obtained the approval by the Minister. The beam is 663mm depth and 325 wide, H-600x200 covered by glulam. This member can realize 12.8m span space. 641 cubic meters of glulam is used in this building.

5. ”Shimouma Project”

”Shimouma Project” is under construction in Setagaya-ku, Tokyo.(Photo 4) This building is five storied timber apartment house.

Timber characteristic appearance is not only finishing member but also a structural member. This lattice-shaped member work as a bracing.



Photo 4 : “Shimouma” Project (Photo by KUS)

Architect	KUS
Structural Design	M.Koshihara, T.Sato, Y.Kirino
Area	122.89m ² (total floor) / 92.83m ² (building)
Use	Apartment
Height	16.200m
Number of stories	5 stories
Structure	RC structure(1st story) Timber structure(2-4 story)

6. CONCLUSION

After completion of M Bldg. various middle-rise timber building were constructed and will be construct. A technology of middle-rise timber building about seismic performance and fire-resistance performance is developing. New technology will create new timber architecture. Eve in the city we have a new choice, timber structure, not only steel structure and RC structure.

REFERENCES

M.KOSHIHARA, H.ISODA, et al.: *A Study of five storied timber based hybrid building for practical use (Part 1-3)*, Summary of Technical Papers of Annual Meeting Architectural Institute of Japan, C-1, pp.201-206, 2005

S. YUSA, T.YOSHIKAWA, et.al: *Research in practice on 5-story fire resistance hybrid wooden structure building*, Summaries of Technical Papers of Annual Meeting Japan Society for Finishing Technology, pp.7, 2005

Study on lightning risk assessment for oil tank area

Boni SU¹, Hong HUANG², Yuntao LI¹ and Fanghui LUO¹

¹Institute of Public Safety Research, Department of Engineering Physics, Tsinghua University, Beijing, China

²Professor, Institute of Public Safety Research, Department of Engineering Physics, Tsinghua University, Beijing, China
hhong@tsinghua.edu.cn

ABSTRACT

Along with economy's growth, energy demand is rising unceasingly. Many countries are increasing oil reserves to satisfy the daily industry and national defense requirements. When unexpected events happen, oil reserves are important to national stability. In recent years, many oil tank accidents caused by lightning occurred, which means that studying on the disaster risk assessment model of the oil tank in lightning weather has practical significance.

In this paper, models of lightning and floating roof tanks were established according to domestic and international standards. The risk probability of lightning hitting oil tanks was calculated using these models. After that, the risk probability of fire when lightning hit oil tanks was estimated according to some experimental results. Finally, practical methods for lightning protection in oil tank areas were given.

Keywords: lightning, floating roof tank, fire, probability, risk assessment

1. INTRODUCTION

With the continuous development of economic, many countries are increasing oil reserves to satisfy the daily industry and national defense requirements. The expansion of oil reservoirs cause safety risks. Oil tanks are often used to store toxic, flammable or explosive chemicals. Once accidents occur, a great deal of heat and dangerous substances will be released, causing serious casualties and economic losses. Among those accidents, lightning-caused accidents account for a large proportion. According to statistics, in 529 oil tank fire incidents, 31% were caused by lightning (Drabkin M. M. and Grosser A, 2006). There were several serious accidents caused by lightning hitting oil tanks, such as the Huangdao oil depot fire in August 12, 1989, and the Orion Noroo Oil refinery fire in July 7, 2001. Therefore, lightning protection in oil tank areas is very important. In this paper, the risk of lightning hit floating roof tanks was evaluated and the probability of fire caused by lightning was calculated.

2. MODELS OF LIGHTNING AND OIL TANKS

2.1 Model of lightning

Thunderclouds contain positive and negative charge. When the electric field strength reaches a certain threshold, the air between thundercloud and ground (or another thundercloud) will breakdown, forming a discharge. This is lightning. The three most common types of lightning are Cloud-to-Cloud (CC) lightning, positive Cloud-to-Ground (CG) lightning and negative CG lightning. CC lightning has little effect on the ground, positive CG lightning only occurs in some particular natural disasters. Therefore, we mainly consider the prevention of negative CG lightning in lightning protection. Each lightning discharge consists of one or more partial lightning strikes (DEHN 2011). The possible combinations of partial lightning strikes are shown in Figure 1.

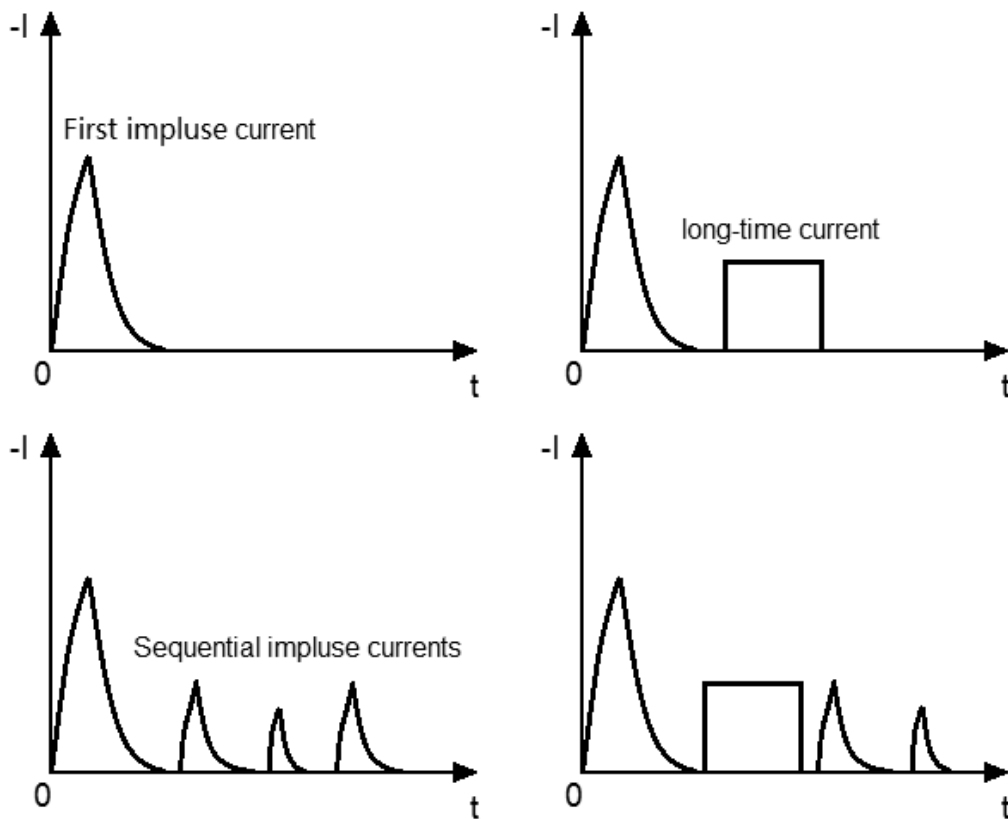


Figure 1: Possible combinations of partial lightning strikes

In a lightning current, first impulse current always exists and is the maximum, so we only consider first impulse currents in this paper.

Lightning currents are load-independent. According to International Electro technical Commission (IEC) standard IEC 62305-1 (IEC 2010), the current shapes of impulse currents in lightning can be approximated as:

$$i = \frac{I}{k} \cdot \frac{(t / \tau_1)^{10}}{1 + (t / \tau_1)^{10}} \cdot \exp(-t / \tau_2) \quad (1)$$

Where i is lightning current (A), I is the peak current (A), t is the time (s), τ_1 is the front time constant (s), τ_2 is the tail time constant (s), k is the correction factor for the peak current. For the first negative impulse, $\tau_1=1.82\mu\text{s}$, $\tau_2=285\mu\text{s}$, $k=0.986$ (IEC 2010).

The amount of charge discharged by lightning, Q (C), equals to i on t integral:

$$Q=I \times 2.872 \times 10^{-4} \text{s} \quad (2)$$

Distribution of peak current can be obtained according to statistical data. As we don't have statistical data, Chinese standard DL/T 620-1997 (Ministry of Electric Power Industry of the People's Republic of China 1997) is used to estimate the distribution:

$$\lg P = -I/88 \quad (3)$$

Where I is current (kA), P is the probability of lightning's peak current exceeding I .

2.2 Model of oil tanks

There are two kinds of oil tanks: metal tanks and nonmetal tanks. Because of their poor electrical conductivity, nonmetal tanks usually bring sparks when hit by lightning. That is dangerous. Furthermore, when a nonmetal tank catches fire, it is hard to put out the fire. The serious fire in Huangdao oil depot was caused by lightning which hit a nonmetal tank, the fire couldn't be put out until it burnt the whole oil tank area. After that accident, constructing nonmetal tanks to store oil is forbidden in China. Nowadays, large oil tanks are usually floating roof tanks made by metal. Unlike nonmetal ones, metal tanks have low resistance and have a good electromagnetic shielding ability. Therefore, induced lightning has little impact on metal tanks. So we only consider direct lightning in this paper.

Basic structure of a floating roof tank is shown in Figure 2.

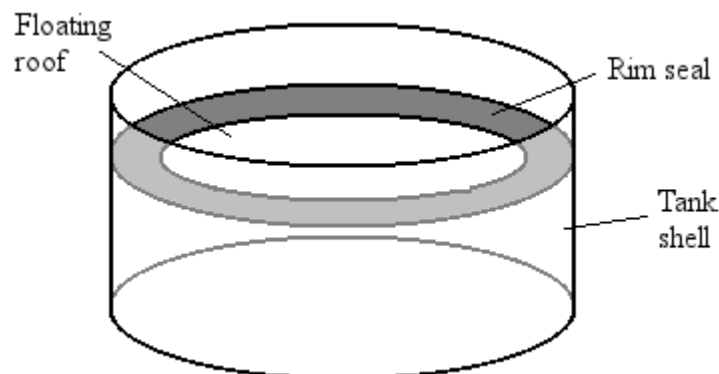


Figure 2: Basic structure of a floating roof tank

The floating roof floats as the liquid level changes. The gap between the floating roof and the tank shell is about 250mm wide. In order to reduce the leakage of oil gas, rim seal is used. Currently, most floating roof tanks use a primary seal and a secondary seal. There are three kinds of primary seal: mechanical seal, elastic seal and tubular seal. Mechanical seal reduces leakage by pushing steel plates against the tank shell using a boom system. Elastic seal and tubular seal are collectively referred to as soft seal. Soft seal reduces leakage by filling the gap with elastic material (foam or liquid).

There are a set of floating roof tanks' dimensions in a manual (Zhengxi Li and Siwen Xu 1997), as shown in Table 1.

Table 1: Standard dimensions of floating roof tanks in reference document

Volume/m ³	Diameter/m	Height/m
10000	28.50	15.85
20000	40.50	15.85
30000	46.00	19.35
50000	60.00	19.35
100000	81.00	21.10

In practice, tanks' volume and dimensions may be adjusted according to local conditions.

3. CALCULATION OF PROBABILITY OF ACCIDENTS

3.1 Probability of lightning hitting a tank

According to IEC standard IEC 62305-2 (IEC 2010), the average annual number of dangerous events due to lightning N_D (a⁻¹) can be calculated using the following formula:

$$N_D = N_G \cdot A_D \cdot C_D \times 10^{-6} \quad (4)$$

Where N_G is the lightning ground flash density (km⁻² · a⁻¹), A_D is the collection area (km²), and C_D is the location factor.

According to Chinese standard GB50057-2010 (China Machinery Industry Federation 2010), when statistical data are unavailable, N_G can be estimated by:

$$N_G = 0.1 T_d \quad (5)$$

Where T_d is the number of thunderstorm days per year. Take Qingdao City (where Huangdao oil depot fire happened) for example, $T_d=23$. So $N_G=2.3/\text{km}^2/\text{a}$ according to the formula, which means that there will be 2.3 events of lightning hit ground in 1.0 km² per year on average.

The collection area A_D of a building with a height of H and a radius of R is:

$$A_D = \pi(R+3H)^2 \quad (6)$$

Large oil tanks are often built near each other, thus they are surrounded by objects of the same height or smaller. So C_D is 0.5 according to IEC 62305-2.

By taking different tank dimensions in Table 1 into these formulas, we got different N_D of tanks of different volume, as shown in Table 2.

Table 2: Average annual number of lightning hitting tanks

Volume/m ³	A_D/m^3	$N_D/km^{-2} \cdot a^{-1}$
10000	1.20×10^4	0.0138
20000	1.44×10^4	0.0166
30000	2.06×10^4	0.0237
50000	2.44×10^4	0.0280
100000	3.38×10^4	0.0389

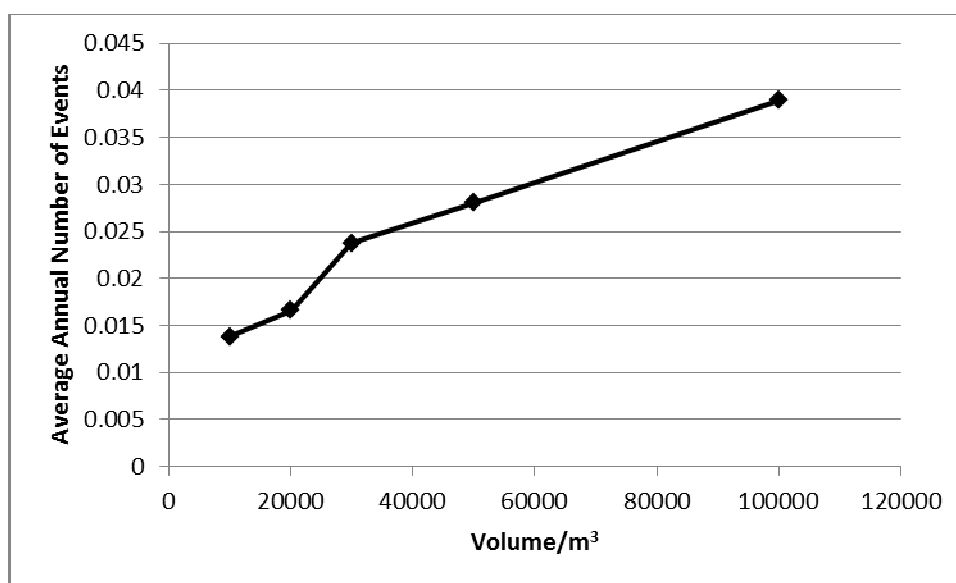


Figure 3: Average annual number of lightning hitting tanks

It can be seen that larger oil tanks are more likely to be hit by lightning.

3.2 Probability of spark causing fire

In recent floating roof tank accidents in China, most of the fires caused by lightning started at the rim seal. Shunts on the secondary seal are the main sources of ignition in floating roof tank fires. In most floating roof tanks, shunts are set up at intervals of 3m or less. The intervals are assumed to be 3m in this paper. We can calculate the number of shunts on tanks of different dimensions by dividing 3m into the circumference. Experimental results show that a shunt will generate sparks when the lightning reaches a peak current of about 400A (Haiyan Hu et al.

2011). The floating roof is metal and is very large, thus it has low resistance. Therefore, we consider the floating roof is equipotential and all the shunts are parallel connected. So lightning should reach a peak current of $n \times 400A$, where n is the number of shunts. According to formula (3), the probability of lightning cause sparks can be calculated. We can get the average annual number of such events by multiplying the average annual number of lightning hit tanks. The result is shown in Table 3.

Table 3: Probability of lightning causing sparks on tanks

Volume/m ³	Number of Shunts	Peak Current Needed/kA	Probability	Annual Number of Events
10000	30	12	0.73	0.0101
20000	43	17.2	0.64	0.0106
30000	49	19.6	0.60	0.0142
50000	63	25.2	0.52	0.0145
100000	85	34	0.41	0.0160

It can be seen that the probability of lightning cause sparks decreases slowly as the tanks get larger. But considering that larger tanks are more likely to be hit by lightning, the average annual number of lightning cause sparks increases as the tanks get larger.

If sparks occur and the concentration of oil gas reaches the explosive limit, the oil gas will explosion. According to statistical data, in 4% of tanks that using soft primary seal and 19% of tanks that using mechanical primary seal, the concentration of oil gas between the primary seal and the secondary seal are beyond the explosive limit (Xuqing Lang et al. 2008).

By multiplying the average annual number of lightning cause sparks by the probability of oil gas reach the explosive limit, we get the average annual number of lightning cause fire by sparks.

Table 4: Annual number of lightning causing fire by sparks

Volume/m ³	Using Soft Primary Seal	Using Mechanical Primary Seal
10000	0.000403	0.01915
20000	0.000424	0.02012
30000	0.000568	0.02700
50000	0.000579	0.02752
100000	0.000640	0.03038

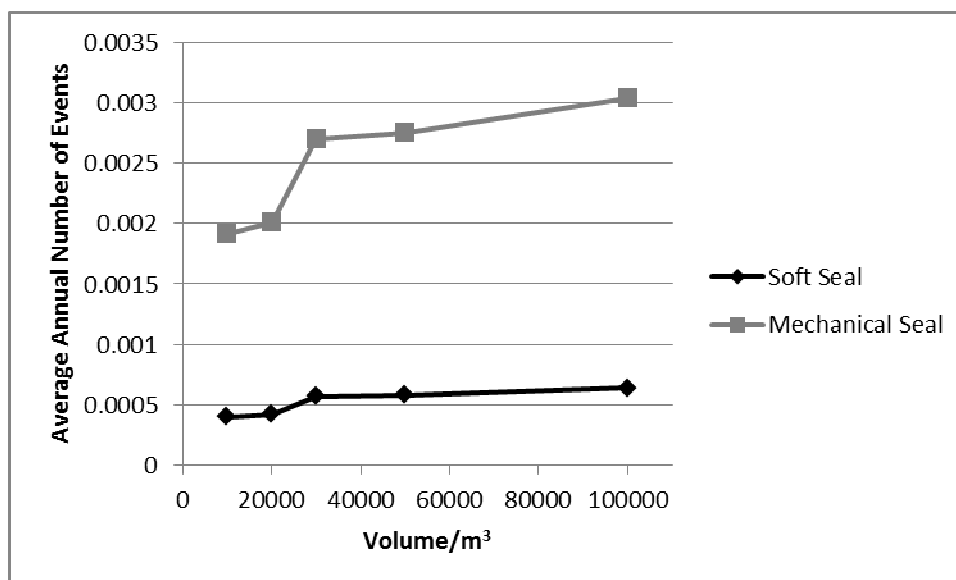


Figure 4: Annual number of lightning causing fire by sparks

In fact, in tanks that using mechanical primary seal, sparks can occur at some parts other than shunts, like the gap between the seal plates and the tank shell. So the actual annual number of accidents in tanks that using mechanical primary seal should be higher than the estimated value in this paper. Comparing to tanks that using soft primary seal, such accidents are much more likely to occur on tanks that using mechanical primary seal. That is in line with the fact that almost all the recent floating roof tank fires caused by lightning in China occurred on tanks that using mechanical primary seal (Hong Gong et al. 2008).

3.3 Other possible accident forms

There are other ways how lightning can cause oil tank fires. For example, oil gas leaks through the rim seal and reaches the explosive limit, and then lightning can ignite the oil gas and cause a fire. However, the leak rate of floating roof tanks is very low under common condition, and the concentration of oil gas is far below the explosive limit. Large amounts of leakage can happen only when loading and unloading oil. This kind of accidents can be avoided by using weather forecast and avoiding loading or unloading oil during a thunderstorm. Therefore, this paper does not consider the probability of such accidents.

4. CONCLUSIONS

This paper computes the probability of direct lightning strokes causing floating roof tank fires by sparks at the rim seal. Based on these data, we can draw the following conclusion: comparing to tanks using soft primary seal, tanks using mechanical primary seal are more likely to catch fire due to lightning. This matches the actual situation of recent floating roof tank fires caused by lightning in China.

To reduce the accident rate of floating roof tank fires caused by lightning, the following methods can be used.

(1) Reduce the probability of lightning struck a tank. Direct lightning strokes can only cause fire when they hit oil tanks. When selecting oil depot sites, try to avoid the lightning-prone areas. For oil depots that have already been built, set up lightning rods to reduce the probability of lightning struck a tank.

(2) Reduce the use of mechanical seals. Although mechanical seals have long life and are easy to maintain, their ability of defense is not as good as soft seals. In lightning-prone areas, less mechanical seals and more soft seals should be used.

(3) Improve shunts on the rim seal. If shunts don't produce sparks any more, the accident rate of floating roof tank fires caused by lightning will decrease significantly. Currently, there are some attempts. For example, the American Petroleum Institute (API) put forward that shunts should be moved to 0.3m below the oil surface (American Petroleum Institute 2009), and China Petroleum & Chemical Corporation put forward that wax scraping device can be used as shunts (Haiyan Hu et al. 2011). Although these ideas are not mature now, it is inevitable that shunts on the rim seal should be improved in the future.

ACKNOWLEDGEMENT

This work was supported by Ministry of Science and Technology of the People's Republic of China under Grant No. 2012BAK03B03 and 2011BAK07B02.

REFERENCES

Drabkin M. M., and Grosser A., 2006. Lighting protection of flammable storage facilities. *International Conference on Grounding and Earthing & 2nd International Conference on Lightning Physics and Effects*.

International Electrotechnical Commission, 2010. *Protection against lightning - Part 1: General principles*. IEC62305-1.

International Electrotechnical Commission, 2010. *Protection against lightning - Part 2: Risk management*. IEC62305-2.

Ministry of Electric Power Industry of the People's Republic of China, 1997. *Overvoltage protection and insulation coordination for AC electrical installations*. DL/T 620-1997.

Zhengxi Li, and Siwen Xu, 1997. *Oil Storage and Transportation Design Manual*. Beijing: Petroleum Industry Press.

China Machinery Industry Federation, 2010. *Code for design protection of structures against lightning*. GB 50057-2010.

DEHN, 2011. *Lightning Protection Guide*. <http://www.dehn-usa.com/dehn-Lightning-Protection-Guide-pubcid4.html>.

Haiyan Hu, Baoquan Liu, Quanzhen Liu, Tingting Zhang, and Xin Gao, 2011. Analysis on Second Sealing Oil and Gas Space Discharge in Floating Roof Tank. *China Safety Science Journal* 21(3): 106-109.

Xuqing Lang, Xin Gao, Hong Gong, Quanzhen Liu, and Ting Wang, 2008. Research on Reducing Oil Gas Concentration in Large Floating Roof Tank Seals. *Journal of Oil and Gas Technology* 30(2): 618-619.

Hong Gong, Quanzhen Liu, Xiangsheng Song, Xuqing Lang, and Jianxiang Li. Analysis of Fire Accidents Caused by Lightning Strike on the Seal Ring of Large Floating Roof Tanks. *Safety Health & Environment* 8(10): 7-8.

American Petroleum Institute, 2009. *Recommended Practice for Lightning Protection of Aboveground Storage Tanks for Flammable or Combustible Liquids*. Washington, DC: API Publishing Service.

Structural damage detection by using hybrid time reversal process method

Usik LEE¹, Ilwook PARK², and Jungsik CHOI³

¹ Professor, Dept. of Mechanical Eng., Inha University, Korea
ulee@inha.ac.kr

² Graduate Student, Dept. of Mechanical Eng., Inha University, Korea
iwpark@inha.edu

³ Graduate Student, Dept. of Mechanical Eng., Inha University, Korea
blue4325@yahoo.co.kr

ABSTRACT

This paper presents a hybrid time reversal process method (HTRPM) for the structural damage detection. The HTRPM is characterized by three key features: (1) In the HTRPM, the forward process of the time reversal process is conducted by the measurement while the backward process is conducted by the computation; (2) For structural damage detection, the damage signal is obtained by extracting the comparison signal from the signal reconstructed by the time reversal process; (3) The imaging method is used to visualize the damage location by using the damage signal. The HTRPM is applied to the aluminum plates and composite laminated plates. Experimental results show that the proposed HTRPM can successfully detect the damages generated in the plate specimen.

Keywords: structural damage, damage detection, hybrid time reversal process method, time reversal, plate

1. INTRODUCTION

Lamb waves are the guided waves which can travel a long distance in the thin-walled structures such as the plates (Viktorov, 1967). When the guided wave travels through a region where damages exist, scattering may occur in all directions to change the characteristics of the guided wave. Thus it is possible to detect structural damages by comparing the response signals measured at the damaged state with the baseline data measured at the intact state. As the baseline data may change due to the change of environmental or operational conditions, the baseline-based damage detection methods often provide inaccurate damage detection results. Thus, recently some researchers (Wang et al., 1998; Park et al., 2007) have proposed some baseline-free damage detection methods by using the time reversal process (TRP) of Lamb waves.

The standard TRP consists of two processes which are conducted by actuator and sensor-based measurements: the forward process and the backward process. In the forward process, an input voltage is applied to a PZT actuator (say, PZT A) and the response signal is measured by a PZT sensor at other location (say, PZT B). The measured response signal is then time reversed and it is used as the input

signal for the next backward process. In the backward process, the role of PZT A and PZT B is reversed: PZT B now plays as the actuator and PZT A as the sensor. The time reversed measured response signal is applied to PZT B and then the response signal is finally measured by PZT A. The response signal measured by PZT A is called the reconstructed response signal. If there are no damages on the paths between PZT A and PZT B, the reconstructed signal will be identical to the initial input signal applied to PZT A: this is the case of the perfect time reversal of the non-dispersive waves. However if there exist damages on the paths between PZT A and PZT B, the time-reversibility of the Lamb waves will be break-down. Thus the difference between the initial input signal and the reconstructed response signal has been used for detecting damages in the baseline-free damage detection methods (Wang et al., 1998; Park et al., 2007).

In the standard TRP, both forward and backward processes of the TRP are all conducted by the actuator and sensor-based measurements. In most existing TRP-based damage detection methods (e.g., Park et al., 2007), the pattern comparison methods have been widely used, where the shape of the initial input signal is compared with that of the reconstructed response signal for detecting damages. Very recently Lee and Choi (2010) and Lee et al. (2012) proposed a hybrid TRP where the measurement-based backward process is replaced by the computation-based process. The advantages of the hybrid TRP over the standard TRP can be referred to Jun and Lee (2012). As the shape of initial input signal can be changed during the TRP by many other reasons than the damage itself, the conventional pattern comparison methods may not be always appropriate.

Thus this paper presents a hybrid TRP-based baseline-free damage detection method where damage signals are used to visualize damage locations by using an imaging technique.

2. GENERAL PROCEDURE OF STRUCTURAL DAMAGE DETECTION

2.1 Computation of the reconstructed signal

The general procedure of the hybrid TRP to obtain the refined reconstructed signal by an actuator-sensor PZT pair is as follows (Lee and Choi, 2010; Jun and Lee, 2012):

(1) Exert a narrowband tone-burst input signal to an actuator PZT placed at a location (location A) of the plate under inspection as illustrated in Figure 1. The center frequency of the input signal is chosen to excite Lamb wave A_0 and S_0 modes only and it is tuned so that A_0 mode becomes dominant over S_0 mode.

(2) Measure the response signal at other location (location B) of the plate by using a sensor PZT.

(3) Refine the measured response signal by removing small S_0 mode which comes first at the sensor PZT.

(4) Reverse the refined measured response signal in time.

(5) Compute the refined transfer function by dividing the refined measured response signal by the input signal applied at the location A.

(6) Compute the reconstructed response signal by multiplying the time reversed refined measured response signal (used as a new input signal applied at

the location B) and the refined transfer function. The result is illustrated in Figure 1.

The above procedure is repeated for all other actuator-sensor PZT pairs or Lamb wave propagation paths. The benefit of the hybrid TRP is to remove excessive unnecessarily wave signals otherwise to be generated by the S_0 mode from the refined reconstructed signal, which will make the signal processing much simple and efficient. In order to improve the damage detection results obtained by using the imaging method (Wang, 1998; Ihn and Chang, 2008; Jun and Lee, 2012), the wavelet transform (WT) is applied to the reconstructed response signals. From the time-frequency responses obtained by WT, the time responses at the center frequency of the input signal are extracted and used as the final forms of the reconstructed response signals.

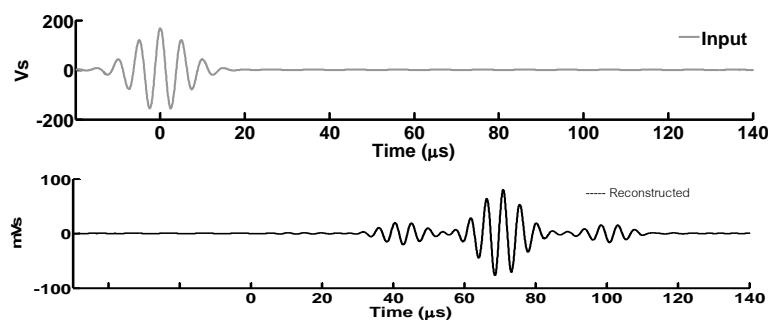


Figure 1: Input signal and reconstructed response signal

2.2 Damage detection method

The reconstructed response signal for a specific actuator-sensor PZT pair in general consists of a main wave packet and single pair (multiple pairs) of sidebands due to a single damage (multiple damages). As a unique feature of the TRP of Lamb waves, the sidebands always appear on both sides of the main wave packet in a symmetric form. For instance, a pair of sideband illustrated in Figure 1 is formed by the wave signals which propagate back to the initial input excitation point (location A) via the damage during the forward and backward processes. Thus, the TOA (time of arrival) of each sideband signal can be computed by using its group velocity and traveling distance. The traveling distance of a sideband is determined by the linear distance between two PZTs used as an actuator-sensor pair and the location of damage. This implies that the TOA of each sideband contains damage information. Thus, the TOA of each sideband can be used to detect damage.

The pattern comparison methods have been used in the previous TRP-based damage detection methods (e.g., Park et al., 2007) where the difference between the initial input signal and the main wave packet part of the reconstructed signal is used to detect damage. However, the difference may come arise due to not only the damage but also the other sources such as the dispersive and damping characteristics of a structure. Thus, instead of using the pattern comparison method based on the difference between the initial input signal and the main wave packet part of the reconstructed signal, the TOFs of the sidebands will be used to detect damage.

Figure 2 shows an input signal and the corresponding reconstructed response signal for a specific actuator-sensor PZT pair. It is obvious from Figure 2 that the shape and magnitude of the reconstructed response signal are not identical to those of input signal due to the effects of damage, damping, and dispersive characteristics of the structure. Thus, in order to use the sideband signals on both sides of the main wave packet for damage detection, the authors propose a method to remove the main wave packet from the reconstructed response signal by utilizing the input signal (Lee and Choi, 2010).

The input signal can be modified in magnitude and phase so as to match with the shape of the main wave packet of the reconstructed response signal. The shape of the main wave packet part is characterized by three parameters as displayed in Figure 3. The input signal modified in such a way is called the comparison signal and it is compared with the reconstructed response signal in the top of Figure 4. In Figure 4, all signals are displayed in enveloped forms. By subtracting the comparison signal from the reconstructed response signal, the main wave packet part can be removed to obtain the damage signal which now contains only the sideband on the right-hand side of the main wave packet. The damage signal for a specific wave propagation path between PZT A and PZT B is displayed in the bottom of Figure 4. The damage signals for other wave propagation paths can be obtained in the similar manner for the use in the damage detection. By applying the imaging method to damage signals, the damage locations can be visualized as a color image (Ihn and Chang, 2008; Jun and Lee, 2012).

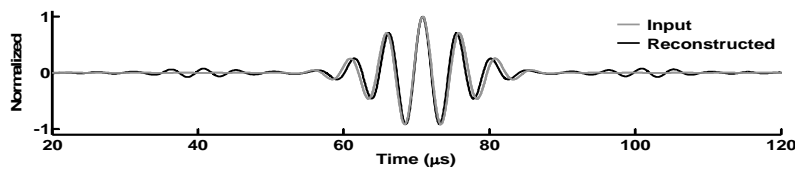


Figure 2: Comparison of the input and reconstructed signals

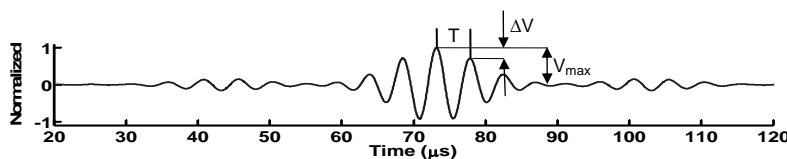


Figure 3: Parameters of the main peak of the reconstructed signal

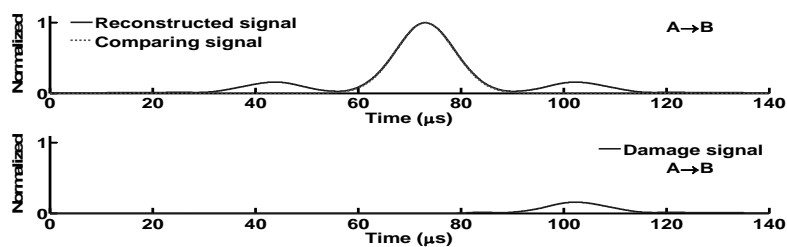


Figure 4: Damage signal for the wave propagation path between PZT A and PZT B

3. EXPERIMENTAL RESULTS AND DISCUSSION

3.1 Experimental set-up

The experimental setup used for the present study is shown in Figure 5. It consists of a data acquisition (DAQ) system, a function generator, a linear amplifier, three digitizers, a personal computer, and the plate specimen with four surface bonded PZTs. The LabView waveform generator is used to generate a narrowband tone-burst analog signal. The analog signal is then transformed into the digital signal and exerted to a PZT by the function generator, after being amplified by the linear amplifier. The response signals are measured by other three PZTs and stored in the DAQ system via the digitizers. The personal computer is used to conduct the signal processing of the measured response signals, the computation-based backward process of the hybrid TRP, and the diagnostic digital imaging process. The damage in the aluminum plate is represented by the added mass (circular steel bar of diameter 10mm) attached on the plate surface.

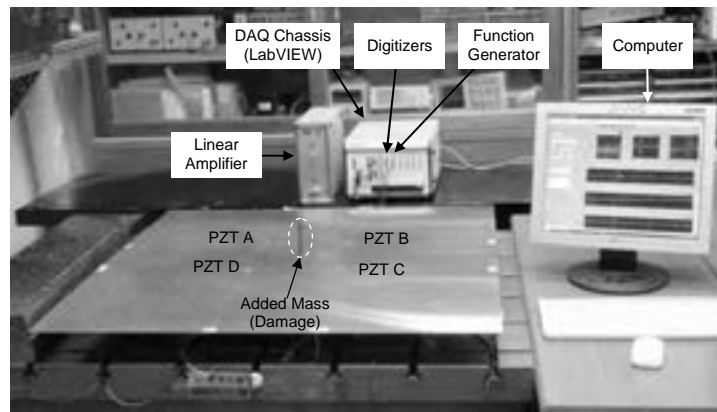
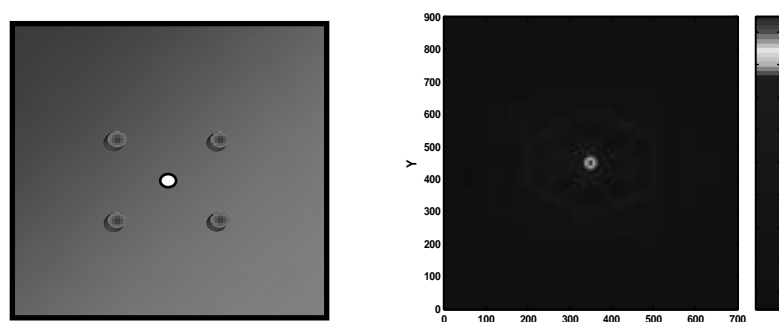


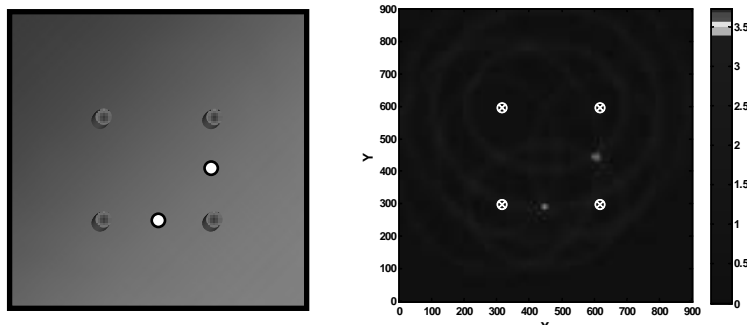
Figure 5: Experimental set-up for the present study

3.2 Experimental results

Experimental results of damage detection are displayed in Figure 6 for the aluminum plates with single damage and two damages and in Figure 7 for the composite laminated plate with single damage.



(a) Single damage



(b) Two damages

Figure 6: Damage detection results for the aluminum plate with (a) single damage and (b) two damages

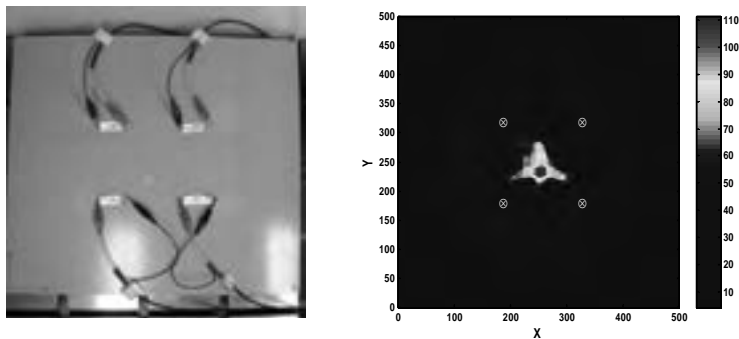


Figure 7: Damage detection result for a composite laminated plate with single damage

Figures 6 and 7 show that the present hybrid TRP and imaging method-based damage detection method is quite successful to detect damages generated in the metallic plate as well as in the composite laminated plate.

4. CONCLUSIONS

A hybrid TRP and imaging method-based structural damage detection method is proposed in this paper. The damage signals obtained by extracting comparison signal from the reconstructed response signal are used for structural damage detection. Experimental results show that the proposed structural damage detection method can successfully detect damages generated in the aluminum and composite laminated plates.

ACKNOWLEDGEMENTS

This research was supported by Basic Science Research Program through the National Research Foundation of Korea (NRF) funded by the Ministry of Education Science and Technology (Grant number 2010-0007741; 2012-004482).

REFERENCES

- Jun, Y. and Lee, U., 2012, Computer-aided hybrid time reversal process for structural health monitoring. *Journal of Mechanical Science and Technology* 26, 53-61.
- Lee, U., Jun, Y. and Park, I., 2012, A computer-aided time reversal process for structural damage diagnosis. *Advanced Materials Research* 393-395, 3-6.
- Lee, U. and Choi, J., 2010, Structural damage diagnosis method by using the time-reversal property of guided waves. *Journal of the Korean Society for Precision Engineering* 27, 64-74.
- Ihn J.B. and Chang, F.K., 2008, Pitch-catch active sensing methods in structural health monitoring for aircraft structures, *Structural Health Monitoring* 7, 5-15.
- Park, H.W., Sohn, H., Law, K.H. and Farrar, C.R., 2007, Time reversal active sensing for health monitoring of a composite plate, *Journal of Sound and Vibration* 302, 50-66.
- Wang, C.H., Rose, J.T. and Chang, F.K., 1998, A synthetic time-reversal imaging method for structural health monitoring, *Smart Materials and Structures* 13, 415-423.
- Viktorov, I.A., 1967, *Rayleigh and Lamb Waves: Physical Theory and Applications*, Plenum Press, NY.

Fire risk study of Ulaanbaatar City

master D.Bayan-Erdene¹, doctoral candidate S.Bazarragchaa²

Head of complex laboratory, major of emergency agency

Researcher and heat engineer, senior officer, major of emergency agency

ABSTRACT

The population of Ulaanbaatar city is increasing rapidly in connection with the economic growth and infrastructure of our country. This leads to the construction of buildings and structures that don't fulfill urban development and fire safety requirements built on areas and grounds that don't fulfill standard requirements, as well as to the formation of carelessly built streets and ger district concentration. These all lead to the situations increasing of possible fire risks and to the troubles to the firefighting measures.

From previously carried out studies we can see that the amount of fire occasions, damage size caused by them, as well as the scope of such incidents is permanently increases. This shows that an urgent situation for performing fire risk research works to incorporate this study and research works to the Ulaanbaatar city's emergency situation map.

During carrying out of this research work the legal environment isn't clear enough for the terminology and definition of buildings and structures including of high buildings, as well as for providing of fire safety. For example, the following don't fulfill the requirements of standards, norms and rules. These are: evacuation road and exits, safety sizes between buildings and structures, internal and external water supply, ventilation, smoke circulation system, firefighting first aid and equipment, auto-mechanic ladder for evacuation and rescue operations, fire resistance of building structures etc. From this we observed the need of implementation of state fire inspection and control, as well as the fire prevention measures and operations. Thus these issues should be solved. This research work is a work that attempts a new approach by covering all above stated factors as a whole issue, assessing of fire risks of Ulaanbaatar city and incorporating the achieved results to the emergency map. As we assessed the fire risks of Ulaanbaatar city based on this research work we came to conclusion that an abrupt renovation works should be implemented urgently at the level of taking measures for risk decreasing. Thus, it is urgently required to carry out the management and measures to eliminate the vulnerable and disadvantageous issues. Furthermore, we came to conclusion that it is inevitably required to incorporate the following issues to the standards, norms and rules. These are the application of modern technic and technologies for providing of fire safety of building and structures, especially of high buildings, as wells the utilization of recent construction materials.

The seismic-engineering survey among multi-store constructions within the territory of Ulaanbaatar City

Batsaikhan TSERENPIL¹, Sergei SEREBRENNIKOV², Baatarsuren GANBOLD³

¹Head laboratory, Research Center of Astronomy and Geophysics MAS,
Ulaanbaatar, Mongolia
batsaikhan@rcag.ac.mn

²Institute of the Earth's Crust SB RAS, Irkutsk, Russia

³Researcher, Research Center of Astronomy and Geophysics MAS, Ulaanbaatar,
Mongolia

ABSTRACT

The article presents brief analysis of data to validate initial seismicity Ulaanbaatar city and engineering-geological conditions for construction. There were built numerous multi-store constructions within the territory of UB in the past 10 years.

The status of soil under construction area of those high buildings had undergone through the analyzes, that were based on the results of seismic-engineering studies made within the territory of those buildings.

The authors give key parameters settlement accelerogram for a platform of buildings(for example Koyoto company building site): the maximum values of acceleration of fluctuations of soil, the frequency of the basic maximum of a spectrum.

Keywords: seismic-engineering, multi-store construction, acceleration, frequency, seismic wave

1. INTRODUCTION

Central Asia is a region with a high level of seismic hazard. The deformation in Mongolia can be attributed to the collision and subsequent penetration of the Indian plate with respect to Eurasia. In northern Mongolia there is extensional tectonics component related to the active Baikal rift system. Continental earthquakes are distributed over large regions and typically have shallow depths, in the range of 10 to 25 km beneath the surface. During last century, Mongolia has been known one of the most seismic active intra-continental regions in the world with several very large earthquakes. Since the year 1900, there were occurred 69 earthquakes with $M \geq 6.0$. Among them 44 earthquakes were with magnitude $6.0 \leq M < 7.0$. In the magnitude range of $7.0 \leq M < 8.0$, there were 20 earthquakes and very large $M \geq 8.0$, 4 earthquakes have taken place in Mongolia so far:

Tsetserleg 1905 with magnitude $M = 8.0$, produced 190 km length of surface rupture;

Bulnai 1905, with magnitude $M = 8.4$, produced 375 km long of surface rupture;

Fu-Yun 1931, with magnitude $M = 8.0$, produced 180 km long of surface rupture; Gobi-Altai 1957, with magnitude $M = 8.2$, km produced 270 km long of surface rupture.

These major continental earthquakes occurred along active faults that have very long recurrence intervals (~3000 years for the 1957 earthquake; Ritz et al 1995). However, the large number of active faults capable of producing a devastating earthquake ($M_w 6.5+$) in Mongolia makes the prospect of strong events very concerning.

2. BRIEF ANALYSIS OF DATA TO VALIDATE INITIAL SEISMICITY ULAANBAATAR CITY

In last few decades, most scientists working in Mongolia focussed on these largest earthquakes and their spectacular impact on the landscape. They considered that the main tectonic and seismic activity takes place in the west of the country, several hundred kilometres from Ulaanbaatar. However, the most recent earthquake with $M_w > 7$ happened near Mogod (1967, $M_w = 7.2$), a mere 250 km from the capital city. Due to the relatively recent settlement of Ulaanbaatar in the Tuul Valley, knowledge of historical earthquakes in the region is limited and only covers a few centuries, i.e. a fraction of the several millennia long recurrence periods.

For an estimation of separate building sites in territory of Ulaanbaatar the reliable justification of its initial seismicity on the basis of the data on a geological structure, tectonics, data on strong earthquakes [1], EQ zones and to their key parameters, the return period and its likelihood estimations (Solonenko, 1985; Solonenko, 1959; Dzhurik, 2004) is necessary.

For territory of Ulaanbaatar now such estimations don't exist, and initial seismicity is accepted according to the acting, confirmed map (the Map of seismic zoning into districts MNP, 1985 (Solonenko, 1985) and Mongolian Building document 22.01*/2006 (БНБД 22.01*/2006). According to this map and the city territory is carried to intensity 7. Return period of EQ with intensity 7 is 1 times per 1000 years.

In relation to size of the accepted initial seismicity it is necessary to notice that the territory of Ulaanbaatar is in the Mongol-Baikal seismic zone, one of the most seismoactive on the Earth (Medvedev, 1971). Therefore to problems of seismic division into districts and seismosafety of a city it is given particular attention.

Last 30 years near of the city there were some notable earthquakes to a power class (K) equal 8-11. Their epicenters are located in radius of 10-60 km and cover presumably sites with the raised seismic potential. Earthquakes (around 10) with $K > 12$, in radius to 300 km, were felt in a city with force of 3-6 intensity, but on considerable damages was not informed. This position is confirmed also with the data of the registered epicenters of earthquakes with 1964 on 2009, with inclusion of the data of registration by a network of modern digital seismic stations. The basic source the zones influencing initial seismicity are located from 75 to 300 km (Figure 1), potential from 0-10 to 300 km. Therefore there are bases to consider that the initial seismicity of a city estimated intensity 7, needs its specification or revision taking into account the received new data on a geological structure, tectonics, seismicity and probability of strong earthquakes (Dzhurik, 1995).

On the basis of told, in the present conclusion initial seismicity is accepted according to operating standard documents for territory of Ulaanbaatar and intensity is equals 7 (Batsaikhan, 2008) though this estimation is not declared on a modern seismic situation of a city. It is necessary for considering to designers and builders.

Today, some recent observations raise strong concerns on seismic activity around Ulaanbaatar. The number of potential and still unknown fault structures in the region beneath a Hustai, Emeelt and Gunjiin active fault area which is located about 10 to 40 km west and 10 km to east of Ulaanbaatar have been discovered. See Figure 2. These scientific findings dramatically altered our view on the relative seismic quiescence about Ulaanbaatar.

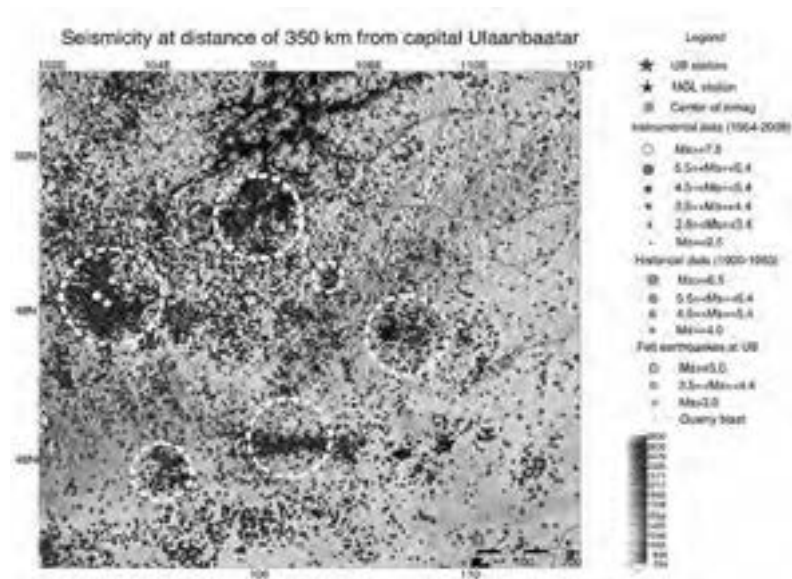


Figure 1: Map of epicenters of EQ between 1964 and 2010 years and the EQ's generation zone (signed by white circle).



Figure 2: Potential active fault structures around Ulaanbaatar city.

The high seismic activity of Ulaanbaatar area starts from middle of 2005 and still continues up to today. The number of earthquakes occurred between 1970 and 2009 contains totally 2420 events, 900 events recorded during 1970 - 2004 and 1340 events occurred from 2005 to 2009. There were 508 earthquakes corresponds only for 2009, and 510 events were already occurred mid of 2010. See Figure 3. These statistics showing seismic activity is increasing and migrating. Distribution of these swarms, with more than 2000 events, has interconnected to the major active structures in Ulaanbaatar area by a steeply dipping fault surface striking East-West Hustai and North-South Emeelt fault. The Hustai fault area is activated by the 2009 and 2010 swarms. It shows probable main potential structure which may produce large earthquakes, starts to be cracking and moving. Most activity is occurring east end of the Hustai active fault and shows somehow connection between these two active faults as well as there is Gunjiin faults in the same structure.

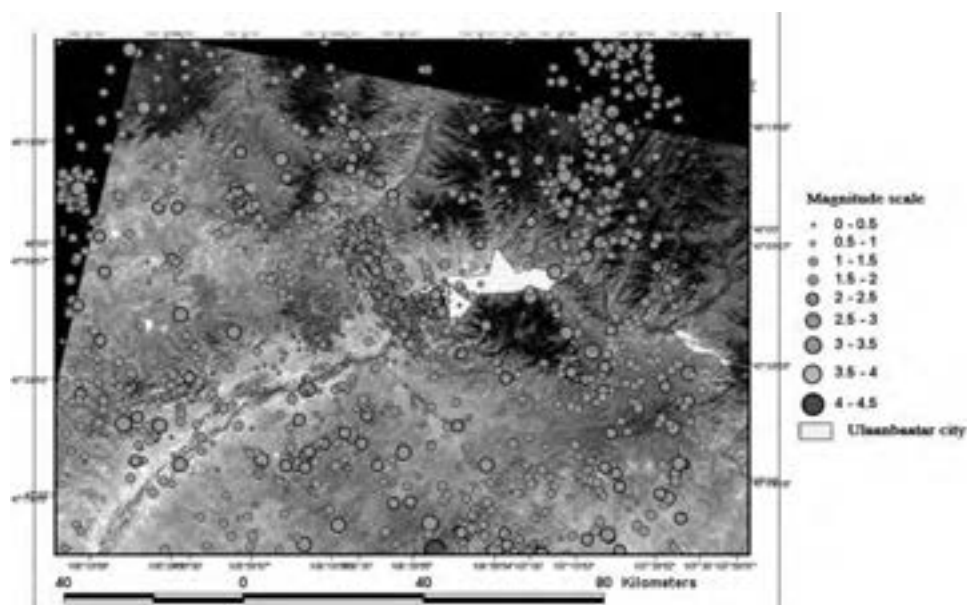


Figure 3: Seismicity around Ulaanbaatar

The facts:

Important seismic activity has been taking place near and within Ulaanbaatar since 2005. This concerns 1) the Emeelt area with small but numerous events perfectly aligned and showing a large deep active fault, 2) several earthquakes of magnitude 4 and more took place during last 5 years in the vicinity of Ulaanbaatar, some of them were actually felt by inhabitants of Ulaanbaatar.

Large active faults have been identified less than 30 km from Ulaanbaatar (e.g. Hustai, Emeelt and Gunjiin, see Figure 4). Their morphology indicates they are capable to produce earthquakes of magnitude 6.5 to 7.5.

An earthquake rupturing one of these faults will produce at Ulaanbaatar severe ground shaking of an Intensity of VIII to X at rock (VIII is associated with many collapses of weak buildings - X is associated with many collapse of buildings well made in concrete without earthquake resistant conceptions). These intensities will

be increased (and the related destructions) for buildings on sediments due to site effect amplification. This is the case for the most part of the city, which sits within a sedimentary basin.

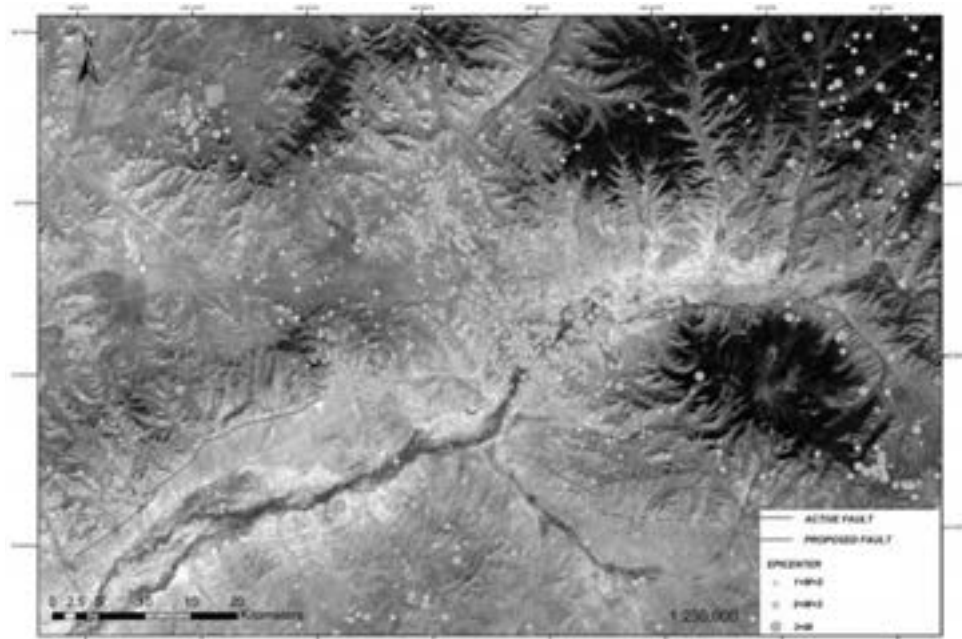


Figure 4: Map of seismic activity and active faults around Ulaanbaatar

3. CALCULATION OF SEISMIC DANGER IN POINTS DEPENDING ON SOIL CONDITIONS OF PLATFORM OF BUILDING

The design procedure of seismic danger in points meets the requirements of existing standard documents, both in Russia, and in Mongolia. For calculations of seismic danger of a platform the acoustic stiffness method was used. The increments of intensities were estimated by comparison of seismic characteristics of soils, received by direct measurements under Medvedev's formula [10] and agree Tables №1:

$$\Delta J_{pV} = 1.67 \lg(\rho_3 \cdot V_3 / \rho_i \cdot V_i) \quad (3.1)$$

where $\rho_3 \cdot V_3$ and $\rho_i \cdot V_i$ - acoustic stiffness reference and investigated of grounds, ΔJ - settlement values of increments of intensities.

For water sated of soils to the formula (3.1) the amendment is entered, agrees expressions:

$$\Delta J_{GWL} = K * e^{-0,04h * h} \quad (3.2)$$

The factor "K" for territories where prevail sandy and clay grounds in the top 10 meters layer, is accepted equal 1; where maintenance of gravel, a pebble, rockwaste, landwaste, boulders is more than 70 %, is equal 0,5. If level of ground waters is located below 10 m from a surface, amendment ΔJ_{GWL} is not entered.

Resonant properties of a layer soul of grounds are estimated through calculation of frequency characteristics (Section 3.2). The amendment for a relief is entered at its inclinations from a horizontal more than 15 degrees. In our case of such amendment it is not required.

Thus, for an estimation of seismic danger in points, are necessary: a standard choice, definition of average speeds of seismic waves in the top 10 meters layer soils, their volume weight and depth Ground Water Level.

Speeds of seismic waves were measured by a method of the refracted waves (Dzhurik, 1998) 24 channels digital station McSEIS-SX 24 XP (Japan). Measurements were spent separate search with maintenance counter and making up hodograph. The length hodograph made 46 m. Excitation of seismic fluctuations by means of blows. The binding on district was carried out on GPS geodesies. Supervision were spent with possibility of registration of longitudinal and cross-section waves. Such measurement technique allows to receive average values of speeds in the top zone of a cut to depth of 10-30 m.



Point measurements	Latitude	Longitude
MS 637	47,90021°N	106,91029°E 1283m
....
MS 649	47,90041°N	106,91038°E 1283m
....
MS 661	47,90061°N	106,91046°E 1283m
Seismic station	47,90017°N	106,91035°E 1283m

Figure-5. Example. The scheme of an arrangement of points of seismosounding near of the territory of “Coyote” company (blue color lines) and mobile seismic station (white color ellips).

By the technique stated above it is direct on a building site it is executed seismosoundings (Figure 5) for studying of speeds of seismic waves in Rock "reference" and average not water sated soul grounds more than 20 searching. Characteristic counter seismograms of records of useful waves are presented in Figure 6, 7.

Speeds of seismic waves in "reference" Rocky grounds were measured on their exposures in a vicinity of Ulaanbaatar. For an estimation of their most probable values were used as the share and literary data about measurements of speeds of

seismic waves in soul and Rocky grounds around Ulaanbaat;ar (Dzhurik, 1998; Dzhurik, 2001; Batsaikhan, 2006) and it is direct in its territory in a vicinity of the platform (Dzhurik, 1980; Dzhurik, 1989; Dzhurik, 1995). The most probable average values of speeds in the top 10 meter layer of Rocky grounds are As a result established. Were for this purpose used and the conclusions drawn authors received earlier (Seismic division into districts., Solonenko, 1971).

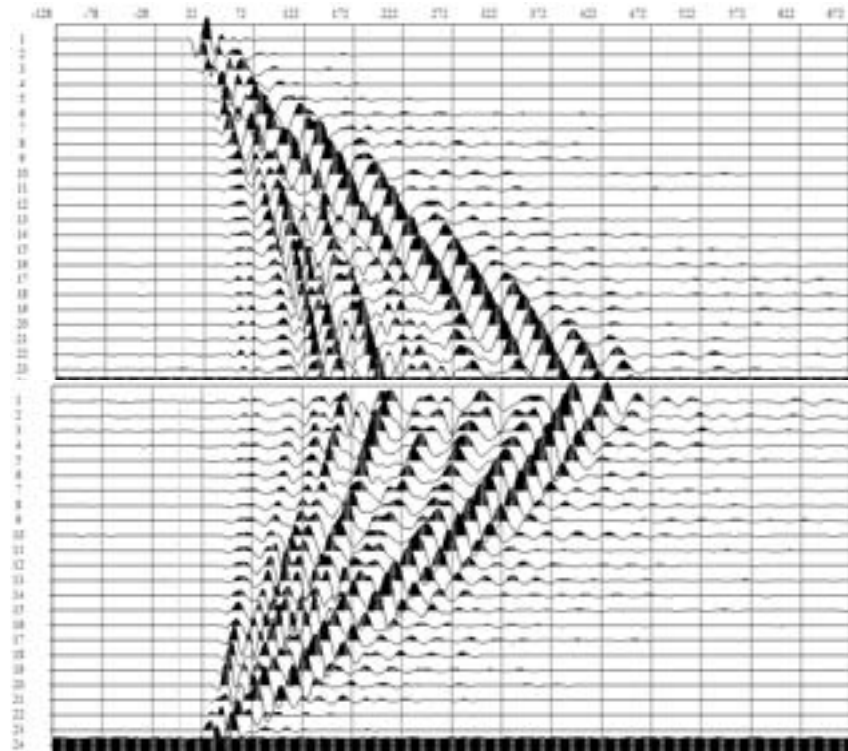


Figure-6. Seismogram (see Figure-5, points MS-637 and MS-661).

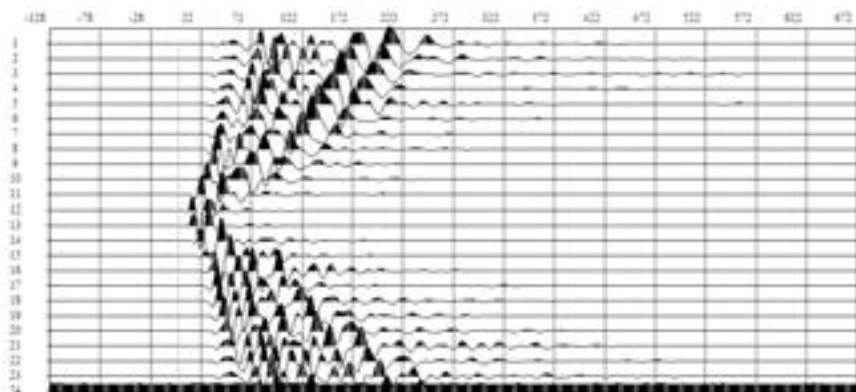


Figure-7. Seismogram (see Figure-5, point MS-649).

Calculation of intensity of seismic danger under the formula 3.1 and 3.2, concerning reference rocky soils, leads to value of an increment of intensity for a platform of building at the expense of seismic rigidity (ΔJ_{pV}) equal 0,834:

$$\Delta J_{pV} = 1.67 \cdot \lg (2,5 \cdot 2400) / (2,11 \cdot 725) = 0,991$$

where: 700 – average speed of P- waves in 30 meter layer on a site of building of a complex.

The amendment at the expense of depth of GWL (ΔJ_{GWL}) is equal 0,451 points at $h=1,6m$:

$$\Delta J_{GWL} = 0,5 \cdot \exp (-0,04 \cdot h^2) = 0,451$$

As a result the total increment of intensity will constitute 1,442, and intensity of seismic danger of a platform of building on a method seismic rigidity is estimated in 7,44.

4. SEISMIC INFLUENCES ON A CASE OF STRONG EARTHQUAKES

The basic maxima of spectra of "accelerations" (spectral density in sm/sec , T - the period in second, $f = 1/T$ – frequency of fluctuations in Hz) have on frequencies 1,27 - 3,3 Hz, and their maximum values are equal 32,9 and 17,7 sm/sec , for component NS and Z. The spectrum of accelerations is specified in the sense that as the initial information for calculations digital record accelerogram set serves in sm/s^2 . Under this data it is possible to calculate a considerable quantity of the spectra, which used for the decision of various tasks, including for calculations of frequency characteristics and spectra of reaction for concrete constructions in sm/sec^2 . For realization of calculations, data on construction attenuation in the latter case are required.

The maximum values of acceleration of fluctuations of soil for EW and Z a component reach values of 136 and 81 sm/sec^2 – according to (Figure 8). It according to scales of intensity is equated to the seismic influence close to 7,44.

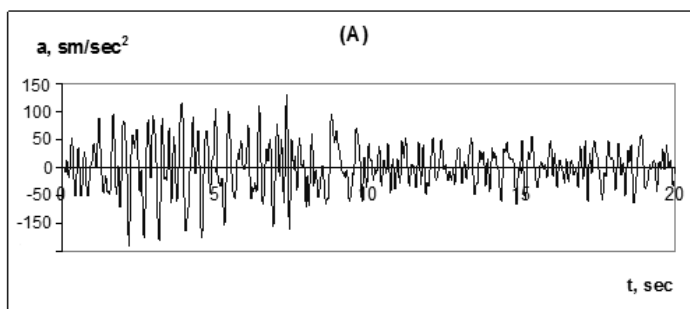


Figure-8. Horizontal a component (EW) of the calculated accelerogram

Concerning the executed theoretical calculations of seismic influences it is noticed that they are conducted in the assumption of elastic deformation, that is all energy is shown in elastic fluctuations soils. Sizes of residual deformations can be determined on seismic scales, on values of the received settlement accelerations. In turn it is approached by the decision as transition from values of characteristics soils in an elastic stage to characteristics in a stage of not elastic deformation practically isn't studied. Therefore the estimation of seismic danger of a platform

of “Coyote” company building was based on a number of known assumptions. The cores from them are reduced to the following provisions, the received relative characteristics of oscillative motions at weak earthquakes can be extrapolated on strong, and the spectral railroad train of strong earthquake can be estimated by extrapolation of the weak. Reliability of these assumptions and the theoretical preconditions used by us can be established only experimentally. In this respect and, to some extent, for confirmation of the received results we will result available data (Medvedev, 1971) about studying of relative sizes of fluctuations soils according to records of weak earthquakes near to a building platform.

5. CONCLUSION

The justification of engineering-seismological conditions of a site of “Coyote” company building in area Sukhbaatar district of Ulaanbaatar city is conducted on the basis of direct measurements, use of the found materials, the data settlement methods and parameters of initial seismicity. The topographic basis of the site and engineering-geological data were provided by the customer in the form of reports. In this conclusion we give resume on seismicity area near of Ulaanbaatar city. It is shown that weak earthquakes in a city vicinity constantly are registered and the parameters of probable strong earthquakes are measured as: epicenter distance 0-240 km, magnitude 5.5-8.0, intensity 8, focus depth 10-20 km and its focal mechanism can be slip and reversed strike-slip fault.

Our calculations provided in the first approximation the initial seismicity of the construction area, which was defined as intensity 7 according to acting normative documents.

For a site of building distribution of speeds of S- and P-waves with depth to radical breeds is established. Reference values of speeds of the seismic waves, corresponding to their probable values for radical breeds of territory of Ulaanbaatar are chosen, seismic models for soil thicknesses of residential buildings serving by bases are constructed. The initial signal for horizontal the components, answering to parameters of probable strong earthquakes for the city territory is generated, as a first approximation. Their spectra and frequency characteristics of fluctuations are calculated on a case of such shake of soul in a basis of a building for maximum horizontal (EW) and vertical (Z) a component accelerogram.

In the seismic relation the site of “Coyote” company building is estimated, as rather homogeneous in intensity 7. When a building is erected, an artificial foundation must be removed from the ground.

The basic settlement parameters of seismic influences is in following limits: seismic danger in intensity 7,44. The maximum value of accelerations at possible strong earthquake can reach 136 and 81 sm/sec², accordingly for horizontal (EW, NS) and vertical (Z) component. Maxima of spectra of accelerations have on frequencies of 1,4 and 3,3 Hz, and their maximum values are equal 32,9 and 17,7 sm/sec accordingly for EW and Z a component.

The calculations are performed with the elastic deformation implied. Concerning the conducted calculations of seismic influences it is noticed that they are conducted in the assumption of elastic deformation and sizes of residual

deformations can be determined on scales of intensity taking into account settlement values of the maximum accelerations.

The established level of seismicity for the territory of Ulaanbaatar city may be exceeded with 10% probability during 50 years ($T=1000$) or with 90% probability of non-exceedance for the same time span. If the class of responsibility of an construction is raised by designers even at the expense of a floors, it is necessary to review and results of calculations of seismic influences on new level of likelihood estimations, intensity 8.

REFERENCE

Ritz, J.-F., E. T. Brown, D. L. Bourle`s, H. Philip, A. Schlupp, G. M. Raisbeck, F. Yiou, and B. Enkhtuvshin, *Slip rates along active faults estimated with cosmic-ray-exposures dates: Application to the Bogd Fault, Gobi-Altay, Mongolia*, *Geology*, 23, 1019–1022, 1995.

В.П. Солоненко, Н.А. Флоренсов. *Землетрясения и основы сейсмического районирования Монголии*. М., Наука, 1985. 224 с.

Солоненко В.П. О сейсмическом районировании территории Монгольской Народной Республики. – *ДАН СССР*, 1959. Т.127, вып.2

Солоненко В.П. О некоторых особенностях землетрясений Монголо-Байкальской сейсмической зоны. *Бюлл. Совета по сейсмологии*. Москва: 1959. №10. С. 414-418.

Dzhurik V.I., Dugarmaa T., Batsaikhan Ts., Serebrennikov S.P., Drennov F.A. The technique of seismic risk mapping for the territories of economic development of Mongolia. *Proceedings of Mongolian Academy of Sciences*.2004, p.16-29.

Глубинное строение и геодинамика Монголо-Сибирского региона. Наука, Новосибирск,1995, 185с.

С. В. Медведев. *Сейсмическое районирование Улан-Батора*. М.: Наука, 1971. 200 с.
Джурик и др. Отчет: «Сейсмическое микрорайонирование площадок Аймачных центров Дзун-Мод и Сухэ-Батор и площадки второго микрорайона г. Улаанбаатара». Иркутск-Улан-Батор,1980. 198 с.

Джурик В.И. и др. Инженерно-сейсмологические условия территории г. Аргалант (площадки гражданского и промышленного строительства). Иркутск-Улан-Батор: 1989. 261 с.

Джурик В.И. *Проект комплексных исследований по сейсмическому микрорайонированию территории г. Улан-Батора*. Иркутск –Улаанбаатар: 1995.

Джурик В.И., Дугармаа Т. и др. Сейсмическое микрорайонирование аймачных центров Монголии. Улаанбаатар: АНМ,1998. 248 с.

Джурик И.И., Дугармаа Т. Вопросы оценки сейсмического риска для Улаанбаатара и его окрестностей. // *Geophysics & astronome*. №1. Улаатбаатар:,2001. С.47-59.

Батсайхан Ц. Инженерно-геофизическая оценка сейсмической опасности грунтов территории г.Улаанбаарара. *Диссертация на соискание ученой степени к.г.-м.н.* Иркутск 2006. 144 с.

Ц.Батсайхан. *Оценка инженерно-сейсмологических условий площадки строительства жилого здания (на левом берегу р. Толы у подножья памятника сов. Воину) г. Улаанбаатара*». 2008, 32с.

Улаанбаатар хот. Хан-уул дүүргийн 1-р хорооны нутагт барих “КОЁОТЭ” ХХК-ний оффис, үйлчилгээний барилгад зортулсан инженер-геологийн судалгааны дүгнэлт. "Жоншит-Уул" ХХКомпани. Улаанбаатар хот. 2012 он.

Газар хөдлөлтийн бүс нутагт барилга төлөвлөх барилгийн норм ба дүрэм. БНБД 22.01*/2006. *Монгол улсын Барилга, хот байгуулалтын яам*. Улаанбаатар хот 2006 он. 42 стр.

Study on recovery curves for temporary housing after the 2011 Great East Japan Earthquake

Osamu MURAO¹ and Kazetaka KOTOKU²

¹ Associate Professor, Faculty of Engineering, Information and Systems
University of Tsukuba, Japan
muraos@risk.tsukuba.ac.jp

² Graduate School of Systems and Information Engineering,
University of Tsukuba, Japan

ABSTRACT

As of the time we are writing this paper, One year and five months have passed since the 2011 off the Pacific coast of Tohoku Earthquake and post-tsunami urban recovery has been progressed in each damaged area. One of the important activities for the victims is construction of temporary housings in the earlier stage of urban recovery process. The authors were provided temporary housing construction data after the event by Ministry of Land, Infrastructure, Transport and Tourism in order to construct recovery curves, which are quantitative tool to compare regional recovery processes. In this paper, the authors firstly present how temporary housing had been constructed in Iwate, Miyagi, and Fukushima since the event. Then they develop recovery curves and compare them. The analysis clarified that the speed of the construction is the highest in Iwate, and the lowest in Fukushima.

Keywords: 2011 Great East Japan Earthquake, temporary housing, recovery process, Iwate, Miyagi, Fukushima

1. INTRODUCTION

1.1 Background

The 2011 off the Pacific coast of Tohoku Earthquake, which occurred on March 11, 2011, catastrophically devastated the eastern part of Japan. It damaged more than one million houses: heavily 129,914, moderately 258,591, and slightly 711,376 (National Police Agency, 2012). More than one year passing, recovery activities started in most damaged areas in the serious aftermath of the event.

1.2 Purpose

Temporary housing construction is one of the most important recovery activities in the early stage of recovery process. However, its construction situation is different according to regional condition of the damaged areas. This paper aims to clarify the difference of temporary housing construction process between the

most affected three prefectures due to the 2011 Great East Japan Earthquake: Iwate, Miyagi, and Fukushima.

In order to gain the purpose, we use the recovery curve method proposed by Murao and Nakazato (2010). Recovery curve is a measure to quantitatively compare the long-term recovery process of the damaged areas after disasters. Using the tool, Murao and Nakazato (2010) clarified the regional differences of reconstruction process in terms of temporary houses and permanent houses in Sri Lanka after the 2004 Indian Ocean Tsunami. Also, Murao et al. (2011) constructed the recovery curves after the tsunami disaster in Thailand and Indonesia, and compared those processes.

2. METHOD

The following procedure is employed to construct recovery curves for each prefecture.

2.1 Data Used

In order to construct the recovery curves for temporary houses, the authors use the temporary housing data provided by Ministry of Land, Infrastructure, Transport and Tourism (MLIT, 2012). The dataset has been weekly updated since April 11, 2011, and the authors arranged the monthly data of Iwate, Miyagi, and Fukushima as of January 2012.

2.2 Recovery Ratio Calculation

To plot the recovery curves, it is necessary to normalize the recovery condition of damaged areas of varying size. This was done by comparing the recovery ratio of the number of buildings constructed per month to the total number of constructed buildings as of January 2012.

2.3 Selection of Optimal Recovery Curve

For the time period of 10 months, the cumulative ratio of building completion is assumed to be fitted a sigmoid curve such as Cumulative Normal Distribution curve, Logistic curve, or Gompertz curve. A curve showing the highest correlation with observed data is considered to represent the most optimal recovery curve for the temporary houses.

2.4 Development of the Recovery Curves

After the optimal curve is determined, prefectural curves are constructed respectively. Finally, the construction conditions of temporary houses between three prefectures are quantitatively compared with the developed recovery curves and probability density functions.

3. TEMPORARY HOUSING CONSTRUCTION SITUATION AFTER THE 2011 GREAT EAST JAPAN EARTHQUAKE

Temporary housing is constructed by Japan Prefabricated Construction Suppliers and Manufactures Association or local construction companies according to order from the damaged local governments, or at the request of MLIT. Sometimes instead of the temporary housing, public housing or rented apartments managed by private companies are used for the victims to save the construction. The number of the affected households by the earthquake in the rented apartments is 67,648 as of July 24, 2012 (Reconstruction Agency, 2012).

As for the construction of temporary housing after the event, there were several problems. One of the critical problems was shortage of available land for the construction. Because of the huge earthquake of March 11, the inundated areas totally extended for 561km² (GSI, 2011), and enormous number of houses became necessary in the affected areas. Nevertheless, it was difficult for some local governments to prepare the spare sites for temporary housing out of the damaged areas because of the geographical condition, especially in the mountainous areas along the Sanriku Rias Coastline. Those governments dealt with the problem by the way of using outer lands or farmlands, but it spent a long time to convince the affected residents and to properly allocate the provided lands. Those were reasons of delay in construction process of the temporary housing in some areas.

Another problem was difficulty of construction material obtention. A link of supply chain was broken, for factories producing materials or manufacture companies themselves located in the damaged areas were devastated by the tsunamis or shaking. They handled it with imported building material and other local governments' supports, yet they faced other difficulties of transportation and arrangements.

The most serious situation arose in Fukushima among the three prefectures. Fukushima Daiichi nuclear disaster forced the residents around to be evacuated from the evacuation zone or the emergency evacuation preparation zone surrounding the Fukushima No.1 nuclear power plant. The complicated situation delayed the temporary housing construction in some municipalities in the prefecture.

4. PREFECTURAL COMPARISON OF TEMPORARY HOUSING CONSTRUCTION

Monthly-completed construction situation of temporary houses in Iwate, Miyagi, and Fukushima Prefecture based on the provided dataset (MLIT, 2012) is shown in Table 1 and Figure 1. The prefecture with the largest number of required temporary house units is Miyagi, and the smallest is Iwate.

In April 2011, Prime Minister Naoto Kan announced that all temporary housing would be constructed by mid-August. Also Iwate prefecture announced that all units would be completed before September 11, 2011, a half year after the event. That timeline can be a mark to evaluate the recovery process.

Iwate estimated the required units to be 18,000 at first. Although the number decreased to 13,984, the construction effort almost achieved the goal in August

2011. In Miyagi, 95.9% of the necessary houses were completed by August 2011, and all the construction had been finished by December. On the other hand, Fukushima still remained in a difficult situation even in January 2012. The emergency evacuation preparation zone surrounding the Fukushima No.1 nuclear power plant, which was regulated on April 22, 2011, was lifted on September 30, and temporary housing construction in the zone got permitted. Although the construction ratio achieved 94.8% as of January 2012, the number of required houses was still increasing.

Table 1: Monthly-completed construction situation of temporary houses in Iwate, Miyagi, and Fukushima Prefecture

Month	Iwate	Miyagi	Fukushima	Total
March 2011	0	0	0	0
April 2011	533	1,426	437	2,396
May 2011	6,869	10,294	6,332	23,495
June 2011	9,694	14,160	9,021	32,875
July 2011	13,112	16,988	11,181	41,281
Aug. 2011	13,983	21,189	13,573	48,745
Sep. 2011	13,984	21,826	14,284	50,094
Oct. 2011	13,984	21,899	15,514	51,397
Nov. 2011	13,984	22,042	15,700	51,726
Dec. 2011	13,984	22,095	15,788	51,867
Jan. 2012	13,984	22,095	15,788	51,867
Required Units	13,984	22,095	16,659	52,738

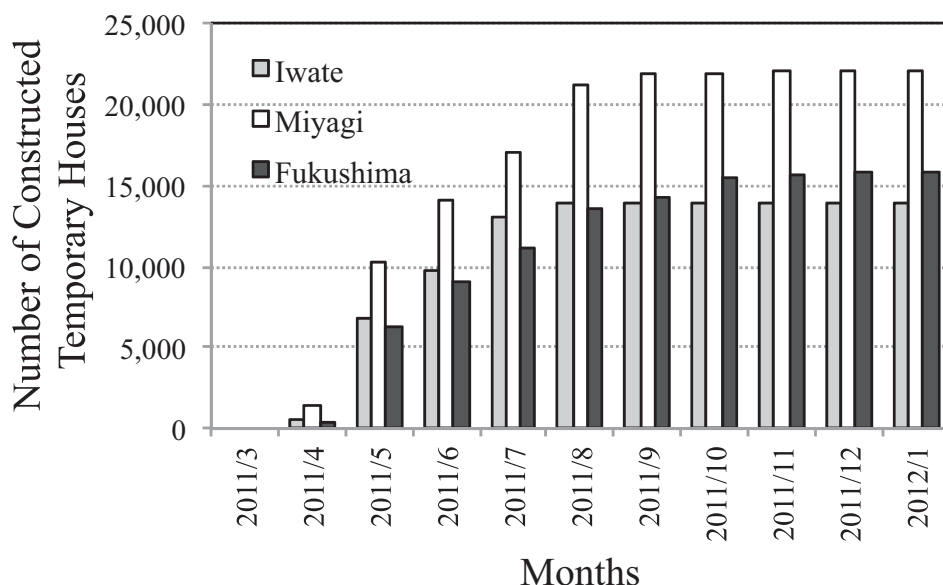


Figure 1: Completed construction situation of temporary houses in Iwate, Miyagi, and Fukushima Prefecture

5. CONSTRUCTION OF RECOVERY CURVES FOR TEMPORARY HOUSING

Optimal approximate recovery curves were then selected for the temporary houses. Assuming that the relationship between elapsed time and recovery ratio closely fits a sigmoid curve, we considered three kinds of Sigmoid Curves; Cumulative Normal Distribution curve, Logistic curve, and Gompertz curve.

As a result, we found that a Gompertz Distribution is the best fit among the three for the temporary house data, as well as the previous research for Sri Lanka by Murao and Nakazato (2010). Then the Gompertz Distribution is used for making the recovery curves for the three prefectures.

The factors of time (months) and the ratio of building completion are used to construct recovery curves. The time period starts in March 2011, with April 2011 being regarded as month “1”, and extends over 10 months until January 2012. The ratio of building completion for a given time period is calculated based on the total amount of completed buildings. For a time period of t (months), the cumulative ratio of building completion $R(t)$ can be described by the Gompertz curves, using the following equation:

$$R(t) = a^{b^t} \quad (1)$$

where a and b , are coefficients.

Recovery curves for the prefectures can now be plotted using the regional construction data. However, it should be noted that the number of buildings constructed in Fukushima was less than that of necessary construction as of January 2012. Since the recovery curves can thus be considered to closely reflect the actual situation, a parameter, K , reflecting the completion realization ratio for each prefecture can be combined with Eq. (1) to give Eq. (2) for the temporary houses, as the final building recovery functions. In addition, Eq. (3) shows the probability density function of the Gompertz curve.

$$R(t) = Ka^{b^t} \quad (2)$$

$$P(t) = Ka^{b^t} b^t \cdot \log a \cdot \log b \quad (3)$$

Thus, the recovery curves and the probability density functions for temporary houses were obtained as shown in Table 2, Figure 2 and Figure 3.

Table 2: Recovery curve parameters for temporary housings in Iwate, Miyagi, and Fukushima Prefecture

Month	a	b	R^2	K
Iwate	0.0000432	0.296	0.986	1.00
Miyagi	0.0002036	0.361	0.986	1.00
Fukushima	0.0001958	0.424	0.974	0.95
Total	0.0001476	0.375	0.991	0.98

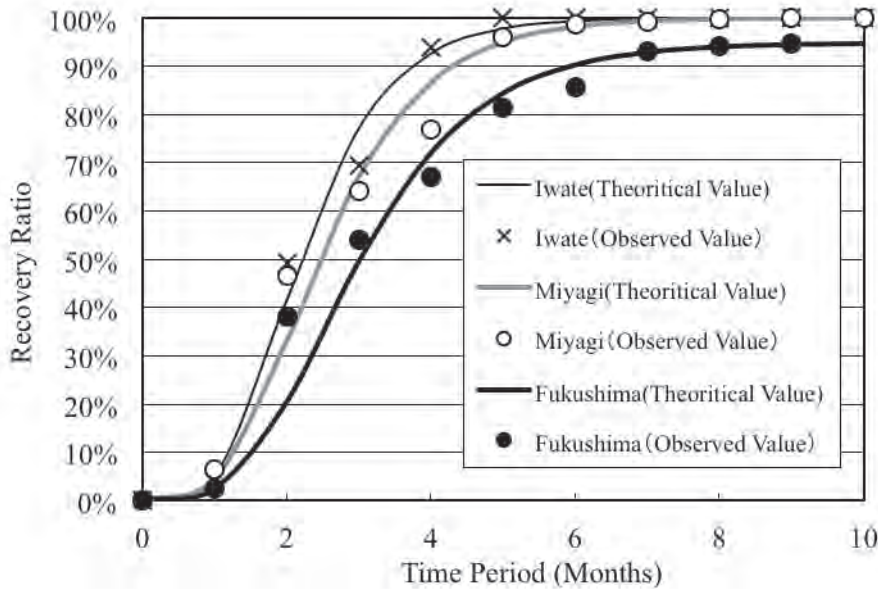


Figure 2: Recovery curves for temporary housing in Iwate, Miyagi, and Fukushima Prefecture

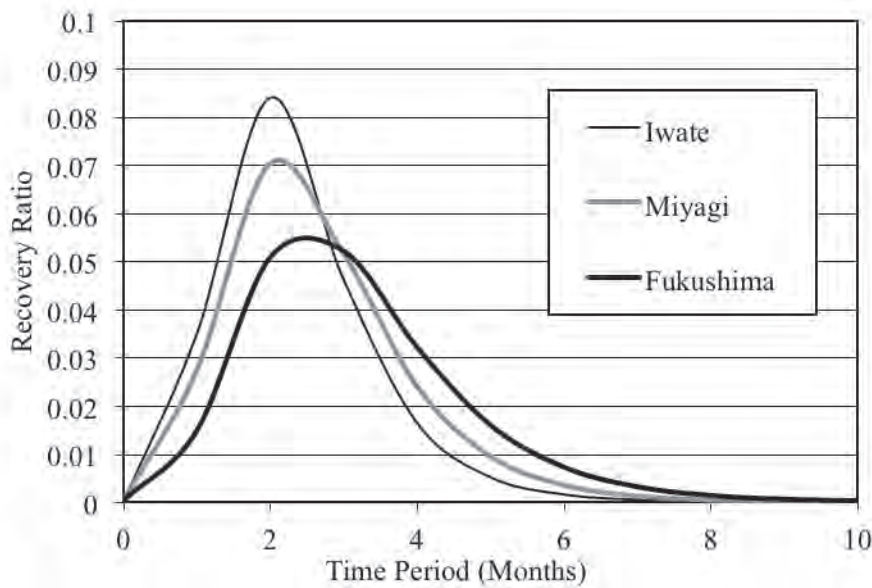


Figure 3: Probability density functions for temporary housing in Iwate, Miyagi, and Fukushima Prefecture

High correlations, more than 0.97, were observed between the curves developed in this study and the observed data, so the curves are considered to properly reflect each recovery condition. The average completion months is 2.19 in Iwate, 2.46 in Miyagi, and 2.92 in Fukushima. The difference between Iwate and Fukushima is 0.73 months.

6. CONCLUSION

In this study, recovery curves for temporary housing in Iwate, Miyagi, and Fukushima, the most seriously damaged prefectures due to the 2011 Great East Japan Earthquake, were developed using the dataset provided by Ministry of Land, Infrastructure, Transport and Tourism. It was found that a Gompertz Distribution was the better fit than Cumulative Normal Distribution curve and Logistic curve. Then the difference of the construction process between the three prefectures was quantitatively clarified: the speed of the construction is the highest in Iwate, and the lowest in Fukushima.

ACKNOWLEDGEMENTS

This research was supported by the recovery support program for the Great East Japan Earthquake granted by University of Tsukuba.

REFERENCES

- Geospatial Information Authority of Japan (GSI), 2011. Information of Inundation Areas by the Tsunami of March 11, 2011, the fifth report, <http://www.gsi.go.jp/common/000059939.pdf>
- Ministry of Land, Infrastructure, Transport and Tourism (MLIT), 2012. Information related to temporary housings, http://www.mlit.go.jp/report/daisinsai_kasetu.html.
- Murao, O., and Nakazato, H., 2010. Recovery curves for housing reconstruction in Sri Lanka after the 2004 Indian Ocean Tsunami. *Journal of earthquake and Tsunami*, Vol.4, No.2, 51-60.
- Murao, O., Sugiyasu, K., and Nakazato, H., 2011. Study on Recovery Curves for Housing Reconstruction in Sri Lanka, Thailand, and Indonesia after the 2004 Indian Ocean Tsunami, *Proceedings of the 10th International Symposium on New Technologies for Urban Safety of Mega Cities in Asia (USB)*, 8p., Chiang Mai, Thailand, 2011.10
- National Police Agency, 2012. Damage by the 2011 Great East Japan Earthquake and Tsunami and Response, <http://www.npa.go.jp/archive/keibi/biki/higaijokyo.pdf>.
- Reconstruction Agency, 2012. Process of the number of households in rented apartments. http://www.reconstruction.go.jp/topics/0724_mincin.pdf.

Disaster management of municipal governments on the Kii Peninsula after flood and sediment disasters caused by the 2011 Typhoon Talas

Shinya KONDO¹, Kazuyoshi OTA² and Yasuhiro KATAIE³

¹ Project Researcher, ICUS, IIS, The University of Tokyo, Japan
kondos@iis.u-tokyo.ac.jp

² Civil Engineering Department, Wakayama Prefecture, Japan

³ Kaiso Branch Office, Wakayama Prefecture, Japan

ABSTRACT

The Kii Peninsula protrudes to the south from the center of Honshu, Japan. This area is surrounded by the Pacific Ocean, and most of the peninsula is mountainous. It is predicted that the Kii Peninsula will suffer huge damage from the Tokai, Tonankai and Nankai earthquakes. However, Typhoon Talas also caused serious damage to the mountainous areas of the Kii peninsula due to large-scale debris flows and river flooding. There were 87 casualties across the three prefectures of the Kii Peninsula (Wakayama, Nara and Mie). In addition, because of communication failures during this disaster, people could not access disaster information. Lessons from this disaster could be useful for future countermeasures before, during and after the Tokai, Tonankai and Nankai earthquakes and for the design of flood and sediment disaster information dissemination systems in Asia.

In this paper, the authors summarized the disaster management activities of three municipalities in the southern part of Wakayama Prefecture during and after Typhoon Talas through interviews with personnel. Their disaster management was organized from two perspectives: “flowchart of disaster information generating process” and “flowchart of disaster information communication process.” As a result, the following three points were clarified. First, municipalities must make an effort to increase residents’ understanding that facilities which aim to mitigate the effects of disasters have the ability to reduce the disaster impact. Second, it is necessary to secure the multiplex communication network, such as telecommunications infrastructure and services (Social Network Service, among others). Third, municipalities need to carry out public relations so that people can decide whether to evacuate before dark without fear of time going to waste.

Keywords: disaster management, flood disaster, sediment disaster, typhoon, evacuation

1. INTRODUCTION

The Kii Peninsula protrudes to the south from the center of Honshu, Japan. This area is surrounded by the Pacific Ocean, and most of the peninsula is mountainous. It is predicted that the Kii Peninsula will suffer huge damage by ground motion, tsunami, and sediment disaster from the Tokai, Tonankai and Nankai earthquakes. However, Typhoon Talas also caused serious damage to the mountainous areas of the Kii peninsula due to large-scale debris flows and river flooding. There were 87 casualties across the three prefectures of the Kii Peninsula (Wakayama, Nara and Mie prefecture). In addition, because of communication failures during this disaster, people could not access disaster information. Lessons from this disaster could be useful for future countermeasures before, during and after the Tokai, Tonankai and Nankai earthquakes and for the design of flood and sediment disaster information dissemination systems in Asia.

In this paper, the authors summarize the disaster management activities of three municipalities in the southern part of Wakayama Prefecture during and after Typhoon Talas through interviews with personnel. Their disaster management is organized from two perspectives: “flowchart of disaster information generating process” and “flowchart of disaster information communication process.” People can consider the design of flood and sediment disaster information dissemination systems in Asia.

2. INVESTIGATION SUMMARY

2.1 Typhoon Talas (Japan Meteorological Agency (JMA) 2011)

On 3 September, Typhoon Talas made landfall on Shikoku Island and reached the Sea of Japan on the next day after crossing Shikoku and Chugoku regions. Because Talas had a large scale strong wind area and moved very slowly, it induced moisture advection for many hours and caused the record-breaking heavy rainfall over a wide area from western to northern Japan, especially along the mountains.

Especially over a wide area of the Kii Peninsula, the total amount of the precipitation from 17 JST, 30 August exceeded 1,000 mm. The observing station at Kamikitayama-village in Nara Prefecture observed 1,652.5 mm rainfall in 72 hours, hitting the record high in Japan. The total amount of the precipitation at the station reached 1805.5 mm and precipitation amount in some areas was estimated to be over 2,000 mm based on Radar/Raingauge Analyzed Precipitation. (Figure 1)

Human casualties caused by this typhoon are 81 people dead (5 people related death) and 16 people missing. Especially in the Kii Peninsula, human casualties are 71 people dead (5 people related death) and 16 people missing (Fire and Disaster Management Agency: FDMA 2012). This means that a large damage occurred around the Kii Peninsula by this typhoon. There were 3 rivers beyond

estimated high-water level, 91 debris flows, 30 landslides, and 80 slope failures (Ministry of Land, Infrastructure, Transport and Tourism: MLIT 2012).

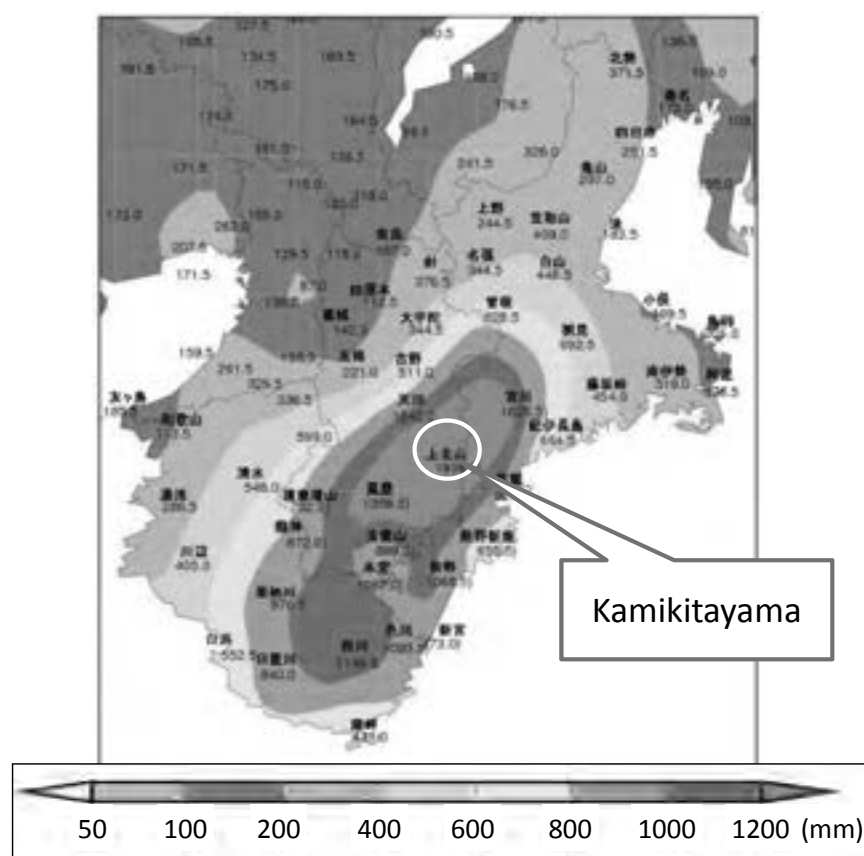


Figure 1: Precipitation during Typhoon Talas coming (30th August – 4th September)

2.2 Investigation area

In this study, investigation areas are Shingu city, Nachi-Katsuura town and Kozagawa town, Wakayama prefecture (Figure 2). These municipalities are located in the southern part of Kii Peninsula. Central area is located in the coastal area. In the mountainous area, there are parts of World Heritage site, Kumano Taisha and Kumano Kodo, and many small districts.

Table 1 shows human casualties. These were caused by inundation by river flooding and sediment disasters. Figure 3 shows the relationship of precipitation, heavy rain warning and landslide warning information at Nishikawa, the mountainous area of Kozagawa town. Rain became heavily at early morning on 2nd September after heavy rain warning issued. Landslide warning information was also issued at 11:45 on 2nd September at Shingu city and at 21:45 on this day at Nachi-Katsuura town and Kozagawa town. Shingu city was damaged by Kumano river flooding and sediment disaster. Nachi-Katsuura town was damaged by debris flow along to Nachi river. Kozagawa town was damaged by Koza river flooding.

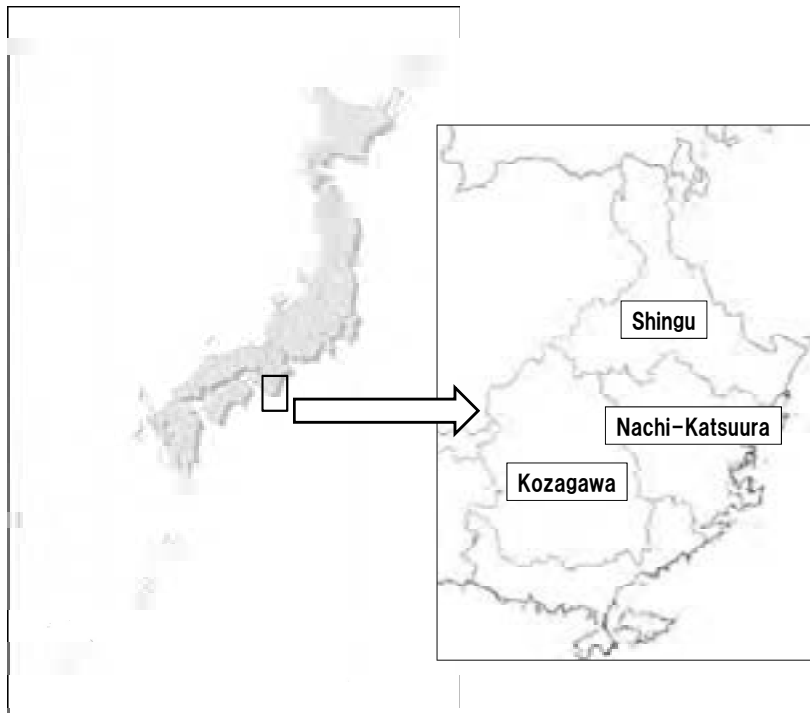


Figure 2: Investigation area

Table 1: Human casualties at three municipalities

	Death	Related death	Missing
Shingu	13	0	1
Nachi-Katsuura	27	3	1
Kozagawa	0	2	0

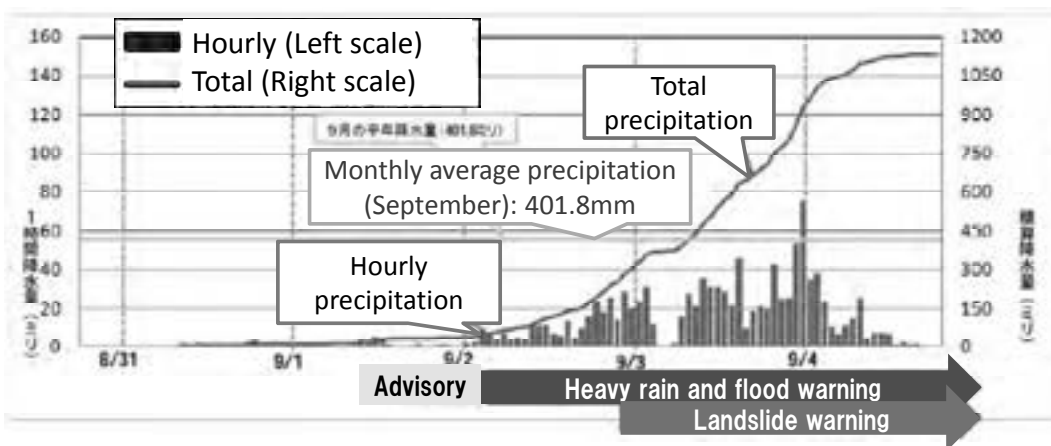


Figure 3: The relationship of precipitation, heavy rain warning and landslide warning information (Kozgawa town)

In this study, the authors conducted interviews about disaster response (from the time that typhoon Talas would affect Kii Peninsula was expected) for disaster management staff of three municipalities.

3. RESULTS OF INTERVIEW

3.1 Shingu city

Shingu city is a municipality that has been established by merged by Shingu city and Kumanogawa town which was at mountainous area of Shingu city. Disaster operation center was opened at main government building at 19:00 on 2nd September. But disaster management staff operated for the people living in Kumanogawa town area at Kumanogawa branch office. For example, when disaster management staff decides evacuation directives for Kumanogawa town area at main government building, Kumanogawa branch officials will tell people to evacuation. At 16:00 on 2nd September, main road leading to Kumanogawa town area were closed to traffic because of heavy rain. At 19:00 on 2nd September, the level of Kumano river became higher beyond embankment. At early morning on 4th September, second floor of Kumanogawa branch office was flooded.

Disaster management officers issued evacuation directives monitoring the level of Kumano river. At 20:40 on 2nd September, evacuation instruction was issued at Kumanogawa town area. On the other hand, evacuation directives were issued step-by-step at dangerous area around coastal area after 20:40 on 3rd September.

There are 10 dams in Kumano river. Objective of dams is not flood control but power generation except one (Sarutani dam). Figure 4 shows the flow and storage of Sarutani dam. We can see inflow and outflow of this dam were equal from early morning on 2nd September. There is an agreement that dam manager sends FAX to disaster management officers once an hour when the outflow of dam becomes three thousand tons per second. At that time, dam manager sent FAX to disaster management officers once thirty minutes. Disaster management officers told residents about dam information by email and public wireless network for disaster prevention. Some residents at Kumanogawa town area had experience of inundation, so they collected river information by themselves using internet.

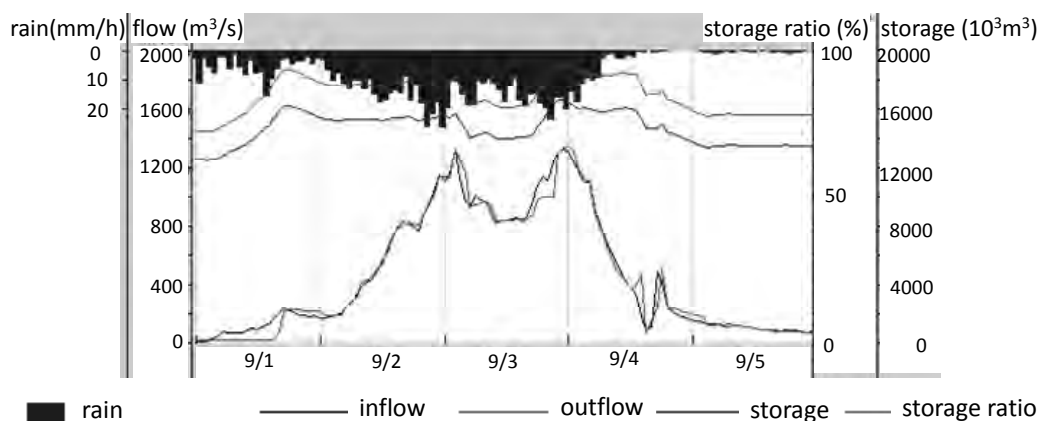


Figure 4: Flow and storage (Sarutani dam)

In this disaster, it was not easy to ensure communication tool. From 3rd to 7th September, fixed-line was interrupted. There were portable radios at meeting place of the districts, but most of them were submerged. Furthermore, mobile phone was interrupted at mountainous area. Web and mail server was not available then anyone could not access to disaster management officers by official. Disaster management officers started to use official twitter account for disaster management (Ishikawa 2012).

3.2 Nachi-Katsuura town

At Nachi-Katsuura town, there is Nachi river at the northern part of there and there is Ohta river at the southern part of there. Disaster management officers thought Ohta river was not better situation. On 2nd September, there was no damage and some residents at mountainous area started to evacuate by themselves. On 3rd September, disaster management officers started to prepare evacuation centers. Disaster operation center opened at 18:00 on 3rd September.

At 22:40 on 3rd September, emergency discharge of Kodakumi dam (upstream of Ohta river) was transmitted to residents in the siren and public radio network. Kodakumi dam is managed by Nachi-Katsuura town. Disaster management officers got the dam information successively. The water level of Nachi river was increased at 1:00 on 4th September then disaster management officer issued evacuation directives at 1:45. At 4:00, entire area was flood.

Town officials dispatched to the evacuation center, and disaster management officers communicated to them by mobile phone but they could not communicate after 3:00 on 4th September. At “A” evacuation center (Figure 5) along Nachi river, evacuee decided to move to “B” evacuation center (upstream of Nachi river) (Figure 6) by themselves. After moving, “A” evacuation center was damaged by debris flow. We can see the damage at the wall of house from Figure 5.



Figure 5: “A” evacuation center (Nachi-Katsuura town)



Figure 6: “B” evacuation center (Nachi-Katsuura town)

3.3 Kozagawa town

The entire Kozagawa town area is the watershed of Koza river. At upstream of Koza river, there is the Shichikawa dam. Kozagawa town officer communicated to dam manager and knew the level of Koza river. Figure 7 shows the flow and storage of Shichikawa dam. It can be seen that the dam earned the time to evacuate.

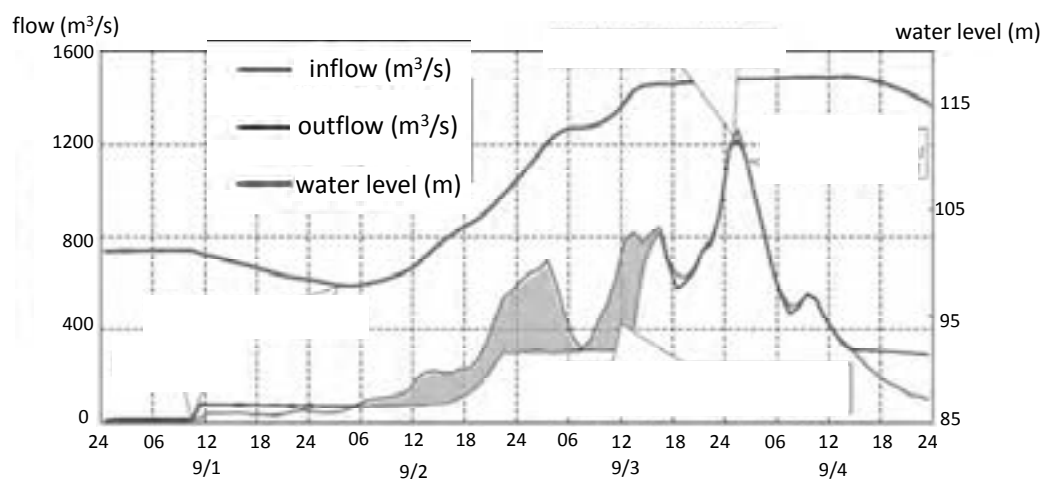


Figure 7: The flow and storage of Shichikawa dam

Kozagawa town officials did anything for evacuation. They did not fear to be a useless. After heavy rain warning issued, in the morning on 2nd September, officials started to prepare evacuation centers, and residents started to evacuate by themselves at 14:00 on 2nd September. At 22:00 on 2nd September, officials told to district leaders to prepare for evacuation instruction because of heavy rain. At 6:00 on 3rd September, some residents started to go back their home. Therefore,

officials continued to call them for evacuation and issued the information prepared evacuation.

In the evening on 3rd September, the outflow and the inflow of Shichikawa dam became equal. Before then, officials knew that situation. So officials issues evacuation instructions at 16:00 on 3rd September. The water level of Koza river rose and all plains along the river were flooded. At 0:00 on 4th September, evacuation directive was issued, but PR car could only go around government building. And government building was isolated because of flood.

From midnight on 2nd September, power outage lasted intermittently. At 2:00 on 4th September, phone was interrupted. Officials could not communicate to residents, but human casualties were kept to minimum because of early evacuation.

4. DISASTER INFORMATION TRANSMISSION SYSTEM

Figure 8 shows “flowchart of disaster information generating process” at investigation area on Typhoon Talas. Central government and prefectural government collectively issued warning and information according to the criteria based on observation information. JMA issued weather information. Local meteorological observatory and prefectural branch office issued flood forecast and landslide warning information. Flood forecast is intended for rivers that are specified in advance. At investigation area, only Koza river was specified. Municipalities got warning, forecast, observation information, dam information, and reports from the field. According to these information and warning, municipalities were issued evacuation instruction/directive. Residents decided their evacuation based on this evacuation instruction/directive. But some residents who had experience of inundation collected river information by themselves using internet. And municipality official urged residents to evacuate.

Figure 9 shows “flowchart of disaster information communication process” at investigation area on Typhoon Talas. Central government and prefectural government sent observation information, forecast and warning to residents using television, radio and internet. Municipalities got dam information and water level of rivers using mobile phone. Municipalities sent evacuation information to residents using public radio network and PR car. Some residents who had experience of inundation collected river information by themselves using internet. However, residents who lived at mountainous area could not get any information because most of all communication service was interrupted. Using PR car and dispatch of officials to evacuation center were difficult because of road traffic interruption. Municipalities could not send any information by official because of fixed-line phone and web server interruption. Some municipality urged residents to evacuate before flood in the daytime. Some evacuee in the other municipality area moved other evacuation center by themselves in the nighttime. Therefore, human casualties were minimized.

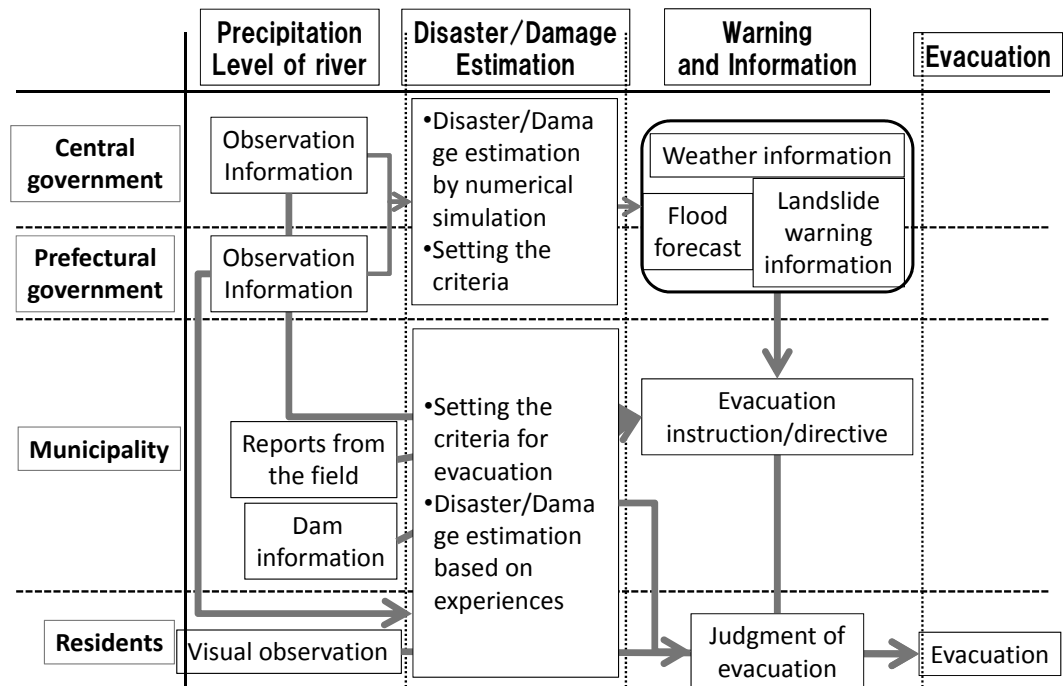


Figure 8: The flowchart of disaster information generating process

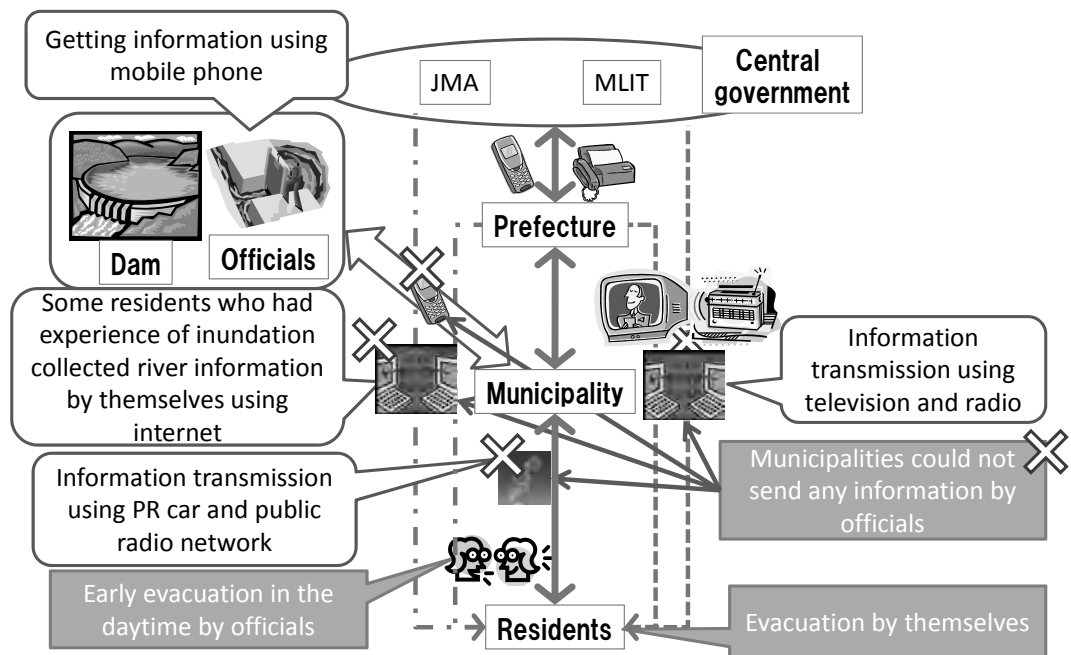


Figure 8: The flowchart of disaster information communication process

5. DISCUSSION

From the results of interview and two types of the flowchart, the following items were revealed. First, municipalities must make an effort to increase residents' understanding that facilities which aim to mitigate the effects of disasters have the ability to reduce the disaster impact. Second, it is necessary to secure the

multiplex communication network, such as telecommunications infrastructure and services (Social Network Service, among others). Third, municipalities need to carry out public relations so that people can decide whether to evacuate before dark without fear of time going to waste.

6. CONCLUSIONS

In this paper, the authors summarized the disaster management activities of three municipalities in the southern part of Wakayama Prefecture during and after Typhoon Talas through interviews with personnel. Their disaster management was organized from two perspectives: “flowchart of disaster information generating process” and “flowchart of disaster information communication process.” From the results of interview and two types of the flowchart, lessons of the design of flood and sediment disaster information dissemination systems in Asia have become clear.

REFERENCES

- Japan Meteorological Agency, 2011. *Typhoon Talas relevant information -Portal-*. http://www.jma.go.jp/jma/en/typhoon_Talas.html
- Fire and Disaster Management Agency, 2012. *Disaster management of fire fighting in 2011 Typhoon Talas. (Japanese)* <http://www.fdma.go.jp/bn/data/%E5%8F%B0%E9%A2%A8%E7%AC%AC12%E5%8F%B7%E3%81%AB%E3%82%88%E3%82%8B%E8%A2%AB%E5%AE%B3%E7%8A%B6%E6%B3%81%E3%81%AB%E3%81%A4%E3%81%84%E3%81%A6%EF%BC%88%E7%AC%AC18%E5%A0%B1%EF%BC%89.pdf>
- Ministry of Land, Infrastructure, Transport and Tourism, 2012. *Summary of Damage caused by 2011 Typhoon Talas, (Japanese)* <http://www.mlit.go.jp/common/000166361.pdf>

Study on implementation of remote building damage assessment system during large scale earthquake disasters

Makoto FUJIU¹, Miho OHARA² and Kimiro MEGURO³

¹ Ph.D. Candidate, Department of Interdisciplinary Information Studies,
The University of Tokyo, Japan
fujiiu@iis.u-tokyo.ac.jp

² Associate Professor, Interfaculty Initiative in Information Studies
/ Institute of Industrial Science,
The University of Tokyo, Japan

³ Professor, Interfaculty Initiative in Information Studies,
/ Institute of Industrial Science,
The University of Tokyo, Japan

ABSTRACT

Building damage assessment is necessary for governments to issue the Victim Certificates for residents who suffered from housing damages. The process of assessment needs accuracy, quickness, objectivity and fairness because the results of assessment are used as criteria for providing public monetary supports for rebuilding of their livelihood. In Japan, several big earthquakes are expected to occur in the near future. A lot of structural damages due to these earthquakes will cause enormous needs for building damage assessment. However, there is a limit action on the number of specialists with adequate assessment skills who can access the damaged area under bad traffic conditions. Delay in building damage assessment by local governments can disturb rapid reconstruction of the damaged area.

Considering these problems during large-scale earthquake disasters, authors proposed the new system for building damage assessment using photos of damaged houses taken by residents or volunteer fire corps in the damaged area. Specialists outside the damaged area confirm these photos on the website and assess their damage levels. All the data used for building damage assessment is managed with GIS database on a management server located outside the damaged area under cloud condition. This kind of digital management system can contribute to enhance the accuracy and efficiency of the procedures for issuing the Victim Certificates for residents.

In this paper, the remote system for specialists to assess the damage levels was developed as a web-based service for supporting building damage assessment. Furthermore, authors conducted operation tests with some local government staffs to evaluate the effectiveness of the developed systems. As a result of these operation tests, it became clear that the developed system could be used for the assessment of the damaged houses.

Keywords: earthquake disaster, building damage assessment, IT system

1. INTRODUCTION

In Japan, several big earthquakes are expected to occur in the near future. A lot of structural damages due to these earthquakes will cause enormous needs for building damage assessment. Building damage assessment is necessary for governments to issue the Victim Certificates for residents who suffered housing damages. However, the current number of human recourses who are trained with the procedures of building damage assessment is not enough. It is necessary to develop the new system which enables quick building damage assessment in case of the next large-scale earthquake disaster.

The guidelines of general procedures for inspecting building damage due to disasters were published by the Cabinet Office in 1968, 2001 and 2009. However, in the past disasters, various problems of building damage assessment have been pointed out such as inaccurate inspection, difficulty in quick inspection and lack of human recourses with sufficient skills of assessment.

In order to solve the past problems and achieve quick building damage assessment, authors proposed new remote system for building damage assessment using IT technologies. So far, a prototype system was developed. But, the functions of the system need to be verified through operation tests. In this paper, authors conducted operation tests with some local government staffs to evaluate the effectiveness of the developed systems.

2. CONCEPT OF NEW REMOTE SYSTEM FOR BUILDING DAMAGE ASSESSMENT

As a new system for achieving all the solutions for the problems reported at the past building damage assessments, we proposed a new remote system for supporting building damage assessments during large-scale earthquake disasters. The concept of the system is illustrated in figure 1.

The total system consists of two sub-systems. The first one is photo upload system in the damaged area. Photos of a damaged house are taken by residents or volunteer fire corps in the damaged area and those data is uploaded to the server. The second one is remote assessment system for specialists. Specialists located outside the damaged area confirm these photos through the website, and assess their damage levels.

All the data used for building damage assessment is managed with GIS database on the management server located outside the damaged area under cloud condition. This kind of digital management system can contribute to enhance the accuracy and efficiency of the procedures for issuing the Victim Certificates for residents.

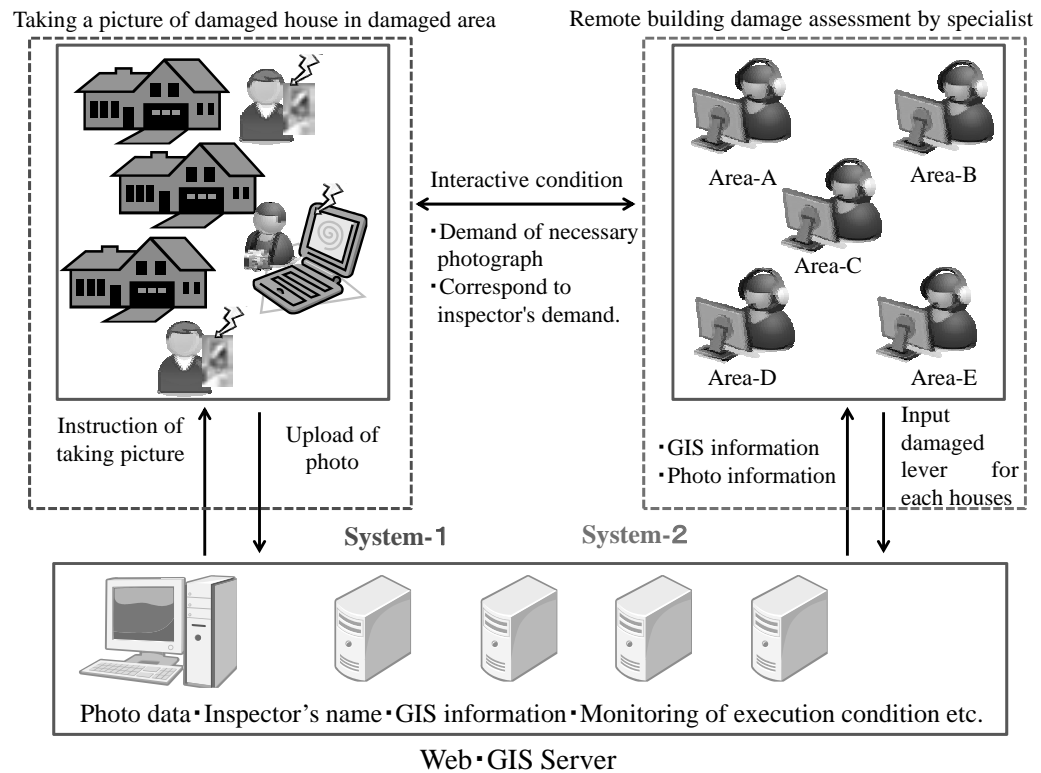


Figure 1: Concept of remote building damage assessment system

3. DEVELOPMENT OF REMOTE BUILDING DAMAGE ASSESSMENT SYSTEM

3.1 Development of photo upload system in damaged area

Photo upload system in the damaged area was developed as an application on smart phones used by residents or volunteer fire corps in damaged area. Prototype of this system was developed by Android as the mobile phone operating system which is installed in almost all the smart phones except iPhone.

Firstly, residents or volunteer fire corps as inspectors input the basic information such as GPS information, an address and an owner name. Secondly, they upload some photos such as an overview of the damaged house, incline of the damaged house and the damaged point of their roofs, walls and fundamentals. Finally, they confirm the input data and some photos.

Method of completing for photo upload in the damaged area using upload application is as follows. Inspectors take some damaged house photos which are full views of the damaged house (north side, east side, south side and west side) and closeup views of the damaged points. Inspectors should take pictures of the damaged house concerning three factors: externals, inclination and building element (roof, exterior wall and foundation). Furthermore, they have to relate closeup views of damaged points to full views using touch screen functions. These photos are uploaded to an exclusive server in cloud condition using upload application. The comments about damage levels and damage locations, etc can be added to the photo, if necessary. The prototype system of photo upload system

was developed based on the data of totally damaged houses due to the 2011 off the Pacific coast of Tohoku Earthquake in Japan.

3.2 Development of remote assessment system for specialists

Here, prototype of “remote assessment system for specialists” was developed as shown in figure 2. Specialists outside the damaged area confirm the photos uploaded on the website and assess their damage levels. All the data used for building damage assessment is managed with GIS database on the management server located outside the damaged area under cloud condition.

Flow of remote assessment system is as follows. Firstly, specialists who are registered architects and experienced workers outside the damaged area confirm the basic information such as shape of the damaged house, location and seismic level on the web system and overview all the photos of the damaged house. Secondary, they assess the damage level and area based on their inclines and the damaged points of roofs, walls and fundamentals. Finally, specialists confirm the input data. Then result of the first assessment is passed to the next specialist to carry out double check.

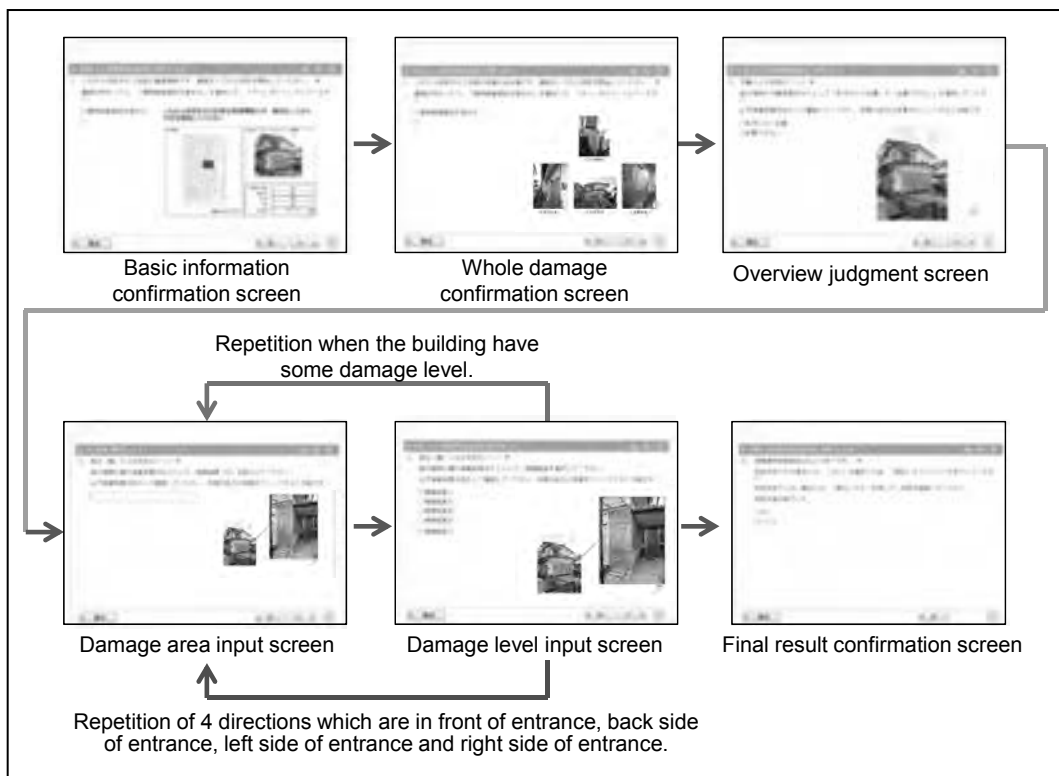


Figure 2: Remote building damage assessment system

Figure 2 shows the prototype system of primary inspection in case of a moderate damaged house as an example. Total damage level of a house is decided based on damage levels of three factors: externals, inclination and building element. The photos taken at the 2011 off the Pacific coast of Tohoku Earthquake were used for describing the damages.

Specialists can see close-up photos, if necessary. They evaluate the photos and select the damage levels and its area from pull down choices in each page. In addition, they can request additional photos for more accurate assessment to inspectors in the damaged area. In final page, they fill in the special or caution comments of the assessed house and pass the result to the next specialist. Assessment for one damaged house should be conducted by two or three specialists to double-check the result for achieving accurate, fair and objective assessment. When the assessment ends here, a Victim Certificates for the resident is issued from the local government.

4. EVALUATION OF EFFECTIVENESS OF REMOTE BUILDING DAMAGE ASSESSMENT SYSTEM

4.1 Condition of Operation tests

Authors conducted operation tests for twenty local government staffs who experienced building damage assessment due to the the 2011 off the Pacific coast of Tohoku Earthquake. They belonged to Yokohama city in Kanagawa Prefecture and Sendai city in Miyagi Prefecture as shown in figure 3. The staffs of Yokohama city were sent to Sendai city after the Earthquake for supporting building damage assessment.

The operation tests were held during April 26-27th, 2012 in Yokohama city, and on May 15th in Sendai city. The total time for one test was about two hours. At the beginning of the operation test, system of remote building damage assessment was briefly explained. After that, the operation test was done using the developed system. When the operation test finished, staffs answered the questionnaire survey regarding usability and feasibility of the developed system.

Table 1 shows the conditions of the operation tests. Seven scenarios including four damage patterns and two cases respectively (except major-moderate damage) were examined by the operation test. Tested damage patterns were major damage, major-moderate damage, moderate damage and minor damage. Two scenarios mean easy or difficult cases for assessing the damage levels. Figure 4 shows examples of damage photos used for moderate damaged houses in the system for the operation tests. These are photos of damages due to the 2011 off the Pacific coast of Tohoku Earthquake which are moderate damaged houses. Scenario 4 is for a moderate damaged house which is easy to assess for everyone, and scenario 5 is for a moderate damaged house which is difficult to assess even for an experienced person.



Figure 3: Operation test in Yokohama city

Table 2: Condition of operation test

Scenario	Damage Level	Test Conditions
1	Major damage	Easy to assess for all test persons
2	Major damage	Easy to assess for all test persons
3	Major-moderate damage	Difficult to assess for experienced person
4	Moderate damage	Easy to assess for all test persons
5	Moderate damage	Difficult to assess for experienced person
6	Minor damage	Easy to assess for all test persons
7	Minor damage	Difficult to assess for experienced person

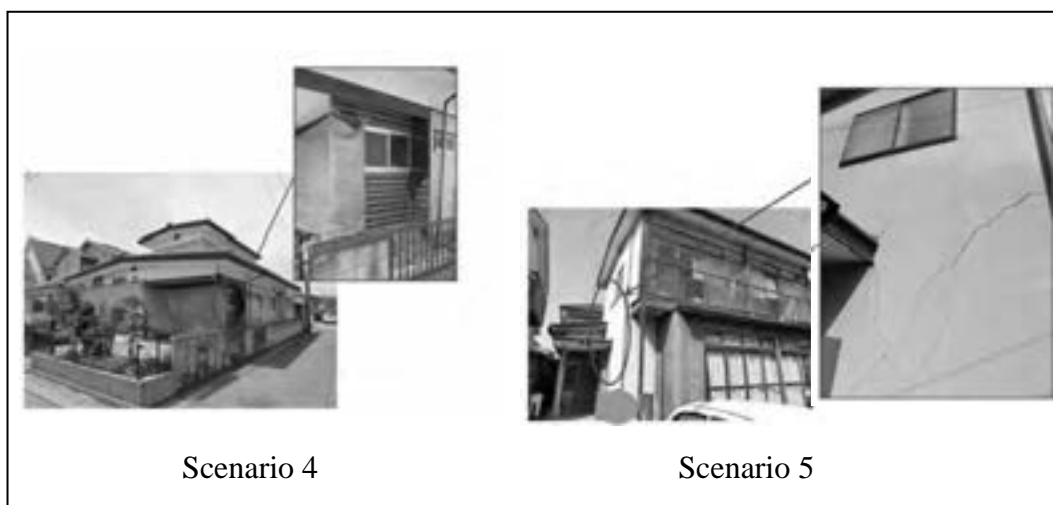


Figure 4: Example of damage photos for remote assessment system

4.2 Result of Operation test

Figure 5 shows the result of the assessment by participants. All the staffs could assess the correct damage level for scenario 1 and 2. On the other hand, scenario 3,4,5,6 and 7 were not assessed perfectly. The correct ratio for scenario 4 was higher than scenario 5. Scenario 4 was an easy case, and scenario 5 was a difficult case to assess even for an experienced person. As a result, the correct ratio of the difficult case was 20% lower than that of the easy case. Scenario 6 and 7 had the same result.

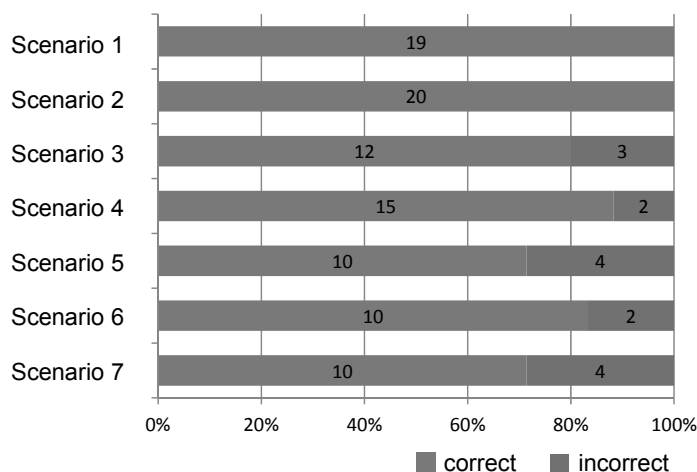


Figure 5: Result of assessment

Figure 6 shows the result of the judged damage level for scenario 7. Scenario 7 was a difficult case to assess even for an experienced person. The house of scenario 7 had three walls which located at the left or back side of entrance. The red circles in the figure 6 indicate correct judgment. As a result, about 70% of the participants could assess the correct damage level of the wall. However, about 30% of the participants could not assess the damage level correctly because they could not identify small cracks.

Figure 7 shows the result of the judged damage area for scenario 7. As a result, the wall 1 and wall 2 was assessed to be larger than the correct area, but the wall 3 was assessed to be smaller than the correct one. This was because participants could not identify small cracks and misjudged the damaged area. These results indicated that small cracks in the photos were difficult to be assessed on the remote assessment system. It is necessary to install the functions that support finding damages and deciding its damaged area such as showing damage examples, showing grid meshes, etc.

Figure 8 shows the result of the questionnaire survey that was conducted after the tests to understand usability and feasibility of the system. The participants answered that the proposed system was very useful because this had more advantages than the present procedures. Especially, participants highly evaluated on “reducing inspection time” and “Result of inspection is managed by digital data.”

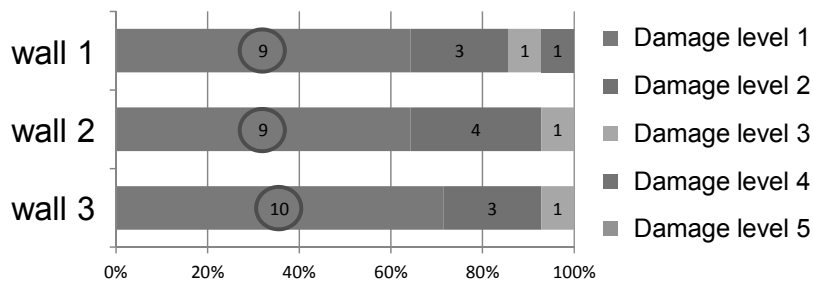


Figure 6: Result of assessment of damage level (wall inspection)

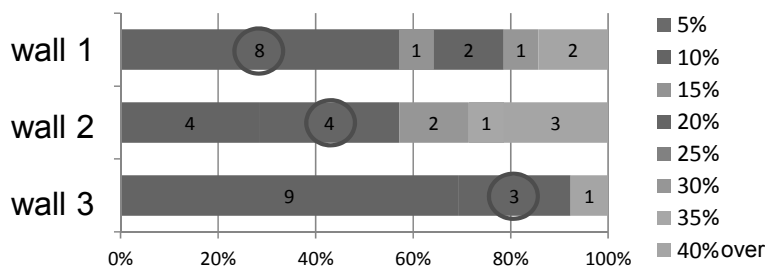


Figure 7: Result of assessment of damaged area (wall inspection)

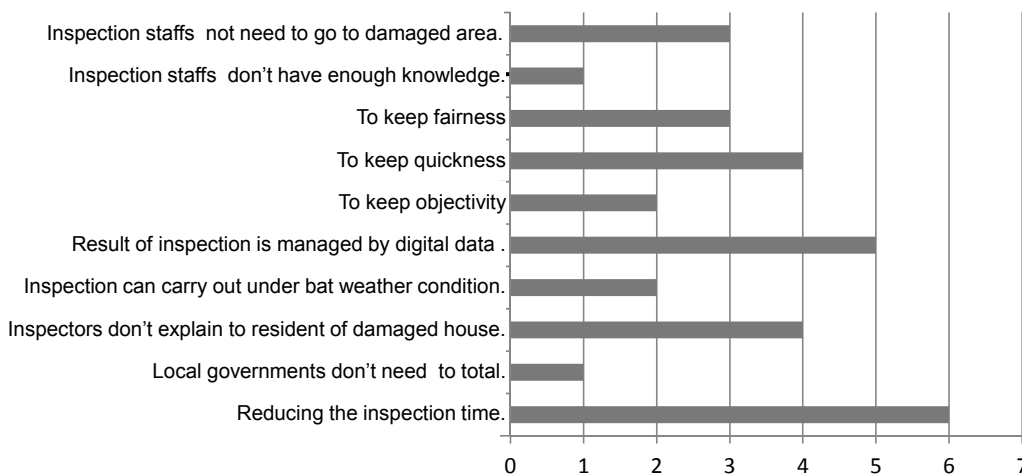


Figure 8: Result of questionnaire survey regarding usability and feasibility

5. Conclusions

In Japan, several big earthquakes are expected to occur in the near future. It is necessary to develop the new system which enables quick building damage assessment in case of the next large-scale earthquake disaster. In this paper, a new system for remote building damage assessment was developed and operation tests were conducted to verify its effectiveness.

The prototype system of remote building damage assessment system was developed using the photos of the damaged houses due to the 2011 off the Pacific coast of Tohoku Earthquake. The operation tests were conducted with local government staffs who experienced the building damage assessment at the Tohoku Earthquake. As a result, it became clear that the developed system could be used for the assessment of the damaged houses and the system had more advantages than the present procedures.

In the future, we plan to evaluate the effect of the proposed system in case of the Tokyo metropolitan Earthquake.

REFERENCES

- Murao, O., Yamazaki, F., 1999, Comparison of Building Damage Evaluation by Local Governments after the 1995 hyogoken-nanbu earthquake, *Journal of Architecture Planning and Environmental Engineering*, No.515, pp.187-194
- Shigekawa, K., Tanaka, S., Horie, K., Hayashi, H., 2005, *Some Regualational Issues on Building Damage Assessment –A Case Study of Niigata-ken Chuetsu Earthquake-*, *Journal of social Safety Science* No.7, pp.133-140
- Horie, K., Shigekawa, K., Maki, N., Tanaka, S., Hayashi, H., 2005, *Application of Damage Assessment Training (DATS) to Ojiya City following 2004 Niigata-ken Chuetsu Earthquake –Through a Disaster Response Support Activity for Issuing Victim Certificate-*, *Journal of social Safety Science* No.7, pp.123-132
- Yoshitomi, N., Hayashi, H., Urakawa, G., Shigekawa, K., Tanaka, S., Horie, K., Matsuoka, K., 2005, *The Development of a Damage Certificate Issuing Support System –A new disaster response database schema created for the Niigata Chuetsu Earthquake-*, *Journal of social Safety Science* No.7, pp.141-150
- Tanaka, S., 2008, *A Study on the Building Damage Assessment Processes for the 2007 Niigata Chuetsu Oki Earthquake Disaster : Kashiwazaki Case Study*, *Proceedings of social Safety Science* No.22, pp.35-38
- Fujiu, M., Ohara, M., Meguro, K., 2011, *Development of remote system for supporting building damage assessment during large-scale earthquake disaster*, *Proceedings of the Eighth International Symposium on New Technologies for Urban Safety of Mega Cities in Asia*, Chiang Mai, Thailand, CD-ROM
- Fujiu, M., Ohara, M., Meguro, K., 2012, *Development of remote building damage assessment system during large-scale earthquake disaster*, *Proceedings of the 15th World Conference on Earthquake Engineering*, CD-ROM, Lisbon, Portugal

News coverage concentration on specific municipalities: Analysis of TV report contents at 2011 Tohoku Earthquake

Muneyoshi NUMADA¹ and Kimiro MEGURO²

¹ Research Associate, ICUS, IIS, The University of Tokyo, Japan
numa@iis.u-tokyo.ac.jp

² Professor, ICUS, IIS, The University of Tokyo, Japan

ABSTRACT

Following the 2011 Tohoku Earthquake in Japan, we have noticed that TV coverage highly emphasized certain municipalities, repeatedly reporting its damage and disaster response activities. Nuclear power plant accident was also extensively highlighted. The news coverage focusing on specific regions induced aid and support – e.g. distribution of relief supplies and donations -- to certain areas only. This problem of unbalanced press coverage has also been witnessed in the past disasters -- Hokkaido Nansei Oki Earthquake in 1993, Hokkaido Toho oki Earthquake in 1994, and the Southern Hyogo prefecture earthquake in 1995. While the same issue arose again in the 2011 Tohoku Earthquake, lopsided media coverage again failed to offer disaster overview or enhance understanding the total damage, both of which are crucial in times of such massive earthquake. We believe that TV media bears heavy responsibility and should therefore play the leading role in providing information that helps people to make appropriate decisions and judgments.

The purpose of this research is to conduct a quantitative analysis of the municipalities that were repeatedly featured in TV news reports. Media coverage rate by municipalities was analyzed to find out the relationship between media coverage amount and damage level.

The result showed that even if the damage levels were equal, the amount of TV news coverage among the municipalities differed -- a common and distinctive feature among all TV stations. One of the reasons can be explained by the fact that TV crew was unable to reach certain cities and towns due to damaged roads and traffic. However, another reason and perhaps the essential problem lie in the longtime tendency of Japanese TV stations: to follow and conform to successful reports which has given impact and sensation. The unbalance occurs because each TV station is driven by the fear of missing out on a scoop. The results of this study, based on quantitative analysis, are an indication of these alarming phenomena.

Keywords: TV news coverage, TV media, disaster information, Tohoku earthquake

1. INTRODUCTION

1.1 Overview of the 2011 Tohoku Earthquake

At 14:46 JST (5:46 UTC) on March 11th, 2011, an earthquake of a moment magnitude 9.0, the largest earthquake ever recorded in Japan, struck off the shore of the Sanriku area in the Tohoku Region. The “*mega tsunami*” followed, deeply hitting indented coastal areas and bringing enormous and devastating damage to many cities and villages in the area. Damage by the “*mega tsunami*” was not only limited to buildings, but the resulting fires destroyed many communities, taking lives of thousands. Moreover, nuclear power plant (NPP) facilities suffered complicated and serious damage. This earthquake was later officially named “*The 2011 off the Pacific coast of Tohoku Earthquake*” by the Japan Meteorological Agency (JMA).

1.2 Importance of TV programs

In this earthquake, people faced difficulty in grasping the full scope of the disaster since the damage was extremely widespread and diverse. To obtain information on damage conditions, safety confirmation, news and announcements from municipalities, all kinds of media were used. In addition to the conventional television, radio and the Internet, new types of information-sharing tools such as Twitter and Facebook were utilized. The Internet TV news sites, such as USTREAM and NICO-NICO DOUGA, were also capable of broadcasting NHK (Japan Broadcasting Corporation) programs and commercial TV stations at no charge. Furthermore, people could watch TV programs in the open air by receiving one-segment broadcasting services.

According to a survey (*Nomura Research Institute, Ltd. 2011*) on “*trends in media contact associated with the 2011 off the Pacific coast of Tohoku earthquake*”, TV was ranked no.1 and no.2 as the important information source. On acquiring earthquake information, about 80.5% considered “*NHK TV*” and 56.9% considered “*commercial TV stations*” as important. “*Newspaper*” and “*Internet*” both ranked below TV.

Likewise, another survey (*My Voice Communications, Inc. 2011*) shows “*how people gathered information on the 2011 Tohoku earthquake*”. Here again, TV was ranked top at 93.5%, followed by newspapers at 44.9%, Internet news sites at 44.8%, Internet portal sites (e.g. Yahoo) at 42.8% and radio at 31.1%. These results evidently show that the majority relied on TV as the main tool to get information.

According to *the Article 108 of the Broadcasting Act and Disaster Countermeasure Basic Act* (Tanaka 2008), broadcasting organizations are obliged to provide useful services in order to prevent and minimizing disasters. Also, the Ministry of Internal Affairs and Communications has requested NHK and the National Association of Commercial Broadcasters in Japan to provide accurate and detailed information to the public as quickly as possible (Ministry of Internal Affairs and Communications 2011).

Considering the above, we can say that the expected role of TV news is not just reports on damages but also to provide useful information that prevent further damage. TV news is indeed counted on as one of the “disaster prevention

organizations” – to make appropriate contributions in disaster management.

1.3 Problems of TV programs

Immediately after the 2011 Tohoku Earthquake, certain affected areas, where TV reporters could easily reach, were repeatedly exposed from an early stage, leaving strong impact on the viewers. Obviously, specific municipalities were intensively covered by TV news than others. High emphasis was also placed on the nuclear power plant accident. We can say that the news coverage was pretty much unbalanced, especially when considering the vast extent of the affected areas. This unfairness eventually led to the uneven allocation of aid activities, with distribution of relief supplies and donations concentrated to limited municipalities while other areas were left neglected.

Although this problem of media coverage concentration has been repeatedly pointed out in the past earthquakes (Nakamori 1995) such as Hokkaido Nansei Oki Earthquake in 1993, Hokkaido Toho oki Earthquake in 1994, and the Southern Hyogo prefecture earthquake in 1995, the same issue arose again in the 2011 Tohoku Earthquake (Nakamori 2011). Unbalanced media coverage on certain topics and areas does not offer the audience comprehensive views or understanding of total damage, both of which are crucial especially at the time of such massive disaster. TV media is heavily responsible for providing information to the public so that they can make correct decisions and take appropriate actions.

Previous studies on TV news coverage and contents after the Tohoku earthquake include: chronological analysis of TV news contents (NHK 2011), verification of early media coverage, confused and disordered reports of the nuclear power plant accident, and analysis of foreign media reports (General incorporated association of Tokyo-sya 2011). But never before had there been any quantitative analysis of TV news coverage unbalance conducted.

1.4 Purpose of this research

The purpose of this study is to conduct a quantitative verification of the unbalance in media coverage by municipalities during the emergency period after the Tohoku earthquake. The correlation between media coverage and damage level during the first ten days after the disaster was analyzed.

2. TV news data

In this study, we selected six major TV stations, namely NHK, NTV, TBS, Fuji TV, TV Asahi, and TV Tokyo. TV content analysis generally requires text data from each program section. Especially for this study, we adopted a database called "*Document-Analyser*" by JCC Corporation, which allowed us to obtain text data of all six TV stations for 365 days a year, 24 hours a day and by the unit of seconds. The database enabled us to comprehend the full details of when, what, where, and how each TV stations reported. Table 1 shows an example of the text data of NHK on March 12th.

The target period of this research covers the ten days from March 11th to 20th, considering the importance of TV news reports at an early stage immediately after

the disaster. We paid attention to how the damage situation became apparent along with how much influence the news reports gave on supply of relief goods.

Table 1: Example of the text data of the TV program (259 characters)

In Miyagi Prefecture, by the earthquake, 53 people were killed. The details is 17 people in the Higashimatsushima city, 12 people in the Kesennuma city, 8 people in the Shichigahama town and 5 people in the Sendai city. In the coastal town of Minamisanriku where was attacked by the tsunami, many buildings and houses were washed away by the tsunami except the hospital building constructed by concrete, and many people were missing. In the area along with the port of Kesennuma in Kesennuma city, the large-scale fire occurred caused by the outflowing oil from the tank at the port. The video of Kesennuma city. (March 12, NHK)

3. Concentration of TV PROGRAMS

Contents of news programs broadcasted by each TV station were more or less similar; no big difference or distinctive feature was observed from the reports produced during the ten days after the disaster.

3.1 Index “C” Definition: Concentration-ratio of municipality news coverage

This chapter analyses by text data the way each TV station focused its reports on specific municipalities. “Concentration-Ratio of the News Coverage on Municipality” is defined as Index “C”. The “C” is indicated by the ratio of "the total number of all municipalities each TV station has picked up" and "the number of each municipality each TV station has picked up." Here, the definition of "pick up" implies the appearance of municipality name in text data as underlined in Table 1. For example, Higashimatsushima City marked “1”, Kesennuma City “4”, Shichigahama Town “1”, Sendai City “1”, and Minami-Sanriku Town “1” respectively in the text given in Table 1.

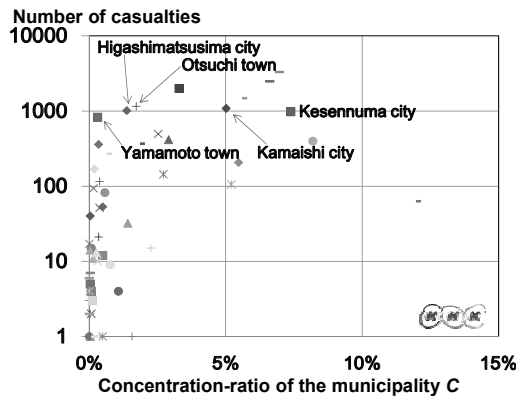
If the Index C scores high, it indicates that the TV station has made intensive reports focusing on a particular municipality. If the Index C is low, it suggests that no specific municipality has received unusual attention. If the Index C is zero, then municipalities got no coverage at all.

3.2 Correlation between “C” value and damage level

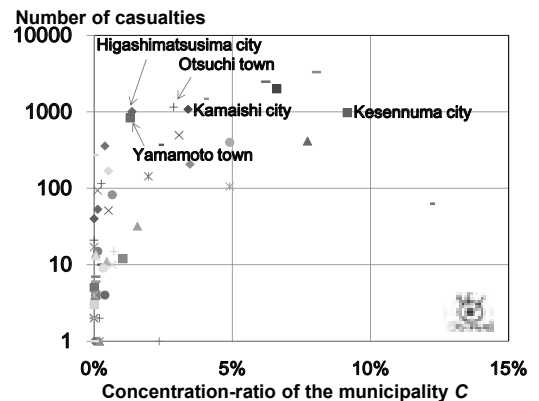
In this section, we discuss the relationship between the “C” value and damage

level. Although previous studies have conducted a quantitative analysis of correlation between newspaper coverage and damage level (Matsumura 1998), the relationship between the TV report coverage and damage level has not yet been studied.

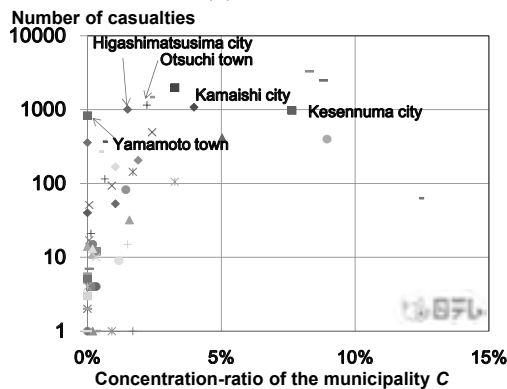
The definition of "earthquake coverage rate" is indicated by the ratio of quake-related reports in all newspaper articles excluding advertisements. The result suggests a high correlation between "earthquake coverage rate" and the number of casualties, but not much correlation with the number of totally collapsed buildings.



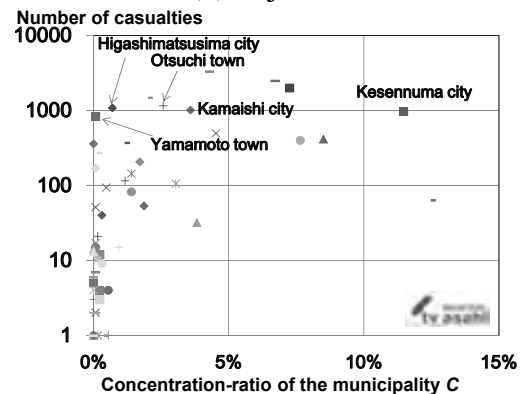
(a) NHK



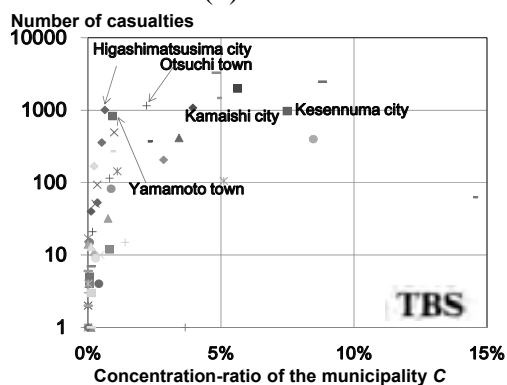
(d) Fuji-TV



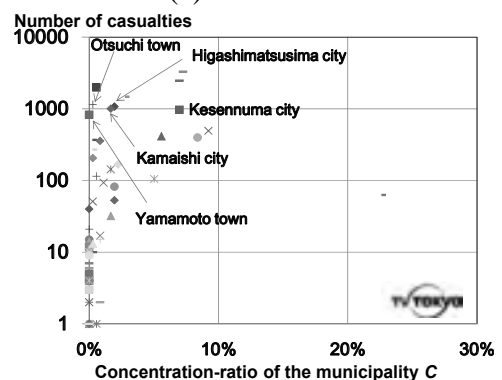
(b) NTV



(e) TV-Asahi



(c) TBS



(f) TV-Tokyo

Figure 1: Relationship between the number of casualties and the concentration-ratio of the municipality

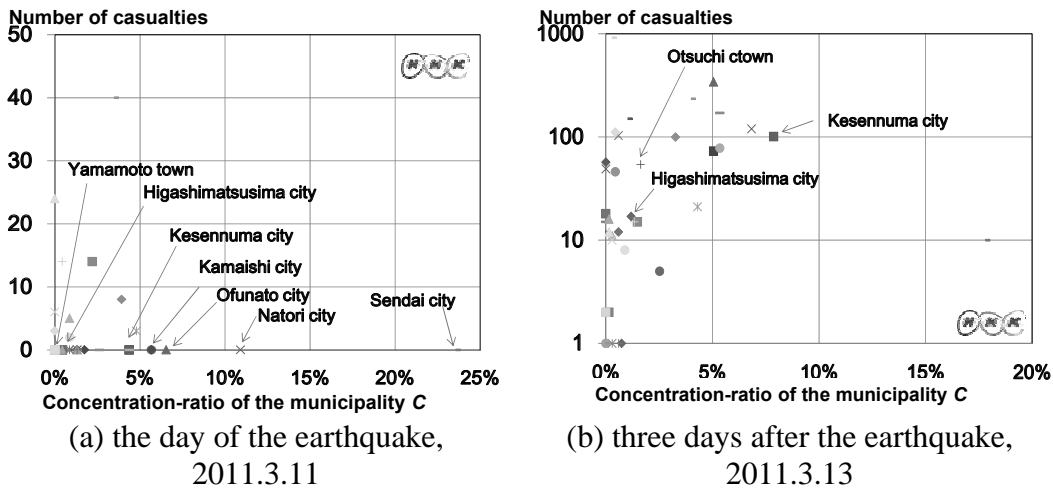


Figure 2: Relationship between the number of casualties and the concentration-ratio of the municipality of NHK

Using the above result as reference, this paper analyses the relationship between casualties and the Index C of TV news coverage. The number of total casualties used here represents the sum of the missing and the dead.

Figure 1 shows the relationship between casualties and the Index C on March 11th. In calculating the Index C here, the total number of news coverage on municipalities from March 11th to 20th is used, and the number of casualties referred to those confirmed by March 20th.

Focusing on the municipalities with over 1,000 casualties, NHK showed the highest Index C score for Kesennuma City, followed by Kamaishi City, Otuchi Town, Higashimatsushim City and Yamamoto Town. This result shows that even though the number of casualties is similar, significant difference is seen in the amount of TV news coverage on municipalities.

Similarly, when looking at Nihon-TV's reports on municipalities with over 1000 casualties, the Index C of Kesennuma shows high value, while Yamamoto and Higashimatsushima show relatively low value. The same tendency is observed in other TV stations. This tendency can also be observed from the chronological analysis as given in Table 2 (a) and (b). On March 14th, in Higashimatsushima City, 152 dead and 400 missing people were found, likewise on March 15th in Yamamoto, 111 dead and 638 missing people were found. Despite these findings of high number of casualties, no obvious reaction was observed in the Index C.

Figure 2 shows the relationship between casualties and the Index C of NHK on the day the earthquake hit, the third and the tenth day after disaster. The C is calculated by the number of coverage on March 11th, the day of the earthquake, the sum of the coverage of the third and the tenth days respectively. The number of casualties used is the sum of dead and missing people on the day of the earthquake, by the third and tenth days since March 11th respectively.

The Index C of the Sendai and Natori cities on the day of the earthquake is high, subsequently followed by Ofunato City, Kamaishi City, Kesennuma City, Higashimatsushima City and Yamamoto Town. At this stage, Otsuchi Town is not covered as seen in Figure 2 (a). Now, we will discuss by comparing two municipalities of Kesennuma City and Otsuchi Town.

On the third day (Figure 2 (b)), both Kesennuma and Otsuchi showed increase in the number of casualties. Nevertheless, the Index C of Kesennuma rose while that of Otsuchi remained unchanged. By the tenth day, the number of casualties of both reached almost the same level, yet a large gap in Index C is observed. These results have proved quantitatively that difference exists in Index C, despite the fact that the casualty level is the same. Therefore, the figures indicate that the news report coverage is unbalanced, and this tendency is common among all TV stations. Of course, one of the reasons may be explained by the accessibility to certain municipalities due to road conditions. However, another reason may be that TV stations tend to conform with reports by major successful TV stations which have managed to deliver news with strong impact because they are driven by the fear of missing out on a scoop. The results of this study, based on quantitative analysis, are an indication of these alarming phenomena.

4. CONCLUSIONS

The concentrated news coverage induced the unfair allocation of relief supplies and donations to some specific areas. This problem has repeatedly happened in the past disasters. This research has proved quantitatively that difference exists in Index C, regardless whether the casualty level is the same or not. This fact has shown the fact that news report coverage is unbalanced among all TV stations. One of the reasons may be the accessibility to certain municipalities due to the road conditions. However, another reason may be that the TV stations have the tendency to conform with reports by major successful TV stations which managed to deliver news with strong impact, and they are driven by the fear of missing out on a scoop. The results of this study, based on quantitative analysis, are an indication of these alarming phenomena.

Led by these results, we propose the following strategy to improve the standard of fairness in TV news reporting ahead of the next disaster. Considering the limited time and human resources at TV stations, we strongly advise them to: (1) grasp the overall damage conditions and perspective accurately, (2) provide information that corresponds to the direct needs of the audience, and (3) promote cooperation among TV stations, pay respect to press freedom, avoid unbalanced news coverage focusing on specific municipalities only, and lastly, improve access to obtain necessary information.

With regards to the role of the press, TV stations are expected to provide useful information, thereby contributing to appropriate disaster response, both from inside and outside the disaster-affected areas (Cabinet Office of Japan 2008). The above-mentioned strategy will serve as the guideline for improvement in this aspect.

In the next phase of this study, we will develop similar analysis using the amount of reporting time, then verifying the difference from text data. Moreover, we will carry out further study to find out what kinds of subject matters were reported intensively.

AKCNOWLEDGEMENT

This research has been supported by Mr. Takatoshi Ishii of JCC Corporation.

REFERENCE

- General incorporated association of Tokyo-sya (2011). Journalism of unprecedented disaster and tribulation, Journal of general journalism research, No.217, pp.9-18, 26-51
- Japan Cabinet Office of Japan (2008). Basic Disaster Management Plan, pp.48-49.
- Kazuo Matsumura (1998). Reaction of society against the earthquake disaster reported by the newspaper, Journal of Architectural Institute of Japan. 511, pp.61-67.
- Ministry of Internal Affairs and Communications (2011). The request for Japan Broadcasting Corporation and National Association of Commercial Broadcasters in Japan about the information providing of the 2011 Off the Pacific Coast of Tohoku Earthquake, http://www.soumu.go.jp/menu_news/s-news/01ryutsu07_01000018.html. [Accessed at 2011.4.1]
- My Voice Communications, Inc. (2011). Questionnaire survey on "How to gather information about the 2011 Off the Pacific Coast of Tohoku Earthquake ", <http://www.myvoice.co.jp/biz/surveys/15417/index.html>. [Accessed at 2011.5.30]
- Nakamori H., (1995). Problems about initial and regional-detail information focused on the city of Hanshin region, Journal of the Institute of Social Safety Science (5), pp.21-28.
- Nakamori H., (2011). Problems of news and mass media in the 2011 Off the Pacific Coast of Tohoku Earthquake. Journal of Urban problems, Vol.102, pp.4-9.
- NHK (2011). What kinds of contents did TV stations provide in the 2011 Off the Pacific Coast of Tohoku Earthquake, NHK broadcasting studies, Vol. 61, No.5, pp.2-7.
- NHK (2011). What kinds of contents did TV stations provide in the 2011 Off the Pacific Coast of Tohoku Earthquake (2), NHK broadcasting studies, Vol. 61, No.6, pp.2-9.
- Nomura Research Institute, Ltd. (2011). Research on trends in media contact associated with the earthquake, <http://www.nri.co.jp/news/2011/110329.html>. [Accessed at 2011.3.29.]
- Tanaka H., and Yoshii A., (2008). Introduction to Disaster Information Theory, Koubundou, pp.164-165, 218-227.

Reconstruction of Kamaishi City after the 2011 Tohoku Earthquake and Tsunami

Maria Bernadet Karina DEWI¹, Sae SHIKITA², Takaaki KATO³

¹ Graduate Student, ICUS, IIS, The University of Tokyo, Japan
dewi@iis.u-tokyo.ac.jp

² Undergraduate Student, ICUS, IIS, The University of Tokyo, Japan
sae.shikita@gmail.com

³ Associate Professor, ICUS, IIS, The University of Tokyo, Japan
kato-t@iis.u-tokyo.ac.jp

ABSTRACT

Hakozaki Peninsula, Kamaishi city, consists of eight villages, located alongside the coastal area of Iwate Prefecture. During the 2011 Tohoku earthquake and tsunami, the casualties were 1,061 dead and missing, 2,954 completely destroyed houses, and 687 partially destroyed houses. Currently, the population lives in temporary houses in scattered locations. As other cities in the Tohoku affected area, this city faces the very significant problem of a declining society, as well as other problems.

Kamaishi city's population data and economic and governance systems are resources that should be considered with regard to reconstruction. Since the 2011 Tohoku earthquake the process of reconstruction with the involved stakeholders—the national government, municipalities, communities, NPOs, and others has been ongoing. This paper analyzes the current situation of the recovery, community activities for reconstruction, and relation between these activities, then finding problem between the process and involved stakeholders.

Keywords: reconstruction, Kamaishi city, Hakozaki Peninsula, community participation, problems, solution.

1. BACKGROUND – KAMAISHI CITY BEFORE THE DISASTER

Kamaishi city is located in the southeastern part of Iwate Prefecture, along the coastal line towards the Pacific Ocean, with total area of 441.43 square kilometers. Kamaishi city was well known for its fishery and iron industry. In 1857, Nambu Domain constructed the Ohashi blast furnace at Kamaishi as the first western-style blast furnace in Japan. In 1934, the Meiji Government established Nippon Steel, the city's population at that time reached 40,388. At the same time, roads and railways were developed, and the role of Kamaishi Port became significant.

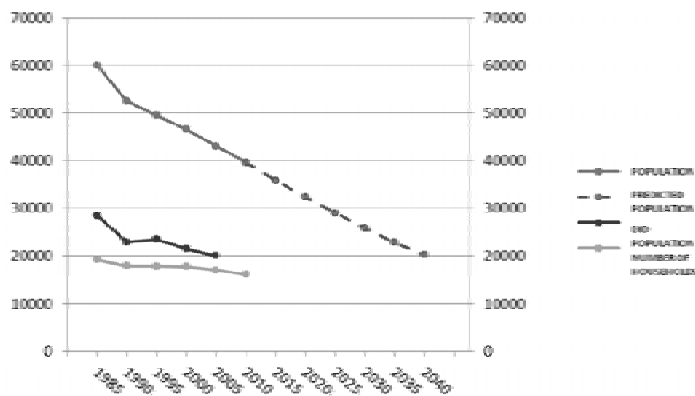


Figure 1: Changes in population and the number of households in Kamaishi (Source: National Census)

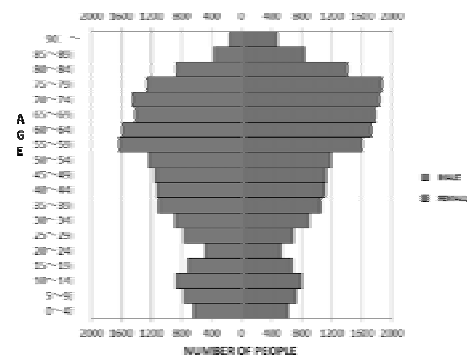


Figure 2: Population pyramid of Kamaishi City in 2010 (Source: National Census)

Figure 1 shows the population trend in Kamaishi City, the densely inhabited district (DID) population, and the number of households, with the data obtained from the National Census. The population is estimated from 2010 until 2040. From this graph, it can be assumed that population will greatly reduce in the future. The decrease can be seen in the general population, as well as in the urbanized area. On the other hand, the declining household rate is smaller compared to rate of population decline. Figure 2 explains how the population has been subject to a declining birth rate with the majority of the population between age of 55 and 79.

The situation of industry in Kamaishi City in 2007 was decreasing, with primary industry becoming 3.8%, secondary industry 33.3%, and tertiary industry 67.6%. The number of employees had been declining about 30% from 1990 until 2010. In particular, the decline of the primary industry was significant, having halved in 20 years. Agriculture has decreased about 65% among others. Though the number of fish caught has not decreased much, the revenue of the fishery industry has been declining, especially from 2000 until 2009.

2. CASUALTIES AND DAMAGE CAUSED BY THE GREAT EAST JAPAN EARTHQUAKE AND TSUNAMI

Kamaishi City suffered great tsunamis in 1896, 1933, 1960 and most recently in 2011. With the highest tsunami wave reaching 10.1 m at Kamaishi harbor during the Great East Japan Earthquake and Tsunami on March 11, 2011, Kamaishi City suffered 885 fatalities, with 176 missing, 9,883 evacuees to other areas, and 633 evacuees inside the city (Kamaishi, 2011). The number of dead and missing in Kamaishi City was the third largest in Iwate Prefecture, after Rikuzentakata and Otsuchi Town. The number of totally collapsed buildings is 2,954, with 396 highly destroyed, 291 partially destroyed, and 907 damaged.

3. CURRENT SITUATION

Refugee location was completed by October 8th, 2011, and temporary housing was completed by August 5, 2011 with 3,164 relocated to 50 sites. An estimated 50% of debris from the total amount of 762,000 tons was removed by April 2012 with a process of 3% (23,000t). Currently, the population is living in temporary housing in scattered locations.

4. RECONSTRUCTION

4.1. AUTHORIZED RECONSTRUCTION PLAN BY THE GOVERNMENT

In September 2011, the Basic Policy for Reconstruction was enacted, which initially consisted of a policy and Reconstruction Plan timetable. Then in December 2011, the Basic Reconstruction Plan (Figure 3) was enacted. However, the detailed landscape plan and land use will be decided after consultation with communities (Figure 4).



Figure 3: The ideal image of the city as per the Basic Reconstruction Plan
(Source: Kamaishi, 2011)



Figure 4: Draft of land use plan for the central area
(Source: Kamaishi, 2012)

4.2. COMMUNITY PARTICIPATION

Sets of interviews were conducted regarding the settlement of Ryoishi and Shirahama by the Crisis & Environmental Management Policy Institute (CeMI) and Kato Takaaki Laboratory of ICUS, the University of Tokyo in order to understand the conditions and expectations of the communities in terms of the reconstruction process. The interviews were conducted with people who had moved to temporary housing, in the reconstruction target area, especially those who left the town right after the earthquake. To reverse the stem the decline is as important as ensuring citizens to live in it. The basic reconstruction of Kamaishi City was organized and meets the needs of stakeholders. However it was not sufficiently transparent in assuring the opinion of representative organizations and

citizens, regarding the details of the residential area plan and disaster prevention measures. Therefore, it should be a matter of policy that residents' awareness plays a role in achieving stakeholders satisfaction.

Community participation across Hakozaki Peninsula is becoming more effective, and the community bond between districts is becoming stronger. This movement began in June 2011 with the combined involvement of four villages, mainly held by fishermen in Ryoishi Village with support from Non-Profit Organization (NPO) CeMI. Community members and NPOs had been working together for the reconstruction process, including discussing the reconstruction plan. Then in October 2011, events were held mainly by residence of Katagishi Village to raise awareness and encourage residents' participation. In March 2012, a new NPO was established, named O-Hakozaki Shimin Kaigi (Community Association of Hakozaki Peninsula) consisting of community members and professionals. The involved community is located across the following villages: Ryouishi, Kuwanohama, Kariyado, Shirahama, Hakozaki, Nebama, Katagishi, and Murohama.

Starting in August 2012, O-Hakozaki Shimin Kaigi's activities are conducted via four working groups. Working Group 1 manages community recovery for the future, including physical, social, and human factors; Working Group 2 addresses economic issues, creating job opportunities and new industries related to fishery; Working Group 3 focuses on human capacity building such as disaster mitigation and response; and Working Group 4 focuses on economic development, based on the resources of this area, and product marketing and value addition.

5. DISCUSSION

Challenges and problems

During the reconstruction process, there have been several challenges for all stakeholders. One positive note is that the community has been quite adaptable to the scattered location of temporary housing and has formed a new community in their new location.

Top-down planning strategies have been applied in this area from the very beginning. Citizens trust the government to develop and implement the reconstruction plan. However, differentiation in the reconstruction division has posed a challenge, since there is no sufficient cohesion between all of the divisions. For example, reconstruction is mainly focused on the physical aspects with some considering the other aspects such as social and economic. However, such interlinked functioning is needed to have a comprehensive approach to the reconstruction process, and to bridge the involved stakeholders. Possible solutions are achievable through citizen participation.

The second challenge is that there has not been much chance for the community to participate and share their aspirations. The reconstruction plan management planned to have consensus building with community, and a public hearing for the

plan was held. The other difficulty is the community has a short-term view regarding their economic, social, and built-environment situation, while the local government has a long-term view. In the area, fishermen and fisheries dominate with local fishermen participating in a cooperative union aimed for their working purpose. The profile of community in the area is fishermen and fisheries industry, with their fishermen cooperative union which aimed for their working purpose.

Japan, now a developed , needs to adopt a different approach for reconstruction than those that were implemented after prior disasters during the developing period. The next challenge is overcoming the issue of the ageing population of Kamaishi City, as well as the deteriorating economic condition. The majority of community leaders and most of the people are aged 70 years old. However, a young generation does exist in Shirahama to support the reconstruction process. In addition, the community members who are elderly tend to stay in their previous place and/or city, and do not want to move to other cities. The interviews result that the community has a strong attachment to the area. The future of the cities lies in ensuring that safety and sustainability issues are addressed in comprehensive ways; how to attract the people to stay in this area also needs to be taken into account. Considering the formation of a compact, smaller town, is also important to maintain the population and sustainability in the future.

6. CONCLUSION

Currently Kamaishi City and the other affected area in Japan are in the early phase of reconstruction. Considering the past of Kamaishi City, and the present situation of the ageing society, Kamaishi City has several challenges to face during the reconstruction process, especially related to the developed state of Japan and the currently applied planning system, as well as in the character of the community to adapt to the new situation.

Further study is necessary to analyze the challenge of the reconstruction process, including finding influencing factors, considering the needs of citizens, and ensuring citizen involvement, and consensus between all stakeholders. Then, analysis can be aimed to find possible suggestions to achieve a comprehensive reconstruction process.

REFERENCES

- Kamaishi City. 2011. *Reconstruction Plan Kamaishi. Basic Town Plan*. Iwate Prefecture, Japan: Kamaishi City. Data obtained on December 22nd, 2011.
- Kamaishi City. <http://www.city.kamaishi.iwate.jp/index.cfm/8,0,76,425,html>
- Iwate Prefecture. 2012. *Iwate Prefecture NPO activities*.
[http://www.pref.iwate.jp/~hp0301/npo-info/ninsho/sinsei-ninshodantaiichiran/ichiran-10\(451-500\).htm](http://www.pref.iwate.jp/~hp0301/npo-info/ninsho/sinsei-ninshodantaiichiran/ichiran-10(451-500).htm). Data obtained on June 2012.
- Website of Reconstruction from the Central Government
<http://reconstruction.go.jp>. Data obtained on June 2012.
- Japan Non-Profit Organization . 2012.
nonprofitjapan.home.jgc.org/npo/mpojp.html. Data obtained on June 2012.

Analysis of disaster information gathering behavior and language ability after the 2011 Tohoku Earthquake

Akiyuki KAWASAKI¹, Michael HENRY², and Kimiro MEGURO³

¹Project associate professor, International Center for Urban Safety Engineering,
Institute of Industrial Science, the University of Tokyo, Japan
akiyuki@iis.u-tokyo.ac.jp

²Assistant professor, Division of Field Engineering for the Environment,
Faculty of Engineering, Hokkaido University, Japan

³Professor and Director, International Center for Urban Safety Engineering,
Institute of Industrial Science, the University of Tokyo, Japan

ABSTRACT

After the March 11 Tohoku Earthquake, people living in Japan were faced with confusing and conflicting messages from differing information sources which created an atmosphere of uncertainty and led many people, particularly foreigners, to relocate to western Japan or leave the country entirely. In order to improve the dissemination of information after future disasters, a survey was conducted to understand how people in the Kanto region – the most populous area of Japan and border the Tohoku region – received their disaster information, what difficulties they encountered related to disaster information and how these may have affected their post-disaster decisions. This paper presents analyses and discussions on the relationship between language ability and disaster information gathering behavior, information difficulties, and demographic characteristics.

Keywords: 2011 Tohoku Earthquake, disaster information, language ability

1. INTRODUCTION

At 14:46 on March 11th, 2011, a magnitude of 9.0 earthquake with a hypocenter in the Pacific Ocean off the Sanriku area of Tohoku struck, causing enormous damage mainly in the eastern area of Japan. This earthquake (which shall be referred to as the “Tohoku Earthquake”) was not only the largest earthquake recorded in Japan and resulted in a massive tsunami which hit the Tohoku and Kanto regions, but also triggered a nuclear power plant crisis which included core meltdown and the release of radioactive material.

The news of this earthquake was immediately delivered all over the world, but differences in the reported urgency level of the crisis and disagreements and contradictions between the contents of overseas and domestic media after the earthquake soon emerged. Under these circumstances, a large number of foreigners residing in Japan hurriedly evacuated for short- or long-term periods either inside the country or outside Japan. This evacuation had broad implications

on socio-economic activities. These effects include the withdrawal of foreign government functions in Japan due to the relocation or closure of embassies, reduction in productivity due to the relocation or stoppage of foreign companies' functions, relocation of supply chain or human resources outside of Japan, and so forth. The educational field was particularly hard-hit, as up to 80% of foreign students in the Tohoku region returned to their country, and many did not return to Japan; this effect was also felt in the Kanto region and other areas of Japan, and the withdrawal of large numbers of foreign student had a large impact on some universities' economic situation. The tourism industry was also affected by the cancellation of trips, tours, conferences, and so forth.

After the Tohoku Earthquake, many important questions about disaster information dissemination – particularly as it relates to foreigners – were raised. How did foreigners residing in Japan collect disaster information? Which sources did they trust when faced with a wide variety of information released from both domestic and overseas sources? Did differences in their Japanese and English language ability affect their information collection behavior or which information sources they trusted the most or least? What aspects of disaster information may have contributed to the widespread flight of foreigners? What should be done to improve disaster information dissemination to foreigners after future disasters?

To contribute to solving these issues, we conducted a questionnaire survey targeted at Japanese and foreigners residing in the Kanto region at the time of the earthquake. Previous analyses have introduced general results focusing on the differences between Japanese and foreigners (Kawasaki et al., 2011; Henry et al., 2011). In this paper, we examine the disaster information gathering behavior and related difficulties considering the language ability in order to better understand how we may improve disaster information dissemination in the future.

2. SURVEY METHODOLOGY & SAMPLE CATEGORIZATION

2.1 Survey design & distribution

We carried out an online questionnaire survey focusing on people in the Kanto region, which is the most populous area in Japan and includes Tokyo and seven surrounding prefectures. In order to collect samples from the major foreign nationalities, we prepared the survey in nine different languages. A detailed overview of the survey contents is provided in Kawasaki et al. (2011) and Henry et al. (2011). The survey was distributed via two methods: first, through social and professional contacts; and second, through direct requests for cooperation with entities such as business communities, universities, embassies, and so forth. Responses were gathered for two weeks beginning roughly 10 weeks after the earthquake occurred.

2.2 Categorization by language ability

A total of 1,357 responses were collected in this survey, of which 497 were from Japanese and 860 were from foreign nationals representing 73 countries. We first

categorized the respondents into groups according to their self-assessed Japanese speaking and listening and English proficiency levels, as summarized in Table 1. Language proficiency was classified into five levels: “native,” “advanced,” “intermediate,” “basic,” and “none.” The purpose of this analysis is to investigate how the difference in language ability levels affected disaster information collection behavior, so the respondents who chose the upper or lower two levels were defined as “skilled” or “unskilled,” respectively. They were then divided into three categories based on language proficiency as follows: “JPN+ENG” for high proficiency in both Japanese and English, and “ENG only” or “JPN only” for high proficiency in only English or only Japanese. This resulted in the extraction of 767 respondents, who were then divided into five groups depending on their language ability category and nationality (Japanese or foreigner).

Table 1: Categorization of respondents according to language ability

		English proficiency				
		Native	Advanced	Intermediate	Basic	None
Japanese proficiency	Native	JPN+ENG F:198 J:76		F:74 J:135	JPN only F:42 J:236	
	Advanced					
	Intermediate	F:152		F:57 J:1	F:30 J:1	
	Basic	ENG only F:215		F:56	F:9 J:1	
	None					

3. ANALYSIS BY LANGUAGE ABILITY

3.1 Disaster information sources

The most-trusted disaster information sources are shown in Figure 1 by nationality and language ability. For foreigners [JPN+ENG] and [ENG only], the most-trusted sources were International Organization, Japanese news source, and Japanese government. For foreigners [JPN only], however, the most-trusted source was Japanese news source, followed distantly by Japanese government and international organization. For Japanese respondents, the most-trusted source was Japanese news sources, followed by the Japanese government and Japanese research/academic institutions.

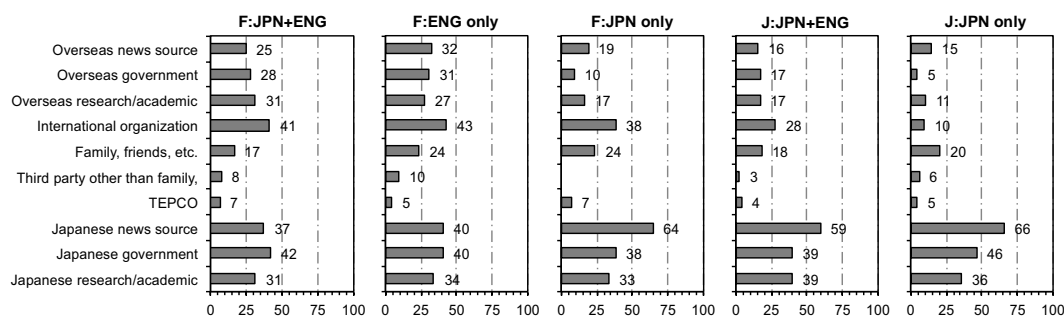


Figure 1: Most-trusted disaster information sources

Figure 2 shows the least-trusted disaster information sources. A similar trend can be seen for foreigners [JPN+ENG], [ENG only], [JPN only] and Japanese [JPN+ENG], with the top least-trusted information source being the Tokyo Electric Power Company (TEPCO), followed by the Japanese government and overseas news sources. For Japanese [JPN only], TEPCO is still the top least-trusted source, followed by the Japanese government and Japanese news sources.

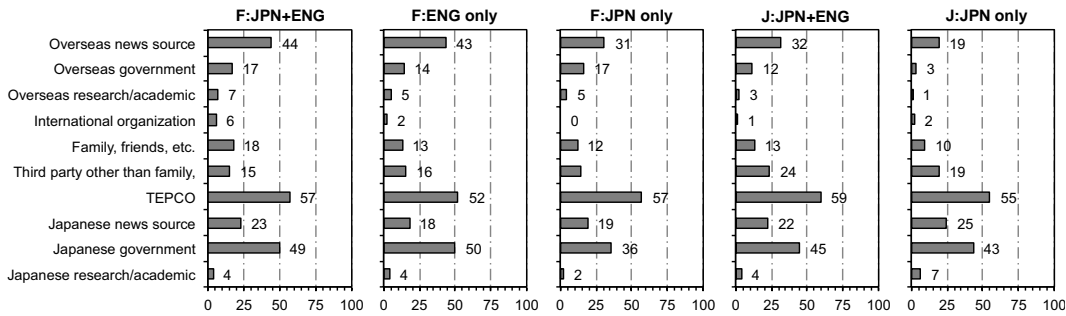


Figure 2: Least-trusted disaster information sources

In order to evaluate the net trust-worthiness of information sources, the percentage of respondents who found a source to be un-trustworthy was subtracted from the percentage who found a source to be trust-worthy. These results are summarized in Figure 3. For foreigners [JPN+ENG] and [ENG only], the source with the highest net trust-worthiness was international organization, and for foreigners [JPN only] and Japanese [JPN+ENG] and [JPN only], the source with the highest net trust-worthiness was Japanese news source. The source with the lowest net trust-worthiness for all groups was TEPCO. Large differences by language ability could be seen for international organization and Japanese news sources: in the case of the former, the net trust-worthiness was much lower for Japanese [JPN only] than for the other groups; conversely, for Japanese news source, the net trust-worthiness was much lower for foreigner [JPN+ENG] and [ENG only] than for the other groups.

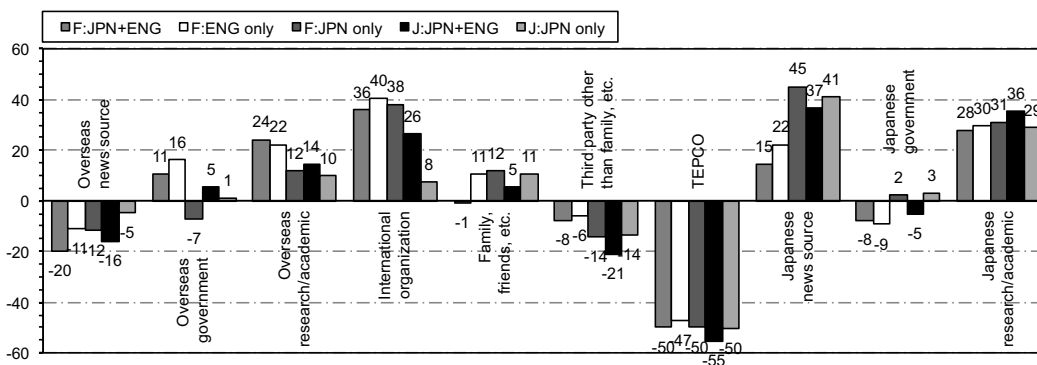


Figure 3: Net trust-worthiness of disaster information sources

3.2 Media & language for disaster information acquisition

The media and language utilized for acquiring disaster information is shown in Figure 4. Foreigners [JPN+ENG] used Japanese TV the most, followed by traditional internet in both English and Japanese. These respondents also tended to

use Japanese more for non-internet media modes and English more for internet media modes. For foreigner [ENG only], however, English was overwhelming used for all media modes, with traditional internet and TV being the most-used. Conversely, foreigners [JPN only] showed the opposite trend, with Japanese being the most-utilized language for nearly all media modes. In this case, Japanese television was the most-used mode, followed by Japanese traditional internet and traditional internet in other languages. The media and language usage pattern for Japanese [JPN+ENG] and [JPN only] was fairly similar, with Japanese television, traditional internet, and printed media as the most-used media modes. Japanese [JPN+ENG] did, however, tend to use English in addition to Japanese much more than Japanese [JPN only].

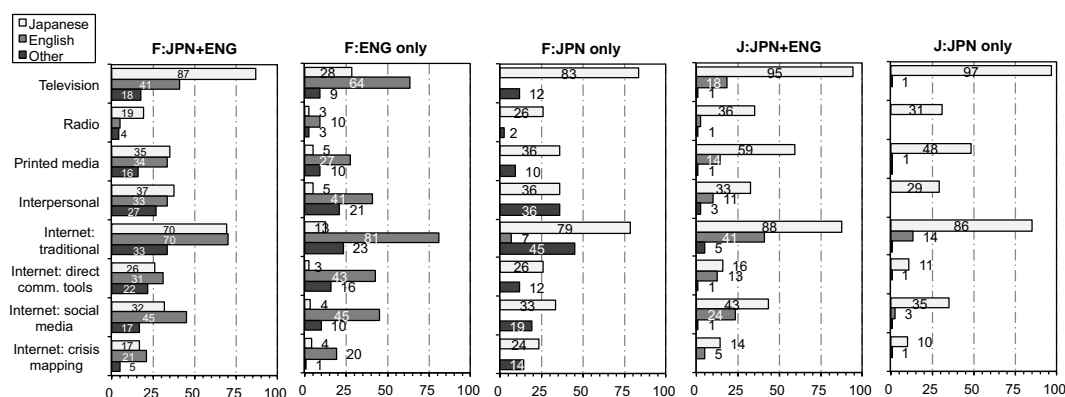


Figure 4: Utilized media and language for acquiring disaster information

3.3 Problems related to disaster information acquisition

Figure 5 shows the reasons why respondents encountered difficulties related to information acquisition. Confused by conflicting or differing information was the reason cited by the highest percentage of respondents for all groups except for foreigners [ENG only], for whom language comprehension was the largest problem, and Japanese [JPN+ENG], for whom inability to access information was just as highly rated as conflicting or differing information. The differences based on nationality and language ability were relatively small for most reasons except for inability to access information and language comprehension. For the former, Japanese respondents appeared to have more trouble with accessing information due to mobile congestion, power outage, and so forth than foreigners did. For the later, foreigners [ENG only] – the only group not skilled in Japanese – cited language comprehension difficulties much more than the other groups.

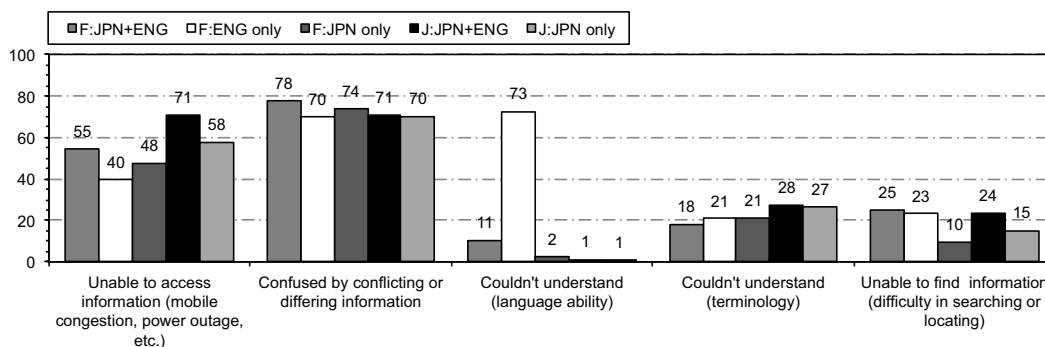


Figure 5: Reasons for problems related to disaster information acquisition

4. DISCUSSION

4.1 Dissemination of disaster information to foreigners in English

After the Tohoku Earthquake, to what extent did information originating from domestic (Japanese) sources get disseminated to foreigners residing in the Kanto region? Were foreigners who can understand Japanese the only ones able to utilize information from domestic sources, whereas those less skilled in Japanese were unable to receive domestic information? We propose the hypothesis that major Japanese information provided by domestic information sources was somehow transmitted to many foreigners in English. If so, then even Foreigner [ENG only] was able to obtain the same Japanese-language information delivered from domestic information sources as Foreigner [JPN+ENG], and this fact led to both groups having a similar pattern for most- and least-trusted information sources. However, Foreigner [JPN+ENG] tended to collect information from both Japanese and English media, whereas Foreigner [ENG only] collected information mainly in English with a very low percentage of information collection in Japanese. Therefore, the hypothesis that “information related to the Tohoku Earthquake provided by domestic information sources was disseminated to foreigners in English” arises. By analyzing the “open response” part of our survey, we found that there were primarily three means by which the information from domestic information sources was disseminated to foreigners in English.

The first was via NHK (Japan Broadcasting Cooperation), Japan’s only public broadcaster. For regular NHK General TV programs, two news programs are translated in English simultaneously using alternative audio, however, after the Tohoku Earthquake two additional news programs were also translated in English simultaneously with extended airtime. In addition, NHK also broadcast the news briefings of TEPCO and press conferences of the Prime Minister with simultaneous English translation using alternative audio. Furthermore, “NHK World,” a 24-hour English news program which normally can only be viewed overseas, was delivered after the earthquake via the Internet and via cable TV in Japan through special arrangements with domestic cable TV companies. Through these supporting activities led primarily by NHK, there were a variety of Japanese news programs choices which could be viewed in English for a period after the Tohoku Earthquake. Although the utilization of television in both Japanese and

English by Foreigner [ENG only] was not as high as other media modes (as shown in Fig. 2), we believe that TV played an important role as one of the useful domestic information sources in English.

The second means was through the use of social media such as Facebook to collect or find domestic information translated into English by a third party. Several respondents cited the “Fukushima Reactor Feed” as a helpful and important information source after the earthquake in their open response comments. The Fukushima Reactor Feed was a Facebook page launched at noon on March 12th by a foreigner residing in Japan, with the intention of sharing information on the nuclear power plant crisis by translating news broadcasts and articles related to situation in Fukushima. Some of this information included URLs referring back to the original information source, whereas some information was from other individuals’ translation of domestic TV broadcasts and news articles. As a result, information translated with a wide range of accuracy was available to many foreign audiences. Similarly, some individuals and groups provided Japanese information by translating it into English on their blogs and websites.

The third means was automatic translation of Japanese text into English using translation software or translation applications via a web browser. In this case, it is difficult to obtain an exact translation of a Japanese sentence into a English one, but some people may believe consider it is possible to understand the approximate meaning by identifying keywords from the translation result.

As described here, an environment was built on the Internet which allowed foreigners to understand the circumstances by collecting secondary English translations of Japanese information or by translated broadcast contents. Thus, Foreigner [ENG only] was able to obtain similar information as Foreigner [JPN+ENG], which may explain why their reliability on domestic information sources was similar.

4.2 Reliance of foreigners skilled in English on overseas information sources

Why did Foreigner [JPN+ENG], who collected domestic information in both Japanese and English, and Foreigner [ENG only], who collected domestic information mainly in English, both tend to place higher reliability on overseas information sources, and why did they both tend to distrust domestic information sources? Through analysis of the open responses provided by foreigners the following reasons were derived.

Both groups (Foreigner [JPN+ENG] and Foreigner [ENG only]) may have felt discomfort or anxiety due to a gap between the actual situation in Japan and the overly urgent and sensationalist reports coming from overseas. In addition, as a result of the Japanese government’s low awareness of crisis management, foreigners may also have distrust in the Japanese government’s and TEPCO’s response due to the government’s lack of involvement or intervention at the nuclear power plant along with a distinct lack of active publishing of specific information. Furthermore, these feelings of anxiety and so forth may have been

exacerbated by the shortage of reliable English information from public institutions. These reasons may have produced higher distrust of domestic information sources (albeit the difference was small) and greater trust in overseas information sources.

The major opinions of foreigners provided in the open response section as related to information from domestic sources are summarized below.

a) Passive attitude of information disclosure to the public

- A lack of proactive information provision based on the precautionary principle. For example, the continual reporting of facts such as “we can see a large amount of smoke in the sky above the Fukushima Daiichi nuclear power plant” or “currently, the measured radiation level is ○○ millisievert” without any analysis, evaluation, verification, or prediction, which forced people to make decisions or take action based on less useful information
- No information about the worst-case scenario and risks which might occur over the medium- to long-term time period, such as response to radioactive contamination, nor information about the expected radiation levels such as the prediction of short- to long-term dispersion considering weather conditions such as wind direction
- Analysis results should have been open and transparent

b) Repetitious, meaningless and ambiguous information

- Difficult to understand the actual meaning due to the high frequency of ambiguous expressions used by many Japanese to avoid being assertive, such as “we can ’ t exclude the fact that ○○ did not occur”
- No consistency in information or large amounts of contradictory information
- Repeated broadcasting of the same images and information seen and given after earthquake

c) Disappointment in the Japanese government’s response to the nuclear power plant crisis

- This is a fundamental problem related to the Japanese government’s crisis management, but many opinions were received in the open response section of questionnaire: “even if the nuclear power plant problem is a national crisis, it is hard to understand why the Japanese government entrusted the resolution of the nuclear problem to TEPCO, which is just a public company – why wasn’t the government more deeply involved;” “the Japanese government was too slow in getting involved;” “we were confused because the government said that it was safe without showing any scientific evidence about the radioactive contamination of soil, water, and food.” From these actions of the government, it gave the impression to many foreigners that the Japanese government lacked the precautionary principle, and that the government underestimated the situation due to poor crisis management ability. In addition, foreigners were very concerned whether the Japanese government and TEPCO were hiding information.

4.3 Reliance of foreigners skilled in Japanese on domestic Japanese information sources

Contrary to other groups of foreigners based on language ability, Foreigner [JPN only] mainly used Japanese media or, in some cases, their native language (except English) for collecting information, but they rarely used English (Fig. 3). There is a large difference between this group's reliance on domestic information sources (57%) versus overseas information sources (32%).

A similar level of reliance (based on percentage) could also be observed for Japanese [JPN+ENG]. The majority of Japanese [JPN+ENG] collected information in Japanese, although there was some limited use of English. Even when the amount of information collected from overseas information sources was small, even if they were able to collect using both English and Japanese language, it resulted in low trust in overseas information sources; this tendency was even greater for Japanese [JPN only].

Foreigner [JPN only] appeared to collect some information in their native language (excluding English), in which the urgency of crisis may have been different from domestic broadcasts. Japanese [JPN+ENG] also collected overseas information in limited manner. As both of these groups collected information in a similar manner in Japanese, both Foreigner [JPN only] and Japanese [JPN+ENG] also tended to trust similar information sources. However, Japanese [JPN only] only collected domestic information, and as such their evaluation of trustworthiness was biased towards domestic information sources.

REFERENCES

- Kawasaki, A., Henry, M., Meguro, K., 2011. Disaster information gathering behavior after the Tohoku Earthquake Part 1: Results of Japanese respondents. *2011 New Technologies for Urban Safety of Mega Cities in Asia (ICUS Report 2011-02)*, Chiang Mai, Thailand, 45-56.
- Henry, M., Kawasaki, A., Meguro, K., 2011. Disaster information gathering behavior after the Tohoku Earthquake Part 2: Results of foreign respondents. *2011 New Technologies for Urban Safety of Mega Cities in Asia (ICUS Report 2011-02)*, Chiang Mai, Thailand, 149-161.

Analysis of traffic situation on urban road network after large-scale earthquake

Shinji TANAKA¹, Daisuke OSHIMA², Takashi OGUCHI³

¹Associate Professor, Institute of Urban Innovation,
Yokohama National University, Japan
stanaka@ynu.ac.jp

²Research Fellow, Institute of Industrial Science, the University of Tokyo, Japan

³Professor, Institute of Industrial Science, the University of Tokyo, Japan

ABSTRACT

This paper analyzed the traffic situation on a road network after the occurrence of a large-scale earthquake.

The Great East Japan Earthquake that occurred in March 2011 brought serious damages including transportation facilities to the Tohoku region, Japan. Even Tokyo metropolitan area, which is more than 300km away from the epicenter, also experienced serious traffic jam and congestion throughout the road network until the next morning, even though there were very few damages of road facilities. If such congestion occurs in case holding physical and human damages, it would make serious influence on a lot of important activities such as evacuation, rescue, inquiry, and so on. It is essential to clarify the mechanism how such congestion occurred.

This study analyzed the traffic situation by this earthquake using a traffic simulator and reproduced the phenomenon observed on the day. As a result, it is found that rapid demand increase of returning home after the earthquake occurrence made gridlocks on the network and they speared out very quickly.

Keywords: traffic congestion in disaster, traffic simulation

1. INTRODUCTION

The Great East Japan Earthquake occurred in March 2011 in the Tohoku region, Japan. It caused huge human and material damages by strong shaking and high tsunami. Transportation facilities such as roads, railways, ports etc. were also seriously damaged in that area, and the movement of people and goods were influenced very much for a long time.

Tokyo metropolitan area is more than 300km away from the epicenter, and there were few damages on the transportation infrastructure. However, all the train operations were suspended and the Metropolitan Expressway was closed for safety check, then very serious traffic jam and congestion occurred throughout the road network after the earthquake until the next morning. A lot of people tried to go home by car or by walk, but they had to spend several hours on the jammed streets. If such congestion happens when there are a lot of human and material damages, it would make serious influence on a lot of important activities such as evacuation, rescue, inquiry, and so on. Therefore, it is essential to clarify and to

understand the mechanism how such serious congestion occurred so as to prepare for future potential earthquakes that may occur around Tokyo.

Based on this background, this paper aims to analyze the situation of traffic congestion on the road network in Tokyo by this earthquake using a traffic simulator. This analysis would become a kind of the basis to make countermeasures such as traffic regulation and traffic control in disaster situation.

2. METHODOLOGY

To reproduce complicated traffic situation, traffic simulation is one of the useful and powerful tools. This chapter describes the outline of the methodology to analyze the traffic situation using traffic simulation.

2.1 Traffic Simulation Model

This study uses a traffic simulation model which can deal with an urban scale network. This model simplifies the representation of link and node properties such as lane configuration, traffic signals etc. but it can treat a relatively large area. Vehicles move along a link according to the FIFO (First In, First Out) principle, and form a queue at the downstream end of the link if the arriving rate is higher than the node (=intersection) capacity, which regulates the outflow rate to the next links.

Based on the input traffic demand (OD table), each vehicle has their origin and destination. Two types of users are modeled, that is, captive group and choice group. The choice group changes their route depending on the traffic situation e.g. travel time while the captive group sticks to the fixed route. Vehicles moves to their own destination according to their route, and some of them (choice group) can change it en route.

As mentioned above, two components of vehicle movement module and route choice module are iterated each other to carry on the simulation calculation. The outlook of the traffic simulation model is shown in the Figure 1.

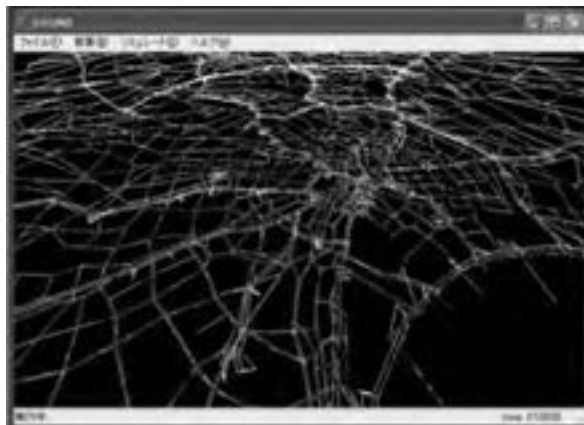


Figure 1: Outlook of traffic simulation model

2.2 Study Network

Figure 2 shows the location of the study area and the road network used for this study. It consists of major arterial streets in Tokyo and it includes the emergency routes that are designated in the disaster prevention plan. The number of the nodes and links are 526 and 1472 respectively, and the total length of the network is 1656.8km. Vehicle trips are generated and attracted at 91 centroids that are set all over the OD zones and the edge of the network. Each link has information of length, number of lanes, and directional outflow capacity to the next link and so on.

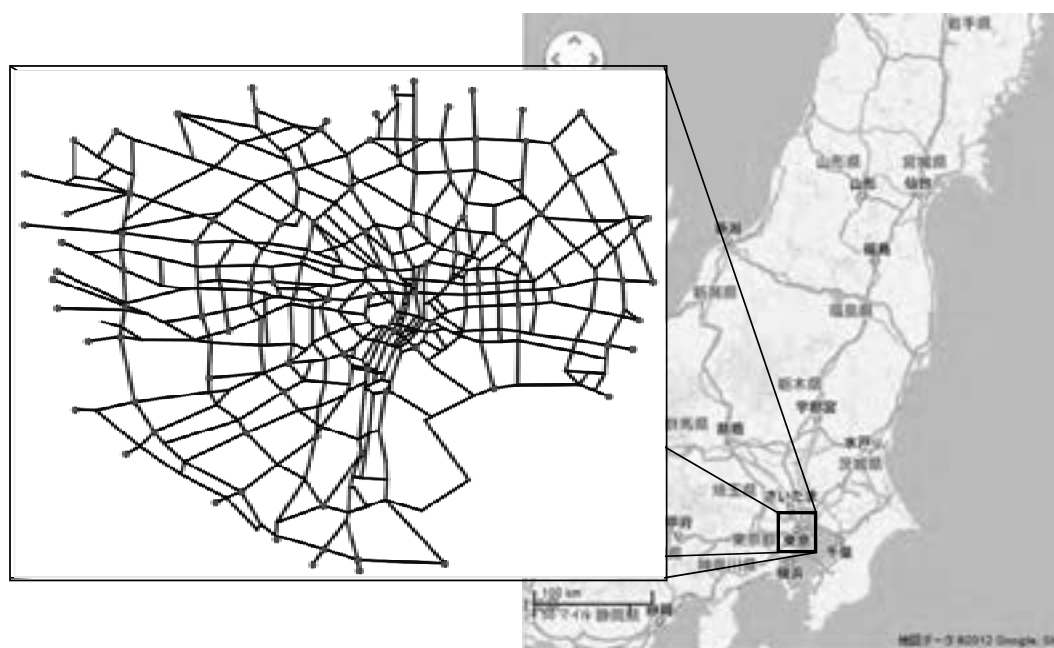


Figure 2: Study area and network

2.3 Demand Estimation

It is necessary to estimate traffic demand as an input to the simulator in order to reproduce the traffic situation in disaster. This study estimated it by applying the result of a questionnaire survey on returning home behavior on the day of the earthquake to the general person trip survey.

First, the increase of vehicle trips due to the train service suspension etc. was estimated. According to the questionnaire survey on the travel mode, the modal share of vehicles on that day that includes private/company vehicles and taxis was 24.0%, whereas the normal vehicle share is 13.4%. Therefore, it was assumed that 24.0% of people who were outside their home used vehicles to go back home. It corresponds to 2.3 million trips, and it is larger than normal vehicle trips by one million. It is estimated that the number of parked vehicles in Tokyo during the daytime normally is approximately one million, so the amount of demand increase in disaster can be explained by those unused vehicles.

Next, the time distribution of the traffic demand was estimated. Another questionnaire survey showed that approximately 50% of people began returning

home before 5pm on that day and very few people began traveling after the midnight. Then, the estimated 2.3 million trips were distributed according to the ratio of the trip start time obtained from the survey between 3pm to 12am. Figure 3 shows the time-series distribution of the estimated traffic demand. It shows a sharp peak just after the earthquake occurrence, which means significant volume of (more than double of the normal) traffic demand was supposed to be generated in a very short time period onto the network. This hourly traffic demand was used as an input for the disaster case simulation.

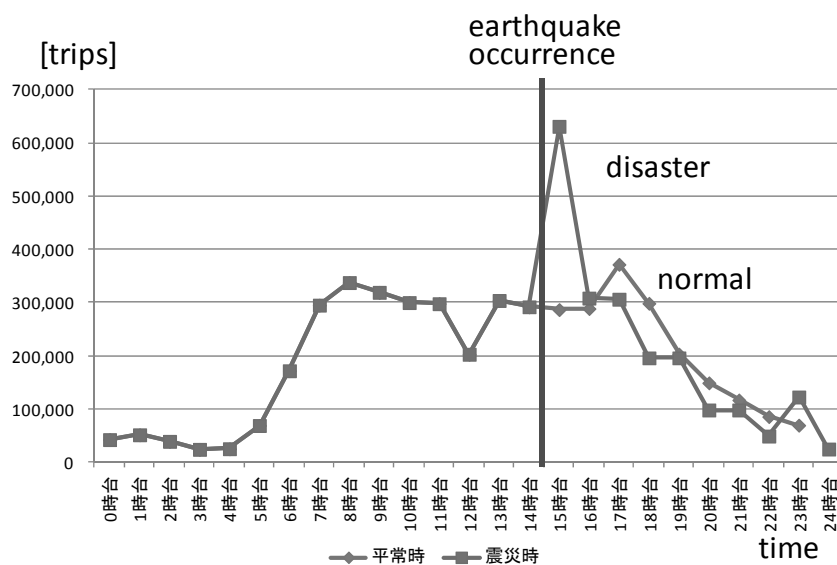


Figure 3: Estimated demand in normal and disaster cases

3. SIMULATION RESULT

This chapter describes the result of the simulation analysis. First, the reproducibility of the simulator was checked by a normal case scenario, and then the disaster case scenario was implemented to analyze the traffic situation.

3.1 Reproducibility Check

First, a normal case scenario simulation was conducted in order to calibrate the simulation parameters and to check the model reproducibility. Here, the result of the person trip survey in Tokyo metropolitan area was used as traffic demand of a normal day. Average vehicle ridership of 1.3 [person/vehicle] was used to convert the unit to the vehicle basis. As the simulation network is simplified and it has less links than actual, the input traffic demand was also reduced for a certain rate.

Figure 4 shows the reproducibility of the normal case scenario at 6pm, showing the link speed by different colors. The left is simulated and the right is observed value. The overall status is quite similar although there are some minor differences. The simulation parameters are shown in Table 1.

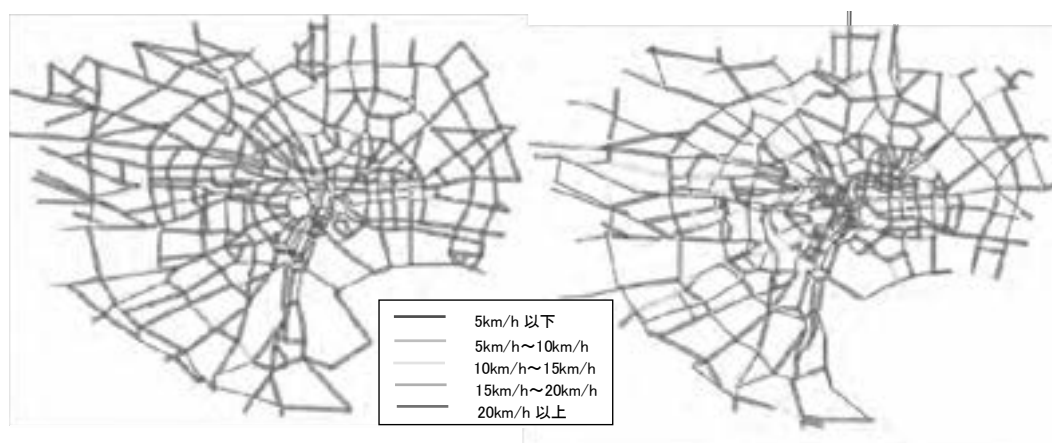


Figure 4: Link travel speed at 6pm (left: simulated, right: observed)

Table 1: Simulation parameters

Parameter	Description	Value
Dial assignment theta	Sensitivity to the link cost	0.01
Maximum speed	Free flow speed of the link	60 km/h
Route choice interval	Update interval of route choice function	60 sec
Scan time	Update interval of vehicle movement	3 sec
Packet size	Group of vehicles of same OD	10 vehicles
Vehicle length	Length of vehicle and headway	8 m

3.2 Estimation of the Traffic Situation after the Earthquake

Using the model parameters and the estimated traffic demand, the disaster case scenario simulation was conducted to reproduce the traffic situation after the earthquake. Figure 5, 6 and 7 show the link speed of the simulated and the observed values in different time periods. These figures show that the general transition of the traffic status is the same both for the simulation and the observation, that is, the congestion started just after the earthquake (4pm), spread out rapidly to the jam (6pm), and dissolve to the normal again (next 5am).

It was revealed that a large part of the network became gridlock situation in the congested time period. The links and nodes were packed with vehicles to the capacity, and only very little movement was allowed. This would be caused by the rapid increase of the unusual traffic demand as well as the reduction of the intersection capacity due to a lot of pedestrians spilled over from sidewalks.

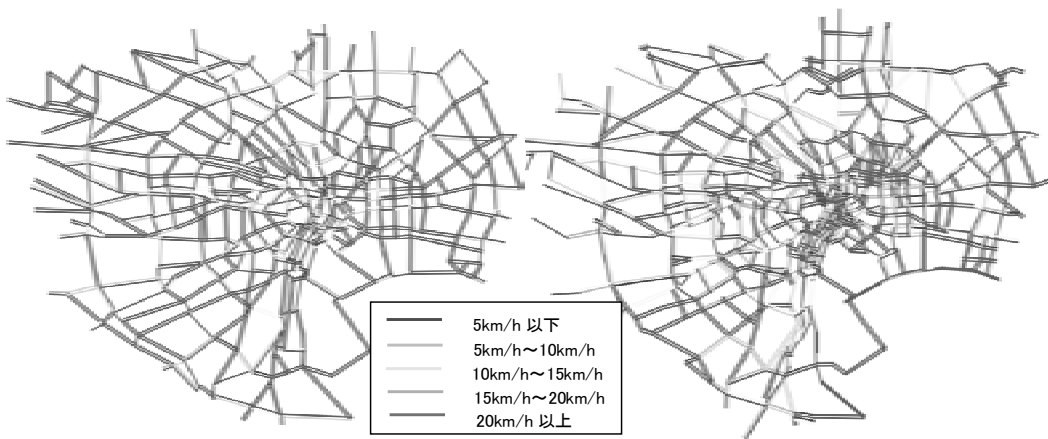


Figure 5: Link travel speed at 4pm (left: simulated, right: observed)

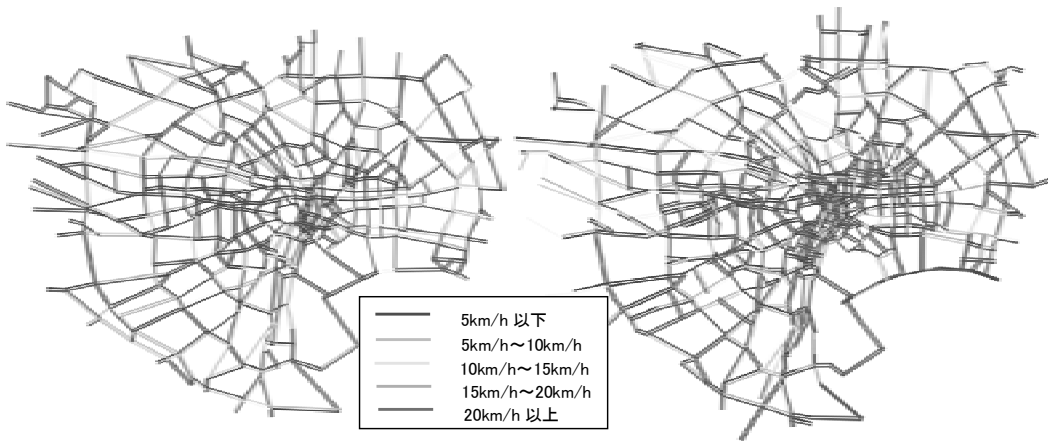


Figure 6: Link travel speed at 6pm (left: simulated, right: observed)

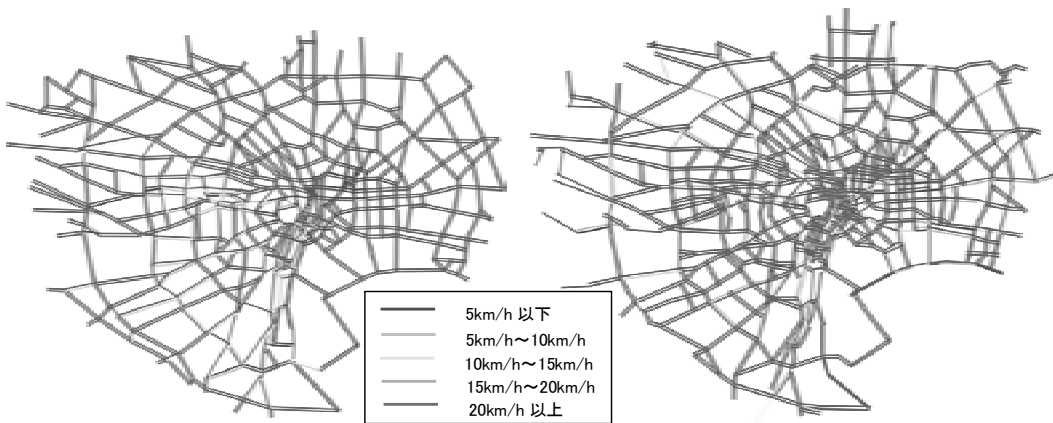


Figure 7: Link travel speed at next 5am (left: simulated, right: observed)

4. CONCLUSION

This study analyzed the traffic situation on Tokyo metropolitan road network after the Great East Japan Earthquake using traffic simulation. The simulation was able to reproduce the traffic situation in disaster as well as its time transition. It was revealed that the serious traffic jam and congestion were formed by the network gridlock, and it would be caused by the rapid demand increase and the intersection capacity reduction.

Based on these results, effective countermeasures to alleviate the congestion and to maintain the network function should be considered and examined for the next steps. Traffic simulation would be useful for such kind of scenario analysis.

REFERENCES

- Yoshii, T., Kuwahara, M. and Morita, H., 1995. A network simulation model for oversaturated flow on urban expressways. *Traffic Engineering*, Vol. 30, No.1, 33-41
- Okamura, H., Kuwahara, M., Yoshii, T. and Nishikawa, I., 1996. Development and validation of surface street network simulation model. *Proceedings of 16th Symposium on Traffic Engineering*, 93-96
- Nippon Research Center, Ltd., 2011. Survey on the residents' response to the Great East Japan Earthquake.
- Marketing Service Co. Ltd., 2011. Survey on attitude to disasters regarding the Great East Japan Earthquake.

Possibility of developing a new special economic zone in Ulaanbaatar City

Oyuntsatsral TSEYENBALJIR

Senior Lecturer, School of Civil Engineering and Architecture, MUST, Mongolia

ts_oyuntsatsral@yahoo.com

ABSTRACT

Developing Special Economic Zone (SEZ) is a commonly used method to improve economic condition of developing countries. Although 4 SEZs have been under construction in the rural areas of Mongolia since 2002, progress of those SEZs is slow. Thus it's better to build a new SEZ in the center of the country where the most of the population lives and infrastructure condition is better. World trend of developing SEZ also shows locating SEZs in the cities or near cities is successful compared to SEZs in rural areas. Ulaanbaatar will have a new international airport as replacement of existing Chinggis Khaan International Airport by 2015. But there is no a proper plan for the existing Chinggis Khaan International Airport after completion of the new airport. If the facilities and infrastructures such as electricity, water, drainage and sewage systems of the existing airport can be used as SEZ infrastructure basics, SEZ development cost will be reduced drastically. This paper analyzes possibilities of developing a SEZ in Ulaanbaatar city.

Keywords: special economic zone, international airport

1. INTRODUCTION

Special Economic Zone (SEZ) is a commonly used method in developing countries to generate economic growth, to attract foreign direct investment, to increase employment and to improve living conditions. There are several important reasons for establishing SEZs, as follows:

- Attract foreign direct investment
- Develop manufacturing
- Develop and diversify exports
- Job creation
- Develop infrastructure
- Regional development

Most developing countries are trying to develop a various types of SEZs for the last four decades. Mongolia, as a developing country, is also included the list of countries which are developing SEZs. But many developing countries are facing a number of problems to develop SEZs, Mongolia as well.

2. SEZs IN MONGOLIA

Mongolia entered a new era of market economy after the 70 years of a socialist economy by the help of the democratic revolution in the early 1990s. Nowadays implementing successful model of development is crucial for development of the country.

Influenced by successful cases in other countries, Mongolian parliament has already approved “The Concept of Establishing Free Economic Zone in Mongolia” in 1995 and law on Free Zones in 2002. The Law on Free Zones consists of 3 chapters and 18 articles. In the Law on Free Zones, the SEZ is defined as follows:

“Free zone” shall mean part of the territory of Mongolia under special conditions for business and investment and which should be considered to be separate in terms of custom and taxation.

And also the law announces that the SEZ in Mongolia will be pure public as follows:

The State Ih Hural (Parliament) shall decide on the creation, forms, location and the size of territory, borders, change and dissolution of free zone in Mongolia upon submittal of respective proposal by the Government.

There are 4 zones under implementation; in the northern, southern, western border areas and along the railway - Altanbulag FTZ, Zamyn-Uud FEZ, Tsagaannuur FTZ and Choir FEZ (Figure 1).



Figure 1: Potential SEZs in Mongolia

Even Mongolia's SEZs projects were started several years ago, number of problems facing these projects such as legal and regulatory framework, lack of funding and lack of experience. These main problems facing to SEZ development in Mongolia can be discussed hereunder.

a) Political problems

Frequent changes of governments are observed in the least developed country like Mongolia. Mongolia uses unicameral parliamentary system and the parliament selects its members every four years by general election. According to the election results, changes of the organizational structure of ministries, agencies and human resource will happen after the every parliamentary election. Key projects also suffer from a change of project personnel along with the change of government which ultimately make difficult to attain the targeted schedule and cost.

b) Financial problems

Government oriented programs are facing lack of financial source dependent on government budget. Due to insufficient amount of budget, given to SEZ projects every year, progress of project is prolonged. Table 1 shows the total investment was given by the Government of Mongolia since the SEZs were announced to develop.

Table 1: Total investment for SEZ development in Mongolia, million tugrug

	2003- 2004	2005	2006	2007	2008	Total
Altanbulag FTZ	224.9	615.9	48.0	109.2	629.0	1627.0
Zamyn-Uud FEZ				1300.0	1892.0	3192.0
Tsagaannuur FTZ			60.0	37.3	1111.5	1208.8
Choir FEZ				35.0	135.0	170.0
Total	224.9	615.9	108.0	1481.5	3767.5	6027.8

Source: Free Zone Committee, 2010

c) Organizational problems

Preparatory work of SEZ project development had not well been done. None of the 4 projects have feasibility study and cost-benefit analysis. Moreover, preparing the necessary studies to implement SEZ projects are suffering from lack of experienced specialists in SEZ projects.

d) Laws and Regulations

The law on Free Zones, approved in 2002, does not have a full set of implementation regulations. The revised law on Free Zones has been discussed since 2005. Approving the laws and regulations related to the zone activities takes time and effort.

3. POSSIBILITY OF DEVELOPING A NEW SPECIAL ECONOMIC ZONE IN ULAANBAATAR

While all existing on-going SEZs in Mongolia are located in very rural areas and their construction is pro-longed, it is crucial to develop a new SEZ with successful features for the development of Mongolia. The author was searching a possibility of developing a new SEZ in the area with more advantages compared to the existing failed SEZs. And she found out that Ulaanbaatar, capital city of Mongolia will have a new international airport as replacement of existing Chingis Khaan International Airport by 2015. The airport will be built with Japanese assistance in Tov province. Japanese Government will be giving a 40-year loan of US\$270 million. The project has already initiated. However the future development plan of existing Chingis Khaan International Airport has not yet decided by the government. And the author noticed that there is high possibility for developing a new SEZ based on the lessons learned from the world successful SEZ cases in the existing international airport. It is possible to use the building facilities and infrastructures such as electricity, water, drainage and sewage systems of existing international airport as SEZ infrastructure basics. The project can reduce its development cost drastically. Ulaanbaatar City is located just 15 km from the existing airport. Therefore it will not difficult to get work resources.

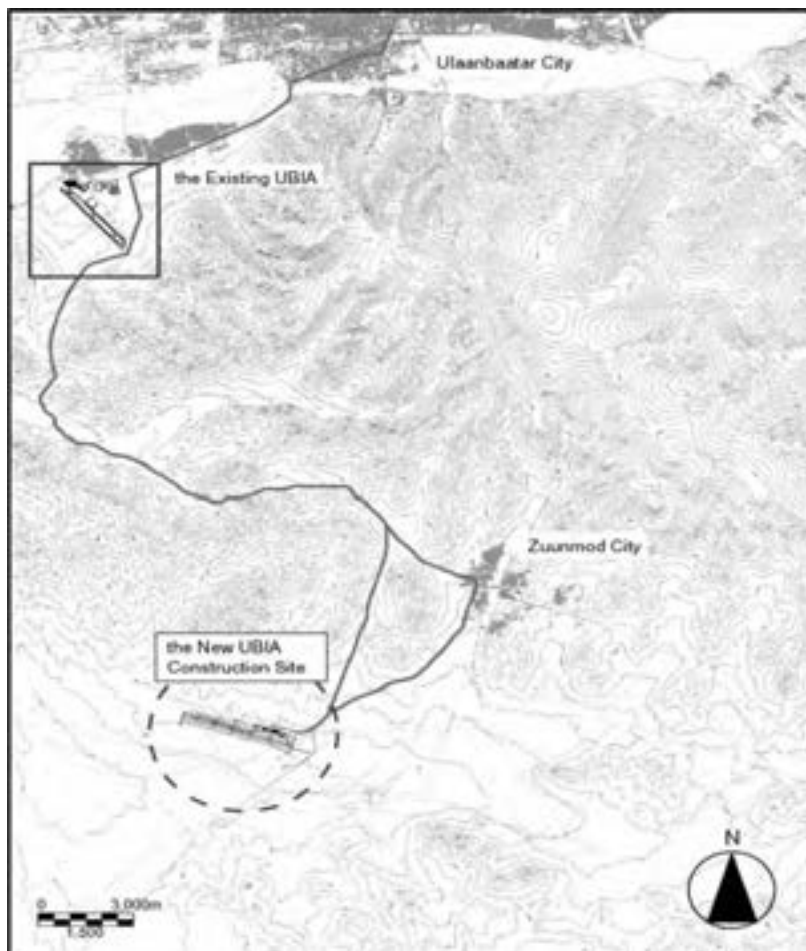


Figure 2: Location of Existing and New Ulaanbaatar International Airports

The author made the preliminary feasibility study of this plan and named this plan as “Ulaanbaatar Airport SEZ” construction project. The author also evaluated the feasibility study level of the new SEZ to-be-built by using the evaluation check list based on the New Scheme of Feasibility Study. Table 2 shows the results of author’s evaluation. It shall be understood that while there is no concrete plan to establish Ulaanbaatar Airport SEZ, evaluation is basically based on the technical features of the location. However this plan has much higher feasibility level than 4 on-going SEZ projects.

Table 2: The feasibility study level of a new SEZ in existing airport

	Description of conditions	New SEZ
Market Demand Feasibility	Competitive advantages of the zone site location	Airport is the world sky gateway and it has more possibility to connect other countries except only the neighboring countries; Russia and China.
	Competitive advantages of the zone offering for investors	NA
Technical feasibility	Distance from capital city	15 km
	Close to international school	Yes
	Close to hospital with international standards	Yes
	Close to stores and supermarkets with international standards	Yes
	Population within 15 km	1,071,700
	Easy to find labour force	Yes (easy to employ from the capital city, Ulaanbaatar where the half of total population lives)
Economical feasibility	Cost of infrastructure development	Less cost to access SEZ site
Financial feasibility	Financing resource	NA
Environmental feasibility		Environment friendly industries should be invited
Concurrence of stakeholders		PPP type scheme should be used

Before establishing SEZ, what kinds of industries should be invited to the SEZ is one of the crucial issues to decide. Most countries make decision based on their

own advantages. Somehow it is possible to make decision by supplier side view. But the emerging globalization issue reminds to consider not only own interests but also international and regional trends. Mongolia is a low-population, landlocked country located between two giant neighbors. In Mongolian case, it is better to consider 3 variants for choosing potential industries to be located in SEZ. Also the author considered that in case developing SEZ on the basis of the airport, the products to be produced should be light weighted.

- Traditional industry based on the agriculture sector of Mongolia
- High tech industry based on the natural resources of Mongolia
- High-tech service industry based on the geographical location of Mongolia

4. CONCLUSION

Based on the world trend there is a demand for adjusted new type of SEZ in landlocked, low population countries such as Mongolia. New type of SEZ in landlocked country such as Mongolia should consider following matters.

1. Near to the international gateway
In case of landlocked country, the location should be next to an airport.
2. Save infrastructure expenditures
Using existing infrastructure for establishing SEZ will be a cost effective way for developing country such as Mongolia.
3. Industries in SEZ should be based on advantages of host country
In Mongolian case, the industries can be based on rich mineral resources and strategic geopolitical location of Mongolia.

For preventing same unsuccessful stories as exist in Mongolia, Mongolian SEZ projects should follow the world trend of private sector participation in SEZ project development so as to avoid reliance on government funding. Attracting private sector participation in SEZ development needs preparation work related to laws, regulations and planning. Especially for the planning, complex feasibility study is crucial to develop SEZs in landlocked developing countries. An appropriate scheme of feasibility study should be prepared for encouraging SEZ development in developing countries.

REFERENCES

- Law on Free Zones, 2002. Ulsiin Ih Khural, Ulaanbaatar, Mongolia
Introduction to Altanbulag FTZ. URL: http://www.altanbulag.gov.mn/index.php?option=com_content&view=article&id=125&Itemid=162
- Law on the Legal Status of Altanbulag FTZ, 2002. Ulsiin Ih Khural, Ulaanbaatar, Mongolia
Introduction to Zamyn-Uud FEZ. URL: <http://www.zufez.mn/preface#content>
- Introduction to Tsagaannuur FTZ. URL: <http://www.tsagaannuur.mn/>
- TFTZ, 2009. "Master Plan of Tsagaannuur Free Trade Zone", Government of Mongolia, Ulaanbaatar, Mongolia

Tseyenbaljir O. , 2009. Current Situation of Special Economic Zones in Mongolia, *Proceedings of the 11th International Summer Symposium, JSCE*, Japan, pp. 165-168

Roadmap from smoke to the development: Airport city as a win-win model for the eco- economical context of the capital city development

S.Davaanyam

Doctorant, Researcher, National Development Institute
Davaanyam1206@yahoo.com

ABSTRACT

The cities around the world occupy 0.4% of the world territory, yet they accommodate 51% of the world's population and generate 83% of the global GDP. Likewise, as of 2010 in the city of Ulaanbaatar, which occupies only 0.3% of the country's territory, reside 45% of the country's population and 62.7% of the national GDP is produced. According to the recent comparative study among the world's 200 major cities, Ulaanbaatar leads with its growth rate in terms of GDP and number of employed population. It is obvious that in order to facilitate sustainable economic growth, a city should ensure healthy and safe environment and competitive infrastructure development. However, in Mongolia the adequate balance of the human settlement is lost. This can be clearly exhibited from the country's leading position in terms of the share of territory per person against the number of the population per city, except the case of island-states and city-states. The national security of Mongolia is negatively affected by the fact that a 45% of its total population is living the city, which has the worst air pollution level globally. Moreover, the intensive population and economic growth in the capital city Ulaanbaatar lead to the overburdened urban infrastructure and other negative impacts such as traffic congestion and environmental pollution. Over concentration around a socio-economic single-center in area of Baga-Toiruu, where there are state administration, healthcare, education and commercial services are concentrated, will likely further magnetize population concentration. For instance, 80% of the central and local government institutions such as ministries, parliament and city government, as well as 68% of the employees and university students are concentrated within the 1.4 km² area of the Baga-Toiruu. In addition the population of vehicles in the capital city has been increasing intensively on an annual basis. If 50% of the total 200,000 vehicles be aligned in 4 lanes along the street, then such a queue would be two fold longer than the length of the most crowded 84.3km long road section. It shows that unless the over concentration around Baga-Toiruu be unbundled, the traffic congestion problem would not be solved. Hence, for the landlocked country – Mongolia it is being proposed to develop an Airport-City with 300,000-400,000 population as a win-win model in terms of competitiveness and eco-economic parameters based on the International Airport in Khushig Vallye in 53 kilometers from Ulaanbaatar and move there a half of the state and public institutions as ministries and agencies, in order to reduce the over concentration pattern around Baga-Toiruu area. It is estimated that it would then enable the reduction of Ulaanbaatar air pollution by 30-40%.

Key words: *Over concentration around a socio-economic single-center, migration and movement, Airport City.*

Review on the definitions of vulnerability, resilience, and adaptation

Yuto SHIOZAKI¹ and Takaaki KATO²

¹ PhD candidate, Department of Urban Engineering,
The University of Tokyo, Japan
yuto@iis.u-tokyo.ac.jp

² Associate Professor, ICUS, IIS, The University of Tokyo, Japan

ABSTRACT

The concepts of resilience, vulnerability, and adaptation are increasingly used in the fields of global climate change, natural disasters, and ecological and social systems. However, each of the concepts has different definitions. This paper reviews the definitions of vulnerability, resilience, and adaptability, and shows that the concepts can be categorized based on some attributes. First, there are two major definitions for the concept of vulnerability: the exposure to hazards and the degree of coping capacity. Most vulnerability concepts involve exposure, sensitivity, and adaptability. Criticality is also an important concept in vulnerability. Second, the concept of resilience is classified into engineering resilience, ecological resilience, and social resilience. Regime shift is also an important concept in ecological resilience. Social resilience includes the aspects of learning and adaptation in addition to engineering resilience and ecological resilience. Third, the concept of adaptation/adaptability is classified into the context of the target to be operated, the degree of system modification, as well as the timing and duration. As a result, the concept is grouped into coping capacity, adjustment capacity, and transformability. Finally, the linkages between the three concepts are demonstrated using a scenario of a city exposed to a natural disaster.

Keywords: vulnerability, resilience, adaptation, catastrophic regime shift, criticality, natural disaster

1. INTRODUCTION

In the recent years, the concepts of resilience, vulnerability, and adaptation have been increasingly used in the context of global climate change, natural disasters, and ecological and social systems. The perspectives of the three concepts are used as approaches for understanding how and why a system responds to hazards. These concepts have been applied to ecological systems, social systems, and socio-ecological systems (coupled human-environmental systems). These concepts can form an interdisciplinary and comprehensive framework. However, since no unified definition exists for these concepts, and the existing definitions are different, the use of these terms may lead to confusion. In Japan, especially after the Great East Japan Earthquake in 2011, these terms have often been used when discussing natural disaster management and reconstruction,

but without clear definitions. As a result, the discussions in this field are subject to confusion.

To prevent such confusion, this work first highlights the fundamental definitions and components of the three concepts by reviewing relevant articles and reports in the fields of global climate change, natural disasters, and ecological and social systems. These components represent the aspects of a system's behavior in response to hazards. Therefore, understanding them is considered to be useful for establishing a framework for analyzing and managing a system. Second, this article uses a scenario of a city responding to a rapid natural disaster to demonstrate the components. This example clarifies the linkage between the three concepts and facilitates a discussion on the focal points of urban analysis and management in preparation for natural disasters.

2. SYSTEM AND HAZARD

The concepts of resilience, vulnerability, and adaptation are used to represent the manner in which a system responds to hazards. Hence, it is necessary to clarify the definitions of system and hazard before the definitions and components of vulnerability, resilience, and adaptation are explained.

2.1 System

A system is generally “a group of related parts that work together as a whole for a particular purpose” (Longman, 2009). Systems focused upon in this work are generally ecological systems, social systems, and socio-ecological systems. The definitions of a system are listed in Table 1. For example, a lake or forest is an ecological system, in which many animal and plant species interact with each other. A community, city, or country are types of social systems. Examples of social-ecological systems are a fishing village or an agricultural community, in which people are both dependent on and influence their surrounding ecological systems. Any system is generally associated with subsystems and higher-order systems (e.g. a tree-patch-forest system or a household-community-city system).

2.2 Hazard

According to Turner et al. (2003), “hazards are defined as threats to a system, comprising perturbation, stress (and stressors), and the consequences they produce. A perturbation is a major spike in pressure beyond the normal range of variability in which the system operates. Perturbations commonly originate beyond the system or location in question. Stress is a continuous or slowly increasing pressure, commonly within the range of normal variability. Stress often originates and stressors (the source of stress) often reside within the system.”

In other words, there are two types of hazards: perturbation and stress. The former is a rapid environmental change that occurs in the short term (e.g., a tidal wave or hurricane), and the latter is a chronic environmental change that influences a system over the long term (e.g., sea level rise, soil degradation). As a result, hazards might cause damage to the system. In social systems, in addition to environmental change, political or social changes may also act as hazards, such as political upheaval, war, and aging of the society.

Table 1: Definitions of Systems

System	Definition
Ecological system (Ecosystem)	All the animals and plants in a particular area, and the way in which they are related to each other and to their environment (Longman, 2009).
Social system	The people in a society are considered as a system organized by a characteristic pattern of relationships (Miller, 1995).
Social-ecological system	A social-ecological system consists of a bio-geo-physical unit and its associated social actors and institutions. Social-ecological systems are complex, adaptive, and delimited by spatial or functional boundaries surrounding particular ecosystems and their problem context (Glaser et al., 2008).

3. VULNERABILITY

3.1 Background of Vulnerability

The word “vulnerability” has been derived from the Latin word “vulnare,” which means “to wound” (Dow, 1992). The concept of vulnerability has its roots in the study of natural disasters (Janssen et al., 2006). It is considered to focus on the relationship between a social system and its surrounding natural environment. From the 1990s, research on natural disasters started to focus on the vulnerability of social systems to environmental change, and particularly, to climate change.

3.2 Definitions of Vulnerability

There are many different definitions of vulnerability, but Dow (1992) has pointed out that there are two major definitions. In the first definition, vulnerability is defined as *exposure* to the hazards of natural disasters and environmental changes. In the second definition, vulnerability is defined as the lack of *coping capacity* to hazards.

In the first definition, the vulnerability of a system can be measured by the degree of potential or actual hazards that the system is exposed to. For example, exposure is the degree of estimated or actual damage to humans, infrastructure, buildings, and other properties in the case of a natural disaster.

In the second definition, the exposure of a social system is a given condition, and the coping capacity, depending on the components or the condition of the social system, is assumed to affect the degree of damage caused to the system by a hazard. Coping capacity is considered to be composed of two types of social system abilities. One is the ability to absorb the impact of hazards and continue to function, and the other is the ability to recover losses. Dow (1992) defines the former ability as *resistance*, and the latter, as *resilience*.

Additionally, there is a combined definition that encompasses those described above, in which a social system with low coping capacity and high hazard exposure is assumed to be the most vulnerable (Cutter, 1996).

According to Adger (2006), the concept of vulnerability is most often conceptualized by three components: *exposure*, *sensitivity*, and *adaptive capacity*.

Exposure is “the nature and degree to which a system experiences environmental or socio-political stress.” Sensitivity is “the degree to which a system is modified or affected by perturbations.” Adaptive capacity is “the ability of a system to evolve in order to accommodate environmental hazards or policy change and to expand the range of variability with which it can cope.”

Gallopín (2006) defines the three components of vulnerability in a similar manner: exposure, sensitivity, and capacity of response. His definitions of exposure and sensitivity are the same as those of Adger (2006), and he defines the capacity of response as “the system’s ability to adjust to a disturbance, moderate potential damage, take advantage of opportunities, and cope with the consequences of a transformation that occurs.”

Turner et al. (2003) also defined exposure and sensitivity in a similar manner, although they distinguish the capacity to cope/respond from the capacity of adaptation, in their framework of vulnerability analysis. Capacity to cope/respond is the ability of a system to moderate potential damage immediately after an environmental change, and to influence the recovery situation of system. On the other hand, capacity of adaptation is the ability of a system to restructure itself after the coping/response action is taken.

Finally, the concept of *criticality* is introduced, which is related to the concept of vulnerability. Even if a system is exposed to a hazard, the system can cope to a certain degree because of its adaptability or capacity to cope/respond. However, the system is considered to be deteriorated in the case of the occurrence of a hazard whose magnitude is beyond the adaptability or the capacity of the system to cope/respond. Kaspersen et al. (1996) defined such a situation as *criticality*, which refers to a situation in which the extent or rate of environmental degradation precludes the continuation of the current system or levels of human well-being, given feasible adaptations and societal capabilities to respond.

4. RESILIENCE

4.1 Background of Resilience

The term resilience was originally used in the field of material science, where it meant “to bounce back to the original point” (De Bruijn et al., 2007). It was introduced by Holling (1973) as a concept for representing an ecological system’s responses to environmental change. At first, resilience was used in the field of population ecology and in the study of ecosystem management, and it was mathematically based and model oriented. Since the late 1980s, the concept has been used increasingly in the analysis of social-ecological interactions and applied to human systems under the umbrella of social-ecological system studies. At present, there are studies in which the concept is applied to only social systems, focusing more on human society or communities than on ecological systems (Janssen et al., 2006; Wilson, 2011).

4.2 Definitions of Resilience

There are also many definitions of resilience; however, they can be grouped under three general categories: (1) *engineering resilience*, (2) *ecological resilience*, and (3) *social/community resilience* (Holling, 1996; Adger 2000;

Wilson, 2011). In this section, we first explain how a system responds to an environmental change and then present the definition for each category.

Assuming that a system is in an equilibrium condition, the system may respond to environmental change in any of the following manners (De Bruijn, 2004):

- i) The system does not react at all.
- ii) The system reacts but soon returns to the equilibrium condition.
- iii) The system reacts and switches to another stable condition.
- iv) The system enters an oscillating unstable condition.

In the first case, the system completely absorbs the impact of environmental change. In the second case, assuming that a system is always dynamically changing, the system is not expected to completely return to the same condition, but the system is expected to change within the domain, wherein its fundamental structure of variables and processes that control system behavior are maintained, and to return to an equilibrium condition. Such a domain is called the domain of attraction of equilibrium. In the third and fourth cases, the system changes to such a great extent that it cannot maintain its fundamental structure. In the third case, as a result, the system switches to another domain of attraction where the fundamental structure of the system is different. In the fourth case, the system does not settle in any domain of attraction.

Engineering resilience is an important attribute in the second case, when a system can return close to the initial equilibrium point after an environmental change. Engineering resilience is defined as the ability of a system to return to the equilibrium situation after an environmental change (Holling, 1973). It can be measured by the time required for a system to return to the equilibrium situation.

Ecological resilience is defined as the ability of a system to persist despite absorbing changes in state variables, driving variables, and parameters (Holling, 1973). In other words, it is the ability of a system to maintain its fundamental structure while undergoing environmental change. Ecological resilience can be measured by the magnitude of environmental change that can be absorbed before the system changes to another domain of attraction. In ecological systems, if a system changes to another domain of attraction by environmental change, the system will restructure by changing the variables and processes that control its behavior. This phenomenon is called *regime shift* (Scheffer & Carpenter, 2003). For example, the abrupt change from a clear-water lake to an algae-dominated lake occurs when the ratio of a nutrient reaches the threshold in the process of eutrophication. Once a regime shift occurs in a system, it is difficult for the system to return to the previous domain of attraction. Understanding the conditions and processes of regime shift is required in order to maintain a system in a desired state, and hence, the concept of ecological resilience is important for the management of a system.

The concept of ecological resilience has been applied to the field of social-ecological systems. The concept is expanded in this field, and it is described as (1) the amount of environmental change a system can absorb and still remain within the same state, (2) the degree to which the system is capable of self-organization (versus lack of organization, or organization forced by external factors), and (3) the degree to which the system can build and increase the capacity for learning and adaptation (Folke, 2006).

In the field of social systems, Adger (2000) focuses on the resilience of human society and communities, terming it *social resilience*. Cutter et al. (2008) defines social resilience as “the ability of a social system to respond and recover from disasters and includes those inherent conditions that allow the system to absorb impacts and cope with an event, as well as post-event, adaptive processes that facilitate the ability of the social system to re-organize, change, and learn in response to threat.” Social resilience has the attributes of engineering resilience and ecological resilience. Additionally, the aspects of learning and adaptation of social systems are more emphasized in social resilience.

5. ADAPTATION

5.1 Background of Adaptation

According to Smit and Wandel (2006), the term “adaptation” has its roots in natural science, and specifically, in evolutionary biology. The definition of adaptation in natural science is “the development of generic or behavioral characteristics, which enable organisms or systems to cope with environmental changes in order to survive and reproduce.” The term “adaptation” is used in the context of anthropology, in which cultures or societies that can cope with environmental change quickly and easily are considered to have high adaptability. Since the late 1990s, the concept of adaptation has been used in the study of climate change. The concept of adaptation/adaptability is usually included in the concept of vulnerability and resilience.

5.2 Definition of Adaptation

In the field of climate change, adaptive capacity is defined as “the ability of a system to adjust to climate change, to moderate potential damages, to take advantages of opportunities, or to cope with the consequences” (Gallopin, 2006). Adaptation is defined by the Intergovernmental Panel on Climate Change (IPCC) as follows: “(it is the) adjustment in ecological, social, or economic systems in response to actual or expected stimuli and their effects or impacts. This term refers to changes in processes, practices, or structures to moderate or offset potential damages or to take advantage of opportunities associated with changes in climate. It involves adjustments to reduce the vulnerability of communities, regions, or activities to climatic change and variability” (Macarthy et al., 2001).

Adaptability is synonymous with some terms such as adaptive capacity, coping capacity (capacity to cope), and response capacity (capacity to respond). Adaptation also has some synonyms: mitigation and adjustment. These synonymous terms are used with the same definitions as adaptability or adaptation in some cases, but they use different definitions in other cases. In the case of different definitions, the synonymous terms are often used to distinguish adaptability or adaptation in the context of the target to be operated, the degree of system modification, as well as the timing and duration.

In the context of the target to operate on, IPCC differentiates between adaptation, by defining it as “actions that operate upon the system itself,” and mitigation, by defining it as “actions that operate upon the origin and attributes of the environmental change” (e.g., greenhouse gases reduction) (Gallopin, 2006).

In the context of the degree of system modification, adjustment can be distinguished from adaptation. Adjustment is the action of a system in response to environmental change that does not essentially alter the system itself, and it tends to result in a short-term and minor system modification. On the other hand, adaptation is the action of a system in response to environmental change that fundamentally alters the system itself, and it shifts the system to a new state (Gallopín, 2006). The definition of adaptability and transformability by Walker et al. (2004) is considered to be related to this viewpoint. For them, adaptability is the collective capacity of the human actors in the system to manage the sensitivity and ecological resilience of system, given that the fundamental characteristics of system are maintained. Transformability is “the capacity to create a fundamentally new system when ecological, economic, or social (including political) conditions make the existing system untenable.”

In the context of timing and duration, coping capacity can be distinguished from adaptive capacity. Coping capacity is the relatively short-term ability of a system to survive crises, whereas adaptive capacity is the ability of a system to achieve more sustainable and relatively long-term adjustment (Smit & Wandel, 2006). Gallopín (2006) indicates that there are generally two types of components in the concept of adaptive capacity. The first is “the capacity of the system to cope with environmental contingencies (to be able to maintain or even improve its condition in the face of changes in its environment(s)).” This is assumed to be a relatively short-time ability and to be manifested immediately after an environmental change. The second is “the capacity to extend the range of environments to which it can adapt.” This is assumed to be a long-term ability and is expected to manifest before an environmental change or after the first one occurs.

As described above, this article classifies the concepts of adaptation into three groups: (1) coping capacity, (2) adjustment, and (3) transformability. (1) Coping capacity is the relatively short-time ability of a system to survive a crisis and cope with contingencies during or immediately after environmental change. This is the ability of a system to prevent the existing fundamental structure from collapsing in an emergency situation. It is also related to resistance and resilience, which Dow (1992) defined, and to engineering resilience. (2) Adjustment is the relatively long-term ability to modify a system, while its fundamental structure is maintained, in preparation for expected environmental changes or after an actual environmental change. The adjustment after an actual environmental change can be also called *learning*. Adjustment includes the ability to extend coping capacity, described as (1). (3) Transformability is the ability to create a fundamentally new system when the existing system is untenable (in the case of a regime shift or criticality).

6. LINKAGE OF THE THREE CONCEPTS

The definitions and components of vulnerability, resilience, and adaptation have been explained. Now, the linkages between the concepts and components are discussed for a city exposed to a rapidly occurring natural disaster.

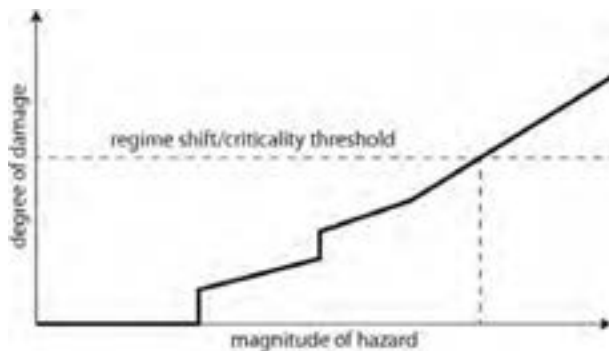


Figure 1: Relationship between the magnitude of a hazard and the degree of damage

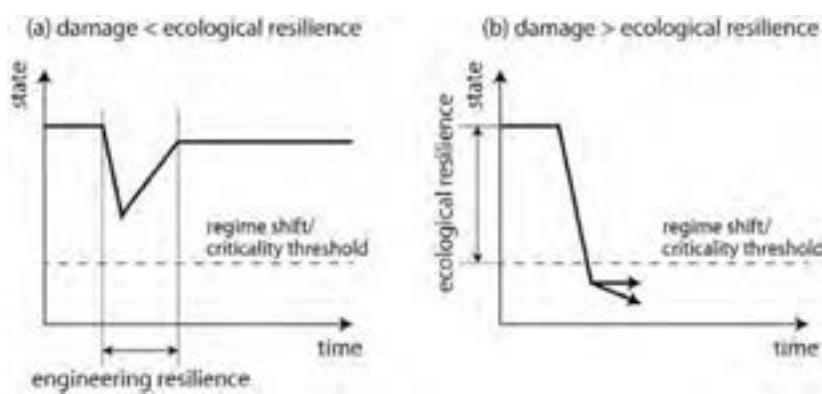


Figure 2: Engineering resilience and ecological resilience

Figure 1 conceptually represents the relationship between the magnitude of a hazard and the degree of damage to a system. The horizontal axis indicates the magnitude of a hazard to which the system is potentially exposed (*exposure*). The magnitude of the hazard gradually increases towards the right, although it is generally thought that a larger magnitude hazard tends to occur with lower probability. The vertical axis indicates the degree of damage that the system undergoes because of the hazard. The function of figure 1 is to indicate the extent to which a system may be damaged if it is subjected to hazards of various magnitudes (Mens et al., 2011).

As the figure shows, the system undergoes no damage up to a certain degree of hazard. For example, assuming that a city is protected against floods by dikes, the city would suffer no damage from small-scale flooding as the dikes can cope with floods to a certain degree. The system starts to undergo damage at a certain magnitude of hazard. In figure 1, the trajectory of the function shown can be discontinuous, and the gradient of the trajectory may not constant, although it is a continually increasing function. This function corresponds to *sensitivity*, which is a component of vulnerability. The higher the *resistance* of a system is, the more gradual the trajectory of the function becomes. In this context, *sensitivity* is related to *resistance*.

Assuming that there is a threshold point of regime shift/criticality, the system can maintain the existing fundamental structure, provided the degree of damage

does not reach the threshold. In this case, the system can recover or regenerate from the damage without losing its structure. The time taken for recovery is the *engineering resilience* or *resilience*, which Dow (1992) has defined (see figure 2.a). After the process of recovery, *adjustment* may be used in preparation for the next hazard. *Adjustment* can also be used before an anticipated hazard. This ability of a system is assumed to improve *sensitivity*, *engineering resilience*, and *ecological resilience*.

Conversely, a system cannot continue and recover if the degree of damage is beyond the threshold. In this case, the system loses its structure and cannot continue to persist. The maximum degree of damage that the system can withstand without resulting in a regime shift or criticality is *ecological resilience* (see figure 2.b). The system enters an untenable situation if a regime shift or criticality occur. In such a case, the system requires to fundamentally modify itself to create a new system. This ability corresponds to *transformability*.

7. CONCLUSION

The concepts of vulnerability, resilience, and adaptability have originated in different fields. However, these concepts have been applied to ecological systems, social-ecological systems, and social systems, and linked with each other. All these concepts are used as approaches for understanding how and why a system responds to environmental change and for managing the system in an appropriate and efficient manner.

Each of the concepts can be divided into some components. There are two major definitions of the concept of vulnerability, while the concept is generally composed of *exposure*, *sensitivity*, and *adaptability*. A system can collapse if the magnitude of a hazard exceeds the adaptability of the system. This situation is called *criticality*. Further, the concept of resilience is classified into *engineering resilience*, *ecological resilience*, and *social/community resilience*. Engineering resilience is the speed of system recovery when the system returns to equilibrium conditions. Ecological resilience is the ability of a system to maintain its existing fundamental structure while undergoing environmental change. *Regime shift* is also an important concept in ecological resilience, and it is similar to *criticality*. Social resilience includes the aspects of learning and adaptation in addition to engineering resilience and ecological resilience. Finally, the concept of adaptation/adaptability is classified based on the target to operate on, the degree of system modification, and the timing and duration. As a result, the concept is divided into three groups: coping capacity, adjustment capacity, and transformability. Finally, the linkages between the three concepts are discussed in the case of a city exposed to a rapid natural disaster.

REFERENCES

- Adger, N., 2006. Vulnerability. *Global Environmental Change*, vol. 16, pp. 268-281.
- Adger, N., 2000. Social and ecological resilience: are they related? *Progress in Human Geography*, 24[3], pp. 347-364.

- Cutter, S. et al., 2008. A place-based model for understanding community resilience to natural disasters. *Global Environmental Change*, vol. 18, pp. 598-606.
- Cutter, S. L., 1996. Vulnerability to environmental hazards. *Progress in Human Geography*, 20[4], pp. 529-539.
- de Bruijn, K. M., 2004. Resilience and flood risk management. *Water Policy*, vol. 6, pp. 53-66.
- de Bruijn, K. M., Green, C., Johnson, C. McFadden, L., 2007. Evolving Concepts in Flood Risk Management: Searching for a Common Language. In: S. Begum, M. J. Stive J. W. Hall (Eds.), *Flood Risk Management in Europe*. Dordrecht: Springer, pp. 61-75.
- Dow, K., 1992. Exploring differences in our common future(s): The meaning of vulnerability to global environmental change. *Geoforum*, 23[3], pp. 417-436.
- Folke, C., 2006. Resilience: the emergence of a perspective for social-ecological system analyses. *Global Environmental Change*, 16[3], pp. 253-267.
- Gallopín, G., 2006. Linkages between vulnerability, resilience, and adaptive capacity. *Global Environmental Change*, vol. 16, pp. 293-303.
- Glaser, M. et al., 2008. Human/nature interaction in the Anthropocene: Potential of social system analysis. *GAIA*, 17[1], pp. 77-80.
- Holling, C. S., 1973. Resilience and stability of ecological system. *Annu. Rev. Ecol. Syst.*, vol. 4, pp. 1-23.
- Holling, C. S., 1996. Engineering Resilience versus Ecological Resilience. In: P. C. Schulze (Eds.), *Engineering Within Ecological Constraints*. Washington DC: The National Academy of Sciences, pp. 31-43.
- Janssen, M., Schoon, M., Ke, W. Börner, K., 2006. Scholarly networks on resilience, vulnerability and adaptation within the human dimensions of global environmental change. *Global Environmental Change*, vol. 16, pp. 240-252.
- Kasperson, J. X., Kasperson, R. E., Turner II, B. L., 1996. Regions at risk: Exploring environmental criticality. *Environment*, 38[10], pp. 4-15, 26-29.
- Longman, P., 2009. *Longman Dictionary of Contemporary English*. 5th edition. Harlow: Longman ESL.
- McCarthy, J. J. et al. (Eds.), 2001. *Climate Change 2001: Impacts, Adaptation, Vulnerability*. Cambridge University Press, Cambridge, UK.
- Mens, M. J., Klijn, F., de Bruijn, K. M. van Beek, E., 2011. The meaning of system robustness for flood risk management. *Environmental Science & Policy*, vol. 14, pp. 1121-1131.
- Miller, G. A., 1995. WordNet: A lexical database for English. *Communications of the ACM*, 38[11], pp. 39-41.
- Smit, B., Wandel, J., 2006. Adaptation, adaptive capacity and vulnerability. *Global Environmental Change*, 16[3], pp. 282-292.
- Scheffer, M., Carpenter, S. R., 2003. Catastrophic regime shifts in ecosystems: linking theory to observation. *TRENDS in Ecology and Evolution*, 18[12], pp. 648-656.
- Turner II, B. L. et al., 2003. A framework for vulnerability analysis in sustainability science. *Proceedings of the National Academy of Sciences of the United States of America*, 100[14], pp. 8074-8079.
- Walker, B. et al., 2004. Resilience, adaptability and transformability in social-ecological systems. *Ecology and Society*, 9[2], art. 5 [online], URL: <http://www.ecologyandsociety.org/vol9/iss2/art5/>

Wilson, G., 2011. *Community Resilience and Environmental Transitions*. 1st edition. New York: Routledge.

Ulaanbaatar City flat region acoustic

S.Barkhas¹, G.Jambalsuren²
Mongolian University of Science and Technology
architecture 2nd course, School Building Engineer and Architecture
ba_james@yahoo.com

ABSTRACT

In architecture, the noise outside of the building is protected by planning, structural, technological and operational way.

Planning ways in architecture are the most common and economical methods to protect rooms from street and industrial noise. The essence of this method is to divide environs into the noisy and quiet region. The city's noise is divided into the 4 zone by noisy level.

- 1. Industrial the zone is the most noisy .it is 80db by sound level.
There are many factories and streets*
- 2. Public and big trading organizations The noisy zone. It is 70db by sound level. Transports are movement*
- 3. Flat region is less noisy. It is 60db by sound level.*
- 4. Quiet zone there are hospitals , libraries and children centers in that zone.*

Key words. Apartments, road of transport, noisy

1. INTRODUCTION

Neiderland and Dany's scientists did research by sound quality. E.Robinson and P.Dadson made research that all animal organization make noises that man's can't hear and can hear abilities

Green structure is the most important planning to struggle against the city noise. The industries and means of transport make noise in city. And means of transport noise is more than others. From the scientists research result, the noise from the transports are:

Trolleybus- 66-76db
Car- 66-86db
Bus- 64-90db
Truck (1.5tn)- 70-90db
Truck (5tn)- 80-98db
Motorcycle- 130-140db

But noise from transport is more than this level. Too much noise is very bad for people's mind and the nervous system. In our research result, there are many buildings and flats along the Ulaanbaatar city arterial magisterial road. From

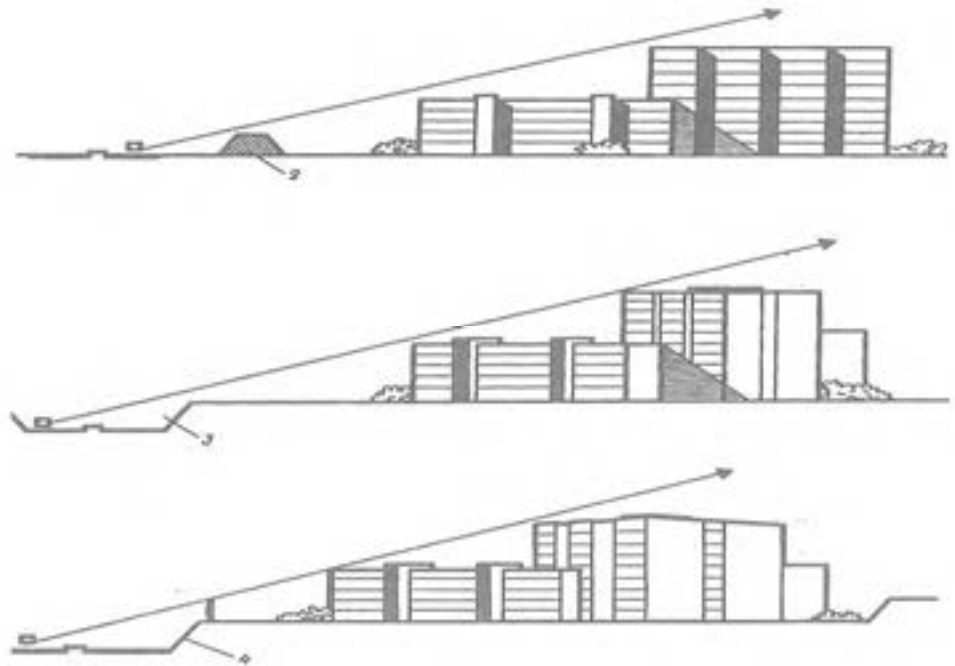
researches, 20-25db leveled that can't influence against human health for a long time.

To see Russian scientist P.E. Leyusheni trees take 26 percent and take away 74 percent. Without green land is get more noisy 5 than green land in 2 metres



To see from the developed countries experience, buildings along the central road are protected by many planning methods.





Elements to protect and separate flats from the road noise



The buildings at center of Ulaanbaatar is along the magisterial road .



The buildings at center of Ulaanbaatar is along the magisterial road .

To do research for a sound wave along the UB city arterial road:

The 12th of the March in 2012

The noise and sound wave along the city arterial road:

5pm-7pm 68-75db

07am-09am 74-79.2db

12pm-02pm 71db

Air humidity 30.8%rh

4 road crossing 68-74db

Bus station 75-80db

To meet to people who live in flat along the arterial road and measure the sound wave:

In No 3, 2nd floor, 1st entrance, 25-30 flat, 5th region, Sukhbaatar district, sound wave was 59.7db at 09pm-11pm. To talk with the citizens, their bedroom is located in road side. And the older people and children live here and there is always noisy at their home.

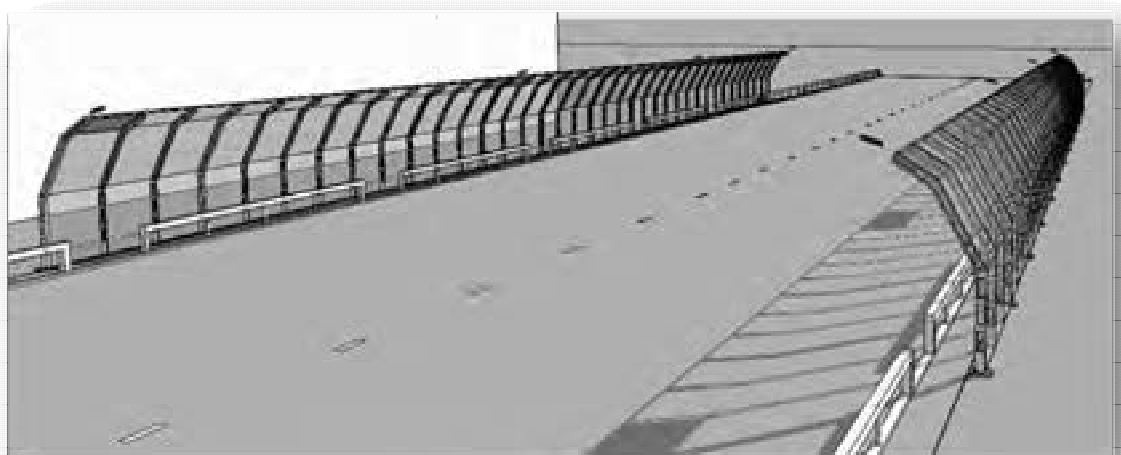
The tools that we have used for the research.

Universal DT-8820
 Light 0-20000lk
 Dampness 25-95%

Temperature 20-750°C
 Sound 35-100db



We offer an idea to save energy and protect people's health for solve the problem of bad influence of transports' noise that the people who live in flats along the arterial magisterial road. It is possible to realize the idea in our country for our own resources and very effective to save energy.



Sun screen

Working temperature -40°C - +40°C

Lamp Working temperature -250°C - +400°C

Average work hours- 6000hr

Storage charge

Working temperature -250°C - +500°C

Capacity 65a.hr

Light power by 50wt Additional source of charge is 11wt

Time to turn on light by energy that storage a day is 100hr

Sun battery system's main advantages:

- No need to constantly care, fuel and professional worker
- Any bad influence for surroundings, ecological clear source of energy
- Comfortable to use in a country where substructure doesn't developed well
- Working years- 20-30years
- There are 7-21days are not sunny in a year and very few cases to be cloudy for more than 2 days

Structural materials that used for our offering idea:

Glass barrier: 12mm thick dried glass

Width 180cm, height is 330cm

1m² 12000□ 4.5 times durable than ordinary glass

Storage sun battery: 60cm width

180 cm long one panel is 20000□ worth

Frame and column:330m height- 4000□

Total money sum: 7,696,000□ in 30m distance

24,320,000 in 100m distance

Assessment

We have done research and report by topic "Ulaanbaatar city flat region acoustic". By this report, we have researched to protect people's health for solve the problem of bad influence of transports' noise that the people who live in flats along the arterial magisterial road.

1. From researches, 20-25db leveled that can't influence against human health for a long time. But in result of our research, nowadays in Ulaanbaatar city, this statistic opposite and people who live in flats along the arterial road is getting hurt by their health, the nervous system and mentally. There is lack to supply people's comfortable environment.
2. Flats window along the Ulaanbaatar city arterial magisterial road is not to be enough to protect from noise influence. So theplace high performed windows that do notconduct noise is very important way to help those people.
3. So we hope that to implement our idea, to summarize and improve the process to grant city places to people and architecture planning, and do researches from professional organizations for make up people's acceptable living environments and following the example of developed countries and make enough level of protecting from noise, will give an effective result.

Resources:

V.V.Aurov "ArchitecturnayaPhysica" 2001

N.M.Gusev "Osnoviistroitelnoyphysicii" 1990

V.M.Ilinelskii "Stroitelnoyphysicii" 1984

Lectures of Magister S.Amgalan

Lectures of Magister B.Mandakh

Writers: architecture 2nd course S.Barkhas

G.Jambalsuren

Leaded teacher: B.Mandakh

Eco fence the improvement of the Ger district living environment

G.Ganbat¹, G.Punsaldulam² and Sh. Enkhtungalag³
University of Science and Technology, Civil Engineering and
Architect School
Architectural and Drawing Department
Ganbat_art0713@yahoo.com

ABSTRACT

Since 21st century started human life development has been intensively increasing. The one view of such development is the wonderful cities which are making the face of each countries. The biggest cities of the world are paying the higher attention to the tendency for the eco – solutions which toward to the communication between the human and the nature, except the construction exterior, façade view and the interior design of the construction development. City development is improving its quality based on the recent requirement of such cities and is creating the eco-development designs for them. According to this tendency we aim to create the development solutions for the ger area in the capital city of Mongolia – Ulaanbaatar, which are really common placed in every area around the city. Recent problems in the Ger districts:

- *Unordered location*
- *The dust from the soil road*
- *Air pollution /smoke/*
- *Open trashes and garbage*
- *The city view*
- *Lighting system*
- *Un safe usage of the water*

As we known, the recent fences are only for the separation of the private-owned land. This influence for the city view harmfully and make a bad design for the modern city. In order to break this traditional style, we offer the mono-usage and multi - beneficial solution. This is the ECO-FENCE, which can solve the city view recent problem

The survey result in the Ger district: By the survey, we have chosen 1500 families in Khan-Uul district, and 1410 families or 94% of them have wooden plate fences, 67 families or 4.5% of them have block-stone fences. The rest 23 families or 0.5% of them have brick and metal fences. We have made the below calculation based on the above survey result, it means for 94% of the ger district families. This eco-fence can design the comfortable living environment in the ger district and solve the messy locations, saves cost and nature-friendly decisions for the life style of people. It also can influence to the beauty and psychological view of people in their living environment. Not only in UB city, in the provinces this solution brings very reliable and comfortable fence generation.

Introduction

This project is the most common project for replanning the ger micro-district of Ulaanbaatar. Therefore it was included in the senior development plan of Ulaanbaatar city 2020 and certified the strategic project “Development of ger micro-district”. Current fences of ger micro-districts are becoming the front side but it’s appearance doesn’t look well. That is why displacement of current fences into eco-fence is beneficial. By the changing fences we can reduce the use of wood in ger micro-district and improve the appearance of Ulaanbaatar city.

Preface

70% of Ulaanbaatar’s citizens are living in ger micro-district also ger micro-district’s expansion raised to 60%. For example in 2000 year 51623 people of all citizens were living in ger district, in 2011 it raised to 103241.60% of population in aimag’s center are living in bad environment. The rise of citizens from countryside raises the ger district’s expansion.

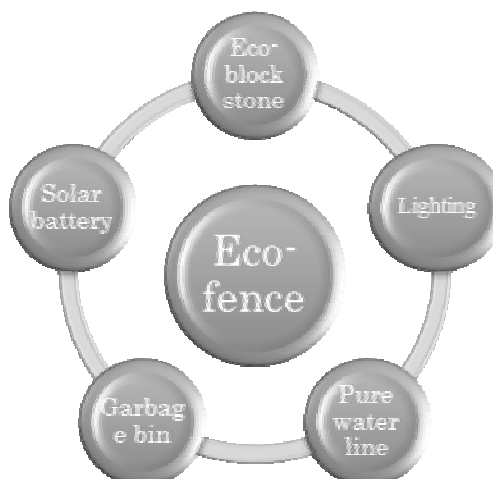
That is why it is the most important issue to decide. Government has started the housing area project but it is cannot house all people who live in ger micro-district. According th international analysis housing raises the population and crime possibility.

Since 21st century started human life development has been intensively increasing. The one view of such development is the wonderful cities which are making the face of each countries. The biggest cities of the world are paying the higher attention to the tendency for the eco – solutions which toward to the communication between the human and the nature, except the construction exterior, façade view and the interior design of the construction development. City development is improving its quality based on the recent requirement of such cities and is creating the eco-development designs for them.

According to this tendency we aim to create the development solutions for the ger area in the capital city of Mongolia – Ulaanbaatar, which are really common placed in every area around the city.

1.Characteristics of eco-fence.

Wooden fences are used as a separator of privet-owned lands. Also this fences are losing it’s quality, form and facade by time. In order to break this traditional style, we offer the mono-usage and multi - beneficial solution



1.1Eco-block stone.

Eco-block stones are made of alabaster material which are specially foraminated. The most important characteristic is not harmful for man, easy to use, resistant and thermal preservation is high. Block stone size is 150x250x1000

Technical details of the physical and chemical characteristic of the Block Stone

	Characteristics	Unit	Meaning of the details			
			Standard	By the Analyze result		
				δ=10sm	δ=15sm	δ=20sm
1	Bar density	kg/m ³	Less than 700	600	600	600
2	Bar weight	Kg/pc	Less than 23	20	20	20
3	Bar capacity	KN	Less than 1.5	1.5	2	2
4	Sound separation	dB	Less than 30	41	42	45
5	Heat separation	Ro (m ² oC/B _T)	-	0.59	0.88	1.18
6	Stability of the pressure	Kg/h/sm ²	-	17	17	17
7	Individual radio activeness	Bk/kg	Less than 370	212.1		
8	Fire Resistance	minute	Less than 180	180<		

1.2 Solar battery.

TiO₂ absorbs the solar energy to produce the electricity, It is usefull and easy to produce. It is a plate made of cooper, silinium and indium also it is semi-conductor solar element.

Domestic use of electricity, cost of electricity:

One house usage is 17000-25000kW:

1. Iron-1monthly-8h*1.4kW=11.2kV*84=940kW
2. Oven-1h-2kW, 1daily-4h=8kW,
1monthly=240kW*84=2016kW
3. Light-1h=100W, 1daily-6h=600W,
1daily=600*30=18000W=18kW
4. Washing machine-1h=330W 1daily=4h=1320W=1.32kW
1monthly=6.6kW
5. Vacuum cleaner -1h=1.5kW
1monthly=7.5kW
6. Rice cooker-1h=0.8W 1monthly=6kW

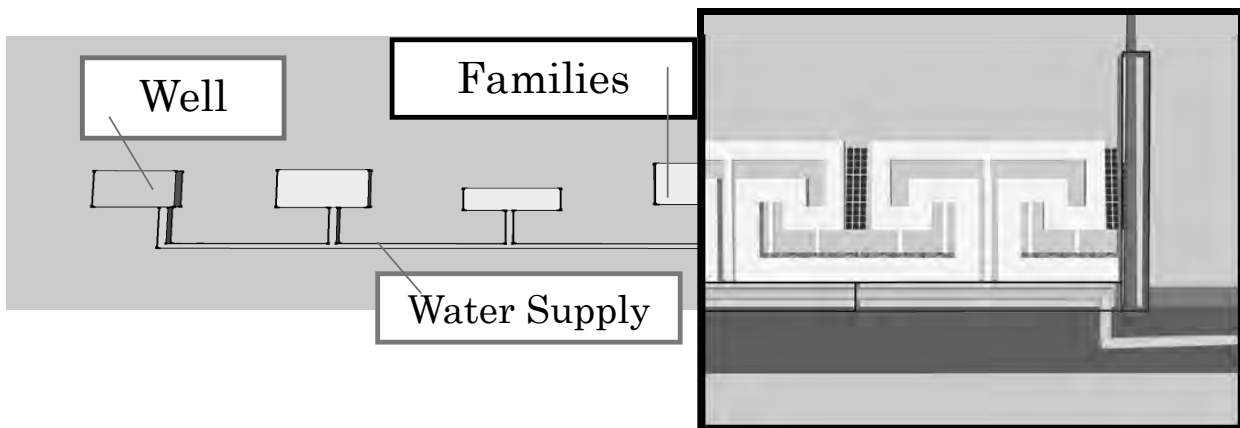
1.3 Garbage bin.

The very important thing in the ger district is the garbage problem. In order to keep the human labor we also offer the garbage assortment solution in this area. The garbage bins will be installed with the Eco-Fence and it would be separated for the below:

- Recyclable garbage
- Bio-Garbage
- Ashes

1.4 Pure water line

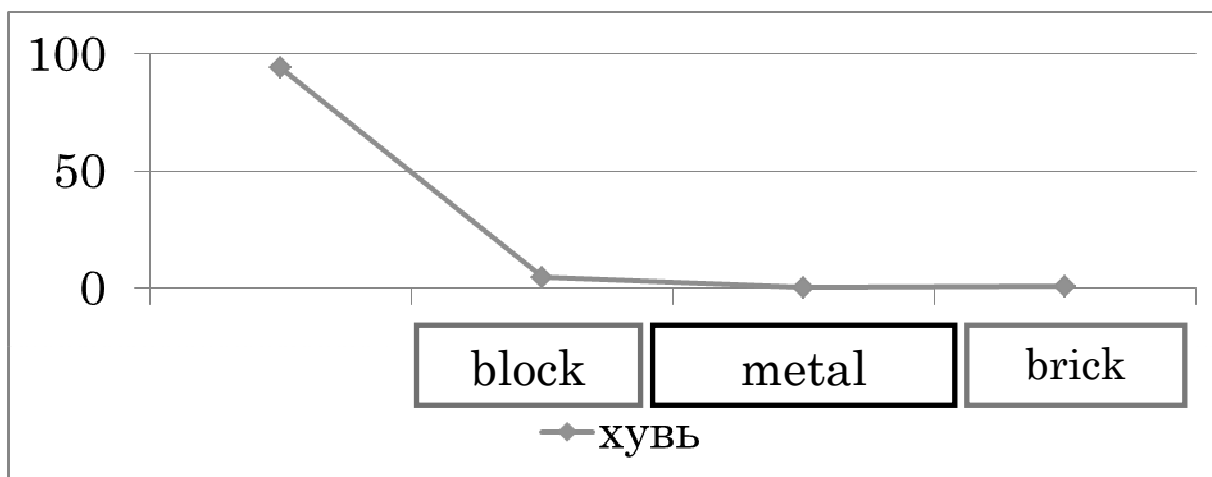
That fence contains pure water lines, and helps to decrease the unclean usage of the well water, and keeps the human labor in ger districts.



Installing all of this instruments makes environment more comfortable for people. Solar battery will be installed to the wall and it will supply lighting and other electric gadgets.

2. The survey result in the Ger micro-district:

By the survey, we have chosen 1500 families in Khan-Uul district, and 1410 families or 94% of them have wooden plate fences, 67 families or 4.5% of them have block-stone fences. The rest 23 families or 0.5% of them have brick and metal fences.



We have made the below calculation based on the above survey result, it means for 94% of the ger district families.



3. Cost:

Total fences of the ger district: 103.241pc

If we estimate that a family has 70m long fence, it must contain 3-4 m³ wood. On the recent market this amount of wooden plate cost 450.000MNT-600.000MNT, which only for the frame usage.

From above, total ger district fence price will be like below:

$$103.241 \times 500000 = 51.620.500.000 \text{MNT}$$

If a family were involved for the apartment program, it would take 20 years at least. It says that during this time, a family has to renew their fence every 7-12 years. In this case the fence cost will be like below:

$$51.620.500.000 \times 2 = 103.241.000.000 \text{MNT}$$

4. Ecological survey:

Total ger micro- district fence requires $103241 \times 4 \text{m}^3 = 412.964 \text{m}^3$

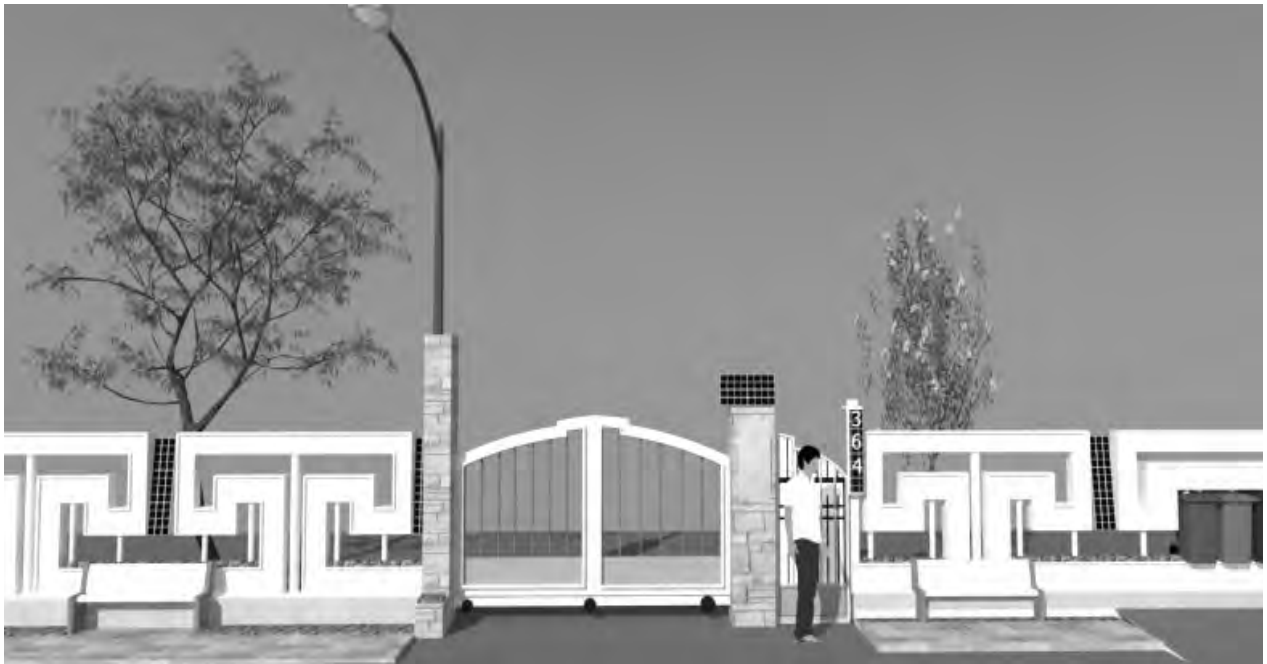
Normally, one tree can be divided into 12 pieces of the wooden plates. It means 1m³ wooden plate destroy 10 trees. In the forest of Mongolia there are 2500-3000 trees in every one hectare area. Until the apartment program will have implemented,

$$412964 \times 10 = 4129640 \quad 4129640 : 3000 = 1377 \text{ hectares}$$

If each family renew their fences twice within 20 years, $2754 \times 3000 = 8.262.000$ trees or $1377 \times 2 = 2754$ hectares of the forest will be destroyed completely.

5. Implementation.

- Eco block stone /25x100cm/ 3.000 MNT-5.000 MNT
- Pure water lines
- Lighting : Street nickel lighter, 3.5 m high , Price 185.000 MNT
- Garbage bin
- Solar battery – 200.000 MNT – 250.000 MNT
- Budget cost: 750.000 MNT – 850.000 MNT for the single family fence , based on the owned area

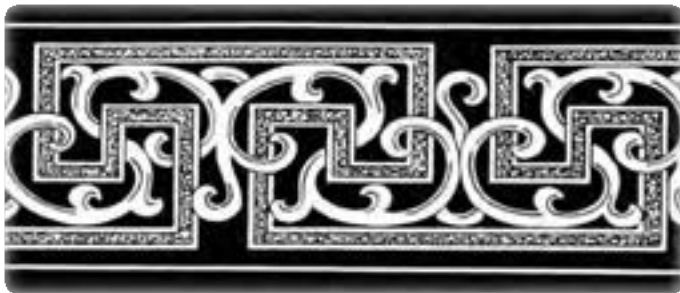
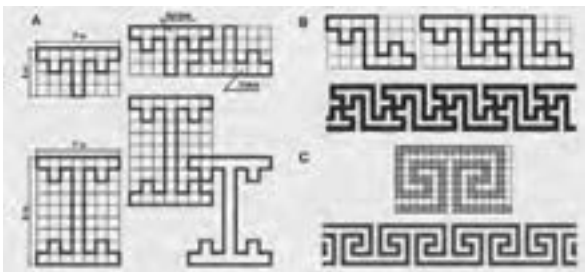
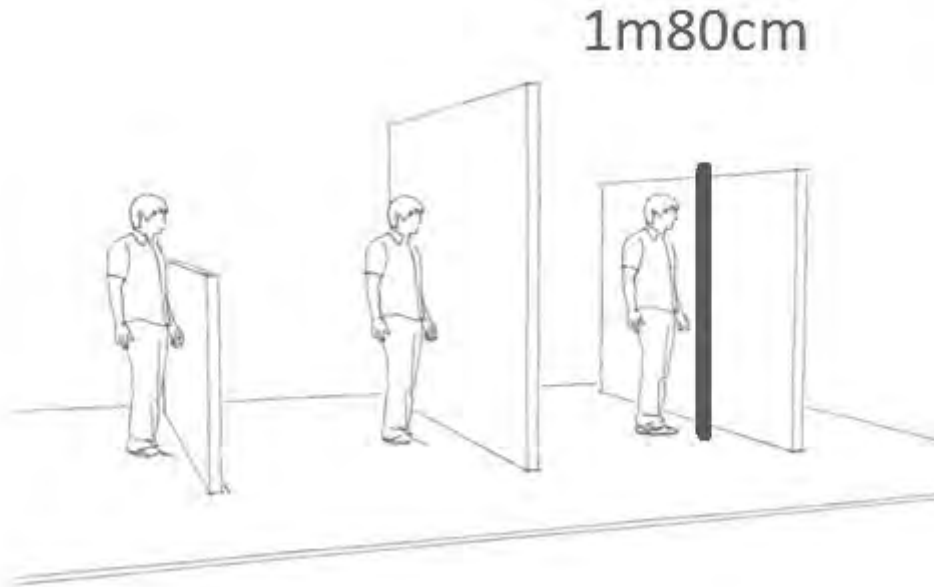


Fence design.Hammer like ornament:

1. National pattern.
2. Lesser material usage.

3. Hammer like ornament never ends.

Our fence height will be 1.8 m which is very confident with the human average height.





Conclusion

This eco-fence can design the comfortable living environment in the ger district and solve the messy locations, saves cost and nature-friendly decisions for the life style of people. It also can influence to the beauty and psychological view of people in their living environment. Not only in UB city, in the provinces this solution brings very reliable and comfortable fence generation.

Used resources:

- <http://ecomngl.posterous.com/1> or [What does the garbage mean?](#)
- <http://www.eaoph.info/pdf/2009papers/P1.pdf> Population prevalence, urban living environment
- Google Earth
- <http://biznetwork.mn/blog/show/id/6147>
- Ornament symbolism
- <http://barilga.mn> Lighting

Issues and challenge in legal framework related to urban redevelopment in Mongolia

Toshiaki KUDO¹, Tomoko ABE²

¹General Manager, Urban & Regional Development Department,
Global Division, Oriental Consultants Co. Ltd., Japan
kudot@oriconsul.com

²Planner, Overseas Department, ALMEC Corporation, Japan

ABSTRACT

This paper describes current issues and challenge of legal framework for urban redevelopment in Mongolia, and mechanism of urban redevelopment projects in Ulaanbaatar. The Urban Redevelopment Law (URL) has been drafted since 2010 and is to be finalized. The law is expected to facilitate urban redevelopment projects in a more proper and smoother manner, though it still requires operational improvement through actual application. Ideas to apply new urban redevelopment mechanisms are proposed by a JICA project, the Project on Capacity Development in Urban Development Sector in Mongolia (MUGCUP) based on studying and monitoring actual urban redevelopment projects in the city since May 2010.

Keywords: urban redevelopment, urban redevelopment law, ger area development, old apartment reconstruction

1. INTRODUCTION

Ulaanbaatar City's population has grown at a 3.3% per annum over the last two decades much faster than the national average of 1.3% per annum. Most of them have settled in so-called *ger* area where engineering and social infrastructure are not develop adequately because the central apartment area in Ulaanbaatar City cannot absorb all the increasing population. Presently in Ulaanbaatar City around 60% of the city population live in *ger* area and the rest live in the central apartment area which is connected to the central utility systems.

This urbanization trend has caused *ger* area sprawling toward outside, and redevelopment in the central area and redevelopment of *ger* area in a rather disorderly and unplanned manner. From safety aspects, *ger* area has been expanded without proper infrastructure that hampers emergency vehicle approach and flash flood control, so on; on the other hand, in the central area, many old apartment buildings are evaluated as non seismic resistant and many infill development are implemented on apartment courtyards.

To cope with these urban developments, the legal framework related to urban development has been reformed by amendment of existing laws and new laws under the *New Development Program* approved in June 2010. Among them, the

Urban Redevelopment Law (URL) has newly been drafted to facilitate urban redevelopment projects.

The JICA Team of the Project on Capacity Development in Urban Development Sector in Mongolia (MUGCUP) has worked with the Mongolian counterparts since June 2010. The project has worked on overall legal framework related to urban development with focus on the Urban Redevelopment Law and its rules and regulation, as well as smooth implementation of urban redevelopment projects in Mongolia based on issues found through monitoring the actual urban development situation in Ulaanbaatar.

2. PROPOSED LEGAL FRAMEWORK OF LAWS RELATED TO URBAN DEVELOPMENT

2.1 Legal framework related to urban development

After having reviewed the legal structure related to urban development in Mongolia, the JICA MUGCUP Team has proposed a legal structure related to urban development with the Urban Development Law as the center with major relevant laws, as shown in Figure 1.

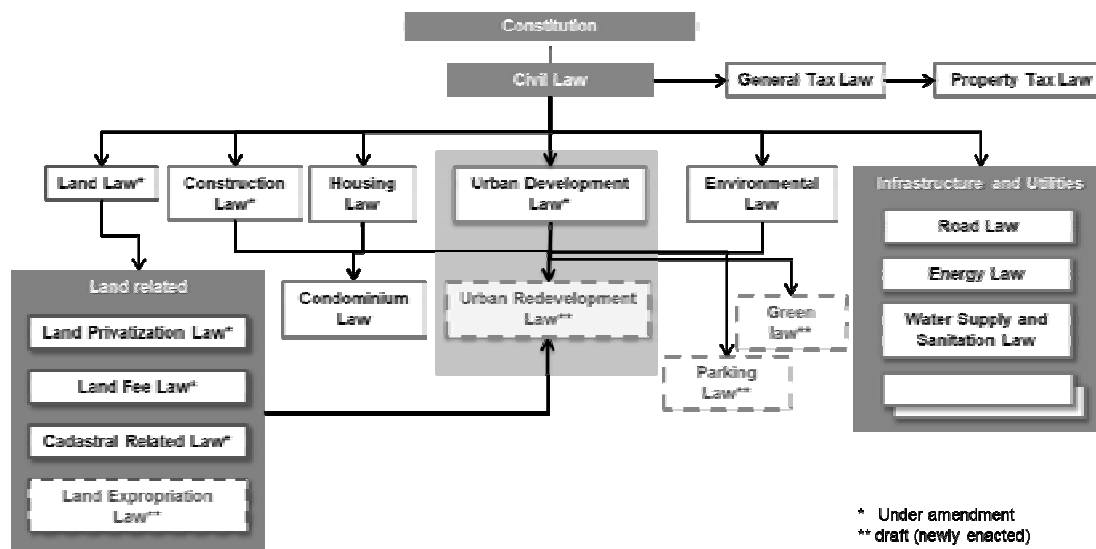


Figure 1: Overall Legal Framework related to Urban Development

2.1.1 Current Legal framework related to urban development

In general, all Mongolian legal frameworks are complied and/or coherent with the Constitution of Mongolia and Civil Code of Mongolia in terms of rights and duties of the Mongolian governments and people.

Construction activities shall follow the technical norms and standards stipulated by the Construction Law. Urban planning and development activities are ruled by the Urban Development Law, which stipulates mandates, powers and duties of the government sector for urban development planning and projects implementation. This law is the core of the legal system for urban development.

Land issues have been complicated in Mongolia since the time when land ownership started being privatized (700m² per person), and are related to several relevant laws, that is: Law of Mongolia on Land; Law of Mongolia on Land Fees, Law on Allocation of Land to Mongolian Citizens for Ownership, Land issues are also related to administration of housing, geodesy and land management, taxation of property tax and other land systems. For these ends, several laws have been newly developed, enacted and amended since 2002 when land privatization policy was executed. Privatization process of land somehow urbanization spreading outward which thereby make it difficult to acquire land necessary for urban engineering and social infrastructures.

Development and construction of urban infrastructures and utilities are regulated by respective law and/or regulations, such as Law on Utilization of Urban Water Supply and Sanitation, Law on Roads, Law on Energy, Law on Telecommunications, so on. In addition to these laws, technical standards for design and construction are regulated by respective “norms.”

2.1.2 Reformed legal structure for urban development

As illustrated in Figure 1, urban development-related laws are composed of three laws with a hierarchy with the Urban Development Law (UDL) which is due to be amended, followed by the Urban Redevelopment Law (URL) under drafting. Needless to say, these laws must be complied with principles of the Mongolian Constitution and Civil Code. The UDL shall cover the basic policies and legal framework of powers, responsibilities, and duties of the government sector for urban planning, land use and urban development. Under this policy umbrella, the URL, or the administrative law for urban redevelopment projects, is to be enacted.

These urban-related laws are interrelated or referred to other relevant laws such as land-related laws, housing-related laws, infrastructure-related and environmental laws.

3. URBAN REDEVELOPMENT LAW

3.1 Urban Redevelopment Law under drafting

In urban development sector, the JICA Team has focused on urban redevelopment projects and worked on the Urban Redevelopment Law (URL) and cooperated with the Mongolian counterpart of Ministry of Construction and Urban Development (MCUD) and Ulaanbaatar City since 2010.

The latest draft of the Law was made in June 2012. The Law consists of nine chapters and 30 Articles with the following: general provisions, plenary power of

government organizations handling urban redevelopment activities, urban redevelopment project types, implementing body, requirements of project and project area, funding, obligations and responsibilities of project participants, real estate and its right conversion in project area, monitoring system, compulsory land acquisition.

The URL covers five types of urban redevelopment projects, namely: (1) land readjustment projects in ger area, (2) redevelopment (ger-to-apartment) project in ger area, (3) reconstruction of old apartment, as well as (4) redevelopment of the area that does not meet the planning standards, and (5) redevelopment project in public land.

3.2. Important issues of Urban Redevelopment Law and related laws

The URL is composed of several vital concepts which shall be coherent with other relevant laws. In this regard, there are several concepts: (1) land use control (zoning) , (2) compulsory land acquisition, (3) compensation, (4) land and property evaluation, (5) right conversion, (6) reconstruction of old apartments, and (7) public participation.

(1) Land use control (zoning)

Urban redevelopment projects should be planned and designed in urbanized area, not in environmentally preventive and/or conserved zones. Thus, the land use zoning policies in the city is consistent with those stipulated in the URL, or more specifically, legal directions deliberated in the Urban Development Law and the Land Law.

(2) Compulsory land acquisition

The URL needs to regulate the procedure of land expropriation process, in case that some land owners or right holders will not participate in the urban redevelopment projects, but move out of the project area, getting the compensation in any form. In general, the urban redevelopment project is undertaken in such a way that all right holders residing in the project area shall gain more comfortable and valuable living environment rather than before, with their property rights being protected. For the sake of compulsory land acquisition for public service facilities, the legal process has not been properly regulated, although this aspect is stipulated by several laws, including the Mongolian Constitution, the Urban Development Law, the Land Law and Law on Allocation of Land to Mongolian Citizens for Ownership. Since the legal framework for this issue is not integrated, but still fragmented, the independent law, named “Law on Land Expropriation” will be soon proposed by MCUD with ADB’s technical assistance. However, the logical consistency between this law and the URL should strictly be kept.

(3) Compensation

The rational compensation scheme, which is mostly related to the land expropriation issue, needs to be cleared for those who are negatively affected by the urban redevelopment project. This aspect is mentioned in the Mongolian

Constitution, the Civil Code, the Land Law and the Urban Development Law. The basic concept should be mutually coherent among those relevant laws.

(4) Land and Property Evaluation

It is clearly stipulated in the Mongolian Constitution that the compensation shall be evaluated at market prices. However, as the market mechanism in the real estate sector is often distorted or not perfect, thereby being likely to be speculated, the rational evaluation of land and property is of a vital issue for land, urban development administrations. Although the Cadastre Law, the Property Evaluation Law and the Condominium Law stipulate this issue with respective purposes, a rational method of the valuation needs to be defined.

(5) Right conversion

The *right conversion* may be a new concept. However, this is the most vital part of procedure attached to urban development projects. The original rights of property owners should be maintained during and after the project, even if the original right is converted to another form, that is: the land to apartment floor, the land to another plot of land, old apartment floor to new apartment floor, so on. The Housing Law, which stipulates right conversion of the old apartment floor to the new apartment floor, is directly pertinent to the URL on this issue.

(6) Reconstruction of old apartments

Since the Housing Law, amended in February 2010, depicts an official procedure of the reconstruction of old apartment buildings, the URL shall basically refer to such a procedure as defined. In this process, the most noteworthy policy is that the tripartite agreement among the apartment owner, the investor and the local government shall be made for the implementation of the old apartment reconstruction project in which the old apartment building is evaluated as “non-seismic resistant and urgently need to be rebuilt” by the State Inspection Agency.

(7) Public participation

A participatory approach in a democratic manner is indispensable to facilitate any types of urban redevelopment activities. This perception has been prevailed in the Urban Development Law. The public participation has two types of involvement: one is the public hearing type where a wide range of stakeholders are involved in planning and decision-making process of the project; and the other is the consensus building type among right holders of and/or directly-affected people by the project. The former is relevant to the Urban Development Law and the latter shall be functionally regulated by the URL and the Housing Law.

4. RULES AND REGULATIONS OF URBAN REDEVELOPMENT LAW

4.1 Rules and regulations stipulated in Urban Redevelopment Law

Mongolian manner for the legalization process is as follows: (1) laws should be drafted in accordance with the “Law on Preparation of Draft Laws & Parliament Resolution and its Submission” and submitted to the Parliament for approval, and

(2) rules/regulations stipulated in the law should be prepared and approved by Minister's Order.

“Rules and Regulations” which are defined and/or stipulated in the draft Urban Redevelopment Law shall be prepared by Agency of Land Administration, Geodesy and Cartography (ALAGaC) under the MCUD in close collaboration with the JICA Project Team. In the draft URL Law (June 2012 version), the following seven rules/regulations are due to be prepared and approved.

- (1) *Methodologies for Calculation of Compensation and Rules for Payment*, which shall be regulated by the Government of Mongolia
- (2) *Rules on Land Reduction and Contribution for Land Readjustment Project*, which shall be regulated by the Government of Mongolia
- (3) *Rules on Selection and Designation of Project Area* which shall be regulated by the Government of Mongolia
- (4) *Rules and Guidelines to Manage Project Implementation Process*” which shall be prepared by MCUD,
- (5) *Rules and Guidelines to Facilitate Old Apartment Reconstruction Projects*” which shall be prepared by MCUD
- (6) *Project Implementation Model*” which shall be prepared by ALAGaC
- (7) *Model Format of Tripartite Contract/Agreement*” which shall be prepared by ALAGaC

4.2.2 Proposed rules and regulations

In addition to the above mentioned seven rules/regulations, the JICA Project Team has proposed that vital issues be stipulated by rules and regulations under the draft URL, including (1) materialization of urban redevelopment basic policy, (2) implementation body, (3) consensus building, (4) participation and protection of right holders, (5) computation and payment of compensation, (6) beneficiary-pay-principle, (7) tripartite contract/agreement, (8) right conversion, (9) land expropriation, (10) establishment of monitoring committee and its responsibility and duties, (11) project financing and subsidy system.

(1) Materialization of urban redevelopment policy

The draft URL stipulates that the Urban Redevelopment Basic Policy must be in accord with the following principle for urban redevelopment projects as well as Urban Development Basic Policy stipulated by the draft URL. To materialize the basic policy, the following shall be ensured: (1) citizens' right to live in a healthy and safe environment, (2) social interest and rights, and (3) prevention and protection from natural disaster based on evaluation of disaster risk and evacuation.

In this regards, the following should be included: secure of land for public facilities in urban redevelopment promotion area and their development, restriction on construction and land right transaction, and special measures in urban redevelopment project area.

(2) Implementation body

The draft URL stipulates that the implementation body of the urban redevelopment project is: (1) aimag or city governor or (2) legal entity. Qualification requirement and selection process of legal person and project-related rights as the implementation body shall be regulated.

The following items should be included as regulation: qualification and capability of implementation body, conduct of competition to select implementation body, independent project account, repeal of approval of implementation body.

(3) Consensus building

To secure smooth implementation of the project, a guideline to build consensus among residents is to be provided. Detailed process for projects of Redevelopment Projects of sub-standard, inadequate urbanized area, Reconstruction of Old Apartments, Land Readjustment Project in ger area, and Urban Redevelopment Project in ger area are to be regulated.

The rules/regulations should include: residents' consensus on urban redevelopment area and draft basic plan, agreement of right holders on project implementation plan and tripartite contract, criteria for execution of compulsory land acquisition.

(4) Participation and protection of right holders

Right which the residents who take part in the urban redevelopment project hold project before the project must be legally protected during and after the project.

Accordingly regulations shall be provided, including scope of right holders to be protected, preservation of original right during construction period, legal base for resident representative organization, resident participation and decision making process by consent of majority.

(5) Computation and payment of compensation

The draft URL defines compensation and provides that the government decides compensation items and their calculation and payment methods. Compensation for the right holders who do not participate in the project and move out or the right holders whose lands are acquired is to be stipulated.

The rules/regulations should include: compensation items in urban redevelopment projects, calculation method of compensation money, payment of compensation money, settlement money.

(6) Beneficiary-pay-principle

Within the extent of economic benefits accrued from the project that the implementation body and right holders receive, it is reasonable and necessary to request them to shoulder some portion of development cost of certain public facilities in order to uplift public welfare and realize an equitable society, which is the base of urban redevelopment projects.

Accordingly rules and regulations on *beneficiary-pay-principle* are proposed, including: cost burden sharing system for development of public facilities, basic principle of land donation in land readjustment projects.

(7) Tripartite contract/agreement

The draft URL stipulates “Tripartite Contract” which shall be concluded among (1) the aimag (city) governor, as project initiator, (2) the implementation body selected through a proper competitive bidding process, and (3) the organization representing the right holders. This contract is the base for the project implementation. Urban redevelopment projects are prescribed as not only an economic activity but also a public social activity.

The tripartite contract should include: legal status of tripartite contract, invalidity of tripartite contract, explicit responsibility of project continuity.

(8) Right conversion

Right conversion, stipulated in the draft URL, is one of the most important procedure in urban redevelopment projects. Accordingly, rational right evaluation method and appropriate rules of right conversion are required for consent of the right holders. A basic rule of right conversion in Japan is equal value based exchange while in Mongolia, the Housing Law stipulates equal-floor-area based exchange of apartment units for reconstruction of old apartment buildings.

The right conversion system should include: land evaluation method and evaluation base, apartment building evaluation method and evaluation base, right conversion between ger (khashaa, or wooden fence) land and apartment, right conversion in old apartment reconstruction projects, right of shops on first floor and its compensation in old apartment.

(9) Land expropriation

The purpose of the URL is to improve living environment by securing land necessary for development of public facilities with consent of the residents, not by compulsory land acquisition. Thus, compulsory land acquisition stipulated in the draft URL should be the last resort to take. This should be coordinated with the Law on Land Expropriation which is now under draft.

(10) Establishment of Monitoring Committee and its responsibility and duties

In order for the Monitoring Committee stipulated in the draft URL to function effectively, establishment, responsibility and power, and operation and management of the Monitoring Committee shall be specified.

The rules/regulations should include: procedure of establishment of monitoring committee, monitoring activities and internal articles of the monitoring committee.

(11) Project financing and subsidy system

As for “Financing for urban redevelopment project” stipulated in the draft URL, the implementation body shall basically finance the project cost. However, development cost of public facilities needs to be shouldered by the administrative

entities of public facilities. In addition, a wide range of subsidy is required to facilitate quality urban redevelopment projects.

Such governmental support should include: government budget for infrastructure projects, utilization of public financing system, technical assistance to formulation of plans of urban redevelopment projects, subsidy system for urban redevelopment projects, tax reduction for urban redevelopment projects, independent project account system.

5. CONCLUSIONS

The rapid urbanization has caused urban sprawl in the ger area without adequate infrastructure on the one hand; many old buildings in the central area should be reconstructed because they have become non-seismic resistant. At the same time, the city suffers from traffic congestion, air pollution and other urban problems.

To solve these urban problems, the Mongolian Government has made an effort to amend or newly enact laws relevant to urban development under the New Development Program. However, Mongolia, which had adopted urban planning system under state-planned economy, has to introduce planning and development concepts under market economy which are new to them. Accordingly, it is rather difficult to develop many urban development related laws with consistency in a short time.

Presently Mongolia is experiencing a transition period in urban planning and development under rapid urbanization pressure accelerated by mining-sector led economic growth. In this situation, the following among others are of importance to promote urban development sector properly in Ulaanbaatar: (1) establishment of comprehensive and coherent legal framework related to urban development, (2) development of proper operational rules and regulations of the URL, (3) adoption of democratic, participatory approach in planning and development process, (4) introduction of new concept of right conversion based on appropriate property evaluation, and (5) strict enforcement of these laws and regulation.

The JICA MUGCUP Project has monitored actual projects of land readjustment projects in ger area, redevelopment projects in ger area, and old apartment reconstruction projects to sort out issues, and has proposed legal framework related to urban development and operational rules and regulations of the URL, and working together with Mongolian counterpart to finalize it. Ulaanbaatar City will be reformed to more safe against disasters such as earthquake and flashflood through proper urban redevelopment projects in ger area and the central area, which are stated in the Urban Redevelopment Law and promoted by the JICA MUGCUP Project.

REFERENCES

JICA, *Final Report, the Study on Master Plan and Urban Development Program*

in Ulaanbaatar City in Mongolia (UBMPS), March 2009

JICA, *Progress Report 4, JICA project, the Project on Capacity Development in Urban Development Sector in Mongolia (MUGCUP)*, May 2012

Working Group of Urban Redevelopment Law, Ministry of Construction and Urban Development of Mongolia (MCUD), *the Urban Redevelopment Law (draft)*, June 2012

A challenge toward application of new urban redevelopment mechanism in Ulaanbaatar City

Tomoko ABE¹, Toshiaki KUDO²

¹ Planner, Overseas Department, ALMEC Corporation, Japan
abe@almec.co.jp

² General Manager, Urban and Regional Development Department,
Oriental Consultants Co. Ltd., Japan

ABSTRACT

This paper describes experiences and current issues, proposed mechanism of urban redevelopment projects in Ulaanbaatar City which are proposed by a JICA project, the Project on Capacity Development in Urban Development Sector in Mongolia (MUGCUP) which has been conducted since May 2011. The basic principle of urban redevelopment projects are aimed to improve living environment with basic infrastructure, by applying of “right conversion” which assess property value fairly and redistribute new properties (land or apartment floor), or resettlement with compensation. However it is still difficult for citizens to understand this concept which is new and unfamiliar to them. After stipulation of the new Urban Redevelopment Law, it is expected that both citizens and developers understand and agree to the process of right conversion with participatory process, and urban redevelopment projects will be further promoted. In parallel with formulation of new legal and institutional system, efforts of promotion of understanding of citizens are indispensable. Proposals and ideas to apply new urban redevelopment mechanisms based on lessons learned from current challenges and issues in the city as well as experiences in Japan are stated.

Keywords: new urban redevelopment mechanism, right conversion, consensus building, public participation, urban redevelopment law

1. INTRODUCTION

The urban structure of Ulaanbaatar City is clearly separated into apartment area where central infrastructure network are connected, and Ger area where urban infrastructure and utility services are limited or not available. Though citizens in Ger area originally immigrated from rural areas, younger generations seek for modern residential types such as detached houses and apartments. Though residents of old apartments in the city center can easily access to water, sewage and heating, they are in danger of collapse and destruction of apartments in the event of strong earthquake, which were constructed from 1930's to 1960's. The central and local governments have implemented policies and projects to redevelop Ger area into apartment areas, and to reconstruct old apartments for citizens' safety and improvement of air pollution.

Since 2011, JICA has implemented “the Project on Capacity Development in Urban Development Sector in Mongolia”, which aims to develop capacities to implement and manage urban development by improving the policy and legal framework for urban development in Mongolia and by enhancing the capacity of organizations and individuals responsible for the urban sector.

In this project, several ongoing urban redevelopment projects in Ulaanbaatar City have been monitored to analyze and review challenges and issues to reflect Urban Redevelopment Law and related regulations which have been drafted by Ministry of Construction and Urban Development (MCUD) and relevant authorities. For implementation of urban redevelopment projects, some issues similar to Japan have been found of whose legal system of urban redevelopment has already been consolidated, while other issues are specific to Mongolia where the city has rapidly urbanized and the legal environment for urban development has not been established yet.

2. TYPE OF URBAN REDEVELOPMENT PROJECT

2.1 Current Situation of Ulaanbaatar City

In the socialism era, many apartments were constructed in the city center. These apartments have been deteriorated and many apartments constructed in 1930’s – 1960’s face risks of collapse in case of earthquake.

Around the apartment areas in the city center, Ger areas have been expanding without urban infrastructure and utilities not being connected and immigrants have settled. It is said more than half of citizens in Ulaanbaatar City settle in Ger areas, and these areas have been uncontrolled by the government (see Figure 1).

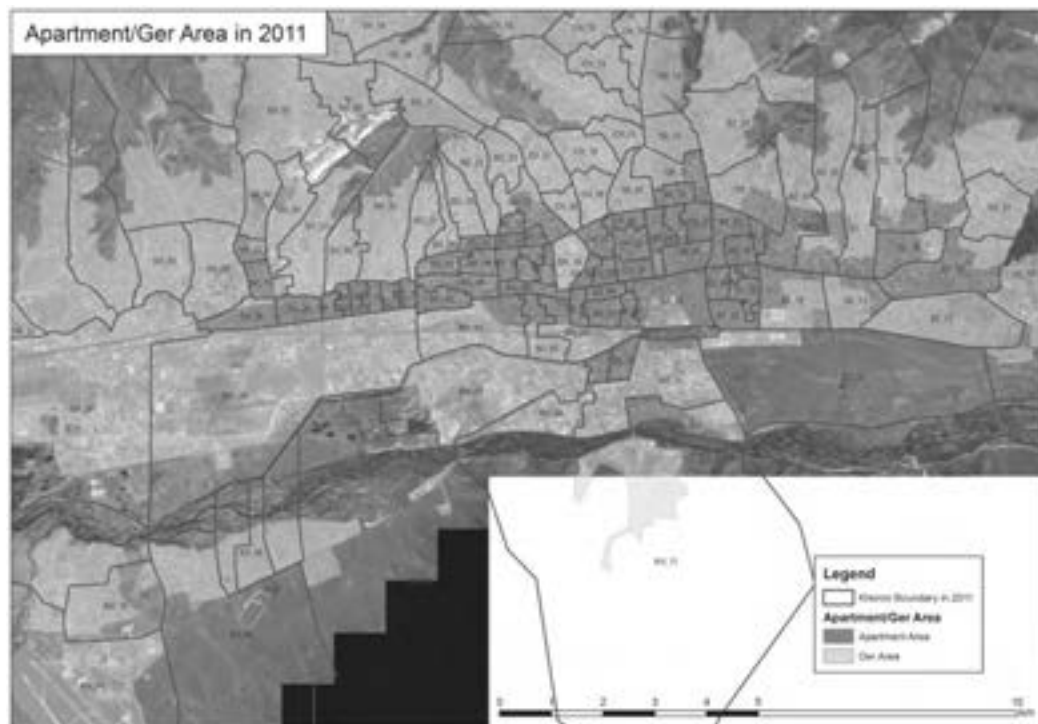


Figure 1: Distribution of Apartment and Ger Area in Ulaanbaatar City, 2011

2.2 Type of Urban Redevelopment Project

According to the draft Urban Redevelopment Law, the basic principles of urban redevelopment project are stipulated as follows: (a) sanitary and safe living environment development for residents, (b) consideration of public interests, and (c) requirement of participation of residents.

To tackle the urban issues in both apartment and Ger areas and to satisfy basic principles of the law above, urban redevelopment projects stated in the draft Urban Redevelopment Law are categorized into five (5) types:

- Reconstruction of areas that do not meet architectural, urban development and urban planning requirements;
- Demolishment of the buildings and structures that do not comply with exploitation requirements, rebuild new buildings;
- Reorganization of Ger area;
- Redevelopment of Ger area for apartment development; and
- Redevelopment of public spaces

Among the five types above, (i) old apartment reconstruction, (ii) land readjustment project in Ger area, and (iii) urban redevelopment (Ger to apartment) projects have been studied in the JICA project (see Figure 2).

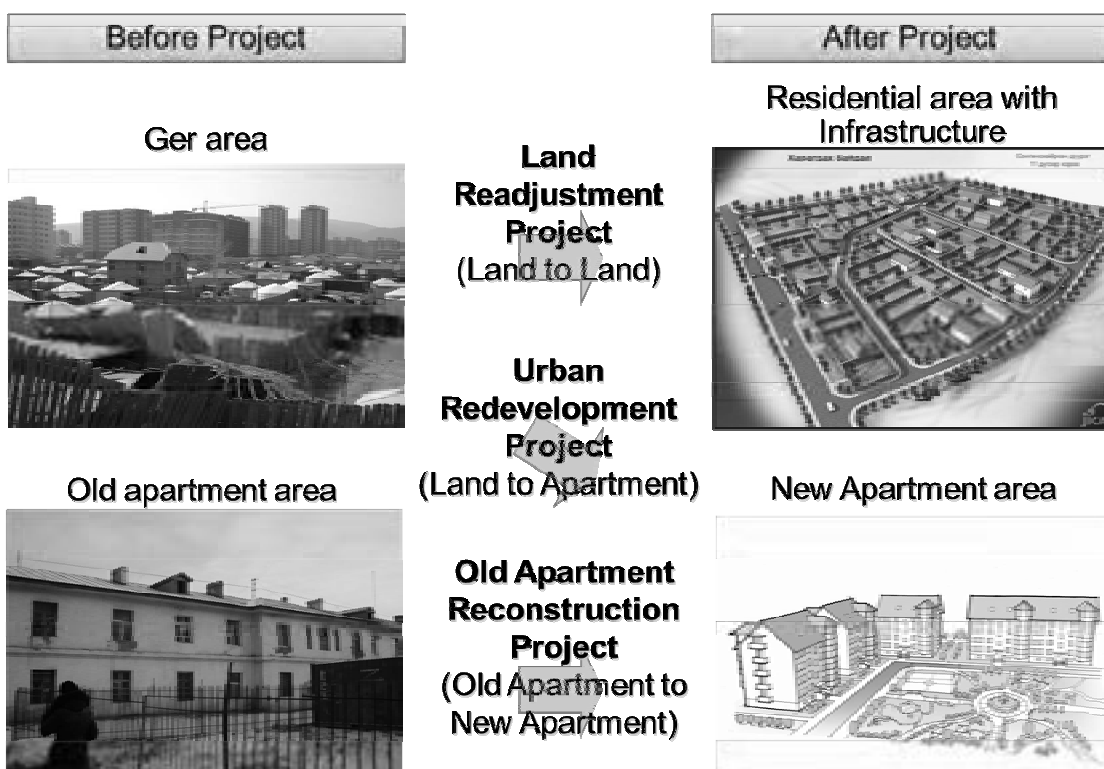


Figure 2: Types of Urban Redevelopment Project

3. FINDINGS AND ISSUES OF URBAN REDEVELOPMENT PROJECTS

3.1 Land Readjustment Project in Ger area

3.1.1 Principle and Methods of Land Readjustment Project

The principle of land readjustment project is to secure public lands for public facilities and to replot and readjust land parcels in order by converting land right and contributing some areas of land for public facilities and sales (“reserve land”). Profit of sale of reserve land is utilized for project finance, while reserve lands for public facilities are used for roads, parks and schools.

In Japan, land readjustment project is called “mother of urban planning”, which have been implemented covering app. 400,000 ha, 1/3 of DID (Densely Inhabited District).

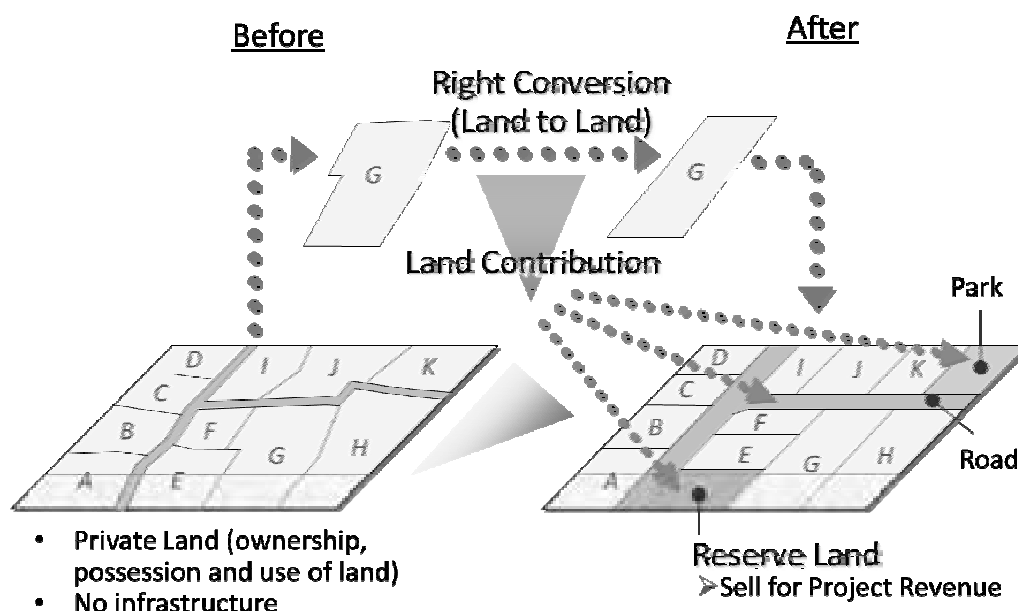


Figure 3: Method of Land Readjustment Project

3.1.2 Land Readjustment Project in Ulaanbaatar

In Ulaanbaatar City, there are no specific methods and systems for redevelopment and living environment improvement in Ger area at this moment. International donors and local NGOs have conducted projects such as water kiosk development, urban utility development (e.g. water pipeline, electricity, improvement of heating equipment, sanitation), and community empowerment, etc. Ironically, these efforts have caused settlement and expansion of Ger area without adequate utility facilities and public services by the government.

To consolidate comprehensive urban redevelopment approaches for Ger area, several pilot projects which have adopted the basic concept of land readjustment project have been implemented by the Land Department of Ulaanbaatar City.

The Land Department of Ulaanbaatar City launched a Land Readjustment Project in Bayankhoshuu, 11th Khoroo of Songinokhairkhan District as the first model

project of Land Readjustment in the city. This project aims to reshape land plots (3.07 ha, 49 households) and develop roads and necessary facilities.

In 2009, the Land Department negotiated with the 49 land owners and got basic agreements for setback (see Figure 4). By the end of 2010, several households along the planned road at the east end already set back the *khasshas* (wooden fences of each plot). Some part of the road was widened ($w=7.5$ m), and some street light poles were installed. Since then, there has been no major improvement because of lack of finance and agreement among relevant departments of the Ulaanbaatar City. After the restructuring of the government due to the national general election and city council election in August 2012, Bayankhoshuu has been selected as a model project by the government, and the city government has started to review current progress and issues to formulate the project with financial resource.

3.1.3 Lessons Learned for Land Readjustment Project

Based on experiences in Bayankhoshuu, the following issues for applying land readjustment project are identified:

- i) *Difficulty of land contribution:* Only small land parcel of several households reduced land size, so reserve land for public facilities and for sales were not secured. It means project finance is not secured by the project itself, and local government bears all financial responsibility.
- ii) *Difficulty in understanding by residents:* The residents cannot understand the land readjustment project mechanism well and are reluctant to reduce land size. As most of Ger residents are low-educated and low-income so it is difficult for them to express own opinions.
- iii) *Difficulty of independent financial allocation for the project:* The Land department of the city initiated the project without enough discussion and coordination among other relevant departments such as Construction and Urban Development Department, Road Department, and Investment Department. Consequently budgets are allocated ad hoc for individual projects by each department, but not for completion of a land readjustment project in a comprehensive manner. In principle, it is necessary that a financial scheme for a land readjustment project should be independent account which should be closed with its revenue and expenditure equal.

3.2 Urban Redevelopment (Ger to Apartment) Project

3.2.1 Principle and Methods of Urban Redevelopment Project

The urban redevelopment project in Japan is applied mainly for renovation of deteriorated areas to construct apartments and buildings with necessary roads and public facilities. While land right is converted to new land right in case of land readjustment project, it is converted to floor right of new apartments in case of urban redevelopment project (see Figure 4).

Features of urban redevelopment projects are to combine individual land rights and convert them to floor rights of mid or high-rise apartments to utilize limited land effectively. After rights of original land owners are converted to the new apartment floors, the remained new floors of apartments (“reserve floor”) are sold for project finance.

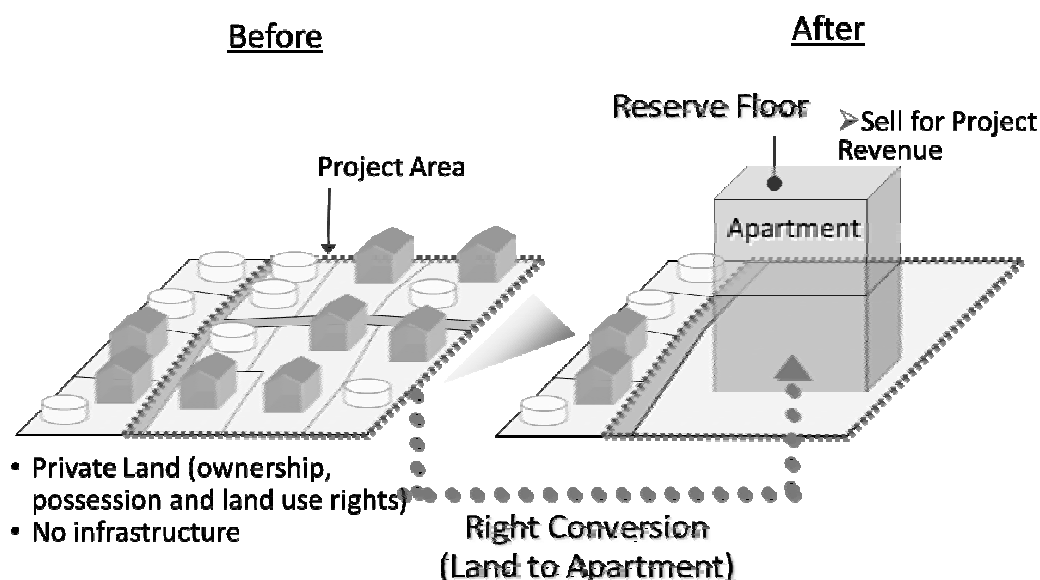


Figure 4: Method of Urban Redevelopment Project

3.2.2 Urban Redevelopment Project in Ulaanbaatar City

There are several ongoing urban redevelopment projects mainly in the central area of the city. These areas are mixed with apartments, detached houses and Gers. Ger residents have settled for long years while apartments have been newly constructed, so socio-economic condition among residents are varied.

The 14th Khoroolol is the first urban redevelopment project in Ulaanbaatar City. In the first phase, 2-story wooden apartments were demolished and high-rise apartments were constructed on that area. At that time, the same floor area of the old apartment was exchanged to the same area of the new apartment without any payment by residents.

In case of the 7th Khoroolol project, which the Ulaanbaatar City initiates, the Ulaanbaatar City allocated the budget for compensation of land acquisition for road and utility development in the first phase. The standard price of the 7th Khoroolol for compensation was 100,000MNT/m², while the official land price was 13,200 MNT/m² at that time.

Though the state allocates budget for compensation to develop road and utilities, the local government does not allocate compensation to develop public and social facilities. According to the Urban Development Law, land can be acquired for the purpose of civil engineering and social infrastructure.

According to the Land Law and the Land Privatization Law, land can be acquired for special needs with compensation for land ownership right, and with or without

compensation for land possession right and land use right. Land for special needs are not clearly defined, what kind of road, infrastructure and social infrastructure are covered.

The Detailed District Plan of East Selbe area was carefully formulated based on experiences of other areas which had not been realized. The planning team consulted with each land and apartment owner if they would agree with the proposed plan, and the proposed draft plan was opened for public in compliance with the Urban Development Law. Originally, it is expected that this would be the first urban redevelopment project with public participation to gather opinions for reconstruction or not. At the end, the plan does not include enough public facilities and road network to serve for future population and the city government cannot enforce land owners to secure lands for public facilities.

3.2.3 Lessons Learned for Urban Redevelopment Project

Based on experiences in East Selbe area and other project sites, following issues for applying urban redevelopment project are identified:

- i) *Difficulty of construction restriction:* In general, the District Detailed Plan is formulated and approved by the city government in compliance with the Urban Development Law. In case of the urban redevelopment project, the District Detailed Plan is formulated covering the whole area, which project implementation plan including implementation body, finance, etc. is not planned in detail. Furthermore, there is no legal power to enforce to restrict land transaction and construction activities in the Detailed Plan area to make it comply with the approved plan. It is found that the District Detailed Plan is the drawing of no practical use under current legal system.
- ii) *Difficulty to secure lands for public facilities and road network:* Public facilities and road network are not planned enough to afford future development and population. Furthermore, since right conversion system has not been established with legal basis, land acquisition and resettlement with compensation is only the measure to acquire lands in compliance with the Land Law and the Urban Development Law.
- iii) *Difficulty to negotiate with property owners for agreement:* It is difficult for the government to negotiate with residents without having standards of land value and land assessment measures for compensation or right conversion. At this moment, the land price of 100,000MNT/m² is a kind of standard for compensation in the central area, but this price cannot be applied to suburban and remote Ger area where infrastructure is not connected. In addition, many land owners in the central area are eager to sell their lands for higher price, or to construct an apartment building by themselves. So it is difficult for the government to control land transaction and construction activities to materialize the approved plan which aims to improve the area as a whole.

3.3 Old Apartment Reconstruction Project

3.3.1 Principle and Methods of Old Apartment Reconstruction Project

In case of Japan, there are many old apartment complexes which were constructed more than 40 years before, during rapid economic growth period in 1950's - 70's. The residents of these apartments are mostly aged, and many of these apartments are vacant and facilities have been deteriorated. In addition, crimes inside the apartment complex happen in these days.

In Mongolia, many apartments were constructed in 1930's to 60's in socialist era. These apartments face danger of collapse in case of earthquake and it is dangerous to live in. The State Inspection Agency of Mongolia has designated many apartment buildings to be lived in and to be reconstructed.

Though the background of reconstruction of the old apartment buildings is different from Japan and Mongolia, the principle of project implementation mechanism is the same, which is based on consensus building and right conversion (see Figure 5). The apartment floor owners exchange original floor right to new floor right, and construct mid or high-rise buildings whose total floor area after the project is increased.

In Japan, the floor area before the project is exchanged to the new floor area whose floor value is the same as before (equal value based exchange). On the other hand, the floor area before the project is exchanged to the new floor area which the floor area size is the same as before (equal size based exchange), in compliance with the Housing Law in Mongolia. After right conversion of right owners, supplemental floor areas are sold to market to cover portion of project finance.

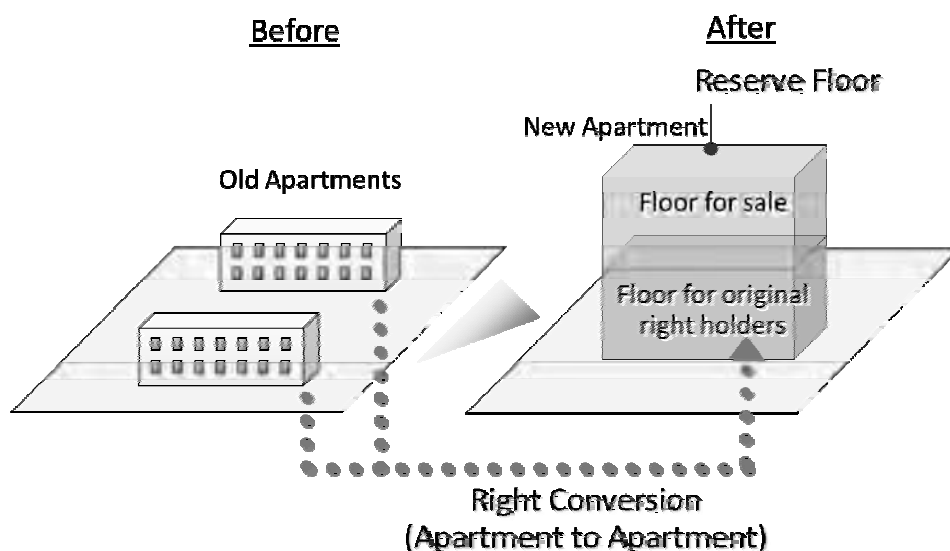


Figure 5: Method of Old Apartment Reconstruction Project

3.3.2 Old Apartment Reconstruction Project in Ulaanbaatar

Some private developers and construction companies have worked for old apartment reconstruction projects. At first, they tried to purchase all floor rights from owners, but it took long time to negotiate with each owner, and the private companies could not afford enough finance to purchase all rights in advance to project implementation.

Even private companies successfully concluded agreement of reconstruction from original owners, they faced financial difficulty in construction cost, compensation cost for resettlement, etc. The initial cost for project implementation is so large that the private company cannot secure it. At this moment, the government does not have a technical and financial support mechanism for most of private companies which work for old apartment reconstruction.

3.3.3 Lessons Learned for Old Apartment Reconstruction Project

Based on experiences in several project sites, following issues for applying old apartment reconstruction project are identified:

- i) *Difficulty to get agreement from residents:* Since the reconstruction project will demolish the original apartment, most of residents are hesitate it and it is difficult for them to understand the project mechanism and roles of residents. Most of residents of old apartment buildings settle for long period, they don't want to move out.
- ii) *Difficulty to get agreement from commercial floor owners:* There are many shops in the 1st floor of apartment, which intrude sidewalks. In principle, they must have a land possession or use right, construction permission, and a commercial license. Business owners claim their business rights no matter whether they have these certificates and titles or not. Private companies need to take into consideration how to compensate commercial activities and to secure new floors for continuation of their activities. It also causes unfairness among residents and business owners in the same apartment building.
- iii) *Difficulty to secure finance:* There is no subsidy system by the government, so it is difficult for private companies to secure project finance to afford from initial stage to completion.

4. CONCLUSIONS

In compliance with the Urban Redevelopment Law under drafting, urban redevelopment projects will be implemented efficiently in a comprehensive development approach. Urban redevelopment projects are featured as follows:

- (a) The urban redevelopment project improves comprehensive living environment including housing, roads and public facilities based on cooperation between the government and residents.

- (b) The tripartite contract among right holders, government, project implementation body (the city governor or legal entity) is a legal basis for a proper project implementation.
- (c) Right conversion is to secure original land and property rights during project implementation period based on a fair property assessment.
- (d) Residents of Ger area who participate in the land readjustment project can select detached houses or apartments, though they need to construct new dwellings by themselves. Residents can choose not to participate in the project and move out with compensation.
- (e) A project implementation body can allocate project finance by selling reserve land or reserve floor.

The urban redevelopment project also enables to strengthen capacity of disaster resistance with appropriate provision of road network, parks and openspace which can be utilized for emergency. In the process of project implementation, a community activity will be also promoted, and it will be sustained even after the project completion to manage the community service and facilities by themselves. The government has a responsibility to support residents and private sectors' initiatives to improve the city environment.

Though the legal structure and project implementation mechanism of Japan and other countries will be good references for Mongolia, it is necessary to take special conditions into consideration. Most of poor Ger residents put priority to earn a living, so it might be necessary to develop a comprehensive program including urban redevelopment and socio-economic development in parallel to promote understanding and agreement of residents for implementation of urban redevelopment project.

It is said that "community" has not been consolidated in Mongolia since a history of Ger settlement in Ulaanbaatar City is not so long. The principle of disaster management of "self-help, community-help and public-help" should be promoted as a common idea for urban redevelopment project which contribute to a comprehensive environment improvement.

REFERENCES

- JICA, *Final Report, the Study on Master Plan and Urban Development Program in Ulaanbaatar City in Mongolia (UBMPS)*, March 2009
- JICA, *Progress Reports 1 to 4, the Project on Capacity Development in Urban Development Sector in Mongolia (MUGCUP)*, May 2012
- Working Group of Urban Redevelopment Law, Ministry of Construction and Urban Development of Mongolia (MCUD), *Draft Urban Redevelopment Law*, June 2012
- Ministry of Land, Infrastructure, Transport and Tourism (MLIT) of Japan, *Outline of Urban Redevelopment Project*

Seismic vulnerability of gravity-load designed buildings

Kiang Hwee TAN¹, T BALENDRA² and Aziz AHMED³

¹Professor, Department of Civil and Environmental Engineering,
National University of Singapore, Singapore
tankh@nus.edu.sg

²formerly Professor, Department of Civil and Environmental Engineering,
National University of Singapore, Singapore

³PhD Candidate, Department of Civil and Environmental Engineering,
National University of Singapore, Singapore

ABSTRACT

Buildings designed primarily for gravity loads are prone to suffer shear failures in walls, columns and beams when subjected to far field effects of earthquakes. In previous studies, pushover analyses carried out on these buildings were terminated when a local shear capacity is reached. However, by considering shear yielding, ductile shear hinges can be used to model the behaviour of such buildings. By comparing the capacity determined with this new modeling feature with the seismic demand due to long distant earthquakes, the performance of a typical gravity-load designed, 25-storey building at critical soil sites in Singapore is investigated in this study.

Keywords: *concrete structure, ductile shear hinge, post local shear failure behavior, pushover analysis.*

1. INTRODUCTION

Many buildings in large Asian cities like Bangkok, Kuala Lumpur, Seoul and Singapore are designed primarily for gravity loads due to little or no local seismic activities. However, it has been realized that such gravity-load designed (GLD) buildings are not totally immune to the effects of far-field earthquakes, especially if they are sited on soft grounds that are likely to amplify the seismic waves.

Research on seismic performance including capacity of GLD reinforced concrete structures has been carried out in Singapore context (Balendra et al. 1999, 2001, Kong et al. 2003). A microscopic model calibrated for shear walls has been used to determine the capacity of full scale shear wall structures (Kong 2004). Also, a macroscopic model for capacity evaluation of shear wall-frame structures was presented in Balendra et al. (2007), with which a pushover analysis of a 25-storey point block was carried out and the analysis was terminated at the onset of shear failure at the base of the shear wall.

This study focused on ductile shear failure using SAP2000 (2009) software, taking advantage of its shear hinge feature to model the post elastic shear behavior

in addition to moment hinges to model the flexural yielding in beams, columns and walls. Shear hinge was incorporated in all the frame elements including the equivalent columns simulating the shear walls in order to detect ductile shear failures. The effects of infill were accounted for and the implication on the performance of the building is shown by superimposing the resultant capacity curve on the demand curve of a critical soil site, for two possible scenarios of earthquakes of moment magnitude $M_W = 8.9$ and $M_W = 9.5$ at 600 km from Singapore.

2. MODELING OF STRUCTURE

2.1 Building under study and simplified model layout

A typical 25-story building with plan view shown in Figure 1 is considered. The plan dimension of the building is 25 m by 20 m and the total height is 65 m (each story of height 2.6 m). Slab thickness is 100 mm and the typical dimensions of beams and columns are 230 mm x 450 mm and 300 mm x 1200 mm, respectively. The structure comprises of moment resisting frames, two I-shaped shear walls located in the center and four L-shaped shear walls located at corners. Details of the floors and beams are identical for all stories, but the dimensions and details of columns and shear walls vary with the height.

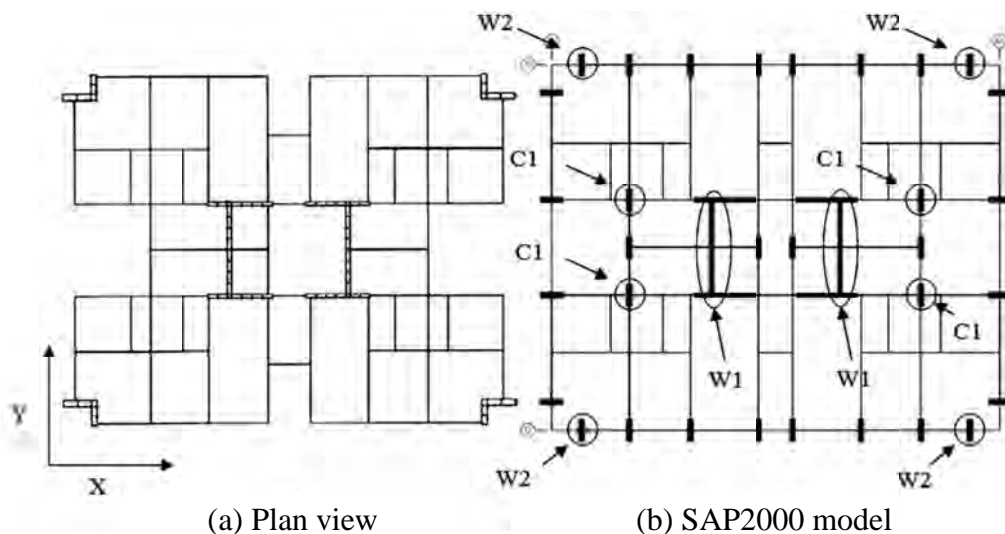


Figure 1: Typical 25-storey building

The building has been designed according to BS8110 (1985), with no seismic provisions. Longitudinal reinforcing bars in members have design yield strength of 460 MPa, and transverse reinforcing bars have design yield strength of 250 MPa. The cube compressive strength of concrete was taken as 25 MPa. The unfactored dead loads (DL) calculated for the typical floors and the roof floor were 4.6 kN/m^2 and 3.6 kN/m^2 , respectively. Unfactored live load (LL) was taken as 1.5 kN/m^2 , and the load combination of $1.0 \text{ DL} + 0.4 \text{ LL}$ was used.

The effects of masonry infill walls, expected to be beneficial in minor to moderate seismic regions were included (Mainstone 1974). Columns and shear walls were assumed to be fixed at the base. The L-shaped shear walls at corners were each simulated by two equivalent columns. The I-shaped shear walls at the center of the structure were each simulated by five equivalent columns. Rigid links were used to connect the equivalent columns simulating the shear wall and also to connect them to the adjoining members. Beams and columns were modeled with frame type RC beam and beam-column element respectively. Flexural rigidity in the local y - y and z - z directions, denoted as EI_{yy} and EI_{zz} respectively, were calculated by multiplying the corresponding values by the reduction factors obtained from tests (Li 2006). Values of 0.58 for columns, 0.8 for shear walls and 0.35 for beams were used. Rigid planar diaphragms were used at each floor level to simulate the slab action.

2.2 Modeling of nonlinear hinges

Five types of nonlinear hinges were used in modeling this building. The orientations of the hinges are presented in Figure 2. Location of these hinges are presented in Figure 3.

P-M2-M3 hinge simulates nonlinear behavior of a column under axial load and biaxial moment. Shear hinges V2 and V3 were used simultaneously in each column to model the shear failure mechanism in two orthogonal directions. For beams, only V2 hinge was used at each end of the beam. Axial hinge P was used in masonry struts to simulate the post compressive failure behavior. M3 hinge was used to simulate the nonlinear flexural behavior of the beam.

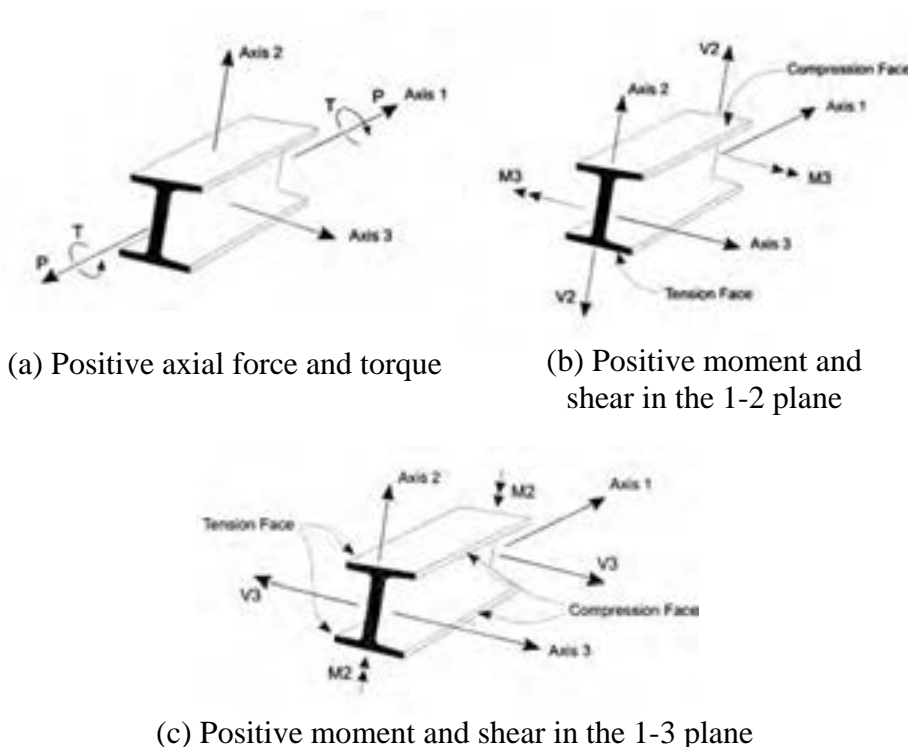


Figure 2: Typical P, M2, M3, V2 and V3 orientations used in SAP2000 (2009)

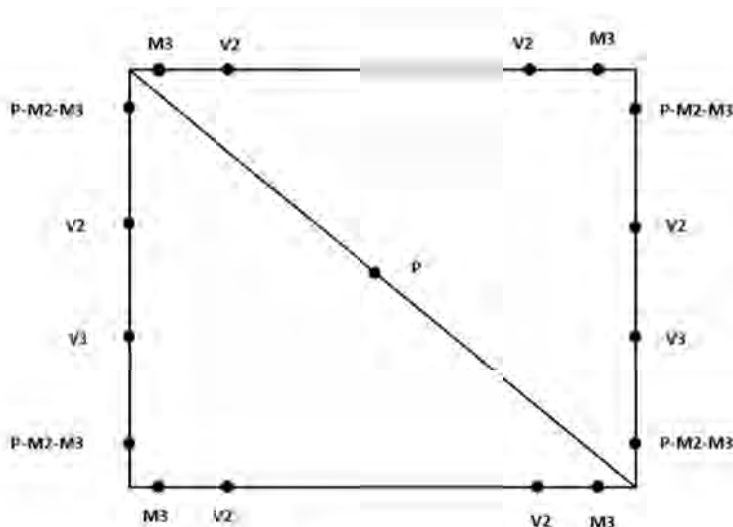


Figure 3: Locations of nonlinear hinges in beams, columns and braces

P-M2-M3 hinges were located at each end of the column. Shear hinges V2 and V3 were located at $0.4L$ and $0.6L$ of the columns, where L is the clear height of the column. This approach is based on the fact that moment is highest at the ends of the column and shear force is constant throughout the length of the column.

Of these five nonlinear hinges, P-M2-M3 and M3 hinges were automatically modeled by SAP2000 using FEMA-356 (2000) Tables 6-7 and 6-8 respectively. The shear and axial hinges were modeled manually based on experimental data.

2.2.1 Shear hinge

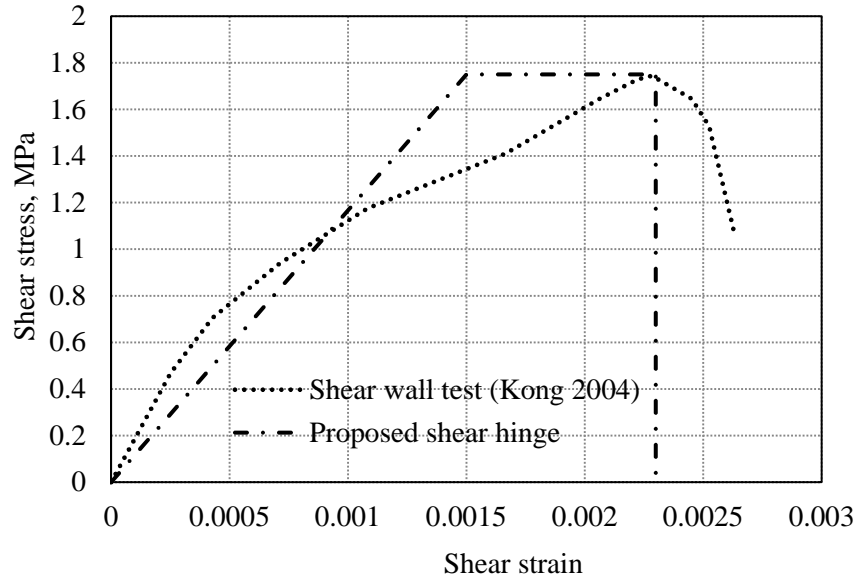
Shear walls and wide columns are likely to fail in shear with a certain degree of ductility, especially with flexural yielding of the longitudinal reinforcement (Chowdhury, 2007; Elwood & Moehle, 2004; Patwardhan, 2005). Considering this fact and based on experimental data, models for ductile shear hinges (that is, displacement-controlled hinges) were proposed as follows.

The constitutive relation for the shear behavior of the shear walls without flexural yielding is based on the experimental study by Kong (2004). The idealized shear stress-shear strain curve for the shear wall is shown in Figure 4(a) and reproduced in Figure 5(a). That is, a bilinear relationship with yield shear strain of 0.0015 and ultimate shear strain of 0.0023 is assumed.

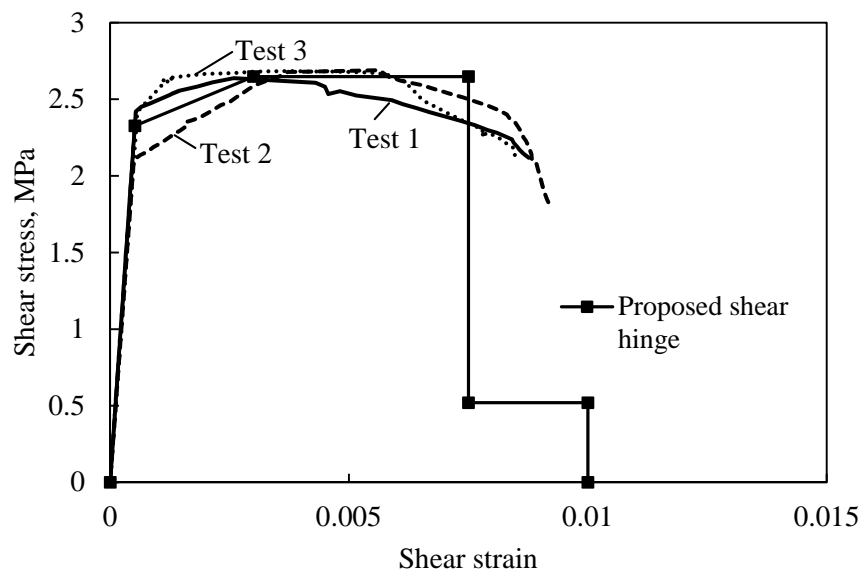
Also, based on tests on three wide columns similar to those in the building considered, an idealized shear stress-shear strain curve is obtained in Figure 4(b). That is, a yield shear strain of 0.003, ultimate shear strain of 0.011 and a post elastic strength of 14% as shown in Figure 5(b) are assumed. The shear strain at initial flexural yield (γ_y) is calculated as (Elwood and Moehle 2003):

$$\gamma_y = \frac{2M_y}{LGA_v} \quad (1)$$

where M_y = column moment at yielding of the longitudinal reinforcement, L is the length of column, G = shear modulus, E = Young's modulus, and $A_V = 5/6 A_G$ is the shear area of the column cross section.



(a) Shear wall



(b) Column

Figure 4: Idealized shear stress-shear strain behaviour

For both shear wall and wide column, the elastic shear strength of each member (V) is calculated according to equations 2 to 4, based on ACI 318 (2005).

$$V = V_c + V_s = \left(1 + \frac{N_u}{14A_g}\right) \left(\frac{\sqrt{f'_c}}{6}\right) b_w d + \frac{A_v f_y d}{s} \quad (2)$$

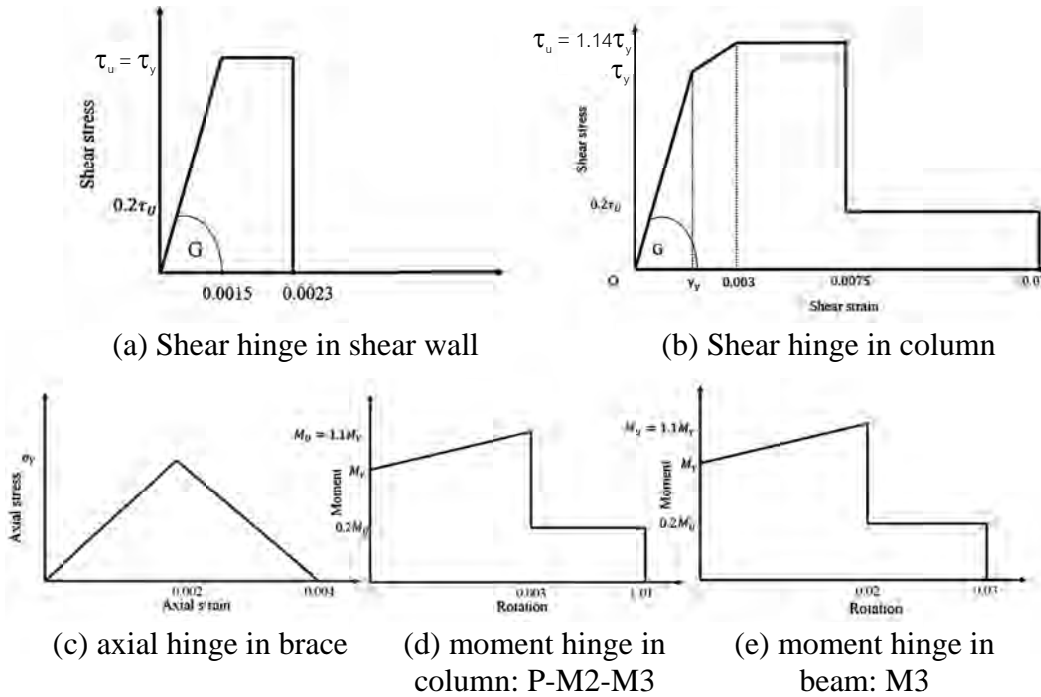


Figure 5: Constitutive relations

where

$$V_c = \left(1 + \frac{N_u}{14A_g}\right) \left(\frac{\sqrt{f'_c}}{6}\right) b_w d \tag{3}$$

$$V_s = \frac{A_v f_y d}{s} \tag{4}$$

where N_u = axial compression force; A_g = area of the cross section; f'_c = cylinder compressive strength of concrete, in MPa; b_w = width of the web; A_v = area of horizontal shear reinforcement at a vertical spacing s ; d = effective depth, taken as $5h/6$; h being the dimension of member in direction of loading, and f_y = yield strength of steel. Also, the ultimate shear strength τ_u is taken equal to V/A_v .

2.2.2 Axial hinge

The stress–strain curve shown in Figure 5(c) is based on the model suggested by Oktem and Pala (2003) and was used in modeling the nonlinear behaviour of the axial hinge. Also, the tension limit for the elements simulating the infill is assigned as zero to represent the inability of infills to act under tension. The compressive strength and elastic modulus of the infill were assumed as 12 MPa and 6000 MPa respectively (Kaushik et al. 2007). Thus the yield strain of the equivalent compression strut was 0.002, and ultimate strain was assumed as 0.004.

2.2.3 Flexural hinge

Using the yield moment and ultimate rotation capacity for non-conforming components as per Tables 6-7 and 6-8 of FEMA356 (2000), the flexural hinges P-M2-M3 for column and M3 for beam were defined as in Figures 5(d) and 5(e).

2.3 Verification of nonlinear hinges

Verification studies were performed to justify the accuracy of flexural and shear hinges in columns. Scaled models of a sub-frame and a shear wall, which were tested under pushover loading by Li (2006) and Kong (2004) respectively, were considered. The dimensions are shown in Figures 6(a) and 7(a). Pushover analyses were carried out as per the tests. Figures 6(b) and 7(b) show that results from SAP2000 compare very well with experimental results and that given by ABAQUS model (Kong, 2004).

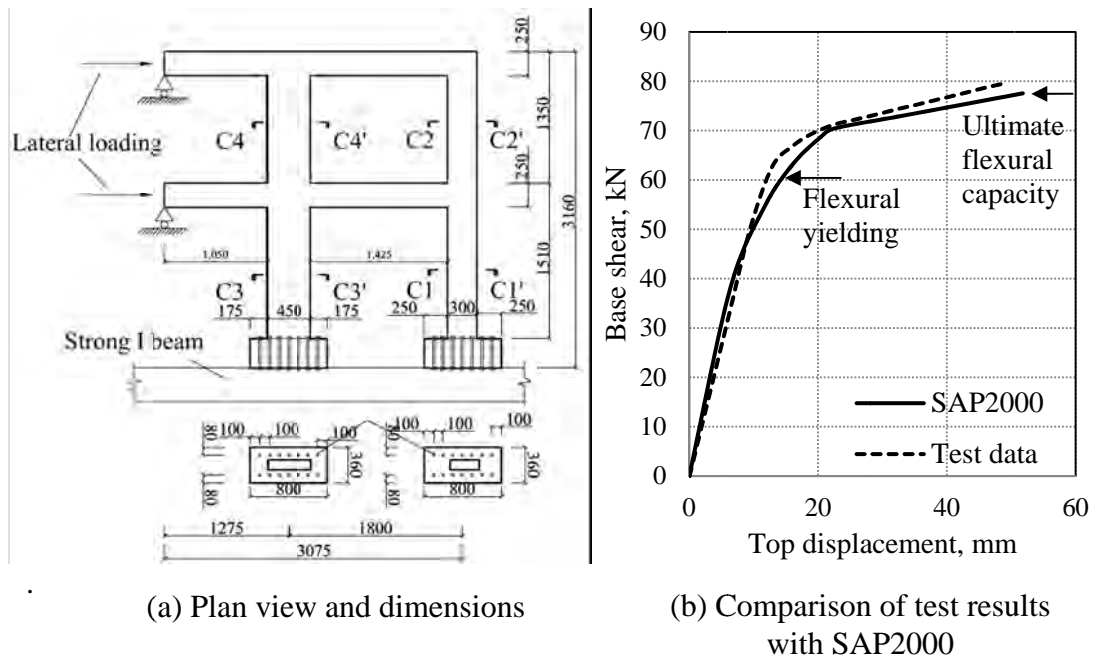


Figure 6: Sub-frame tested by Li (2006)

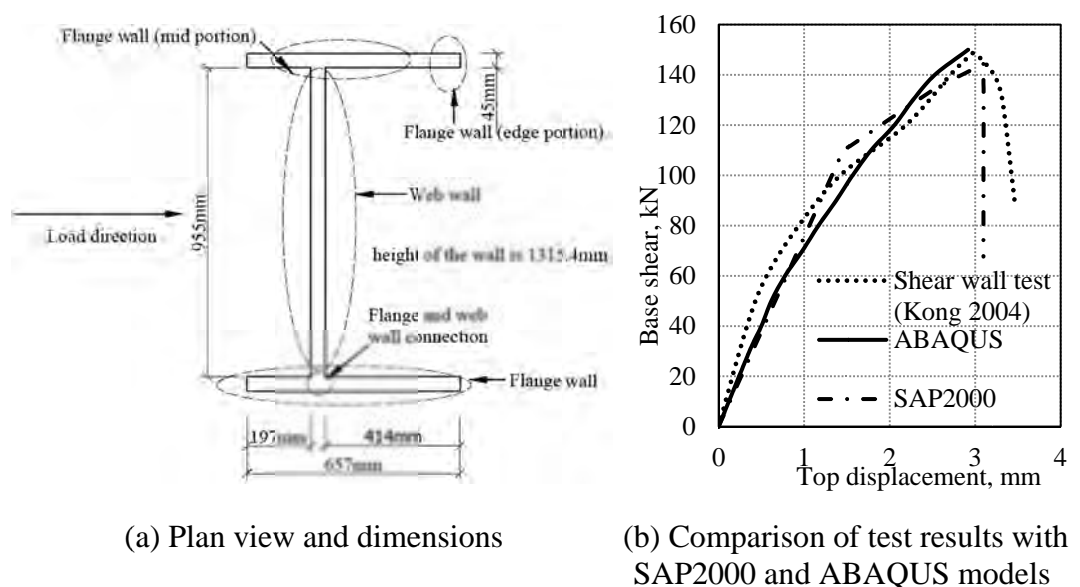


Figure 7: Shear wall tested by Kong (2004)

3. CAPACITY EVALUATION

To obtain the capacity of the structure, nonlinear pushover analysis was carried out. This is a simple option for estimating the strength and displacement capacities in the post-elastic range and it can also be used to highlight the potential weaknesses in the structure. In the pushover analysis, lateral loads were applied in one direction at the master nodes of the floor levels and were increased until the collapse of the structure. From modal analysis, computed modal participation ratio justified the adequacy of considering only the fundamental mode to estimate the seismic behavior of the structure by static pushover analysis.

The variation of lateral load applied along the building height was based on the first translational mode shape of that direction. The capacity curves obtained from the pushover analysis were for a multi-degree-of-freedom (MDOF) system. In order to compare with the demand curves, the capacity curves were converted into the spectral acceleration-spectral displacement (A-D) format for an equivalent single-degree-of-freedom (SDOF) system (Freeman et al. 1975; Freeman 1978).

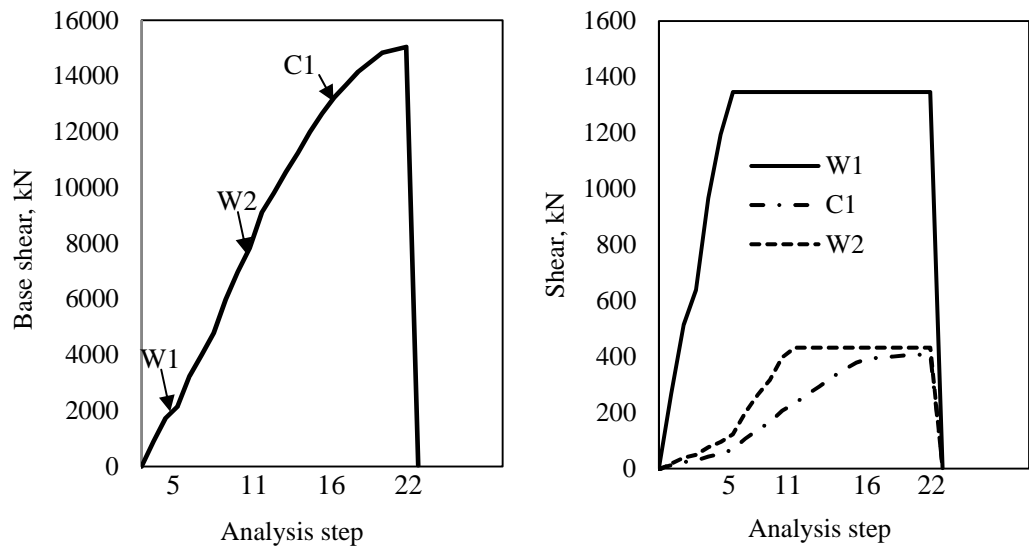
3.1 Ductile shear failure behavior

Figure 8(a) shows the stepwise base shear in the building for loading in the critical y-direction (see Figure 1), and Figure 8(b) shows the shear carried by three critical components, W1, W2 and C1 at various loading stages. At Step 5, first local shear capacity is attained in the first storey at the web of the shear wall W1. Due to displacement ductility, W1 maintains the shear strength in subsequent loading steps, and any additional base shear demand is carried by W2 and C1. At Step 11, W2 reaches its strength capacity and thereafter C1 carries the additional demand.

At Step 16, C1 reaches its shear strength capacity and the additional increase in base shear demand is carried by other columns. Finally, at Step 22, the displacement capacity is reached at the first storey of component W1, and the load drops, causing a soft-storey-like failure mechanism. This point corresponds to the ultimate capacity in Figure 9. It demonstrates that the capacity would be grossly underestimated if the first local shear strength capacity was to be considered as the ultimate capacity. It is worth noting that based on the shear strength capacity the ultimate capacity would have been only 8% of the self weight of the building, whereas it is 27% when shear failure is based on the displacement concept.

3.2 Performance of the structure

Figure 9 superimposes the demand curves obtained for a critical site affected by $M_W = 9.5$ and $M_W = 8.9$ earthquakes. At the performance point for the $M_W = 9.5$ scenario, the base shear is 13% of self weight and the spectral displacement is 55 mm which is equivalent to 0.1% drift. At this performance point, shear strength capacity is reached at the web of the shear wall at the first storey and several beams have yielded in flexure. All other components along with non structural masonry walls remain in the elastic range. This suggests that although initiation of some shear cracks may be observed at the base of the shear wall, overall the life safety of inhabitants is not compromised under these two earthquake scenarios.



(a) Steps at which shear capacity of W1, W2, and C1 is reached

(b) Shear resistance provided by W1, W2 and C1

Figure 8: Base shear carried by building and its critical components

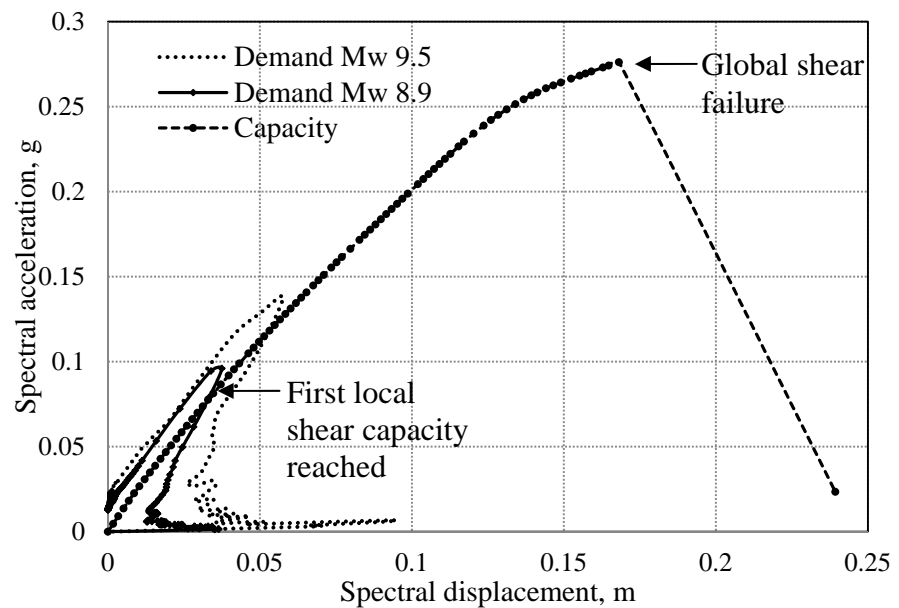


Figure 9: Performance of the structure

4. CONCLUSIONS

The proposed FEA model incorporating ductile shear hinge for walls and columns is a reliable and elegant tool to determine the seismic performance of full-scale buildings. Using this model, the seismic vulnerability of a typical GLD shear

wall-frame building was evaluated for two earthquake scenarios on a critical soil site. The ultimate capacity of the building was found to be significantly higher than the demand under assumed earthquake scenarios.

REFERENCES

- ACI318, 2005. *Building Code Requirements for Structural Concrete and Commentary*. American Concrete Institute, Farmington Hills, Michigan, USA
- Balendra, T., Li, Z. J., Tan, K. H., and Koh, C. G., 2007. Vulnerability of Buildings to Long Distance Earthquakes from Sumatra. *J. Earthquake and Tsunami* 1(1), 71-85.
- Balendra, T., Tan, K. H., and Kong, K. H., 2001. Ultimate Strength of a Reinforced Concrete Frame-Wall Structure Designed According to BS8110", *ICCMC/IBST International Conference on Advanced Technologies in Design, Construction and Maintenance of Concrete Structures*, Hanoi, Vietnam, 66-72.
- Balendra, T., Tan, K. H., and Kong, S. K., 1999. Vulnerability of Reinforced Concrete Frames in Low Seismic Region, When Designed According to BS 8110. *J. Earthquake Engineering and Structural Dynamics* 28(11), 1361-1381.
- BS8110, 1985. *Structural Use of Concrete: Parts 1, 2 and 3*, British Standards Institution, UK.
- Chowdhury, T., 2007. *Hysteretic Modeling of Shear Critical Reinforced Concrete Columns*. M.Sc. Thesis, The Ohio State University, Columbus, Ohio.,UK
- Elwood, K. J., and Moehle, J. P., 2004. Evaluation of Existing Reinforced Concrete Columns, *Thirteenth World Conference on Earthquake Engineering*, Vancouver, B.C. Paper no. 579.
- Elwood, K. J., and Moehle, J. P., 2003. *Shake Table Tests and Analytical Studies on the Gravity Load Collapse of Reinforced Concrete Frames*. PEER Report Series 2003/01.
- FEMA356, 2000. *Prestandard and Commentary for the Seismic Rehabilitation of Buildings*. Federal Emergency Management Agency, Washington, D.C.
- Freeman S. A., 1978. *Prediction of Response of Concrete Buildings to Severe Earthquake Motion*. Special Publication SP-55, American Concrete Institute, Farmington Hills, Michigan, USA.
- Freeman S. A., Nicoletti J. P., and Tyrell, J. V., 1975. Evaluation of Existing Buildings for Seismic Risk — A Case Study of Puget Sound Naval Shipyard, *1st US National Conference on Earthquake Engineering*, Berkeley, California, USA.
- Kaushik, H. B., Rai, D. C., and Jain, S. K., 2007. Stress-Strain Characteristics of Clay Brick Masonry Under Uniaxial Compression. *J. Materials in Civil Engineering* 19(9), 728-739.
- Kong, K. H., 2004. *Overstrength and Ductility of Reinforced Concrete Shear-Wall Frame Buildings Not Designed for Seismic Loads*. Ph.D. Thesis, National University of Singapore, Singapore.
- Kong, K. H., Tan, K. H., and Balendra, T., 2003. Retrofitting of Shear Walls Designed to BS8110 for Seismic Loads Using FRP, *6th International Symposium on FRP Reinforcement for Concrete Structures*, Vol. 2, 1127-1136.
- Li, Z., 2006. *Seismic Vulnerability of RC Frame and Shear Wall Structures in Singapore*. Ph.D. Thesis, National University of Singapore, Singapore.
- Mainstone, R. J., 1974. *Supplementary Note on the Stiffness and Strengths of Infilled Frames*. Current Paper CP 13/74, Building Research Station, Garston, Watford.
- Oktem, O. and Pala, S., 2003. Nonlinear Analysis of RC Frames with Masonry Infill Wall, *13th Mechanical Congress*, Gaziantep, Turkey.

Patwardhan, C., 2005. *Strength and Deformation Modeling of Reinforced Concrete Columns*. M.Sc. Thesis, The Ohio State University, Columbus, Ohio.
SAP 2000, 2009. *CSI Analysis Reference Manual*. Computers and Structures, Inc, Berkeley, California.

Study on the effects of chemical and physical properties of concrete on the behavior of internal water

Chohji NAKAMURA¹, Yuya SAKAI² and Toshiharu KISHI³

¹ Graduate Student, School of Engineering,
The University of Tokyo, Japan
choji@iis.u-tokyo.ac.jp

² Assistant Professor, IIS, The University of Tokyo, Japan

³ Professor, IIS, The University of Tokyo, Japan

ABSTRACT

A lot of deterioration in the concrete structures are caused by liquid water existing inside of the structures. For evaluation of durability of the concrete structures, it is important to understand the behavior of liquid water in pores in order to predict precisely the deterioration caused by water. In this paper, the effects of chemical and physical properties of concrete on the behavior of internal liquid water are discussed by using the apparent contact angle and the threshold pore radius as chemical indicator and physical one, respectively. The apparent contact angle is measured by water and ethanol absorption test. The threshold pore radius is measured by mercury intrusion porosimetry by using epoxy coated samples.

As a result, it is indicated that the difference of chemical property by the kind of admixture affects scarcely the capillary pressure of penetrating water into concrete. Instead, physical property such as pore structure dominates the behavior of water in the case of water transport driven by pressure gradient.

Keywords: behavior of water, Washburn's equation, contact angle, threshold pore radius

1. INTRODUCTION

A lot of deterioration, such as drying shrinkage, creep and chloride ion ingress in concrete structures are closely related to liquid water existing inside of the structures. Therefore, for evaluation of durability of the concrete structures, it is important to understand the behavior of liquid water in pores of concrete in order to predict the deterioration precisely. So far, some researchers have tried to quantify the behavior of liquid water in cementitious material in different ways (Maekawa et al., 2009; Okazaki et al., 2011). The objectives of this study are to understand the effects of chemical property, e.g. the surface charge of pore wall, and physical property, e.g. pore structure, on the behavior of liquid water in concrete by conducting some tests on the specimens which have different curing conditions and mix proportions.

2. THE EFFECT OF CHEMICAL PROPERTY ON THE CAPILLARY PRESSURE

2.1 Contact angle

When a drop of liquid is put on an ideal solid surface, liquid forms into the curved shape by own surface tension shown as Figure 1. The shape of liquid/vapor interface is determined by the Young-Laplace equation as follows (Young, 1805),

$$\gamma_{SV} = \gamma_{LV} \cdot \cos \theta_E + \gamma_{SL} \quad (1)$$

Where γ_{SV} is the solid/vapor interfacial energy, γ_{LV} is the liquid/vapor interfacial energy (i.e. the surface tension), γ_{SL} is the solid/liquid interfacial energy, and θ_E is the equilibrium contact angle. Therefore, the contact angle is the angle between the tangent of a drop of liquid and a solid surface when a thermodynamic equilibrium between the three phases is established. It is used as the indicator of the wettability of a solid surface by a liquid. It also quantifies the capillary pressure which is the driving force when a liquid penetrates into a hydrophilic porous material like concrete. Therefore, if the contact angle is measured between water and concrete which have different curing conditions and mix proportions, the effect of chemical property of concrete on the capillary pressure could be evaluated. However, it is difficult to measure the contact angle between a liquid and a porous material because a liquid penetrates into the material as soon as a drop of liquid is put on the surface. Besides, the contact angle is extremely sensitive to contamination and smoothness of a solid surface. In order to avoid these problems, we have measured the apparent contact angle by using Letey's method as reference (Letey et al., 1962).

2.2 Method to measure the apparent contact angle between water and concrete

We assume that pores in concrete are several capillaries shown as Figure 2. Therefore, weight of absorbed liquid during the liquid absorption test on horizontal condition is expressed as follows,

$$M = \rho n \pi r^2 L \quad (2)$$

Where M is weight of absorbed liquid, ρ is density of liquid, n is the number of channels, r is radius of channels, and L is absorbed length. Absorbed length L is considered to be expressed as equation (3) which is derived from Washburn's

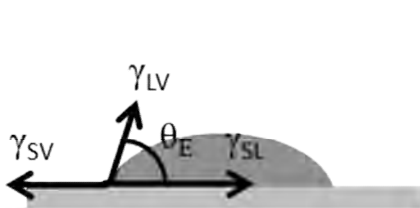


Figure 1: Contact angle

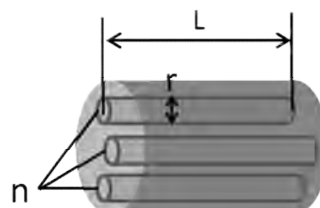


Figure 2: Conceptual diagram of pores in concrete

equation and Hagen-poiseuille's equation (Washburn, 1921).

$$L = \sqrt{\gamma \cos \theta / 2\mu} \cdot \sqrt{t} \tag{3}$$

Where γ is the surface tension, θ is the contact angle, μ is the viscosity of liquid, and t is time. Because Haneveld (2008) has reported that this law is established in a 5nm height channel, there would be no problems to apply this law to pores in cementitious materials. Then, substituting Equation (3) into Equation (2), we obtain,

$$M = C\rho \sqrt{\gamma \cos \theta / 2\mu} \cdot \sqrt{t} \tag{4}$$

$$C = n\pi r^{5/2} \tag{5}$$

Where C is the pore structure parameter of concrete. When these properties of a liquid are known, parameters except C and θ can be obtained by measuring weight of absorbed liquid during absorption test. Here, it is considered that the contact angle between ethanol and every solid surface is zero. Therefore, the value of C parameter can be obtained by ethanol absorption test. If the same specimens as ethanol absorption test are used for water absorption test after they are dried enough, the contact angle θ between water and concrete can be calculated by using the value of C parameter.

2.3 The absorption test

Mix designs of the specimens are shown in Table 1. AE water reducing agent and air entraining agent is added with 0.2% and 0.004% of cement weight, respectively. Specimens are demolded 3 days after the casting and under-water curing is given until the age of 28 days, and after that, all specimens are cured in a room of 20 degree Celsius for 2.75 years. Figure 3 shows the diagram of the absorption test. After the specimens are dried in a drying stove at 105 degree Celsius for 3 days, they are put in 95% ethanol which is kept 6cm depth and 20 degree Celsius. The weight of absorbed ethanol is measured at given intervals for 3 hours. Then, the specimens are again put in drying stove at 35 degree Celsius and 20% humidity and after the weight of them become the same as before ethanol absorption test, water absorption test is conducted with the same conditions. Though there is possibility that micro cracks are induced in the specimens during drying at 105 degree Celsius, it scarcely affects the results since the same specimens are used in ethanol and water absorption tests.

Table 1: Mix designs of the specimens

(kg/m ³)	W	C	FA or BFS	S	G
N40	180	450	-	708	978
N55	180	327	-	805	984
N70	180	257	-	886	960
FB55	172	251	62	791	1007
FC55	169	216	92	783	1017
BA55	179	260	65	787	1002
BB55	174	159	159	792	1008

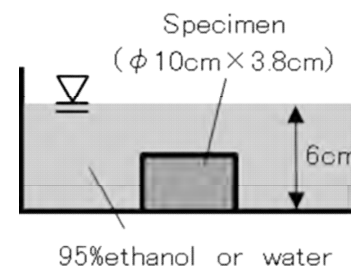


Figure 3: The diagram of absorption test

2.4 The results of measured apparent contact angles

Figure 4 shows the result of absorption test of N40. As shown in Figure 4, the slope decreases as the weight of absorbed liquid increases. The main reason is considered that the area of seepage face decreases as liquid ingress is progressed since liquid is absorbed into the specimens three-dimensionally. In order to avoid this, we use the data 5 minutes after the beginning of the test.

Figure 5 shows the result of calculated apparent contact angles between water and concrete by using the method explained in previous chapter. The apparent contact angles are 60 degree approximately in any specimens though the contact angle between water and concrete has been considered to be zero in many previous papers. This result also indicates that the admixture, such as fly ash and blast furnace slag, affects scarcely the apparent contact angle. In other words, the admixture affects scarcely the capillary pressure as driving force during water ingress into concrete. Therefore, if the admixture affects behavior of water in concrete, the viscous friction as resisting force or the physical property such as the pore structure are considered to be the main influencing factors.

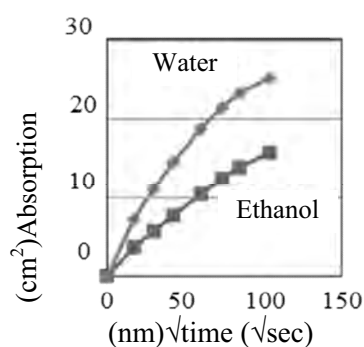


Figure 4: Absorption weight vs. square root of time

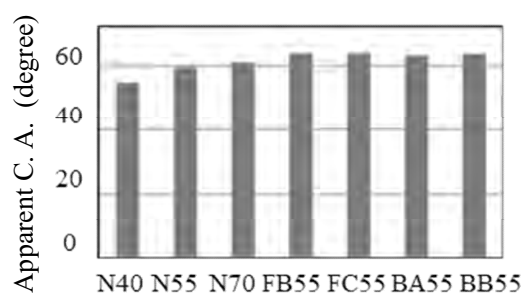


Figure 5: Apparent contact angle

3. THE EFFECT OF PHYSICAL PROPERTY ON WATER PERMEABILITY

3.1 Threshold pore radius

So far, many researchers have pointed out that there is a good correlation between threshold pore radius and water permeability. Powers and Metha studied relationship between pore structures and water permeability. Powers (1955) has found correlation between volume of capillary pore and water permeability, and Metha (1980) has reported a good correlation between threshold pore radius and water permeability. It is considered that threshold pore radius represents the minimum radius of pores which are geometrically continuous throughout all regions of the hydrated cement paste (Winslow et al., 1970). In this paper, we conduct water permeability test and mercury intrusion porosimetry (MIP) to obtain water permeability coefficient and threshold pore radius and study on how physical property of concrete affects water permeability.

3.2 Water permeability test

We conduct water permeability test to the specimens shown in Table 2 added to Table 1 which is used in absorption tests. AE water reducing agent and air entraining agent is added with 0.2% and 0.004% of cement weight, respectively. L55, M55 and H55 represent low-heat cement, moderate-heat cement and high-early-strength cement, respectively. Specimens are demolded 3 days after the casting and under-water, sealed, or in-wind curing are given until the age of 28 days, and after that, all specimens are cured in a room of 20 degree Celsius. Here, in in-wind curing, specimens are winded by a fan for faster drying. Figure 6 shows the diagram of water permeability test. The cylindrical specimens with 10cm in diameter and 20cm in height are cut into 3.8cm thickness from casting side. They are saturated with vacuum for 24 hours until the test. 2.5 MPa pressure is given to the specimens for water penetrating. Figure 7 shows the result of water permeability coefficient k_{wl} calculated by Equation (6) as follows.

$$k_{wl} = l\mu Q / AAP \tag{6}$$

Where l is the thickness of the specimen, μ is the viscosity of liquid, Q is the flow rate, A is the cross-section area of the specimen, and ΔP is the pressure gradient. As the result, it is indicated that higher W/C gives higher k_{wl} and better curing condition gives lower k_{wl} . Therefore, it is considered that this test can catch the property of concrete reasonably.

Table 2: Mix designs of the specimens

(kg/m ³)	Curing condition	W	C	FA or BFS	S	G
N70	Wind	180	257	-	886	960
FB40	Water	172	345	86	694	998
FB70	Wind	172	197	49	873	985
BB40	Water	174	218	218	695	1001
BB70	Wind	174	124	124	873	985
L55	Sealed	180	327	-	807	987
M55	Sealed	180	327	-	807	987
H55	Sealed	180	327	-	804	984

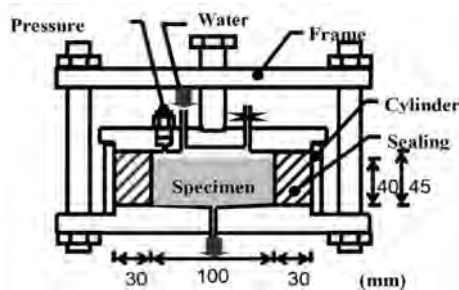


Figure 6: Permeability test set-up

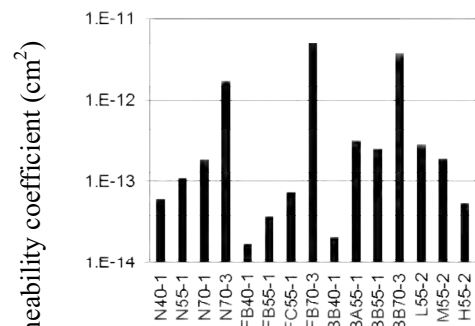


Figure 7: Water Permeability coefficient

3.3 New method to evaluate threshold pore radius

We measured threshold pore radius of concrete sample with MIP following the previous research (Winslow et al., 1970) and in this method, threshold pore radius is the corresponding pore radius where the MIP curve shows the largest tangent. The obtained threshold pore radius is shown in Table 3. Figure 8 shows the relationship between the threshold pore radius and water permeability coefficient, however, the correlation is poor. As a possible cause of the poor correlation, in the first place, threshold pore radius is not extracted correctly. According to the definition, when pressure increases enough to push mercury into the threshold pore of a sample, the intruded volume of mercury must increase rapidly. However, in some samples, the increase is very gentle as shown in dotted line in Figure 9, and it may be difficult to obtain the threshold pore radius in such results. Then, a new method to obtain threshold pore radius more correctly is proposed and discussed.

Table 3: Measured threshold pore radius

	TR (normal) (nm)	TR (Epoxy-coated) (nm)
N40-1	99.35	52.50
N55-1	152.55	52.55
N70-1	51.9	52.70
N70-3	372.05	301.25
FB40-1	41.65	23.75
FB55-1	41.55	15.75
FC55-1	99.2	42.25
FB70-3	881.85	866.95
BB40-1	41.4	52.40
BA55-1	488.75	126.75
BB55-1	871.6	99.30
BB70-3	1108.9	577.45
L55-2	41.5	437.55
M55-2	41.5	59.25
H55-2	41.45	99.35

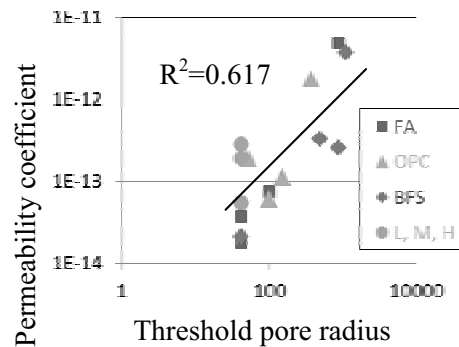


Figure 8: Threshold pore radius vs. water permeability coefficient

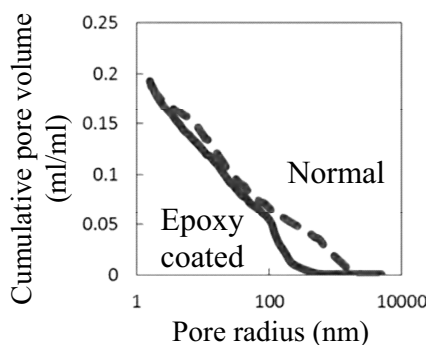


Figure 9: MIP results of normal and epoxy-coated samples

Here, threshold pore radius in MIP means the largest pore radius to push mercury into the core of a sample, and when the pressure corresponds to the threshold pore radius is applied, much mercury is intruded suddenly into the sample. At this time, in normal MIP method, samples are small and mercury is intruded three-dimensionally. As a result, the volume not intruded yet is small and the threshold pore size is not clear, as shown in dotted line in Figure 9. Therefore, special treatment is given to the cubic samples which usually used in MIP, 5mm in a side. They are covered with epoxy-resin leaving small area, about 4mm² as shown in

Photo 1, and MIP analysis is conducted on them. As shown in Figure 10, this treatment will keep larger not-intruded area when the pressure reaches the value which corresponds to the threshold pore radius. Figure 9 is a comparison between the measured results of a normal and an epoxy-coated sample. The result of an epoxy-coated sample shown in solid line is adjusted to coincide with pore volume corresponding to 1.5nm pore radius in the result of a normal sample. It is obvious that epoxy-coated sample shows a clear jump and the corresponding pore radius indicates threshold pore radius. Threshold pore radius measured with the above method is shown in Table 3, together with the results by normal samples, and the relationship with water permeability coefficient is shown in Figure 11. Threshold pore radius measured with the proposed method has a more strong correlation with water permeability in any mix proportions and curing conditions. The above results show that threshold pore radius is obtained by the proposed method reasonably, and the threshold pore governs water permeation. In other words, it is indicated that physical property such as pore structure dominates the behavior of water in the case of water transport driven by pressure gradient. However, it is reported that there is other phenomena occurred in case of deadly slow water permeation, such as the existence of static and kinetic yielding hydraulic gradients (Okazaki et al., 2011). Since they cannot be explained by this result, more detailed consideration is required.

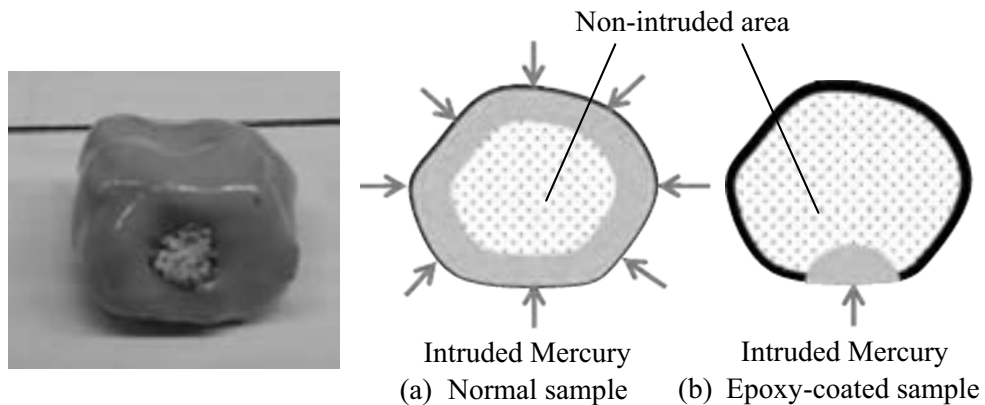


Photo 1: Epoxy-coated sample

Figure 10: Conceptual diagram of mercury intrusion into normal and epoxy-coated samples

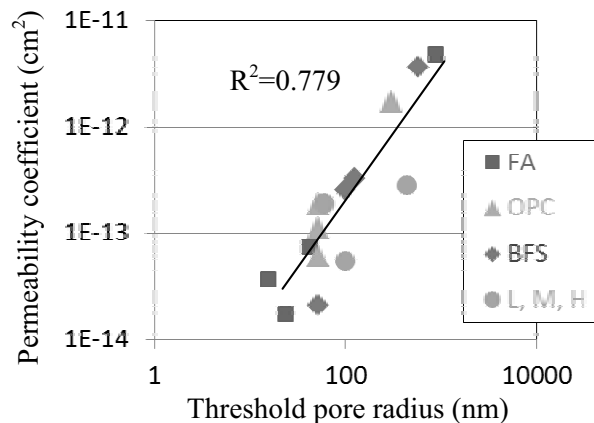


Figure 11: Threshold pore radius vs. water permeability coefficient (Epoxy-coated samples)

4. CONCLUSION

In this paper, the effects of chemical and physical properties of concrete on the behavior of internal liquid water are discussed by using the apparent contact angle and the threshold pore radius as chemical indicator and physical one, respectively. As a result, it is indicated that the difference of chemical property by the kind of admixture affects scarcely the capillary pressure of penetrating water in concrete. Instead, physical property such as pore structure dominates the behavior of water in the case of water transport driven by pressure gradient.

REFERENCES

- Maekawa, K., Ishida, T., and Kishi, T., 2009. *Multi-scale Modeling of Structural Concrete*. Taylor and Francis.
- Okazaki, S. and Kishi, T., 2011. *A study on the mechanism of dead slow permeation of water and modelling in saturated concrete*. Journal of JSCE, Vol.67, No.3, 396-410.
- Young, T., 1805. *An essay on the cohesion of fluids*, Philos. Trans. Roy. Soc. London, Vol.95, 65-87.
- Letey, J., Osborn, J., and Pelishek, R., E., 1962. *Measurement of liquid-solid contact angles in soil and sand*, Soil Sci., Vol.93, 149-153.
- Washburn, E. W., 1921. *The dynamics of capillary flow*, Physical Review, Vol.17, 273-283.
- Haneveld, J., Tas, N. R., Brunets, N., Jansen, H. V., and Elwenspoek, M., 2008. *Capillary filling of sub-10nm nanochannels*, J. Appl. Phys 104, 014309.
- Powers, T. C., Copeland, L. E., Hayes, J. C., and Mann, H. M., 1955. *Permeability of Portland cement paste*, Journal of the American concrete institute, Vol.51, 285-298.
- Mehta, P. K. and Manmohan, D., 1980. *Pore size distribution and permeability of hardened cement paste*, 7th International Congress Chemistry Cement1 Paris, Vol.3,7.1-7.5.
- Winslow, D. and Diamond S., 1970. *A mercury porosimetry study of the evolution of porosity in Portland cement*, Journal of Materials, Vol.5, 564-585.

The fire resistance issue of reinforced concrete beam

Duinkherjav Yagaanbuyant, Erdenedavaa Bat-Ochir
The School of Civil Engineering and Architecture,
The Mongolian University of Science and Technology,
daamt@must.edu.mn

ABSTRACT

The study of fire resistance limit and the study of load bearing capacity of structure after fire exposure have been carried out up to date by researchers. This paper is devoted to the second part. Why we chose this study topic? Unfortunately, in Mongolia we still have tendency to demolish buildings exposed to the fire. We aim to study possibility of safe occupation of those buildings through adequate strengthening of the structures on the basis of thorough diagnosis and investigation of the state of the structure.

Keywords: concrete testing, diagnosis, fire-resistance, loading,

INTRODUCTION

By 2004, the capital city of Mongolia had population of 915531 and this number has increased up to 12000000 by 2008 due to intense movement of population from rural areas. This increase of population is also contributes to the unavoidable hazards. Fire call ranks in the second after traffic accident among emergency call and its percentage is 12 from the total [1].

In 2004-2009, total of 7402 fire incidents in buildings and 141 fire incidents in forestry are registered that damaged 3900 hectar of forest areas and 476.2 hectar areas of farming; the total loss of these reached 6.4 billion MNT. If we see the classification of fire incidents; 422 cases of 2.1 billion MNT belong to state owned companies, 6980 cases of 4 billion MNT belong to private companies and people, 3 million MNT cases belong to joint venture with foreigners or foreigner owned entities. The death toll is 172 and the number of the injured is 152; apartments and houses of 2392 households, 472 vehicles and 3400 buildings and 138 farm buildings have been damaged in certain scale [1].

Even though reinforced concrete is considered as a material having relatively good fire resisting capacity, its improper design and poor operational condition lower its reliability level and it does not confirm the requirements of the Building Code. In this year there have been large scale fires in Apartment building No.14 of Darkhan city, silo of wheat grain, commercial building in Ulaanbaatar city, storage building of furniture market, hotel building and all these building had reinforced concrete frames.

The fire occurrence in the buildings is frequently observed after strong earthquake and explosion and this brings enormous financial loss to the economy.

Fire resistance is the relatively new field of the study in Mongolia especially related with building structure. In this paper some test results of fire resistance of

some simple structural elements are discussed and the research significance can be determined as an improved building design that could bring more safe environment to citizens.

1. Fire resistance limit of building structures

From many years of practice it is observed that fire exposure on building structure develops different level of damage. Some of the structures had been fully damages; some are just heated experiencing small sized deflection and crack development. In the first case replacement of the structure and in the latter case limited occupancy are possibly can be suggested.

The degree of structural damage due to fire exposure is determined by fire resistance limit of structural element in one side and the time length of fire and temperature created in other side. Therefore it is necessary to estimate the time length of fire and the limit of fire resistance of the structure first. V.E.Murashev formula can be used to establish the required value of the limit of fire resistance as shown in equation (1).

$$R \geq K_0 \cdot \tau \quad (1)$$

R – the required value of the limit of fire resistance, hrs;

K_0 – fire resistance coefficient;

τ – estimated time length of fire, hrs.

Depending on type, size and complete burn period of material, the time length of fire can be determined by equation given in (2).

$$\tau = q/m \quad (2)$$

τ – estimated time length of fire, hrs;

q – quantity of material combustible, kg/m²;

m – combustion rate kg/m².

Eq (2) can be looked as a simple but actual time length of fire is not so easily determinable. What this means? The rate of combustion depends heavily on air flow condition and location in fire zone. The material can also contain noncombustible minerals in it. This should be considered in quantity of material combustible in eq (2). The main drawback of equation (2) is that it doesn't take account of temperature of fire. For example when rubber and paper burned up in an hour the former can create temperature of 1100°C but the latter's can be 500°C. Depending on this effect of fire exposure into building structure is different. Therefore in the above equation an estimate of fire resistance limit uses time length of fire in a unit temperature scale.

2. Research methodology

From the experiments carried out in different countries different structural elements such as beam, slab, column, trust etc. are chosen for fire test. We tested reinforced concrete beam in our study. Beam section is shown in Fig 2, 3 and design scheme of beam as flexural element is considered as statistically determined element. Before fire loading beam was loaded by static load of 2 κH/M² as work load. Fire load was chosen according to the curve of 'standard fire' as shown in Fig 1.

Physical and mechanical properties of beam is determined before fire test and temperature and strain are measured during the testing. After testing visual

inspection was done and change in actual length, section dimensions and location of rebars are examined and measured. The depth of cover of rebars is chosen as 15, 25, 35mm respectively in the testing.

3. Experimental part

3.1. Temperature of fire and structure

Fire temperature in the test should follow 'standard fire' curve as given in Fig 1. Actual temperature created by fire is measured by thermocouple of alumel and chromel and it was located in a distance of 70 to 100mm from the surface of element. Diameter of thermocouple is 3mm and 5mm at the end.

Inside temperature of beam is also measured by the same thermocouple of alumel and chromel and it was located inside before cast. Diameter of thermocouple is 0.7mm.

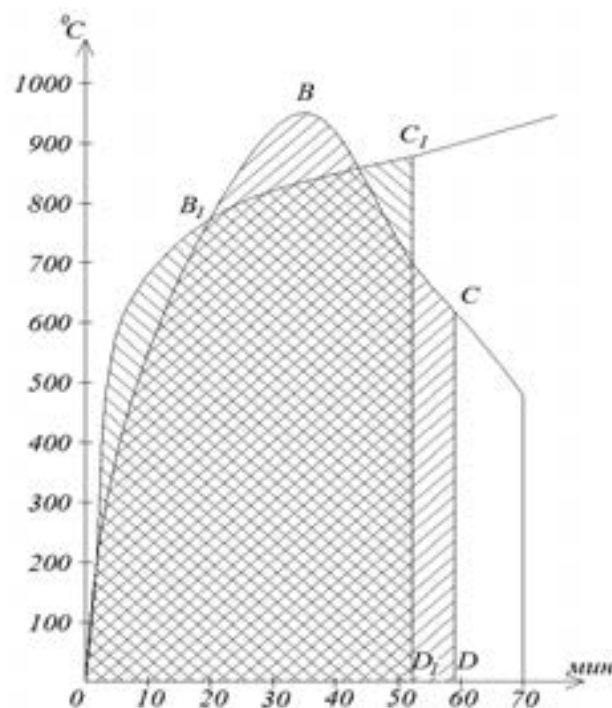


Fig 1. Temperature scheme of standard fire and experimental fire

3.2. Beam strain and stress

The major significance of this paper is the study of the stress and strain state of loaded beam and load bearing capacity of the beam after fire exposure.

There are two types of the study in this field, one is study of fire resistance limit and the other is the study of load bearing capacity of structure after fire exposure. This paper is devoted to the second part. The reason is in the country there is still strong tendency to demolish buildings after fire exposure. One example is Revolutionary Party Building, as an expert provided diagnostics of the building status I can assure that there was still possibility to reinforce the building structure through strengthening.

3.3. Tested Beam Details

Reinforced concrete beam was designed by Structural Testing Laboratory of MUST, the OPC 42.5 from Khutul cement was used, tension rebars of $\Phi 13\text{mm}$ of Grade SD390 from Darkhan and shear rebar of Grade Q235 from China are used also. Water cement ratio is 0.45 and 28 day strength of the concrete is 32.5MPa. The formwork of the beam was carried out using plywood. The section design is shown in Fig 3.

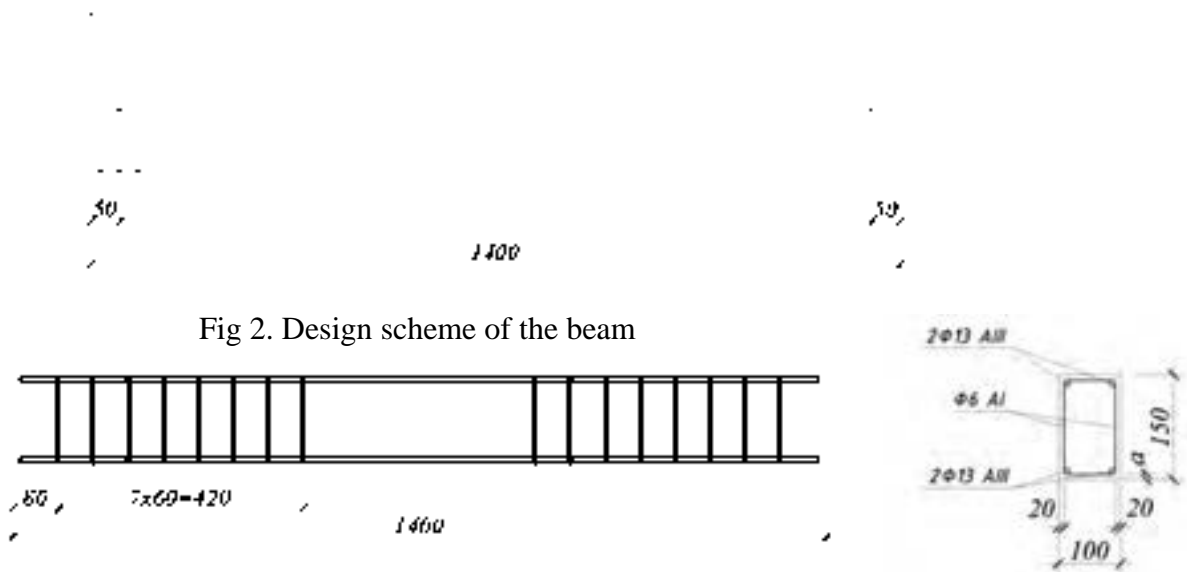


Fig 2. Design scheme of the beam

Fig 2. Rebar location in beam

3.4. Experimental work

Fire resistant test was carried out in the area of Building No.2 of MUST. The experiment was designed as stated above that beam had kept in open fire for 1 hr in the temperature of 600°C. The crack with width of 0.08mm was developed in tension zone of the beam. Beam deflection was measured by displacement measure made in Japan. After cooling of the beam it was tested under loading to test its load bearing capacity as shown in Fig 4 and 5.

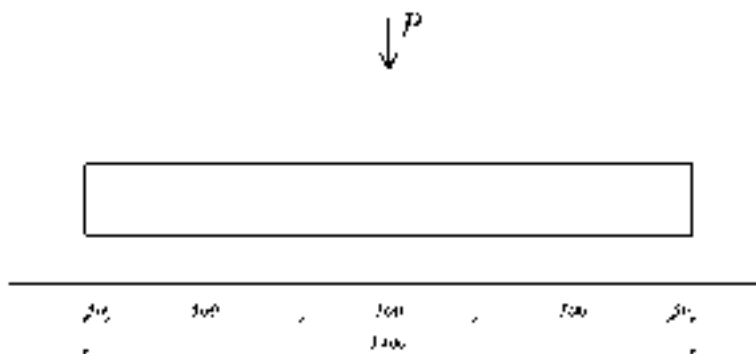


Fig 4. Testing design scheme of the beam



Fig 5. Testing of the beam

3.5. Results discussion

Crack development and deflection relationship of the beam during loading after fire exposure is shown in Fig 6. There have been developed cracks with width of 0.08mm and 0.04mm respectively in two beams that had been tested in fire. During loading of the beams it was observed that 0.3mm cracks are developed under 60kN load in the beam not exposed to fire and under load of 50kN and 45kN for the beams exposed to fire.

Table1. Width of cracks developed in beams and load tested

Load, κH	Crack width, mm		
	Not exposed to fire	Exposed to fire	
		1	2
0	0	0,08	0,05
10	0	0,08	0,05
20	0	0,1	0,075
30	0,01	0,15	0,125
40	0,1	0,2	0,2
50	0,2	0,3	0,325
60	0,3	0,4	0,45
70	0,4	0,45	0,5

Table 2. Deflection of beams and load tested

Load, κH	Beam deflection, mm		
	Not exposed to fire	Exposed to fire	
		1	2
0	0	0,2	0,15
10	0	0,2	0,15
20	0,2	0,8	0,3

30	0,8	1,2	1,3
40	1,2	2,2	2,5
50	2	3,5	3,8
60	3,6	5,1	6,0
70	5,0	7,5	8,0

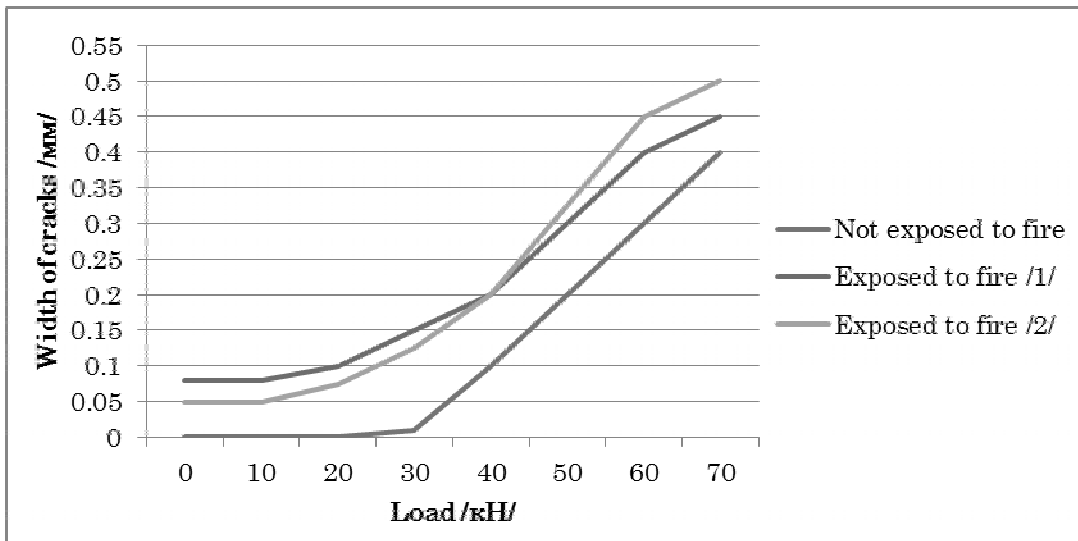


Fig 6. Width of cracks developed in beams and load tested

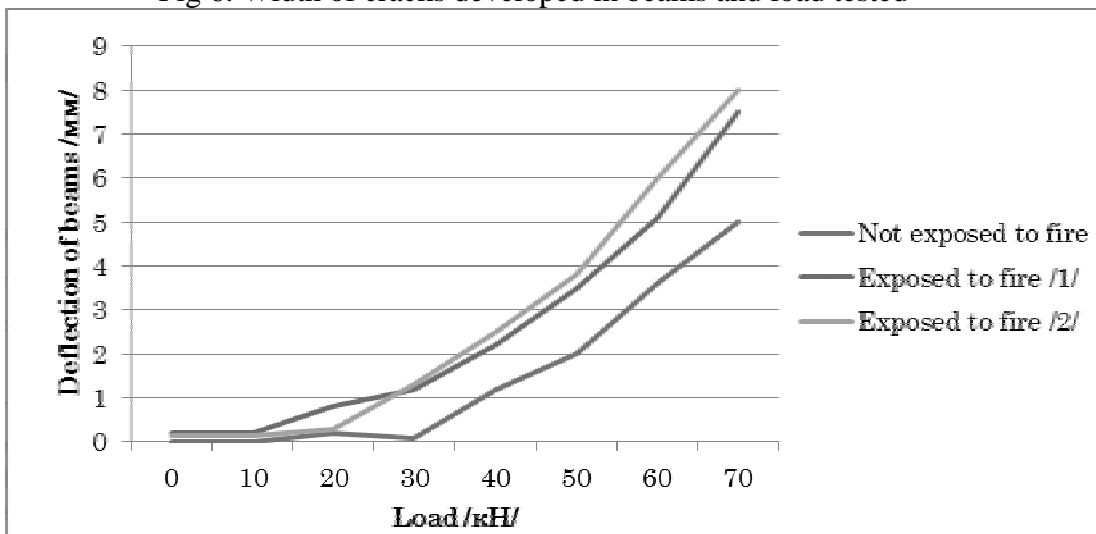


Fig 7. Deflection of beams and load tested

Conclusion

Test results are very consistent for 16 beams tested. Therefore, in this paper results of two beams are discussed. Beam deflection and crack width results show that load bearing capacity of beams are within acceptable limit after testing in fire. In other words beams can be re-used. These beams can be reinforced using strengthening methods to improve its load bearing capacity.

Reference

1. Hazard Report: Hazard faced in the city in 2004-2008, causes of technical incidents and prevention measurements, UB, 2009,
2. Butcher E. G, Parnell A. C., Smoke control in fire safety design. London E.& F.N. Spon. 1980
3. А.П.Кричевский. “Расчет железобетонных инженерных сооружений на температурные воздействия”. 1984. М /in Russian/
4. Ройтман М. Я.: Противопожарное нормирование в строительстве. – М.: Стройиздат, 1985: -590с., ил. /in Russian/
5. Ройтман В. М. Инженерные решения по оценке огнестойкости проектируемых и реконструируемых зданий. Издат. АВС. М. 2008/in Russian/
6. Ройтман В. М,ТеличенкоВ. И.: Стойкость объемов строительного комплекса при комбинированных особых воздействиях с участием пожара – важный элемент их комплексной безопасности. В кн.Безопасность эксплуатируемых зданий и сооружений. Под ред. В. И. Теличенко и К. И.. Ерёмина. М.: Магнитгорский дом печати. с.58-86./in Russian/
7. А.Ф.Милованов. “Стойкость железобетонных конструкций при пожаре”. 1999. М/in Russian/
8. BS 8110 Structural use of concrete. Part 1, part 2, part 3.
9. СНиП 21-01-97. Пожарная безопасность зданий и сооружений. /in Russian/

Modeling of diffusive and advective transport of ionic species in cemented soil

Hayato IKOMA¹, Taiju YONEDA², Tetsuya ISHIDA³

¹Master Course Student, IIS, The University of Tokyo, Japan
ikoma@iis.u-tokyo.ac.jp

²Researcher, Department of Civil Engineering, The University of Tokyo, Japan

³Associate Professor, Department of Civil Engineering, The University of Tokyo, Japan

ABSTRACT

Stabilization of the contaminated soil with cementitious materials is regarded as an effective and economical method. Since this method has possibility of elution of pollutant ions, it is necessary to simulate and evaluate the process quantitatively. Authors' research group has developed a computational model under hydrostatic condition considering the equilibrium of ions in solid and liquid phase. In this research, Authors improve this model which can evaluate elution under advective environment, on the basis of elution experiment with rapid water flow. In the experiment, Cl⁻ is used as tracer in cemented soil, and one-dimensional flow is applied with changed velocities. The result indicates that the equilibrium is lost, and Cl⁻ is eluted more slowly than predicted. The authors proposed an improved model. In the improved model, the equilibrium is not achieved instantly, and the elution rate depends on the amount of fixed Cl⁻. Since fixed Cl⁻ consists of two types, their elution speeds are dealt with respectively. The simulation of elution process with the improved model shows consistent result with the test. Hence, it is concluded that ion elution under advection environment can be properly simulated by considering the elution rates of fixed ions. The proposed approach is promising for the future application to other pollutant ions such as Cr(VI).

Keywords: soil pollution, advective transport, cemented soil, chloride diffusion, Cr(VI)

1. INTRODUCTION

1.1 Background

Solidification of the contaminated soil with cementitious materials is regarded as an effective and economical method to stabilize the pollutants in the soil. In the cement hydrates, the bounded amount of the pollutants may vary depending on the amount of free ions in pore water. And, when ground water flows through the solidified soil, the concentration of ions in pore water changes and the elution of ions may occur. Therefore, it is necessary to simulate and evaluate the elution process quantitatively.

In order to predict time-dependent behaviors of cement hydrates and ions, a multi-scale constitutive model, DuCOM, has been developed in Concrete Lab, the University of Tokyo. In this model, based on the equilibrium of ions in solid and

liquid phases, the amount of fixed ions in cement hydrates can be calculated. Recently, this model has been expanded to deal with the phenomena in soil field, such as soil pollution with Cr(VI). However, Sakimura et al. suggests that the current model cannot be attained to the situation under advection dominant condition. In hardened cement paste, which are the main target of the model, pore structure is dense and water flow is slow enough to be treated the as the completely equilibrium state. However, as to cemented soil the pore structure is quite coarse and the water flow is relatively fast. In cemented soil, under advective situation, the amounts of ions in pore water change too rapidly before achieving the equilibrium state. In this study, for the purpose of evaluating elution process with rapid water flow, the authors carried out experiments and improved the existing model under Semi-equilibrium states.

1.2 Stabilization model

Equation (1) shows the governing equation for ion equilibrium and transportation in current DuCOM model.

$$\frac{\partial}{\partial t}(\phi \cdot S \cdot C_{ion}) - Q - divJ_{ion} = 0 \quad (1)$$

Where, ϕ is porosity [m^3/m^3] and S is degree of saturation. C_{ion} represents the amount of ions in pore water [mmol/l]. Q represents the amount of bounded amount of ions and J_{ion} represents flux vector of ions [mmol/($m^2 \cdot s$)]. Q is decided by the amount of fixed ions and the equilibrium of ions in solid and liquid phases as follows.

$$Q = C_{bound} - C_{bound_eq} \quad (2)$$

Where, C_{bound} is the current amount of bounded ions at specific time and C_{bound_eq} is the amount of bounded ions after bounded amount will be balanced with C_{ion} in the equilibrium [mmol/l]. Since in current model, ions are assumed to achieve equilibrium state instantly, Q is independent from time. And, the equilibrium state of ions in solid and liquid phases can be decided experimentally. In this research, Cl^- is used as tracer in cemented soil. For Cl^- , the equilibrium has been studied by Portland cement pastes with various w/c ratios and mineral admixtures such as fly ash cement and slag cement. In cement materials, Cl^- ions are fixed in two different forms; Friedel salt ($Ca_2Al(OH)_6(Cl, OH) \cdot 2 H_2O$) and adsorbed Cl^- . With ordinary Portland cement (OPC), the equilibrium state was defined as equation (3) considering the different fixed forms (Ishida and Lan Anh, 2005).

$$C_b = \frac{\alpha \times C_f}{1 + 4.0C_f} \quad (3)$$

$\alpha = 11.3$ (OPC)

Where, C_b is the amount of Cl^- in solid phase and C_f is the amount of Cl^- in liquid phase. α changes with the type of cement materials.

2. EXPERIMENTAL

2.1 Material properties

To confirm the reliability of current model under advection dominant conditions, elution experiments with Cl^- were conducted.

Table 1: Mix proportion

Description	W/C (%)	C (kg/m^3)	W (kg/m^3)	S (kg/m^3)	NaCl (kg/m^3)
C100	100	100	100	1493	20
C200	100	200	200	1493	20

Table 2: Specimen condition

	Void (%)	Permeability (cm/s)	Cl^- ion (g)
C100	39%	0.068	3.58
C200	21%	0.062	3.89

The mix proportion is shown in Table 1. Two groups of mortar specimens (C100 and C200) are cast with varied cement volume and much higher w/c ratio than normal case. OPC and natural sand are used. The specimens contain NaCl in advance. In this experiment, the Cl^- is used as a tracer ion considering the experimental safety, ease of treatment and the numbers of past research, although the final goal of this research is the soil pollution phenomena with Cr(VI) .

The specimen data which is important on the elution phenomena are given in Table 2. To unify the compaction degree of the specimens, Specimens are compacted with specific methods, such as dropping a steel stick from an altitude of 15cm in 25 times.

2.2 Equipment and test program

The equipment and test program is shown in Figure 1. The length of the specimen is 200mm and the diameter is 50mm. But the available maximum length of mold is 100mm considering the size of the vacuum saturation equipment, so, two 100mm specimens are connected after curing and vacuum saturation treatment. The actual degree of saturation is 75-85%. Water head difference is applied to provide one-dimensional flow into specimens at a uniform speed. Water flowing out of the specimens is collected and the density of Cl^- in the collected water is measured by the potentiometric titration machine.

The water head is changed to provide different flow speeds. For C100 the flow speed is 0.020 and 0.010 (cm/s), and for C200, the speed is 0.012 and 0.004

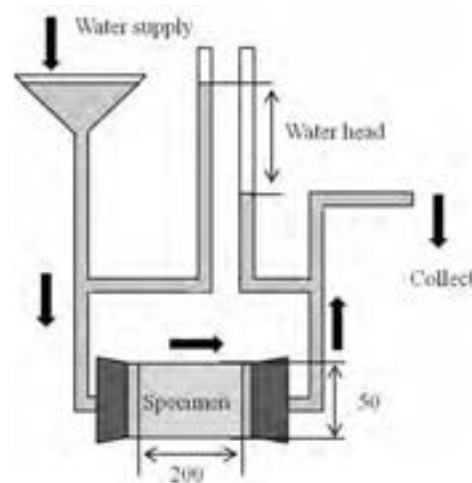


Figure 1: Equipment

(cm/s). A part of tubes is broken during the experiment so the data of C200, 0.004 (cm/s) flow speed is lost.

2.3 Elution experiment

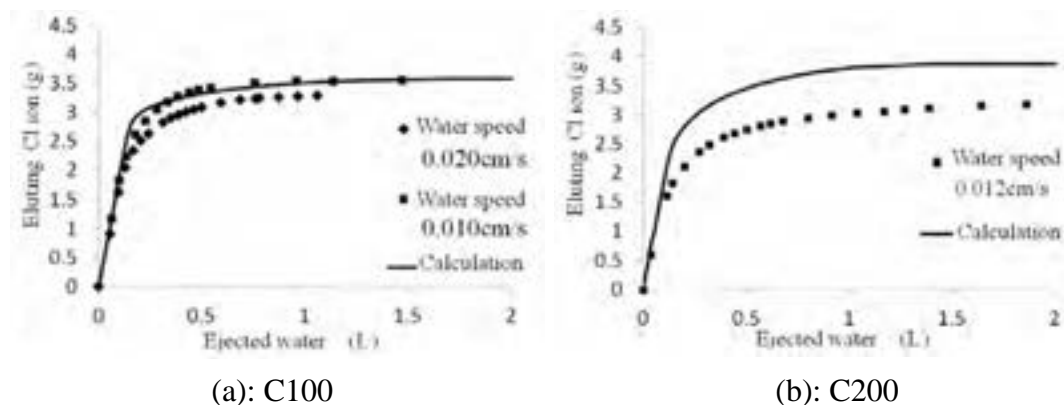


Figure 2: Result of elution experiment

The experimental results are shown in Figure 2. In the figures, analytical results with DuCOM are also plotted with line. The vertical axis is the amount of eluting Cl^- (g), and the horizontal axis represents the ejected water (L). The data was measured every five minutes at the first one hour, and then measurement interval becomes longer with 10 minutes, 30 minutes, and 1 hour. And it took around 2 hours to run 1 L of water through the specimens.

In this calculation, the current model assume the complete equilibrium state at each time steps, so cannot consider the effect of water flow on the equilibrium, the result is the same in different water flow speed.

Fig. 2-(a) shows the result of C100. It can be seen that there is only little difference between different water flow speeds. This difference cannot prove the influence of advection if considering the error generated by the equipment. It is supposed that the difference of the water flow speeds and the amount of fixed Cl^- are not large enough to observe the influence of advection. According to this figure, the existing model seems to simulate the elution process well.

Fig. 2-(b) shows the result of C200. In this case, Cl^- is eluted slower than the calculation. In the elution of hydrostatic condition, the existing model, which considering the equilibrium of ions between solid and liquid phase, can simulates the elution process properly. However, In Fig. 2-(b), this is the advection dominant condition, Cl^- ions do not dissolve enough to achieve the solid-liquid equilibrium. Some part of Cl^- ions remains in the specimen because water flow is too fast. In this experiment, it took about 15 minutes for flowing water to go through the specimen, which may be too short for chloride in solid and liquid phases to become the equilibrium state. Here, we can find the advection influence on elution phenomena.

3 IMPROVED ANALYSIS MODEL

3.1 Current model

In the calculation, and the amount of eluting Cl^- increases at a constant speed in the early stage and then elution becomes slower. In the existing model, it is premised that ions move with only advection and diffusion, so, the blending of pore water and flowing water in the specimen is ignored. In the early stage, according to this premise, the ejected water is pore water which exists before water flowing. After all the original pore water is ejected, chlorides start to elute in the flowing water which is ejected afterwards.

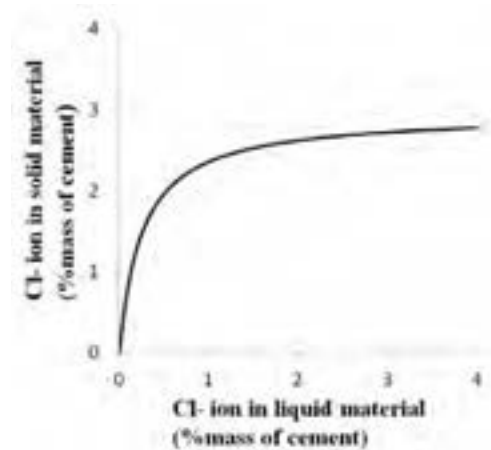


Figure 3: Equilibrium of ions in solid and liquid phase

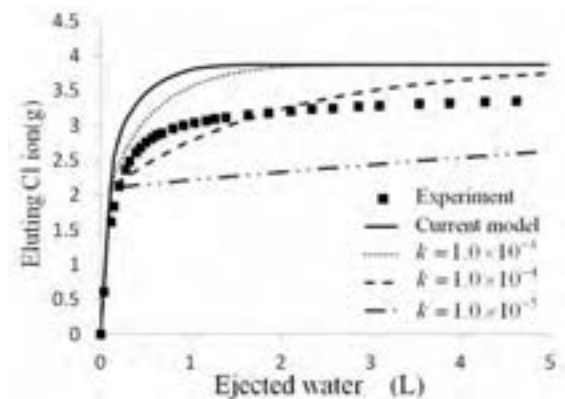


Figure 4: Analysis of the model with single coefficient

Following Equation (3), the equilibrium between ions in solid and liquid phases in cement paste is plotted in figure 3. The vertical axis represents fixed Cl^- in solid hydrates, and the horizontal axis represents Cl^- in pore water. In the existing model, the relationship between fixed Cl^- and free Cl^- is always on this equilibrium line. When the amount of Cl^- in pore water decreases, the amount of fixed Cl^- also decreases along the curve in Figure 3 to keep the equilibrium.

Accordingly, when pure water flows into the upper stream part of specimen, first, in upper stream part, the concentration of Cl^- in the pore water decreases and chlorides in the solid elute out to pore water. This elution is completed instantly and the state of new equilibrium state is achieved immediately. Next, downer stream part begins to elute, and finally, final part begins.

However, in existing model, that Cl^- elution from cement matrix part to pore water finishes instantly. However, as mentioned beforewards, this assumption seems not work well in advective situation.

3.2 Modified model with single coefficient

In order to simulate elution in advective situation properly, it is necessary to consider the speed of elution from solid to liquid phase. For advective condition, the Cl^- concentration in pore water at specific control area is changed instantly by advection flow. Accordingly, elution of ions from cement hydrates to pore water starts, and it would take some time until the equilibrium state. This implies the elution speed should be considered. Especially if the flow speed is fast enough, elution speed becomes the principal factor of affecting the concentration of chlorides. Here, equation (2) was modified as equation (4).

$$Q = \frac{\partial C_{bound}}{\partial t} \tag{4}$$

$$\frac{\partial C_{bound}}{\partial t} = k(C_{bound} - C_{bound_{eq}})$$

Herein, fluctuation term Q is dominated by the coefficient k . k represents the influential factor of elution which is related to water flow speed. If ions in solid phase are assumed to elute instantly, k becomes enormous. k depends on several factors such as the type of ions, solid materials temperature, or other parameters. In this study the value of the coefficient k was derived from the test result of C200. First, different value of k is given to the modified model and the results are compared in figure 4. It shows that smaller k value provides smaller analytical result. For advective situation, the modified model with coefficient k implies that Cl^- ions in solid phase dissolve gradually as time passes, which is different from the original model.

However, none of the modified models can reproduce the whole elution process with enough accuracy. In the analysis of the model with smaller k such as 1.0×10^{-5} , the elution speed becomes much slower after all the original pore water is flushed out by the water flowing, so the final value is greatly underestimated. However, in reality some chlorides in solid phase may continue to dissolve and the volume of eluting ions still increases. In this study the authors assume that different elution process exist depending on the bounding forms of chlorides. Hence it is necessary to improve model additionally considering the bounding forms of chlorides.

3.3 Improved model with multiple coefficient

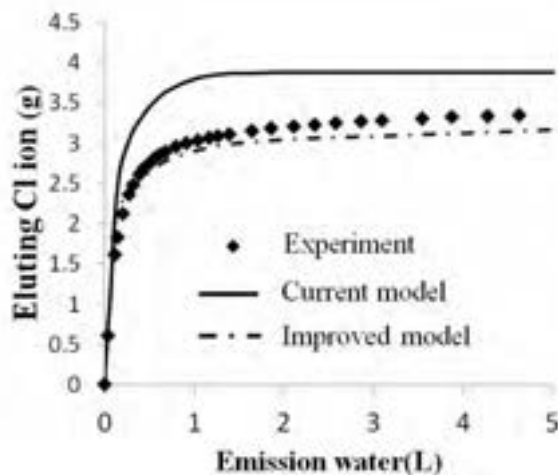


Figure 5: Analysis of the model with multiple coefficients

Chlorides bounded to cement hydrates principally have two bounding forms, one is crystallized chlorides, which is represented by Friedel salt ($Ca_2Al(OH)_6(Cl, OH) \cdot 2 H_2O$) and the other is adsorbed Cl^- . Since the elution process of these two bounding forms may be different, it is necessary to describe

them separately. Therefore equation (5) and (6) are given to describe the amounts of adsorbed Cl⁻ and crystallized chlorides per unit time respectively.

$$\frac{\partial C_{bound_ads}}{\partial t} = k_{ads}(C_{bound_ads} - \beta C_{bound_eq}) \quad (5)$$

$$\frac{\partial C_{bound_fix}}{\partial t} = k_{fix}(C_{bound_fix} - (1 - \beta)C_{bound_eq}) \quad (6)$$

$$\frac{\partial C_{bound}}{\partial t} = \frac{\partial C_{bound_fix}}{\partial t} + \frac{\partial C_{bound_ads}}{\partial t} \quad (7)$$

Where, k_{ads} and k_{fix} represents the influential factor of elution related to adsorbed Cl⁻ and crystallized chlorides respectively. Since crystallization is relatively stable form of solidification, it can be assumed that the elution is slower and k_{fix} is given smaller value than k_{ads} . And β is the rate of each bounding forms of Cl⁻. In this research, β is assumed 0.5, and it means that half of the total bounded Cl⁻ is crystallized form and the other half is adsorbed form. The amount of total bounded Cl⁻ is the summation of those equations (Equation (7)). Coefficients k_{ads} and k_{fix} are assumed with the experimental results.

With the trial and error analyses, from the experimental result, model with $k_{ads} = 1.0 \times 10^{-3}$ and $k_{fix} = 1.0 \times 10^{-5}$ can estimate the elution process most realistically. Analysis with current model and improved model are compared in Figure 5. It shows that improved model can estimate the elution under advective situation more properly than the existing model. Furthermore, the point where elution speed changes can be well reproduced by the improved model.

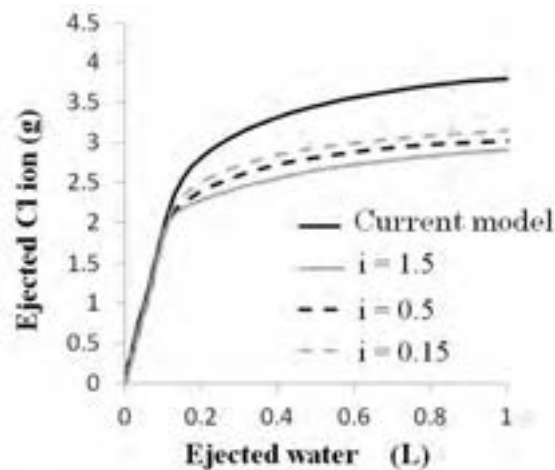


Figure 6: Sensitivity analysis of the improved model

In Figure 6, the results of sensitivity analysis with different hydraulic gradient are shown. In the figure the parameter i represents the hydraulic gradient, and with different i value, we can get the different elution behaviors. The value 1.5 is the actual hydraulic gradient value in the experiment of C200. In order to distinguish the influence of water speed, much smaller values of hydraulic gradient such as 0.5 and 0.15 are also given in the sensitivity analysis.

The results show that only when the water speed difference is as large as around 10 times, can obvious difference of eluting process be observed. On the other

hand, in the test of C100 in this study, no obvious difference of eluting process with varied flowing speed exists as mentioned before. One of the reasons may be that the equipment in this research can only produce water head difference in 2-3 times. Therefore in the future research the influence of water speed on the elution should be verified experimentally. Furthermore, it is important to apply the improved model which considering elution speed and different forms of fixed ion, to other species of ions. Although this research used Cl^- as tracer, this model was investigated in the scope of estimating the behaviors of heavy metal ions which cause soil pollution, such as Cr(VI) . It is supposed that Cr(VI) are also fixed in two form like Cl^- ; adsorbed ion and crystallized ion. The improved model in this research can be applied also for the Cr(VI) . But the values of coefficient must be different from the species of ions, so in future research, the coefficients of elution speed need to be estimated with the experiments using Cr(VI) .

4 CONCLUSIONS

Based on the results of elution experiments under advective condition and simulations considering elution speed and forms of fixed ions, the following conclusions are obtained:

- (1) Based on the elution experiment under advective condition, the characteristic elution process with water flow is clarified experimentally. The existing model which is established for hydrostatic condition cannot simulate the elution process under advective condition.
- (2) The improved model considering elution speed can simulate the experimental elution process properly under advective situation, by considering elution speeds for two fixed forms of Cl^- separately. Sensitivity analysis suggests that only by changing the flow speed largely can the process of elution be obviously influenced.
- (3) The model considering elution speed and fixed form can apply to other pollution ions. Especially, since behaviors of Cr(VI) is not so different from Cl^- ion in the fixed forms, the value of coefficient can be decided with similar experiments using Cr(VI) .

5 REFERENCES

- Maekawa, K., Ishida, T., Kishi, T., 2008. *MULTI-SCALE MODELLING OF STRUCTURAL CONCRETE*, Taylor and Francis.
- Sakimura, T., Ishida, T., Nakarai, K., Usui, T., 2005. *Analysis of calcium ion based on multi-scale pore model*, Annual meeting of JCA, Japan (in Japanese).
- Ho Thi Lan Anh., 2005. *Modeling of chloride transport under arbitrary temperature*, Master Thesis, University of Tokyo.
- Takahashi, Y., Ishida, T., 2011. *Leaching analyses of cement-solidified soil contaminated with Cr(VI) using multi-scale thermodynamic analytical system*. Japan National Conference on Geotechnical Engineering, (in Japanese).

Shear performance of PVA-coarse aggregate-ECC beams under a rotating stress field

Yoshiyuki TAKANO¹, Benny SURYANTO² and Kohei NAGAI³

¹ Graduate Student School of Eng., The University of Tokyo, Japan
y-takano@iis.u-tokyo.ac.jp

² Researcher, The University of Tokyo, Japan

³ Associate Professor, IIS, The University of Tokyo, Japan

ABSTRACT

This paper reports the results of two series of experiments on PVA-ECC and PVA-Coarse Aggregate-ECC beams under static and fatigue loading conditions. The primary objective was to study the beneficial effects of aggregate interlock at a structural member level. The first experiment series involved the testing of shear-critical beams under center-point fatigue loading. Despite lowering tensile capacity and ductility, coarse aggregate was found to preserve the shear fatigue performance of the beam, indicating a trade-off between tensile and shear mechanical properties. The second experiment series involved the testing of shear-critical beams subjected to anti-symmetric four-point static and fatigue loading. The effects of precracks were investigated to represent the possible rotation of stress field. While the advantage of aggregate interlock under static loading was not quantified, it was observed that it is effective to influence the stress state in the ECC, to lengthen fatigue life, to control crack angle, and to limit the magnitude of shear slip under repeated cycles. Instead of these potential advantages, detailed crack observation along the failure crack surface indicates that the aggregate was not able to protect the rupturing of fibers in shear.

Keywords: PVA-ECC, aggregate, shear fatigue, rotating stress

Table 1: Series of experiments

Series of experiments		Name of specimen	Material	Size of specimen(mm)	Longitudinal reinforcement (%)	a/d	Reinforcement	
Bending			Normal ECC	100×100×400				
			ECC + Aggregates					
Compression			Normal ECC	φ100×200				
			ECC + Aggregates					
Simple beam	Fatigue		ECC-F-S	150×300×1800	3.80	3.10	3D25 USD685	
			CA-F-S					
Anti-symmetric four point shear test	Static	Precracked	ECC-S-P	100×200×1200	4.59	2.29	4D16 USD685	
			CA-S-P					ECC + Aggregates
		Non- precracked	ECC-S-N					Normal ECC
			CA-S-N					ECC + Aggregates
	Fatigue	Precracked	ECC-F-P					Normal ECC
			CA-F-P					ECC + Aggregates

1. INTRODUCTION

Polyvinyl Alcohol Engineered Cementitious Composite (PVA-ECC) is a unique example of Strain Hardening Cementitious Composites (SHCCs). In this material, the strain hardening property is realized through the formation of fine, multiple cracks. Across each of these cracks, tensile stresses exist and are transmitted by the PVA fibers (typically 2% by volume) bridging each of the two crack surfaces. Not only may tensile stress, but also shear stress may develop across the cracks. Nevertheless, the later has not been investigated in-depth. Recently, the authors found that coarse aggregate, when added to the ECC, improves the material behavior in terms of cracking and load-carrying resistance, particularly when subjected to a complex stress field.

In response to this material-level behavior finding, experiments were conducted on PVA-ECC and PVA-coarse aggregate-ECC beams, in order to investigate the beneficial effects of aggregate interlock at structure-level behavior. Two different test configurations were considered: beams subjected to center-point fatigue loading, to provide a preliminary insight into the benefit of aggregate interlock, and beams subjected to anti-symmetric four-point static and fatigue loading, to investigate the problem on a better shear state. In the second test configuration, some beams were also preloaded prior to testing, in order to simulate a complex stress situation such as under the continuous rotation of stress field as generally experienced by a bridge deck under traffic loading. Interests were on the ultimate load capacity, fatigue life, crack pattern, and average strains across cracks.

2. EXPERIMENTAL PROGRAM

2.1 Material

Two materials were tested: PVA-ECC (hereafter abbreviated “ECC”) and PVA-ECC mixed coarse aggregates (hereafter abbreviated “ECC+CA”). For the later, coarse aggregate was added at about 10% by volume, which was found to be the optimum amount (Suryanto et al 2009). The maximum size of the coarse aggregate was 9.5 mm. A summary of the experimental program is shown in Table.1.

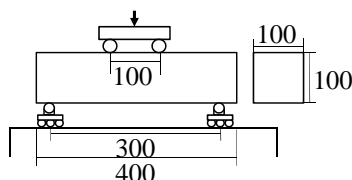


Figure 1: Bending test

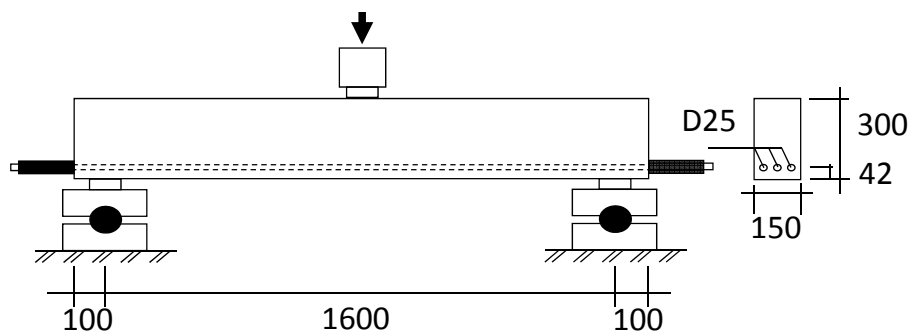


Figure 2: Beam test under center-point loading

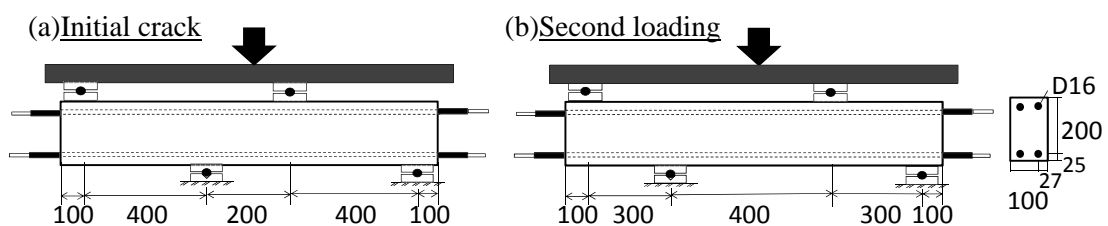


Figure 3: Anti-symmetric four-point-shear test

All dimensions are in mm

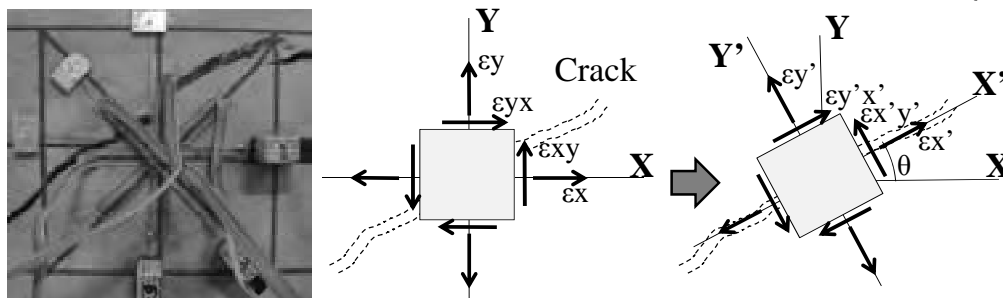


Figure 4: Instrumentation: (a) Strain measurement at the center span
(b) Strain transformation into the crack coordinate

2.2 Material tests

The material properties of the ECC were obtained from 4-point bending and uniaxial compression tests. Bending tests were carried out to obtain ECC tensile properties. A total of four ECC specimens and five ECC+CA specimens were tested. The test setup and typical specimen geometry are shown in Figure 1. Compression tests were performed on three 100×200-mm cylinders to determine the mean compressive strength.

2.3 Beam test: Center-point fatigue loading

Two beams were tested under fatigue loading. The details of the beams are shown in Figure 2. Three high-strength D25 reinforcements (USD685) were used for the tension reinforcement, with the end being extended past the both ends of the beam and then being secured with steel nuts. The maximum and minimum load was kept constant at 60% and 10% of the ultimate shear capacity, obtained from the corresponding control beam (ECC: 284 kN, ECC+CA: 276 kN).

2.4 Beam test: Anti-symmetric four-point static loading

The anti-symmetric four-point loading was considered to achieve a pure shear state at the midspan. Four beams were tested: two beams of different materials (ECC, ECC+CA; served as control specimens), were loaded to failure and two other similar beams were preloaded and then tested to failure. The objective of the preloading stage was to investigate the shear performance under a rotating stress field.

Details of the test setup are shown in Figure 3. In all beams, four 16-mm high strength reinforcements (USD685) were used, two for the compression bars and the other two for the tension bars. All beams had no web reinforcement. Two test configurations were considered. In the first configuration [see Fig. 3(a)], the load was applied to the beam at the four points; the shear span was 200 mm, while the two side spans were 400 mm. When the load reached about 55% the static capacity, a number of diagonal cracks had established and the beam was then fully unloaded. Following this preloading stage, the inner loading points were then moved apart by 200 mm, leaving a 300 mm span at each side (see Fig. 3(b); the second test configuration). The beam was then reloaded to failure.

2.5 Beam test: Anti-symmetric four-point fatigue loading

In this test series, only precracked beams were tested. The same loading protocol as used in the previous section was considered. The static strength was assumed to be the same as the shear strength of the control beams that were 267 kN and 210 kN, for ECC and ECC+CA, respectively.

In addition to the measurement of displacement and load level, it was of interest to measure the strain field across the precracks during the course of the fatigue loading. For this purpose, potentiometers and strain gauges were glued on the beam surface at the center span's height (see Figure 4), but only the recorded data from the potentiometers will be discussed. These strain data were firstly transformed into the precrack coordinate to determine the average behaviors along and across the pre-cracks's planes. Optical microscope was also used to check the condition of the PVA fibers on the failure crack surface after being subjected to fatigue.

3. MATERIAL TEST RESULTS

Figure 5 shows the result of bending test for each material. As can be seen, coarse aggregate appears to lower tensile strength and ductility (there was also less numbers of multiple cracks). It appears that this happened as there was less numbers of PVA fibers bridging the cracks (as a result of the presence of the aggregate) and due to the fact that the aggregate increased the matrix toughness. The compressive strength was 37.8 and 31.6 MPa, for ECC and ECC+CA, respectively. The reduction of compressive strength in ECC+CA was likely caused by the variation in

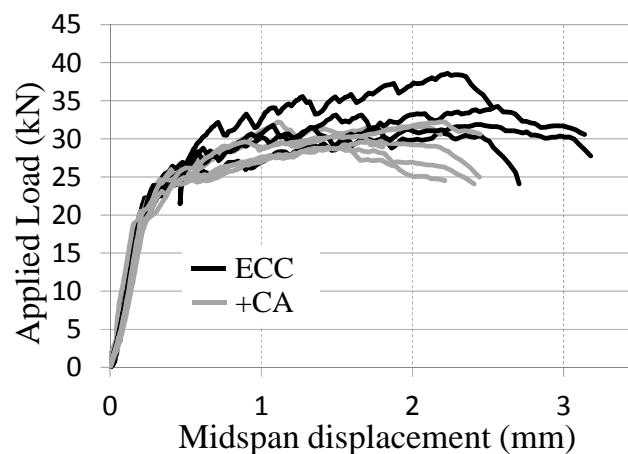


Figure 5: Result of bending test

air content, and/or the more heterogeneous stress field in the matrix.

4. TEST RESULTS

4.1 Beams under center-point fatigue loading

Figure 6 shows the results of fatigue tests on Beams ECC and ECC+CA. Note that Beam ECC was accidentally loaded to about 85% of its static capacity at around 7,500 cycles. It appears that the beam would survive longer if this accident did not happen. By looking at the rate of the deflection increase before the accident, it appears that the fatigue life of the two beams might be at approximately the same order of lifetime.

Interestingly, the coarse aggregate in Beam ECC+CA appears to bring a trade off to the fatigue life performance of the beam, since the tensile property and the compressive strength of the ECC+CA were in fact lower.

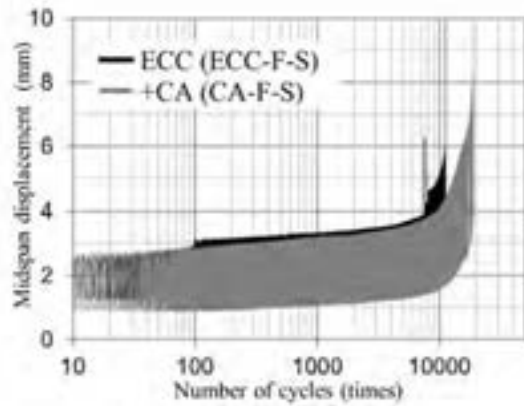


Figure 6: Result of fatigue test in simple beam test

4.2 Beams under anti-symmetric four-point static loading

Figure 7 shows the result of static load test in anti-symmetric four-point-shear beam. For the ECC beam series, the shear capacity of Beam ECC-S-P is lower as compared with Beam ECC-S-N, with no precracks. The failure of Beam ECC-S-P is also more brittle. These two findings indicate that PVA-ECC is more susceptible to shear.

The shear capacity of Beam CA-S-N appears to be much higher than Beam ECC-S-N, suggesting that the contribution of the aggregate interlock. The repeatability of this trend is still being investigated as the variation in shear capacity is generally large.

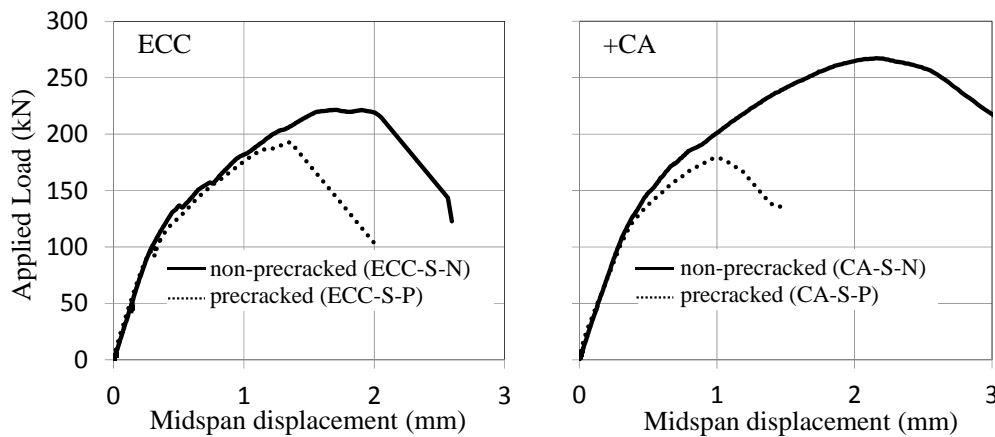


Figure 7: Result of static load test in anti-symmetric shear beam

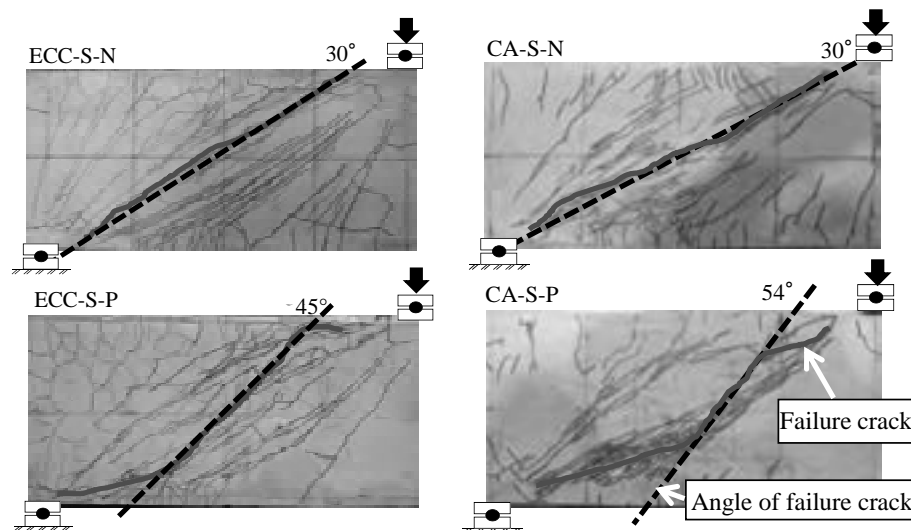


Figure 8: Crack observation after the failure

When the results of the precracked beams are compared, it appears that the effects of aggregate interlock is only minor, being the shear capacity of Beams ECC-S-P and CA-S-P are nearly the same. In fact, the effects of precracking tend to be more significant in

beams with coarse aggregate. It is likely that this happened as the aggregate might not well distributed; further tests are clearly necessary to confirm this phenomenon. Figure 8 shows the crack pattern of each beam after failure. For the control beams, it appears that failure occurred once the diagonal shear crack propagated toward the top and bottom loading plates. For the precracked beams, it is apparent that the effects of the precrack were significant. In both cases, a Z shape crack is observed, involving the precrack and the secondary crack that was formed during the second loading stage. It is interesting to note that, there are, however, more cracks connecting the top and bottom loading plates in Beam ECC+CA-S-P than in Beam ECC-S-P. This implies that there must be a stress field acting perpendicular to these diagonal cracks as a result of better shear being transmitted across the precrack planes.

4.3 Beams under anti-symmetric four-point fatigue loading

Figure 9 shows the result of fatigue load tests for beams loaded under anti-symmetric four-point fatigue. As compared to the static capacity, it appears that the contribution of aggregate interlock is more remarkable in fatigue than in static loading conditions. Fatigue life of Beam ECC+CA appears to be longer than Beam ECC, which is likely to be attributed to the added contribution of aggregate interlock under fatigue loading.

To investigate this macroscopic behavior more details, the strain measurement spanning

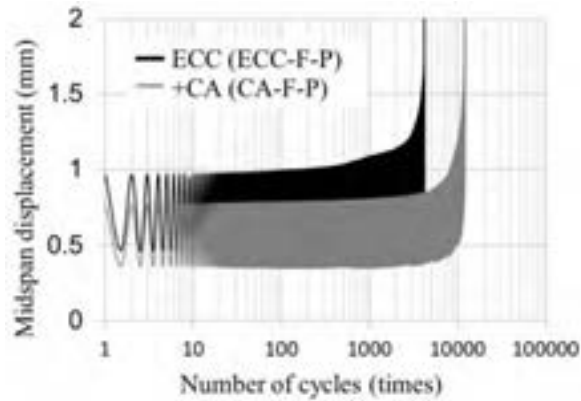


Figure 9: Result of fatigue load test in anti-symmetric shear beam

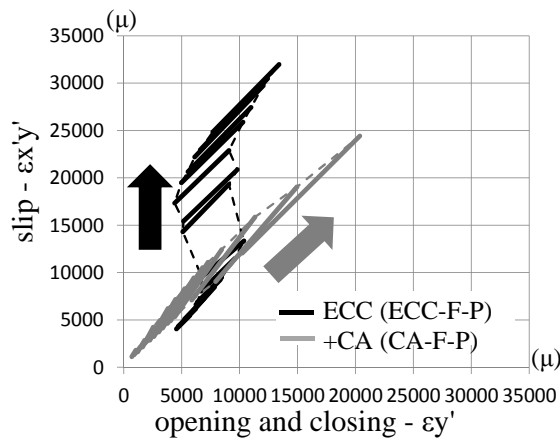


Figure 10: “opening-closing” and “shear-slip” relation on crack

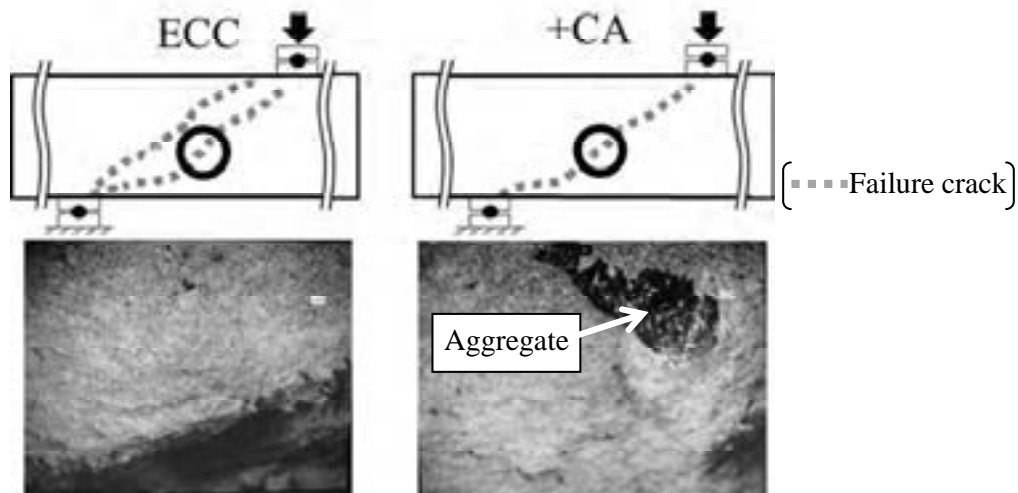


Figure 11: Observation of crack surface by microscope

over of about 10 cm at the center span’s height of the beams are discussed. Figure 10 shows the relation between the opening-closing behavior and the shear friction behavior of the cracks.

At the beginning stage of fatigue loading, it appears from the two beams that both crack opening and slip increase with increasing load cycles. After a number of cycles, a different tendency can be observed. From Beam ECC, the shear slip

component increases dramatically after about 3000 cycles, with little increase in the crack opening component, possibly due to the breakdown of shear transfer mechanism. The slip eventually gets stabilized, and the two components increase together. On the other hand, a more stable behavior of crack-opening and -slip components can be observed, suggesting the beneficial effects of aggregate interlock. The measurement was, however, very tedious, as the instruments could only capture the average phenomenon inside a 10 cm square. Further measurements using image data analysis is currently being performed to obtain better insight into the local and global behavior of multiple cracks under fatigue. Finally, the failure surface of the diagonal crack was observed by microscope and the results are shown in Figure 11. As can be seen, there is almost no PVA fibers remain on the surface in both materials, suggesting that the fibers were rubbed by the opposing two crack surfaces during the fatigue cycles. The aggregate interlock is seen not adequate to protect the PVA fibers from rupturing due to shear.

5. CONCLUSIONS

- 1) Coarse aggregate decreases the flexural capacity and ductility of ECC.
- 2) From the beams subjected to center-point fatigue, it was found that coarse aggregate, despite lowering the tensile property, appears to be beneficial to the shear fatigue performance of the beam.
- 3) From the precracked beams subjected to anti-symmetric four-point static loading, it was found that the precracks dictated the ultimate shear capacity significantly. The formation of a Z-shape crack indicates that the failure was initiated from the tip of the precracks, given that the shear demand was higher on this crack plane.
- 4) The beneficial effects of coarse aggregate tend to be more significant under fatigue than under static loading conditions. It was found that aggregate interlock is useful to limit crack slip under fatigue.
- 5) Coarse aggregate is not adequate to protect the PVA fibers under repeated shear.

REFERENCES

- Victor C. Li., 2003. On Engineered Cementitious Composites (ECC), A Review of the Material and its Applications, *Journal of Advanced Concrete Technology*, Vol. 1, No.3, pp.215-230.
- Suryanto, B. Nagai, K. and Maekawa, K., 2010. Modeling and Analysis of Shear critical ECC Members with Anisotropic Stress and Strain Fields, *Journal of Advanced Concrete Technology* Vol. 8, No. 2, pp.239-258.
- Suryanto, B. Nagai, K. and Maekawa, K., Role of Coarse Aggregate in High Performance Fiber Reinforced Cementitious Composite, *Proceedings of JCI*, Vol.31, No.1, pp.385-390, 2009
- Shimizu, K. Kanakubo, T. Kanda, T. and Nagai, S., 2006. Evaluation of Tensile Properties of PVA-ECC Using Bending Test, *J. Struct. Constr. Eng., AIJ.*, No.604, pp.31-36.
- Suryanto, B. Dalimunthe, M. Nagai, K. and Maekawa, K., 2011. Shear Fatigue Performance and Crack Surface Observations in PVA-ECC Beams without Web Reinforcement, *Proceedings of JCI*, Vol.33, No.2, pp.1279-128.

Pushover analysis of RC bare frame: Performance comparison between ductile and non-ductile detailing

B. Narender¹ and Ramancharla Pradeep Kumar²

¹P.hD Student, Computer Aided Structural Engineering, IIIT Hyderabad,
Hyderabad, India.

Narender.b@research.iiit.ac.in

²Associate Professor, Earthquake Engineering Research Centre,
IIIT Hyderabad, Hyderabad, India.

ramancharla@iiit.ac.in

ABSTRACT

The objective of this paper is to compare pushover response of ductile and non-ductile frames using AEM (Applied Element Method). Pushover analysis is non linear static analysis, a tool for seismic evaluation of existing structures. Unlike FEM, AEM is a discrete method in which the elements are connected by pair of normal and shear springs which are distributed around the elements edges and each pair of springs totally represents stresses and deformation and plastic hinges location are formed automatically. In the present case study a 1 x 1 bay four storied building is modeled using AEM. Gravity loads and laterals loads as per IS 1893-2002 are applied on the structure and designed using IS 456 and IS 13920. Displacement control pushover analysis is carried out. The effect of ductile detailing, change in grade of concrete and bar sizes in columns is also compared.

Keywords: Pushover analysis, AEM, ductile detailing.

1. INTRODUCTION

There is an urgent need to assess the seismic vulnerability of buildings in urban areas of India as an essential component of a comprehensive earthquake disaster risk management policy. Detailed seismic vulnerability evaluation is a technically complex and expensive procedure and can only be performed on a limited number of buildings. It is therefore very important to use simpler procedures that can help to rapidly evaluate the vulnerability profile of different types of buildings, so that the more complex evaluation procedures can be limited to the most critical buildings.

Nonlinear static (pushover) analysis is used to quantify the resistance of the structure to lateral deformation and to gauge the mode of deformation and intensity of local demands. The static pushover analysis is becoming a popular tool for seismic performance evaluation of existing and new structures. The expectation is that the pushover analysis will provide adequate information on seismic demands imposed by the design ground motion on the structural system and its components. The existing building can become seismically deficient since

seismic design code requirements are constantly upgraded and advancement in engineering knowledge. Further, Indian buildings built over past two decades are seismically deficient because of lack of awareness regarding seismic behavior of structures. The widespread damage especially to RC buildings during earthquakes exposed the construction practices being adopted around the world, and generated a great demand for seismic evaluation and retrofitting of existing building stocks.

The objective of this paper is to study the performance of building designed without considering earthquake forces and by considering the earthquake forces. A newly developed method called AEM is used for this study. In the present case study a 1 x 1 bay four storied building is modeled. Gravity loads and laterals loads as per IS 1893-2002 are applied on the structure and designed it using IS 456 and IS 13920. Displacement control pushover analysis is carried out in both cases and the pushover curves are compared. The effect of ductile detailing, change in grade of concrete and bar sizes in columns is also compared.

2. Applied Element Method

Numerically, it is important to know the damage of the structure till collapse. Applied element method (AEM) is an efficient technique to deal this kind of problems accurately. In this method, the elements are connected by pair of

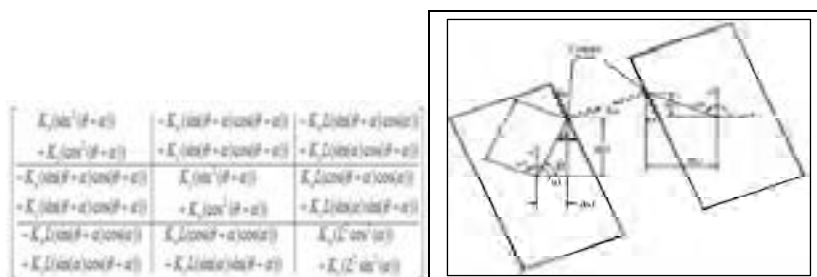


Figure 1: Element shape and degrees of the freedom

normal and shear springs which are distributed around the element edges. These springs represents the stresses and deformations of the studied element. The elements motion is rigid body motion and the internal deformations are taken by springs only. It is advisable to increase the number of elements than connecting springs for improving the accuracy. The general stiffness matrix components corresponding to each degree of freedom are determined by assuming unit displacement and the forces are at the centroid of each element. The element stiffness matrix size is 6x6. The first quarter portion of the stiffness matrix is given by equation (1). The stiffness matrix components diagram is shown in Figure.1. However the global stiffness matrix is generated by summing up all the local stiffness matrices for each element.

Case study

Description of structure

A ground plus three storey RC building of plan dimensions 3.3 m x 3.3 m and height of building is 12 m located in seismic zone II and on hard soil is considered.

It is assumed that there is no parking floor for this building. Seismic analysis is performed using the IS 1893-2002 seismic coefficient method. Since the structure is a regular building with a height less than 12 m, as per Clause 7.8.1 of IS 1893 (Part 1): 2002, a dynamic analysis need not be carried out. Detailed design of the beams along longitudinal and transverse as per recommendations of IS 13920:1993 has been carried out.

Plan of the building and sectional elevations of four story RC frames are shown in Figures 2. The sizes of the beams and columns are given in Table 1.

Material property

For this study material property has been used as follows

Grade of concrete: M20, M25 and M30

Grade of steel = Fe 415 and Fe250

Live load on floors = 2 kN/m²

Floor finish = 1 kN/m²

Brick wall on peripheral beams = 230 mm thick

Density of concrete = 25 kN/m³

Density of brick wall including plaster = 20 kN/m³

Column		Beam	
C1	360 X 300	B1	300 X 240
C2	360 X 300	B2	300 X 240
C3	360 X 300	B3	300 X 240
C4	360 X 300	B4	300 X 240
Slab thickness: 120			

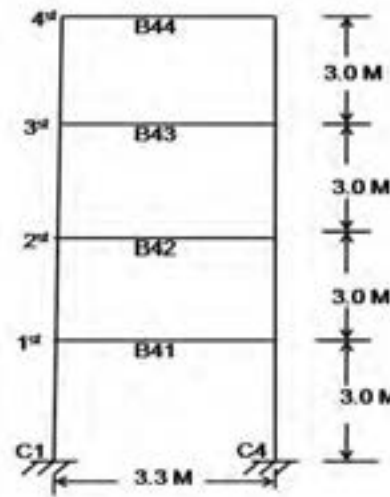
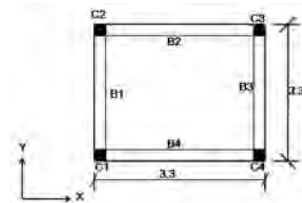


Figure 2 Plan of building (All dimension are in meters)

Load Combinations

Load combinations are considered as per IS 456: 2000 and are given in Table 2. EQX implies earthquake loading in X direction and EQY stands for earthquake loading in Y direction. The emphasis here is on showing typical calculations for ductile design and detailing of building elements subjected to earthquakes. In practice, wind load should also be considered in lieu of earthquake load and the critical of the two load cases should be used for design. This analysis only three combination were used.

Beams parallel to the Y direction are not significantly affected by earthquake force in the X direction (except in case of highly unsymmetrical buildings), and vice versa. Beams parallel to Y direction are designed for earthquake loading in Y direction only. Torsion effect is not considered in this example. The dead load of slab, beam and wall and live load and floor finishing

load on slab were calculated and total load of dead load and live load on beam have been used 22.7 kN/m and 9.9 kN/m respectively. Due to symmetry plan all floor beams had same load.

The seismic weights are calculated in a manner similar to gravity loads. The weight of columns and walls in any storey shall be equally distributed to the floors above and below the storey. Seismic analyses were evaluated and base shear was calculated and it is distributed according to IS: 1893 which were from first floor to top floor distribution like inverted triangle. The base shears of structure were obtained 26.73KN. Due to symmetry similar frame can be used for further analysis

Design and Detailing

The design of all beams and columns are based on IS: 456 and IS 13920. The longitudinal, transverse reinforcement and spacing of both beam and column as shown in Figures 3 (a)-(b) respectively.

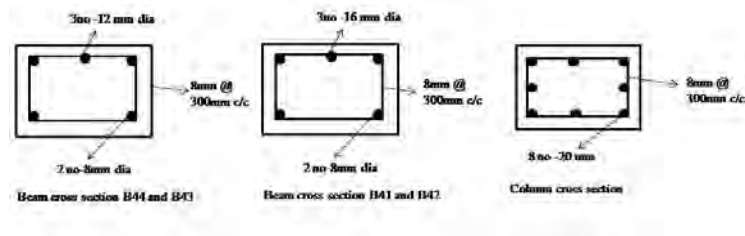


Figure 3 (a) IS: 456 design details

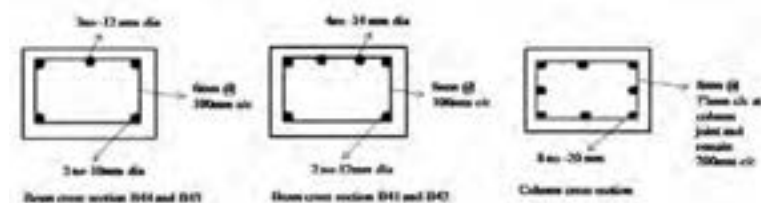


Figure 3 (b) IS: 13920 ductile design details

Pushover Analysis

Pushover Analysis is performed using applied element method on a 2D frame to obtain the capacity curve for three frames, viz., design only for gravity loads, designed earthquake loads without ductile detailing and designed for earthquake loads and also with ductile detailing.

Case I: Gravity Design Pushover Curve

Lateral displacement is applied according to force distribution given in IS 1893. A total of 0.2 m is applied in 100 load steps. Base shear at every displacement step is captured. Maximum base shear obtained 32 kN at 10mm of displacement pushover (See Figure 4). After reaching maximum load, frames lost its capacity significantly, which can be seen as a steep fall in load carrying capacity. It is obvious that without considering the earthquake forces, frame’s capacity to resist lateral displacement is very low.

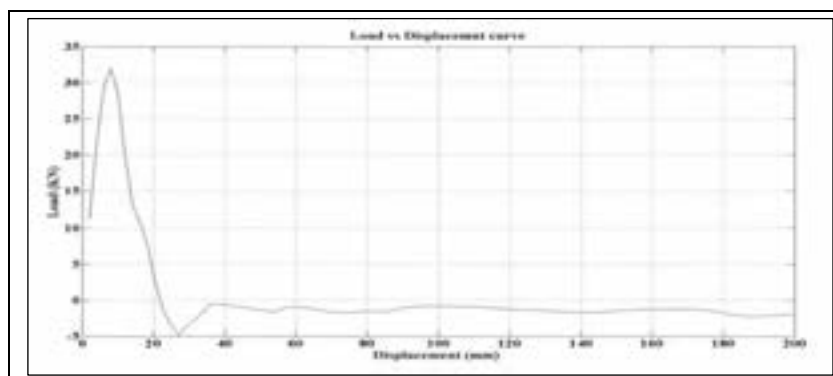


Figure 4: Load vs displacement curve

Case II: Non Ductile Detailing Pushover Curve

Second case study was for non-ductile detailing structure. The members were design according IS: 456 and reinforcement details were shown in Figure 3(a). Ductile detailing is not considered in this frame. Pushover analysis is performed on this frame using displacement pushover approach. Maximum displacement applied at top of roof element as 2.4m and its collapse behavior as shown in Figure 5. Maximum base shear occurred at 118KN and drift ratio of 0.019 %. After reaching the drift ratio, the first failure occurred at top roof beam joint members in, hinges forming at top floor elements. The sequence of failure shown in Figure 5 as top beam joint element to bottom beams joint and it followed by left column joint. In figure vertical drops indicate the steel failure and incline lines indicate the elements behavior.

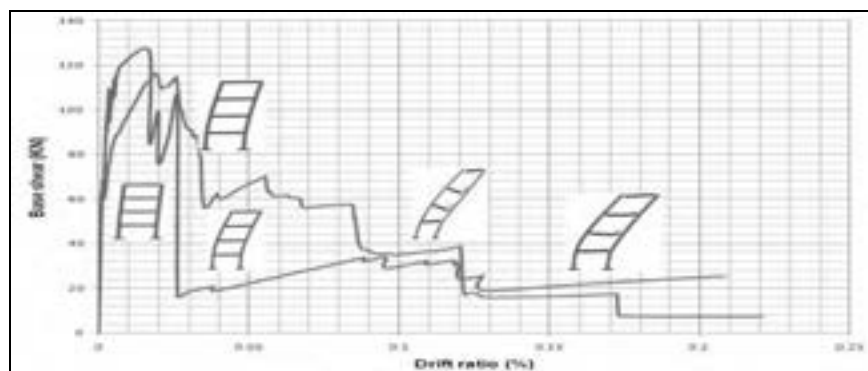


Figure 5: Non ductile detailing Load vs displacement curve

Case III: Ductile detailing Pushover Curve

Members were design according IS: 13920 and reinforcement details were shown in Figure 3(b). Pushover analysis has been performed and the results were shown in Figure 6. It can be clearly seen from the results that ductile detailing is increasing the capacity of the frame significantly. Up to significant deformation, structure is not losing its load carrying capacity. The maximum base shear was obtained as 125KN but this base shear is maintained same up 1.3m after that sudden drop took place. This sudden vertical drop indicate that joint member failed at time and the sequence of failure like beam-column joint at top to bottom beam but column joint still stand. The resistance capacity more compare to non ductile design.

Case IV: Effect of concrete grade

As a case study affect of concrete grade on load deformation capacity of the frame is studied. Three cases were considered i.e., M20, M25 and M30 grade. Figure 6, it can be clearly seen that the yield strength of the structure is higher for higher grades of concrete however; the capacity to deform is lower when the grade of the concrete is higher. It was found that M 25 grade of concrete slight to high base shear and smooth decreasing curve compare to other grade of concrete. From observation of all combination, M25 grade of concrete has slight high resistance capacity compared M20 and M30. It can be concluded that grade of the concrete has less affect on the capacity of building under lateral loads.

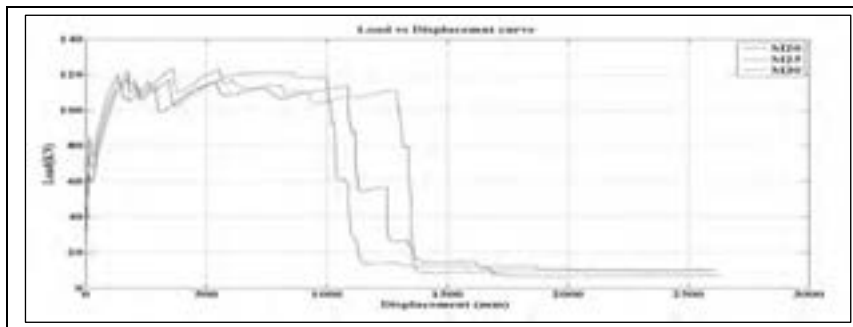


Figure 6: Effect of grade of concrete

Case V: Effect of change in diameter of column bars

As a second case study affect of steel grade on load deformation capacity of the frame is studied. Two cases were considered i.e., Fe 250 and Fe 415 grade. Results are illustrated in Figure 7. It indicates that load deformation curve is same for both the cases upto 115 kN, there after as the deformation is increasing, the load carrying capacity of Fe 250 is lower than Fe 415, however ductility is higher.

Along with this another study has also been conducted to understand the affect of number of reinforcing bars. It can be concluded from the analysis that if the number of bars are increasing, capacity is also increasing slightly, however, care must be taken because large number of reinforcing bars increase congestion in concreting.

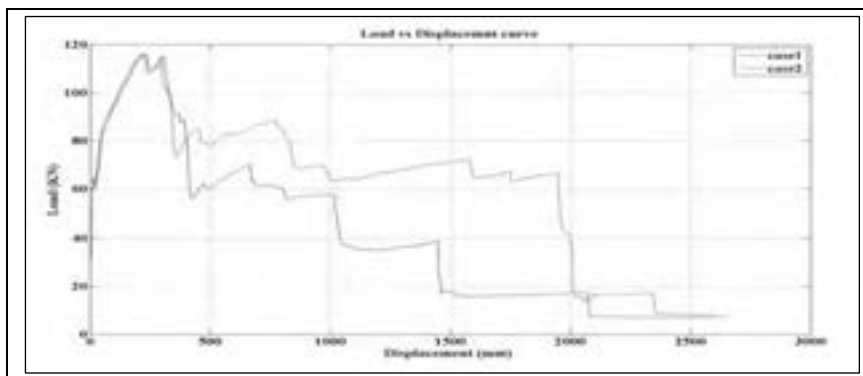


Figure 7: Effect of Steel Grade

Conclusion

In the present case study a 1 x 1 bay 2D four storied building is modeled using AEM (applied element method). Gravity loads and lateral loads as per IS 1893-2002 are applied on the structure and designed it using IS 456 and IS 13920. Displacement control pushover analysis is carried out in both cases and the pushover curves are compared. As an observation it is found that AEM give good representation capacity curve. From the case studies it is found that capacity of the building significantly increases when ductile detailing is adopted. Also, it is found that affect on concrete grade and also steel are not that significant.

REFERENCES

1. Hatem Tagel-Din and Kimiro Meguro: Applied Element Method for Simulation of Nonlinear Materials: Theory and Application for RC Structures, Structural Eng./Earthquake Eng., International Journal of the Japan Society of Civil Engineers (JSCE) Vol. 17, No. 2, 137s-148s, July 2000.
2. _____ IS 456: 2000; Criteria for Plain and Reinforced Concrete Design of Structures, BIS, India.
3. _____ IS 1893: 2002; Criteria for Earthquake Resistant Design of Buildings, BIS, India.
4. _____ IS 13920: 1993; Code of Practice for Ductile Detailing of Buildings, BIS, India.

How remote sensing data were used for the Tohoku Earthquake

Haruo SAWADA
Professor, ICUS, IIS, The University of Tokyo, Japan
sawada@iis.u-tokyo.ac.jp

ABSTRACT

Thousands of digital aerial photos were taken by private survey companies for the Tohoku Earthquake under the special agreement in case of disaster between GSI (Geospatial Information Authority of Japan) and the air-survey group of Japan. Although they were very useful to identify the damage level by visual interpretation, it took time and needed many technicians to interpret the whole damaged area. As for satellite remote sensing data, the International Disaster Charter (IDC) as well as the Sentinel Asia also made contributions for this event and offered more than a few thousands of satellite images. The JAXA kept producing the PALSAR images of inundated area which was caused by the Tsunami until the satellite stopped its regular operation in April 2011. High resolution satellite images were well used for identifying the damages. The combination of images of pre- and post- earthquake makes us easy to identify the damage situations. Remote sensing data have much potential for the large earthquake disaster management and the Tohoku Earthquake event clearly showed us the importance of appropriate preparation for remote sensing.

Keywords: Tsunami, review, remote sensing, large disaster

1. INTRODUCTION

The Tohoku Earthquake of M9.0 which occurred on 11 March 2011, was the biggest earthquake known ever to have hit Japan. It directly damaged buildings, houses, dams, railways, road and other infrastructures and also became the trigger of huge Tsunami that reached heights of up to 40 meters. This event directly damaged eleven prefectural governments. The National Police Agency (<http://www.npa.go.jp/archive/keibi/biki/index.htm>) reported (on 5th Sep., 2012) that the total number of dead, missing and injured person were 15,870, 2,846 and 6,110 persons, respectively. The number of missing person indicates the sever Tsunami. The number of fully, half and partially collapsed residential houses were 129,291, 264,004 and 725,918, respectively. 63,574 non-residential houses were also damaged. Heavy destructions at roads, bridges, railways and levees were reported 4,200, 116, 29 and 45 places, respectively. About 190 km of the coastal levees out of 300 km were damaged. Various remote sensing data have been introduced to collect information for damage assessment and for new rehabilitation plans. This report summarizes the use of remote sensing data for this huge disaster.

2. AERIAL PHOTOGRAPHY

2.1 Taking aerial photos

GSI (Geospatial Information Authority of Japan) and APSAT (Association of Precise Survey and Applied Technology) made a contract on taking emergency aerial photograph in 2005. Then GSI called APSAT to request stand ready 44 minutes after the earthquake and 10 minutes later officially requested emergency aerial photograph (Tanioka, 2011). According to this call the APSAT made contact with contracting 22 survey companies if they could fly over Tohoku. However, the telephone line between GSI and APSAT was not stable and only one way communication from GSI to APSAT was established because both GSI and APSAT offices were also located in the damaged area by the earthquake. The survey airplane had to fly for a long distance because Sendai airport, the main airport in Tohoku area, was also damaged by Tsunami. Next day six survey companies started to take aerial photos according to the agreement with GSI and covered almost all the area within 2 days, about 4,820km². However we had to wait until on 19 March to cover 100% of the Tsunami damaged area because of the weather condition.

2.2 Distribution of aerial photos

GSI has an airplane KUNIKAZE for aerial photography but the airplane was under the periodic inspection until the end of March 2011 and GSI could start flying the KUNIKAZE on 1st April. The aerial photos were taken by digital camera and normal camera depending on their availability suitable for 1/10,000 scale images. Their geo-coded photos (with Japanese coordinate system) were distributed through the website of GSI. These aerial photos were also converted to orthophotos and open to public in digital format through web site with 50 cm resolution one day after as well as printed images to governmental uses. Higher resolution digital images were also available by request.

2.3 Products and other activities by GSI

GSI published the Tsunami affected area map with the scale of 1/25,000 a few weeks later. We interpreted the Tsunami lines on the orthophotos just after GSI opened them on the web site and started offering the Tsunami Aerial photo Map with the scale of 1/10,000. The main interpretation key was the debris.

The ground level is important information for rehabilitation of the area and some survey companies used LiDAR and created DEM with 5m spatial resolution. The ground sinks caused by the earthquake were found in many coastal areas and that made worse the impact of Tsunami.

Mukouyama (2011) mentioned that a tsunami simulation was useful to identify the damaged area on remote sensing images quickly and accurately. However, lack of machines and electric power made their works difficult because their office was also damaged by the earthquake and the electric power was under the

governmental control. We need to think about our business continuity under these situations especially at rescue stage.

The aerial photo survey was conducted again through May to November 2011. These aerial photos are commonly used as the important source of information for damage assessment and rehabilitation plans for local government and residents. GSI provided base map with the scale of 1/25,000, 1/50,000 and 1/200,000. The digital web mapping system was also introduced for further uses.

GSI dispatched the emergency mapping team for one and a half months to the emergency mapping center in a special meeting room at the Cabinet Office and another team (TEC-FORCE) with big printing systems to Sendai, Tohoku, for helping the disaster management center and distributing the aerial photos and their products (Furuya, 2012).

3. SATELLITE DATA

3.1 Capability of satellite data

Satellite images were suitable to overview the whole damage situations along the coastal lines of 600km caused by the Tsunami. Because broad agricultural lands including paddy fields kept Tsunami water for a long time, many satellite images enhanced the inundated areas. Even MODIS was useful to detect debris caused by the Tsunami (Aoyama, 2012).

High resolution satellite images were well used for identifying the damages. The GeoEye image with 50cm resolution identifies the debris along the coastline. Its object-type classification combined with elevation data enabled us automatically delineate the Tsunami affected area. Because the combination of images of pre- and post- earthquake makes us easy to identify the damage situations, image dataset of normal days must be created for the whole country as a base data. Although remote sensing data have much potential for the large earthquake disaster management, the Tohoku Earthquake event clearly showed us the importance of appropriate preparation for remote sensing data.

3.2 Private survey companies

The Asia Survey Ltd. reported that the pan-sharpen AVNIR-2 image was useful to identify large buildings washed away by the Tsunami but it was difficult to identify the damage levels of remaining buildings. The Hitachi Solutions Ltd. provided GeoPDF files to the Cabinet Office and local government which were mapped from QuickBird and WorldView1 and 2. The Image One Ltd. used Radarsat-2 to show the land cover changes and damages of fisheries caused by the Tsunami. The Japan Space Imaging Ltd. started the formulation of the emergency structure and successfully obtained the satellite images, such as COSMO SkyMed on 12 March, GeoEye-1 on 13 March and IKONOS on 12 March (Li, 2011). The emergency condition continued until the end of April 2011. The KKG (Kokusai Kogyo Group) showed the aerial images, satellite images, other data and Tsunami simulation CG videos. The PASCO Ltd. showed panoramic photos, inundation

map derived from TanDEM-X, TerraSAR-X, EROS-B images, topographic change maps and other information related to nuclear power plant problems.

4. INTERNATIONAL ACTIVITIES

4.1 IDC: INTERNATIONAL DISASTER CHARTER

The IDC stands for the Charter on Cooperation to Achieve the Coordinated Use of Space Facilities in the Event of Natural or Technological Disaster. The IDC aims at providing a unified system of space data acquisition and delivery to those affected by natural or man-made disasters through Authorized Users. Each member agency has committed resources to support the provisions of the Charter and thus is helping to mitigate the effects of disasters on human life and property (<http://www.disasterscharter.org/home>). The IDC was established in 1999 and started their activities in 2000. JAXA as the representative of Japan participated in 2005 and the number of participating institution is 21 organizations in 2012. There are tens of requests every year from various regions and there were 31 actions in 2011 including the Tohoku Earthquake.

4.2 Activation of IDC for the Tohoku Earthquake

JAXA requested IDC to activate the emergency observation on March 11, 2011. A few day later IDC products came out on the web site, ex. WorldView (33 products), RapidEye (32 products), SPOT (17 products), Landsat (9 products), TerraSAR-X (9 products), GeoEye (8 products), IKONOS (7 products), QuickBird (4 products), Radarsat (4 products), Formosat (1 product).

The images were observed during March 12 to April 14, 2011. In total, 94 satellite image maps were uploaded on the web site and high resolution images were commonly used. The actual observation dates were depended on satellite systems; WorldView: 6days, SPOT: 3 days (12 to14 March), RapidEye: 2 days (12 and 13 March), IKONOS: 2 days (12 and 14 March), GeoEye: 2 days (13 and 19 March). More than 5,000 satellite images were also sent directly to JAXA although they were not shown on the web site. It was one of the successes of IDC program. As for the timing, for example, the SPOT image on 12 March was uploaded on the web site next day as a processed image showing the Tsunami damage with the scale of 1/100,000 (Charter call ID359, Product No. 05). It was a very rapid action comparing with the previous 10 years average (7.8 days) in IDC.

4.3 Use of IDC products

Although there were a lot of requirements to the maps which indicated damaged area, very few maps were available and hand drawn maps were commonly used for showing various places at the damaged sites. We could not hear that local government staffs or volunteers used the IDC products at the sites. There were several reasons as follows:

- the IDC was not well known; no local government staff knew about the ID

- no print was available; printed images were required under no electric power supply
- the maps were explained in English; Japanese characters are necessary on the map
- all the data were not easily accessible although thousands of GSI aerial photos were available through a web site

We felt a lot of difficulties in introducing the IDC products directly to the local government sites. Volunteers who interpret English and revised maps in Japanese are necessary to make the IDC product useful for disaster management. Otherwise these products are useful only for foreign persons who are far from the disaster with no restriction of internet condition and electric power supply. In addition, we felt that the duration of the IDC activation was too short because most of the emergency observation activities were stopped within a few weeks. Especially we felt so after the ALOS stopped its operation in April 2011. Government should have some agreement with foreign institutions to continue satellite observation for a certain period of time in case of these huge disasters. And the agreement must be signed before the disaster.

5. ACTIONS OF JAXA

5.1 Satellite observation

JAXA played important role in supporting the disaster management center in the Cabinet Office and provided not only various satellite data but also satellite communication system to both Cabinet and local government.

JAXA changed the ALOS operation soon after the Earthquake and provided about 450 scenes during 72 paths. On March 12, JAXA brought into the Cabinet Office 70 satellite geographic maps which were created by overlaying digital maps on existing ALOS images. The emergency observations by ALOS were conducted and satellite images and products (ex. Statistical information about Tsunami inundation areas) were uploaded on their web site 33 times. Two days after the Earthquake, the inundation map created from the AVNIR-2 on 12 March and pre-event PRISM image and the inundation map derived from FORMOSAT-2 were released.

5.2 Damage assessment

The PRISM, AVNIR-2, PALSAR, TerraSAR-X and RapidEye images were used 3 times, 17 times, 17 times, 2 times and once, respectively in the 33 times of upload. JAXA provided pre-event satellite images as well. The combination of images of pre- and post-event clearly showed the Tsunami damages. These products were related to the Tsunami damages and the liquefaction, for example, was reported ten days after the event.

Because the AVNIR-2 is an optical sensor and cloud and atmospheric conditions influenced the images. However, the images in fine weather clearly showed the

Tsunami damages. The characteristic of cyclic satellite observation with high resolution optical sensors was quite useful for monitoring the influences of the Tsunami event. PALSAR is little influenced by cloud and hazes and showed inundation areas. These inundation data were sent to the Ministry of Agriculture, Forestry and Fisheries every week.

5.3 Further study is needed

PALSAR, however, has difficulty in clear delineation of Tsunami damaged areas. It was early March and no agricultural activities were performed at paddy field. Therefore, the inundated agricultural fields were reasonably considered as damaged area by the Tsunami. Then how we can delineate the Tsunami damages in growing season of paddy field by PALSAR? The inundated areas were summarized by JAXA and the figures showed that the inundation area was about a half of damaged area. It must be studied to automatically delineate the Tsunami damaged area so that the information becomes useful for rescue purposes as well as monitoring damages in agriculture fields.

The Tsunami produced a huge amount of floating objects and JAXA explained on March 23 that the PALSAR was useful to detect floating material with exact coordinates using the data of March 13. They explained that the image was useful for ships to take care their routs to navigate. As we mentioned before, one of the characteristics of the Tsunami disaster is the large number of missing people. One dog was found survive after three weeks on a floating object. How were people? It is not only we who wondered if the PALSAR or other remote sensing data were used to detect floating objects for rescue purposes. Even for ships, the information derived from an image of ten days before is not appropriate for finding safe routes. It is no meaning to show the capability of remote sensing data in a particular disaster stage. To the contrary, it is necessary to give useful and practical information. We strongly recommend that disaster management groups think about the operational systems to process and deliver remote sensing data for large disasters.

5. ACADEMIC SOCIETY

Academic societies, such as AJG (The Association of Japanese Geographers), GISAJ (GIS Association of Japan), JASDIS (Japan Society for Disaster Information Studies), JSCE (Japan Society of Civil Engineering), JSPRS (Japan Society of Photogrammetry and Remote Sensing), RSSJ (The Remote Sensing Society of Japan) have made various projects on this event and opened web sites to show their activities. The JSPRS published a special edition journal to summarize the list of remote sensing data (Tsuru, 2012), which shows a list of vertical air photograph, oblique photograph, elevation data derived from aerial laser, vehicle installation field measurement data, optical satellite data, SAR data. Activities of private companies were also summarized in a special edition (Vol. 50, No.4, 2011). The RSSJ (2011) also published a special edition journal and summarized the usage of high resolution satellite images.

Workshops and seminar were held in all over the country as well as Tohoku. The Forest Conservation and Management Group checked all the coastal forest using satellite remote sensing data and proposed rehabilitation plans according to the site condition (<http://www.hozen-ken.jp/index.html>). They used Landsat and SPOT-5 for comparison between pre- and post- disaster situation.

The GeoGrid had a web site from on April 1 to July 16, 2011, to offer ASTER image data and information about damages derived from ALOS data. ASTER images are often used in Japan now because no other Japanese satellite has high resolution sensors to observe the land covers.

5. DISCUSSION

Hundreds of digital aerial photos were taken by private survey companies under the special agreement in case of disaster. Their geo-coded photos (with Japanese coordinate system) were distributed through the website of GSI. Although they were very useful to identify the damage level by visual interpretation, it took time and needed many technicians to interpret the whole damaged area. Many survey companies also contributed to the event using satellite images.

The International Disaster Charter as well as the Sentinel Asia also made contributions for this event and offered more than a few thousands of satellite images. However, because the products were written in English and the supporting actions were stopped after a few weeks, there was little significant contribution to the suffering sites. Although International collaboration like IDC is still important and useful, we would like to recommend to strengthening its activity.

We would like to add two more recommendations. One is the collaboration in normal situation and the other is the standardization of products. We are very much encouraged by many web sites because there were many volunteers who analyze remote sensing images. Therefore, remote sensing data must be open to public as soon as obtained so that any person contributes at each stage of disaster mitigation activities. The “satellite observation calendar” which shows the observation possibilities of all the orbital satellites at a site is also expectant. I would like to recommend establishing networks or agreements on collaboration among related institution before a big disaster because we do not have time to duplicate the same activity at the emergency stage.

As for the standard products, it is necessary to prepare a list of request at each disaster stage and location. The standard products may depend on disaster types and management stage (before a disaster, during a disaster (rescue stage), after a disaster (evacuation), and rehabilitation stage). The standard products must be mentioned related to the request list so that both producers and users can expect what products will be come out in geocoding type, scale, color, language, etc. These products should be used in disaster mitigation drill so that people become familiar with the remote sensing products.

REFERENCES

- Aoyama, Takashi, 2012, Monitoring of debris flowing to the ocean by mega-tsunami caused by the 2011 off the Pacific coast of Tohoku Earthquake, *Proceeding of the 52nd Conference of the Remote Sensing Society of Japan*, 269 - 270
- Furuya Takashi, Reo Kimura, Munerari Inoguchi, Keiko Tamura and Haruo Hayashi, 2012, Visualization skill for common operational picture aimed for the effective disaster response - Via practical activities in Tohoku district Pacific Ocean earthquake emergency mapping team in cabinet office, *Journal of Disaster Information Studies*, No. 10, 68 -76
- Li Yunqing, Mamoru Sugawara and Jun Shibata, 2011, Disaster monitoring of the great east Japan earthquake using high resolution satellite, *Journal of the Japan Society of Photogrammetry and remote sensing*, 50(4), 210- 215
- Mukouyama, Sakae, Yoichi Murashima, Noritoshi Kamagata, Yukio Akamatsu and Yasuteru Imai, 2011, Rapid extent grasp of the disaster area by The 2011 Off the Pacific Coast of Tohoku Earthquake through tsunami simulations and multiple satellite image analyses,? *Journal of the Japan Society of Photogrammetry and Remote Sensing*, 50(4), 192-197
- Ochi, Shiro, Haruo Sawada, Naoki Mitsuzuka, Yoshinobu Nonoguchi, 2012, Remote Sensing application to damage assessment of coastal forest damaged by the Tsunami in 2011, *Proceeding of 21st Forum on Global Environment and Disaster Risk Information*, 33-36
- Sawada, Haruo, 2012, Contribution of remote sensing data for the Tohoku Earthquake, *Proceeding of 21st Forum on Global Environment and Disaster Risk Information*, 29-32
- RSSJ, 2011, High resolution satellite remote sensing concerning the 2011 off the Pacific Coast of Tohoku Earthquake and Tsunami Disaster, *Journal of the Remote Sensing Society of Japan*, 31(3), 344-367
- Takenaka, Hideaki, Takashi Y. Nakajima, Hiroaki Kuze, Tamio Takamura, Teruyuki Nakajima, 2011, The Japan Earthquake Disaster Observed by Geostationary Satellite "HIMAWARI", *Journal of the Remote Sensing Society of Japan*, 31(3), 338-343
- Tanioka, Seiichi, 2011, An urgent air photographing for the 2011 off the Pacific coast of Tohoku Earthquake, *Journal of the Japan Society of Photogrammetry and Remote Sensing*, 50(1), 185 -191
- Tonooka, Hideyuki, 2011, Great east Japan earthquake seen in ASTER nighttime thermal infrared imagery, *Journal of the Remote Sensing Society of Japan*, 31(3), 334-337

REFERENCED WEB SITES

AA: Aero Asahi Corporation (in Japanese)
<http://ec2-175-41-208-71.ap-northeast-1.compute.amazonaws.com/>

AAS: Asia Air Survey Corporation
http://www.ajiko.co.jp/bousai/touhoku2011/touhoku_eng.htm

AIST: The National Institute of Advanced Industrial Science and Technology
(AIST): Global Earth Observation Grid

ASTER data distribution through WMS, ASTER time series data, PALSAR InSAR for crustal deformation

<http://disaster.geogrid.org/>

ATR-Promotions Inc.

Software and data set distribution for iPad

<http://eq.stroly.com/maps/support>

AJG: The Association of Japanese Geographers

http://www.ajg.or.jp/disaster/201103_Tohoku-eq.html

DCRC: Disaster Control Research Center, Tohoku University

Building damage map derived from the interpretation of post- and pre-event aerial photos

http://www.tsunami.civil.tohoku.ac.jp/tohoku2011/mapping_damage.html

Center for Satellite Based Crisis Information, DFD, Germany

TerraSAR-X Change Analysis of Sendai Area, Japan

<http://www.zki.dlr.de/article/1893>

Interactive view of RapidEye satellite images on ZKI GIS-Viewer

http://www.zki.dlr.de/flexviewer2.5/index.html?config=config_japan201103.xml

KKG: Kokusai Kogyo Group (in Japanese)

http://www.kk-grp.jp/english/csr/disaster/201103_touhoku/index.html

GISAJ: GIS Association of Japan

Aerial photographs, tectonic activity, geographic base maps, DEM, Tsunami affected area map, traffic information

<http://rarmis.jp/dpgissig/>

GSI: Geospatial Information Authority of Japan, Ministry of Land, Infrastructure, Transport and Tourism (in Japanese)

http://www.gsi.go.jp/BOUSAI/h23_tohoku.html

HU: Harvard University

Japan Sendai Earthquake Data Portal

<http://cegrp.cga.harvard.edu/japan/?q=content/home>

Digital archive of 2011 Tohoku Earthquake

<http://worldmap.harvard.edu/japanmap/>

IDC: International Disaster Charter

http://www.disasterscharter.org/web/charter/activation_details?p_r_p_1415474252_assetId=ACT-359

IIS: Institute of Industrial Science, The University of Tokyo

PNG and KML files of GSI aerial photo, KML and SHP files of the Tsunami line interpreted by the laboratory

http://stlab.iis.u-tokyo.ac.jp/eq_data/index_e.html

JASDIS: Japan Society for Disaster Information Studies

<http://www.jasdis.gr.jp/11link/index.html>

JAXA: Japan Aerospace Exploration Agency

ALOS and other satellite images /emergency

<http://www.eorc.jaxa.jp/imgdata/practical/natural/earthquake/east-japan-20110311.php>

Image gallery 3) Disaster

http://www.eorc.jaxa.jp/ALOS/gallery/lib_data/j3disaster.htm

Summary of the activities for the Tohoku Earthquake

http://www.jaxa.jp/info_support_j.html

JFA: Forest Conservation and Management Research Group

<http://www.hozen-ken.jp/menu/2012-01siryou4.pdf>

JSCE: Japan Society of Civil Engineering

<http://committees.jsce.or.jp/2011quake/>

JSI: Japan Space Imaging Corporation

<http://www.spaceimaging.co.jp/EastJapanEarthquake/tabid/576/Default.aspx>

JSPRS: Japan Society of Photogrammetry and Remote Sensing
<http://www.jsprs.jp/action.html>

Mapion
Aerial Photo and Information on Land marks
<http://www.mapion.co.jp/feature/eq2011/hisaichi.html>

NICT: National Institute of Information and Communications Technology
airborne Pi-SAR2 images on 2011/03/12 and 2011/03/18
<http://www2.nict.go.jp/pub/whatsnew/press/h22/announce110312/index.html>

NARO: National Agriculture and Food Research Organization
GSI aerial photo distribution through WMS
<http://www.finds.jp/independent/tohoku/index.html>

NIED: National Research Institute for Earth Science and Disaster Prevention
Aerial photos and ALOS data distribution through WMS (tentative)
<http://bosai-drip.jp/alos/wms.htm>
Satellite images, aerial photography, traffic information, map of evacuation center,
other geographic maps, list of related sites
<http://all311.ecom-plat.jp/>

NTNU: National Taiwan Normal University
Web Map Service
http://140.122.82.87/2011_Japan_Earthquake/index.htm

PASCO Corporation (in Japanese)
http://www.pasco.co.jp/disaster_info/110311/

RSSJ: Remote Sensing Society of Japan
<http://www.rssj.or.jp/sinsaihenotorikumi/sinsaihenotorikumi.htm>

Tokyo University of Information Science
MODIS support of SAR and Nuclear pollution for 3.11 quake disaster
<http://e-asia2.tuis.ac.jp/browse/Sanriku/indexSanriku.html>

The investigation on a potential chemical incident risk in the area of Ulaanbaatar

Ganzorig TSOGTBAATAR¹, Chimedtseren PUREVJAV¹, Sodnomragchaa DAGVA² and Algirmaa ERDENE-OCHIR³

¹Researcher-chemist, Doctor (Ph.D), The Disaster Research Institute under the National Emergency Management Agency (DRI under NEMA) of Mongolia

¹Researcher-chemist, Master (M.Sc), DRI under NEMA

²Specialist of Geo-Hazard Sodnomragchaa Dagva, Master (M.Sc), DRI under NEMA

³Laboratory assistant, Master (M.Sc), DRI under NEMA

ts_ganzorigmn@yahoo.com , pchimdee@yahoo.com

ABSTRACT

Mongolia has become a large importer and user of chemical substance. About 500 types of chemical, amounting to hundred-thousand tones in total were imported in 2010-2011. The majority of them are still being stored, traded and used within Ulaanbaatar city, in which approximately 40 percent of the total population of Mongolia lives. For these reasons, a significant portion of Mongolian population is at chemical incident risk of exposure to toxic and dangerous chemicals.

This study shows the locations of 34 industries and companies that have permission to store, trade and use extreme toxic and dangerous chemical substances, using GPS, and illustrates them on a map of Ulaanbaatar city. The chemical risk levels in Bayangol and Khan-Uul districts were higher than of other seven districts, but in within the “acceptable risk level” according to definition system of the international risk definition. With regard to the other 6 districts (excepting Songinokhairkhan) chemical incident risks were at “an extreme low level”.

Keywords: *chemical incident, hazard, vulnerability, assessment of chemical risk, chemical toxic and dangerous chemicals (TDCs)*

1. INTRODUCTION

Due to the intensive development of the mining, metal refining and other heavy industries in Mongolia, in the last decade the import, use and variety of toxic and dangerous chemicals has increased rapidly. Recently, technological or man-made incidents involving these chemicals have been occurring routinely due to the rapid development of science, techniques and technology. From 2006 to 2011 approximately 69 chemical incidents were reported in Mongolia, of which 65% occurred in the metropolitan area of Ulaanbaatar, the capital. In the last few years, the most highly developed countries have been reducing the improper usage of toxic and dangerous chemicals (TDCs), through new technology or substitution by non-toxic, safer substances. In developing countries, however, TDCs are still utilized in mining, heavy

and light industries, and daily life. In Mongolia, heavy and light industries and mining had been extensively developed, and subsequently the country has become a large user of chemicals. Therefore, the assessment of the chemical incident risk and hazard created by TDCs must be carried out in the country.

The aims of this study were to find the location of those industries and other entities that have permission to store, trade and use TDCs in the 9 districts of Ulaanbaatar city, to classify the relevant chemicals according to their hazard and toxicity effects, to determine the amount used, stored and traded, to assess potential hazards, vulnerabilities and risks, and to map these on Ulaanbaatar city.

Basic concepts concerning chemical incident risk

Directly or indirectly, chemical incidents affect the health and life-expectancy of humans and animals, and can contaminate the environment. The effects can last from a few minutes to many decades. In this they are very different to other man-made or natural disasters. Chemical incidents can be caused by people, or by the impact of flood, fire, earthquake, lightning or other natural phenomenon [1]. If air and water are contaminated by chemicals, the effects of chemical incidents can be wide-ranging, being felt well beyond the actual location of the incident. These contaminated environments negatively affect the routine of daily human life, and completely destroy the ecological balance and natural stability [2].

Chemical incidents are generated mostly by disasters or natural hazardous phenomenon, human fault and accidentally activity, errors in industrial processes and through the wear and tear of equipment and devices. TDCs released for the above reasons have a hazardous effect on humans and the environments. There are several pathways for human exposure to TDCs, including dermal, inhalation and ingestion.

Generally, in the event of an incident the hazard zone is defined by the exposed area and site. In contrast, a chemical hazard is classified by permissible human exposure limits to TDCs. Chemical substances show the following effects on humans, animals, the environment and property:

1. Exposure hazard
2. Fire hazard and exposure hazard to a toxic substance generated by the fire
3. Explosion and exposure hazard to a toxic substance generated by the explosion.

Chemical incident risk is defined commonly by the probability of human death (by number per year) as a result of exposure to the chemical substance in the incident zones. Sometimes, however, this number cannot be estimated for each risk [3,4]. In order to calculate the chemical incident risk, the following factors must be determined:

- Hazard of TDCs
- Vulnerability of human and environments exposed to TDCs
- Probability of chemical incidents occurring
- Capacity to fight and respond to a chemical incident and its consequences.

Further, an assessment of chemical incident hazard (ACIH) can determine the source of potential hazards. In particular, environmental conditions, geo-location, geographical information, human settlement patterns, population density, information about chemical storage, manufacture, utilization and sales, pathways of exposure to the chemicals, probability of exposure, information concerning dangerous chemical industry and enterprise, reports on previous assessments of chemical incident hazards and risks, and information of damage etc,

are used in ACIH. As well, factors that can increase the strength of the hazard must be revealed. For ACIH it is necessary to create a methodology for reducing possible hazards, to map hazard zones, to study hazard frequency, to compare primary and secondary negative effects of hazards with relevant standards and norms.

As defined by the Law on Disaster Protection of Mongolia, disaster vulnerability means that humans, animals, property and the environment are exposed to possible hazards. The vulnerability of exposure to chemicals is determined by numerous factors, such as the hazard type and characteristics of exposure, the capacity to combat and recover from chemical incidents, and human population within the relevant area [5]. Commonly, the assessment of chemical incident vulnerability (ACIV) is done using the measurement of a statistical probability. Some Chinese scientists have created a two-fold classification of general vulnerability, by the following [6,7]:

1. Physical
2. Social

These vulnerabilities do not only depend on the chemical and physical nature of the incident, but also on the social and economic characteristics of those exposed to the chemicals. In order to have the capacity to mitigate a chemical event, it is necessary to not only co-ordinate the various responses, but also to adequately assess the character of the incident. The capacity to mitigate a chemical incident is affected by the assessment of the incident scenario, the utilization of response forces, the adequacy of relevant rules, laws and guidelines, and the effectiveness of integrated training, public announcements and the skills of responsible agencies.

2. MATERIALS AND METHODS

Materials and objects

In this study, the following materials and objects were selected and used carefully:

1. Industries, companies and enterprises that have permission to store, trade and use toxic and dangerous chemicals in the territory of Ulaanbaatar city (excepting import, export, and transit of explosive substances).
2. Dangerous chemical facilities
3. All information, reports and statistical data about the population of Ulaanbaatar city, its districts and sub-district (khoroo), its territory and location, and other crucial factors
4. All information, reports and MSDS about chemical substances

Methods

Basic research methods such as statistical analysis, comparison and deduction were used in this study. The assessment of the chemical incident risk in the territory of Ulaanbaatar city were carried out using the below-mentioned 6 methods used by Russia, Canada, India and some European countries that could be applied to Mongolian social, environmental and economic conditions.

1. The methodology for previous estimations of the area of exposure to TDCs and hazard zones when incidents have happened involving dangerous chemical objects and facilities [8, 9].
2. The methodology to assess the quantitative risk to human health preliminary by chemicals [10].
3. The methodology to assess chemical incident vulnerability [7].
4. The methodology for chemical incident risk assessment. Chemical incident risk consists of chemical hazard, vulnerability and probability of death by exposure to chemicals. It is estimated 2 ways.

$$CR = (H * V)F \quad (1.1)$$

$$CR = (H * V)P \quad (1.2)$$

Where:

CR – Chemical incident risk

H – Number of people exposed to chemicals (exposed people/total people)

V- Vulnerability (as from 1 to 4 points)

P- Quantitative probability of death from incident

F- Incident probability (number of incidents per person)

Quantitative probability of death by incident was estimated by the following formula:

$$P = \frac{K}{Y_a * TP} \quad (1.3)$$

Where:

K- number of deaths

Ya- number of total years that incident happened

TP- total population

Incident probability (number of incidents per person) was estimated by the following formula::

$$F = \frac{A}{Y_a * TP} \quad (1.4)$$

Where:

A- number of chemical incidents

Ya- number of total years that incident happened

TP- total population

5. Risk ranking matrix. TDCs released by chemical incidents badly affect human health and cause environmental contamination. Therefore, the assessment of acute exposure of humans is the most important for assessing impacts of chronic exposure to CTDSs. Based on the following 2 factors, the matrix reveals whether the location of dangerous chemical industries, companies and enterprises would be suitable or not [11,12].

IRF (individual risk factor)= [as risk potential per year]

GSRF (geo-social risk factors) = [KM²/year]

6. Disaster risk levels. The risk level based on disaster risk quantitative assessment is used to design a risk management strategy [3].

3. RESULTS

- **The research on CTDSs used in the range of 9 districts of Ulaanbaatar city**

In the last few years, the usage of TDCs and the number of chemical incidents that have occurred in Mongolia have increased significantly. Between 2004 and 2007, there were 20 reported chemical incidents, and between 2008 and 2010 this number increased to 48 [13,14]. According to data given by the Ministry of Nature, Environment and Tourism, approximately 360 enterprises and individuals had permission to use, sell and store TDCs, excepting explosive substances, in 2010. 15% of these were located in the provinces, while 85% (approximately 260 companies or individuals) were in the Ulaanbaatar area. About 30% of the latter have immediately transported chemical substances to the provinces, but 182 store the chemicals in the Ulaanbaatar area. As this study found, about 80% of those relevant companies registered in the territory of Ulaanbaatar city are located in Bayangol, Khan-Uul and Songinokhairkhan districts (figure 1).

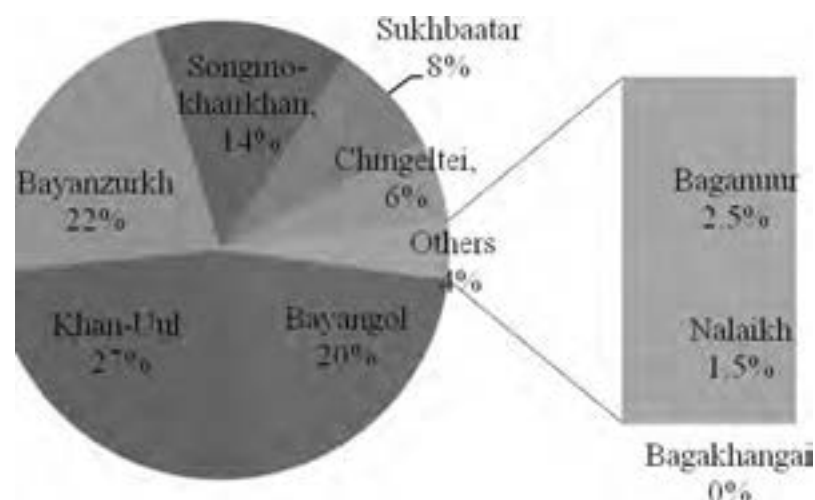


Figure 1: Distribution of industries, companies, enterprise and individuals had permission for use, sell and store CTDSs located in Ulaanbaatar city

In order to map chemical hazard, vulnerability and risk, firstly the toxicological data and amount of CTDS used and stored in a certain area have to be characterized and determined. Therefore, 34 industries and entities that have permission to store, trade and use chemical extreme toxic and dangerous chemicals in Ulaanbaatar city were placed using GPS, and research on the hazard, vulnerability and risk of 18 companies was carried out.

Ammonium, sodium cyanide, organic and non-organic acid and alkali, and organic solvents for cooling and freezing systems, the leather, fur and wool factories, mining, laboratories and cleaning have been used and stored commonly in the area of Ulaanbaatar city. In the area of the 9 districts, 17 individuals that use ammonium, classified as a toxic and flammable substance, 5 individuals that use cyanide, classified as extremely toxic, 65 individuals that use acid and alkali, classified as toxic, corrosive and oxidative, and 17

individuals that use organic solvents classified as extremely toxic and flammable have been mapped in this study (table 1) [15,16].

Table 1: The number of companies that use and store some widespread high-toxic and dangerous substances

District	Ammonium	Sodium cyanide	Acid	Alkali	Organic solution	Total
Bayangol	4	1	8	4	4	21
Chingeltei	-	1	3	1	1	6
Sukhbaatar	-	-	11	3	4	18
Khan-Uul	4	1	10	9	2	26
Songinokhairkhan	6	2	8	3	4	23
Bayanzurkh	1	-	4	1	2	8
Total	15	5	44	21	17	102

Generally, extreme toxic and hazardous substances have been used and stored in highly-populated districts of Ulaanbaatar city such as Khan-Uul, Songinokhairkhan, Bayangol and Bayanzurkh. Therefore, it is necessary to organize government and private enterprise to ensure the safe use and storage of hazardous chemicals and eliminate weak points.

- **Potential exposure and hazard areas from the direct release of toxic or dangerous chemical liquids and volatile substances from dangerous chemical objects in Ulaanbaatar**

The exposure and hazard areas from an incident involving liquid and volatile chemical substances were estimated by methodology 1 above. A mapping of exposure and hazard areas from the direct release of toxic or dangerous liquids and volatile substances from dangerous chemical objects located in Ulaanbaatar city was made based on this estimation, as is shown in figure 2.



Figure 2: Exposure and hazard area by the direct release of toxic and dangerous liquids and volatile substances from dangerous chemical objects in Ulaanbaatar

• **A mapping and assessment of chemical hazard, vulnerability and risk in Ulaanbaatar city**

The chemical incident risk was carried out with methodology 4, and illustrated in Table 2. Based on results shown in this table, it was determined by methodology 5 whether the location of chemical manufactures and users, as well as market and storage facilities in a certain area were suitable or unsuitable for that area (shown in Table 3). The chemical risk level of 9 districts, determined, based on this chemical incident quantitative risk, according to methodology 6, is presented in table 4. The mappings of possible chemical incident hazard, vulnerability and risk in Ulaanbaatar city are shown in figures 3, 4 and 5, respectively.

Table 2: Chemical incident risk level (by districts)

No	District	Sub-district number ^{1, 2}	Territory size exposed to hazard (km ²) ³	GSRF	Human number of exposure/hazard rate (person exposed/total people) ⁴	Vulnerability (0-3 points) ⁵	Incident probability per person (F) (person ³ *incident number)	Potential risk (person exposed/total people/year) (IRF and CR)
1	Khan-Uul	16	34.6 km ²	7x10 ⁻²	6 x 10 ⁻¹	3	2.1x10 ⁻⁵	0.37x10 ⁻⁴
2	Baganuur	4	0.2 km ²	3x10 ⁻⁴	1 x 10 ⁻³	1	5.4x10 ⁻⁵	0.5x10 ⁻⁸
3	Bayanzurkh	24	1.2 km ²	9x10 ⁻⁴	1 x 10 ⁻⁴	1	4.5x10 ⁻⁶	0.45x10 ⁻⁹
4	Bayangol	20	29,5 km ²	1x10 ⁻¹	10 x 10 ⁻¹	3	4.8x10 ⁻⁶	0.14x10 ⁻⁴
5	Bagakhangai	2	0	0	4 x 10 ⁻⁴	1	2x10 ⁻⁴	0.8x10 ⁻⁷
6	Songinokhairkha	32	30 km ²	2.5x10 ⁻²	6 x 10 ⁻¹	3	3.6x10 ⁻⁶	0.65x10 ⁻⁵
7	Sukhbaatar	18	1 km ²	4x10 ⁻³	3 x 10 ⁻²	1	1.5x10 ⁻⁶	0.45x10 ⁻⁷
8	Chingeltei	19	3.5 km ²	4x10 ⁻²	1 x 10 ⁻²	2	1.5x10 ⁻⁶	0.3x10 ⁻⁷
9	Nalaikh	6	0.2 km ²	3x10 ⁻⁴	1 x 10 ⁻³	1	1.4x10 ⁻⁵	0.14x10 ⁻⁷

¹-The report on Ulaanbaatar city by 2011

²- Enhancing Policies and Practices for Ger Area Development in Ulaanbaatar (2010)

³- The results of estimation of the area of exposure to CTHSs and hazard zones if a chemical incident happened at a dangerous chemical object facility that use massive liquid and volatile substances

⁴- Human number in possible hazard zone and exposure area (person exposed/total people)

⁵- Human vulnerability based on human situation in the area of exposure to CTHSs and hazard zones (as points)

⁶- Incident probability based on chemical incident occurring between 2006-2011 (person/year)

Table 3: Chemical risk rank of 9 districts

GSRF	IRF			
	High risk (IRF > 10 ⁻⁴)	Medium risk (10 ⁻⁴ >IRF>10 ⁻⁵)	Low risk (10 ⁻⁵ >IRF>10 ⁻⁶)	Very low risk (IRF <10 ⁻⁶)
Low risk zone (GSRF < 10 ⁻³)	CS	S	S	S: Bayanzurkh, Baganuur, Nalaikh, Bagakhangai
Medium risk zone (10 ⁻³ ≤ GSRF <10 ⁻²)	U	CS: Khan-Uul	S	S: Sukhbaatar
High risk zone (10 ⁻² ≤ GSRF <10 ⁻¹)	U	U: Bayangol	CS: Songinokhairkhan	S: Chingeltei
Extreme high risk zone (GSRF > 10 ⁻³)	U	U	U	CS

U- unsuitable, CS-conditionally, S-suitable

Table 4: Chemical risk of districts by a disaster risk level

Risk level	Quantitative meaning	Risk classification	Risk level as color
Remote	10 ⁻⁸ -10 ⁻⁷	1	Other 6 districts
Low	10 ⁻⁷ -10 ⁻⁶	2	Songinokhairkhan
Permissible	10 ⁻⁶ -10 ⁻⁴	3	Khan-Uul, Bayangol
Dangerous	10 ⁻⁴ -10 ⁻³	4	
Emergency	10 ⁻³ -10 ⁻²	5	

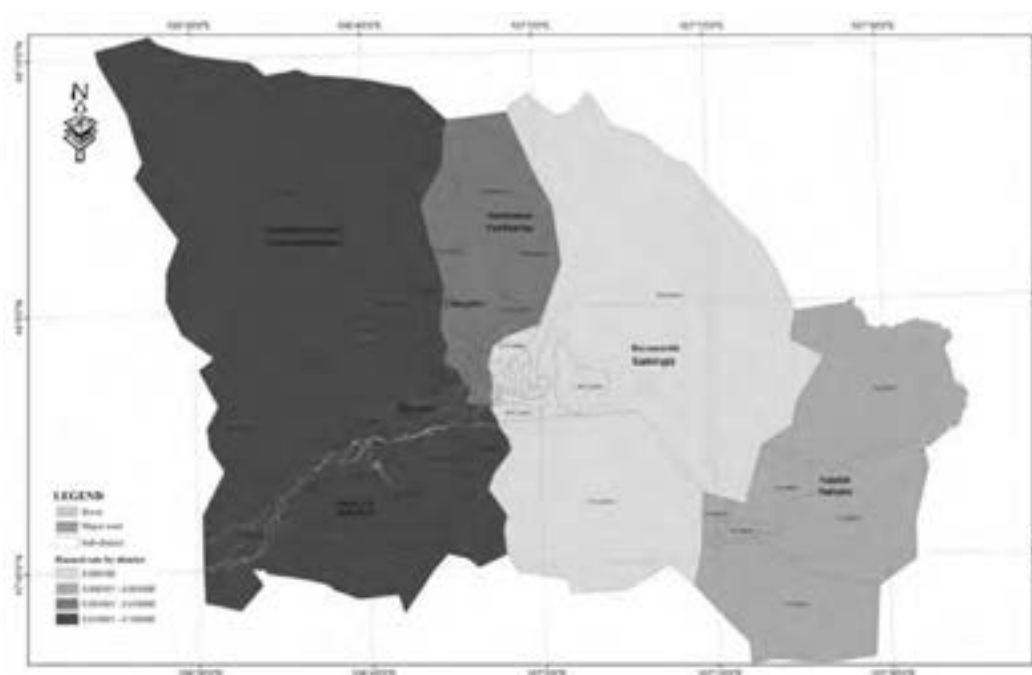


Figure 3: A mapping of chemical incident hazard

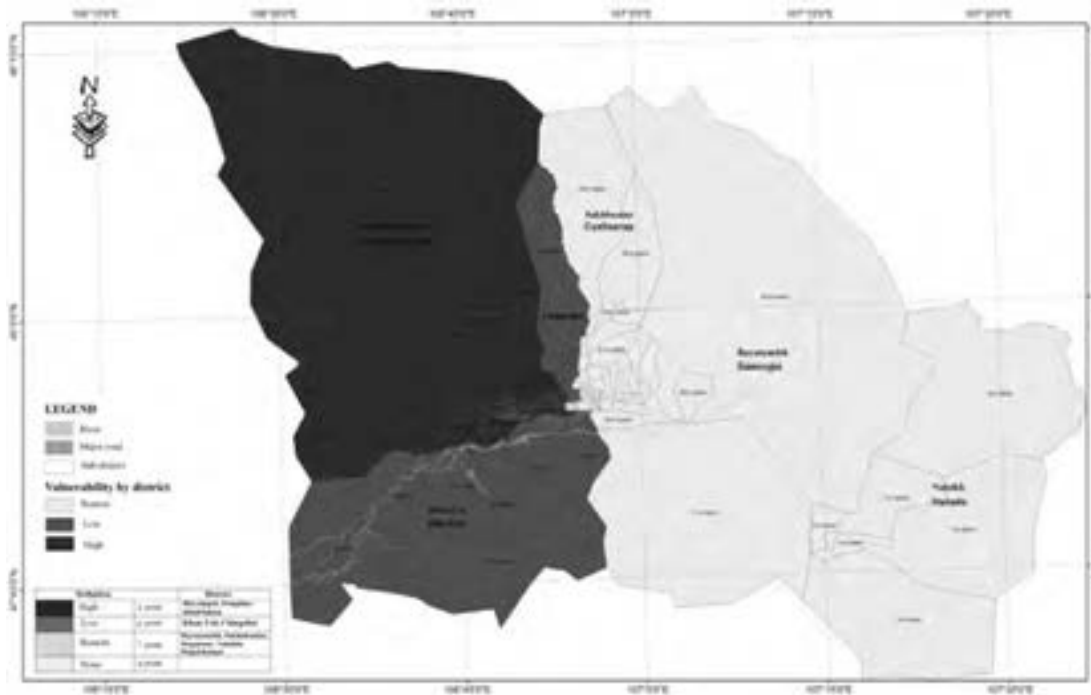


Figure 4: A mapping of chemical incident vulnerability



Figure 5: A mapping of chemical incident risk

CONCLUSION

The aims of this study were to find the location of industries and entities that have permission to store, trade and use TDCs in the 9 districts of Ulaanbaatar city,

to classify them according to the hazard and toxicity effects of the chemicals utilized by them, to determine the amount of usage, storage and trade, and also to assess the potential chemical incident hazard, vulnerability and risk, by mapping them in the territory of the 9 districts of Ulaanbaatar city. The following results were revealed as this study.

1. Large amounts of chemical substances with high hazard rate were used and stored in Bayangol, Khan-Uul, Songinokhairkhan, Bayanzurkh districts.
2. The estimation of the human population who live in areas of high chemical exposure and hazard was done for each district. Human numbers exposed to potential chemical incident hazards in Bayangol district was the highest or 10×10^{-1} , and Songinokhairkhan and Khan-Uul were 6×10^{-1} , respectively. In contrast, human numbers exposed to potential chemical incident hazards in Sukhbaatar, Chingeltei, Baganuur and Nalaikh districts was much lower than these, at 10^{-2} - 10^{-3} . With regard to Bayanzurkh and Bagakhangai districts, they were the lowest at 10^{-4} .
3. The vulnerability of the population of Bayangol and Songinokhairkhan to TDCs was the highest, with Khan-Uul and Chingeltei districts lower and other five districts the lowest.
4. Comparing the results of this study to the international risk level, the chemical risk levels of Bayangol and Khan-Uul districts were higher than of other seven districts, but within acceptable risk levels according to the definition system of the international risk level. With regard to other 6 district, except Songinokhairkhan, chemical incident risks were in extreme low level.

SUGGESTIONS

Based on above-mentioned results, the following suggestions could be presented officially:

- To develop a policy on potential chemical incident hazards and risk prevention, and preparedness and capacity to fight such incidents by the National Emergency Management Agency (NEMA);
- To control chemical substance seller and buyer, as well as to improve control on the usage, utilization and storage of toxic and dangerous chemical substances by NEMA
- To improve cooperation and relation between governmental organizations such as NEMA, the Police Department, State Professional Inspection Agency and others;
- To exchange practice and information and to organize training and seminar periodically within governmental organizations in order to improve knowledge and skill of related inspectors and staffs concerning the inspection and control on the usage, utilization and storage of toxic and dangerous chemical substances;
- Scientific institutes and governmental organizations should co-operate in deciding zoning for companies and industries that use, store and sell

chemical substances in order to provide for the safety and security of society and the population;

- To enhance activities of training and education of the public about chemical hazards.
- To tighten regulations concerning the usage, storage and transportation of chemical substances;
- To do assessments of chemical incident risk by related organizations;

These suggestions could support the reduction of chemical hazard and risk in Ulaanbaatar city.

REFERENCE

1. Battogtokh, P., Bayarjargal, B., 2006. Guide on Disaster and accident protection. Reserarch Institute under the National Emergency Management Agency, Ulaanbaatar
2. Anand S Arya., Anup Karanth., Ankush Agarwal., 2008. Hazards, Disasters and Your Community. *Gol-UNDP Disaster Risk Management Programme*. New Delhi, India.
3. Bayarjargal, B., Khurelsukh, S., Serjmaydag, D., 2010. Disaster Management. The Disaster Research Institute, Ulaanbaatar.
4. Renjith, V, R., Madhuh, G., 2010. Individual and societal risk analesis and mapping of human vulnerability to chemical accidents in the vicinity of an industrial area. *International Journal Of Applied Engineering Research*, Dindigul, Vol 1, №1, ISSN-0976-4259.
5. Cutter, S, L., 1996. Vulnerability to environmental hazards. *Progress in Human Geography*, Vol. 20.
6. Cutter, S, L., Mitchell, J, T., Scott, M, S., 2000. Revealing the vulnerability of people and places: a case study of Georgetown County, South Carolina. *Association of American Geographers*, Vol. 90.
7. Fengying Li., Jun Bi., Lei Huang., Changsheng Qu., Jei Yang., Quanmin Bu., 2010. Mapping human Vulnerability to chemical accidents in the vicinity of chemical industry parks. *Journal of Hazardous Materials*, Vol.179.
8. Law of Mongolia on chemical toxic and hazardous substances, 2006. Ulaanbaatar
9. “Методика прогнозирования масштабов заражения сильнодействующими ядовитыми веществами при авариях (разрушениях) на химически опасных объектах и транспорте”. (1991). РД52.04.253-90.
10. Part I: Guidance on Human Health Preliminary Quantitative Risk Assessment, 2004. *Environmental Health Assessment Services Safe Environments Programme*, Canada.
11. Gurjar, B, R., 1999. Environment Risk Analysis for Industrial Sitting, Planning Management. *PhD Thesis*, Centre For Atmospheric Sciences, Indian Institute of Technology, New Delhi.
12. Gurjar, B, R., Manju Mohan., 2003. Integrated risk analysis for acute and chronic exposure to toxic chemicals. *Journal of Hazardous Materials*, Vol. A103.

13. The report on hazardous phenomena and incident happened in Mongolia in between 2000-2009
14. “The report on disaster situation of Mongolia in between 2004-2011
15. Guideline on chemical toxic and hazardous substance, 2010. Ulaanbaatar
16. List of companies and industries that have permission to use chemicals by Ministry of Nature, Environment and Tourism, 2011

The application of geoinformation for emergency management and hazard

CPT. D.Sodnomragchaa¹
CPT. Doc.V.Batsaikhan², Ts.Naranbolor³, CPT. Ts.Ganzorig³, Justin D Pummil⁴
Disaster Research Institute under NEMA of Mongolia^{1,2}
US Army corps of Engineers⁴
E-mail: Sodnomragchaa@msn.com
vbatsaikhan@yahoo.com
Tel: +976-98888148

ABSTRACT

Mongolia is an ancient nation with nomadic origin. It has an area of 1.565 million square km, and is located between Russia and China. Mongolian total population is approximately 3 million. The main administrative divisions are in Ulaanbaatar city region, the 21 provinces. The Provinces are subdivided into Soums and Bags. Ulaanbaatar city is divided by Districts and Sub-Districts. Ulaanbaatar is the capital city of Mongolia and has close to 1.5 million registered population in 2015 and 470 thousand hectares of territory. The city administrative units include 9 districts, which are subdivided into sub-district. Two districts are located outside of the city boundary. Ulaanbaatar have more than 40 percent of the country's population. In Mongolia, which has a total population of 3 million, this implies that floods are not only natural hazards, but also an issue of national security. Changes of local and statistics say 60% of populations are community on human made disaster, natural disaster mostly flood and earthquake risk area of Ulaanbaatar. Therefore, human made disaster chemical accident and radical's accident. The climate warming in Ulaanbaatar over the last 65 years has been 2.4°C, which is 30% higher than national average. Faster the climate change, greater the risk of disasters. Forest area around the city decreased significantly since early 1990s, due to forest fires and particularly due to the consumption of "free of charge" natural resources (including aggressive woodcutting for housing, furniture and firewood). Ground water levels increased while permafrost thickness decreased by 20-30 cm in the last 8 years. Heavily degraded soil leads to increase in floods and related damages. There is an increasing tendency of runoff coefficient that indicates increased degradation of vegetation cover in the river basins of the city.

The aim of work is to make emergency hazard zone maps of Ulaanbaatar city by using time series data derived from SAR data and GIS layers (LULC, Canal, Road, Bridge) derived from high resolution Worldview image, ALOS PALSAR, disaster information data. Software are used the ERDAS, ArcGIS, Google hybrid map downloader. Most important is to detect how much people and area will be affect by disaster. therefore I m trying to detect emergency zone of Ulaanbaatar city for example to detect hazard zone using result of object fire, chemical and radical accident, earthquake and geographic information system.

Keywords: remote sensing, geographic information system, erdas, arcgis, alos palsar, lulc-land use land cover, aster and landsat data

1. INTRODUCTION

Urbanization is a worldwide phenomenon. While urbanization pattern has not been determined academically across different areas, it is essential to understand urban development to avoid environmental problems due to urban sprawl. Urban sprawl, excessive spatial growth of cities, is caused by complex driving forces (social, economical, political, and physical ones), their interactions, and associated processes¹. The pattern of urban sprawl should therefore be considered in each area in order to realize desirable landscape and manage the natural environment.

Although Mongolia has abundant natural lands and a traditional nomadic culture, its population is mainly concentrated in Ulaanbaatar, the capital of Mongolia, where it increased rapidly from 0.58 million in 1992 to over 1.3 million in 2012 due to migration (National Statistical Office of Mongolia).

Some parts of the privatized areas are called “*ger-areas*” because most of the immigrants build *gers* (traditional and portable Mongolian residences) or block houses enclosed by fences, shown in Fig.1, and these areas account for about 60% of Ulaanbaatar city’s population (UN-Habitat 2010). Some of them live dangerous area. Although it is easy for people to build *fence* on a land and acquire it, modern infrastructures, such as piped water, sanitation, proper roads, public transportation, and heating systems, have not been improved. *Ger-areas* also have negative impacts on the human and natural environment due to unplanned and haphazard expansion. One of matter is discompose which inadequate new higher building area in center of Ulaanbaatar city.

Accordingly, to use new space technology for to monitor dangerous area, to detect emergency zone for emergency situation this will be affect. The aim is how Geo-information application is useful for emergency management. Likewise to make emergency hazard zone maps of Ulaanbaatar city by using time series data derived from SAR data and GIS layers (LULC, Canal, Road, and Bridge) derived from high resolution Worldview image, ALOS PALSAR, disaster information data. Software are used the ERDAS, ArcGIS, Google hybrid map downloader. Most important is to detect how much people and area will be affect by disaster. Therefore I’ m trying to detect emergency zone of Ulaanbaatar city for example to detect hazard zone using result of object fire, chemical and radical accident, earthquake and geographic information system.

Rationale

- ✓ Planning and management of disaster process requires data as a support to take decision.
- ✓ If the data is on paper or even in computers in tabular format, it can’t be as useful as data represented on maps because this can’t enable us to create various thematic analyses ad hoc.

It is said that –A Picture is worth a Thousand Words...

Objective

- ✓ To create emergency zone maps using conventional and remote sensing data
- ✓ To create the emergency maps based on multi-temporal emergency maps integrated with other GIS thematic layers
- ✓ To create an emergency database for disaster situation and disaster research work.



Fig. 1: Ger-areas in the sprawling areas of Ulaanbaatar

2. METHODOLOGY

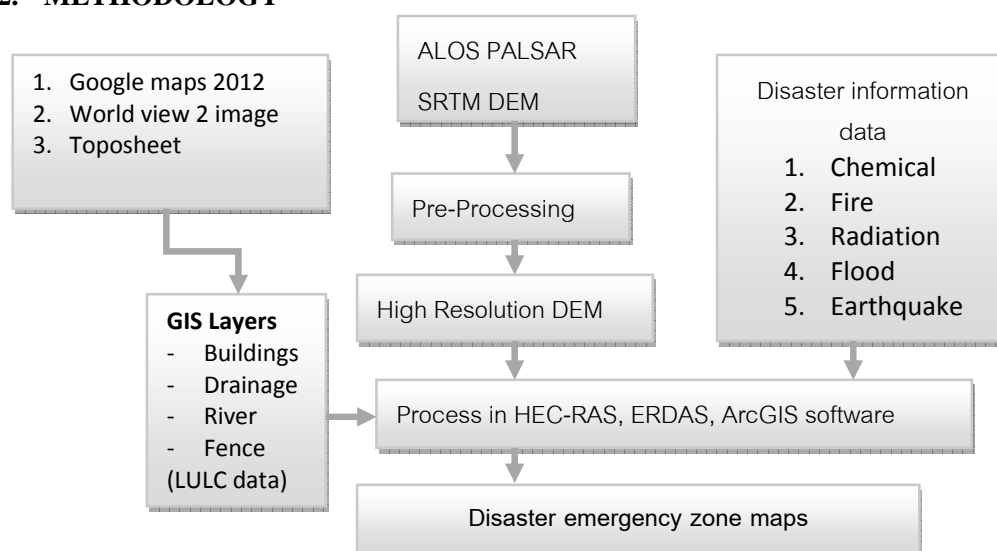


Fig. 2. Methodology to identify the areas subject to Emergency zone creation

3. Geo-Information for disaster

3.1. Remote Sensing is a technology that detects and monitors the movement of natural hazards and their parameters and disaster situation by measuring the electromagnetic waves reflected or emitted from the related natural object. Space information derived through remote sensing methods is divided into two types: active-radar and inactive-optic.

Remote sensing is now widely used in all sectors of Mongolia. NEMA cooperates with many foreign and domestic organizations, which are engaged in geo-information.

Currently, NEMA receives information from NOAA AVHRR and TERRA MODIS satellites whose precision is 250-1000 meters to monitor forest and steppe fires, droughts, dzud (heavy snow) and strong snow and dust storms, and evaluate disaster situations. Those data are very useful for monitoring natural disaster supported from Environment information center. Also NEMA is using WINDS satellite ground antenna for disaster situation supported from JAXA. Fig.3

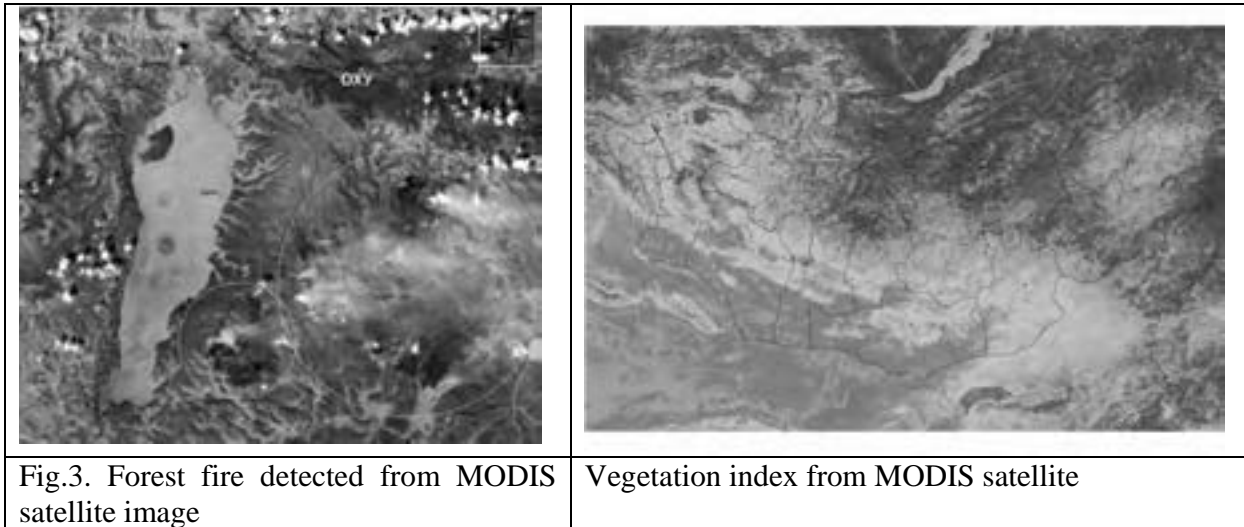


Fig.3. Forest fire detected from MODIS satellite image

Vegetation index from MODIS satellite

Forest fire risk. The risk of forest fires is high in Mongolia during the dryer seasons of the year. Fire risk in the Bogd Mountain forests has been analyzed using high precision 3-dimensional 5RTM satellite imaging. (Figure 4 and 5)



Fig.4. Vegetation index of Bogd khan mountain, Ulaanbaatar (the result is classification of ASTER and Landsat DATA)

Through spatial analysis by GIS and coding certain attributes of GIS images by their contribution to the risk of catching fire, we have sorted the total forest areas of Bogd Mountain into smaller segments by their risk of catching fire. The following mathematical and statistical formula has been used in the process:

$$\text{Risk of catching fire} = 1 + 100\text{Vegetation} + 50\text{Slope} + 40\text{Winddirection} + 30\text{Altitude} + 20 \text{ Distance from a road} + 10\text{Distance from the nearest settlement}$$

The above formula and its risk coefficients of 100, 50, 40, 30, 20 and 10 were devised based on experiments conducted in the cold and dry territories of Canada. Based on this formula, Bogd Mountain does not have a forest segment that has no or very little risk of forest fires. The Mountain is under high risk of forest fires because it is surrounded by human settlements and is under the constant influence of human activities. Therefore, forest fires in the Bogd Mountain area tends to increase, which is related to the socio-economic development, poverty, and density of human settlements around the mountain. The table below shows the sizes of areas that are under different levels of risk of forest fires.

Level of risk of forest fires	Area size(ha)	Percentage of the area on the satellite image
High	16 760. 6 ha	28. 17%
Medium	18 765. 69 ha	31.54%
Low	23 971. 77 ha	40. 29 %
Very low	0.00 ha	0%
Total	59 498. 06 ha	100.00%

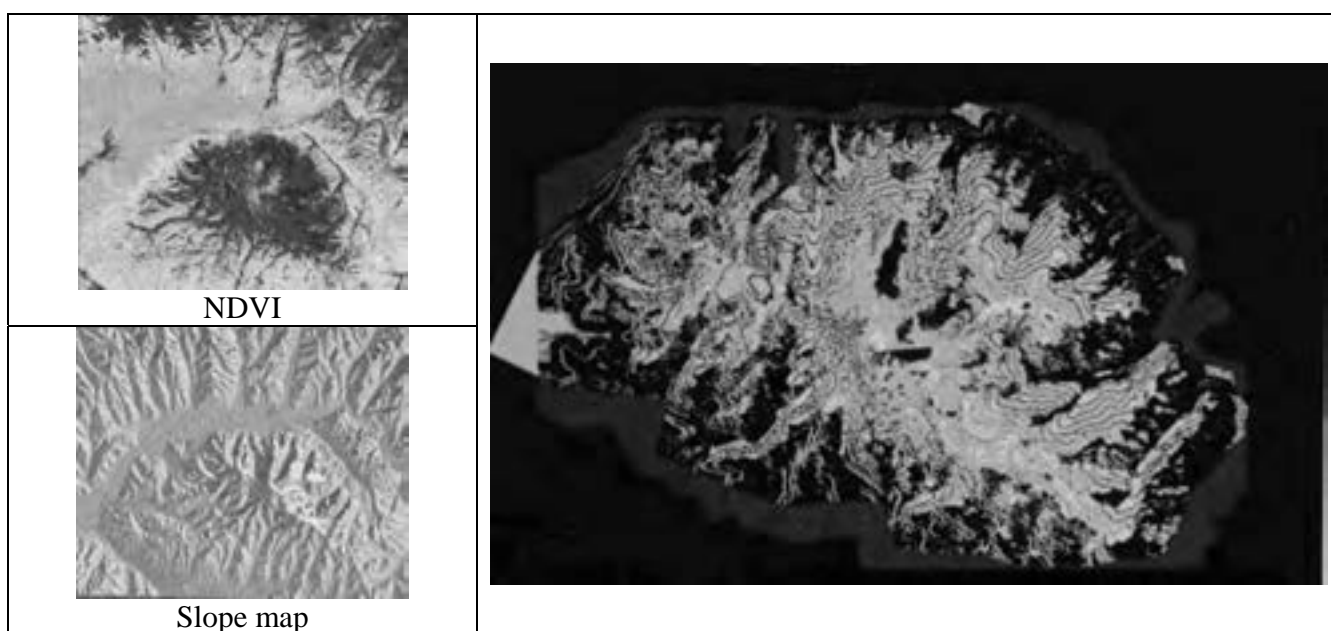


Fig.5. Areas of Bogd Mountain with high risk of forest fires (areas depicted in red have high-risk.)

The table divides the territory of the Bogd Mountain into segments by the level of risk of forest fires based on satellite information, and shows the area size of each category. High precision data from satellites is essential in forecasting and monitoring possible disasters through remote sensing technology. In order to take full advantage of remote sensing technologies, the emergency management institution of Mongolia needs to introduce the modern LIDAR system. LIDAR is a system that monitors earthquake and flood disasters that has occurred in densely populated settlements, by monitoring the area through laser camera, installed in hand-manipulated helicopter, which has the precision to a centimeter.

2.1. Geographic information system

Geographic information system produces both spatial and characteristic data and information, which are used for various planning, research and analysis purposes. In the disaster management field, geographic information systems can play an important role in correcting and preventing from repeating of any previous mistakes and mishandlings, strengthening disaster protection capacities, and reducing vulnerabilities and risks.

In my work I have done emergency zone by using RS and GIS data and software, it is possible to pinpoint areas with high disaster risk, assess risks and vulnerabilities, promptly plan search and rescue measures during disasters, manage communication and information during disasters, and provide timely information to the decision makers and end users during disasters. GIS can be used not only for exchanging information on natural hazards, but also on economic phenomena and environmental situation. Displaying and analyzing disaster hit areas in 3-dimension through computer programs makes information easy to understand and utilize.

Moreover, GIS is useful in predicting natural and man-made disasters, and facilitates a certain level of preparedness by making prompt planning of prevention, response and recovery measures possible. (Figures 7, 8, 9 and 10)

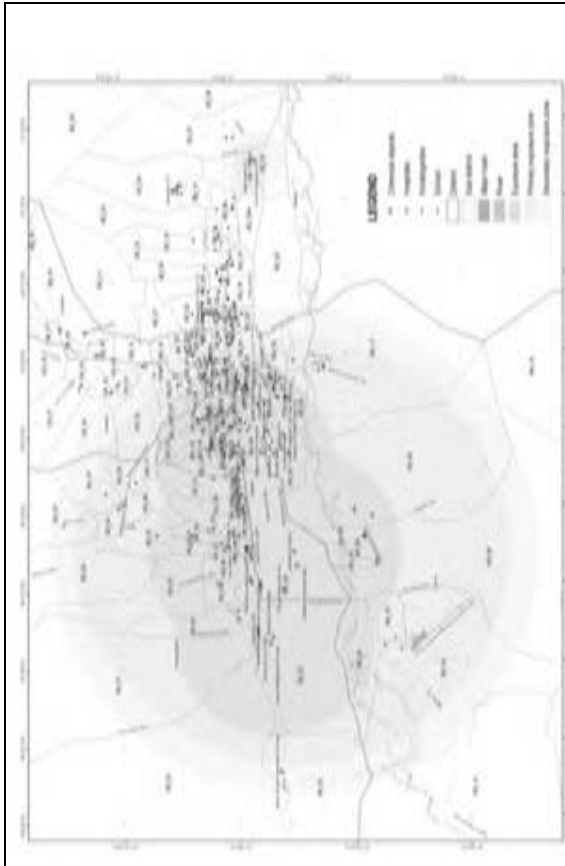


Fig.7. Chemical risk zone in Ulaanbaatar city



Fig.9. Radiation risk zone of hospital ontological

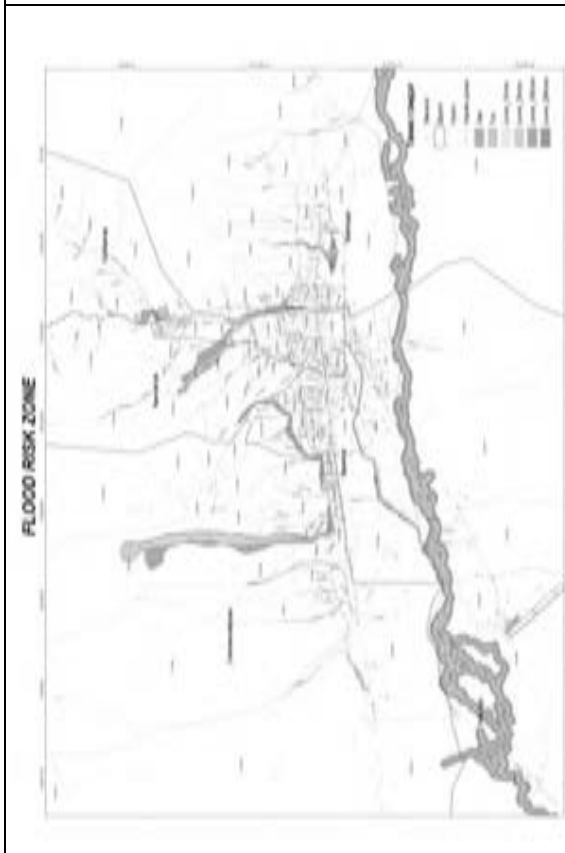


Fig.6. Flood risk zone in Ulaanbaatar city

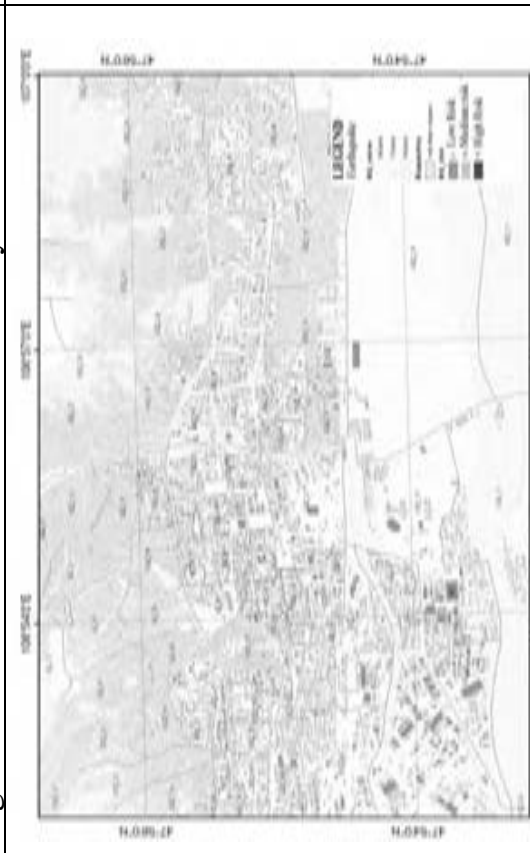


Fig. 8 Earthquake risk zone in Ulaanbaatar city

Mongolia have 13 type of disaster like Drought, Dzud, Wind storm, Forest fire, Earthquake etc.. mostly happen forest fire in Mongolian east north. Mongolia vegetation is divided by 4 types Forest region, orkhon-selenge region, touchwood region and field region. Fig.10.



Fig.10. Forest fire zoning

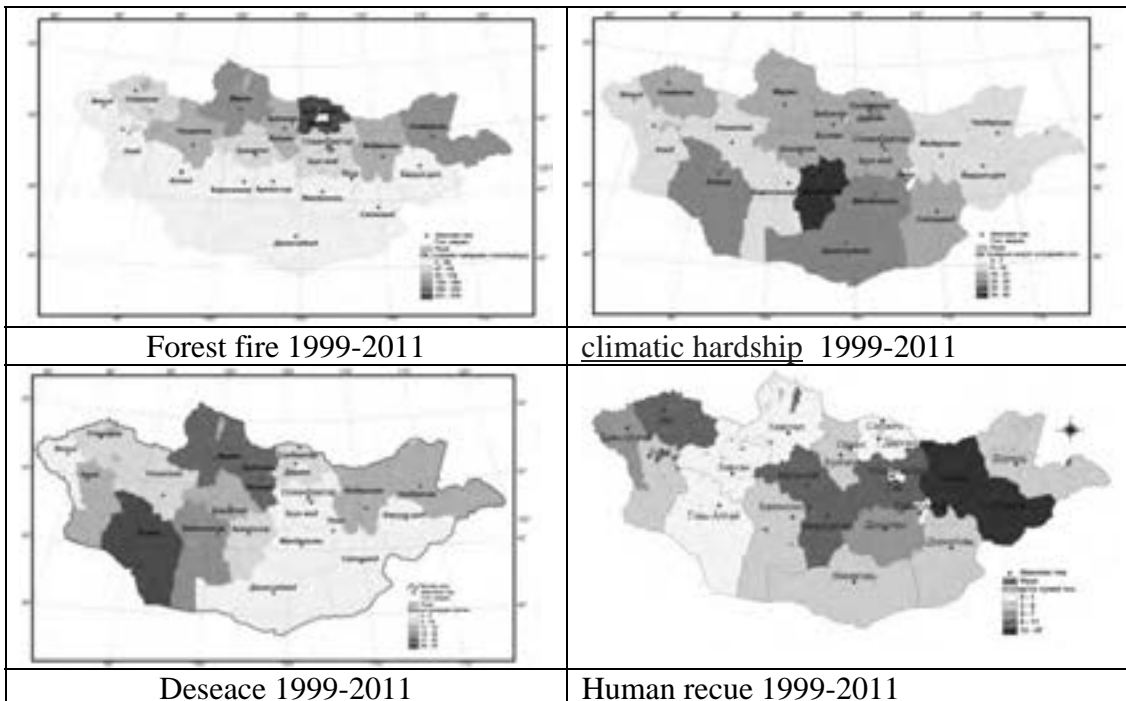


Fig.11. Natural hazards that have occurred nationwide in 1999-2011

Precision of geographic information is vital in preventing and planning for preparedness against small-scale disasters, hazards, and accidents that usually happen at a single structure or construction. Therefore, it is important to create an

integrated geographic information database with scales from 1:5000 to 1:100,000 at the national level.

Conclusion

Geographic Information Systems and Remote Sensing systems need to be introduced to and expanded at the emergency management institutions of Mongolia to improve prevention from possible disasters, supply decision makers with accurate information during disasters, strengthen the national disaster protection capacities, and to organize appropriate response and recovery measures.

Although Geographic Information System and Remote Sensing are still new acquaintances to the emergency management system of Mongolia, the need for more and better of them is constantly increasing. Therefore, it is necessary to train the provincial and city level officers of the emergency management organizations in using the GIS and remote sensing technologies, increase the number of GIS and remote sensing specialists, expand partnership and cooperation with organizations in the field of geo-informatics, and promote projects and programs in this field. Most important one is we need high resolution satellite image, small scale vector file for analyzing and preparing maps (disaster management) for who decide during the disaster and planning for disaster. Particularly It will help to save time, money and workforce.

Also NEMA should have to establish a disaster geo-database and a Disaster Geo-Database Center in this era of information and communication technologies would be a huge stride forward in promoting the usage of the GIS and remote sensing technologies in disaster reduction endeavors.

REFERENCES

- [1] Amarsaikhan D., Blotvogel H.H., Chinbat B. Study on Land Use in Industrial and Green Production Zones of Ulaanbaatar City Using Quickbird Image. Map Asia 2008. 2008.
- [2] Bruun O., Odgaard O. Mongolia in transition. RoutledgeCurzon, 1996.
- [3] Amarsaikhan, D., Ganzorig, M. and Moon, T.H., 2005. Application of multitemporal RS and GIS data for urban change studies. *Proceedings of the Korean GIS Conference*, Busan, Korea, pp. 190-215.
- [4] Bumerdene, Ch. and Chinbat, B, 2003. Some problems in functional zoning and land use of Ulaanbaatar city, Free press. Ulaanbaatar, Mongolia.
- [5] Chinbat, B., 2005. On a new land use classification and zoning scheme of Ulaanbaatar, Mongolia. *Proceedings of Mongolia- Korea Conference in Urban Planning*, Ulaanbaatar, Mongolia.
- [6] ERDAS, 1999. Field guide. 5th Ed. ERDAS, Inc. Atlanta, Georgia, USA.
- [7] Gonzalez, R. C. and Woods, R. E., 2002. *Digital Image Processing*. 2nd ed. Upper Saddle River, New Jersey: Prentice-Hall.
- [7]. Herro, M, Onon, N, et al., 2003. Ulaanbaatar rapid needs assessment. USAID report, Ulaanbaatar, Mongolia.
- [8]. Hofstee, F., Radnaabazar, G. and Kuffer, M., 2004. Monitoring the development of informal settlements in Ulaanbaatar, Mongolia. Ulaanbaatar, Mongolia.

[9]. Pohl, C., and Van Genderen, J.L., 1998. Multisensor image fusion in remote sensing: concepts, methods and applications. *International Journal of Remote Sensing*, 19, pp. 823-854.

ⁱ Fang et al. 2005; Gimblett et al. 2001; Weber 2003

Successful solution of water ecology and economy in consumption of apartment

Enkhtungalag SH., Batbileg Enkhbat and Bulgan Zorig
Department of Architecture and cartography
The School of Construction Engineer and Architecture,
The Mongolian University of Science and Technology,

REVIEW

Urgent issues

Water shortage problem is facing to the world and especially the urgent problem in Mongolia. Because of the water shortage, 1.1 billion people are using poor quality water all over the world and 1.8 million children pass away per year 4900 per day.

According to the Ikh Zasag Law of Chinggis Khan, a person who damages the water along the mountain, trees along the water and entail shall sentence to death. If use the water only for the pureness, you won't know the benefits of water. Our body consist of water. All cells are covered of water and 70% of our body consists of water.

Trees and water are connected. The tree is the important thing to save the water.

According to the study: By 2011 the forest decreased by 30%. If consider this degeneration continues as upon speed, there are no forest after 20 years and small rivers will dry.

The Purest Tuul River which is too deep to be crossed by a horseman, is dried to the soil of the ground because of insufficient water to feed its fish. The River treated the black shadows of this city. Supplying bushes were cut and waste water with chemical toxic from industries of machine techniques and fur and leather production are flowing to Tuul River. There are many species of animals are being destroyed along the river. This sorrowful event are facing to the all rivers of Mongolia.

The water resources are non-renewable and we are going to buy the water. Because of the inappropriate utilization of Tuul's water, the fish and other species are completely extinct, but Mongolians are still singing "The Stream of River Tuul is beautiful during the night".

STUDY

Resources of surface ground water of Mongolia are 500 m³ and 85% of these are pure water. According to the study of 2011, there are 4276 rivers, 6857 fountains, 3800 lakes and 225 ice-rivers in Mongolia, but 1662 dried only for year.

12,5% for agriculture, 8,25% for industry, 22,1% for mining, 15,3% for population and 24% used for the electrical power from the total water consumption.

Total water supply of our country is from the underground water resources. There is no other country like Mongolia. We should economically use our water resources, but:

- Thousand of cars washed by drinking water
- Sauna and swimming pools limitlessly using the drinking water
- Agriculture is being watered by drinking water
- And washing our toilet by drinking water

We should stop to clean the toilet by drinking water!!!

But other countries use recycled water named “grey water” for the toilet. Our country were talking about it for many years. The government made the amendments to the law of water supply and sewage. In this law, stated that the wastewater from home water consumption shall be named the “Grey water”. Home wastewater is the wastewater from sink, shower, bath, water closet and other pipes of apartments and industries. The grey water is possible to be used in newly constructed apartments. But the Water Administration Office noticed that the grey water is not possible to be used in apartments in further 10 years.

The apartment resident uses 204 liters of water per day and “Ger” district resident uses 7 liters per day. /Water Administration Office/

10 liters of water need for one toilet flush. And we use one person water usage for one toilet flush.

Averagely 4 people live in 1 family. /According to study of 2010/.

1 person goes to toilet 3 times per year and 1 family uses 120 liters of water per day for toilet flushes.

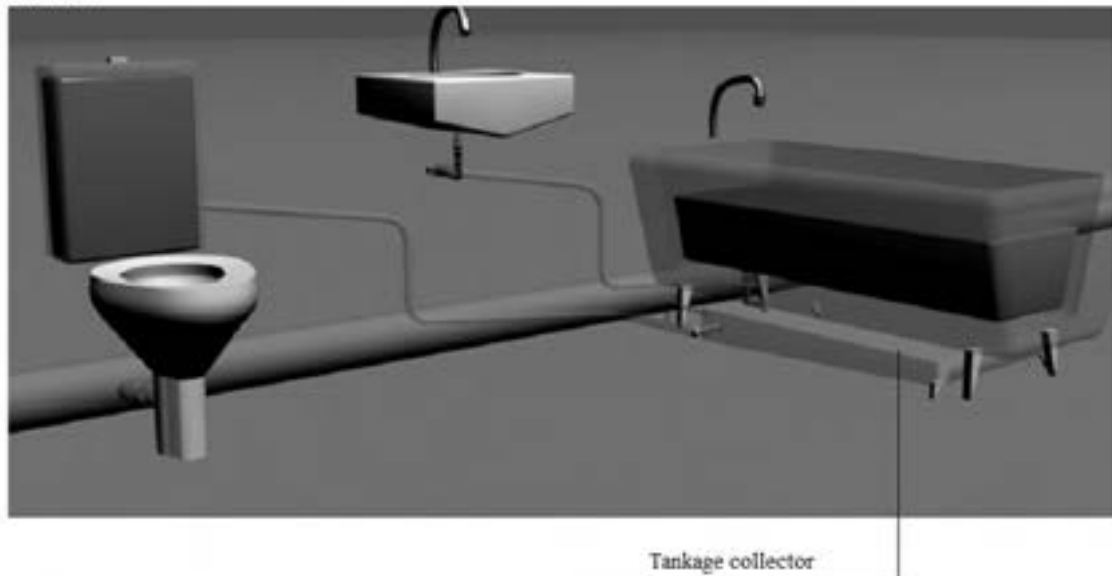
100, 000 families live in apartments in Ulaanbaatar, and they use 12,000,000 drinking water for toilet flushes, it is 1,500,000 people’s drinking water consumption.

PURPOSE

We invented the technology and equipment to use the grey water for toilet flushes in order to protect our nature and economy, to keep the ecological stabilization of drinking water and to reach the international standard.

APPROACH TO EXECUTE

Picture 1



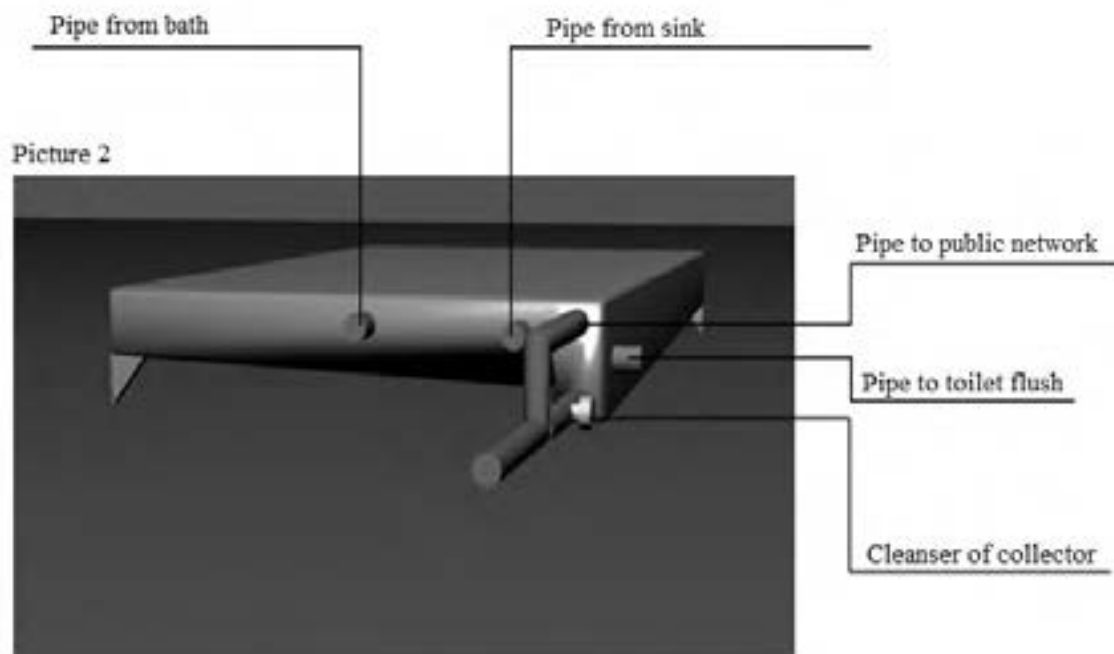
We are going to install the grey water equipment at each apartment without installing the grey water pipe. We will install the grey water equipment at the toilet room of each family. The space is most important in this period when the apartment price is high. And we are planning to install grey water tank in the unused space where under the bath. The grey water tank consists of pipe to public network, tankage collector, pump of toilet flusher and receiver pipe from sink and bath. And the grey water tank is made by the plastic in order to waterproof and anti-bacterial and 5° slant from left to right and north to south. The water tank capacity will be 45 liters under the bath and the tankage collector will be installed at the minimum level of grey water tank. We will make the tank with 3 feet in order to separate and extract the heavy cells from grey water and tankage will be collected in footless side. Its required to open and clean the tankage collector 1-2 times per month.

The pipe to public network extracts the wastewater after the tank is full. Also extracts the bubbles and soap above the water. Bottom of grey water tank is slant from left to right, in order to collect the tankage and to completely extract the wastewater.

It' s required to open and clean the tankage collector 1-2 times per month. To extract the wastewater after take a shower or after woke up. And completely empty the grey water tank in case of leave home for a long time.

Use vacuum pump when pumps water to toilet. The vacuum pump has pressure sensor and it will automatically pumps the water when water level is low. The vacuum pump requires 220 W and pumps 10 liters of water in 10 seconds. The water of toilet flusher is from the middle of grey water because the purest water will be in middle of the tank. Because the bubbles and soap floats in above and heavy cells sinks to the below of the tank. Water tank capacity is 45 liters. Water resources of the tank is renewable because people wash their hand after go to toilet. And vacuum pump has the sensor and works automatically. Filters will be located in start of sink and bath. These filters consists of 2 layers and top filter has small holes and bottom one has big holes, they filter the wastes of tank and protect

from block.. The filters are possible to be replaced and cleaned. The grey waters can meet to the standard requirements by adding the chemical compounds to toilet. And add the anti-bacterial fluid to the flange of bath in order to protect from bacteria.



Total apartment use 12,000,000 liters of water for the toilet flush per day.
1 liter water=1 tugrugs and we use 12, 000,000 tugrugs for the toilet flush per day.

If this project will successfully run we will save:
360, 000, 000 tugrugs per month
And 4.3 billion per year.

SUMMARY

We can save the daily wasting drinking water by executing this project. And we can save the total drinking water of Ulaanbaatar by executing this project. Water shortage problem is not only faced to Mongolia, this is the global issue, the project can extend the period of water resources of Mongolia by 2 times. If cannot execute this project, we are still wasting 1,500,000 people's drinking water per day. But we can save 12,000,000 tugrugs which only for the toilet flush and. Ulaanbaatar's people can share the huge investment to water resources and the future generation. We can build-up the appropriate use of water which meet to the international standard.

Spatial distribution of heavy metal contamination in urban soil of Ulaanbaatar

Byambasuren Ts¹, Otgontuul Ts¹, Shabanova.L.B²,
O.A Proydakova², I.E Vasileva², Khuukhenkhoo¹, Tsedenbaljir D¹

¹ Institute of Physics and Technology, MAS, Ulaanbaatar, Mongolia

² Vinogradov Institute of Geochemistry, SB RAS, Russia

tttuuulll@yahoo.com

ABSTRACT

Over than last ten years technogenic environmental pollution of Ulaanbaatar has become a critical issue due to its rapid growth of population. The surface soil of Ulaanbaatar is heavily contaminated through air deposition. Therefore, surface soil contamination with heavy metals could be a good indicator for environmental pollution. The spatial distributions of heavy metals in Ulaanbaatar soil were performed in order to evaluate pollution and risk control. In the present work has been studied the heavy metal contamination of soil samples of Ulaanbaatar collected in 2003 and 2010 years. The pseudo total concentrations of Pb, Zn, Cu, Cr, Mn, Ni and Co were determined by FAAS. The pollution index of heavy metals was calculated on basis of World Clark value and the inverse distance weighting method of pollution index applied as spatial interpolation technique was performed by ArcGIS program.

The pollution index was analyzed by number of soil samples and sampled area. According to the histogram obtained by the number of samples, the pollution index of soil samples from 2003 and 2010 years showed an ascending order as Ni < Mn < Co < Cu < Cr < Zn < Pb and Mn < Cr < Ni < Co < Cu < Zn < Pb, respectively, indicating the similar tendency as function of heavy metals. The results of the spatial distributions of heavy metals in soil samples of 2003 show that Ulaanbaatar soils are attributed to low level of pollution with Ni < Co < Mn, moderate level of pollution with Cr < Cu, high and extremely high levels of pollution with Zn and Pb elements, respectively.

Keyword: spatial distribution, Ulaanbaatar, heavy metal

1. INTRODUCTION

According to numerous studies[1-4], soil pollution with heavy metals is mainly due to the anthropogenic sources caused by industrial and energy production, construction, vehicular traffic and road infrastructures, waste disposal, as well as coal and fuel-oil combustion. Heavy metals are particularly dangerous pollutant, because they do not neutralize and decompose like organic and other toxicants, so they tend to accumulate and persist in urban soils for a long time. On the other hand, from an environmental point of view, the heavy metals in urban soil can be used as an indicator for air pollution due to their existence for long time. Heavy metals play a significant role in ecosystem. The soil highly polluted with heavy metals loses its ecological function to buffer and neutralize toxic substances, and becomes a secondary source of air and water pollution itself. [4-5]

The surface soil contamination of Ulaanbaatar with heavy metal has attracted serious attention in recent years due to massive migration of rural residents to city

resulting in the high-density of urbanization. The urbanization causes the increase in fuel and energy industry such as power plants and low-pressure heating stoves, moreover, the vehicular traffic and road infrastructure. The largest power plant-3, consumes about 3.5 million tons of coal per year. In Ulaanbaatar, there are more than 400 low-pressure heating stoves, which use about 1. million tons of low-grade fuel per year, delivering waste to the atmosphere without any treatment [6]. In addition, the about 60% of Ulaanbaatar territory is referred to Ger region, which burns 572 thousand ton of low-quality coal and 700 cubic meters of wood for heating. These all energy and heating sources consume about 5.2 million tons of coal and emit about 200 different types of substances such as ash and slag for each year. According to the survey of World Bank [7], 47% of air pollution in the Ger region is due to smoke of coal combustion, while 48% of that is due to soil pollution. In addition, environmental pollution causes an increase of allergy and cancer among the people, especially children. For example, it has been reported that 93.77% of respiratory disease and 90.91% of bronchitis among the children are caused by air pollution. However, there are not enough fundamental researches on the soil pollution of Ulaanbaatar for the pollution risk control management. The soil contamination with heavy metals has been only studied for a particular [8-12] and limited [13-16] area of Ulaanbaatar.

The main objective of the present study was to analyze sufficient number of soil samples collected and measured under the same standards, methods and lab conditions. The spatial distribution of soil pollution of Ulaanbaatar for Ni, Co, Mn, Cu, Cr, Zn and Pb elements was obtained by interpolation method using ArcGIS program. The surface soil of Ulaanbaatar is considerably polluted by Co, Cu, Cr and heavily polluted by Zn and Pb.

2. MATERIALS AND METHODS

2.1 Study site and sample collection

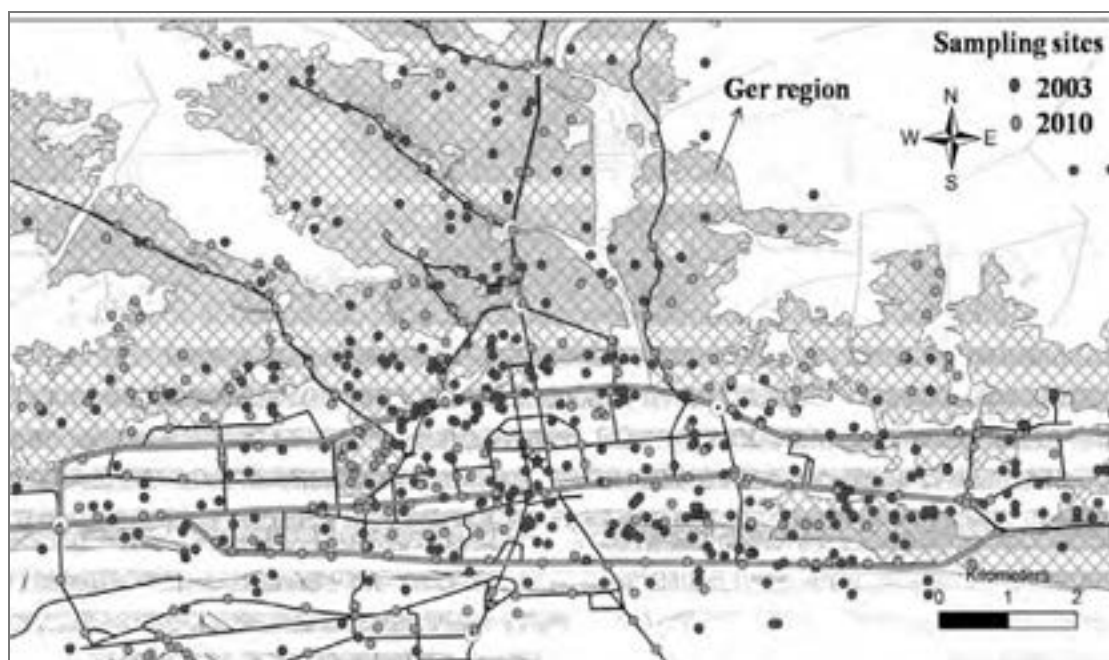


Figure 1: Soil sampling sites in 2003 (660 sites) and 2010 (330 sites).

Ulaanbaatar, the capital city of Mongolia stretches about 20 kilometers along the Tuul River, and located at an altitude of 1350 m above sea level and in northern Mongolia. In the Figure 1 is shown the major central part of Ulaanbaatar. Ger region localized in northern part of city uses untreated coals for heating. In the last 10 years the population of Ulaanbaatar increased rapidly due to migration of rural populations to the city (the population of city was 600,000 in 1989, while it has increased to 1,204,000 in 2010 [17]), resulting in uncontrolled expansion of Ger area (especially in northern part of city) and in increase the number of constructions, industries and traffic infrastructure.

About 600 samples in 2002-2003 and 70 samples in 2010 were collected, which sampling points are marked in the Figure 1 with “filled” and “open circles”, respectively. The samples were collected from the different areas: near power plants, highways and residential area. The all samples were collected by “envelope” method from the 0-10 cm upper layer according to the MNS 3298-90 standard [18]. Soil samples were dried at room temperature in air-dry condition and the large inclusions such as manually stones, glass, and plant roots were removed then sieved and grounded on the instrument Fritsch.

2.2 Chemical analysis

The soil samples are decomposed in various acids solution before determination of the pseudo-total concentration of elements by AAS. Concentrated chemically pure acids (HNO_3 and H_2O_2) and deionised water were used for the decomposition of soil samples and for standard solutions; The calibration standard solutions for all elements were prepared by diluting the “Ventron” standard solutions (998-1000 mg/l). The samples treated with a mixture of $\text{HNO}_3 + \text{H}_2\text{O}_2$ acid. The contents of the beaker were heated on a hot plate for 3 hours at a temperature of about 100°C [19-20].

2.3 Determination of the elements concentration by AAS

All measurements were performed on Perkin-ELMER Model 5000 atomic absorption spectrophotometer with flame atomization (FAAS). For atomization and determination of heavy metals were used air-acetylene flame and the standards calibration methods, respectively. The detailed experimental conditions are given in Table 1.

Table1. Experimental parameters used for FAAS measurements of heavy metals

Lamp	HCl system						
Carrier gas	Air						
Flow rate	$40 \text{ dm}^3 \text{ min}^{-1}$						
Fuel gas	Acetylene (H_2C_2)						
Flow rate	$20 \text{ dm}^3 \text{ min}^{-1}$						
Element	Cu	Pb	Zn	Co	Ni	Cr	Mn
Wavelength, [λ / nm]	324.8	217.0	213.9	240.7	232.0	357.9	279.5
Spectral bandwidth, [nm]	0.7	0.7	0.7	0.2	0.2	0.7	0.2
Lamp intensity, [I / mA]	15	15	15	20	20	15	20

2.4 Interpolation method

The accuracy of heavy metal spatial distribution maps is critical for risk control. Contaminants always vary greatly over the land surface, so it is very difficult to

acquire an accurate spatial distribution of heavy metals. The mapping of special distribution requires the spatial interpolation methods. In the present work, the inverse distance weighting was used as interpolation method and the interpolation was acquired by ArcGIS program [21-23]. The inverse distance method based on the premise that the prediction is a linear combination of available data.

$$Z(x) = \frac{\sum_{i=1}^n \frac{1}{d(x,x_i)^p} Z_i}{\sum_{i=1}^n \frac{1}{d(x,x_i)^p}}$$

where $Z(x)$ is the predicted value at an interpolated point, Z_i is value at a known point, n -total number of known points used in interpolation, $d(x,x_i)$ is the distance between point i and predicted point and p is positive real number.

2.5 The pollution index of heavy metals in surface soil

The pollution index (PI) of heavy metals is defined as the ratio of the metal concentration in the urban surface soil and the background concentration of the corresponding metal /ref/:

$$PI = \frac{C_i}{B_i} \quad (1)$$

where, C_i and B_i are the element concentration and natural background value, respectively. We used the World Clark content of microelements [24] as natural background value, since approved standard specification of background soil for Ulaanbaatar region does not yet exist. The pollution index (PI) classified into four categories [25-27] as shown in Table 3.

5 Table2: Classification of the Pollution Index of heavy metals

$PI \leq 1$	low level of pollution
$1 < PI \leq 2$	moderate level of pollution
$2 < PI \leq 5$	high level of pollution
$PI > 5$	extreme high level of pollution

3. RESULTS AND DISCUSSION

3.1 The pollution index

The pollution index calculated by equation (1) for all samples collected in 2003 and 2010 are classified according to the pollution levels given in Table 2. The obtained results (2003) summarized in Table3 show that the heavy metal pollution level in Ulaanbaatar surface soils increase as $Ni < Mn < Co < Cu < Cr < Zn < Pb$. 96.8% and 91 % of samples found to be unpolluted and the only 2.8% and 8.7% are moderately polluted by Ni and Mn, respectively. 50.2% and 37.1% of samples are unpolluted, 45.1% and 42.7% are moderately polluted by Co and Cu. For Cu, the amount of samples are associated to highly and extreme highly pollution level significantly increased to 16.4% and 3.7%, respectively. The most of samples were moderately (47.9%) and highly (43.6%) polluted by Cr, while for Zn and Pb the extreme highly polluted samples are considerably increased to 23.2% and 43.3%, respectively.

The all samples collected in 2010 found to be low level of soil pollution with $Mn < Cr < Ni$ elements. For Co and Cu, 59% and 70.5% of the soil samples found

unpolluted and 41% and 16.4% of the samples are associated to moderate level of pollution, respectively. 9.8% and 11.5% or considerable amount of the samples are highly polluted by Cu and Zn, respectively, while the large amount of the samples (44.5%) and (14.7%) are highly and extreme highly polluted by Pb, respectively.

The pollution level of samples collecten in 2003 and 2010 are compared In the Figure 2. The obtained results show that the overall pollution index of samples collected in 2010 were found to be lower than that in 2003 (specially for Cr), which may be due to fact that relatively low amount of samples being analyzed. However, the trend of the soil pollution levels according to elements was found similar, particularly for Zn and Pb associated to high and extremely high levels.

Table 3: The pollution index calculated by number of samples collected in 2003 and 2010

(n- number of samples being analyzed)

Elements	The amount of sample classified by pollution level %, (2003), n=600				The amount of sample classified by pollution level %, (2010), n=70			
	Low	Moderate	High	Extreme high	Low	Moderate	High	Extreme high
Ni	96.8	2.8	0.2	0.2	100	-	-	-
Mn	91.0	8.7	0.3	-	100	-	-	-
Co	50.2	45.1	4.2	0.5	59.0	41.0	-	-
Cu	37.1	42.7	16.4	3.7	70.5	16.4	9.8	3.3
Cr	4.6	47.9	43.6	3.9	100	-	-	-
Zn	6.6	24.5	45.7	23.2	39.3	42.6	11.5	6.6
Pb	5.5	15.1	36.1	43.3	8.2	32.8	44.3	14.7

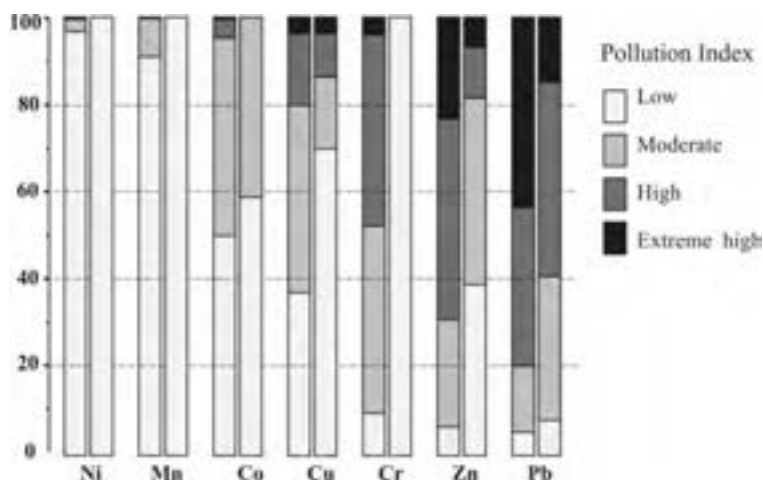


Figure 2: The pollution level of samples collected in 2003 (1-st column) and 2010 (2-nd column)

3.2 Spatial distribution of soil pollution

The contour maps of the spatial distribution of heavy metals pollution of Ulaanbaatar was obtained by interpolation methods (based on inverse distance weighting) using ArcGIS program for above mentioned elements. The distribution of the pollution levels for these heavy metals was classified according to pollution level given in Table 2. The derived results are summarized in the Table 4 and in histogram (Figure 2), while the obtained distribution maps are presented in Figure 3.

Table 4: Pollution level associated with Spatial distribution map

	The surface soil area classified by pollution level %, (2003)			
Pollution level	Low	Moderate	High	Extreme high
Ni	94.5	4.2	0.7	0.6
Co	47.8	49.1	3.1	0.0
Mn	96.2	3.6	0.2	0.0
Cu	29.4	31.6	15.7	3.2
Cr	1.9	52.1	42.0	3.8
Zn	6.0	18.4	60.9	14.7
Pb	3.8	9.1	37.7	49.4

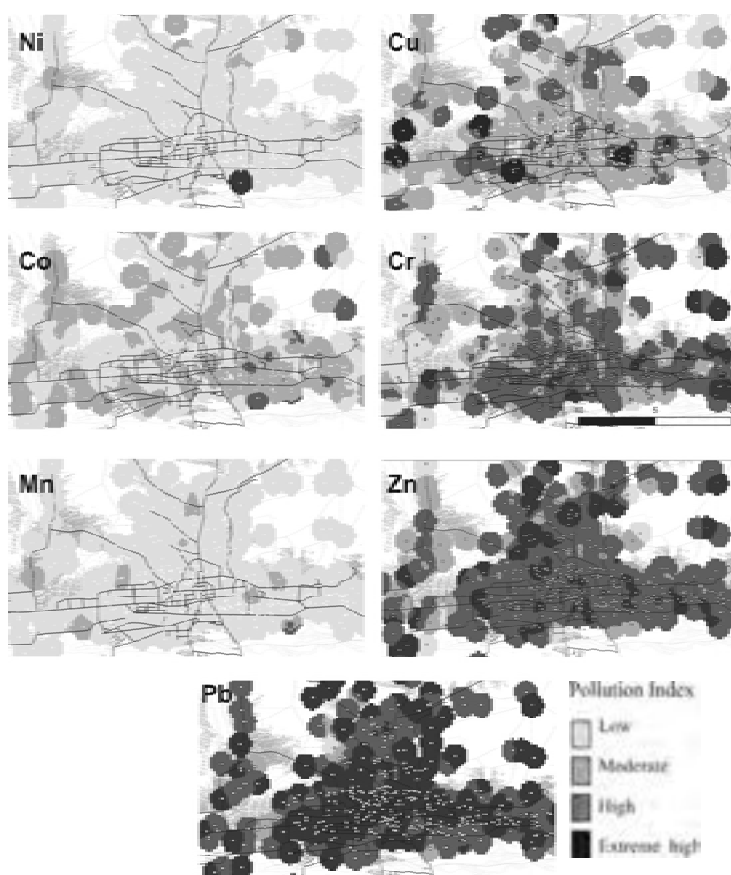


Figure 3. Spatial distribution map for pollution level of heavy metals in Ulaanbaatar soil (2003).

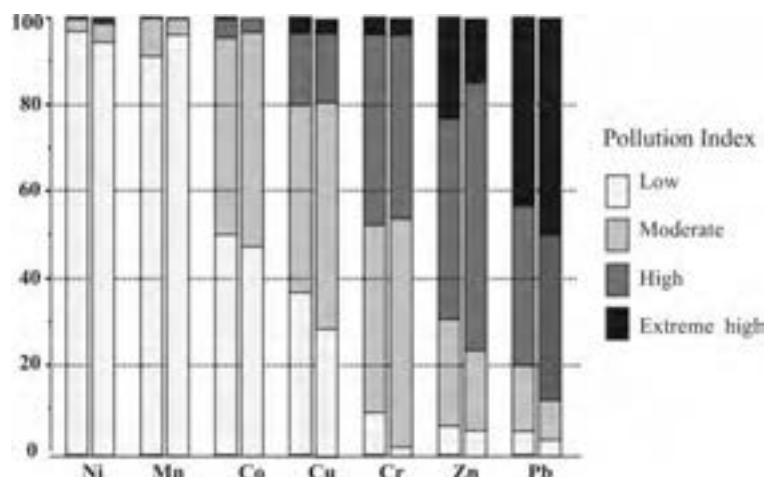


Figure 4: Pollution index associated with Spatial distribution map

From Figure 3 it can be seen that the pollution index of surface soil increases in the following order: Ni <Co <Mn <Cu <Co <Zn <Pb. The according to the present study, the territory of Ulaanbaatar are unpolluted by Ni as the 96.2% of studied area associated to low level of soil pollution. The only certain points in the Ger region are moderately (3.3%), highly (0.4%) and extremely high (0.5%) polluted by Ni. In case of Co, the amount of low and moderate levels found almost the same and equal to about half of studied area and the only small part (3.3%) of area refers to high pollution level. The distribution of the moderate polluted level is found more densely in the central east region of city associated to the Ger region. The pollution distribution of Mn as compared with the Co, the low level decreased to 37.8%, moderate level increased to 58.5% and high level (3.5%) has changed slightly. The moderately polluted area is found more dense in all studied region expect of southern part of the centre of city. The pollution distribution of Cu as compared with the Mn, the highly polluted area increased significantly to 16.6% due to decrease of the low and moderate polluted area to 31.8% and 48.6%, respectively. The most central and central east region of the city is moderately polluted by Cu and the highly and extreme highly polluted area mainly associated to heavy traffic and crossword, industrial and Ger regions. The present study shows that the territory of Ulaanbaatar is heavily polluted by Cr, Zn and particularly by Pb. The almost all studied area to be found moderately, highly and extremely high polluted by these elements. The 53.3% and 43.3% of studied area are associated to the moderate and high pollution levels. The high pollution level is more frequently distributed for the central east and particularly central region.

The distribution of soil pollution level of Zn as compared with the Cr, extremely highly polluted area are increased from 3.6% to 15.7% as moderately polluted area decreased from 53.3% to 20.8%. The central and central east regions are highly polluted, while the central north region is highly and extreme highly polluted by Zn. For capital of Mongolia, Pb should considered as extremely dangerous pollutant, because about 86.4% of the studied area found to be highly and extreme highly polluted by Pb. Furthermore the most part of the central region of the city is extreme highly polluted by Pb.

4 CONCLUSION

The large number of soil samples collected in 2002-2003 and measured under the same experimental conditions was analyzed for the counter mapping to evaluate the statement of pollution risk. The spatial distribution of soil pollution of Ulaanbaatar was evaluated by interpolation method using ArcGIS program for Ni, Co, Mn, Cu, Cr, Zn and Pb elements. The surface soil of Ulaanbaatar is considerable polluted by Co, Cu, Cr and heavily polluted by Zn and Pb. In addition, the obtained results of the present work could be used as fundamental materials to control the pollution risk and remediate the highly contaminated soils.

Acknowledgement

The authors would like to acknowledge the financial support provided by the Department of Environmental Pollution and Trash Management of the Ulaanbaatar service affair for soil sampling and measurements.

References

1. Tokalioglu et al. An Assessment on Metal Sources by Multivariate Analysis and Speciation of Metals in Soil Samples Using the BCR Sequential Extraction Procedure Clean – Soil, Air, Water, 2010, 38 (8), 713– 718
2. Lena Q. Ma, Gade N. Rao, Chemical Fractionation of Cadmium, Copper, Nickel, and Zinc in Contaminated Soils, *Journal of Environmental Quality* Volume 26, no. 1, 1997,
3. Ijeoma L. Princewill-Ogbonna, Princewill C. Ogbonna, Heavy Metal Content in Soil and Medicinal Plants in High Traffic Urban Area Pakistan *Journal of Nutrition* 10 (7): 618-624, 2011
4. Akoto, O., Ephraim, J. H. Darko, G. Heavy Metals Pollution in Surface Soils in the Vicinity of Abundant Railway Servicing Workshop in Kumasi, Ghana, *J. Environ. Res.*, 2(4): 359-364, 2008
5. Moura et al, **Analysis and assessment of heavy metals in urban surface soils of Teresina, Piauí State, Brazil: a study based on multivariate analysis**, *Comunicata Scientiae* 1(2): 120-127 2010
6. Statistical bulletin-2007 //
7. S. Lodoisamba City soil pollution more than air pollution //Newspaper Gerelt tsadig №11(42) 2010-8
8. Tserennaym Batjajgal, Enktur Otgonjajgal, Kitae Baek, Jung-Seok Yang. “Assessment of metals contamination of soils in Ulaanbaatar, Mongolia” *Journal of Hazardous Materials*, 2010. 184 (1-3): p.872
9. Kosheleva.N.E., Kasimov.N.S., Baja.S.N., Gunin.P.D., Golovanov.D.L., Yamnova.I.A., Enkhamgalan.S. Contamination of soil with heavy metals in the industrial centers of Mongolia, // *Vestnik. Moscow Mock. university. Issue. 5. Geography. 2010. № 3. C. 20-27.*
10. Ts.Byambasuren, Z.Tseveen, B.Khuukhenkhoo, Ts.Otgontuul. Heavy metal soil pollution Ulaanbaatar city // *Proceeding of conference on soil and water contamination of Ulaanbaatar, Ulaanbaatar 2010. p 49*
11. Byambasuren Ts., Tsedenbaljir D., Khuukhenkhoo B., Tseveen Z. Application of atomic emission and atomic absorption methods for determination of some heavy metals in soil // *Тез. докл. научного семинара "Современный атомно-эмиссионный анализ и науки о Земле". Иркутск: ИГХ СО РАН, 2009. С. 32-33*
12. Z. Tseveen, Z.Damdinsuren, D. Tsedenbaljir, Ts.Byambasuren Determination of heavy metal in Ulaanbaatar city by AAS method , *proceeding IPT, 1 30. 2003*
13. D.Dorjgotov, O.Batkhisig, The soil condition and pollution study of Chingeltei district of UB, 2003
14. Ts.Otgontuul, Ts.Byambasuren, D.Tsedenbaljir, B.Khuukhenkhoo, “Pollution and Geoaccumulation Index of Heavy Metals in the Soil from Ulaanbaatar for the Different Areas“, *Institute of Physics and Technology 38, MAS, 2011*

15. Ts.Byambasuren, B.Khuukhenkhuu, D.Tsedenbaljir, I.E.Vasileva “Pollution of surface soil from Ulaanbaatar with heavy metal”, III International Scientific Conference on Soil as connecting Part for Natural and Anthropogenic-Transformed Ecosystems Co-functioning, August 2011, 37-40, Irkutsk, Russia
16. O. Battulga, I.Myagmarjav. The soil pollution study of building part in Khanuul district, 2007, UB
17. Mongolia National Census 2010 preliminary results
18. MNS-3298-1991 Soil quality: The general requirement in the selection of soil samples
19. Nomeda Sabiene, Dalia Marija Brazauskiene “Determination of heavy metal mobile forms by different extraction methods” *EKOLOGIJA*. 2004. Nr. 1. p36–41
20. USEPA (United States Environmental Protection Agency) (1996): Method 3050B: Acid digestion of sediments, sludge’s and soils
21. Y.Xie et al. Spatial distribution of soil heavy metal pollution estimated by different interpolation methods: Accuracy and uncertainty, *Chemosphere* 82(2011), 468-476
22. M. Imperato et al. Spatial distribution of heavy metals in urban soils of Naples city (Italy) *Environmental Pollution* 124(2003) 247–256
23. Kholoud Mashal, Mohammed Al-Qinna, Yahya Ali Spatial Distribution and Environmental Implications of Lead and Zinc in Urban Soils and Street Dusts Samples in Al-Hashimeyeh Municipality, *Jordan Journal of Mechanical and Industrial Engineering Volume 3, Number 2, June. 2009*
24. Vinogradov.A.P. Clark content of chemical elements in Earth crust // *Geochemistry*, № 7.p 555 – 571
25. W. Grzebisz¹, L. Cieśła², J. Komisarek³, J. Potarzycki¹ Geochemical Assessment of Heavy Metals Pollution of Urban Soils, *Polish Journal of Environmental Studies Vol. 11, No. 5 (2002), 493-499*
26. t. B. Chen, J. W. C. Wong, H. Y. Zhou, M. H. Wong , Assessment of trace metal distribution and contamination in surface soils of hong kong, *Environmental Pollution*, Vol. 96, No. 1, pp. 61- 68, 1997
27. Wei, B. and L. Yang, A review of heavy metal contaminations in urban soils, urban road dusts and agricultural soils from China. *Microchemical journal.*, 2010. 48(2): p. 99

Estimation of global anthropogenic PM_{2.5} by integrating remote sensing and modeling

Hirotoishi Kishi¹, Wataru Takeuchi² and Haruo Sawada³

¹Graduate student, Department of Civil Engineering,
The University of Tokyo, Japan
kisshi@iis.u-tokyo.ac.jp

²Associate professor, Institute of Industrial Science,
The University of Tokyo, Japan

³Professor, ICUS, Institute of Industrial Science,
The University of Tokyo, Japan

ABSTRACT

This study is estimating global atmospheric conditions focusing on PM_{2.5} by integrating remote sensing measurement and model estimation with bottom-up approach. Firstly, emitted PM_{2.5} inventory is estimated according to emissions sources such as exhaust gas and biomass burning. They are estimated by developed model with paper review and land cover properties obtained by satellite measurements. Exhaust emissions is estimated by total numbers of diesel vehicles in use, population and emission standards regulated by governmental law. Biomass burning emissions is estimated by active fire events observed from Moderate resolution imaging spectroradiometer (MODIS), fuel loading equivalent to the amount of field biomass, combustion factors estimated by vegetation moisture conditions and PM_{2.5} emission factors. Secondly, integrated exhaust and biomass burning PM_{2.5} is compared with Aerosol Optical Depth (AOD) measurement which is equivalent to total column amount of PM_{2.5} to analyze spatio-temporal patterns. It is shown that estimated PM_{2.5} is quite different in each global countries and spatio-temporal changes are tolerable comparing to MODIS AOD.

Keywords : Emission inventory, exhaust emissions, biomass burning and MODIS AOD.

1 INTRODUCTION

1.1 Backgrounds and objective

Air pollution is a serious problem over urban and even rural areas of the world because of emissions from vehicles, factories, dusts, forest fires and poor legal regulations which are not prepared precisely or poor force (JICA, 2005). Particulate matter (PM) is a complex mixture of solid and liquid particles which remain suspended in the air. It is one of the major pollutants that affects air quality in urban and even rural areas of the world (Gupta, *et al.*, 2006). PM whose aerodynamic diameters is less than $2.5\mu\text{m}$ (PM_{2.5}) remains in the inner part of lung and results in asthma, bronchitis and even cancer. Exposure experiments concluded that long term exposure to combustion related fine particulate air pollution is an important environmental risk factor for cardiopulmonary and lung cancer mortality (Pope *et al.*, 2002). It is reported that PM_{2.5} mainly produced by exhaust emissions are estimated about 40% of all PM_{2.5} emissions in Tokyoⁱ, and forest fire events

ⁱMinistry of the environment (<http://www.env.go.jp/>)

about 30% in USAⁱⁱ, about 20 % in Canadaⁱⁱⁱ. However, they were estimated and measured by different methodologies and assumptions. Our previous studies are reporting spatio-temporal patterns of exhaust emissions and biomass burning PM_{2.5} by integrating bottom-up approach model development and satellite remote sensing over asian mega cities (Kishi *et al.*, 2011). However, The investigation in global scale especially for in developing countries is not enough.

Based on these backgrounds, the objective of this study is to estimate global anthropogenic PM_{2.5} emissions and evaluate spatio-temporal patterns compared with observed MODIS AOD.

2 METHODOLOGY

2.1 Framework and data used in this study

Figure 1 shows a framework of estimation of global anthropogenic PM_{2.5} by integrating remote sensing and modeling. Firstly, exhaust emissions and biomass burning PM_{2.5} are estimated by developing bottom-up approach model with literature survey, statistical datasets and land cover properties observed from satellite. Secondly, integrated exhaust gas and biomass burning emissions are compared with MODIS AOD measurement which is equivalent to ambient PM_{2.5} conditions to analyze spatio-temporal patterns.

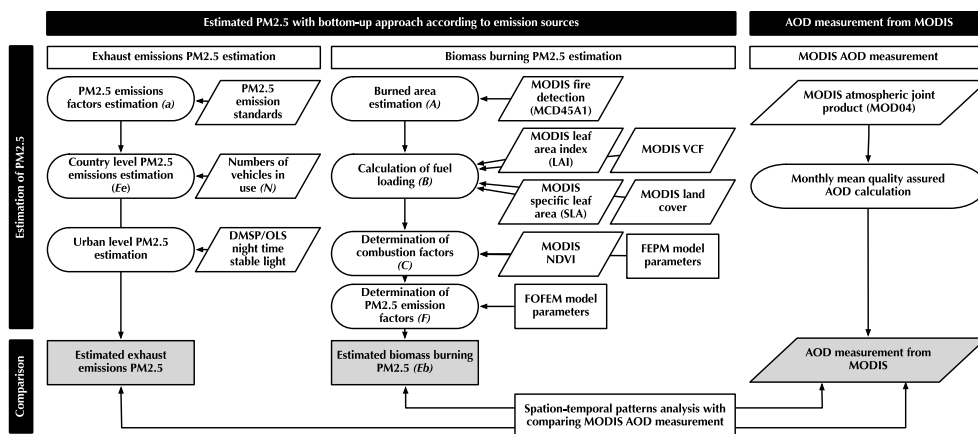


Figure 1 : Flowchart of estimating global anthropogenic PM_{2.5} by integrating remote sensing and modeling.

2.2 Estimation of exhaust emissions PM_{2.5} with bottom-up approach

Firstly, Total exhaust emissions PM_{2.5} in 2007 are estimated by equation 1 (Kishi *et al.*, 2011);

$$E_e = \sum_{i=p,c} N_{ijk} a_{ijk} b_{ijk} \quad s.t. \quad b^* = 1 \quad (1)$$

where E_e is estimated total amount of exhaust emissions PM_{2.5} in each country (denoted as j) and year (k). i stands for car types including passenger car (p), commercial car (c). N is the number of vehicles in use^{iv}. a is the emission factor which represents an exhaust

ⁱⁱU.S. Environmental Protection Agency (<http://www.epa.gov/>)

ⁱⁱⁱEnvironment Canada (<http://www.ec.gc.ca/>)

^{iv}Japan Automobile Manufacturers Association. World motor vehicle statistics 2008.

regulation by law^v ^{vi}. b is defined as the ratio of diesel vehicles to that of gasoline. It is supposed that all vehicles are diesel one in this study because not all data is available among global countries.

PM_{2.5} emission factors are defined by government restrictions in each country. European emission standards, EURO 1 to 4^{vii} are widely employed as national emission standards in many countries. Countries those who have no emission standards are regarded as EURO 0 and it is estimated by exponential approximation (Kishi *et al.*, 2011).

Secondly, DMSP/OSL night time stable light data is employed as a indicator of spatial exhaust emissions PM_{2.5} distribution. Estimated country by country PM_{2.5} is distributed according to OLS data because it can be performed as population and energy related greenhouse gas emissions (Elvidge, *et al.*, 1997).

2.3 Estimation of biomass burning PM_{2.5} with bottom-up approach

Total biomass burning PM_{2.5} emissions in 2007 are estimated by equation 2. Proposed approach for monitoring of biomass burning particulate emissions across contiguous United States (Zhang *et al.*, 2008) is applied to global countries with MODIS remote sensing data by following formula (Kishi *et al.*, 2011);

$$E_b = \sum_{k=1} \sum_{l=1} \sum_{j=1} \sum_{i=1} A_{ijk} B_{ijl} C_{ijkl} F_{ijkl} \quad (2)$$

where E_b is the biomass burning PM_{2.5} emission in a certain time period and location (Mg), A is burned area (km^2), B is the amount of fuel mass available for combustion (Mg/km^2), C is the combustion factor (%), F is the emission factor for PM_{2.5} (kg/Mg), k is the time period, l is the fuel type. i and j define the detected fire location in column and row. They are determined with literature survey and MODIS land cover products shown by Table 1.

Table 1 : Satellite data used for estimating biomass burning PM_{2.5} emissions

Corrected satellite data with MODIS	Temporal and spatial resolution	Year	Data source
Hotspot data	Monthly and 500m	2007	Boston university
Land cover type	Static and 1km	2007	Boston university
Leaf area index	Monthly and 1km	2007	Boston university
Specific leaf area	Static and 60km	2002	University of Tokyo
Vegetation continuous field	Static and 1km	2001	Global land cover facility
NDVI	8days and 2 km	2007	Lille University

2.4 Measurement of quality assured aerosol optical depth with MODIS

Terra/MODIS 10km resolution daily Level-2 atmospheric product (MOD04 L2) is employed to measure AOD at 0.55 μm over land and ocean according to quality assurance confidence flag (QAC). QAC flag value ranges are from 3 to 0, where 3 means good quality and 0 means bad quality (Levy *et al.*, 2009). Quality assured AOD means QAC flag

^vMarklines.com (<http://www.marklines.com/ja/regulation/environment/>)

^{vi}Asian Development Bank.

Country/City Synthesis Reports on Urban Air Quality Management in Asia.

^{vii}European Union: Air pollution

(http://europa.eu/legislation_summaries/environment/air_pollution/)

is 3 over land and 1, 2, 3 over ocean. It is reported that AOD measured by MODIS at $0.55\mu\text{m}$ corresponds to $\text{PM}_{2.5}$ density (Gupta, *et al.*, 2006). Extremely high ($\tau_{0.55} > 3$) and low ($\tau_{0.55} < 0$) measured AOD is excluded to estimate monthly mean AOD and standard deviation per day. AOD measurement accuracy is $\Delta t = \pm 0.03 \pm 0.05\tau$ over ocean and $\Delta t = \pm 0.05 \pm 0.15\tau$ over land (Levy *et al.*, 2009).

3 RESULTS AND DISCUSSIONS

3.1 Spatio-temporal patterns of global anthropogenic $\text{PM}_{2.5}$

Figure 3 and Figure 2 show spatio-temporal patterns of estimated global exhaust and biomass burning $\text{PM}_{2.5}$ in 2007. Maps show spatial distributions of exhaust, biomass burning and integrated $\text{PM}_{2.5}$. A line graph shows country by country integrated $\text{PM}_{2.5}$: Australia, Brazil, China, France, India, Japan, Mexico, Mongolia, South Africa, Taiwan, Thailand and United States.

- Figure 2 shows monthly temporal patterns of integrated exhaust and biomass burning $\text{PM}_{2.5}$ in 2007. Large seasonal changes are found in Brazil, Mexico, Mongolia and Thailand because of fire events. On the other hand, $\text{PM}_{2.5}$ emissions are relatively stable in France, India, Japan, South Africa and Taiwan. Exhaust emissions is dominant emission source in these countries.
- Exhaust emissions $\text{PM}_{2.5}$ is spatially distributed in urban and populated areas including East USA, Japan, Korea, East China and Europe shown by figure 3 (a). These areas are economically developed and motorized. Large exhaust emissions is also estimated in Middle and South America including Mexico, Colombia and Chili, South East Asia including SriLanka, Middle East including Iran and Saudi Arabia, Turkey, and North Africa including Egypt and Tunisia. These areas are not so highly motorized but emissions regulations are not well prepared.
- Large amount of biomass burning $\text{PM}_{2.5}$ is estimated around Amazon, South East Asia including Laos, Thailand and Myanmar, North Australia and Sahel and forest regions in Africa shown by figure 3 (b). Large number of fire events are detected from satellite in these tropical areas. On the other hand, cool-temperate areas such as South Siberia also have much fire events. Peatland fire can be considered because there are many fire events in summer season.
- According to spatial patterns of global integrated $\text{PM}_{2.5}$ emissions shown by figure 3 and temporal ones shown by figure 2, anthropogenic emissions is spatially and temporally distributed all over the world. On the other hand, main emissions areas are highly developed urban areas and forest area mainly in Amazon and Africa.

3.2 Comparison of MODIS AOD and anthropogenic $\text{PM}_{2.5}$

Figure 4 shows country level analysis by comparing observed MODIS AOD and estimated anthropogenic $\text{PM}_{2.5}$ in Japan, India, South Africa and Brazil. In the scatter plots, X-axis shows observed MODIS AOD and Y-axis shows estimated $\text{PM}_{2.5}$ with logarithmic plots.

- In Tokyo, a spatial distribution pattern of estimated $\text{PM}_{2.5}$ is similar to observed MODIS AOD. The scatter plot shows not bad correlation. However, estimated $\text{PM}_{2.5}$ may be saturating comparing to MODIS AOD. There are few count of fire events so that exhaust gas is main emission source of $\text{PM}_{2.5}$.

- In India, a spatial pattern is not similar between observed AOD and estimated $PM_{2.5}$. Its correlation shows negative. Large AOD is observed in large $PM_{2.5}$ estimated area around Deccan plane. On the other hand, large AOD is observed but small $PM_{2.5}$ is estimated around Hindustan plane. There may be atmospheric convection and suspending around Hindustan plane because there lies Himalaya mountains in the northern part of the plane.
- In South Africa, large AOD and $PM_{2.5}$ are found in northern part especially around Pretoria and Johannesburg city. On the other hand, large amount of emissions is estimated but small AOD is observed in Southern part of the country. Overestimation of biomass burning may be considered because this southern part of South Africa is mountain and forest area.
- In Brazil, large amount of $PM_{2.5}$ is estimated around Campos in Brazil plane because of many fire events are detected from satellite. However, MODIS measures high AOD around Mato Grosso, West side of the plane. Atmospheric convection event may be considered because the elevation around west side is lower than east side.

3.3 Discussions and future works

Compared with exhaust emissions, biomass burning has much larger impact for global $PM_{2.5}$ emissions. However, both exhaust and biomass burning emissions estimation model should be refined more. Exhaust emissions model is so simple that it may need much work to represent real atmospheric conditions, for example, the ratio of diesel car vehicles, government force of emissions regulation and vehicle congestion. Our previous research shows comparing total amount of exhaust emissions $PM_{2.5}$ is overestimation in some countries but too small in the others countries (Kishi *et al.*, 2011). In case of biomass burning model, estimation accuracies of fuel loading and burned area should be evaluated properly because these results are not compared with ground measurements or reported inventories. In addition to model refinement, employing atmospheric convection model is required to consider actual atmospheric conditions. Meteorological and topographical features may have large impact to consider the correlations between estimated $PM_{2.5}$ and observed MODIS AOD. AOD measures total column of pollutants that means actual ambient conditions, on the other hand, estimated $PM_{2.5}$ in this research means emissions inventory dataset.

4 SUMMARY

This study estimated global anthropogenic $PM_{2.5}$ by integrating remote sensing and modeling. Spatio-temporal patterns of anthropogenic $PM_{2.5}$ is revealed in global scale. On the other hand, refinements of estimation model and considering atmospheric convection model is required for the future works.

References

Elvidge, C. D., Baugh, K. E., Hobson, V. R., Kihn, E. A., Kroehl, H. W., Davis, E. R. and Cocero, D. Satellite inventory of human settlements using nocturnal radiation emissions: a contribution for the global toolchest, *Journal of Global Change Biology.*, Vol.3, Issue5, pages 387-395. 1997.

Gupta, P., Christopher, S. A., Wang, J., Gehrig, R., Leed, Yc. and Kumare, N. Satellite Remote Sensing of Particulate Matter and Air Quality Assessment over Global Cities, *Atmospheric. Environment.*, 40, 5880-5892. 2006.

Japan International Cooperation Agency. An effective approach for development agenda -Air pollution-. 2005.

Kishi, H., Takeuchi, W. and Sawada, H. Evaluation of model estimated anthropogenic PM_{2.5} emissions over Asia. *Proceeding of 32nd Asian conference on remote sensing.* CD-ROM. 2011.

Pope, C. A. III, Burnett, R. T., Thun, M. J., Calle, E. E., Krewski, D., Ito, K., Thurston, G.D., Lung cancer, cardiopulmonary mortality, and long-term exposure to fine particulate air pollution. *The Journal of the American Medical Association.* 287(9), 1132-1141. 2002.

Robert C. Levy, Lorraine A. Remer, Didier Tanre , S. Mattoo, Yoram J. Kaufman. 2009. Algorithm for remote sensing of tropospheric aerosol over dark targets from MODIS: Collection 005 and 05: Revision 2; Feb 2009 Product ID: MOD04/MYD04.

Zhang, X., Kondragunta, S., Schmidt, C., Kogan F. Near real time monitoring of biomass burning particulate emissions (PM_{2.5}) across contiguous United States using multiple satellite instruments, *Atmos. Environ.*, 42, 6959-6972. 2008.

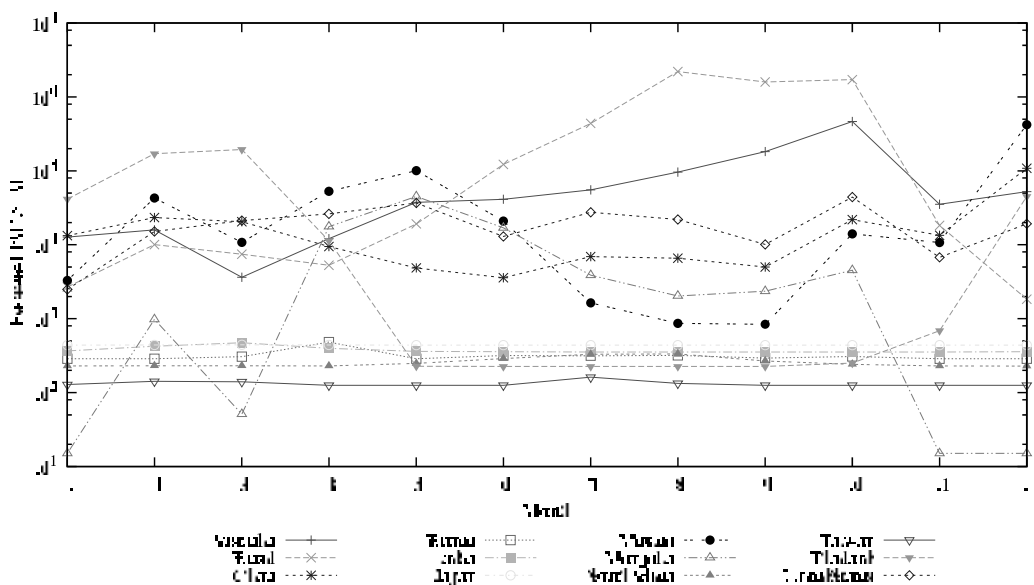
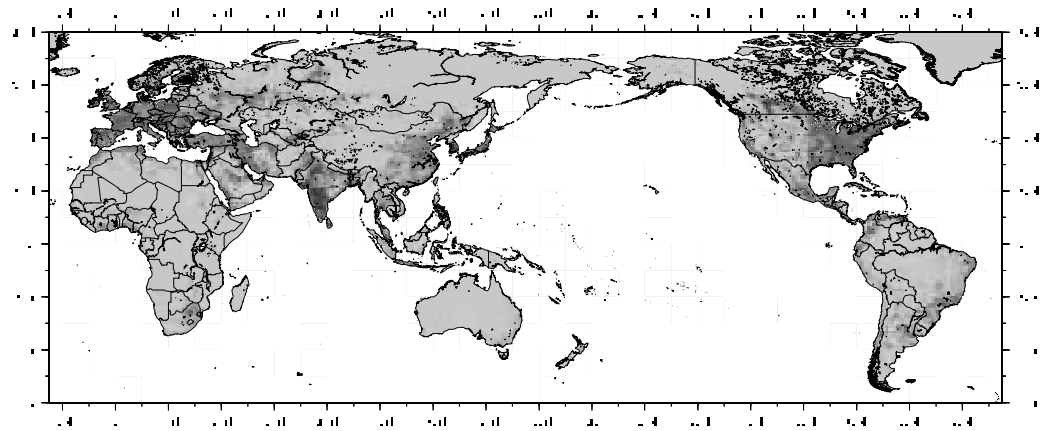
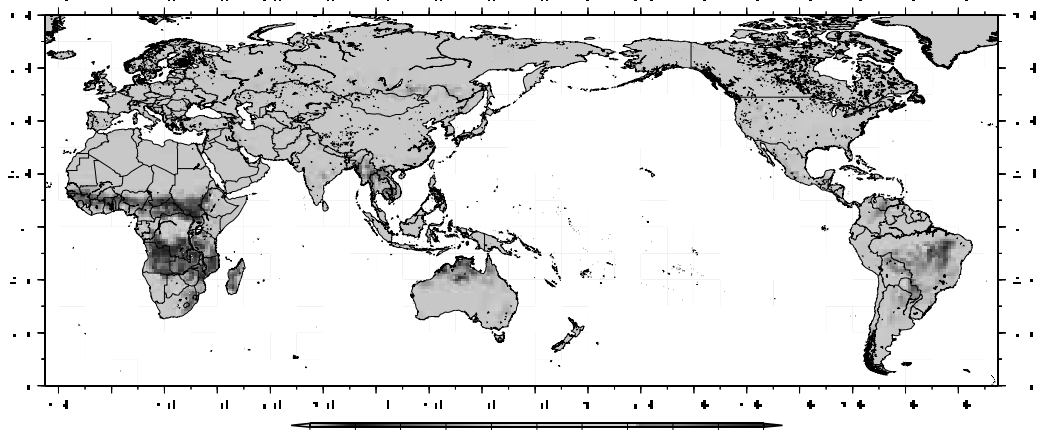


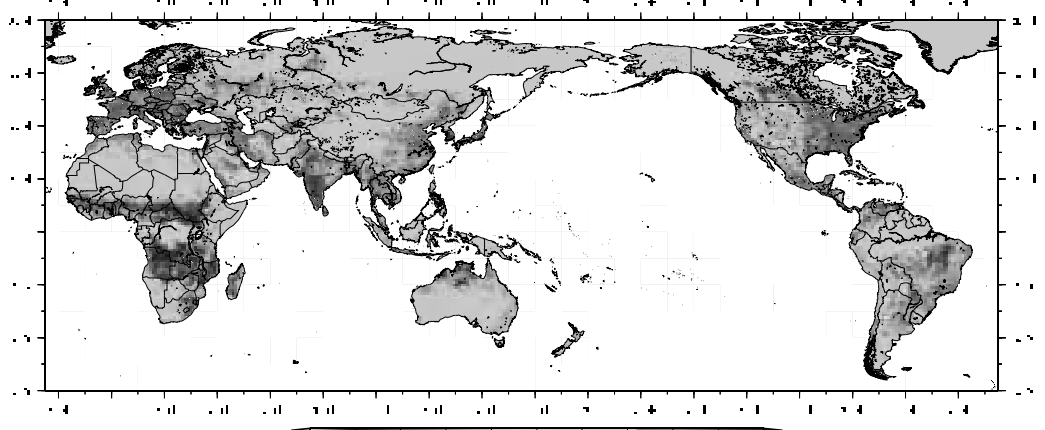
Figure 2 : Estimated integrated PM_{2.5} emissions in 2007.



(a) Estimated exhaust emissions PM_{2.5} in 2007 (kg/yr)



(b) Estimated biomass burning PM_{2.5} in 2007 (kg/yr)



(c) Estimated exhaust and biomass burning PM_{2.5} in 2007 (kg/yr)

Figure 3 : Estimated global exhaust and biomass burning PM_{2.5} emissions map.

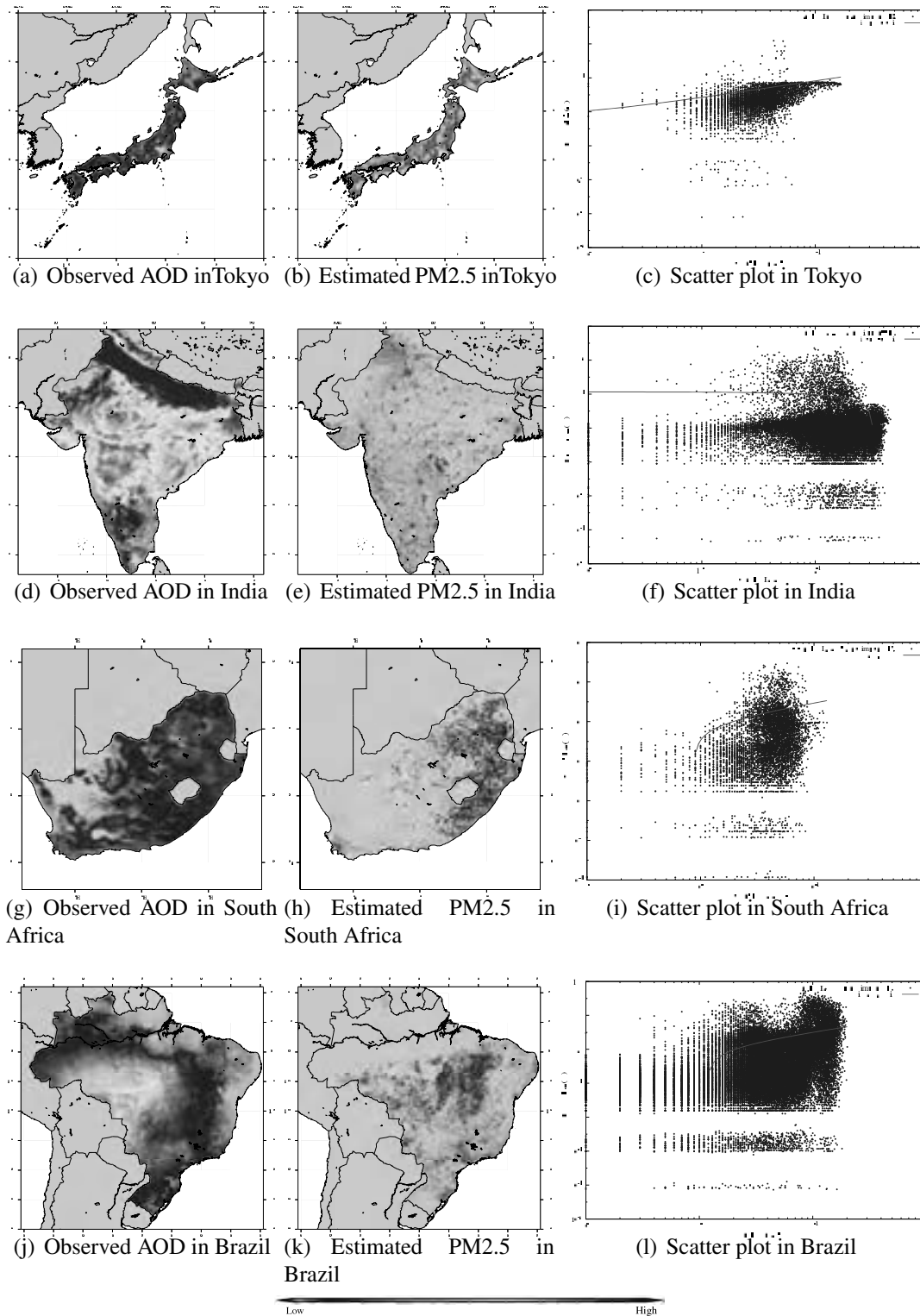


Figure 4 : Observed MODIS AOD (QAC=3), estimated anthropogenic PM2.5 and scatter plot in Japan, India, South Africa and Brazil in 2007.

Reinforced soil walls damaged by tsunami impact in the 2011 Tohoku Earthquake

Jiro KUWANO¹ and Junichi KOSEKI²

¹ Professor, Geosphere Research Institute, Saitama University, Japan
jkuwano@mail.saitama-u.ac.jp

² Professor, IIS, The University of Tokyo, Japan

ABSTRACT

The 2011 off the Pacific coast of Tohoku Earthquake of $M_w=9.0$ with a huge source region of about 450km by 200km caused extensive damage of various structures. Damage caused by tsunami was tremendous and a lot of lives were lost. Besides the damage of concrete structures, seawalls were seriously damaged probably due to scouring. On the other hand some reinforced soil walls were found to be damaged little, though they were inundated with tsunami. Such reinforced soil walls are introduced in this paper together with the reinforced soil which was seriously damaged by the tsunami. Some reinforced soil walls have concrete facing panels, but some have metal mesh facing panels. The walls with the mesh facing were not seriously damaged with limited sucking out of backfill owing to vegetation and protection sheet. However, some damage was found at the backfill and facing panels where the soil was not properly covered and protected against erosion.

Keywords: reinforced soil wall, tsunami, erosion, backfill, facing

1. INTRODUCTION

The 2011 off the Pacific coast of Tohoku Earthquake (The 2011 Tohoku Earthquake) of $M_w=9.0$ with a huge source region of about 450 km by 200 km occurred on March 11, 2011 as shown in Figure 1 (USGS, 2012a). It is the largest earthquake ever recorded in Japan and the fourth largest in the world after 1900 (USGS, 2012b). Almost 20,000 people are dead or missing by this earthquake. Tsunami was the most serious impact of the earthquake. Figure 2 is a tsunami height survey result map (Tsunami Joint Survey Group, 2012) showing that inundation

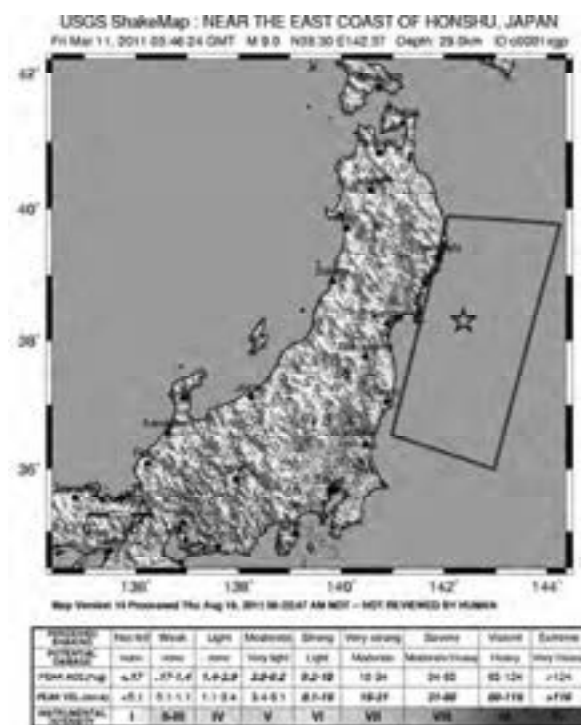


Figure 1: Source region and seismic intensity

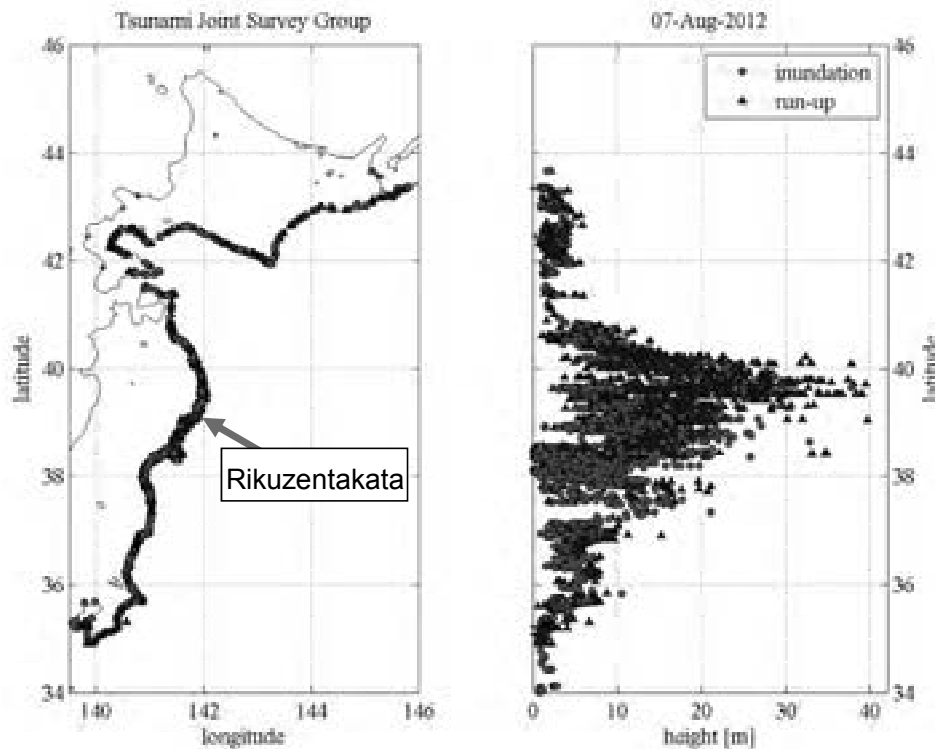


Figure 2: Modified map of tsunami height survey results

height and run-up height were as high as about 40 m. It killed thousands of lives and caused extensive damage of various structures such as seawalls and bridges. Many seawalls and river dikes were washed out by the tsunami. However, many reinforced soil walls survived the tsunami impact, though they were partly or fully submerged.

Reinforced soil walls are usually constructed with soils of high permeability and sufficient drainage. Therefore, effects of ground water are not taken into account in most of the reinforced soil wall design. However, a few trials were made to apply reinforced soil walls to the structures in water environment, such as a river dike (Moriguchi et al., 2002), a seawall (Recio-Minila et al., 2001; Yasuhara et al., 2002) and a temporary structure at a reservoir (Ito and Saito, 2004) and they showed high resistance to water. For example, Moriguchi et al. (2002) reported that the river dike remained stable as a structure after the flood of the 2000 Tokai heavy rain, though a part of the dike was slightly damaged by scouring and outflow of soil at the facing.

There are numbers of reinforced soil walls in Tohoku region. Miyata (2012) reported the damage of the walls by the direct impact of the earthquake (shaking) and summarized that just less than 1% of the walls were seriously damaged but more than 90% of the walls did not show any damage. As mentioned before, most of the reinforced walls were constructed without considering effects of water. However, some of them were exposed to the direct impact of tsunami, as the height of the tsunami by the 2011 Tohoku Earthquake was extraordinarily high.

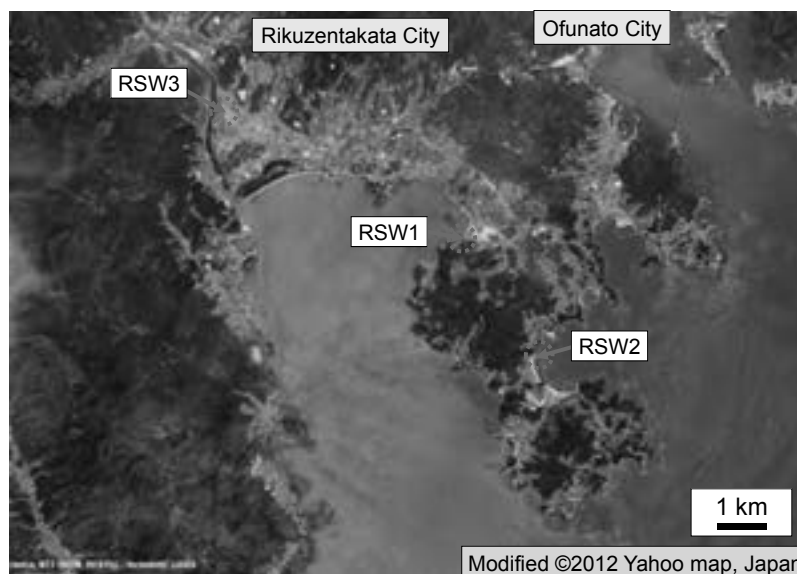


Figure 3: Reinforced soil walls in Rikuzentakata City

Although some of them were seriously damaged by the tsunami, many of them survived with a little damage.

Rikuzentakata City is located at the south end of Iwate Prefecture as shown in Figure 2. The main part of the city was washed out by the tsunami with the inundation height of about 15 m, which is almost the height of four to five stories building. About 2,000 people are dead or missing in the city. Damage of three reinforced soil walls, RSW1~3, in Rikuzentakata City indicated in Figure 3 is reported in this paper.

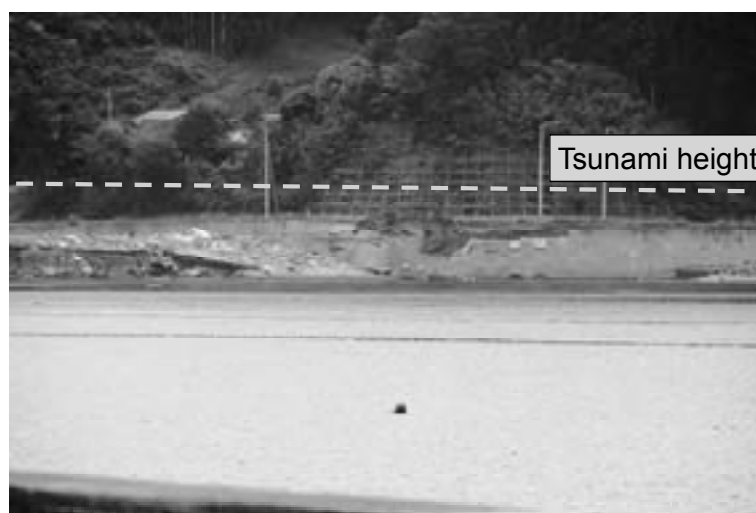


Figure 4: Front view of damaged RSW1

2. REINFORCED SOIL WALL, RSW1, AT HIROTA RECLAMATION DIKE

Terre Armee wall, indicated as RSW1 in Figure 3, with the maximum wall height of 6 m was constructed at the junction of Hirota reclamation dike and the road



Figure 5: Close-up view of damaged RSW1

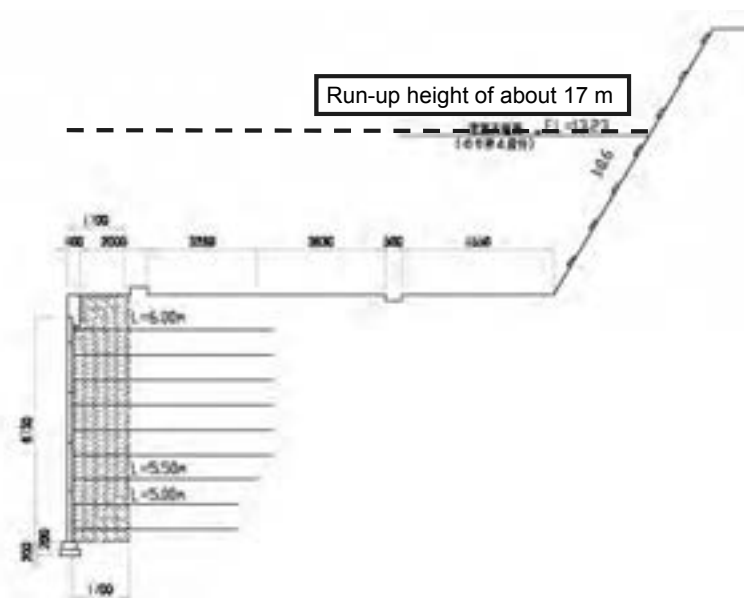


Figure 6: Cross section of RSW1 (by courtesy of Dr. Otani, Hirose Corp.)

embankment on the slope. The area was hit and fully submerged by the tsunami with the estimated run-up height of 17 m. Most of the about 500 m long reclamation dike was washed out by the tsunami except the small part which is near the RSW1 side end where the floodgate was located. Figure 4 is the front view of the damaged RSW1. It is seen that the only a part of the wall near the dike is seriously damaged. Figure 5 is a close-up view of the wall. The upper part of the wall collapsed. Many facing panels fell down and the backfill of the wall was lost. Though not clearly seen in this figure, the lower part of wall was also damaged due to the scouring at the footing. Some of the footing members were brought out and part of soil was lost. Figure 6 is a typical cross section of the wall. Although the cross section is ordinary, the depth of embedment was probably about 40 to 50 cm and a bit too small as a coastal structure. It resulted in the damage of the lower part of the wall as mentioned above. However, it is to be pointed out that the most of the damaged part of the RSW1 was covered with the



Figure 7: Erosion of the backfill of damaged RSW1
(by courtesy of Dr. Otani, Hirose Corp.)

soil of reclamation dike before the earthquake, and probably therefore the footing depth was thought to be enough when designed. Another and more serious problem with the RSW1 was that the wall was not constructed continuously from the sea side to the land side. It was interrupted at the junction of the wall and the dike. The soil of the dike was probably washed out by the tsunami first. Then the backfill of the wall was eroded from the interruption of the wall toward the back of facing panels of the reinforced soil wall as seen in Figure 7. Once the backfill was lost, the facing panels and reinforcing members, which used to support the backfill, were not supported by the backfill and the panels fell down. If the wall was constructed continuously without any interruption, damage of the wall is thought to have been much less.



Figure 8: Location of RSW2 (by courtesy of Dr. Otani, Hirose Corp.)



Figure 9: Close-up view of RSW2 (by courtesy of Dr. Otani, Hirose Corp.)

3. REINFORCED SOIL WALL, RSW2, ON THE EAST SIDE OF THE PENINSULA OPPOSITE TO RSW1

Although the Terre Armee wall, RSW1, was seriously damaged by the tsunami as mentioned above, it is probably not fair to conclude that Terre Armee does not resist tsunami impact. Another Terre Armee wall, RSW2, was located on the east side of the peninsula opposite to RSW1 as shown in Figure 3. The tsunami hit the peninsula from both east and west sides. The RSW2 was constructed on the beach to support the road as shown in Figure 8. The maximum wall height of RSW2 is 10.5 m. The wall was submerged in the tsunami with the estimated run-up height of 14.9 m. However, in contrast to the RSW1, the damage of the RSW2 was negligibly small as seen in Figure 9. There could be two possible primary factors of the small damage. The first one is that the depth of embedment is more than 1.5 m, much bigger than that of the RSW1. Therefore, the backfill of the RSW2 was not lost from the bottom of the wall. The second factor is that the backfill of the reinforced soil wall was fully covered with rigid concrete panels without interruption seen in the RSW1 which was seriously damaged by the tsunami.

4. REINFORCED SOIL WALL, RSW3, AT THE ABUTMENT OF NANAKIRI OVERPASS OF ROUTE 340 ACROSS THE OFUNATO LINE

The downtown of Rikuzentakata City spread over the lowland around the mouth of the Kesen River at the innermost portion of the Hirota Bay. The main part of the city was washed out by the tsunami with the inundation height of about 15 m, which is almost the height of four to five stories building as mentioned before. Takata-matsubara, the famous beautiful forest of 70,000 pines along the beach was completely washed out by the tsunami as shown in Figure 10 and the seawalls were seriously damaged as seen in Figure 11. According to the aerial video taken by Iwate Prefectural Police, the tsunami went upstream along the Kesen River besides the invasion from the coastline. Nanakura overpass of Route 340 across

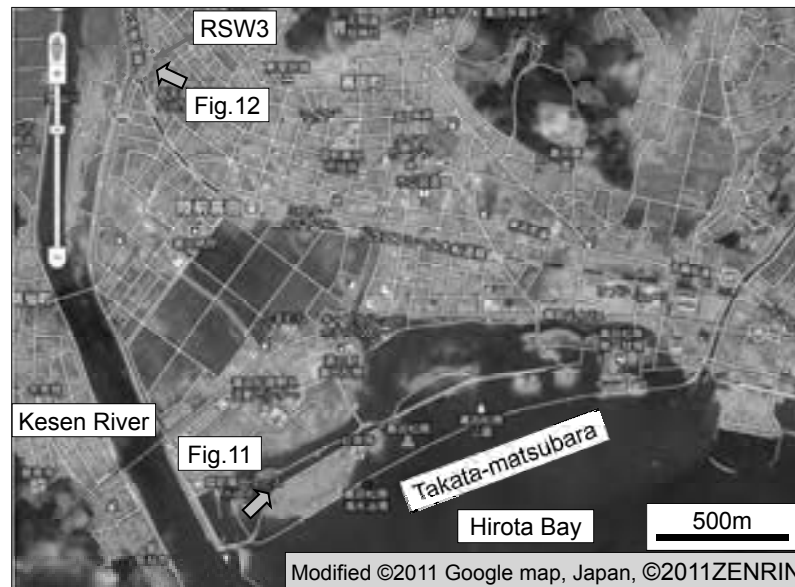


Figure 10: Main part of Rikuzentakata City after the earthquake



Figure 11: Destroyed seawall at Takata-matsubara

the Ofunato Railway Line. The overpass was located near the Kesen River as shown in Figure 10. As the handrails of the bridge were bent down toward the river, the overpass was fully submerged and the power of tsunami was more from the sea side than the river side. Four reinforced soil walls were constructed at the abutments of the bridge as seen in Figure 12. Figure 13 is a cross section of the wall at the maximum height of 7.7 m. It has wire mesh facing units with layers of geogrids for reinforcement and geotextiles for horizontal drain. Scouring was found at the foundation of the abutment as shown in Figure 14. This scouring and the damage of handrails indicate huge impact of the tsunami on the bridge. However damage of the walls was very limited, e.g. a small scoop of backfill as seen in Figure 15. Thin vegetation sheets behind the wire mesh facing panels probably protected backfill from erosion by the tsunami.

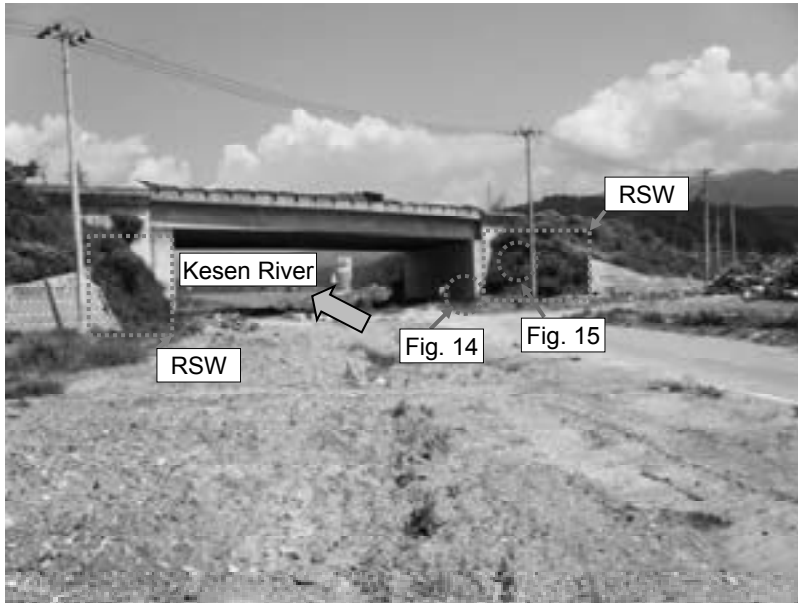


Figure 12: RSW3 at the abutments of the Nanakura overpass

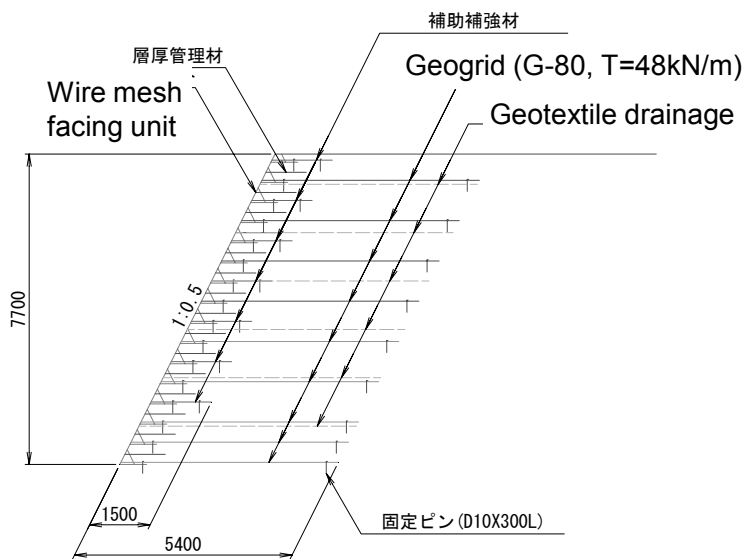


Figure 13: Cross section of RSW3 at the maximum height

5. SUMMARY

The 2011 off the Pacific coast of Tohoku Earthquake caused extensive damage of various structures. Damage caused by tsunami was tremendous and a lot of lives were lost. Besides the damage of concrete structures, seawalls were seriously damaged probably due to scouring. On the other hand some reinforced soil walls were found to be damaged little, though they were inundated with tsunami. Such reinforced soil walls are reported in this paper together with the reinforced soil which was seriously damaged by the tsunami.



Figure 14: Scouring at the abutment of the Nanakiri overpass



Figure 15: Slight damage at the wire mesh facing of RSW3

The facing panels, though concrete, of the seriously damaged soil wall, RSW1, were interrupted and the backfill of the wall was eroded from the interruption. Once the backfill was lost, the facing panels and reinforcing members, which used to support the backfill, were not supported by the backfill and the panels fell down. On the other hand, the reinforced soil wall with simple wire mesh facing units, RSW3, showed little damage. Although the wire mesh has a lot of openings, thin vegetation sheets protected backfill from erosion by the tsunami.

Stability of a structure is usually estimated by mechanics such as equilibrium of force, FEM, etc. However, the damage of reinforced soil walls reported in this paper indicates the details of structure sometimes govern its overall stability.

REFERENCES

- Ito, H. and Saito, T., 2004. In situ construction and measurements of new type of geogrid-reinforced retaining wall combined with soil cement and fiber, *Geosynthetics Engineering Journal, JC-IGS*, 19, 161-166 (in Japanese).
- Miyata, Y., 2012. Reinforced soil walls during recent earthquakes in Japan and geo-risk-based design. Keynote Lecture, *Second International Conference on Performance-Based Design in Earthquake Geotechnical Engineering*, May 28-30, 2012, Taormina, Italy, draft.
- Moriguchi, S., Yashima, A., Sawada, K., Yumira, T., Maeda, H., Matsumoto, N. and Hazama, A., 2002. Full-scale destruction experiments and reconstruction of reinforced river dike, *Geosynthetics Engineering Journal, JC-IGS*, 17, 195-200 (in Japanese).
- Recio-Molina, J.A., Yasuhara, K. and Murakami, S., 2001. Model tests on a geosynthetic reinforced sand revetment subjected to assailing waves, *Geosynthetics Engineering Journal, JC-IGS*, 16, 239-246.
- Tsunami Joint Survey Group, 2012. Tohoku Earthquake Tsunami Information, <http://www.coastal.jp/ttjt/>, viewed on September 11, 2012.
- US Geological Survey, 2012a. Magnitude 9.0 - Near the east coast of Honshu, Japan, <http://earthquake.usgs.gov/earthquakes/eqinthenews/2011/usc0001xgp/>, viewed on September 11, 2012.
- US Geological Survey, 2012b. Magnitude 8 and Greater Earthquakes Since 1900, http://earthquake.usgs.gov/earthquakes/eqarchives/year/mag8/magnitude8_1900_mag.php, viewed on September 11, 2012.
- Yasuhara, K., Recio-Molina, J.A., Murakami, S. and Komine, H., 2002. A design procedure for geosynthetic-reinforced soil walls as revetments protecting coastal area, *Geosynthetics Engineering Journal, JC-IGS*, 17, 201-206 (in Japanese).

Evaluation of internal erosion by turbidity of drained water

Mari SATO¹, Reiko KUWANO²

¹Ph.D Student, Dept. of Civil Engineering,
Faculty of Engineering, the University of Tokyo, Japan
msato@iis.u-tokyo.ac.jp

² Associate Professor, ICUS, IIS, the University of Tokyo, Japan

ABSTRACT

Internal erosion causes various ground disaster such as cave-in accidents and landslides^{1,2)}, which are supposed to happen due to water penetration under the ground with rainfalls. Underground water penetration is sometimes concentrated at a certain area such as a boundary of soil layers, and surroundings of an underground structure. Therefore internal erosion may happen at peculiar areas repeatedly with rainfalls. In this research, turbidity of drained water is supposed to be a good index for evaluation of internal erosion, because finer particles flow out first and it makes drained water from the ground turbid, which has been considered as a warning of the ground disaster. To find clear relationships between turbidity of drained water and degree of internal erosion, simple column test simulating concentrated water flow through the ground was conducted. This column was possible to put high hydraulic gradient and soil and water drainage from the bottom plate was allowed. After finishing the test, cone penetration test was conducted to measure the soil stiffness. As a result, it was shown that weight of drained soil is relative to turbidity of drained water, which was suggested that measuring turbidity of the ground was effective to evaluate the degree of internal erosion. Moreover, internal erosion caused decreasing of penetration resistance.

Keywords: internal erosion, landslides, cave-in accident, turbidity, soil drainage

1. INTRODUCTION

Many ground disasters are caused by underground water flow. Water flow sometimes concentrates at the gaps between original fills and buried fills, where internal erosion happens. In Great Tohoku Earthquake, many landslides occurred at these gaps (see Figure 1.) and it was supposed that these gaps became weak by repetition of internal erosion. This process was schematically shown in Figure 2. Therefore, quantitative evaluation of internal erosion is necessary and this research aimed at turbidity of drained water which is one of the famous threats of ground disaster.

Relationships between turbidity of drained water and degree of internal erosion were investigated due to simple column tests. In addition, decreasing of the stiffness of the ground after internal erosion was measured by cone penetration tests.



Figure 1. Landslide in Yamamotocho, Miyagi-ken

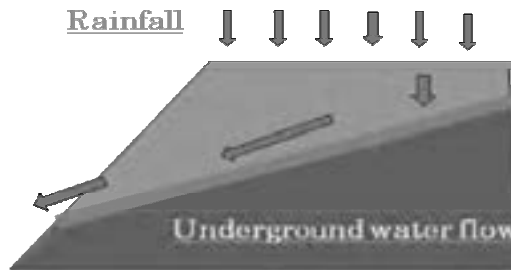


Figure 2. Internal erosion at the boundary of a buried fill and an original fill

2. TEST APPRATUS AND PROCEDURE

2.1 Test apparatus

Test apparatus was shown in Figure 3. The apparatus was composed of a upper plate, a bottom plate and an acrylic cylinder. Diameter of the acrylic cylinder is 8cm and height of that is around 31cm. The apparatus is connected from the upper plate to the outer water tank, which is possible to put high water pressure from the surface. Water in the outer tank is degassed condition. The bottom plate has many 5mm diameter's holes. 1mm mesh cloth was put on the bottom plate. Turbidimeter was 2100P, made by ©Hach, which applied nupherometry method. (Referring to Figure 4) Turbidity was automatically measured by putting a 15ml sample cell to the turbidimeter.

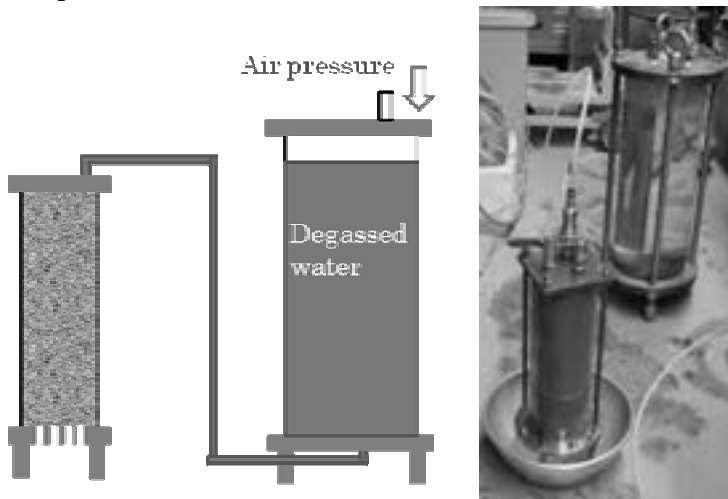


Figure 3. Test apparatus (Left: Schematically figure, Right: picture)

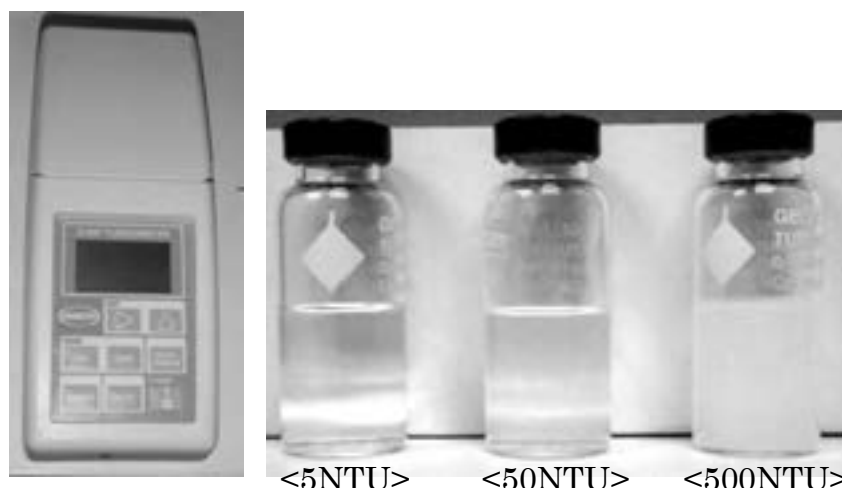


Figure 4. Turbidimeter and sample cells

2.2 Test procedure

Test material was compacted at every 5cm layer, 6 times (30cm height). Hime gravel was put on the surface of the specimen at 1cm thickness for the uniform water penetration. Then the apparatus was submerged in a bucket for 1 day. After the submergence, the apparatus was taken out from the bucket and water flow from the tank was started. Drained water and soil from the bottom plate were gathered in a bowl which was changed at certain period (represented as “time” in Table 1) and turbidity was measured.

3. TEST CONDITIONS

All experimental conditions are shown in Table 1. Test material was Edosaki sand ($\rho_{dmax}=1.76\text{g/cm}^3$, $W_{opt}=14.2\%$, $\rho_s=2.705\text{g/cm}^3$, $e_{min}=0.868$, $e_{max}=1.383$) and particle size distribution of that was shown in Figure . From Figure , Edosaki sand was “unstable material” which was suggested by Kenny et al. (1985). Each test conditions: Hydraulic gradient, Dc, time and cycle were explained with test results of next chapter.

Table 1. Test conditions

Case	Hydraulic gradient	Dc(%)	time (min.)	cycle(times)
Step-Dc90	Step	88.1	20	6
Step-Dc80	Step	79.1	10	9
Const-180kpa	Constant	89.3	10	6
Const-90kpa	Constant	89.4	10	10

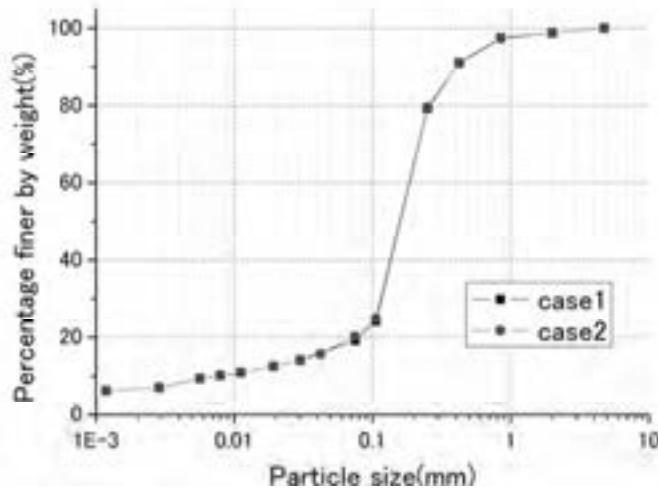


Figure 5. Particle size distribution of Edosaki sand

4. TEST RESULT

4.1 Step increasing of hydraulic gradient

In case “Step-Dc90” & “Step-Dc80”, hydraulic gradient (pressure putting on the water tank) was increased step by step. “Time” represents the continuous time to keep the constant hydraulic gradient. Then increase the hydraulic gradient and repeat certain cycles. (Represented as “Cycle”)

4.1.2 Results of Step-Dc90

Figure 6 is shown that the relationships between weight of drained water and hydraulic gradient (same as “water pressure” putting on the outer tank). Figure 7 is shown the result of weight of drained soil and turbidity. Figure 8 represented photos of sample cells. Figure 6 suggested that weight of drained water increased acceleratory due to rise of hydraulic gradient. On the other hand, weight of drained soil increased suddenly over 120kPa. Turbidity is relative to weight of drained soil. (See Figure 7) Sample cells over 120kpa also got muddy over 120kPa in Figure 8, which is corresponding to the amount of turbidity.

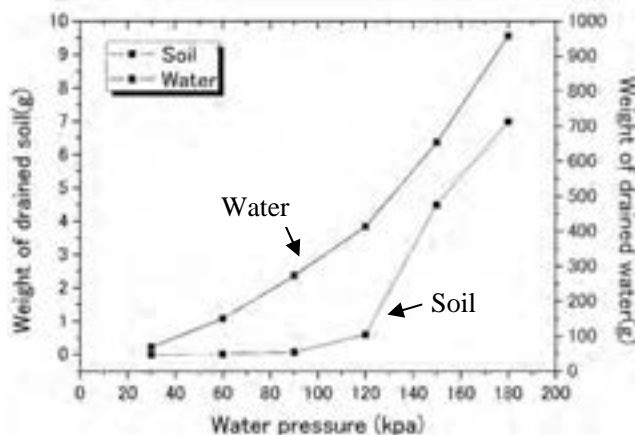


Figure 6. Weight of drained water and soil in Step Dc-90



Figure 8. Pictures of sample cells (Right is higher water pressure)

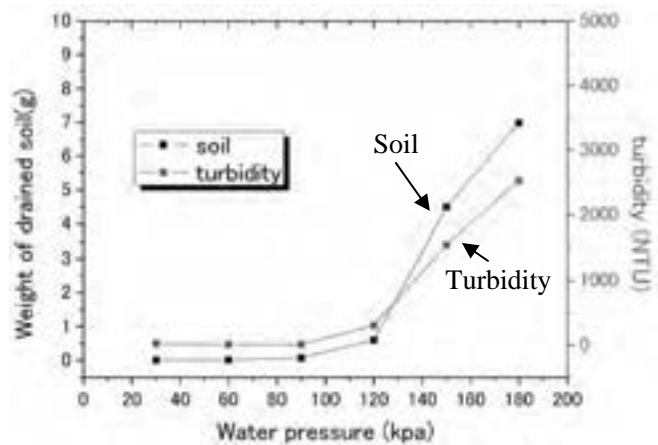


Figure 7. Weight of drained soil and turbidity in step Dc-90

4.1.2 Results of Step-Dc80

Figure 9 is shown that the relationships between weight of drained water and hydraulic gradient (same as “water pressure” putting on the outer tank). Figure 10 is shown the result of weight of drained soil and turbidity. In this case, consolidation which Dc increased around 5% occurred while increasing hydraulic gradient.

Weight of drained soil increased over 45kpa, which is much lower than the result of Step-Dc90. Repetition of increasing and decreasing of weight of drained soil was happened over 45kPa. On the other hand, weight of drained water was constant over 45kPa. Figure 10 proposed that turbidity is relative to weight of drained soil, which is similar tendency as Step-Dc90.

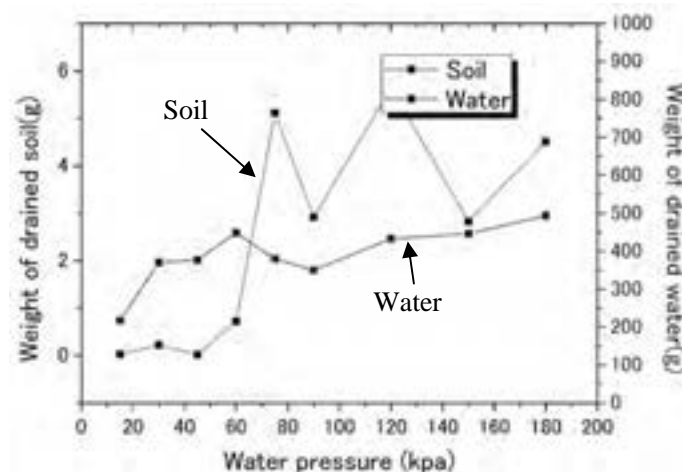


Figure 9. Weight of drained water and soil in Step Dc-80

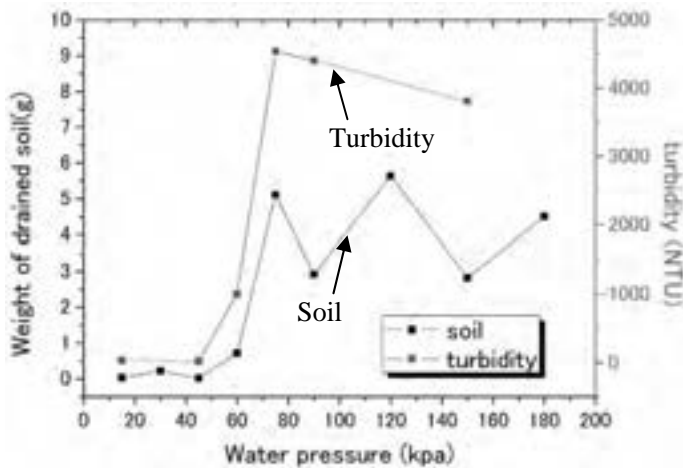


Figure 10. Weight of draind soil and turbidity in Step Dc-80

4.2 Constant hydraulic gradient

In Const-180kPa and Const-90kPa, hydraulic gradient kept constant during the test and indices: weight of drained soil, weight of drained water and turbidity were measured at the certain interval. (Represented as “time”) Then this “Cycle” was repeated.

4.2.1 Results of Const-180kPa

Results of weight of drained water and weight of drained soil with time progress was shown in Figure 11. That of turbidity and weight of drained soil was shown in Figure 12. Figure 11 suggested that weight of drained soil increased slightly after time progressing and weight of drained water decreased once and then recovered. Turbidity was corresponding to the weight of drained soil (Referring to Figure 12)

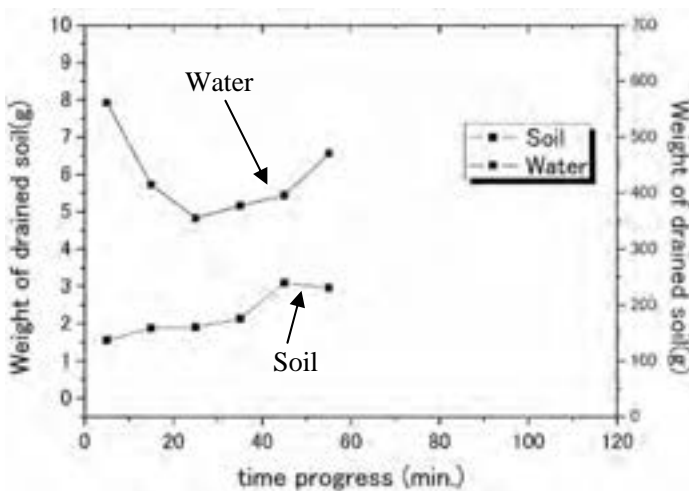


Figure 11. Weight of draind water and soil in Const-180kPa

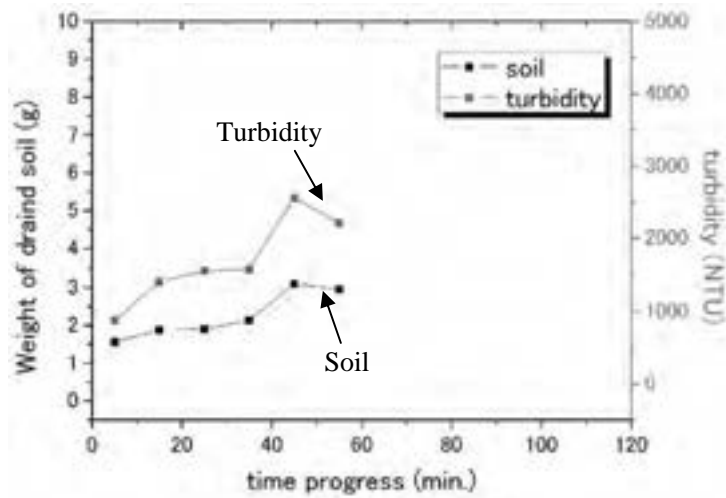


Figure 12. Weight of drained soil and turbidity in Const-180kPa

4.2.1 Results of Const-90kPa

Results of weight of drained water and weight of drained soil with time progress was shown in Figure 13. That of turbidity and weight of drained soil was shown in Figure 14..

Figure 13 suggested that weight of drained soil increased and decreased repeatedly, and weight of drained water was constant. Turbidity was corresponding to the weight of drained soil and gradually increased by continuous water flow (See Figure 14)

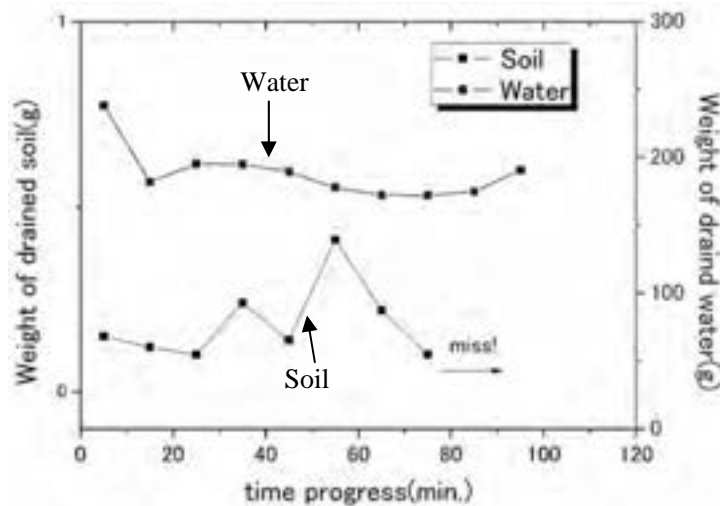


Figure 13. weight of drained water and soil in Const-90kPa

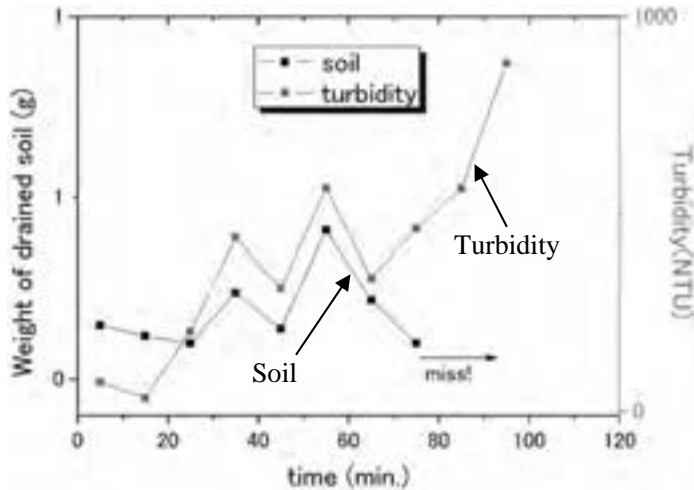


Figure 14. weight of drained water and soil in Const-90kPa

4.3 Permeability Coefficient k

Permeability coefficient k was calculated by water temperature, weight of drained water, length of specimen and hydraulic gradient. Permeability coefficient k during water penetration was shown in Figure 15. Figure 15 suggested k was changed in gradually increasing of hydraulic gradient cases (Step-Dc80 and Step-Dc90). Especially in Step-Dc80, k was decreased because consolidation happened. On the other hand, in constant hydraulic gradient cases (Const-180kPa and Const-90kPa), k was kept constant during water penetration.

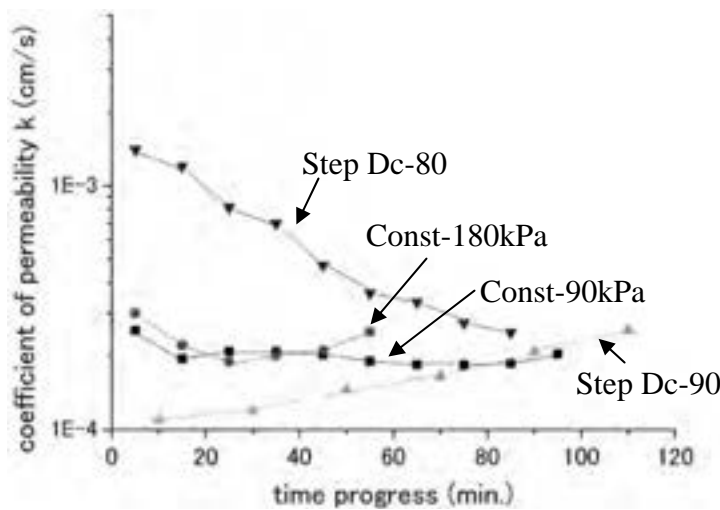


Figure 15. Permeability coefficient

5. CONE PENETRATION TEST

Small scale cone penetration test was conducted to evaluate the influence of internal erosion on soil stiffness. Test apparatus was shown in Figure 16. 3mm diameter's metal stick on which load cell was put, was penetrated at certain speed and penetration resistance was measured by load cell after finishing water penetration test.

Cone penetration test was done in 4 test cases represented in Table 2. Const-180kPa case was explained chapter4 but other 3 were additional test cases: Const-180kpa20m, Const-180kpalim, No_outflow.

Figure 17 suggested Step-Dc90 had large penetration resistance. On the other hand, Step-Dc80's penetration resistance was small. Table 2 suggested ratio of weight of drained soil in whole specimen is relative to degree of decreasing of penetration resistance. In addition, decreasing of resistance in bottom part was clearer than that in upper part, which declared bottom part caused internal erosion at first and loss of resistance.

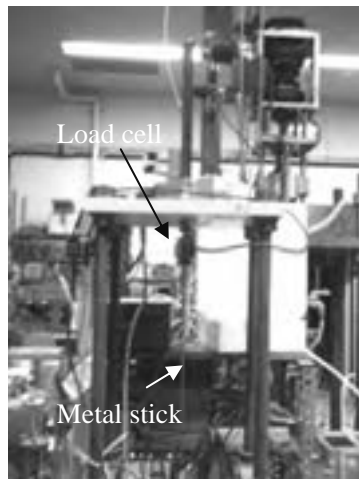


Figure 16. Test apparatus of cone penetration test

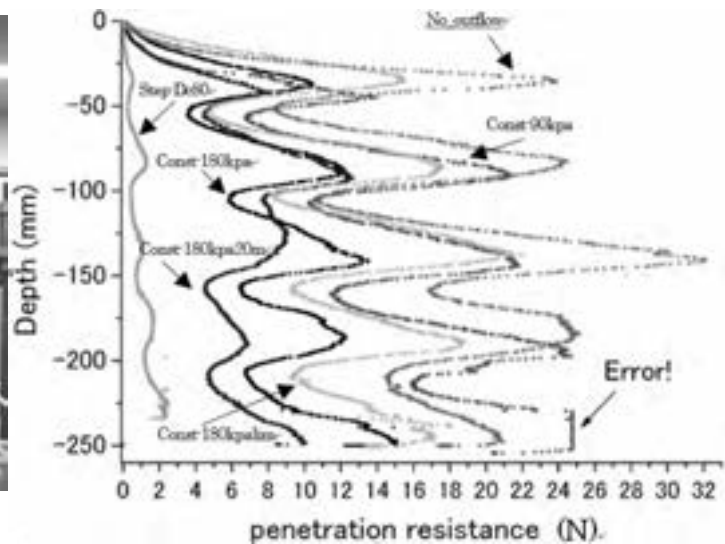


Figure 17. Result of penetration resistance

Table 2. Test conditions of cone penetration test

Case	Hydraulic gradient	Dc (%)	time (min.)	Cycle (times)	Ratio of soil loss (%)
Const-180kpa	Constant	89.3	10	6	0.5
Const-180kpa20m	Constant	89.6	10	2	0.75
Const-180kpalim	Constant	89.6	10	6	0.09
Const-90kpa	Constant	89.4	10	10	0.05
No_outflow	non	88.3	0	0	0

6. DISCUSSION AND CONCLUSION

- Turbidity was corresponding with weight of drained soil, therefore turbidity can become valid index of evaluation of internal erosion.
- Weight of drained soil was most affected by hydraulic gradient. There was a boundary of hydraulic gradient which made drained water turbid suddenly. This boundary was much smaller in loose ground than that in dense ground.

- Weight of drained soil gradually increased during water penetration in constant hydraulic gradient.
- Maeda et al.(2012) suggested clogging and drainage were repeated during soil outflow, and simulated decreasing of soil stiffness by DEM analysis.³⁾ Increasing and decreasing of weight of drained water and soil happened due to this clogging and drainage in the specimen.
- Cone penetration resistance decreased even by 1% soil loss in the specimen. Samanthi et al.(2011) suggested that penetration resistance decreased in large area due to collapse of small cavity in the ground⁴⁾. Internal erosion changed soil particles Skelton and might have caused similar phenomena.

REFERENCES

- 1) Sato, M. & Kuwano, R. *Model Tests for the Evaluation of Formation and Expansion of a Cavity in the ground*. Proc. of the 7th International Conference on Physical Modelling in Geotechnics 2010. Zurich, June 2010, pp.581-586
- 2) Kuwano, R, Yamauchi, K., Horii, T. and Kohashi, H. 2006. *Defects of sewer pipes causing cave-in's in the road*. Proc. of 6th International Symposium on New Technologies for Urban Safety of Mega Cities in Asia. Phuket: No.H63.
- 3) Maeda,K, Wood.D.M, and Kondo, A. Micro and macro modelling of internal erosion and scoring with fine particle dynamics, Proc. of 6th International Conference on Scour and Erosion. 2012, Paris, France: ISCE-000197
- 4) Renuka,S. & Kuwano,R. Formation and evaluation of loosened ground above a cavity by laboratory model test with uniform sand, Proc. of 13th International Summer Symposium, 2011,Uji, Japan: pp211- 214

Application of microbial calcite to hemp fiber reinforced soils to combat desertification

Sookie S. BANG
Professor, Department of Chemical and Biological Engineering
South Dakota School of Mines and Technology, USA
sookie.bang@sdsmt.edu

Sangchul BANG
Professor, Department of Civil and Environmental Engineering
South Dakota School of Mines and Technology, USA

Josh ANDERSON
Graduate Student, Department of Civil and Environmental Engineering
South Dakota School of Mines and Technology, USA

Seok J. LEE, Nam Y. DHO, and Seong R. CHOI
Managers, Lotte Engineering & Construction, Korea

Sung-Hwan KO
President, EcoPhile, Korea

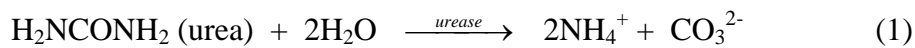
ABSTRACT

*Airborne dust and sand particles caused by wind erosion have been associated with serious problems in human health as well as natural environment. In particular, sand particles originated from Mongolia and northern China due to increasing desertification have been the main cause of frequent such problems. In the past, the majority of control methods have been either chemical or mechanical, resulting in certain degrees of health hazard or frequent applications. An alternative method, surface vegetation, becomes increasingly popular but it is very slow and costly. Recently, a biological technique utilizing a naturally occurring microorganism, *Sporosarcina pasteurii*, has been introduced. This soil microorganism is ureolytic, expressing the urease enzyme that hydrolyzes urea to ammonium and carbonate ions. The ammonium ions raise the surrounding pH, in turn promoting calcium carbonate (calcite) precipitation in the presence of calcium ions. This precipitate has shown great dust suppression potential. The main objective of this study is to examine the application of microbial calcite with bio-degradable fibers to reduce the wind erosion potential, using *S. pasteurii* mixed with medium containing urea and calcium chloride in order to develop an environmentally safe and economically feasible technique to minimize the spread of desertification.*

Keywords: *Microbially induced calcite precipitation, bacteria, hemp fibers, wind erosion, mass loss*

1. INTRODUCTION

Calcium carbonate (CaCO_3) precipitation induced by *Sporosarcina pasteurii* is a potentially long-lasting, environmentally innocuous process that can be used to suppress dust particles from becoming airborne. *S. pasteurii* produces the urease enzyme (Benini et al., 1996; Braissant et al., 2003), which hydrolyzes urea to produce both ammonium and carbonate ions (Reaction 1 below). This reaction raises the pH of the surrounding environment (Stocks-Fischer et al., 1999; Warren et al., 2001), ultimately precipitating calcite from carbonate and calcium ions (Reaction 2 below). The reactions are summarized as follows.



Microbial calcite induced by *S. pasteurii* has been well-documented as an agent used for mineral plugging (Gollapudi et al., 1995), concrete crack remediation (Bang et al., 2001), and improved cement mortar strength and longevity (Ghosh et al., 2005; DeMuyck et al., 2008). Furthermore, a genetically engineered microorganism that can produce organic polymer as well as induce calcite precipitation has been developed in our laboratories as a bio-sealant (Bergdale et al. 2012). This microbially induced cementation process also slows contaminant leaching in soils (Fujita et al., 2000; Mitchell and Ferris 2006) and has been shown to stabilize loose sand structures (DeJong et al., 2006). In particular, *S. pasteurii* has recently been explored as a potential dust palliative when applied to the surfaces of different soils including poorly graded commercial sandblasting sand, silt, and clay soils (Bang et al., 2008; Bang et al., 2009; Meyer et al., 2011). This study utilized poorly graded sand with bio-degradable fibers that were treated with medium containing bacteria. After 96 hours of incubation at 40°C, the soil samples were weighed before and after wind erosion tests at three different wind speeds of 32, 48, and 64 km/hr for 2 minutes to determine the percent mass loss. Untreated soil and soil mixed with fibers only were used as controls. In order to optimize the resistance against the wind erosion, the following conditions and treatments were examined: a) application volume of the medium and b) soil preparation method (treated with medium containing bacteria and fibers).

The main objective of this study is to examine the application of microbial calcite with bio-degradable fibers to reduce the wind erosion potential, using *S. pasteurii* mixed with medium containing urea and calcium chloride in order to develop an environmentally safe and economically feasible technique to minimize the spread of desertification.

2. PREPARATION AND TREATMENT OF BACTERIA

The following briefly describes how the medium and bacteria were prepared. Complete details of the preparation of medium and bacteria are well described elsewhere (Bang et al., 2001).

2.1 Procedures

Urea-NB medium (20 g urea and 3 g nutrient broth per 1 L of distilled water) was prepared by autoclaving, to which filter-sterilized CaCl_2 was added to a final concentration of 100 mM CaCl_2 . Then, *S. pasteurii* was aseptically suspended to the urea-NB- CaCl_2 medium to obtain a concentration of 1×10^8 cells/ml. The medium added with all necessary ingredients was then mixed with sand thoroughly to ensure an even distribution of medium and sand. Fibers were added at this point. The sand mixture was added to a specimen cup and placed in an oven at 40°C for four days before being tested. All samples were prepared in triplicate.

2.2 Wind erosion tests

Two different mixtures of sand were tested. The first mixture consisted of only sand and the second was a mixture of sand, medium containing bacteria, and fibers. The sand used in these tests was HM 106 Gilson sand, commercially available from Gilson Co., Inc., Lewis center, OH. It has a specific gravity of 2.65, uniformity coefficient less than 2.0, and few particles passing US standard sieve #200 or retained on #10.

The fibers used in these tests were hemp fibers. The nominal dimensions of the fibers are 60.1 mm in length and 0.09 mm in diameter. The fibers were obtained by de-stranding a Sisal Manila rope (stock number 74389, Knechts Hardware, Rapid City, SD). The first mixtures were used as controls, i.e., the experimental results of the second mixtures were compared against those of the controls.

The wind erosion specimen preparation began with mixing cultured bacteria at 10^8 cells per ml concentration with the medium. Medium amounts were set at 0.025, 0.05, 0.1, 0.5, 1, 2, and 3 ml per 100 grams of sand. Concentration of fibers was set at 0.25% by the weight. The mixes were hand-stirred with gloves attempting for even distribution of fibers, medium, and bacteria (Fig. – 1).

The containers had dimensions of 75 mm in height and 65 mm in diameter with a total surface area of 3,320 mm². The mix was then compacted into containers while aiming for a density close to 16.34 kN/m³. After striking off excess protrusion from the containers, they were placed in an oven (Fischer Scientific, Hampton, NH) at 40°C for four days. Afterward, the specimens were removed from the oven. Fig. – 2 shows specimens ready for wind erosion tests.

The specimens were then placed in front of a wind tunnel (Aerolab, Laurel, MD, USA, Fig. - 3) that had been set to the appropriate velocity for the test by a digital Turbometer wind speed indicator (Davis Instruments, Inc., Hayward, CA, USA, right photo of Fig. – 4) and a wind meter (Dwyer Instruments, Inc., Michigan City, IN, USA, left photo of Fig. – 4). The specimen was exposed to wind erosion for two minutes and then weighed afterward.

3. RESULTS

Fig. – 5 shows photos of specimens after the wind erosion tests that were treated with medium containing bacteria and fibers. As can be seen, surface crusts were formed that are clearly visible. Please note that the holes on the surface of the



Fig. – 1 Sand mixed with fibers and medium containing bacteria



Fig. – 2 Various sand specimens for wind erosion tests



Fig. – 3 Aerolab wind tunnel



Fig. – 4 Digital Turbometer wind speed indicator and Dwyer wind meter



Fig. – 5 Specimens after wind erosion tests

specimens were created by a surface penetrometer to determine the approximate soil surface shear strength, not by the wind erosion.

Results of mass loss from the wind erosion tests were averaged among triplicate specimens. From the data, the mass loss due to wind erosion was represented by the loss of material in grams per square centimeters of the surface area. Table – 1 and Fig. – 6 show the summary of entire test results. Under 32 km/hr wind for 2 minutes, sand-only samples experienced the highest weight loss of 0.828 g/cm^2 . In general, sand treated with medium containing bacteria and fibers experienced much smaller amounts of mass loss. Although there are minor scatter in data, it is clearly obvious that as the amount of medium containing bacteria increases, the mass loss due to wind erosion becomes noticeably less. As the wind velocity increased, the corresponding mass loss increased substantially.

Under 32 km/hr wind for 2 minutes, when the sand treated with 0.05 ml of medium containing bacteria and fibers were tested, the weight loss was reduced to

Table – 1 Summary of mass loss (in g/cm²) from wind erosion tests

	Wind velocity (km/hr)	Medium (ml) added to 100 g of sand							
		0.0	0.025	0.05	0.1	0.5	1.0	2.0	3.0
sand	32	0.828							
	48	1.034							
	64	1.718							
sand + fibers + bacteria	32		1.047	0.692	0.165	0.029	0.028	0.015	0.008
	48		1.091	1.034	0.710	0.169	0.082	0.035	0.019
	64		1.459	1.035	0.958	0.933	0.812	0.163	0.028

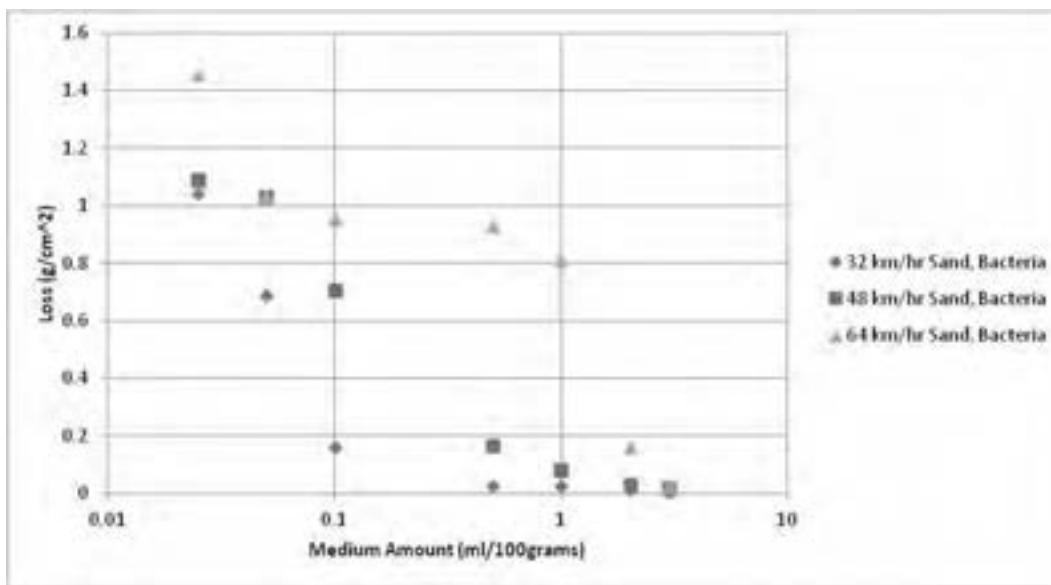


Fig. – 6 Mass loss vs. medium amount relationship of sand with fibers and Bacteria

16.4% of that of sand-only. With 0.1 ml and 0.5 ml of medium, this reduction becomes more pronounced, i.e., 80.1% and 96.5%, respectively.

Under 48 km/hr wind for 2 minutes, when sands treated with 0.1 ml and 0.5 ml of medium containing bacteria and fibers were tested, the weight losses were reduced to 31.3% and 83.7%, respectively, of that of sand-only.

Under 64 km/hr wind for 2 minutes, when the sand treated with 0.05 ml of medium containing bacteria and fibers were tested, the weight loss was reduced to 39.8% of that of sand-only. With 0.1 ml and 0.5 ml of medium, this reduction becomes more pronounced, i.e., 44.2% and 45.7%, respectively.

When the sand was treated with 1.0 ml or more of medium containing bacteria and fibers, the mass loss due to wind velocity of up to 48 km/hr is virtually zero. As expected, when the wind velocity was 64 km/hr, more amount of medium was required to obtain similar mass losses to those at lower wind velocities.

4. CONCLUSIONS

A potentially innovative biological approach in solving one of the most difficult and persistent geotechnical problems, resistance against the wind erosion, has been developed. This technique utilizes microbially induced calcite precipitation with bio-degradable fibers to bond soil particles together so that they are more resistant to becoming airborne. Results indicate that the soil samples treated with *S. pasteurii* form a crust-like layer on the soil surface and that the addition of fibers further enhances the effectiveness significantly. This calcite-rich layer resulted in significant reduction in mass loss as compared to that of untreated soil, indicating that this microbially induced calcite together with fibers can indeed be used as a means of reducing the wind erosion, thus potentially be used to minimize the desertification.

In the future, additional different types of bio-degradable fibers will be tried and tested to identify their respective effectiveness in reducing the wind erosion potential.

5. ACKNOWLEDGEMENTS

The authors are grateful for the technical contributions of Emily Squillace and Ian Prichard, undergraduate research assistants, at the South Dakota School of Mines and Technology and for the financial support provided by Lotte E&C, Korea.

REFERENCES

- Bang, S. S., Galinat, J. K., and Ramakrishnan, V., 2001. Calcite precipitation induced by polyurethane-immobilized *Bacillus pasteurii*. *Enzyme and Microbial Technology* 28, 404–409.
- Bang, S. S., Bang, S., Frutiger, S., Nehl, L. M., and Comes, B. L., 2008. Application of novel biological technique in dust suppression. *Proc. Annual Meeting of Transportation Research Board* (CD-ROM), Washington D.C.
- Bang, S. S., Leibrock, C., Smith, B., Pinkelman, R. J., Frutiger, S., Nehl, L. M., Comes, B. L., Coleman, D., and Bang, S., 2009. Geotechnical values of microbial calcite in dust suppression. *Proc. of NSF Engineering Research and Innovation Conference* (CD-ROM), Honolulu, HI.
- Benini, S., Gessa, C., and Ciurli, S., 1996. *Bacillus pasteurii* urease: A heteropolymeric enzyme with a binuclear nickel active site. *Soil Biol. Biochem.* 28, 819–821.
- Bergdale, T. E., Pinkelman, R. J., Hughes, S. R., Zambelli, B., Ciurli, S., and Bang, S. S., 2012. Engineered biosealant strains producing inorganic and organic biopolymers, *Journal of Biotechnology* 161, 181–189.
- Braissant, O., Cailleau, G., Dupraz, C., and Verrecchia, A. P., 2003. Bacterially induced mineralization of calcium carbonate in terrestrial environments: the role of exopolysaccharides and amino acids. *J. Sediment Res.* 73, 485–490.

- DeJong, J. T., Fritzges, M. B., and Nusslein, K., 2006. Microbially induced cementation to control sand response to undrained shear. *J. Geotechnical and Geoenvironmental Engineering* 132, 1381–1392.
- DeMuyck, W., Debrouwer, D., De Belie, N., and Verstraete, W., 2008. Bacterial carbonate precipitation improves the durability of cementitious materials. *Cement and Concrete Research* 38, 1005–1014.
- Fujita, Y., Ferris, F. G., Lawson, R. D., Colwell, F. S., and Smith, R. W., 2000. Calcium carbonate precipitation by ureolytic subsurface bacteria. *J. Geomicrobiology* 17, 305–318.
- Ghosh, P., Mandal, S., Chattopadhyay, B. D., and Pal, S., 2005. Use of microorganisms to improve the strength of cement mortar. *Cement and Concrete Research* 35, 1980–1983.
- Gollapudi, U. K., Knutson, C. L., Bang, S. S., and Islam, M. R., 1995. A new method for controlling leaching through permeable channels. *Chemosphere* 30, 695–705.
- Meyer, F. D., Bang, S., Min, S., Stetler, L. D., and Bang, S. S., 2011. Microbiologically-Induced Soil Stabilization: Application of *Sporosarcina pasteurii* for Fugitive Dust Control. *Proceedings of the American Society of Civil Engineers' Geo-Frontiers Meeting*, Paper No. 1189, Dallas, TX, March.
- Mitchell, A. C. and Ferris, F. G., 2006. The influence of *Bacillus pasteurii* on the nucleation and growth of calcium carbonate. *J. Geomicrobiology* 23, 213–226.
- Stocks-Fischer, S., Galinat, J. K., and Bang, S. S., 1999. Microbiological precipitation of CaCO₃. *Soil Biol. Biochem.* 31, 1563–1571.
- Warren, L. A., Maurice, P. A., Parmar, N., and Ferris, F. G., 2001. Microbially mediated calcium carbonate precipitation: implications for interpreting calcite precipitation and for solid-phase capture of inorganic contaminants. *J. Geomicrobiology* 18, 93–115.

Sliding disaster in Vietnam and a new proposed design method of reinforced soil wall

Nguyen Hoang Giang¹, Jiro Kuwano²

¹Ph.D, Deputy Director, International Cooperation Department,
National University of Civil Engineering, Vietnam
giangnh@nuce.edu.vn

²Professor, GRIS, Saitama University, Japan
jkuwano@mail.saitama-u.ac.jp

ABSTRACT

Vietnam has a relatively complicated territory: Countless mountains, numerous rivers, long and meandering coastline. It has faced a great deal of difficulties to overcome the landslide disaster which has taken many lives of civilians and damaged properties. Lack of proper design and reinforced structures has caused some severe landslide disasters. Some retaining walls are in bad conditions such as: large displacement, deformation, crack, and some were not proper designed. The repairing work for these structures thus has become very important. This paper will give data of current condition of retaining structures then will introduce a new method for design to improve the quality of these structures. The residual stage of pullout resistance of reinforced soil wall will be introduced in the redesign of damaged soil wall to improve stability number as well as save costs.

Keywords: landslide disaster, reinforced soil wall, geogrid

1. INTRODUCTION

Vietnam has a relatively complicated territory: Countless mountains, numerous rivers, long and meandering coastline. The terrain is different among regions. Moreover, Vietnam lies in the tropical region which is the meeting place of many atmosphere blocks therefore Vietnam is greatly suffered from Asian monsoon regime. Each year Vietnam experiences about 6-10 typhoons and tropical depressions causing heavy rain, whirlwinds and landslides...etc with its complicated and diversified terrain as well as severe storms, Vietnam has faced a great deal of difficulties to overcome the landslide disaster which has taken many lives of civilians and damaged properties. Landslide protection like retaining walls is very important method to against sliding. However, many among them have been severely damaged due to over life operation as well as natural impacts such as typhoons, heavy rain and so on. As Vietnam is in bad economic conditions thus investments to rebuild all of those constructions will become a great challenge. Thus, repair work for these damaged retaining walls has become

very important task not only to improve the stability of construction but also to save cost.

The damaged reinforced soil wall (RSW) must be evaluated by a simple index such as the wall displacement, the crest settlement, and soil-geogrid interaction conditions. To evaluate the condition of RSW which was suffered from a certain damage caused by temporary external load such as earthquake and heavy rain, the unloading-reloading process on the pullout resistance were applied then used to investigate its effects on the safety of RSW. Thank to the results of unloading-reloading effects on the pullout resistance, it was possible to evaluate the factor of safety for RSW at peak, at peak in reloading after the unloading-reloading and at the residual parts. There are many types of centrifuges and geotechnical centrifuge is one of them and it was used in this research. The special geotechnical modeling is to produce the soil behavior in terms of strength and stiffness. In the experimental container soil has free unstressed upper surface and the strength magnitude increases with depth and a rate related to soil density and the strength of the acceleration field.

Centrifuge was used for the shaking table tests and tilting table tests. The special equipment was attached to model to prevent it from total collapse when it was subjected to dynamic loading by using the centrifuge shaking table tests. After the sliding was observed the model was moved to the centrifuge tilting table tests to apply unloading-reloading process and evaluate effects of the peak and residual pullout tests on damaged RSW. There were two test series: Shaking – tilting table test series to investigate the damaged RSW before peak value and tilting - tiling table test series to investigate the residual value of pullout resistance on the stability of damaged RSW.

Vietnam risk

Vietnam is located in the tropical monsoon area in South East Asia (figure 1). Vietnam is one of the most hazard-prone areas in the Asia Pacific Region. Because of its topography, Vietnam is susceptible to typhoons, floods, droughts, sea water intrusion, landslides, forest fires and occasional earthquakes. The storm season lasts from May to December with storms hitting the northern part of the country in May through June and moving gradually south from July to December. Every year, Vietnam suffers directly from 6-10 storms and tropical depressions which causing heavy rain and flood after that.



Figure 1. Map of Vietnam

According to Vietnam report, every year, natural disasters cause an average of 750 deaths, and result in annual economic losses equivalent to 1.5 percent of GDP. However, damage and loss data is chronically underreported, so real totals may be much higher. As most of the population is living in low-lying river basins and coastal areas, more than 70 percent of the population is estimated to be exposed to risks from multiple natural hazards. The frequency of disaster is listed in table 1.

Table 1. Relative disaster frequency. (Source: EM-DAT : The OFDA /CRED International Disaster Database.)

High	Medium	Low
Flood	Hail rain/tornado	Earthquake
Typhoon	Drought	Accident (technology)
Inundation	Landslide	Frost
	Flash flood	Damaging cold
	Fire	Deforestation

Among them landslide has become more and more serious causing lives and economic losses due to poor retaining wall system and earth reinforced soil walls. Disaster Severity in Different Geographic Areas and in the Coastal Economic Zone of Vietnam is listed in table 2.

Table 2. Assessment of Disaster Severity in Different Geographic Areas and in the Coastal Economic Zone of Vietnam.

Disaster	Geographic Areas and Economic Zones							
	North east and north west	Red River Delta	North central coast	South central coast	Central highlands	North east south	Mekong River Delta	Coastal Economic Zone
Storm	+++	++++	++++	++++	++	+++	+++	++++
Flood	-	++++	++++	+++	+++	+++	++++	++++
Flashflood	+++	-	+++	+++	+++	+++	+	+++
Whirlwind	++	++	++	++	+	++	++	++
Drought	+++	+	++	+++	++	+++	+	+++
Desertification	-	-	+	++	++	++	+	++
Saline intrusion	-	+	++	++	+	++	+++	++
Inundation	-	+++	++	++	-	++	+++	+++
Landslide	++	++	++	++	+	++	+++	++
Storm surge	-	++	++	++	++	++	+++	++
Fire	++	+	++	+++	-	+++	+++	+++
Industrial and environmental hazard	-	++	++	++	+++	+++	++	+++

Very severe (++++); Severe (+++); Medium (++); Light (+); None (-)

One of reasons making this sliding disaster become huge problem is due to low quality RSW. Many among them were designed with conventional gravity wall model. Under heavy rain, these types of RSW were seriously damaged (figure 2). The new design of reinforced soil wall with geosynthetics has been introduced and become more popular. However, under huge natural disasters, these reinforced soil wall types were affected and showed partial damage. To save cost, these types of damaged structures should be repaired with simple and reasonable expense. The experiment for stability of damaged reinforced soil wall was carried out at Saitama University and Tokyo Institute of Technology, Japan.



Figure 2. Slope sliding in Quang Ngai province, 2010.

2. TWO-WEDGE ANALYSIS

The pseudo-static two-wedge method (Ismeik and Güler 1998) to evaluate the factor of safety of GRSW against sliding and overturning was used to evaluate the static and seismic stability of the GRSW considering effects of unloading-reloading on pullout resistance of geogrid at peak and residual stage. This method has been studied by several researchers such as Jewell et al. (1984). Parameters obtained from pullout tests that presented by Giang et al. (2010) at peak and residual stages were used for Two-Wedge analysis of GRSW with 7.5 m height, five layers of 4.5 m length geogrids and 1.5 m interval. The backfill material was Toyoura sand. Figure 3 shows the relationship between the factor of safety against the sliding and the horizontal seismic coefficient at failure. It can be observed in Figure 3 that when ϕ_{peak} reduces to ϕ_{residual} the factor of safety is also decreased for all the cases. For example, the SG case with $\phi_{\text{peak}} = 33.8^\circ$, the critical horizontal coefficient k_h is 0.62. At the residual value when ϕ_{peak} decreased to $\phi_{\text{residual}} = 27.6^\circ$, the critical horizontal coefficient k_h is 0.54. This suggests that in a large earthquake, if the GRSW could resist the seismic activities and show some deformation and displacement of geogrids, the pullout resistance of geogrids in some deformed part of the damaged GRSW might work in residual condition. The unloading-reloading process of geogrid reduces the pullout resistance of geogrid in backfill soil resulting the factor of safety of the damaged GRSW reduces from factor of safety at peak to factor of safety at residual. In order to investigate this behavior of damaged GRSW, a series GRSW centrifuge shaking and tilting model tests were carried and the experimental results were compared with the predicted results of Two-wedge method.

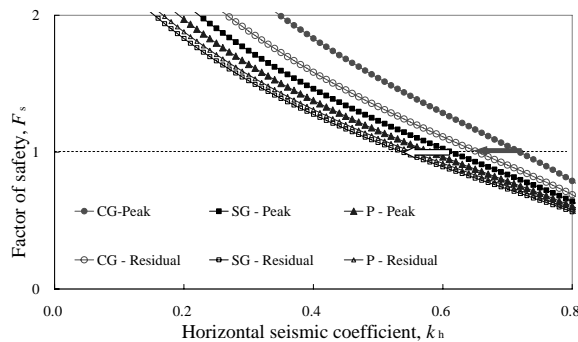


Figure 3. Safety factor vs horizontal seismic coefficient at peak and residual values, against sliding

3. OUTLINE OF THE TEST

A series of centrifuge tilting and shaking table tests was carried out using Mark 3 centrifuge at Tokyo Institute of Technology. Toyoura sand with the relative density of 80 % was used as backfill material. Model geogrids were made of polycarbonate plates with 0.5 mm thickness. The shape of the model geogrid was the same in all cases as shown in Figure 4. Figure 5 shows the schematic diagram of the model GRSW used in both centrifuge tilting and shaking table tests. Five layers of 90 mm long geogrids were laid in the backfill at 30 mm interval. Five pieces of plastic plates were used as a model wall and one geogrid was attached to one plate. Some optical targets were set on the surface of the transparent side wall for detailed observation of deformation. Both tilting and shaking table tests were conducted in the centrifugal acceleration of 50G. In the centrifuge tilting table tests, pseudo static horizontal loading usually used in the design was achieved by tilting the model. On the other hand, in the centrifugal shaking table tests, cyclic loading as in the seismic events with frequency of 100Hz, which corresponds to 2Hz in prototype, were applied to the model. The parameters of geogrid pullout test at peak and residual stages in GRSW are shown in Table 3.

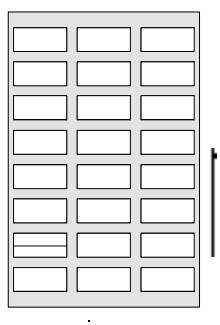


Figure 4. Geogrid model for centrifuge tests

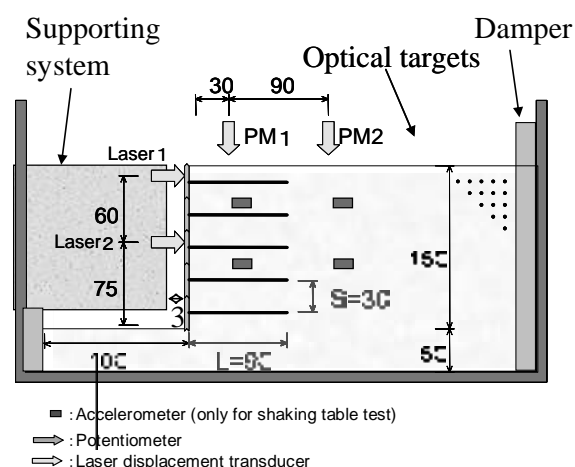


Figure 5. Schematic view of the model GRSW

In 50G centrifuge condition, the GRSW model is equal to GRSW with height of 7.5 m. Using the above mentioned two-wedge method with parameters obtained from Table 3, the GRSW has horizontal coefficient at peak and at residual stages, $k_h^p = 0.47$, $k_h^r = 0.43$, respectively. The reduction of the factor of safety of GRSW decreases when from ϕ_{peak} to $\phi_{residual}$. Factor of safety and failure surfaces of predicted results are shown in Figure 6.

Table 3. Material and pullout resistance properties at peak and residual values

	peak	residual
c_{peak} (kPa)	0.93	-0.75
ϕ_{peak} (deg)	21.4	18.2
$\tan \phi_p / \tan \phi$	0.45	0.38

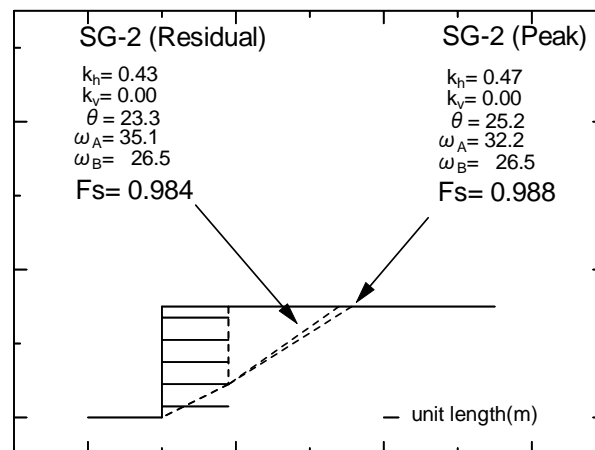


Figure 6. Predicted two-wedge analysis failure of GRSW at peak and residual values.

4. TESTING PROCEDURE

The displacement of wall facing of the GRSW was controlled by the supporting system as shown in Figure 5. According to Izawa and Kuwano (2008), the damage of the GRSW would be evaluated from the surface deformation that is observed from the wall displacement or from the settlement of the crest. The supporting system in this model will prevent the GRSW from total collapse at peak and achieve the residual stage basing on the distance between the wall facing and the system.

There are two types of testing:

First type, Centrifuge Shaking-Tilting test: The GRSW was subjected to shaking in centrifuge test to achieve some deformation. Then the damaged GRSW was moved to tilting test and the tilting-untilting process was applied.

The centrifuge tilting - tilting test: The GRSW was subjected to tilting to achieve residual stage. The supporting system prevented the GRSW from total collapse and the GRSW was then un-tilted. The supporting system was then removed and the GRSW was tilted in centrifuge test again until the full collapse was obtained.

5. RESULT AND DISCUSSION

This GRSW model test was collapsed at tilting angle of 21° as reported by Izawa and Kuwano (2008). In the first test series, the GRSW showed some deformation however the pullout resistance of geogrids had not reached residual value. The GRSW was tilted and un-tilted causing the unloading-reloading process of geogrids in GRSW. In the geogrid pullout tests, the unloading-reloading process did not affect the pullout resistance before the peak value. In the GRSW shaking-tilting model tests, the tilting – untilting process also did not affect the stability of the GRSW. Even the GRSW showed some deformation, the tilting - untilting process with tilting angles $\eta = 5^\circ, 15^\circ, 20^\circ$ did not cause the failure as shown in Figure 8. Therefore, this agrees well with the results of the geogrid pullout test with unloading-reloading process.

In the second type of centrifuge tests, the GRSW showed deformation and the pullout resistance of geogrids had reached residual stage. After the first tilting, the

supporting system was removed. The damaged GRSW was tilted again until full collapse. The damaged GRSW was then collapsed at tilting angle $\eta = 18.3^\circ$ (shown in Fig 7b). It was about 3° less than the critical tilting angle at peak $\eta = 21^\circ$ as shown in Figure 8. This agrees well with the results of geogrid pullout tests and the predicted behaviour by the two-wedge method that when in residual stage, the pullout resistance of geogrid can not reach peak after the unloading-reloading process and the factor of safety of GRSW decreases from ϕ_{peak} to ϕ_{residual} . The maximum shear strain and volumetric strain at the backfill of GRSW before failure are shown in Figure 9a, 9b. The Figure 9a shows that the shear strain concentrates behind the geogrid reinforcement and the failure surface has a two-wedge type.

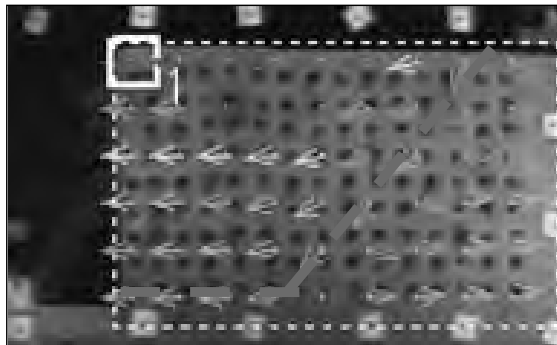


Figure 7a. Potential sliding surface before the collapse

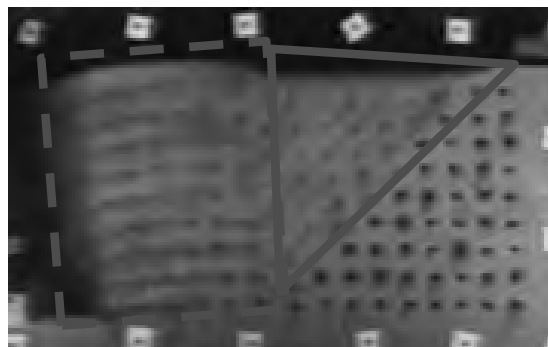


Fig 7b. Two-wedge sliding surface

Even though both the predicted failure of peak value and residual value give higher critical horizontal coefficient than the experimental one but the predicted residual stage has closer critical horizontal value as well as failure surface with the experiment results in compare with the predicted peak value does. This could be explained that during the first tilting, some part of the GRSW had reached peak value of pullout resistance due to displacement and reduced to residual values while other parts were still working in peak value of the pullout resistance. The deformed plane was formed when the other part of potential failure was mobilized to a new failure plane. Thus, after the event, factor of safety and failure plane of GRSW could not reach to peak value. Therefore the residual value of pullout resistance is more suitable to use for re-evaluating the factor of safety of damaged GRSW when some part of GRSW has reached residual stage.

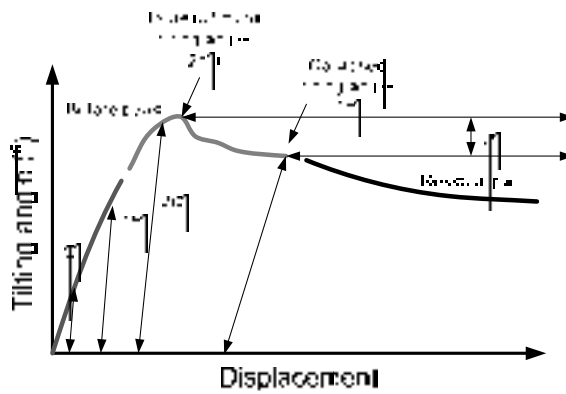


Fig 8. Horizontal seismic coefficient (k_h) where GRSW was subjected to unloading-reloading process.

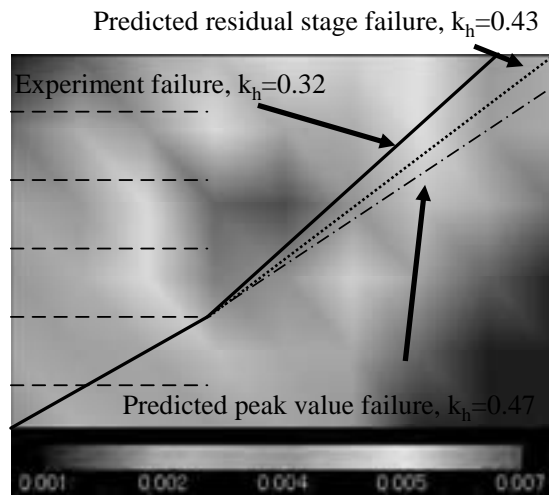


Figure 9a. Maximum shear strain

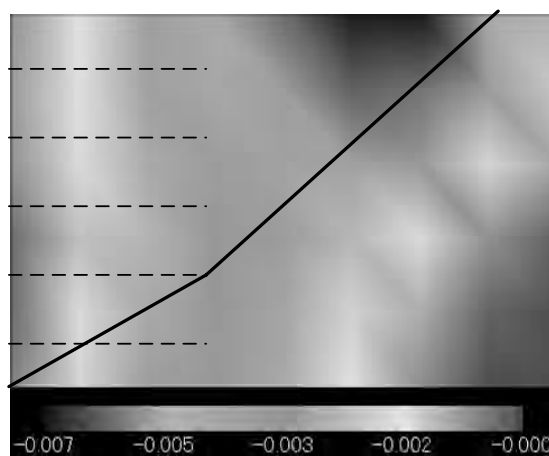


Figure 9b. Volumetric strain

6. CONCLUSIONS

Series of centrifuge GRSW shaking and tilting table tests were carried out to study the effect of unloading-reloading processes on factor of safety and failure surface of damaged GRSW. The two-wedge method analysis was used to predict stability of GRSW at peak and residual stage. The results were then compared with the experimental result. The following conclusions are achieved:

- The unloading-reloading process does not affect the stability of GRSW when the pullout resistance of geogrid is still before the peak.
- The GRSW was collapsed in two-wedge form suitable with the proposal two-wedge analysis.
- The residual value of pullout resistance should be used to re-evaluate the stability of damaged GRSW when part of it has reached residual stage.
- This design and repair method should be used to evaluate stability of reinforced soil wall in Vietnam and propose a repair procedure.

7. REFERENCES

- Giang, N. H., Kuwano, J., Izawa, J. & Tachibana, S. (2010). Influence of unloading–reloading processes on the pullout resistance of geogrid. *Geosynthetics International*, 17, No. 4, 1–8.
- Ismeik, M. and Güler, E. 1998. Effect of wall facing on the seismic stability of geosynthetic-reinforced retaining walls, *Geosynthetics International*, 5(1&2), 41-53.
- Izawa, J. and Kuwano, J., 2008, "Evaluation of damage of geogrid reinforced soil wall based on wall displacement," *Proceedings of 4th European Geosynthetics Conference*, September 7-10, Edinburgh, UK, CD-ROM No.117.
- Jewell, R. A., Paine, N. and Woods, R. I. 1984. Design method for steep reinforced embankments, *Polymer Grid Reinforcement*, Thomas Telford, pp. 70-81.

Estimation of stress distribution in a model ground using bender elements

Reiko KUWANO¹, Sho OH²

¹ Associate Professor, ICUS, IIS, the University of Tokyo, Japan
kuwano@iis.u-tokyo.ac.jp

²Ph.D Student, Dept. of Civil Engineering,
Faculty of Engineering, the University of Tokyo, Japan

ABSTRACT

Elastic wave tomography using bender elements was conducted to evaluate stress distribution in a model ground. Bender element, BE, method has been widely applied in laboratory soil element testing such as triaxial test, oedometer test, or direct shear test. When BEs are used in a model test, it was found that the signal processing was essential to obtain clearer waveforms as the amplitude of received signal was not large enough due to generally lower level of confining stress. The effects of chamber side wall should be also taken into account in the arrangement of the elements location.

In a densely compacted model ground in a trapdoor testing soil chamber, the distribution of stress in the ground was estimated using tomography technique and it agreed well with the results of physically measured stresses at the base. Shear planes observed during the trapdoor test also coincided well with the boundary of the ground between fast and slow wave paths. On the other hand, for a loosely compacted ground, the estimation of stress distribution was not successfully conducted, probably due to moderate change of the stress, i.e. the change of wave velocity.

Keywords: shear wave, tomography, bender element, trapdoor test, stress distribution

1. INTRODUCTION

It is difficult to measure actual stress distribution in the ground for both in the laboratory and in the field, due to the fact that an interaction between an earth pressure cell and soil grains easily changes the contact situation. In this study, the stress distribution in the model ground was roughly estimated using elastic wave tomography technique. The shear wave velocities propagating through soil generally reflect the soil's density and effective stress states, as empirically obtained relationship of equation (1).

$$V_s = \frac{1}{\sqrt{f(e)}} \sigma_i^m \sigma_j^n \quad (1)$$

Where V_s is shear wave velocity, $f(e)$ is void ratio function for normalizing the effects of void ratio, i is the direction of wave propagation, j is the direction of particle motion, m and n is constants. Assuming that the density of soil remains constant, the distributions of shear wave velocities indicate the distribution of current stress state.

For the measurement of V_s , bender element, BE, method was used. BE is piezo-ceramic bimorph elements, which can convert electric signal to physical motion and vice versa. BE has been widely used for the V_s measurement in the laboratory soil specimen, but the application to model tests has not been well reported.

2. APPLICATION OF BE METHOD TO THE MODEL GROUND

The magnitude of received wave signal of BE depends on the confining stress level of soil. Generally, signal of greater than 10mV can be obtained in the soil element test with applied confining stress of at least 10kPa. On the other hand, confining stress of model test is usually less than 10kPa and the received signal is as small as 10^{-2} mV. Therefore the signals are subjected to the effect of electric noise, as shown in Figure 1a. In this study, frequency of received signal was found to be less than 10kHz in most cases. Removing high frequency noise by FFT filter gives clearer wave signal as shown in Figure 1b.

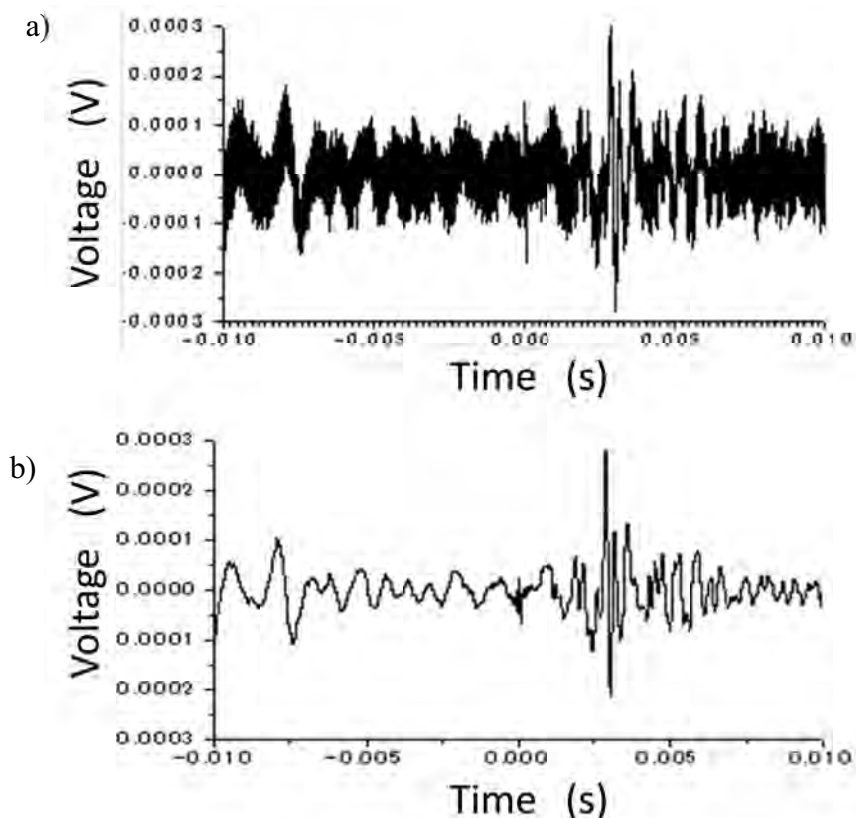


Figure 1: Example of received signal a) before and b) after applying FFT filtering

Arrival of the shear wave was interpreted by the first rise of the main wave, i.e. the wave with maximum amplitude, in the received signal. However, it was often difficult to identify the main wave.

When the transmitter and receiver elements are located near the wall of soil chamber, the wave transmitting near the chamber wall may arrive faster than the wave transmitting the minimum distance of the elements, and the shear wave velocity may be overestimated. In order to evaluate such phenomenon, Shv wave measurements (Fig.2) were conducted with pairs of BE located at different distances from the chamber wall in the dry Toyoura sand model ground. The location of the BE in the soil chamber is shown in Figure 3. The relative densities of the model ground were 60 to 75 %. Distances between transmitter and receiver were 10 to 20cm. The depth of soil cover was 16cm.

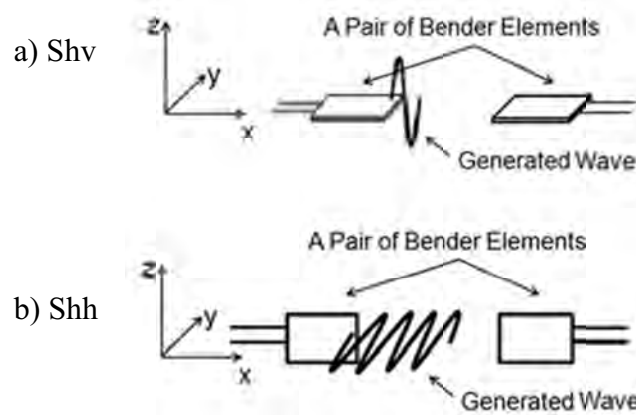


Figure 2: S_{hv} wave and S_{hh} wave generated by BE

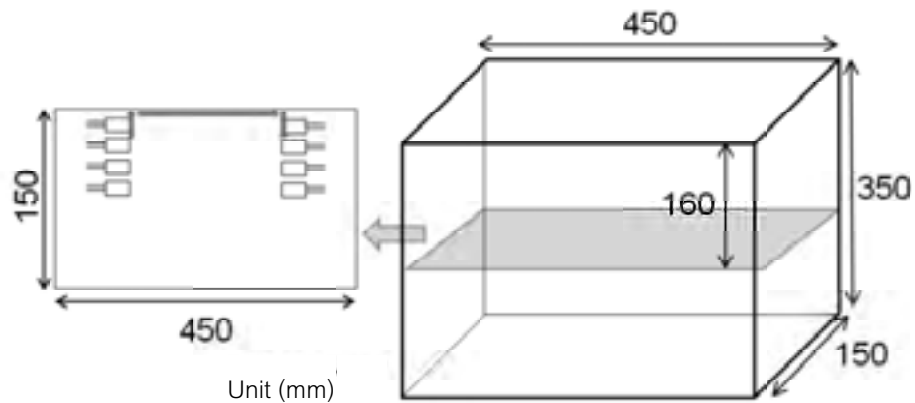


Figure 3: BEs location in the model ground in a soil chamber

An example of the result is shown in Figure 4. Apparent shear wave velocity was calculated by equation (2), assuming that the wave pass through the area near the chamber wall where the wave propagates faster due to the effect of confinement by the wall, as indicated by the arrow in Figure 3.

$$V_c = \frac{d}{l/v_s + d/v_b} \quad (2)$$

V_b, wave velocity near the wall, and V_s, wave velocity in soil, were assumed to be 320m/s and 120m/s, respectively. V_c is an apparent velocity, d is a distance between transmitter and receiver, l is a distance from the wall. Figure 4 indicated that conventional way of interpretation, i.e. the first rise of the received signal, agreed to the apparent wave velocity, while the interpretation adapted in this study was not affected by the chamber wall.

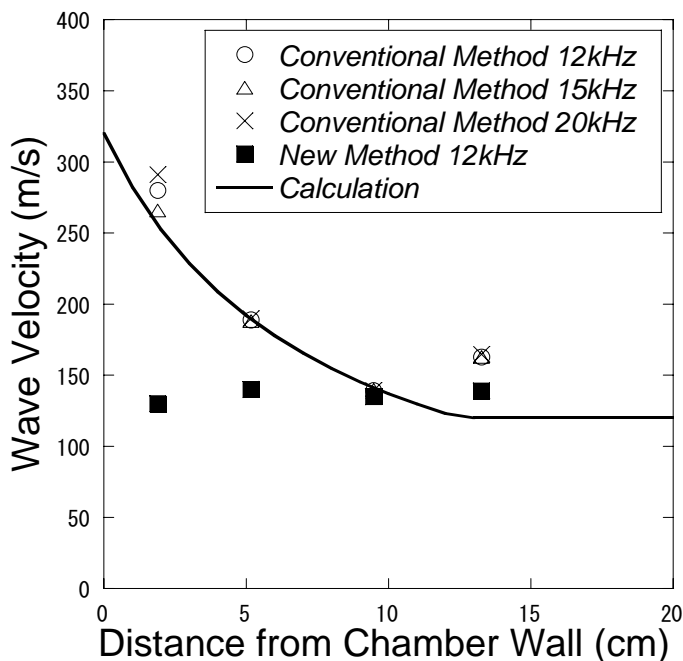


Figure 4: The effect of chamber wall in the BE measurement

3. DISTRIBUTION OF SHEAR WAVE VELOCITIES

3.1 Trap door apparatus

BE measurements were conducted in the trap door test. A trap door apparatus used in this study was developed by Ebizuka et al. (2010). A soil chamber for trap door testing is shown in Figure 5. It can accommodate model ground of 700mm wide, 294mm long and 555mm high. The base of the chamber consists of five separated movable blocks whose size is 100 mm wide, 294mm long and 105mm high, and fixed parts in both sides, in order to create uneven settlement in the model ground. Each base block is equipped with five two-way load cells to measure the load distribution on the base. When some of the base blocks are moved, the stress distribution in the ground should change. Tomography of shear wave velocity measurement was attempted in this soil chamber. Magnitude of shear wave velocity in soil generally reflects its small strain stiffness, which is mainly dependent on current state of density and stress. Technically speaking, then, the distribution of shear wave velocity may give some important information on the stress condition in the ground.

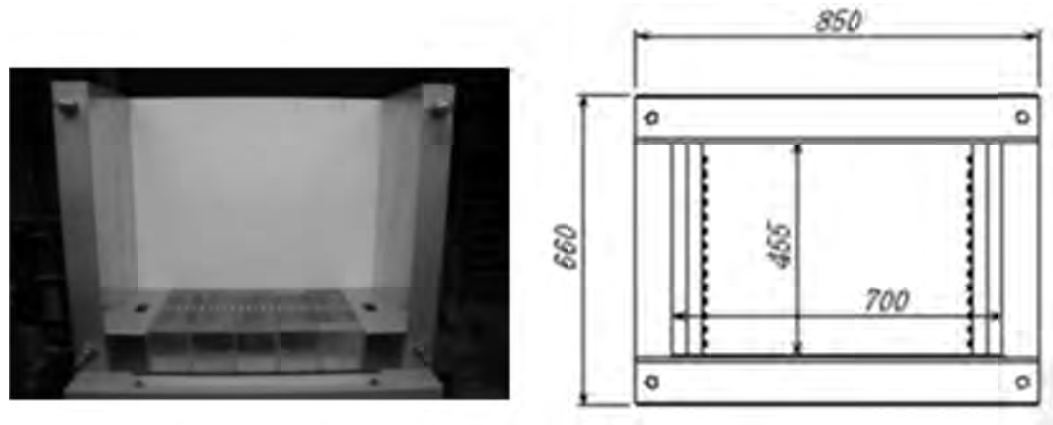
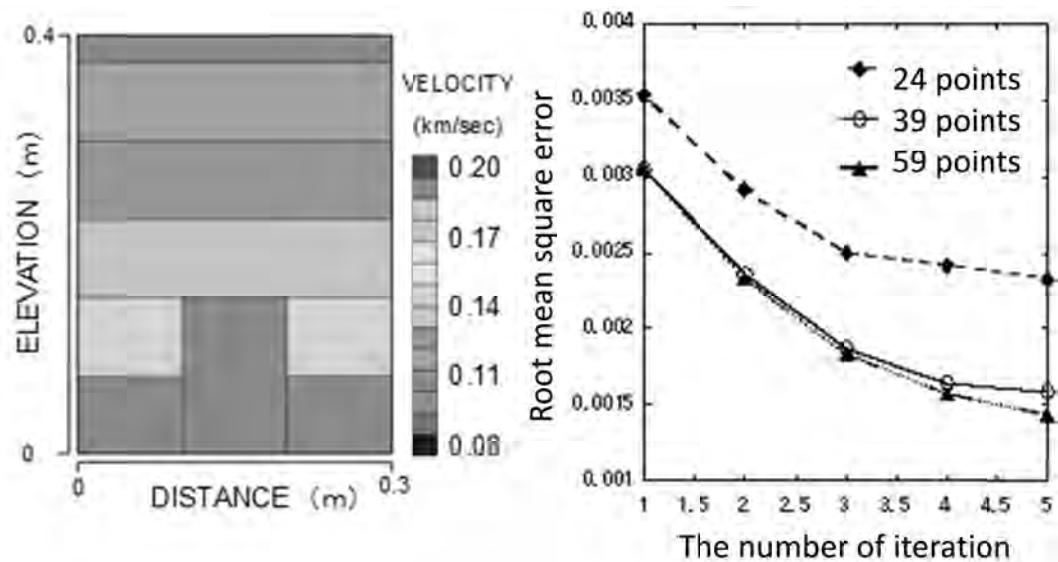


Figure 5: Soil chamber for trap door test apparatus

3.2 Required resolution in tomography analysis

A software called “E-tomo” developed by Dia Consultants Co. Ltd was used for tomography inversion analysis. In order to determine the number of BEs required for the estimation of shear wave velocities distribution, trial calculation was conducted assuming the model ground shown in Figure 6a. The number of measurement points was set to be 24, 39 and 59, and travel time was calculated for each case. Then, based on the calculated travel time, using E-tomo, the ground model was back calculated. Root mean square errors between original ground model and estimated model were plotted in Figure 6b, showing that increase in the number of measurements resulted in higher resolution of the model. Considering that measurement of 39 and 59 points did not show significant difference in RMS error, 39 points of measurement were selected in this study.



a) Wave velocities in assumed model ground b) Errors in estimated results

Figure 6: Preliminary calculation for determining the number of measurement points

4. SHEAR WAVE TOMOGRAPHY IN THE TRAP DOOR TEST

A uniform model sand ground was prepared in the trap door soil chamber using Toyoura sand. A set of shear wave measurements was carried out in the initial condition. Then two base blocks in both sides in the chamber was descended by 1mm, while only the center base block was remained. A set of measurements was conducted again to estimate the difference of wave velocity distribution. The arrangement of BEs in the soil chamber is shown in Figure 7.

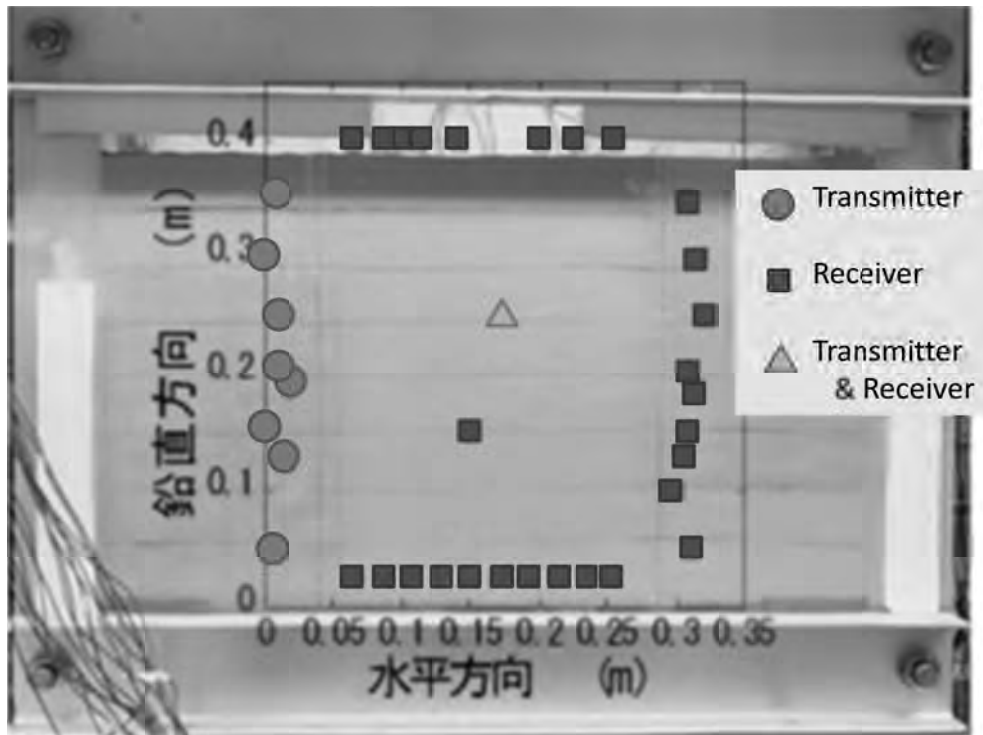


Figure 7: BEs arrangement in the trap door test chamber

4.1 Dense ground ($D_r=70\%$)

Figure 8 shows result of tomography analysis for a dense ground. Figure 8a, 8b and 8c present before and after the base blocks movement and wave travel paths, respectively. Shear wave velocities in the initial state were slower in upper part and faster in lower part, which agreed well to the feature of stress distribution in a uniform ground. Figure 8b shows that wave velocities are faster in the center and slower in sides. Difference of wave velocities of before and after the base block movement are shown in Figure 9 together with the shear plane appeared in the model ground when the base blocks was further descended to 10mm.

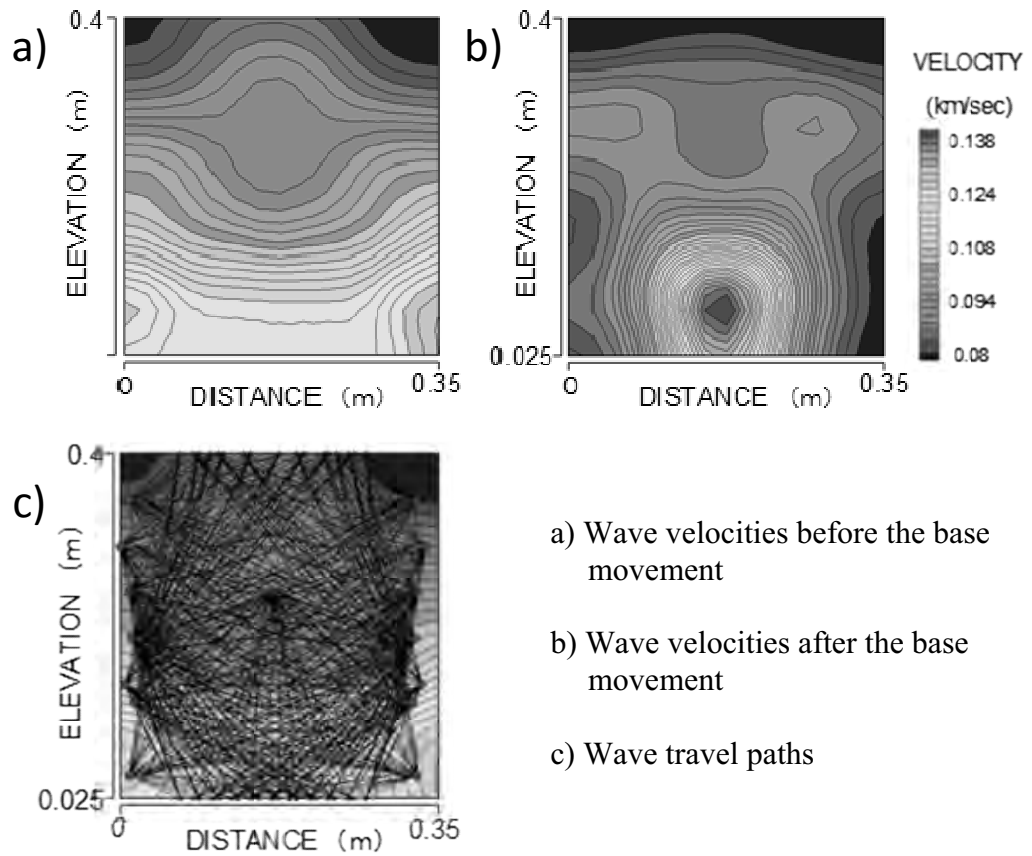


Figure 8: results of tomography analysis for dense ground

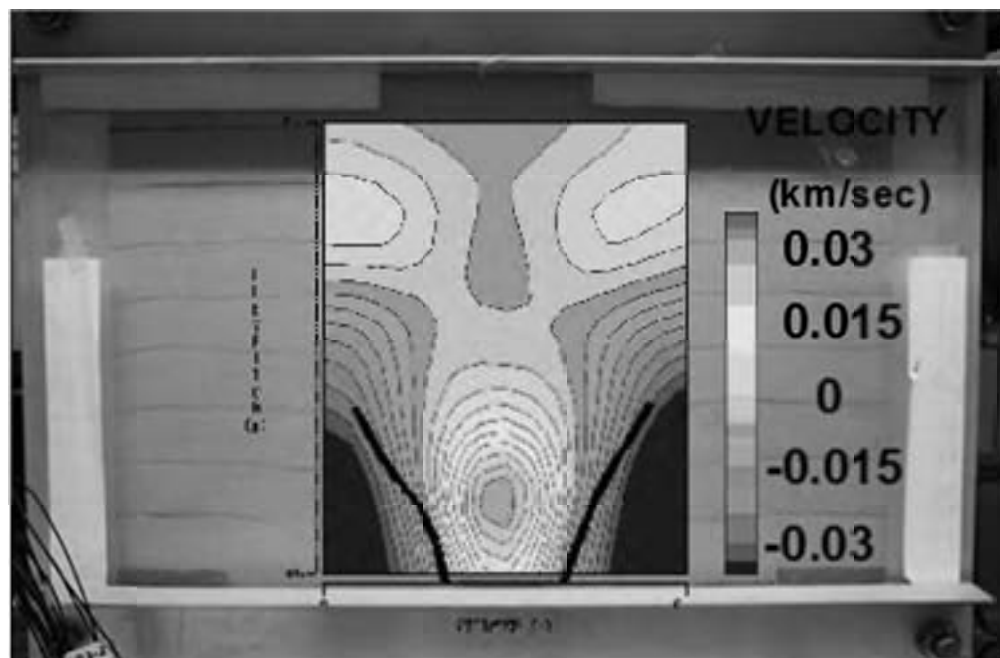


Figure 9: Comparison of tomography result and shear planes observed in the trapdoor test

Estimated wave velocities at the base are compared to the measured stresses in the trap door test. Using equations 3 to 5, estimated wave velocities are converted to mean principal stresses, where equation 4 is empirical relation for Toyoura sand.

$$G = \rho V_s^2 \quad (3)$$

$$G = 8919f(e)\sigma^{0.96} \quad (4)$$

$$f(e) = \frac{(2.17-e)^2}{1+e} \quad (5)$$

Comparisons of estimated and measured stresses at the base before and after the base block movement are shown in Figure 10a and 10b respectively. Although the estimated values did not agree completely in Figure 10, the tendency of stress increment and decrement are well captured and stress re-distribution by the block movement can be detected to some extent.

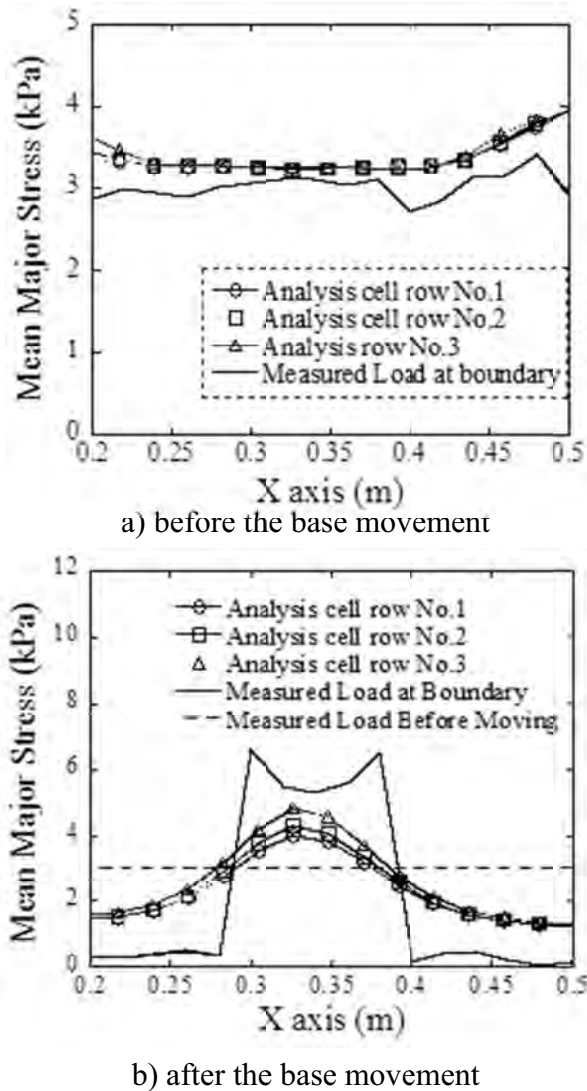


Figure 10: Comparison of estimated and measured stresses at the base

4.2 Loose ground ($D_r=40\%$)

For the loose ground, shear wave tomography did not give appropriate results as shown in Figure 11. Possible reason is that received signals of BE measurements in the loose ground were very weak and errors in the shear wave measurement may be significant.

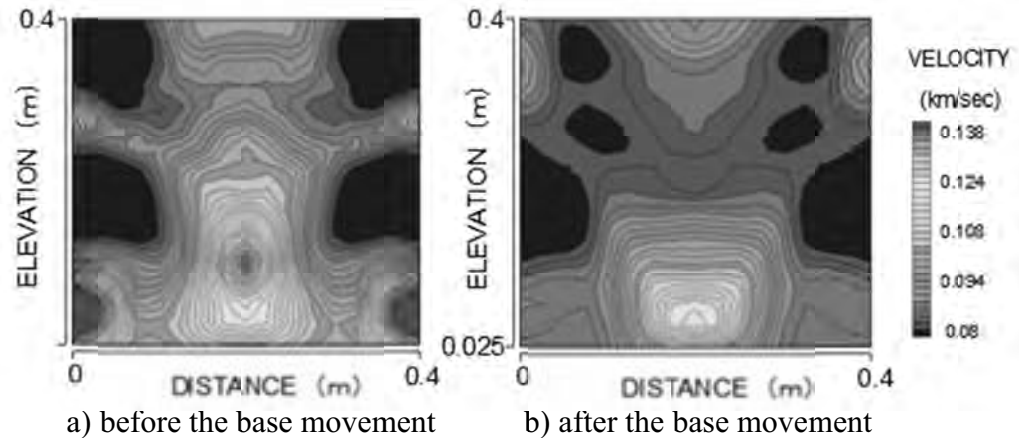


Figure 11: results of tomography analysis for loose ground

5. SUMMARY

Elastic wave tomography using bender elements was conducted to evaluate stress distribution in a model ground and following conclusions were obtained.

- When BEs are used in a model test, it was found that the signal processing was essential to obtain clearer waveforms as the amplitude of received signal was not large enough due to generally lower level of confining stress.
- The effects of chamber side wall should be taken into account in the arrangement of the elements location.
- In a densely compacted model ground in a trapdoor testing soil chamber, the distribution of stress in the ground was estimated using tomography technique and it agreed well with the results of physically measured stresses at the base. Shear planes observed during the trapdoor test also coincided well with the boundary of the ground between fast and slow wave paths.
- For a loosely compacted ground, the estimation of stress distribution was not successfully conducted, probably due to moderate change of the stress, i.e. the change of wave velocity.

Regulatory framework for modern urban housing

Sudhir MISRA
Professor, Dept of CE, IIT Kanpur, India 208016
sud@iitk.ac.in

ABSTRACT

Emergence of multi-storeyed flats as perhaps the only alternative in urban housing in view of the acute shortage of available land and concentration of infrastructural facilities in urban areas, has opened an entirely new paradigm from the point of view of regulatory mechanisms. It has also thrown a challenge to redefine concepts of ownership, property and insurance, to name only a few. The issues raised are equally relevant whether the discussion is on one room studios or luxury apartments. In the different phases of these projects – design, construction and maintenance – various agencies such as real-estate developers, architects, structural designers and contractors are involved, other than the owner of the flats. Government agencies or departments are expected to play a largely regulatory role in ensuring quality in design and construction and compliance with existing provisions. Further, with different flats in a building (or complex) being owned by different persons, the concept of ‘joint ownership’ of the complex and the ensuing ‘community living’ has become a reality, which also raises several questions relating to mutual understanding and responsibilities. Given the service life of apartment buildings and the need to maintain common systems such as electrical, plumbing, sanitation, etc. accurate record keeping and archival and retrieval of information for as-built drawings and construction records has also become important. The paper discusses common scenarios of multi-storeyed flat construction in India and also presents a brief summary of the relevant regulatory framework. Some difficulties in the latter are discussed in light of common practices and the need to urgently draw codes of regulation and defining roles and responsibilities of different stake holders is highlighted.

Keywords: multi-storeyed flats, regulation, laws, quality control, owner, builder developer, government, housing, urban, infrastructure

1. INTRODUCTION

Housing is a key component of infrastructure and developing economies across the world are struggling to provide affordable housing to their populace, and India is no exception. Several factor and processes that are closely associated with development, such as industrialization and urbanization, have led to migration of populations from rural to urban areas. This has placed infrastructural facilities such as housing in urban areas under even greater pressure.

In view of the acute shortage of available land and concentration of infrastructural facilities in urban areas, several cities around the world have seen the emergence of multi-storeyed flats as perhaps the only viable alternative in urban housing. This, in turn, has opened an entirely new paradigm from the point of view of regulatory mechanisms and thrown a challenge to redefine concepts of ownership, property and insurance, to name only a few. The issues raised are as relevant for one room studios as for luxury apartments. In other words, they encompass the entire breadth of the urban populace, regardless of their means.

Now, like in any other area of infrastructure development, there are several stakeholders – the owners (users), builders and regulators, to name the principal ones in a very simplified scheme of things. Further, during the different phases of these projects – design, construction and maintenance – these agencies play different roles, as is discussed later in this paper. In the specific case of the housing sector, the agencies involved could be identified as real-estate developers, architects, structural designers and contractors, other than the owner and user of the flats. Government agencies or departments play a regulatory role in ensuring quality in design and construction and compliance with existing provisions, etc.

Further, with different flats in a building (or complex) being owned by different persons, the concept of ‘joint ownership’ of the complex and the ensuing ‘community living’ has become a reality, which also raises several questions relating to mutual understanding and responsibilities. The Maharashtra Apartment Ownership Act, 1970 [*Maharashtra is one of the states in Western India with Mumbai as it's capital city*], and later the Delhi Apartment Ownership Act, 1986, are two of the early attempts in India to address issues related to citizens living in apartment complexes. They provide a framework for Associations of Apartment Owners, defined their structure and roles, and laid down model byelaws.

This paper discusses common scenarios of multi-storeyed flat construction in India and also presents a brief summary of Maharashtra and Delhi apartment ownership acts. The paper also discusses some concerns of the owners and possible remedies.

2. STAKEHOLDERS AND PROJECT LIFE CYCLE

2.1 Stakeholders

As mentioned briefly in the paragraphs above, the principal players in the housing sector in urban areas can be identified as the builder, owner and regulator, and the following paragraphs put their basic responsibilities in perspective.

Builder: in a generic sense, the term encompasses real-estate developers, architects, structural engineers and designers and contractors. In other words, an agency that is part of the system that plans, designs, builds, markets and sells the product (i.e. the apartment) to the user has been identified as a builder for convenience in this document.

Owner: this is the actual user of the apartment. No distinction is being made at this stage between a landlord and a tenant.

Regulator: the government or its agencies such as Municipal Corporations, etc. are responsible for the safety and welfare of the citizens, and are expected to

fulfill a very important role of ensuring a check on compliance with provisions of structural and functional safety, etc. Their role includes approving plans and designs in the pre-construction stage, inspection during construction and finally issuing a 'good for occupancy' certificate at the end of construction. In the maintenance phase, the regulator plays an important role through periodic inspections and approving major modifications.

2.2 Life cycle of an apartment block

Planning, design, construction and operation, are clearly the most common phases of the life cycle of an apartment block. In the planning phase, the builder acquires the land and draws up a master plan with the help of an agency making sure that the plan conforms to the Master Plan, and other requirements of the area or the city where the apartment is to be located. 'Design' phases involve drawing up of architectural and structural plans for buildings and other related facilities in accordance with prevailing regulations, codes and specifications. The construction phase is essentially the part where the facility is physically built by an appropriate agency. The owner comes into the picture directly only after the completion of construction, and begins to use the facility, which then enters the operation phase.

3.0 ROLES OF THE STAKEHOLDERS AT DIFFERENT STAGES

A closer examination of the stages in the life cycle above clearly shows that, in principle, planning, design and construction can all be completed by the 'builder' with approvals and compliance certificates coming from appropriate regulatory agencies. Once construction is complete, builders have only a limited role and the function of maintaining the facility is performed by Association of Apartment Owners, again within the ambit of the prevailing social and regulatory norms.

It can be said that the builder is the service provider for the owner, who does not have the expertise or resources to plan, design and construct the apartment. However, the owners take the responsibility of maintaining the built facility through the Association of Apartment Owners. It is therefore obvious that following proper processes during the planning, design and construction, is very important to facilitate proper maintenance during the operation phase. Given that the builder has only a limited role in the maintenance phase, and the owner may often be ignorant of the finer details of the earlier phases, it is the regulator's role to ensure that the interests of the owners are appropriately protected. Of course, the regulator also needs to ensure that the Owners also abide by the prevailing rules during the operation of the facility.

Clearly that whereas the role of builder is greatest during the initial stages (planning, design and construction) it rapidly diminishes in the maintenance phase, the converse can be stated for the involvement of the Owner. The role of Regulator is important throughout, though it acquires a different hue during operation compared to the earlier phases, and largely involves ensuring compliance with appropriate standards. Though the basic picture has been discussed above, the following sections briefly mention important steps in some of the common scenarios of flat building in India.

3.1 Scenario 1

1. Builder acquires land
2. Builder hires architects, designers for concept development of township, etc. which, in turn, involves the architect completing the concept plan and a structural designer completing the structural design
3. Builder approaches regulatory authorities and obtains required clearances
4. Builder identifies a contractor and commences the construction – at times the builder has his own construction division and carries out the construction activity in-house.
5. Marketing division of the builder sells flats to prospective owners
6. Builder obtains ‘occupancy certificate’ from regulatory authorities upon completion
7. Flat owners occupy the flats
8. Flat owners form an association or society for maintenance of the complex

3.2 Scenario 2

1. Prospective flat owners form a group or association
2. The group registers itself as a society or association, buys a plot of land, identifies an architect, structural designer, contractor, and obtains clearance from regulatory agencies (Steps 2 to 4 in Scenario 1)
3. The group supervises construction (may hire a consultant)
4. The group obtains the ‘occupancy certificate’ from regulatory authorities
5. The members of the society occupy the flats upon completion and jointly ‘manage’ or ‘maintain the premises.

3.3 Scenario 3

1. Government agencies announce and develop housing colonies.
2. Clearances become an ‘internal’ matter within the government agencies
3. Prospective flat owners apply to the government and are allotted flats
4. The government agency identifies the architect, designer, contractor
5. The government agency does the construction supervision
6. An occupancy certificate is obtained upon completion
7. Flat owners occupy the flats
8. Flat owners form an association or society for maintenance of the premises

4.0 THE REGULATORY FRAMEWORK

Though the Maharashtra and Delhi apartment ownership acts are only two of the several documents in the regulatory or government machinery, it is important to discuss some of the important clauses therein.

4.1 Association of Apartment Owners

The Acts lay great emphasis on the importance and role of the Association of Apartment Owners, and the following is a summary of its role.

- a) Provide for repair and maintenance of the facility
- b) Handling common resources and making appropriate investments
- c) Retain or rent on license common areas or facilities for commercial purposes
- d) Function as 'Employer' of workers, who may be employed for the purpose of maintenance of the property

4.2 Apartment Owners

The Delhi Act also seeks to define the role of the individual owners in the process of the community and shared living in apartment buildings. Some of the important points are mentioned below.

- a) Pay regularly towards maintenance of common facilities
- b) Perform maintenance and repair work within the apartment, including those for air-conditioning, etc.
- c) Facility to be used only for residential purposes
- d) Not carry out any structural modification without informing the association in writing.
- e) Not place any furniture, package, etc in the common area
- f) Rules of conduct such as playing the music, hanging garments, etc.
- g) Cannot have a line for telephone, etc. on the exterior of the building

5.0 INTERESTS OF OWNERS AND THEIR CONCERNS

Since the Owners are the long term users of the facility, it is important that their interests are accorded the top priority in all processes, and in fact the regulatory framework should ensure that. In other words it needs to be ensured that owners get a safe and good quality place to stay, and there are safeguards to insist that they maintain it in that manner. In this discussion it should be important to note that the issues related to quality of design, materials used in construction, workmanship, etc. are all very important and affect the overall durability of the facility. Some of the concerns that owners may have are given as examples in the following paragraphs.

Flow of information and proper checks: From the sequence of events given above (Section 3), it is obvious that only in Scenario 2 the Owners are involved in all steps and have complete knowledge about the details. In the other scenarios the owners only get to see the finished product and have very little real understanding of details of the material used, the specifications actually followed, the quality of workmanship, etc. In fact the final 'as built' drawings are only rarely available and properly archived. This is very important considering that: (1) the expected life of the facility is long and the need for serious repair action may arise several years later, when it may be difficult to trace the persons actually involved with the project, and, (2) having handed over the facility to the owners, the builder may not be inclined to get involved.

In Scenario 3, the regulatory authorities have a serious 'conflict of interest' in that the plans are being drawn up either by them (or directly on their behalf)

and being approved by another wing also under their direct or indirect control. Their continued role in the maintenance phase only compounds the difficulty.

Role of the Association of Apartment Owners: it should be remembered that the association need not have too many members who can understand the technical details of construction, maintenance and repair, and to vest the association with powers to take (technical) decisions may not be very wise, though very democratic. Two examples of this lacuna are given below.

Example 1: Though a provision that an owner can only carry out structural modification after informing the association in writing, is laudable, making it mandatory for the latter to respond within a stipulated period (failing which the owner can proceed with his plans) places the association under avoidable pressure.

Example 2: Granting the association a right to allow commercial activity in common areas can be understood in terms of resource generation for the facility, but there is no safeguard on evaluation of how an activity could affect the long term performance of the structure, and the association could make a genuine error, even if the activity has the 'support' of all the owners. Installation of small communication towers or hoardings on roofs or balconies, etc. could be relevant examples in this regard.

Rights to common areas and future expansion: common areas such as those left around building blocks or the roofs of buildings are prime examples where future 'expansion' may take place. This could be on account of changes in laws governing ground area coverage or the floor-area-ratio, over time. A greater protection than afforded at present is needed to ensure that the interests of the owners are adequately taken care of in this regard.

6. CONCLUDING REMARKS

It is clear that the provisions of the apartment ownership acts basically address the post construction regime and, are not adequately integrated with the provisions applicable at the time of planning, design and construction. The owner associations are thus handicapped in the discharge of their function of maintaining the apartment complexes for want of required drawings, details of construction, lack of technical expertise, etc. There is an urgent need to integrate and strengthen all provisions related to different aspects of apartment complexes. Given the scarcity of manpower in regulatory bodies, the possibility of involving and empowering professional organizations also needs to be actively explored.

Acknowledgement: Support from HUDCO for the study initiated in the area of regulatory framework for multistoreyed flat-type housing in urban areas is gratefully acknowledged

REFERENCES

Delhi apartment ownership act (1986): http://www.dda.org.in/tendernotices_docs/july09/THEDELHIAPARTMENTOWNERSHIPACT1986.pdf (Accessed September 25, 2012)

Maharashtra apartment ownership act (1970): http://www.bricksandbonds.com/downloads/pdf/MAO_1970.pdf, (Accessed September 25, 2012)

Conducting advanced technology of public transportation in Ulaanbaatar City

Mr V. Munkhjargal, Specialist of Construction, Urban Development and Planning Agency of Ulaanbaatar
munjigai@yahoo.com

ABSTRACT

It is an important matter that to discover based on research whether it is possible to conduct an advanced technology of public transportation named monorail in Ulaanbaatar ,which is attracted world countries in recent times and can be manner for the modern metropolis, while General Development Plan for Ulaanbaatar city until 2030 will be legalized and proved.

Conducting monorail research drafted in order to coordinate researches, projects and plans in public transportation for International Organizations, government and private sectors, further contribute to provide conditions of transport easily for citizens and solve urgent issues by applying complex system of public transportation.

GLOSSARY:

<i>Light Rail Transit /LRT/:</i>	<i>Type of metro, high capacity, small size /2 rail-tracks/</i>
<i>Metro /MRT/:</i>	<i>Type of metro, high capacity, large size /2 rail-tracks/</i>
<i>Bus Rapid Transit /BRT/:</i>	<i>A bus which has a high capacity and transit only insulated way</i>
<i>Monorail:</i>	<i>Type of metro, normal capacity, small size /1 rail-track/</i>

INTRODUCTION

We have resulted to research issues of developing public transportation by conducting advanced technologies in order to solve urgent issues in road traffic and public transportation of Ulaanbaatar city since recent years, especially 2008.

Experts, scientists, some well experienced international organizations such as Japanese JICA, The Asian Development Bank, government and private organizations have been studying the matter and introducing its results.

We have studied to choose this argument because, conducting advanced technologies such as monorail has main importance of solving urgent issues, making our city as one of world cities, on the other hand monorail provides people compatibility and safety of public transportation.

By conducting monorail in UB, has significant that to become free from traffic jam in order to reach from one place to another, save your time and use it for doing a kindness to others. In this research observation and comparative method were usually used.

MAIN PART

1. Planning monorail in UB which is advanced technology of public transportation

Monorail line will be planned as a circle; coordinate with subway, which are main lines are planned from west to east parallel as a Peace avenue, from north to south. We have already agreed this subway line solution.

Advantages of monorail are no need to free land to build monorail facilities, low cost, short time implementation. It is possible to build not to break a protective line which is an engineering line and settled under the main road of capital according to urban planning.

Choosing double pillar road for parts, which has seclusion lines in the middle of the road, is the best choice and it is possible that service points, which are on 1st floor of buildings beside the road, are settled under the bridge road with double pillar lines.

Monorail, which is able to implement for the shortest time, is planned to have 1-2 pillars and double bridge roads.

1.1. Monorail Line Planning

Monorail lines are planned to start from behind Peace avenue go through 3rd, 4th division's road, Ikh toiruu, Tsaiz market, then Officer palace's circle, which is about 12.3 km, "10 station", front side of Peace avenue to National park, 19th division, Gobi factor, through "Triangle bridge" and the Sapporo's circle parallel with subway basic line, turn around Moscow micro district.

Figure1. Monorail Line plan



- Monorail lines were planned behind a Peace avenue, which is about 12.3km, 10 stations, in front part is about 14.1 km, 10 stations, total length is about 26.4 km, 20 stations and the length between stations is 1.32km.

1.2. Monorail Station Plan

Monorail stations are planned to cooperate with features and their future planning. See more in followed table.

Table 1

Features and their future planning of Monorail stations

Stations code	Stations name	Length between stations /meter/	Features and their future planning	Tendency of station selection
M1	Way behind 1 st division- 1	331	It is planned to construct ger areas in south, front side of Unur division	Present, future
M2	Way behind of 1 st division - 2	1028		Present, future
M3	End of 3 rd , 4 th division	1637	There has the most passengers in this sector in 3 rd , 4 th divisions	Present
M4	10000 goods store	1300		Present
M5	Bayanburd's circle	1572	It is planned to construct south side of Denjiin 1000 and front side of 5 th division	Present, future
M6	3 rd school	1052	It is planned to construct south side of 7 th division and apartments in front, vertical transit station of metro	Present, future
M7	100 ail	838	Passengers of 11 th division and 100ail are concentrated.	Present
M8	Computer science and management school	1176	It is planned to construct apartment division of Sansar in front, Manba datsan in south	Present , future
M9	Tsaiz market	1867	It is planned to construct ger areas and has the most passengers in this sector	Present, future
M10	Officer palace's circle	1456	There has the most passengers in this sector, horizontal transit station of metro	Present, future
Line length of south side		12257		
M11	14 th division	1098	It is planned to construct 14 th division and Chuluun-Ovoo	future
M12	Narantuul market	1663	It is the most crowded market in the city	Present
M13	National park	1830	It is planned to construct apartment division and National park	Future
M14	120 thousand's circle	1535	There has the most passengers in this sector, is planned to reconstruct, vertical transit station of metro	Present, future
M15	White gate	1098		Present, future
M16	Gobi factory	1689	There has the most passengers in this sector	Present

M17	Loading and in loading brigade of railway	2091	There has the most passengers in this sector and large markets	Present
M18	Sapporo's circle	901	There has the most passengers in Unur division , It is planned to be minor center of the city in General Plan, horizontal transit station of metro	Present, future
M19	Kharkhorin market	1002	There is a market which has the most passengers, it is planned to construct apartment division in front and Unur division in south, horizontal transit station of metro	Present, future
M20	Moscow division	829	Unur division in east, Moscow division in west	Present, future
Depot	Hillside behind 1 st division	393	It is an ger area and the most convenient place to be settled depot	Present
Line length of front side		14129		
Total length		26386		

It is planned:

- For 7 locations based on its current environment and passenger concentration: end of 3rd, 4th division, 10000 goods store, 100 ail, Narantuul market, Gobi factory, stations near Railway brigade of loading and in loading and depot settled hillside behind of 1st division
- Planning of station near 14th division and National Park is based on future planning according to municipality,
- For other 12 stations based on its current environment and prosperity planning

Figure2. Coordinating manner of monorail stations and constructions



1.3 Planning of monorail road design, wheel and number of chain

It is planned to locate in separated side in the middle of road and build bridge beside road. It is planned to be 4.6 m from ground to bridge, width of bridge base is 1.5m, width of double way on bridge is 4.9 m, and sight of bridge construction and wagon is small. Also it is possible to use space under the bridge. There have 2-8 wagons in a chain. 14 passengers can sit, 18 passengers can stand in a wagon. In another word, maximum number of passenger in a wagon is 256. Nowadays, monorail wheels are made from compressed rubber to damp the noise.

Figure3. Road design, number of chain, and sight of wheel

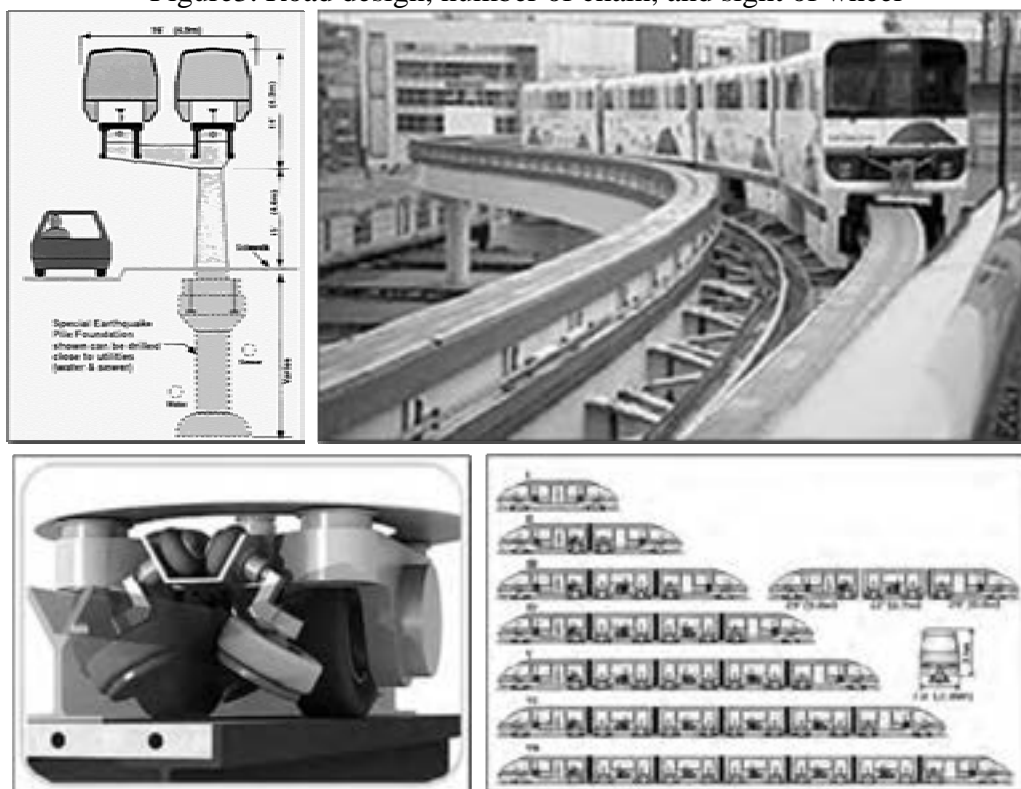


Table 2

Speed selection and available number of chain									
№	Type of speed	Speed Km/hour	Duration to north side (min)	Duration to south side (min)	Total duration (min)	Possible number of chain	Number of turn	Total number of output	
1	Slower	40	46.77	54.39	101.6	20	8	160	
2	Slow	50	39.42	45.91	85.33	17	10	170	
3	Middle	60	34.51	40.26	74.77	14	12	180	
4	High	70	31.01	36.22	67.23	13	13	169	
5	Higher	80	28.39	33.19	61.58	12	14	168	

Explanation:

- Train stops at station for 1-2 minutes
- Train spends 5 minutes between outputs
- Train travels for 15 hours (900 min) a day or from 7.00 to 22.00.

If average speed of monorail is 60 km/hour, monorail travels north side for 34.51 min, and south side for 40.26 min. (total 74.77)

1.4 Location planning of monorail depot

It is planning to build monorail depot at hillside behind of 1st division which is the most compatibility place. But now there is ger-area and it can be solved to free the land.

Figure4. Location of monorail, sight of depot design



1.5 Projects implementing in UB and comparative research

In recent years, there are many projects, which is dedicated to develop public transportation, have been implementing in Ulaanbaatar. Such as:

- “Technical assistance credibility to build subway in UB” done by Su Son group, South Korea
- “Urban transport development project” implementing on credit from Asian Development Bank
- ‘Development project of Railway and public transportation near Ulaanbaatar’ done by Bileg Capital LLC
- Report of implementing “Research of implementing public transportation project in Ulaanbaatar” by JICA which is combined projects.

1.5.1 “Technical assistance credibility to build subway in UB” or metro-LRT

According to 174th order of mayor, tender was announced for advising service with ‘Technical assistance credibility to build subway in UB’ on May, 2010. And ‘Geodesy’ company in Su Son group has won the tender and implemented. The main object of the project “Drafting technical assistance credibility of subway” is to make required research for planning subway line, which connects suburbs and across the city center, to decrease automobile growth in UB and environment pollution. According to planning, it is concluded that light metro is compatibility, and it is estimated to build subway in 5 years and yield in 30 years.

Figure5. Sight of LRT metro, station planning



Line planning:

It is planned to have 2 main lines: length of horizontal line across Peace Avenue is 28.38 km and length of vertical line from north to Chinggis Khan airport is 21.03 km. Also according to prospect, it is possible to build 26.48 km length line from new international airport which will be built in ‘Hushigtiin

hundii' . And it is planned to build bridge in suburb and build subway under 15m depth in city centre.

Figure6. Line planning of LRT and BRT



Station planning: It is planned that average length between station is 1-1.5 km, 21 stations along vertical line, 14 stations along horizontal line. Also there are 2 types of station which are beside of line and middle of line.

In forecast, it is necessary to spend 2 trillion 993 billion tugrugs to build horizontal subway. It included costs of administration, metro structure work, system, and engineering line system. 4 trillion 917 billion tugrugs is required to build 2 ways of metro. If the project starts to implement, construction will be finished to build in 2017 and it is estimated to yield in 2047.

1.5.2 “Urban transport development project” or BRT

In the framework of technical assistance of Asian Development Bank, “Urban transport development project”, which drafted in 2009-2010, was contained research to conduct BRT in UB public transportation.

According to research, it is concluded to conduct BRT and change current bus arrangement. Research team planned to build subway from north to south and from right to left or from Haniin material, Electric transmission to Ikh toiruu, Baga Toiruu, Sharkhad and Narantuul market.

Figure7. Planning BRT in UB



In most countries BRT is established by 2 types. First one is in the middle of road. Another one is public transport which transit on first line. It is estimated there are 22km, 28 stations bus for the first line of seclusion way. Asian Development Bank estimated 19.9 million dollars to build first line of seclusion way.

The project will be implemented 2012-2015. The second level of construction BRT will continue 2015-2018 and require 75 million dollars. And it is estimated that last level will continue in 2018-2020.

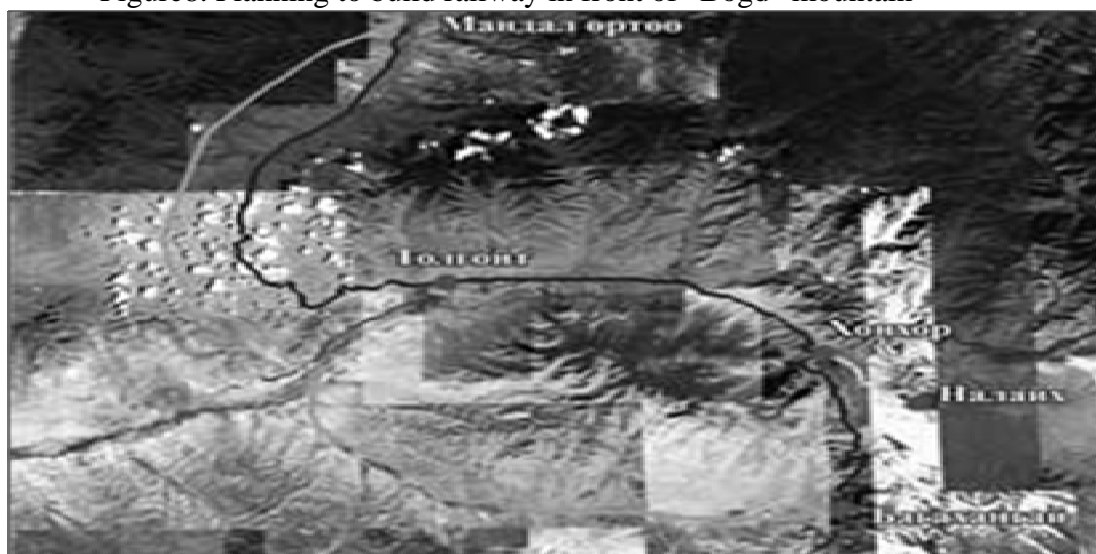
It is estimated that BRT will work by electricity not diesel fuel, length of BRT is 18 m and it contains 145 passengers.

1.5.3 “Development project of Railway and public transportation near Ulaanbaatar” or use current railway in public transportation.

“Bilig Capital” LLC drafted itself “Development project of Railway and public transportation near Ulaanbaatar”. This project will be helpful for fastening baggage turnover and widening railway surrounding UB. Also it is planned to decrease traffic jam by using railway in public transportation of UB. This project is estimated to implement in UB and Mandal, Sergelen and Bayan sum in Tuv Aimag.

Project makers: capital is surrounded by mountains. So it is inconvenient to pass baggage through the current railway, which constituted to coordinate with nature manners, without any artificial constitution such as bridge and subway. There’s too much waste to pass baggage through UB or mountainous region. Also there’s another solution not to transport explosive and poisonous baggage in centre of capital by building a new railway which surrounds UB from Mandal to Bagakhangai. According to planning ‘To develop project’, it is necessary to build 168 km length new railway.

Figure 8. Planning to build railway in front of “Bogd” mountain



After building this new railway, it is possible to use current railway in UB's right region or from Tolgoit to Amgalan by public transportation. There will be 23 km length way, and 27 stations. This will be a main line that average length between stations is 1.095 km. According to research, there will be a new railway from north of UB (from Bayankhoshuu, Baruun and Zuunsalaa) to centre of the city in second level. According to urban planning, there will be a new residence region in Nisekh and Yarmag. So traffic toward city centre will increase rapidly. It is possible to build new line by using roads derived from main line with low-cost.

It is estimated to waste totally 756.950 million tugrugs to implement the project. It includes road, stations, bridge constitution and trains.

1.5.4 Process of 'Research of implementing public transportation project in Ulaanbaatar'

The object of the research is to implement and operate project by becoming research object "first line or horizontal line (right to left line)", and comparing with other types of transportation, suggesting the best solution to cooperate between government and private sector and define every term and requirement to involve with technology and profit from private sector and ODA.

The research has started on Sept, 2011. It will finish on March, 2013. In another word, studying period is 19 months and the research has 3 goals. By now, 1st and 2nd goals are implemented generally.

Goal 1: To define social, economy and project implementing environment in Mongolia

Goal 2: To suggest and discuss a plan of implementing project "Cooperation between government and private sector"

Goal 3: To suggest structure and personnel of implementing project

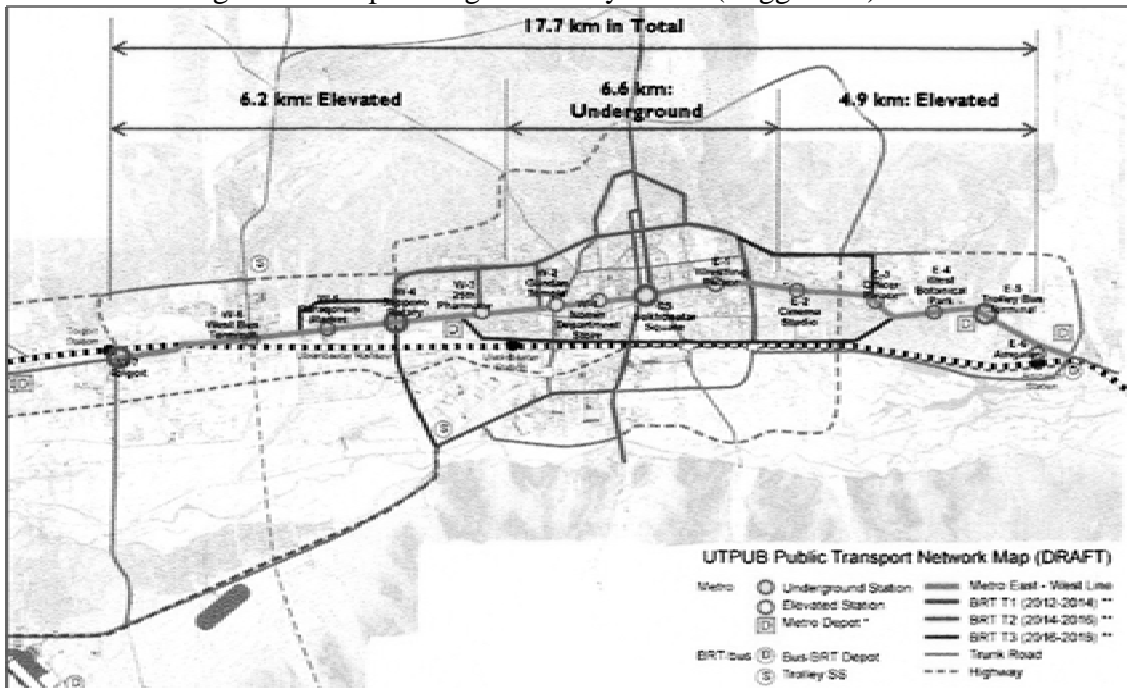
Main concept of constituting subway in Ulaanbaatar

40% of UB residents live near the Peace Avenue and there is constituted part near Sukhbaatar Square which includes public constitution, trade, service, and apartments. There's 3rd power plant located in right and supply apartments by heat and water under the ground.

Urban activities and transportation concentrate following Peace Avenue because Ulaanbaatar located from right to left, surrounded by mountains in north and south and the only main road from right to left is Peace Avenue. Research shows 2 million passengers transport in UB per a day and 700000 passengers (app 35%) pass through Peace Avenue. Also there are 58 main bus routes in UB and 21 routes (36%) of them passes Peace Avenue.

So the Peace Avenue is a main axis of city, which contains wide development opportunity for urban constitution strategy, plays an important role in urban activity, road transportation, and public enterprises. So as a result of research, MRT or railway is the most convenient transport system.

Figure9. First planning of subway in UB (Suggestion)

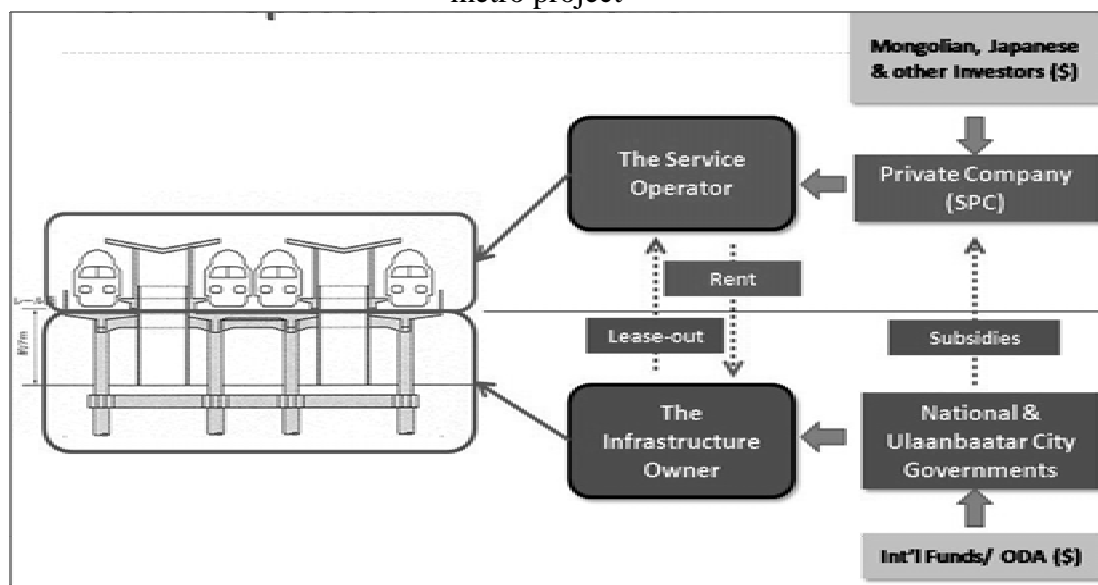


Resource: JICA research team

Structure of metro design:

There have 3 main metro structures: bridge, subway and on the ground. And we select it displacement variation depending on social, economy, environment influence, possibility of transportation, and flexibility with constitutions. Result of it, we have chosen the structure “subway in city centre and bridge in suburb”.

Figure10. Cooperation mechanism between government and private sector of metro project



It would be the best choice if subway constituted by state property and private sectors rent trains.

4 main terms to implement project:

1. Policy from Mongolian Government and its participation
 - The policy about implementing project of “Cooperation between government and private sectors”
2. Policy about constituting public transportation system
 - Constituting complex public transportation system that contain next 100 years
 - The main axis of the city metro infrastructure
 - Constituting efficient system of metro, bus, technical and order act
 - Efficient system that government cooperate with private sector
 - Constituting required legal environment
3. Government financing in infrastructure project
 - Planning to finance infrastructure related economic growth
 - Infrastructure frame and financing opportunity
4. Providing participation of private sector
 - Investment of private sector: Distributing available quantity, costs and investment risk
 - Implementing project method: Operating construction, activities and service of metro, trade service around the metro and providing surroundings efficiently.
 - Type of participation: Sort out, Tender, Unsolicited Private Proposal, Direct Appointment , Strategy Partnership
 - Choosing well experienced country in this sector for partner

1.5.5. Comparative research

Table 3

Comparison between metro line along horizontal axis and circle line frame

Content		Horizontal axis		Closed circle line	
		South Korea- Technical assistance credibility - LRT	JICA- Technical assistance credibility- LRT/MRT	South Korea- Technical assistance credibility -LRT	JICA- Technical assistance credibility- LRT/MRT
Structure	Land level	1.62 km	0	18.4 km	0
	Bridge	14.64 km	12.73 km	0	26.39 km
	Underground	12.12 km	6.62 km	0	0
	Total	28.38 km	19.3 km	18.4 km	26.39 km
Number of stations	Land level	1	1	20	0
	Bridge	8	8	0	20
	Underground	12	5	0	0
	Total	21	14	20	20
Cost/million \$/km/		80-150	67-88	1-15	40
Available period of construction		5 years	7 years	7 years	5 years
Method of making a subway		Digging /open/	Drilling machine	Digging /open/	Digging /open/

- It is smaller than MRT, LRT and investment and operation costs are lower because road is a concrete bridge. It is estimated that closed circle line that length is 26.39 km will be built for 5 years because there are short time implementation and lower excavation.

Table 4

Comparison between horizontal metro line and closed circle line planning

Content	Horizontal metro line			Closed circle line	
	South Korea- Technical assistance credibility	JICA- Technical assistance credibility		Project of ADB	Offering variant
		2020	2030		
Total length	28.38 km	17.64 km		18.4 km	26.39 km
To start operation	2017 year	2020 year		2020 year	2018 year
Demand	20.858 travel/hour	312.016 person/hour	486.975 person/hour	5.000-20.000 passenger/hour	7.000-25.000 passenger/hour
Maximum of passengers	4.135	10.729	17.767	20.000	25.000
Type	LRT	LRT/MRT		BRT	Monorail

Length between stations	1.32 km	1.36 km		0.4 km	1.32 km
Wagon	18 trains/4 wagons in the train/	10 trains/6 wagons in the train/	15 trains/6 wagons in the train/	128	15 trains/2-8 wagons in the train/
Filling	120%	180% /max/	180% /max/	-	180%
Number of passengers in chain	469	1.430	1.430	-	192-256
Rush-hour output	Per 6.7 min	Per 8.0 min	Per 5.0 min	-	Per 5.0 min
Average speed	35 km/hour	39 km/hour			40-80 km/hour
Output/per a day, one direction/	129	71	109	54	160-180
Period	47.5 min /one side/	27 min /one side/		-	31-50 min /one side/

- It is possible to arrange monorail chain depends on passenger flow and it saves your time and money.

Table5

Comparative SWOT analysis between Bus Rapid Transit /BRT/ and Monorail

Indicator	Project of ADB – BRT	Offering variant – Monorail
Advantages	<ul style="list-style-type: none"> - Short-time working, flexible line selection because of lower cost - Short term implementation - Low risk due to get accustomed for passenger’s consumption 	<ul style="list-style-type: none"> - Traffic jam can’t effect and passengers needn’t wait to transit easily - It is convenient to plan a closed circle road, because traffic radius minimum is 30 meter - Low vibration, low sound and low exhaust. - Smaller than MRT, LRT, lower investment cost and operational cost because road is a concrete bridge - Excavation is lower, short term implementation - Constant transit hour because it is fully automatic and has own road.
Disadvantages	<ul style="list-style-type: none"> - To obstruct because it is driven on public road. - Harmful to nature because it makes a noise and generates vibration 	<ul style="list-style-type: none"> - It is impossible to plan acclivity and declivity because slope quantity is 6 percent. -Passengers must transit on bridge stations .
Opportunity	<ul style="list-style-type: none"> - It is possible to connect bus service. - It is possible to use the road 	<ul style="list-style-type: none"> - It is possible to control and arrange depends on passenger flow. - It is possible to plan to build stations in

	as a normal road if there is a lower demand.	constructions. - It is possible to use space under the bridge.
Risk	- Other transports might follow rule of insulated way.	- It is stopped when it damages on the way.

- It is shown by SWOT analysis that choosing monorail is more effective than closed circle line.
- It is necessary to plan stations with best terms for passengers and to prevent external influence for the design.

Table 6

Total cost comparison between bus, LRT and monorail

№	Operation cost	LRT	Monorail
1	Cost and income per 1 km/mile	\$6.95/\$11.17	\$1.55/\$2.50
2	Cost and income per a hour	\$150.00	\$38.00
3	Total cost /a year/	\$12,621,150.*	\$4,000,000.*

Resource: O&M project which implemented abroad

- It is estimated that monorail operation cost is less than LRT by 4 times but it has lower capacity.

Table 7

Comparison between construction work cost and operation cost

№	Indicator	To plan LRT subway, its depth is 15meter	To plan bridge monorail
1	Construction work cost /per 1 km/	66 billion tug	40.1 billion tug
2	Operation cost /per 1 km/	1 billion tug	700 million tug

Resource: Technical assistance credibility drafted by “Su Son” group

- It is shown that construction work cost of bridge monorail is less by 26 billion tugrugs per 1 km than LRT subway.

Table 8



Investment comparison required public transportation systems

№	Indicator	Horizontal axis		Closed circle line	
		South Korea- Technical Assistance Credibility	JICA- Technical Assistance Credibility	Project of ADB	Offering variant
1	Type of system	LRT	LRT/MRT	BRT	Monorail
2	Line length /km/	28.38	17.64	18.3	26.39
3	Required investment /tugrugs/	3 trillion	1.7 trillion	566 billion	1.1 trillion
4	Operation cost / per a year, per 1 km/	1 billion	1 billion	800 million	700 million
5	Period of yielding	30 years	6.7 years /EIRR/	26 years	21 years
6	Average sale of tickets /per a day/	-	200 million	100 million	200 million

- Cost of 1km length of monorail line is estimated and taken from Korean Technical Assistance Credibility.
- Cost of unit of BRT is taken from researches of ADB.
- It is estimated that supposed ticket price is 400 tugrugs and 500000 passenger transit per a day.
- It is estimated that there will be 2 million transits in 2011, 4.5 million transits in 2012 and 6.4 million transits in 2030 by JICA research.

Table 9

Coordinated manner of planned monorail stations and metro stations planning

№	Type of transit stations	Depiction	Stations code	Stations name	Description
1	Unequal level transit station of metro and monorail		M6 M10 M14 M18	- 3 rd school, - Officer's palace's circle, - 120 thousand's circle, - Sapporo's circle,	Transit stations M6, M14, M15 is along horizontal axis, M10, M18, M19 is along vertical axis
2	Equal level transit station of metro and monorail		M15 M19	- White gate - Kharkhorin market	

- It is possible that transit stations of metro and monorail are located on unequal level or equal level of line.

Coordinated manner of planned monorail stations and road planning

- It is necessary that the bridge road cooperated with M5 or Bayanburd's circle; M16 or Gobi factory station, M18 or Sapporo's circle and it is possible to discuss unequal and equal level line while processing.
- M18 or Sapporo's circle is necessary to detail where settled road, metro and monorail lines.

Figure11. Required location of cooperated with monorail stations metro line and bridge road

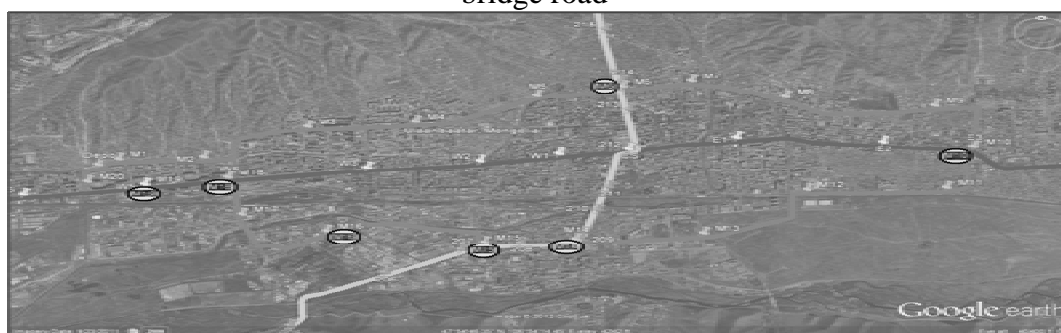


Figure12. Sight distance comparison between monorail lines and road



- It is possible to plan on seclusion line and beside road.

SUMMARY

- It is important to solve and implement to conduct beneficial, convenient public transportation system in Ulaanbaatar based on combining the projects.
- Public transportation system such as metro, monorail require much primary investment and it is possible to generate income from ticket moreover, from service centers under the bridge and real estate market along the lines.
- Public transportation investment, which prefers social benefit into human than ecological benefit, economical benefit and others, is different between other investments as any investment is implemented for economic benefit.
- It is absolutely necessary that government consider to be developed with private sector because metro and public transportation system is a strategy development issue of the city.
- Finally, If Ulaanbaatar city was an apartment, 12 floors even 30 floors apartment wouldn't have an elevator according to general plan of 1950 which planned no elevator for 5 floors apartment.

REFERENCES

- "Underground city" research, 2011 year.
- "Opportunity of conducting monorail in UB" research, 2011 year.
- "Building metro in UB - Technical Assistance Credibility", SU SON group, South Korea, 2011 year.
- "Urban Transport Development Project", Asian development bank, 2010 year.
- "Development project of railway and public transportation near Ulaanbaatar" "Bileg capital" Co., LTD, 2010 year.
- "Research of implementing public transportation project in Ulaanbaatar", JICA, 2012 year.
- <http://www.wikipedia.org/> <http://www.google.com/>

The relationship between pedestrian perception and characteristics of sidewalk environment in case of the central area of Ulaanbaatar City

Amgalan SUKHBAATAR¹, Noboru HARATA², Nobuaki OHMORI³

¹ Lecturer, SCEA, Mongolian University of Science and Technology, Mongolia
amgalans@gmail.com

² Dean of the School of Engineering, Professor, Dept. of Urban Eng., School of Eng., The University of Tokyo, Japan

³ Associate Professor, Dept. of Urban Eng., School of Eng., The University of Tokyo, Japan

ABSTRACT

Walking is basic mode of transportation, recommendable for the city center, especially for the city center with continuous increase of car traffic and high traffic congestion, like central Ulaanbaatar. Most of sidewalks in central Ulaanbaatar have not been designed based on pleasure to pedestrians but mostly on considerations of completing a construction of footpath anyway due to the mainly economic constraints. Even in constraint of given budget, pleasant sidewalks would be designed based on the consideration of its user's preferences. Addressing this situation, the research aims to identify physical and operational aspects of sidewalk environment affecting people's preference of pleasant sidewalks. People's perception was assessed from the questionnaire survey with area based sample size of total 200 samples. Physical and operational features of sidewalk environment were measured during the field measurement at 12 sidewalk segments from 3 city blocks, as well as at the laboratory. After summarizing collected data, applicable statistical method, ordered probit models were developed to analyze respondent's rating for sidewalk environment factors depending on the combination of sidewalk attributes and characteristics of each individuals. Based on model results, physical and operational features of sidewalk environment affecting people's preference were signified quantitatively.

Keywords: walking, pedestrian perception, sidewalk environment, central district

1. INTRODUCTION

Walking is basic mode of transportation recommendable for the city center, especially for the city center with continuous increase of car traffic and high traffic congestion, like central Ulaanbaatar. Within the central district of the city, walking level of pedestrians can be increased by good quality of pedestrian environment. On the other hand, pedestrian's satisfaction level depends on their perception of the characteristic of pedestrian environment such as physical component ratio of sidewalks they use. Therefore, it is important to understand the

relationship between pedestrian perception and characteristics of sidewalk environment in order to increase people's walking level and to provide good quality of environment.

According to the Study on City Master Plan and Urban Development Program of Ulaanbaatar City, over 1 million trips are generated by mode of walking per day. It is 31 percent out of total trips generated daily. However, walk trip duration and distance are short. The quality of walk trip is also unsatisfactory due to the poor quality of environment. Most of sidewalks in the central area of Ulaanbaatar city have not been designed based on pleasure to pedestrians but mostly on considerations of completing a construction of footpath anyway due to the mainly economic constraints. Even in constraint of given budget, pleasant sidewalks would be designed based on the consideration of its user's preferences. Another, functional problem in practice is lack of coordination or comprehensive researches on urban development plans and urban transportation programs of Ulaanbaatar city for small scale. Urban development plans on street level are not clearly coordinated with any other comprehensive plans, affective engineering techniques.

1.1 Research Objectives

The main objective of this research is to identify the physical and operational aspects of the sidewalk environment affecting people's preference of pleasant sidewalks for walking in the central area of Ulaanbaatar city, by exploring the relationship between pedestrian perception and characteristics of sidewalk environment. Specific objectives:

1. Assess the physical elements and operational aspects of selected sidewalk segments from the central area of Ulaanbaatar city in terms of required factors for the existing sidewalk environment
2. Quantify how well sidewalk elements influence to the pedestrian perception of sidewalk environment
3. Identify which physical elements and operational aspects tend to generate more walkable sidewalk environment for all users in the central area of Ulaanbaatar city

2. METHODOLOGY

2.1 Selection of Sidewalk Segments

Based on the characteristics of city blocks in the central area of Ulaanbaatar, 12 sidewalk segments from 3 blocks were selected to assess the physical and operational aspects as well as pedestrian perception of sidewalk environment (Figure 1).

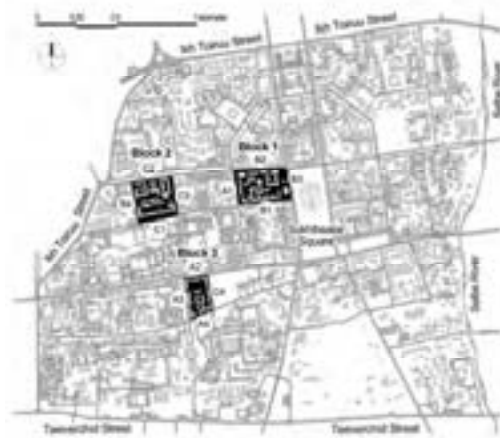


Figure 1: Map of selected sidewalk locations

Block-1 consists from predominant office, public administration, health care and other institutional land-uses. Block-2 consists from mixed use with institutional and commercial land-uses. Block-3 consists from predominant residential land-uses with 5 storey apartment buildings surrounded by retail or commercial land uses with one storey variety of small shops, cafe, fast foods, and small restaurants. Sidewalk segments on surrounding streets of the city blocks were selected and classified into 3 types by similarity of physical components and operational condition. Original street names were represented as block-letter mark with ordered numbers in order to recognize easily for further steps of analysis. Guide mark for the street names and description of the current condition of sidewalk environment as follows:

A1 – Segment of Baga Toiruu Street: It is most typical street in central Ulaanbaatar with variety of small shops, fast foods and small restaurants serving to the adjacent area. Concrete sidewalk path with narrow effective width caused by entrances of these small service spots becomes crowd mainly during lunch time or after work hours.

A2 – Segment of Enkhtaivan Avenue: Sidewalk on Enkhtaivan Avenue, the busiest street of Ulaanbaatar, has relatively high crowd of pedestrians among selected sidewalk segments in both day and evening time due to its link characteristic of major arterial road and existence of commercial facilities.

A3 – Segment of Tserendorj Street: Along the sidewalk segment of Tserendorj Street, variety of small commercial facilities exists. Since utilization of the sidewalk environment from city establishments is inadequate, small enterprises of these facilities provide some part of physical improvements only for the front space of their facility.

A4 – Segment of Seoul Street: Many service and retail facilities exist in this street. Security concerns are implicated by some types of service facilities such as cafe, bar and karaoke rooms working till night in this street segment.

B1 – Segment of Khuulichid Street: It is a typical street with predominant office and institutional land-uses in central Ulaanbaatar. Existence and utilization of physical components of this sidewalk environment is relatively well enough comparing other selected street segments.

B2 – Segment-1 of Sambuu Street: Mostly office and institutional buildings exist in this segment. Pedestrian flow rate of this sidewalk segment is relatively high due to the characteristics of major arterial road as well as physical environment characteristics including wider sidewalk path.

B3 – Segment of Sukhbaatar Street: This street segment exists adjacent to the most primary places of the city. Therefore, presence and utilization of physical components are relatively adequate among selected street segments.

B4 – Segment of Tumurchin Street: Even though physical environment of Tumurchin Street is being improved in recent years, general image of the street among its users is still unpleasant seeing the environment with disordered features.

C1 – Juulchin Street: Among selected street segments, this street has the widest footpath. Safety concern of pedestrian-vehicle conflict is considered as safe enough due to its car-free street characteristics.

C2 – Segment-2 of Sambuu Street: Physical characteristic of this segment is somewhat similar with the characteristic of B2. However there are some specific differences which are the absence of green strip, poor utilization of road lighting, busy vehicle access ways and narrow footpath width than B2's.

C3 – Segment of Baruun Selbe Street: Due to the surrounding mixed developments and the existence of one particular commercial center in this segment, amount of parking space is relatively high. Well utilized street furniture and wider footpath are the pleasant characteristics of this segment. However, there are some types of poor operational condition such as unauthorized parking on vehicle access ways.

C4 – Segment of Khanddorj Street: A sidewalk on this street segment has typical characteristics of collector road sidewalks in central Ulaanbaatar with narrow concrete footpath, few physical components and relatively less rate of pedestrian flow.

2.2 Survey Design

The questionnaire survey has been designed to ask pedestrian's subjective evaluation of 12 different sidewalk segments by 7 factors for each, in 5 point scale with 1 being low and 5 being high score. Sidewalk environment factors required to the current situation of the central area of Ulaanbaatar were used for the evaluation. Factors are: (i) Convenience, (ii) Comfort, (iii) Safety of pedestrian-vehicle conflict, (iv) Security, (v) Access to the Service, (vi) Visibility and (vii) Attractiveness of sidewalk environment. As for the identification of sidewalk segments on the questionnaire sheet, photographs taken at each sidewalk section were used to identify sidewalk segments. In addition, the survey has been designed to ask respondent's socio-economic and walk trip characteristics by questions with answer options.

2.3 Data Collection

Field survey data collection including questionnaire survey data collection and field measurement or observation process was continued from August to September 2010. Previous research papers and relevant studies were reviewed to define attributes of sidewalk environment. Although numerous variables were considered in during research review, total 18 of physical and operational

variables have been determined as important characteristics for the study area of this research.

A paper based questionnaire survey was conducted among sidewalk users traveling and working in the central area of Ulaanbaatar with area based sample size of total 200 samples. 103 questionnaire surveys were conducted in the selected city blocks. 97 questionnaire surveys were conducted among the general public of Ulaanbaatar city. Survey sheets were distributed at work places of respondents then collected back after two days. Questionnaire survey data consist of numerical values from the subjective evaluation on 7 factors of selected sidewalk segments, qualitative data from the information of respondent's individual characteristics and open comments describing urgent issues related with the sidewalk environment of Ulaanbaatar city.

Physical attributes of sidewalk environment were measured during the field measurement and at the laboratory. The footpath effective width was measured on site considering a 'shy distance' and obstacles on the sidewalk path. A footpath actual width and the building front space were measured at the laboratory using sidewalk map. Amount of each footpath surface material was calculated based on the sidewalk map and photographs. The adjacent land-use type, vehicle access ways, distance from moving vehicle and street furniture were counted from the map as well. Sky area ratio was calculated at the laboratory using photographs.

Operational condition of each sidewalk was observed during the field measurement as well as at the laboratory using photographs and video records of sidewalks. Photographs were taken in both of day and evening times. Video records were recorded at sidewalk section, for 15 minutes, weekday and weekend days. Pedestrian flow counting process records how many sidewalk users are walking on the sidewalk path while the pedestrian counter participants are assessing the selected section of the sidewalk. Volume of pedestrian flow, in both directions primary flow and counter flow was counted for 15 minutes in day time, 20 minutes in evening time, weekdays and weekend days. Presence of street vendors and on street parking was counted during the field observation. At the laboratory using photo elevation of sidewalk segments, open entrances of adjacent building were counted for both of day and evening time.

3. DATA SUMMARY AND ANALYSIS

3.1 Data summary

After the field survey data collection, subjective evaluation scores for each sidewalk segment were summarized by each factor. Descriptive statistics result shows that two particular sidewalk segments, B4 and C2, have relatively low evaluation scores for all factors. Due to the consideration of subjective evaluation score for the sidewalk segment B4 potentially affected by the limited identification of photograph used on the questionnaire sheet, data of B4 was excluded from analyses. As for remaining sidewalk segments, two types of assumption for how pedestrians perceive the sidewalk environment were assumed in further analysis:

1. Pedestrians perceive the sidewalk environment as a section - the component ratio of section or segment of the sidewalk

2. Pedestrians perceive the sidewalk environment as a whole - the component ratio of whole length of the sidewalk

Meantime, necessary variables of sidewalk attributes were transformed into module variables depending on assumptions.

3.2 Factor Analysis

The linear regression analysis was performed in order to determine the correlation between factors and attributes of the sidewalk environment. Using the sidewalk section assumption, sum of subjective evaluation scores for each factor of sidewalk segments and module value of related objective measures were used in regression analysis. In addition, using the sidewalk length assumption, sum of subjective evaluation scores for each factor and sum (or mean value for some attributes) value of related objective measures were used in regression analysis. The results from two types of regression analyses between access to the services and evening time service entrances show that the coefficient of determinations, R^2 (s), are relatively high at 0.65 and 0.43 among other correlations. It suggests that people's perception of access to the service in the sidewalk environment of the central area is correlated with mainly evening time service entrances. Next relatively high values of the coefficient of determination, R^2 0.37 and 0.49, were found in regression analyses between attractiveness of sidewalk environment and presence of recreational land-use. The result of total 50 regression analyses shows that coefficient of determinations, R^2 (s), range from 0.0005 to 0.65, still low values. It was presumably caused by summation of different types of pedestrian characteristics.

3.3 Model Estimation and Comparison

Based on results of factor analyses and the applicability to analyze information of people's perception and characteristics of sidewalk environment, the quantitative statistical method, ordered probit model was selected to analyze respondent's rating for sidewalk environment factors depending on the combination of sidewalk attributes and characteristics of each individuals. Using above mentioned two assumptions, two types of ordered probit model for all factors were developed. Dependent variable y was identified by the observed score of respondent's subjective evaluation for sidewalk environment factor from the questionnaire survey. As for the model with sidewalk length assumption, explanatory variables x were identified by the combination of sum (for all attributes except footpath width) and mean (for average width of all sub-segments) values of sidewalk attribute measures and respondent's socio-economic characteristics. As for the model with sidewalk section assumption, explanatory variables x were identified by the combination of module (for all attributes except footpath width) and real (for footpath width at the section) values of sidewalk attribute measures and respondent's socio-economic characteristics. Total 14 models were tested. Number of observations varies from 2177 to 2183.

Comparing determination coefficients, the Pseudo R -Squared for the goodness of fit of models, more fitting model in the set of observed measures for each factor was selected. The Pseudo R -Squared values of the model using sidewalk length measures are slightly higher than values from the model using sidewalk section

measures for Convenience (0.062 > 0.043), Comfort (0.055 > 0.043), Security (0.015 > 0.008) and Access to the Service (0.059 > 0.055). Contrary to these results, the Pseudo R-Squared values of the sidewalk section model are slightly higher than values from the sidewalk length model for Safety (0.057 > 0.056), Visibility (0.007 > 0.004) and Attractiveness (0.036 > 0.032). However, models have limited explanatory competence, the Pseudo R-Squared values range from 0.007 to 0.062. Based on the comparison of determination coefficients, models using sidewalk length measures for Convenience, Comfort, and Security; and the model using sidewalk section measures for Safety were selected. Model results show that most of physical/operational variables are statistically significant at the 95% level. Additionally, marginal effects on subjective scores were tested.

4. FINDINGS AND RECOMMENDATIONS

4.1 Findings and recommendations on Physical / Operational variables

Comparing the coefficients of footpath actual width (-0.03) and effective width (0.32) from the length model for convenience (Table 1), it can be seen that not only fully paved sidewalks, the sidewalk type that has more effective width is much convenient for walking in pedestrian's view point.

Table 1: Summary of Results from the Length Model for Convenience

Variable class	Variable	Coefficient	t statistics
	Constant	0.74	7.34***
Physical	Tree	0.01	1.33
	Footpath actual width	-0.03	-1.02
	Footpath effective width	0.32	9.35***
	Trash can	0.01	0.77
Operational	Day time ped. flow	-0.0062	-13.57***
	Evening time ped. flow	0.0030	13.29***
Socio - economic	Age	0.04	2.23*
	Gender (Male)	-0.02	-0.44
	Daily walk duration	0.0012	1.47
	Winter effect	-0.12	-3.52***
	Trip purpose (Leisure)	-0.09	-1.87
	Primary mode (Walking)	0.02	0.25
Threshold parameter index			
	μ 1	0.83	31.08***
	μ 2	1.73	61.98***
	μ 3	2.70	71.45***

*p < .05, **p < .01, ***p < .001

The result of marginal effect shows that the increase of footpath effective width is associated with the increased choice of higher subjective scores (0.065 y=4, 0.057 y=5) for convenience. In order to improve subjective evaluation for convenience

by using the estimated model, change for the increase of existing effective width is applicable, particularly for the street segment A1 and C2.

From observation and subjective evaluation of selected sidewalk segments, it can be seen that high volume of pedestrian flow does not directly indicate better sidewalk environment. From the length model for convenience (Table 1), coefficients of day time pedestrian flow (-0.006) and evening time pedestrian flow (0.003) indicate that people do not feel convenient with other pedestrians during day time. Underlying reasons should be explored in more specific studies.

As a result of length model for comfort (Table 2), negative coefficient of the concrete surface material (-0.0005) indicates that increase of concrete pavement has negative impact on subjective evaluation.

Table 2: Summary of Results from the Length Model for Comfort

Variable class	Variable	Coefficient	t statistics
	Constant	1.26	15.52***
Physical	Tile surface material	0.0002	11.28***
	Stone surface material	0.0036	11.52***
	Concrete surface material	-0.0005	-9.64***
	Age	0.05	2.33*
Socio - economic	Gender (Male)	-0.02	-0.40
	Daily walk duration	-0.0004	-0.53
	Winter effect	-0.11	-3.20**
	Trip purpose (Leisure)	-0.12	-2.59
	Primary mode (Walking)	-0.01	-0.22
Threshold parameter index			
	μ 1	0.80	31.30***
	μ 2	1.73	60.76***
	μ 3	2.78	65.94***

*p < .05, **p < .01, ***p < .001

In order to improve subjective score of comfort, it is necessary to pay more attention for the utilization and reconstruction of concrete sidewalks in the central area including sidewalk segment A1, A3, B1 and C4. Result of marginal effects on subjective scores for comfort shows that the increase of natural stone surface material is associated with increased choice of higher subjective score (0.001 y=4, 0.001 y=5).

Positive coefficient of the distance from moving vehicles (0.03) shows that people feel safer in the street with green strips (Table 3). Contrary to this result, negative coefficient of adjacent parking area (-0.17) indicates that people are more likely to feel unsafe in the street with large parking space. Result of the marginal effect shows that the increase of distance from moving vehicles is associated with increased choice of higher subjective scores (0.004 y=4, 0.006 y=5) for safety. In order to improve subjective evaluation score of safety, plant of the green strip separation with proper width is applicable for the street segment C2 and C3.

Table 3: Summary of Results from the Section Model for Safety of pedestrian-vehicle conflict

Variable class	Variable	Coefficient	t statistics
	Constant	1.78	17.24***
Physical	Adjacent parking area	-0.17	-9.99***
	Dis. from moving vehicle	0.03	2.84**
	Vehicle access ways	-8.56	-1.71*
Operational	On street parking	-0.83	-12.92***
Socio - economic	Age	-0.0021	-0.11
	Gender (Male)	0.05	1.17
	Daily walk duration	-0.0023	-2.81**
	Primary mode (walking)	0.17	2.67**
Threshold parameter index			
	μ 1	0.78	30.46***
	μ 2	1.50	55.34***
	μ 3	2.33	65.76***

*p < .05, **p < .01, ***p < .001

Negative coefficient of vehicle access way (-8.56) shows that people's perception of safe environment decreases when number of vehicle access ways increase. During the field observation, day time, it was being seen that most of these vehicle access ways (in A2, A3, B2, B4 and C3) are occupied by temporary parking. Therefore, responsible agencies should pay more attention on unauthorized parking on vehicle access ways.

The comparison of coefficients of road lighting (0.1) and sidewalk lighting (0.03) shows that road side lighting can be more effective element than sidewalk lighting to increase pedestrian perception of security in high priority (Table 4).

Table 4: Summary of Results from the Length Model for Security

Variable class	Variable	Coefficient	t statistics
	Constant	0.42	3.12**
Physical	Road lighting	0.10	5.77***
	Sidewalk lighting	0.03	6.71***
Operational	Street vendors	-0.02	-1.74
Socio - economic	Age	0.06	2.80**
	Gender (Male)	0.12	2.54*
	Daily walk duration	0.00	-1.04
	Trip purpose (Leisure)	-0.17	-3.73***
	Primary mode (walking)	-0.02	-0.24
Threshold parameter index			
	μ 1	0.82	33.12***
	μ 2	1.73	61.27***
	μ 3	2.72	63.04***

*p < .05, **p < .01, ***p < .001

From the result of section model for attractiveness, positive higher coefficient (266.2) for arts, entertainment, and recreational land-use shows that the sidewalk type adjacent to the art or recreational facilities is more pleasant for walking in pedestrian perception. However, this affect is related with good utilization of surrounding environment and general image of the area.

Negative coefficient of cross direction advertising stands (-2.99) indicates that the increase of road side advertising stand has negative impact on the visibility of sidewalk environment. Accordingly, advertising stands that are not necessary to the function of the street should be reduced.

4.2 Findings and recommendations on Socio – Economic variables / Walk trip characteristics

Coefficients at significant level for age variable (0.045, 0.047, and 0.06) indicate that younger people do not feel existing sidewalks are convenient, comfortable, secure, and attractive. There are no significant influences regarding to the gender. Only, as it is natural for security concerns, male (0.12) feel existing sidewalk environment of the central area of Ulaanbaatar as secure. The result shows that people's consideration of better safety for pedestrian-vehicle conflict and access to the service decreases due to their walk duration increases. Negative coefficients of winter affection (-0.12 for convenience, -0.11 for comfort and -0.09 for attractiveness all in significant level) indicate that people highly affected by winter condition feel existing sidewalks are uncomfortable, inconvenient, and not attractive. Therefore concerns related with weather condition such as non-slip footpath surface tiles and availability of public recreational facilities on the sidewalk environment should be taken into consideration in further design processes.

5. CONCLUSION

Statistical models used in this research describe the relationship between pedestrian perception and characteristics of sidewalk environment by using subjective evaluation and objective measures of existing environment. Results suggest that both of physical and operational characteristics should be taken into consideration for street level improvement programs of Ulaanbaatar city. More statistically reliable factors to the pedestrian perception might be taken into consideration for further relative studies. Although most of findings are quite natural, overall findings of this research might draw attention on the pleasance of sidewalk environment for street level improvement programs of Ulaanbaatar city.

REFERENCE

Almec Corp., Japan International Cooperation Agency (JICA), Ministry of Road Transportation, Construction, and Urban Development of Mongolia (MRTCUDM): *The Study on City Master Plan and Urban Development of Ulaanbaatar City*, Final Report, Vol. 2, 4-26, 2009.

Relation between urbanization and natural disaster risk in mega cities - Lessons from Tokyo -

Takaaki KATO
Associate Professor, ICUS, IIS, the University of Tokyo, Japan
kato-t@iis.u-tokyo.ac.jp

ABSTRACT

At present, the Tokyo metropolitan region has two kinds of natural mega hazards: M.7 class inner-plate earthquakes and large-scale floods. The Central Disaster Prevention Council, which is the supreme organization of disaster affairs in Japan, has warned about both in published reports. It stated that Tokyo has enormous exposed risks, and tremendous amounts of damage were estimated in the disasters. The present natural hazard risk in Tokyo is closely related to the process of urbanization in the city. As for earthquake disasters, Tokyo has broad wooden crowded areas that are vulnerable to the spread of post-disaster urban fires. The risk has accumulated in two periods of rapid urbanization. The reason primarily lies with urban planning, which does not include the concept of natural hazard risk management—that is to say, urban planning yields to the high pressure of urbanization. This problem has been the main issue with urban earthquake disaster planning in Tokyo for the last four decades. On the other hand, the risk of large-scale floods is not apparent at present. Tokyo has not experienced a large-scale flood for the last century thanks to river management; however, the risk will surely grow in response to climate change. Tokyo has what is called a “below-sea-level city,” which is hugely vulnerable. I can point to two failures that account for why it has been generated: urban planning and hazard control. These cases show that urban planning is significant in natural hazard risk management. In this study, I show the structure of natural hazard risk in mega cities and discuss the role of urban planning in risk management, as well as present necessary countermeasures to consider in urban planning.

Keywords: urbanization, natural disasters, urban vulnerability

1. MEGA-HAZARD IN TOKYO

Tokyo has two kinds of mega hazards: earthquakes and large-scale floods corresponding to climate change. The earthquake probability in the next thirty years is estimated at 70% by the government. On the other hand, large-scale floods present only a small risk at present, thanks to flood control by river management, but the risk will surely increase in response to forthcoming climate change. A few decades from now, it will be a serious problem.

1.1. Earthquake Hazard

In Japan, earthquake damage estimation is a common feature of a municipality's disaster prevention plan and includes the latest damage estimation by the Tokyo metropolitan government. In this estimation, four earthquakes are assumed as an earthquake scenario. The damage situation is influenced by time and weather conditions; for example, they may be assumed as occurring at 18:00 in winter under a wind velocity of 8m/s. Figure 1 shows the results of ground shaking for a Northern Tokyo Bay earthquake scenario, which creates maximum damage. Maximum intensity will be JMA Seismic Intensity upper 6, which is the level at which tremendous damage occurs. The area of intensity upper 6, colored orange in the figure, covers 70% of the entire ward districts where urban stock is concentrated. Most of the area covers the eastern region of Tokyo, in which the possibility of liquefaction is also greater. We understand that the cause for this is that the ground structure in the east area of Tokyo is relatively weak.

Ground shaking and liquefaction cause buildings to collapse. The spatial distribution of building damage is shown in figure 2 and is concentrated in east Tokyo. Two reasons for this are the high seismic intensity and the possibility of liquefaction. Another reason is the unplanned accumulation of many crowded old wooden houses in the highly dense area. Vulnerability to building damage is seen in structures in which the buildings were constructed on weak ground.

Moreover, post-earthquake urban fire spread might occur in a mega-city. The firefighting power in Tokyo is adequate; however, the number of fires that break out after an earthquake is estimated to be much greater than the available firefighting power, resulting in an enormous amount of fire damage. Burnt areas in Tokyo are estimated to total approximately 100 square kilometers. For reference, the 1995 Hanshin-Awaji earthquake disaster resulted in some amount of damage being caused by post-earthquake urban fire spreading; however, it was approximately 65 ha, which was much less than the estimated amount of damage in Tokyo. Figure 3 shows pictures of the current situation of the typical vulnerable districts to post-earthquake urban fire. Large numbers of flammable houses were built and spread with narrow roads across wide-ranging areas. The spatial distribution of fire damage is different from collapsed buildings. It distributes in a doughnut-shaped pattern, centering on CBD of Tokyo.

The history of urbanization in Tokyo shows that it has had two periods of rapid urbanization. The first is a recovery period that occurred after the Kanto earthquake disaster in 1923. Many fires broke out after the earthquake, and due to strong winds, the fires spread, burning down most of the urbanized areas in Tokyo and Yokohama. A lot of people lost their houses, and an absolute shortage of houses occurred. To supply temporary residences for the large number of evacuees became a priority issue. At the same time, the government had to reconstruct the central district of Tokyo and therefore could not afford to plan and construct urban infrastructure. As a result, the fringe of the central district, which had been farmland, had been urbanized by huge numbers of poor-quality houses.

The second period was a high economic growth period that began in the early 1960s, after World War II. In the war, Tokyo was burned down again by bomb attacks. The situation was similar to the 1923 Kanto earthquake disaster. Tokyo had suffered from a lack of housing. Furthermore, Japan entered into a high economic growth period after the Korean War in the early 1950's Tokyo's economic growth promoted immigrants from across the country to flock to Tokyo.

The situation caused the housing shortage to worsen. Tokyo had to continue to provide temporary housing for residents for a long time. In the same manner as the 1923 Kanto earthquake disaster, numerous poor-quality houses began accumulating in the absence of urban planning.

The areas formed in these periods are nearly equal to the current vulnerable areas, as shown in Figure 4; therefore, we can say that Tokyo failed to control vulnerability in the periods of rapid urbanization. There are two reasons for this failure. The first is that, at the time, urban planning commissions had little knowledge about how to control for disaster risks because economic growth had taken priority.

The second is that the speed of urbanization was so high that there was no time or ability to make urban plans and construct urban infrastructures. As a result, urban planning for disaster mitigation adopted a style that assumed it would always be able to keep pace with problems as they occurred. Up until now, as I mentioned, the problems have not yet been solved. It takes a long time to solve past urban problems.

A lesson learned from Tokyo is that it is important to prevent problems before they occur or to mitigate problems when they occur. Japan should have had long-range plans and should have incorporated the concept of risk management into urban planning in a period of rapid urbanization.

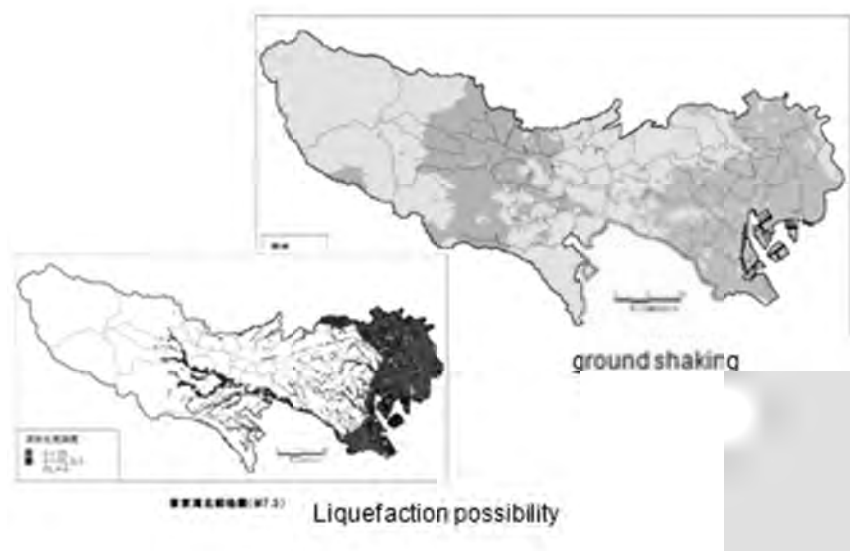


Figure 1 Spatial distribution of ground shaking and the possibility of liquefaction in Tokyo in an earthquake scenario (TMG, 2012)

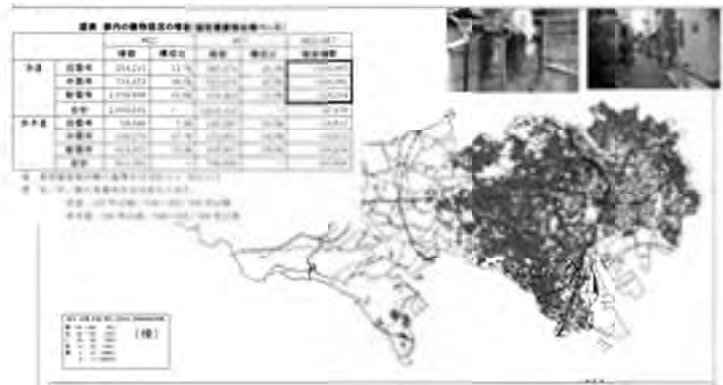


Figure 2 Spatial distribution of collapsed buildings in Tokyo (TMG, 2012)

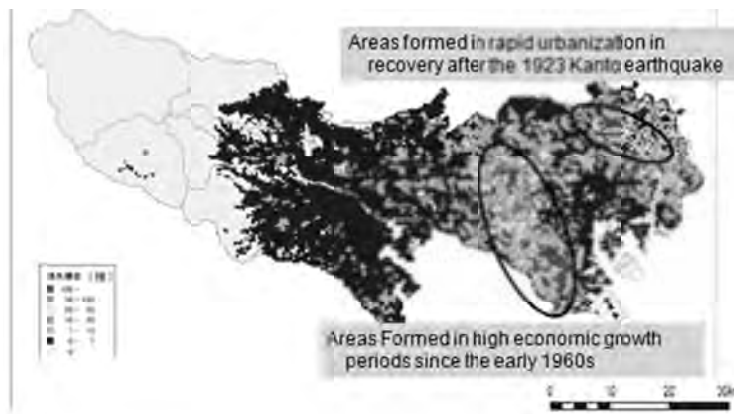


Figure 2 Spatial distribution of post-earthquake urban fire spreading in Tokyo (TMG, 2012) and in urbanization areas in two rapid urbanization periods.

1.2. Large-Scale Floods

Tokyo has below-sea-level areas in the eastern area, as shown in Figure 4. The pink area in the figure is under sea level. The deep pink shows the area under the low tidal level. This area has an accumulation of low-rise buildings and approximately two million people live in the area. Tokyo is obviously very vulnerable to flooding. Figure 5 is a zoom shot of the area. It has many black or red buildings, which are estimated to be under water in case of flooding. In the picture on the right, the red arrows show the water level in the event of a flood. It can be understood that the water level will reach very high levels if a flood occurs.

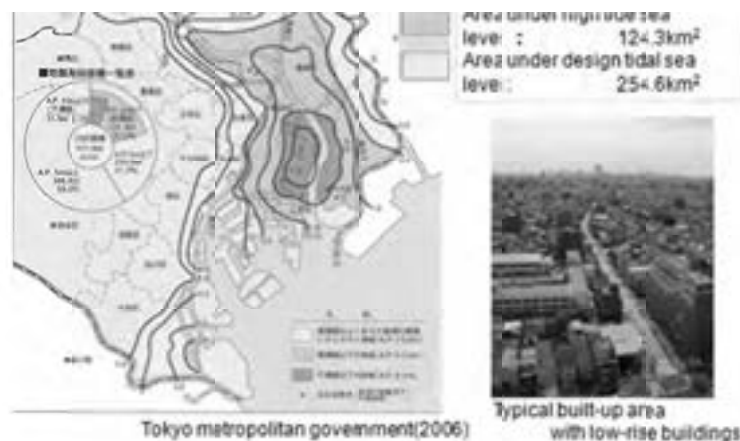


Figure 4 Ground level in Tokyo and a picture of a typical area in Tokyo



Figure 5 Inundation of below-sea-level city in case of flood, focusing on buildings

At present, the municipality has a legal obligation to publish a hazard map. A hazard map of Katsushika city, which is located in the east area of the Tokyo metropolitan area, shows that there is no evacuation space in the neighborhood because the entire city area will be inundated in the event of a flood.

Approximately 300,000 people should evacuate to another city located more than 10km from their hometowns. Mass transit such as buses and railways is the planned means of transportation. It is nearly impossible for huge numbers of citizens to evacuate because of the capacity limitation of transportation. Moreover, even if evacuation is successful, they will have to remain in the evacuation area for a long period of time; estimations suggest they will remain in the evacuation area for more than 20 days after the bank is repaired. The current situation means that the city fundamentally has no acceptable solution for a below-sea-level city.

Failure to control large-scale flooding is the result of two past failures related to industrialization and urbanization. One is ground subsidence corresponding to industrialization. The graph in Figure 6 shows a history of ground subsidence. Subsidence continued until thirty years ago, when regulations were established to forbid ground water pumping. Regulations came too late, however. The maximum length of subsidence is about 5 meters on the report, but it may actually be longer. The second reason for failure is urbanization. Figure 7

shows maps from 100 years ago to the present. The current urbanized area was a rural zone until only sixty years ago. It is already a recognized ground subsidence in this region. In spite of this situation, urbanization in the form of low-rise houses had expanded into the area under sea level for these sixty years. If urban planning in those days had included the concept of risk management for flooding, or if urban planning had prevented urbanization in the areas, or if urban planning had built up the area with high-rise buildings, the present risk would likely be dramatically smaller. We can say that failures of hazard control and urban planning created a “below-sea-level city.” The reasons for a large-scale flood risk are basically the same as for an earthquake.

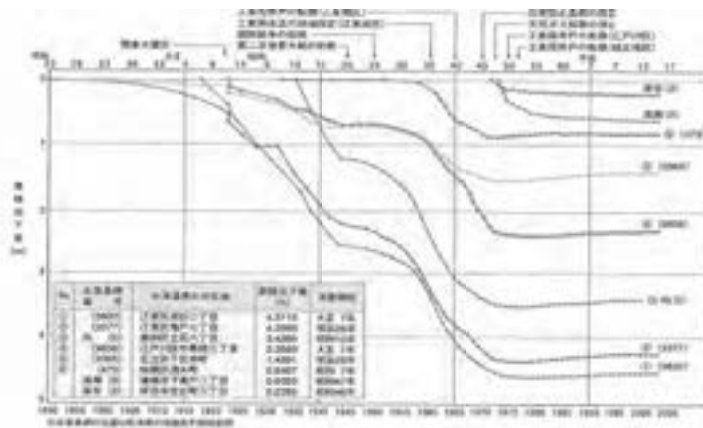


Figure 6 Historical record of ground subsidence in Tokyo (TMG)

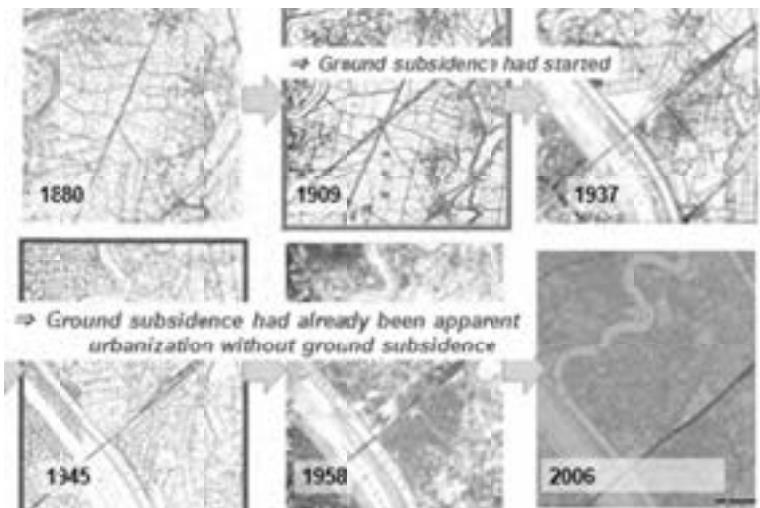


Figure 7 Urbanization in a typical area of Katsushika city over the past 100 years

2. STRUCTURE OF DISASTER RISK

It is understood that the current risk in Tokyo is related to past urbanization. I consider the structure of disaster risk in a mega city. Natural disaster risk can primarily be explained by four factors, as shown in Figure 8: hazard control, a city’s location, accumulation, and vulnerability.

Hazard existence is the fundamental factor. Japan must consider earthquakes and floods as hazards.

The first risk factor is hazard control, such as construction of a river dike in the event of flooding, but it obviously has limitations. Hazard control for earthquake hazards is inherently impossible, although control for large-scale floods has proved valid. In fact, large-scale floods have occurred for over the past fifty years; however, climate change will weaken limitations. The amount of risk that hazard control cannot cover is pushed to urbanized areas.

Risk in urbanized areas can be explained by three factors: location, accumulation, and vulnerability. The second risk factor is the location of the urbanized area. If an urbanized area overlaps the spatial distribution of the hazard, it produces a risk. The typical cases involve urbanized areas that are located in flood-prone areas and in weak ground that produces earthquake shaking, as previously mentioned. Expansion of urbanization should be controlled by urban planning.

The third risk factor is accumulation of urban stock, such as building facilities and lifelines. If accumulation is small, the entire amount of damage will necessarily be small. If the entire amount of damage is small, it is easy to rescue the afflicted area and support its recovery. However, accumulation is one of the fundamental and unique characteristics of mega cities; therefore, it is appropriate to consider that it is uncontrollable. In addition, the functions of urban planning include density control of urbanized areas; therefore, controlling accumulation would be possible.

The term, “exposure risk,” which is generally used to explain the process, is considered to be equivalent to location multiplied by accumulation.

The fourth and most important risk factor is vulnerability—in other words, the quality of the urbanized area from the viewpoint of disaster risk. Vulnerability can be explained by balancing two factors: physical fragility, such as building fragility and lifeline fragility; and the resilience and response abilities of society, such as the firefighting and evacuation abilities of local communities. For example, an old town is generally fragile, but if young people work and live there, their resilience and response abilities are high; therefore, we can say that the town may be not vulnerable. In contrast, if old people, who are vulnerable in terms of physical strength, live in modern buildings, such as high-rise apartments, they will suffer from even slight outages of lifelines. Moreover, the resilience and response abilities of society are supported by two factors: physical factors, such as evacuation areas, roads, and firefighting facilities; and social systems, such as evacuation planning and community-based education. Recent urban planning includes community-based improvements, management, and activities for the future, which are called *machidukuri* in Japanese. It deals with all of the abovementioned sub-factors. Urban planning can control vulnerability.

I consider these four factors basically as explanatory parameters of mega risk in a mega city. All of the factors, except hazard control, are parameters that can be controlled by urban planning; therefore, I can say that the present actual disaster mega risk is capable of being solved in theory by urban planning. Therefore, we should consider future urban planning by focusing on this viewpoint over the next decades. At the same time, we should pay attention to the current balance of these factors and the monitoring system of disaster risk that will be needed in planning.

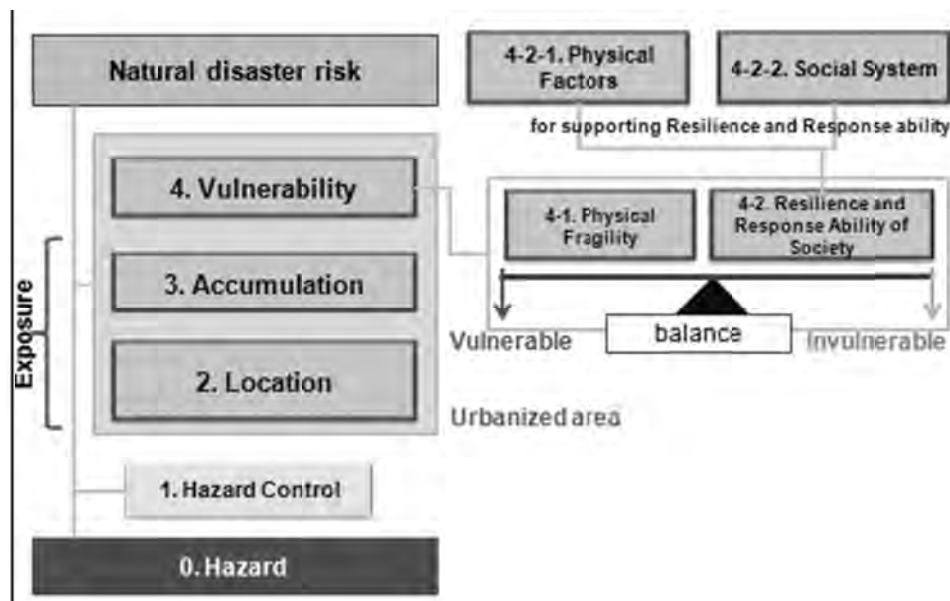


Figure 8 Structure of Natural Disaster Risks

3. CONCLUSION AND DISCUSSION

The important lessons learned from Tokyo are that rapid urbanization without urban planning would itself result in disaster risk, which means that disaster risk is closely related to urbanization. More attention should be paid to the rapid urbanization period. Whether urban planning includes the concept of risk management or not at this time will determine future disaster risks. In the case of a city having no concept of risk management, the city will have a huge amount of risk. Long-range plans are needed to consider this fact.

The structure of natural disaster risk can be constructed with four main keywords: hazard control, a city's location, accumulation, and vulnerabilities, including physical fragility and the resilience and response activities of local communities. All keywords, except hazard control, can be controlled by urban planning. The role of urban planning is significant in disaster risk management.

Developing cities, including Ulaanbaatar, are presently facing rapid urbanization. Present urban planning may be readjusted if based on the above context. However, urban planning should inherently be comprehensive; disaster risk management is also an important issue that urban planning should consider. Better direction should be pursued in balance with other urban planning issues.

REFERENCES

- Tokyo Metropolitan government. 2012. Report on earthquake damage estimation. Tokyo Metropolitan government, Japan.
 Cabinet Office. 2005. Report on Tokyo inner-plate earthquake damage estimation, Japan.

POSTER SESSION

The study to simplify the assessment of earthquake-proof of construction by comparing the first planning of construction to the measurement

Tsend-Ayush Badmaev

Geoinformation application for emergency management and hazard

Sodnomragchaa Dagva

Water ecology, efficient water usage for households

Batbileg Enkhbat

Conducting advanced technology of public transportation in Ulaanbaatar City

Munhjargal Victor

Introduction of intelligent transport system in vehicle parking management of Ulaanbaatar

Erdenetulga Jargalsaikhan

Ulaanbaatar City flat region acoustic

Barkhas Sukhbaatar

ECO FENCE-The improvement of the Ger district living environment

Ganbat Gantulga

The regulation of soil moisture and watering greenery of Ulaanbaatar City

Nasanbayar Narantsogt

Гал түймэр

Bazarragchaa Sodnom

Roadmap from smoke to the development: Airport city a win-win model for the economical context of the capital city development

Davaanyam Surenjav

The investigation on a chemical incident to be occurred in territory of Ulaanbaatar City

Ganzorig Tsogtbaatar

Disaster information collection by Thai and foreigners during the 2011 Thai flood

Michael Henry

Vulnerability assessment of snow disaster based on traffic system: A case study of Chenzhou city in Hunan, China

XU Xiaoge

Hanoi environmental planning to build resilience to climate change and natural disaster – A multi-institutional approach

Lan Huong Nguyen

An analytical investigation of applicability of mechanical anchorage system to beam-column joint by 3D discrete model

Koichiro Ikuta

Study on implementation of remote building damage assessment system during large scale earthquake disaster

Makoto Fujii

Reconstruction of Kamaishi City after the 2011 Tohoku earthquake and tsunami

Sae Shikita

Review on the definitions of vulnerability, resilience, and adaptation

Yuto Shiozaki

Study on the effects of chemical and physical property of concrete on the behavior of water

Chohji Nakamura

Modeling of diffusive and advective transport of ionic species in cemented soil

Hayato Ikoma

Static and fatigue shear performance of PVA-ECC beams with coarse aggregate in damaged condition

Yoshiyuki Takano

Estimation of global anthropogenic PM2.5 by integrating remote sensing and modeling

Hirothoshi Kishi

Evaluation of internal erosion by turbidity of drained water

Mari Sato

Sliding disaster in Vietnam and a new proposed design method of reinforced soil wall

Nguyen Hoang Giang

Seismic risk assessment of some historical mosques of Dhaka using non-destructive testing methods

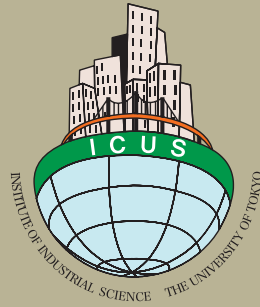
Mehedi Ahmed Ansary

Application of microtremor array for estimating shear wave velocity in Bangladesh

Mehedi Ahmed Ansary

Sea level rise impact on coastal aquifers: A case study in South West region of Bangladesh

Dushmanta Dutta



International Center for Urban Safety Engineering
Institute of Industrial Science, The University of Tokyo

4-6-1 Komaba, Meguro-ku,
Tokyo 153-8505, Japan

Tel: +81-3-5452-6472

Fax: +81-3-5452-6476

<http://icus.iis.u-tokyo.ac.jp>

E-mail: icus@iis.u-tokyo.ac.jp

ISBN 4-903661-61-X

